NUSANTARA BIOSCIENCE

ISEA JOURNAL OF BIOLOGICAL SCIENCES

| Nusantara Biosci | vol. 16 | no. 2 | pp. 149-303 | November 2024 |
| ISSN 2087-3948 | E-ISSN 2087-3956|

Doriprismatica atromarginata (Cuvier, 1804) photo by Budak

Society for
Indonesian Biodiversity

Sebelas Maret University
Surakarta

Published semiannually

PRINTED IN INDONESIA

ISSN 2087-3948 E-ISSN 2087-3956

NUSANTARA
BIOSCIENCE
ISEAJournal of Biological Sciences
| Nusantara Biosci | vol. 16 | no. 2 | pp. 149-303 |November 2024 |
|ISSN 2087-3948| E-ISSN 2087-3956|

PUBLISHER: Smujo International

ASSOCIATION: Society for Indonesian Biodiversity

INSTITUTION: School of Graduates, Sebelas Maret University, Surakarta

FIRST PUBLISHED: 2009

ADDRESS:
Bioscience Program, School of Graduates, Sebelas Maret University
Jl. Ir. Sutami 36A Surakarta 57126, Indonesia. Tel. & Fax.: +62-271-663375, email: editors@smujo.id

ONLINE: smujo.id/nb

List of reviewers: https://smujo.id/nb/reviewers

Society for Indonesian Biodiversity **Sebelas Maret University Surakarta**

Published by Smujo International for The Society for Indonesian Biodiversity and Sebelas Maret University Surakarta

GUIDANCE FOR AUTHORS

Aims and Scope ***Nusantara Bioscience*** (Nusantara Biosci) encourages submission of manuscripts dealing with all aspects of biological sciences that emphasize issues germane to biological and nature conservation; especially for the research conducted in the Islands of the Southeast Asian reign or Nusantara, but also from around the world.

Article types The journal seeks original full-length: (i) **Research papers**, (ii) **Reviews**, and (iii) **Short communications**. Original research manuscripts are limited to 8,000 words (including tables and figures) or proportional to articles in this publication number. Review articles are also limited to 8,000 words, while Short communications should be less than 2,500 words, except for pre-study.

Submission: The journal only accepts online submissions through the open journal system **(https://smujo.id/nb/about/submissions)** or, for login problems, email the editors at unsjournals@gmail.com (or editors@smujo.id). Submitted manuscripts should be the original works of the author(s). Please ensure that the manuscript is submitted using the template, which can be found at (https://biodiversitas.mipa.uns.ac.id/D/template.doc). The manuscript must be accompanied by a cover letter containing the article title, the first name and last name of all the authors, and a paragraph describing the claimed novelty of the findings versus current knowledge. Please also provide a list of five potential reviewers in your cover letter. They should come from outside your institution and better from three different countries. Submission of a manuscript implies the submitted work has not been published (except as part of a thesis or report, or abstract) and is not being considered for publication elsewhere. When a group writes a manuscript, all authors should read and approve the final version of the submitted manuscript and its revision; and agree on the submission of manuscripts for this journal. All authors should have made substantial contributions to the concept and design of the research, acquisition of the data and its analysis, drafting the manuscript, and correcting the revision. All authors must be responsible for the work's quality, accuracy, and ethics.

Ethics Author(s) must be obedient to the law and/or ethics in treating the object of research and pay attention to the legality of material sources and intellectual property rights.

Copyright If the manuscript is accepted for publication, the author(s) still hold the copyright and retain publishing rights without restrictions. For the new invention, authors must manage its patent before publication.

Open Access The journal is committed to free-open access that does not charge readers or their institutions for access. Readers are entitled to read, download, copy, distribute, print, search, or link to the full texts of articles, as long as not for commercial purposes. The license type is CC-BY-NC-SA.

Acceptance Only articles written in US English are accepted for publication. Manuscripts will be reviewed by editors and invited reviewers (double-blind review) according to their disciplines. Authors will generally be notified of acceptance, rejection, or need for revision within 1 to 2 months of receipt. Manuscripts will be rejected if the content does not align with the journal scope, does not meet the standard quality, is in an inappropriate format, or contains complicated grammar, dishonesty (i.e., plagiarism, duplicate publications, fabrication of data, citations manipulation, etc.), or ignoring correspondence in three months. The primary criteria for publication are scientific quality and significance. **Uncorrected proofs** will be sent to the corresponding author by system or email as .doc or .docx files for checking and correcting typographical errors. The corrected proofs should be returned in 7 days to avoid publication delays. The accepted papers will be published online in chronological order at any time but printed at the end of each month.

Charges Publishing costs waiver is granted to foreign (non-Indonesian) authors who first publish the manuscript in this journal. However, other authors are charged USD 150 (IDR 2,100,000). **Reprint** Authors or other parties may freely download and distribute. However, a printed request will be charged, especially regarding postal charges.

Manuscript preparation Manuscript is typed on A4 (210x297 mm^2) paper size, in a single column, single space, 10-point (10 pt) Times New Roman font. The margin text is 3 cm from the top, 2 cm from the bottom, and 1.8 cm from the left and right. Smaller lettering sizes can be applied in presenting tables and figures (9 pt). Word processing program or additional software can be used; however, it must be PC compatible, use the template, and be Microsoft Word based (.doc or .rtf; not .docx). **Scientific names** of species (incl. subspecies, variety, etc.) should be written in italics, except in italicized sentences. Scientific names (genus, species, author) and cultivar or strain should be mentioned completely for the first time mentioning it in the body text, especially for taxonomic manuscripts. The genus name can be shortened after the first mention, except in early sentences, or where this may generate confusion; name of the author can be eliminated after the first mention. For example, *Rhizopus oryzae* L. UICC 524 can be written hereinafter as *R. oryzae* UICC 524. Using trivial names should be avoided. **Biochemical and chemical nomenclature** should follow the order of the IUPAC-IUB. For DNA sequences, it is better to use Courier New font. Standard chemical abbreviations can be applied for common and clear used, for example, completely written butilic hydroxyl toluene (BHT) to be BHT hereinafter. **Metric measurements** should use IS denominations, and other systems should use equivalent values with the denomination of IS mentioned first. A dot should not follow abbreviations like g, mg, mL, etc. Minus index (m^{-2}, L^{-1}, h^{-1}) suggested being used, except in things like "per-plant" or "per-plot." **Mathematical equations** can be written down in one column with text; in that case, they can be written separately. **Numbers** one to ten are written in words, except if it relates to measurement, while values above them are written in number, except in early sentences. The fraction should be expressed in decimal. In the text, it should be used "%" rather than "percent." Avoid expressing ideas with complicated sentences and verbiage/phrasing, and use efficient and effective sentences.

The title of the article should be written in compact, clear, and informative sentence, preferably not more than 20 words. Name of author(s) should be completely written, especially for the first and the last name. **Name and institution** address should also be completely written with street name and number (location), postal code, telephone number, facsimile number, and email address. We choose local names in Bahasa Indonesia for universities in Indonesia. The mention of "strata" program, should be avoided. Manuscript written by a group, author for correspondence along with address is required (marked with "♥"). **The title page** (first page) should include title of the article, full name(s), institution(s) and address(es) of the author(s); the corresponding authors detailed postage and e-mail addresses (P), and phone (O) and fax numbers (O).

Abstract A concise abstract is required (about 200 words). The abstract should be informative and state briefly the aim of the research, the principal results and major conclusions. An abstract is often presented separately from the article, thus it must be able to stand alone (completely self-explanatory). References should not be cited, but if essential, then cite the author(s) and year(s). Abbreviations should be avoided, but if essential, they must be defined at their first mention. **Keywords** are about five words, covering scientific and local name (if any), research themes, and special methods used; and sorted from A to Z. **Abbreviations** (if any): All important abbreviations must be defined at their first mention there. **Running title** is about five words.

Introduction is about 600 words, covering the aims of the research and provide an adequate background, avoiding a detailed literature survey or a summary of the results. **Materials and Methods** should emphasize on the procedures and data analysis. **Results and Discussion** should be written as a series of connecting sentences, however, for a manuscript with long discussion should be divided into subtitles. Thorough discussion represents the causal effect mainly explains why and how the results of the research were taken place, and do not only re-express the mentioned results in the form of sentences. **Concluding** sentence should be given at the end of the discussion. **Acknowledgements** are expressed in a brief; all sources of institutional, private and corporate financial support for the work must be fully acknowledged, and any potential conflicts of interest are noted.

Figures and Tables of a maximum of three pages should be clearly presented. The title of a picture is written down below the picture, while the title of a table is written above the table. Colored figures can only be accepted if the information in the manuscript can lose without those images; the chart is preferred to use black and white images. The author could consign any picture or photo for the front cover, although it does not print in the manuscript. All images property of others should be mentioned the source. Author is suggested referring to Wikipedia for international boundaries and Google Earth for satellite imagery. If not specifically mentioned, it is assumed to refer to these sources. **There is no appendix**, all data or data analysis is incorporated into Results and Discussions. For broad data, it can be displayed on the website as a supplement.

References Preferably 80% of it comes from scientific journals published in the last 10 years. In the text, give the author names followed by the year of publication and arrange from oldest to newest and from A to Z; in citing an article written by two authors, both of them should be mentioned; however, for three and more authors only the first author is mentioned followed by et al. For example, Saharjo and Nurhayati (2006) or (Boonkerd 2003a, b, c; Sugiyarto 2004; El-Bana and Nijs 2005; Balagadde et al. 2008; Webb et al. 2008). Extent citation should be avoided, as shown with the word "cit." Reference to unpublished data and personal communication should not appear in the list but should be cited in the text only (e.g., Rifai MA 2007, pers. com. (personal communication); Setyawan AD 2007, unpublished data). In the reference list, the references should be listed in alphabetical order. Names of journals should be abbreviated. Always use the standard abbreviation of a journal's name according to the **ISSN List of Title Word Abbreviations** (www.issn.org/2-22661-LTWA-online.php). Please include DOI links for journal papers. The following examples are for guidance.

Journal:

Saharjo BH, Nurhayati AD. 2006. Domination and composition structure change at hemic peat natural regeneration following burning; a case study in Pelalawan, Riau Province. Biodiversitas 7: 154-158. DOI: 10.13057/biodiv/d070213.

The usage of "et al." in long author lists will also be accepted:

Smith J, Jones M Jr, Houghton L et al. 1999. Future of health insurance. N Engl J Med 965: 325-329. DOI: 10.10007/s002149800025.

Book:

Rai MK, Carpinella C. 2006. Naturally Occurring Bioactive Compounds. Elsevier, Amsterdam.

Chapter in the book:

Webb CO, Cannon CH, Davies SJ. 2008. Ecological organization, biogeography, and the phylogenetic structure of rainforest tree communities. In: Carson W, Schnitzer S (eds.). Tropical Forest Community Ecology. Wiley-Blackwell, New York.

Abstract:

Assaeed AM. 2007. Seed production and dispersal of *Rhazya stricta*. 50th annual symposium of the International Association for Vegetation Science, Swansea, UK, 23-27 July 2007.

Proceeding:

Alikodra HS. 2000. Biodiversity for development of local autonomous government. In: Setyawan AD, Sutarno (eds.). Toward Mount Lawu National Park; Proceeding of National Seminary and Workshop on Biodiversity Conservation to Protect and Save Germplasm in Java Island. Universitas Sebelas Maret, Surakarta, 17-20 July 2000. [Indonesian]

Thesis, Dissertation:

Sugiyarto. 2004. Soil Macro-invertebrates Diversity and Inter-Cropping Plants Productivity in Agroforestry System based on Sengon. [Dissertation]. Universitas Brawijaya, Malang. [Indonesian]

Information from the internet:

Balagadde FK, Song H, Ozaki J, Collins CH, Barnet M, Arnold FH, Quake SR, You L. 2008. A synthetic *Escherichia coli* predator-prey ecosystem. Mol Syst Biol 4: 187. DOI: 10.1038/msb.2008.24. www.molecularsystembiology.com.

NUSANTARA
BIOSCIENCE
| Nusantara Biosci | vol. 16 | no. 2 | pp. 149-303 | November 2024|
| ISSN 2087-3948 | E-ISSN 2087-3956|
ISEAJournal of Biological Sciences

THIS PAGE INTENTIONALLY LEFT BLANK

NUSANTARA BIOSCIENCE
Vol. 16, No. 2, pp. 149-153
November 2024

ISSN: 2087-3948
E-ISSN: 2087-3956
DOI: 10.13057/nusbiosci/n160201

Assessing the levels of heavy metals Cd, Cr, and Pb in the naturally occurring red seaweed *Gracilariopsis heteroclada* in Iloilo Province, Philippines, for potential mass cultivation

RILEY A. BEUP[1], SAMANTHA GRACE E. FELONGCO[1], SHARMAINE JOY C. CAILIN[1], NICOLAS G. GUANZON JR.[1], RAYMUND N. FANTONALGO[1], ROLANDO V. PAKINGKING JR.[1,2,♥]

[1]Life Sciences Department, College of Arts and Sciences, Central Philippine University. Jaro, Iloilo City 5000, Iloilo, Philippines
[2]College of Medical Laboratory Science, Central Philippine University. Jaro, Iloilo City 5000, Iloilo, Philippines. Tel.: +63-917-3228772, ♥email: rolando102969@gmail.com

Manuscript received: 20 February 2024. Revision accepted: 1 June 2024.

Abstract. *Beup RA, Felongco SGE, Cailin SJC, Guanzon Jr NG, Fantonalgo RN, Pakingking Jr RV. 2024. Assessing the levels of heavy metals Cd, Cr, and Pb in the naturally occurring red seaweed* Gracilariopsis heteroclada *in Iloilo Province, Philippines, for potential mass cultivation. Nusantara Bioscience 16: 149-153.* The Philippines, a leading exporter of seaweed, has incorporated strategies in its Philippine Industry Seaweed Roadmap (2022-2026) to boost seaweed production. Therefore, to achieve this, potential sites for seaweed cultivation must undergo assessment for heavy metal content. A pilot study assessed heavy metals Cd, Cr, and Pb levels in red seaweed (*Gracilariopsis heteroclada*) sourced from three locations in Iloilo Province, Philippines: Site 1, a fishpond in Brgy, Nabitasan, Leganes; Site 2, along Dumangas Port coastline in Brgy, Sapao, Dumangas; and Site 3, a fishpond in Brgy, Talokgangan, Banate. Flame atomic absorption spectrometry was employed to analyze heavy metal concentrations. The mean concentrations of Pb in *G. heteroclada* from Sites 1, 2, and 3 were 5.0129±0.0896, 5.0388±0.8749, and 3.5119±0.9262 mg/kg, respectively; for Cr, they were 3.3002±0.1436, 4.0464±0.3800, and 2.8027±0.1436 mg/kg, respectively. The mean Cd concentrations were also 0.8518±0.0349, 0.8115±0.0202, and 0.5423±0.0419 mg/kg, respectively. Although Cd levels met safety standards, Pb and Cr concentrations exceeded the maximum permissible levels set by the European Union (EU) and China Food and Drug Administration (CFDA), respectively. This suggests that the examined sites may not be suitable for large-scale cultivation due to potential health risks from Pb and Cr exposure through seaweed consumption. Continued monitoring of toxic metal levels in these areas is therefore imperative.

Keywords: Cadmium, chromium, *Gracilariopsis heteroclada,* lead, Philippines, red seaweeds

INTRODUCTION

Gracilaria is a versatile species commonly found in brackish water, mangrove swamps, and the sea, owing to its broad tolerance for changing environmental conditions, including varying salinities. Certain *Gracilaria* species exhibit rapid growth and can absorb high levels of nutrients, making them a valuable source of bioactive substances for multiple products (Wu et al. 2018). *Gracilaria* spp. are utilized in various ways, serving purposes in healthcare and acting as food, fodder, feed, and fertilizer. In Hawaii, fresh *Gracilaria* spp. has been collected and sold as a salad vegetable for many years, and coastal communities in Indonesia, Malaysia, the Philippines, and Vietnam have been gathering *Gracilaria* for food (Mahadevan 2015). Regarding trade, seaweed exports are expanding moderately, with the Philippines as one of the top export sources alongside Indonesia, Ireland, Chile, Korea, and China. The Philippines, following China, is the second-largest supplier of semi-processed and processed carrageenan in Asia (Bureau of Fisheries and Aquatic Resources 2022). According to the Bureau of Fisheries and Aquatic Resources (2022), there has been a noticeable increase in the Philippines' seaweed exports from 1996 to 2019. Specifically, there was a 29% growth observed, with total volumes reaching 37,148 metric tons in 1996 and 48,026 metric tons in 2019.

Seaweeds, including *Gracilaria* spp., can absorb heavy metals from the aquatic environment due to erosion, industrial activities, and domestic sewage (Sadhasivam et al. 2012). The accumulation of these contaminants over time can lead to elevated levels of heavy metals in seaweed, indicating a higher risk of heavy metal exposure during consumption. Sadhasivam et al. (2012) found that eight seaweed species could absorb seven types of heavy metals in varying quantities based on the species and collection areas. Additionally, prolonged ingestion of seaweed, even at low concentrations, may pose potential health risks, as heavy metals are considered non-essential. Consequently, consuming significant quantities of seaweed could result in adverse gastrointestinal, neurological, and carcinogenic effects (Asensio et al. 2021).

Gracilaria spp. play a crucial role in Philippine aquaculture, contributing significantly to both domestic and international production. Among these species, *Gracilariopsis heteroclada* stands out as particularly abundant, thriving in various natural habitats such as fishponds, estuaries, and bays, typically in intertidal or

shallow subtidal areas less than 1 meter deep, where it attaches to rocks or floats freely. Despite its importance, pertinent information regarding the heavy metal contents of *G. heteroclada* in the Philippines is scarce. Therefore, with its prevalence in specific municipalities of Iloilo Province and its widespread utilization as a bioproduct, it is imperative to assess the presence of heavy metals in *G. heteroclada* due to its ability to accumulate these contaminants. Recognizing the Philippines as a leading seaweed exporter, the government has integrated strategies into its Philippine Industry Seaweed Roadmap (2022-2026) to enhance seaweed production (Bureau of Fisheries and Aquatic Resources 2022). This initiative underscores the need to evaluate potential heavy metal content cultivation sites. In the current study, a pilot investigation aimed at determining the concentrations of lead (Pb), cadmium (Cd), and chromium (Cr) in *G. heteroclada* samples collected from selected sites in the municipalities of Leganes, Dumangas, and Banate within Iloilo Province was conducted. Resolute results generated from this study would be crucial in assessing the suitability of these sites for large-scale cultivation of red seaweeds.

MATERIALS AND METHODS

Sampling sites

G. heteroclada specimens were gathered from three distinct locations within the Iloilo Province, Philippines. These selected sites included: (i) Site 1, a fishpond in Brgy. Nabitasan, municipality of Leganes, Iloilo (10° 47' 6.828" N, 122° 38' 13.4376" E), (ii) Site 2, positioned along Dumangas Port in Brgy. Sapao, municipality of Dumangas, Iloilo (10° 46' 50.4372" N, 122° 42' 31.6476" E), and (iii) Site 3, a fishpond located in Brgy. Talokgangan, municipality of Banate, Iloilo (11° 0' 52.4952" N, 122° 49' 58.1952" E) (Figure 1). These sites were selected primarily based on the abundance of naturally occurring red seaweeds and their proximity to nearby establishments, which could potentially serve as sources of heavy metal contamination in the surrounding water bodies.

Water physicochemical parameters

In-situ temperature, pH, and salinity measurements were conducted using a portable multiparameter tool (WalkLAB Professional pH and Temperature Meter HP 9010) and a handheld refractometer (RHS-100ATC), respectively. Dissolved oxygen analysis of water samples was performed at the Chemistry Laboratory of the Central Philippine University.

Collection of seaweed samples

Four kilograms of fresh weight of *G. heteroclada* were gathered from each of the three sampling sites, following a method adapted from Khaled et al. (2014) to ensure an adequate quantity of thalli. Wild thalli found within the sampling areas were manually collected and placed in plastic ziplock bags. Only mature thalli were selected for sampling, and collection occurred during low tide at the shoreline of Dumangas Port. The collected samples were promptly transported to the Research Laboratory at Central Philippine University for preparation. Upon arrival, the seaweed samples underwent thorough washing with running tap water to eliminate sand, salts, and other external particles adhering to the surface. Subsequently, distilled water was used for a final rinse. Drying and homogenization procedures followed the methods outlined by Baghazadeh et al. (2021) and Khandaker et al. (2021), with slight modifications. Briefly, the fresh weight of the samples was recorded before they were divided based on their sampling areas. Air drying was conducted at room temperature (28°C) for 72 hours, followed by further drying in a closed system microwave oven set at 70°C for two days to eliminate remaining moisture. The dried samples were then blended using a heavy-duty blender, resulting in homogenized seaweed powder stored in ziplock bags at room temperature until further analysis.

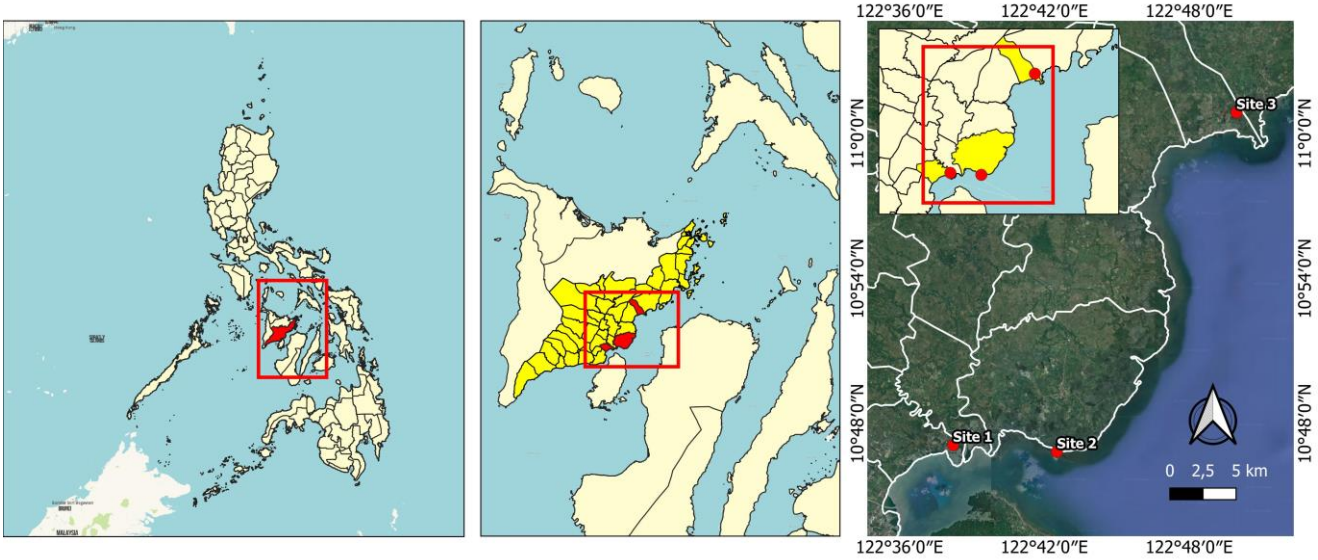

Figure 1. Map of the Philippines indicating the locations of the three sampling sites within the Iloilo Province, Philippines

Heavy metal analysis

The dry-weight replication method outlined by Khaled et al. (2014) was employed with slight modifications. Ten grams (10 g) of dried seaweed from each sample were placed into a crucible in triplicate and weighed using a top-loading analytical balance. The ash extraction technique for seaweed samples described by Rasyid (2017) was slightly modified. Briefly, to determine ash content, *G. heteroclada* samples were heated in a muffle furnace at 450-550°C for 2 hours, followed by cooling at room temperature after removal from the furnace.

Sample digestion was conducted following the method detailed by Qari (2015) and Uddin et al. (2016), utilizing the nitric-hydrochloric acid digestion 1:3 method. Triplicate samples of seaweed species (10 g each) were digested in a freshly prepared acid mixture of one (1) mL 65% HNO_3, 3 mL 37% HCl, and 50 mL H_2O. The resulting mixture was gently boiled over a water bath (95°C) for 5 minutes. Following digestion, the cooled solutions were filtered using Whatman filter paper (No. 41) and transferred to volumetric flasks, with distilled water added to reach a final volume of 50 mL for instrumental analysis. Blank flasks underwent the same treatment using identical volumes of acid and distilled water, with the digestion process repeated for each replicate.

Furthermore, following the procedure outlined by El-Said and El-Sikaily (2013), all digested solutions were analyzed in triplicate for Pb, Cd, and Cr using a flame atomic absorption spectrometer (Agilent 55 AA Spectrometer G8430A). Standard precautions for element analysis were adhered to throughout the process, and analytical-grade reagents were utilized to prepare calibration curves. The detection limits for the studied metals were as follows: Pb (0.1 ppm), Cr (0.1 ppm), and Cd (0.01 ppm).

Statistical analysis

The gathered data underwent statistical analysis employing One-Way Analysis of Variance (ANOVA) to assess potential variations in heavy metal levels among the three sampling sites. After identifying significant differences among the sampling sites, Post hoc analysis was conducted using Duncan's Multiple Range Test (DMRT). The level of significance was set at $P < 0.05$.

RESULTS AND DISCUSSION

Moreover, to effectively achieve the objectives outlined in the Philippine Industry Seaweed Roadmap (2022-2026), which aims to enhance seaweed production in the country, it is imperative to conduct assessments for heavy metal content at potential seaweed cultivation sites in the Philippines. In our current investigation, we delved into the presence of three common heavy metals (Pb, Cr, and Cd) in seaweeds, alongside analyzing the water parameters at three designated sampling sites. Our findings, as depicted in Table 1, reveal notable concentrations of Pb and Cr exceeding the maximum permissible limits required by both the European Union (EU) (European Commission 2020) and China Food and Drug Administration (CFDA) (USDA FAS 2017). Conversely, Cd concentrations remained within acceptable regulatory thresholds. Across the three sampling sites, Pb concentrations ranged from 3.5119±0.9262 mg/kg to 5.0388±0.8749 mg/kg, with Dumangas (Site 2) displaying the highest mean and Banate (Site 3) exhibiting the lowest. Similarly, Cr concentrations varied from 2.8027±0.1436 mg/kg to 4.0464±0.3800 mg/kg, with Dumangas showcasing the highest level and Banate registering the lowest mean compared to the other sampling sites. Cd concentrations ranged from 0.5423±0.0419 mg/kg to 0.8518±0.0349 mg/kg, with Leganes (Site 1) recording the highest mean and Banate the lowest among the three sampling sites. Our findings suggest that while Cd pollution levels were relatively lower than Pb and Cr across all sampling sites, the presence of Pb and Cr remains a concern. pH values across the sampling sites fell within the normal range, while salinity, dissolved oxygen, and water temperature exhibited expected variations typical of marine environments, as shown in Table 2. The lower levels of dissolved oxygen in the bodies of water may have been attributed to a combination of factors such as the presence of fertilizers, excess amounts of nutrients, and organic matter, all of which exacerbate oxygen depletion. Additionally, samples were collected early in the morning, hence the amount of light to drive photosynthesis may be limited.

The elevated levels of Pb and Cr, particularly observed at Dumangas and Leganes, are likely attributed to nearby anthropogenic sources such as local businesses, residences, and maritime activities. Improper waste disposal and industrial processes in these areas could contribute significantly to heavy metal contamination. For instance, maritime vessels operating near Dumangas Port could introduce substantial amounts of fuel, paint, coatings, and other pollutants, contributing to the observed high lead and chromium content in seaweed samples. Similarly, observations at Leganes pointed to potential sources of heavy metal contamination, including effluents from local businesses, residences, and educational institutions. Additionally, agricultural practices near the fishpond and the possibility of corroded leaded pipelines in residential areas may further exacerbate lead contamination in seaweed samples collected from Leganes. Comparatively, Banate exhibited the lowest heavy metal concentrations among the three sites, attributed to its more secluded location with less vehicular and marine traffic. However, despite the relatively lower concentrations, the presence of Pb and Cr still exceeded maximum limits. Our current findings plausibly corroborate with the research conducted by Gangoso et al. (2022), which highlighted that industrial processes, improper waste management, fuel combustion, and the degradation of leaded pipelines were the primary sources of Pb contamination identified in three specific sampling locations in the southern Philippines. Similarly, the elevated levels of Cr could originate from natural sources like weathering rocks containing Cr, as well as from domestic pollution and the prolonged deposition of Cr. Furthermore, the study reported by Gangoso et al. (2022) indicated that Cd, particularly sludge, can travel

long distances, contaminating surface waters and accumulating in sediments. Additionally, our findings are consistent with the study conducted by Karthikeyan et al. (2020), which examined the concentrations of priority metals (Cr, Cd, and Pb) in water, sediment, and biota in the Ennore estuary along the southeast coast of India. Karthikeyan et al. (2020) observed higher levels of these metals than other estuaries in India, suggesting significant bioaccumulation of non-essential metals such as Cd and Pb in marine organisms. The presence of these heavy metals was attributed to various anthropogenic activities, including industrial operations, dredging, thermal power plants, petrochemical industries, vehicular emissions, port activities, and urban expansion, encompassing both residential and fishing communities.

The current study shows that the three sampling sites contained high levels of Pb and Cr but relatively low levels of Cd, indicating that *G. heteroclada* can accumulate substantial quantities of heavy metals over time. Notably, following safety standards, concentrations of Pb and Cr surpassed the maximum permissible limits established by the European Union (EU) (European Commission 2020) and the National Food Safety Standard for Maximum Levels of Contaminants in Foods (GB 2762-2017) of the China Food and Drug Administration (CFDA) (USDA FAS 2017). Consequently, even at low concentrations, prolonged consumption of seaweed may pose health risks due to the toxicity of heavy metals, which are non-essential elements. Lead, for instance, is a toxic heavy metal that adversely affects various bodily systems, including the kidneys, hematopoietic, and nervous systems (Charkiewicz and Backstrand 2020). Assi et al. (2016) reported a range of physiological, biochemical, and neurobehavioral effects associated with Pb ingestion, with severe consequences on the cardiovascular, reproductive, hematopoietic, and peripheral and central nervous systems, as well as organs like the liver, bone, and kidneys. Chakraborty et al. (2022) noted its accumulation in organs, such as the lungs, liver, and kidneys, with detrimental effects on human health. Similarly, increased Cr accumulation in organs has been linked to deteriorating organ functions and overall human health. Chromium exposure is associated with liver and kidney damage, widespread dermatitis, gastrointestinal tract disorders, respiratory tract cancers, cardiovascular disorders, and alterations in DNA methylation status (Chakraborty et al. 2022). At lower levels, cadmium can harm the liver, kidneys, skeletal, and cardiovascular systems. Additionally, Genchi et al. (2020) noted that environmental Cd exposure may elevate the risk of osteoporosis. Epidemiological data suggest that occupational and environmental exposure to Cd may be related to various cancers, including those affecting the breast, lung, prostate, nasopharynx, pancreas, and kidneys (Genchi et al. 2020). Given the adverse effects of consuming contaminated seaweed, it is clear that harvesting and distributing red seaweed from these sampling sites is not recommended. However, large-scale efforts can be targeted towards bioremediation of the polluted sampling sites instead. For example, Rahhou et al. (2023) extensively documented the bioaccumulation and restoration capabilities of *Ulva lactuca*. This species exhibits a remarkable affinity for a wide array of metals, including iron (Fe) and manganese (Mn), as well as essential nutrients like nitrogen and phosphorus. Such characteristics render *U. lactuca* effective in remediating heavy metal contamination and mitigating eutrophication, underscoring its significant potential for bioremediation purposes (Rahhou et al. 2023).

Table 1. Concentrations of heavy metals in *G. heteroclada* collected from the three sampling sites in Iloilo Province, Philippines

Heavy metal	Mean (±SD) concentration (mg/kg)*			Maximum permissible limit (mg/kg)	
	Site 1. Brgy. Nabitasan, Leganes, Iloilo	Site 2. Brgy. Sapao, Dumangas, Iloilo	Site 3. Brgy. Talokgangan, Banate, Iloilo	European Union[a]	China Food and Drug Administration[b]
Pb	5.0129±0.0896[a]	5.0388±0.8749[a]	3.5119±0.9262[a]	1.5	1.5
Cr	3.3002±0.1436[b]	4.0464±0.3800[a]	2.8027±0.1436[c]	NA	2.0
Cd	0.8518±0.0349[a]	0.8115±0.0202[a]	0.5423±0.0419[b]	3.0	2.0

Note: *Limit of detection (mg/kg dry weight): Pb: 0.1; Cr: 0.1; Cd: 0.01. Different letter superscripts denote significant differences at $P < 0.05$. (NA): Not available. [a]European Commission (2020). [b]United States Department of Agriculture Foreign Agricultural Service (2017)

Table 2. Water physicochemical characteristics (mean±SD) of the three sampling sites

Site	Water physicochemical parameters			
	pH	Salinity (‰)	Temperature (°C)	Dissolved Oxygen (mg/L)
Site 1 (Brgy. Nabitasan, Leganes, Iloilo)	8.04±0.00	34±0.00	26.0±0.00	4.0±0.20
Site 2 (Brgy. Sapao, Dumangas, Iloilo)	8.14±0.23	29±0.00	25.8±0.20	4.9±0.15
Site 3 (Brgy. Talokgangan, Banate, Iloilo)	8.12±0.00	29±0.00	24.4±0.23	3.9±0.15

Our current study presents preliminary data on heavy metals Pb, Cr, and Cd concentrations in red seaweeds collected from selected sites in Iloilo province, identified as potential areas for large-scale cultivation. *G. heteroclada* has shown the ability to gradually absorb and accumulate heavy metals from its aquatic surroundings, making it a valuable bioindicator for heavy metal contamination. Our current data, therefore, emphasizes the necessity for ongoing investigation and regular monitoring of seaweed cultivation areas due to the frequent association between high seaweed consumption and human poisoning. Distribution and consumption of *G. heteroclada* from the sampled sites are strongly discouraged, given the elevated heavy metal levels indicating widespread contamination across water bodies. Consequently, these sites studied are presently unsuitable for extensive production and consumption due to high levels of Pb and Cr in the red seaweeds naturally growing in these sites. Therefore, to augment our understanding of trace metal concentrations comprehensively, future investigations should prioritize the exploration of pollution indices, particularly to elucidate the pollution status within the sediment and water of the presently studied sites. Continuous monitoring of heavy metal content in harvested *G. heteroclada* is therefore recommended to ensure safety. Local Government Units (LGUs) should proactively educate communities about the risks associated with consuming metal-contaminated seaweed and encourage alternative sourcing for businesses and restaurants. Collaboration between government agencies and the private sector is essential to enforce regulations and screening measures for water and environmental quality, addressing concerns highlighted by this study within the seaweed industry. Ultimately, concerted efforts from LGUs and the private sector are imperative to tackle pollution sources in water bodies, securing the long-term sustainability of the seaweed sector in the Philippines.

ACKNOWLEDGEMENTS

We express our heartfelt gratitude to the Research and Development Laboratory staff and the Chemical Engineering Technicians of Central Philippine University, Philippines for their invaluable assistance during the study's conduct.

REFERENCES

Asensio JP, Arnaiz UD, Navarro PJ. 2021. Studying inorganic arsenic, heavy metals, and iodine in dried seaweed. Spectroscopy Suppl 36: 24-34.

Assi MA, Hezmee MN, Haron AW, Sabri MYM, Rajion, MA. 2016. The detrimental effects of lead on human and animal health. Vet World 9 (6): 660-671. DOI: 10.14202/vetworld.2016.660-671.

Baghazadeh DL, Samsampour D, Bagheri A, Sohrabipour J. 2021. High content of heavy metals in seaweed species: A case study in the Persian Gulf and the Gulf of Oman in the southern coast of Iran. Phycol Res 4: 544-560.

Bureau of Fisheries and Aquatic Resources. 2022. The Philippine Seaweed Industry Roadmap (2022-2026). Bureau of Fisheries and Aquatic Resources, Quezon City, Philippines. https://www.pcaf.da.gov.ph/wp-content/uploads/2022/06/Philippine-Seaweed-Industry-Roadmap-2022-2026.pdf.

Chakraborty R, Renu K, Eladl MA, El-Sherbiny M, Elsherbini DMA, Mirza AK, Vellingiri B, Iyer M, Dey A, Valsala Gopalakrishnan A. 2022. Mechanism of chromium-induced toxicity in lungs, liver, and kidney and their ameliorative agents. Biomed Pharmacother 151: 113119. DOI: 10.1016/j.biopha.2022.113119.

Charkiewicz AE, Backstrand JR. 2020. Lead toxicity and pollution in Poland. Intl J Environ Res Public Health 17 (12): 4385. DOI: 10.3390/ijerph17124385.

El-Said GF, El-Sikaily A. 2013. Chemical composition of some seaweed from Mediterranean Sea coast, Egypt. Environ Monit Assess 185 (7): 6089-6099. DOI: 10.1007/s10661-012-3009-y.

European Commission. 2020. Commission Regulation (EC) No. 1881/2006 setting maximum levels for certain contaminants in foodstuffs. FAO, Rome, Italy. https://www.fao.org/faolex/results/details/en/c/LEX-FAOC068134/

Gangoso SJ, Del Rosario RM, Walag AM. 2022. The concentrations of selected heavy metals in the surface sediments in three locations of southern Philippines. Asian J Biol Life Sci 11 (2): 514-519. DOI: 10.5530/ajbls.2022.11.69.

Genchi G, Sinicropi MS, Lauria G, Carocci A, Catalano A. 2020. The effects of cadmium toxicity. Intl J Environ Res Public Health 17 (11): 3782. DOI: 10.3390/ijerph17113782.

Karthikeyan P, Marigoudar SR, Mohan D, Nagarjuna A, Sharma KV. 2020. Ecological risk from heavy metals in Ennore estuary, South East coast of India. Environ Chem Ecotoxicol 2: 182-193. DOI: 10.1016/j.enceco.2020.09.004.

Khaled A, Hessein A, Abdel-Halim AM, Morsy FM. 2014. Distribution of heavy metals in seaweeds collected along Marsa-Matrouh beaches, Egyptian Mediterranean Sea. Egypt J Aquat Res 40 (4): 363-371. DOI: 10.1016/j.ejar.2014.11.007.

Khandaker MU, Chijioke NO, Heffny NB, Bradley DA, Alsubaie A, Sulieman A, Faruque MR, Sayyed MI, Al-Mugren KS. 2021. Elevated concentrations of metal (loids) in seaweed and the concomitant exposure to humans. Foods 10 (2): 381. doi: 10.3390/foods10020381.

Mahadevan K. 2015. Seaweeds: A sustainable food source. In: Tiwari BK, Troy DJ (eds). Seaweed Sustainability. Academic Press, San Diego. DOI: 10.1016/B978-0-12-418697-2.00013-1.

Qari R. 2015. Heavy metals concentrations in brown seaweed *Padina Pavonia* (L.) and *P. tetrastromatica* at different beaches of Karachi Coast. Indian J Geo-Mar Sci 44: 1200-1206.

Rahhou A, Layachi M, Akodad M, El Ouamari N, Rezzoum NE, Skalli A, Oudra B, El Bakali M, Kolar M, Imperl J, Petrova P, Moumen A, Baghour M. 2023. The bioremediation potential of *Ulva lactuca* (chlorophyta) causing green tide in marchica lagoon (NE Morocco, Mediterranean Sea): Biomass, heavy metals, and health risk assessment. Water 15 (7): 1310. DOI: 10.3390/w15071310.

Rasyid A. 2017. Evaluation of nutritional composition of the dried seaweed *Ulva lactuca* from Pameungpeuk waters, Indonesia. Trop Life Sci Res 28 (2): 119-125. DOI: 10.21315/tlsr2017.28.2.9.

Sadhasivam S, Seedevi P, Ramasamy P, Subhapradha N, Vairamani S, Shanmugam A. 2012. Heavy metal accumulation in seaweeds and sea grasses along southeast coast of India. J Chem Pharm Res 2012: 4240-4244.

Uddin AH, Khalid RS, Alaama M, Abdualkader AM, Kasmuri A, Abbas SA. 2016. Comparative study of three digestion methods for elemental analysis in traditional medicine products using atomic absorption spectrometry. J Anal Sci Technol 7 (1): 6. DOI: 10.1186/s40543-016-0085-6.

United States Department of Agriculture Foreign Agricultural Service (USDA FAS). 2017. National Food Safety Standard for Maximum Levels of Contaminants in Foods (GB 2762-2017). National Health and Family Planning Commission (NHFPC, currently the National Health Commission) and the China Food and Drug Administration (CFDA, currently the State Administration of Market Regulation). https://fas.usda.gov/data/china-china-releases-standard-maximum-levels-contaminants-foods.

Wu H, Shin SK, Jang S, Yarish C, Kim JK. 2018. Growth and nutrient bioextraction of *Gracilaria chorda*, *G. vermiculophylla*, *Ulva prolifera*, and *U. compressa* under hypo- and hyper-osmotic conditions. Algae 33 (4): 329-340. DOI: 10.4490/algae.2018.33.11.13.

NUSANTARA BIOSCIENCE
Vol. 16, No. 2, pp. 154-168
November 2024

ISSN: 2087-3948
E-ISSN: 2087-3956
DOI: 10.13057/nusbiosci/n160202

Shallow water sea slugs (Gastropoda: Heterobranchia) from Andhra Pradesh, India

J.S. YOGESH KUMAR[1,♥], ARYA SEN[1], C. RAGHUNATHAN[2], C. VENKATRAMAN[3]

[1]Zoological Survey of India, Sunderban Regional Centre. Canning, West Bengal 743329, India. Tel.: +91-9476006830,
♥email: yogeshkumarzsi16@gmail.com
[2]Zoological Survey of India. M-Block, New Alipore, Kolkata, West Bengal 700053, India
[3]Zoological Survey of India, Marine Biology Regional Centre. Chennai, Tamil Nadu 600028, India

Manuscript received: 10 March 2024. Revision accepted: 1 June 2024.

Abstract. *Kumar JSY, Sen A, Raghunathan C, Venkatraman C. 2024. Shallow water sea slugs (Gastropoda: Heterobranchia) from Andhra Pradesh, India. Nusantara Bioscience 16: 154-168.* The current manuscript explores the initial underwater survey findings, revealing 19 heterobranch species across 10 genera, 6 families, 2 suborders, one order, and one superorder within the Visakhapatnam coast of Andhra Pradesh, India. While, the heterobranchs fauna of Andhra Pradesh has been studied by several authors, it has been observed that underwater surveys to discover this marine group are lacking from the region, and therefore, the present study has been done. These species from the study site include *Coryphellina exoptata*, *Pteraeolidia semperi*, *Dendrodoris krusenstenii*, *Doriprismatica atromarginata*, *Glossodoris* sp. cf. *cincta*, *G. rufomarginata*, *Goniobranchus alius*, *G. setoensis*, *G. fidelis*, *G. trimarginatus*, *Hypselodoris bullockii*, *H. nigrostriata*, *H. sagamiensis*, *H. kanga*, *Jorunna funebris*, *Phyllidia ocellata*, *P. polkadotsa*, *Phyllidiopsis phiphiensis*, and *Elysia marginata*. Remarkably, 13 of these heterobranchs species are documented for the first time in the Andhra Pradesh region, with 12 belonging to the order Nudibranchia and one to the superorder Sacoglossa. The manuscript provides a comprehensive analysis of morphometric characteristics, detailed descriptions, photography, and distribution trends of 19 heterobranchs species, as well as a comprehensive literature record of sea slugs found in Andhra Pradesh, India. Sea slugs, being the butterflies of the ocean, are a great part of the ecosystem, although based on economic valuation, they are regarded as a low-value bycatch, trash. The bottom trawl is one of the major threats to the habitat destruction for these animals. Thus, the habitats along the Andhra coastline should be known so that fishing activities in these parts could be restricted for the better survival of sea slugs.

Keywords: East Coast, Heterobranchia, Nudibranchia, sea slugs, Visakhapatnam

INTRODUCTION

Heterobranchs, also known as different-gilled snails, sea slugs, sea hares, sea rabbits, and nudibranchs, are a diverse group of marine gastropod mollusks. The term "nudibranch" originates from the Latin "nudus," which translates to naked, and the Greek "brankhia," which means gills. This name reflects the absence of a protective shell and the existence of exposed gills or gill-like structures found in numerous species. This fascinating group belongs to the subclass Heterobranchia. It encompasses various colorations and growth forms, including head-shield slugs (Cephalaspidea), sap-sucking slugs (Sacoglossa), sea hares (Anaspidea or Aplysiida), side-gill slugs (Pleurobranchomorpha or Pleurobranchida), nudibranchs (Nudibranchia), and umbrella shells (Umbraculida) (Gosliner and Behrens 2015; Apte and Desai 2017). Approximately 6,000 species of heterobranchs have been described worldwide, although around 5,194 species are currently considered valid per the WoRMS (World Register of Marine Species). Among these, nudibranchs are particularly diverse, with approximately 2,520 species identified. Nudibranchs are further classified into two suborders: Cladobranchia and Doridina. The suborder Cladobranchia comprises seven superfamilies, 49 families, 158 genera, and 1,034 species, while the suborder Doridina consists of two infraorders, six superfamilies, 20 families, 108 genera, and 1,486 species (Gosliner et al. 2008; Gobbeler and Klussmann-Kolb 2011).

This classification underscores the vast diversity and intricacy of the nudibranch group, emphasizing the ongoing need for research and exploration to deepen our understanding of these captivating marine organisms (Gosliner and Behrens 2015). Recent studies have focused on monitoring and assessing sea slug communities globally and at regional levels, including India (Raghunathan et al. 2016; Apte and Desai 2017). Fortunately, the colorful sea slugs were observed by recreational SCUBA divers, underwater photographers, and researchers (Nimbs et al. 2015, 2016). Research has identified approximately 400 species spanning seven orders within the Heterobranchia subclass in India. Among these, 213 species have been documented in the Andaman and Nicobar Islands, 88 species along the Tamil Nadu coast, 76 species in the Lakshadweep Islands, 56 species along the Gujarat coast, 55 species along the Andhra Pradesh coast, 28 species in Maharashtra, 9 species in Orissa, 8 species in Kerala, 6 species in Karnataka, 6 species in West Bengal, and 2 species in Goa (Raghunathan et al. 2016; Apte and Desai 2017).

The current investigation was conducted along the Visakhapatnam coast in Andhra Pradesh, which boasts

India's second longest coastline (975 km) and forms part of the Coromandel Coast along the eastern seaboard. Sea slugs were initially documented along the Visakhapatnam coast in the 1880s by Alder and Hancock, along with Eliot, who reported 42 species (Alder and Hancock 1864; Eliot 1906). Subsequently, Sarma (1974) recorded 26 species from this area, while Ramakrishna et al. (2007) reported five species from Andhra Pradesh. Additionally, Srinivasulu et al. (2012) documented the presence of the blue sea slug (*Glaucus atlanticus* Forster, 1777) along the Visakhapatnam coast. Bhave and Apte (2013) updated the current status of the Indian Opisthobranch and mentioned 40 species belonging to 26 genera, 18 families from the Andhra Pradesh coast. Venkataraman et al. (2015) listed 47 species, and Raghunathan et al. (2016) reported an updated list of opisthobranchs from the Indian coast with 55 species from Andhra Pradesh. Apte and Desai (2017) recently published a field guide with good underwater photos, including 26 species from the Andhra Pradesh coast.

Numerous researchers have studied the distribution of heterobranchs along the Indian coastline. However, the authors of this study identified 19 species of heterobranchs, among which 13 species had not been previously recorded. Therefore, this study intends to document these previously unrecorded species from coastal parts of Andhra Pradesh and to furnish a comprehensive and updated list of heterobranch sea slugs in this state.

MATERIAL AND METHODS

The current research was conducted across nine sub-tidal study sites spanning from Rushikonda beach to Chinthapalli beach along Visakhapatnam, Andhra Pradesh State, India (Figure 1, Table 1). Coral reefs and associated fauna surveys were conducted between 24 February to 2 March 2019 and 13 to 20 December 2019. Sub-tidal surveys were conducted at depths ranging from 8 to 24 meters with the assistance of SCUBA diving. Specimens were collected through direct searches within reef and rocky ecosystems, and those collected were anesthetized using a solution containing 72 g L^{-1} of $MgCl_2$. After morphological examinations, the anesthetized specimens were preserved in 100% ethyl alcohol. Underwater photographs were taken of live specimens to record their colors accurately. Identification of specimens was based on morphological characteristics (Jensen 1992; Gosliner 1995; Gosliner et al. 2008; Apte and Desai 2017), and afterward, they were placed in the National Zoological Collections at the Marine Aquarium Regional Centre of the Zoological Survey of India, located in Digha, West Bengal, with each specimen assigned a voucher number.

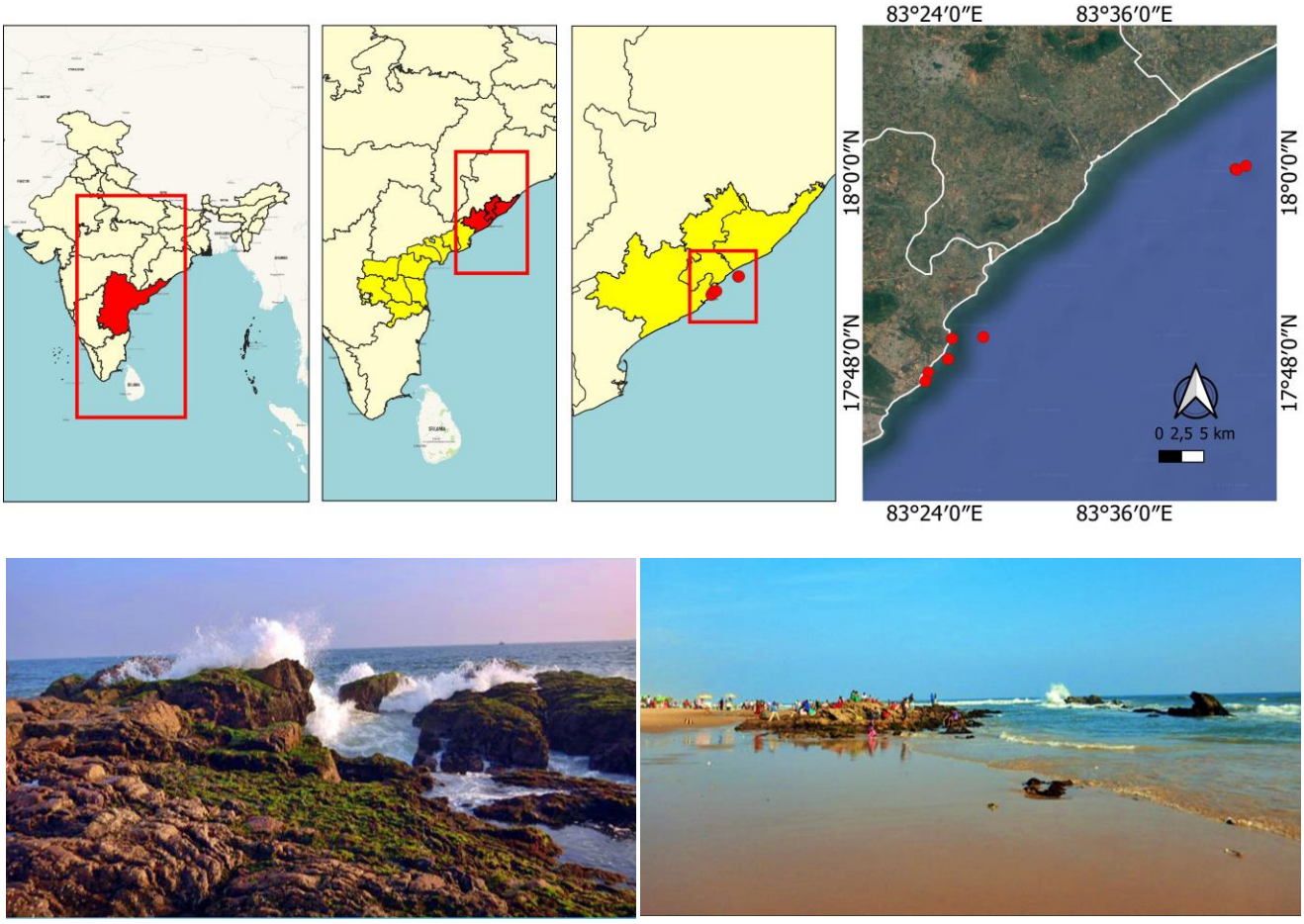

Figure 1. Study site map and surveyed habitats along Visakhapatnam coast of Andhra Pradesh, India; rocky shore and sandy shore

Table 1 Detail of the study areas with GPS coordinates

Date	Name of the place	GPS coordinates	Depth	Habitat
26.02.19	Off Chinthapalli village Shipwreck	Lat. N 18° 00.249', Long. E 83° 43.026’	9 m	Rocky Bottom
27.02.19	Off Chinthapalli village	Lat. N 18° 00.265', Long E 83° 43.022'	12 m	Rocky Bottom
27.02.19	Off Chinthapalli village	Lat. N 18° 00.199', Long. E 83° 43.108’	22 m	Rocky Bottom
01.03.19	Off Chinthapalli village	Lat. N 18° 00.457', Long. E 83° 43.683’	24 m	Sandy Bottom
14.12.19	Off Vammivanipalem	Lat. N 17° 47.421’, Long. E 83° 23.618’	9 m	Rocky Bottom
15.12.19	Off Rushikonda	Lat. N 17° 46.868', Long. E 83° 23.426’	8 m	Rocky Bottom
16.12.19	Off Mangamari Peta	Lat. N 17° 49.558', Long. E 83° 25.110’	9 m	Rocky Bottom
18.12.19	Off Timmapuram	Lat. N 17° 48.272', Long. E 83° 24.869’	12 m	Rocky Bottom
19.12.19	Off Mangamari Peta	Lat. N 17° 49.656', Long. E 83° 27.096’	15 m	Rocky Bottom

RESULTS AND DISCUSSION

During the underwater exploration conducted on the Visakhapatnam coast of Andhra Pradesh, 19 species of heterobranchs from 10 genera and 6 families were discovered (Figures 2-9). Notably, 13 of these species were documented for the first time in the study sites. These newly reported species include *Hypselodoris bullockii* (Collingwood, 1881); *H. sagamiensis* (Baba, 1949); *Phyllidia ocellata* (Cuvier 1804); *P. polkadotsa* (Brunckhorst, 1993); *Phyllidiopsis phiphiensis* (Brunckhorst, 1993); *Glossodoris cincta* (Bergh, 1888); *G. rufomarginata* (Bergh, 1890); *Goniobrachus alius* (Rudman, 1987); *G. decorus* (Pease, 1860); *G. trimarginatus* (Winckworth, 1946); *Coryphellina exoptata* (Gosliner & Willan, 1991); *Pteraeolidia semperi* (Bergh, 1870); and *Elysia marginata* (Pease, 1871).

In terms of higher-order classification, the majority of the identified species belonged to the order Nudibranchia, with the suborder Doridina comprising the highest number (16 species, 8 genera, 4 families) and the suborder Cladobranchia featuring the lowest number (2 species, 2 genera, 2 families). Additionally, the superorder Sacoglossa was represented by one species from the genus *Elysia* and the family Plakobranchidae. Among the study sites, the highest number of species was reported from Off Chinthapalli (12 species), followed by five species from Off Rushikonda beach, four species from Off Vammivanipalem, two species from Off Mangamari Peta, and one species from Off Timmapuram (Table 2).

This comprehensive study revealed 103 species of Heterobranchs belonging to 59 genera, 33 families, and 4 orders in Andhra Pradesh (refer to Table 3). Notably, all authors in the updated list commonly reported two species, *Dendrodoris krusensternii* (Gray, 1850), and *Jorunna funebris* (Kelaart, 1859. The majority of the species (77 species) belonged to the Order Nudibranchia, followed by the Superorder Sacoglossa (13 species), Order Cephalaspidea (6 species), Order Aplysiida (4 species), Order Pleurobranchida (2 species), and Superorder Ringiculimorpha (1 species). The systematic features of the 19 species of Heterobranchs collected in this study are outlined accordingly.

Table 2. Heterobranchs distribution from the present study sites in Visakhapatnam coast, Andhra Pradesh, India

Species	1	2	3	4	5
Coryphellina exoptata (Gosliner & Willan, 1991)	+	-	-	-	-
Pteraeolidia semperi (Bergh, 1870)	-	+	-	-	-
Dendrodoris krusenstenii (Gray, 1850)	-	+	-	-	-
Doriprismatica atromarginata (Cuvier, 1804)	+	+	-	-	-
Glossodoris sp. cf. *cincta* (Bergh, 1888)	-	+	+	-	-
Glossodoris rufomarginata (Bergh, 1890)	+	-	-	-	-
Goniobranchus alius (Rudman, 1987)	-	-	+	-	-
Goniobranchus setoensis (Baba, 1938)	-	-	+	-	-
Goniobranchus fidelis (Kelaart, 1858)	-	+	-	-	-
Goniobranchus trimarginatus (Winckworth, 1946)	-	+	+	-	-
Hypselodoris bullockii (Collingwood, 1881)	-	+	-	+	-
Hypselodoris nigrostriata (Eliot, 1904)	+	+	-	-	-
Hypselodoris sagamiensis (Baba, 1949)	-	-	-	-	+
Hypselodoris kanga (Rudman, 1977)	+	-	-	-	-
Jorunna funebris (Kelaart, 1859	-	+	-	-	-
Phyllidia ocellata (Cuvier, 1804)	-	-	-	-	+
Phyllidia polkadotsa (Brunckhorst, 1993)	-	+	-	-	-
Phyllidiopsis phiphiensis (Brunckhorst, 1993)	-	+	-	-	-
Elysia marginata (Pease, 1871)	-	+	-	-	-
Total	5	12	4	1	2

Note: + Present; - Absent; Study sites 1. Off Rushikonda; 2. Off Chinthapalli; 3. Off Vammivanipalem; 4. Off Timmapuram; 5. Off Mangamari Peta

Table 3. List of Heterobranchs reported from the Andhra Pradesh, India

Species	R1	R2	R3	R4	R5	PS
Superorder Nudipleura (Wagele & Willan, 2000)						
Order: Nudibranchia (Cuvier, 1817)						
Family: Arminidae (Iredale & O'Donoghue, 1923)						
Armina formosa (Kelaart, 1858)	-	-	-	+	-	-
Armina taeniolata (Bergh, 1866)	-	-	-	+	-	-
Armina variolosa (Bergh, 1904)	-	-	-	+	-	-
Suborder Doridina						
Family Discodorididae (Bergh, 1891)						
Asteronotus cespitosus (van Hasselt, 1824)	-	-	-	+	-	-
Family Discodorididae (Bergh, 1891)						
Atagema carinata (Quoy & Gaimard, 1832)	+	-	-	-	-	-
Atagema intecta (Kelaart, 1859)	-	-	-	+	-	-
Atagema osseosa (Kelaart, 1859)	+	-	-	-	-	-
Atagema spongiosa (Kelaart, 1858)	-	-	-	+	+	-
Atagema tristis (Alder & Hancock, 1864)	+	-	-	+	-	-
Family Chromodorididae (Bergh, 1891)						
Ceratosoma trilobatum (J.E. Gray, 1827)	-	-	-	+	-	-
Chromodoris inopinata (Bergh, 1905)	-	-	-	+	-	-
Doriprismatica atromarginata (Cuvier, 1804)	-	-	-	+	-	+
Hypselodoris bullockii (Collingwood, 1881)	-	-	-	-	-	+
Hypselodoris infucata (Ruppell & Leuckart, 1828)	-	-	-	+	-	-
Hypselodoris kanga (Rudman, 1977)	-	-	-	+	-	+
Hypselodoris nigrostriata (Eliot, 1904)	-	-	-	-	+	+
Hypselodoris sagamiensis (Baba, 1949)	-	-	-	-	-	+
Hypselodoris zebrina (Alder & Hancock, 1864)	+	-	-	+	-	-
Family Phyllidiidae (Rafinesque, 1814)						
Phyllidia ocellata (Cuvier, 1804)	-	-	-	-	-	+
Phyllidia polkadotsa (Brunckhorst, 1993)	-	-	-	-	-	+
Phyllidiella zeylanica (Kelaart, 1859)	-	-	-	+	-	-
Phyllidiopsis phiphiensis (Brunckhorst, 1993)	-	-	-	-	-	+
Family Dendrodorididae (O'Donoghue, 1924)						
Dendrodoris areolata (Alder & Hancock, 1864)	+	-	-	-	-	-
Dendrodoris atromaculata (Alder & Hancock, 1864)	+	-	-	-	+	-
Dendrodoris fumata (Ruppell & Leuckart, 1830)	+	-	-	+	+	-
Dendrodoris fusca (Alder & Hancock, 1864)	+	-	-	-	-	-
Dendrodoris krusensternii (Gray, 1850)	+	-	-	+	+	+
Dendrodoris nigra (Stimpson, 1855)	+	+	-	+	+	-
Dendrodoris punctata (Alder & Hancock, 1864)	+	-	-	-	-	-
Dendrodoris pustulosa (Alder & Hancock, 1864)	+	-	-	-	-	-
Dendrodoris tuberculosa (Quoy & Gaimard, 1832)	+	-	-	+	+	-
Doriopsilla miniata (Alder & Hancock, 1864)	+	+	-	-	-	-
Family Discodorididae (Bergh, 1891)						
Discodoris concinna (Alder & Hancock, 1864)	+	-	-	-	-	-
Discodoris pardalis (Alder & Hancock, 1864)	+	-	-	+	-	-
Jorunna funebris (Kelaart, 1859)	+	-	-	+	-	+
Platydoris ellioti (Alder & Hancock, 1864)	+	-	-	+	+	-
Platydoris formosa (Alder & Hancock, 1864)	+	-	-	+	-	-
Platydoris scabra (Cuvier, 1804)	-	-	-	+	-	-
Platydoris striata (Kelaart, 1858)	+	-	-	+	-	-
Sclerodoris apiculata (Alder & Hancock, 1864)	+	-	-	+	+	-
Sclerodoris tuberculata (Eliot, 1904)	+	-	-	-	-	-
Sebadoris fragilis (Alder & Hancock, 1864)	+	-	-	-	+	-
Sebadoris nubilosa (Pease, 1871)	-	-	-	+	-	-
Tayuva lilacina (Gould, 1852)	-	-	-	+	+	-
Thordisa villosa (Alder & Hancock, 1864)	+	-	-	-	+	-
Family Doridiidae (Rafinesque, 1815)						
Doris immonda (Risbec, 1928)	-	-	-	-	+	-
Doris rusticata (Alder & Hancock, 1864)	+	-	-	-	-	-
Glossodoris sp. cf. *cincta* (Bergh, 1888)	-	-	-	-	-	+
Glossodoris rufomarginata (Bergh, 1890)	-	-	-	-	-	+
Goniobrachus alius (Rudman, 1987)	-	-	-	-	-	+
Goniobranchus setoensis (Baba, 1938)	-	-	-	-	-	+
Goniobranchus fidelis (Kelaart, 1858)	-	-	-	+	-	+

Goniobranchus gleniei (Kelaart, 1858)	-	-	-	+	-	-
Goniobranchus preciosa (Kelaart, 1858)	-	-	-	+	-	-
Goniobranchus tennentanus (Kelaart, 1859)	-	-	-	+	-	-
Goniobranchus trimarginatus (Winckworth, 1946)	-	-	-	-	-	+
Family Goniodorididae (H. Adams & A. Adams, 1854)						
Goniodoris aspersa (Alder & Hancock, 1864)	+	-	-	-	-	-
Goniodoris citrina (Alder & Hancock, 1864)	+	-	-	-	-	-
Goniodoris modesta (Alder & Hancock, 1864)	+	-	-	-	-	-
Family Polyceridae (Alder & Hancock, 1845)						
Gymnodoris bicolor (Alder & Hancock, 1864)	+	-	-	-	-	-
Gymnodoris ceylonica (Kelaart, 1858)	-	-	-	+	-	-
Kalinga ornata (Alder & Hancock, 1864)	+	-	+	+	-	-
Plocamopherus ceylonicus (Kelaart, 1858)	+	+	-	-	-	-
Suborder Cladobranchia						
Family Arminidae (Iredale & O'Donoghue, 1923)						
Pleurophyllidiella paucidentata (O'Donoghue, 1932)	-	+	-	-	-	-
Family Bornellidae (Bergh, 1874)						
Bornella stellifera (A. Adams & Reeve, 1848)	+	+	-	+	+	-
Family Facelinidae (Bergh, 1889)						
Coryphellina exoptata (Gosliner & Willan, 1991)	-	-	-	-	-	+
Favorinus japonicus (Baba, 1949)	-	-	-	+	-	-
Phidiana militaris (Alder & Hancock, 1864)	+	+	-	+	+	-
Phidiana unilineata (Alder & Hancock, 1864)	+	-	-	-	-	-
Pteraeolidia semperi (Bergh, 1870)	-	-	-	-	-	+
Family Eubranchidae (Odhner, 1934)						
Eubranchus ocellatus (Alder & Hancock, 1864)	+	-	-	-	-	-
Family Glaucidae (Gray, 1827)						
Glaucus atlanticus (Forster, 1777)	-	-	-	+	+	-
Glaucus forsteri (Lamarck, 1819)	+	-	-	-	-	-
Family Madrellidae (Preston, 1911)						
Madrella ferruginosa (Alder & Hancock, 1864)	+	-	-	-	+	-
Family Tethydidae (Rafinesque, 1815)						
Melibe viridis (Kelaart, 1858)	+	-	-	-	+	-
Family Samlidae (Korshunova, et al. 2017)						
Samla bicolor (Kelaart, 1858)	-	-	-	+	-	-
Family Scyllaeidae (Alder & Hancock, 1855)						
Scyllaea pelagica (Linnaeus, 1758)	+	-	-	-	+	-
Superorder Nudipleura						
Order Pleurobranchida						
Family Pleurobranchidae (Gray, 1827)						
Berthella stellata (Risso, 1826)	-	-	-	-	+	-
Family Pleurobranchaeidae (Pilsbry, 1896)						
Pleurobranchaea morula (Bergh, 1905)	-	+	-	-	-	-
Order Cephalaspidea (P. Fischer, 1883)						
Family Bullidae (Gray, 1827)						
Bulla ampulla (Linnaeus, 1758)	-	-	+	+	-	-
Family Haminoeidae (Pilsbry, 1895)						
Lamprohaminoea cymbalum (Quoy & Gaimard, 1833)	-	-	+	-	+	-
Lamprohaminoea ovalis (Pease, 1868)	-	+	-	-	-	-
Haminoea elegans (Gray, 1825)	-	-	+	-	-	-
Bakawan rotundata (A. Adams, 1850)	-	+	-	-	-	-
Family Tornatinidae (P. Fischer, 1883)						
Acteocina townsendi (Melvill, 1898)	-	+	-	-	-	-
Order Aplysiida						
Family Aplysiidae (Lamarck, 1809)						
Aplysia argus (Ruppell & Leuckart, 1830)	-	+	-	-	-	-
Aplysia oculifera (A. Adams & Reeve, 1850)	-	+	-	-	-	-
Bursatella leachii (Blainville, 1817)	-	+	-	-	-	-
Stylocheilus striatus (Quoy & Gaimard, 1832)	-	-	-	-	+	-
Superorder Sacoglossa						
Family Juliidae (E.A. Smith, 1885)						
Berthelinia limax (Kawaguti & Baba, 1959)	-	+	-	+	+	-
Elysia bangtawaensis (Swennen, 1998)	-	-	-	-	+	-
Elysia bengalensis (Swennen, 2011)	-	-	-	-	+	-
Elysia grandifolia (Kelaart, 1858)	-	+	-	+	-	-
Elysia marginata (Pease, 1871)	-	-	-	-	-	+

Family Oxynoidae (Stoliczka, 1868)						
Lobiger nevilli (Pilsbry, 1896)	-	+	-	-	-	-
Oxynae viridis (Pease, 1861)	-	+	-	-	+	-
Family Hermaeidae (H. Adams & A. Adams, 1854)						
Polybranchia orientalis (Kelaart, 1858)	+	+	-	+	-	-
Family Volvatellidae (Pilsbry, 1895)						
Ascobulla fischeri (A.Adams & Angas, 1864)	-	+	-	-	-	-
Volvatella pyriformis (Pease, 1868)	-	+	-	-	-	-
Family Limapontiidae (Gray 1847)						
Stiliger viridis (Kelaart, 1858)	-	-	-	+	-	-
Family Plakobranchidae (Gray, 1840)						
Thuridilla coerulea (Kelaart, 1857)	-	-	-	+	-	-
Family Aplustridae (Gray, 1847)						
Hydatina zonata (Lightfoot, 1786)	-	-	-	-	+	-
Superorder Ringiculimorpha						
Family Ringiculidae (Philippi, 1853)						
Ringicula propinquans (Hinds, 1844)	-	-	+	+	-	-
Total	40	20	5	45	27	19

Note: + Present; - Absent. R1: Alder and Hancock (1864), R2: Sarma (1974), R3: Ramakrishna et al. (2007), R4 - Venkataraman et al. (2015), R5: Apte and Desai (2017), PS: Present study

Phylum Mollusca Linnaeus, 1758
Class Gastropoda Cuvier, 1795
Order Nudibranchia Cuvier, 1817
Family Facelinidae Bergh, 1889
Genus *Caloria* Trinchese, 1888

Coryphellina exoptata (Gosliner & Willan, 1991) (Figure 2.A)

Synonyms: *Flabeltina exoptata* Gosliner & Willan, 1991.

Material Examined: ZSI/MARC M7359, Off Rushikonda (Lat. N 17°47.421'; Long E 83°23.618'), Visakhapatnam coast, Andhra Pradesh, 15.12.2019.

Diagnosis: Underwater, the live animal is translucent violet colored; long cerata are arranged in 6-8 clusters with creamy white tips and blue bands. The oral tentacles are also the same color, with a blue band and creamy white tip. Rhinopores are bright orange colored. This particular species is defined by having a prominent central purple, occasionally violet-blue, ring on its cerata, which are capped with opaque creamy yellow tips. Its rhinophores display vibrant shades of orange to red. The front corners of its foot are notably enlarged, forming sharply pointed tentacles, while its oral tentacles are elongated and cylindrical.

Size: 12 mm.

Habitat: Rocky bottom with algae.

Distribution: Australia, Indonesia, Russell Island, Solomon Island, Indonesia, South Africa, Malaysia, South China, Reunion Island, Korea, Japan, Christmas Island, Papua New Guinea, Philippines, India (Andaman and Nicobar Island).

Remarks: New distribution report to Andhra Pradesh State.

Genus *Pteraeolidia* Bergh, 1875

Pteraeolidia semperi (Bergh, 1870) (Figure 2.B)

Synonyms: *Flabellina ianthina* Angas, 1864.

Material Examined: ZSI/MARC M6251, Off Chinthapalli (Lat. 18°00.265'N; Long 83°43.022' E), Vizianagaram, Andhra Pradesh, 27.02.2019.

Diagnosis: The animal is commonly called a blue dragon, and the colors differ from place to place. The present study reveals that the animal is light brown, and its oral tentacles have 3 purple bands. The first two bands are close to each other and got fused. A blue line runs from rhinophores to the end of the ceratal cluster and has diamond-shaped blur spots intermittently. Cerata is short compared to body length. White markings are present overhead. The lateral side of the body is also covered with spots.

Size: 75 mm

Habitat: Artificial shipwreck ecosystem with rocky bottom covered in algae.

Distribution: Indo-West Pacific, Tropical, Subtropical, and India (Gulf of Mannar, Gujarat, Lakshadweep Islands, Andaman and Nicobar Island).

Remarks: New distribution report to Andhra Pradesh State.

Family Dendrodorididae O'Donoghue, 1924
Genus *Dendrodoris* Ehrenberg, 1831

Dendrodoris krusensternii (Gray, 1850) (Figure 3)

Synonyms: *Actinodoris krusensternii* Gray, 1850; *Dendrodoris clavulata* (Alder and Hancock, 1864); *Dendrodoris denisoni* (Angas, 1864); *Dendrodoris gemmacea* (Alder and Hancock, 1864); *Doridopsis gemmacea* Alder and Hancock, 1864; *Doris denisoni* Angas, 1864

Material Examined: ZSI/MARC M6253, Off Chinthapalli (Lat. 18°00.265'N; Long 83°43.022' E), Vizianagaram, Andhra Pradesh, 27.02.2019.

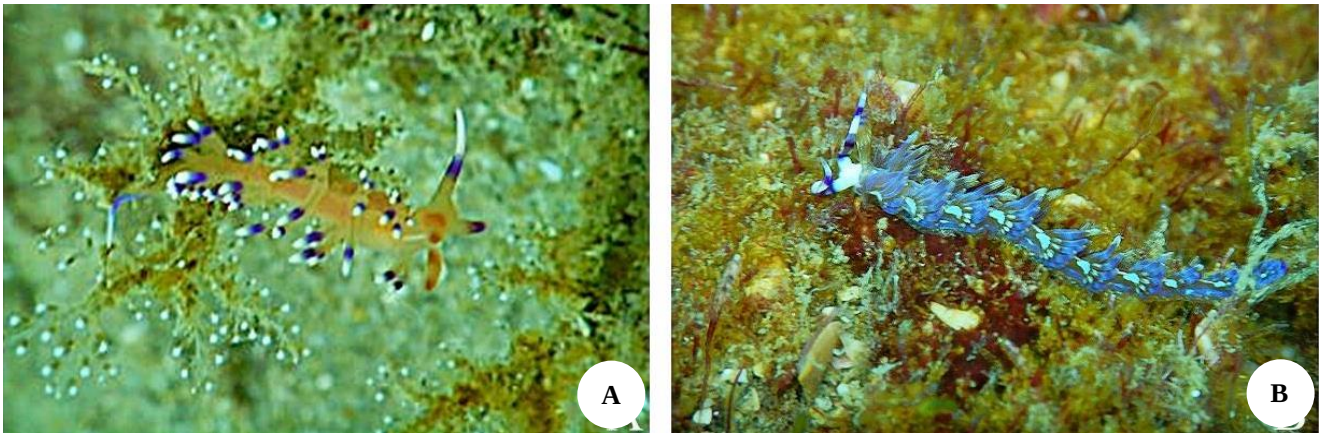

Figure 2. A. *Coryphellina exoptata* (Gosliner & Willan, 1991), B. *Pteraeolidia semperi* (Bergh, 1870)

Figure 3. *Dendrodoris krusenstenii* (Gray, 1850)

Diagnosis: The species is often called ornate elysia or leaf slugs. They exhibit a translucent greenish-yellow hue adorned with white and black speckles. The dorsal surface, or notum, is adorned with fleshy tubercles, while blue spots appear amid these tubercles. Along the body's periphery is an orange band and a black margin. The rhinophores, which are sensory structures, are robust and club-shaped, displaying orange coloring with dark tips.

Size: 25 mm

Habitat: Artificial shipwreck ecosystem with rocky bottom covered in algae.

Distribution: Australia, South Africa, Thailand, Indonesia, South Korea, Reunion Island, Singapore, New Zealand, Taiwan, Hawaii, Philippines, India (Goa, Andhra Pradesh, Andaman and Nicobar Islands).

Remarks: The species documented along the Coromandel Coast by Alder and Hancock (1864) was found in the current study off Chinthapalli, Visakhapatnam, on the Coromandel Coast after 1864, which is 155 years ago.

Family Chromodorididae Bergh, 1891

Genus *Doriprismatica* d' Orbigny, 1839

Doriprismatica atromarginata (Cuvier, 1804) (Figure 4)

Synonyms: *Casella atromarginata* (Cuvier, 1804); *Casella pallida* Bergh, 1905; *Casella maccarthyi* (Kelaart, 1859); *Casella philippinensis* Bergh, 1874; *Doris atromarginata* Cuvier, 1804; *Doris maccarthyi* Kelaart, 1859; *Glossodoris atromarginata* (Cuvier, 1804); *Glossodoris maccarthyi* (Kelaart, 1858); *Goniodoris atromarginata* (Cuvier, 1804).

Material Examined: ZSI/MARC M6243, Off Chinthapalli (Lat. 18°00.265'N; Long 83°43.022' E), Vizianagaram, 27.02.2019; ZSI/MARC M6868, Off Rushikonda (Lat. 17°46.868' N; Long. 83°23.426' E), Visakhapatnam, Andhra Pradesh, 15.12.2019.

Diagnosis: The specimens obtained from the study site exhibit a creamy white to pale yellow hue, with a sinuous mantle edge clearly adorned with a black band. The edges are raised compared to the body. The feathery gills and rhinophores are notable for their black-edged appearance and smooth surfaces. Additionally, the base of the rhinophores features several circular dark rings.

Size: 35 - 40 mm

Habitat: Artificial shipwreck ecosystem with rocky bottom covered in algae.

Distribution: It occurs throughout tropical and subtropical Indo-Pacific water in India (Tamil Nadu, Andhra Pradesh, Kerala, Andaman and Nicobar Islands).

Remarks: Ramakrishna et al. (2010) documented the presence of *G. atromarginata* along the Andhra Pradesh coast. In our current investigation, after a gap of nine years, we report the same species with underwater live photographs from Visakhapatnam, Andhra Pradesh.

Genus *Glossodoris* Ehrenberg, 1831

Glossodoris* sp. cf. *cincta (Bergh, 1888) (Figure 5.A)

Synonyms: *Casella cincta* Bergh, 1888; *Casella foxi* O'Donoghue, 1929

Material Examined: ZSI/MARC M6244, Off Chinthapalli (Lat. 18°00.265'N; Long 83°43.022' E), Vizianagaram, 27.02.2019; ZSI/MARC M6899, Off Vammivanipalem (Lat. 17°47.421' N; Long. 83°23.618' E), Visakhapatnam, Andhra Pradesh, 14.12.2019.

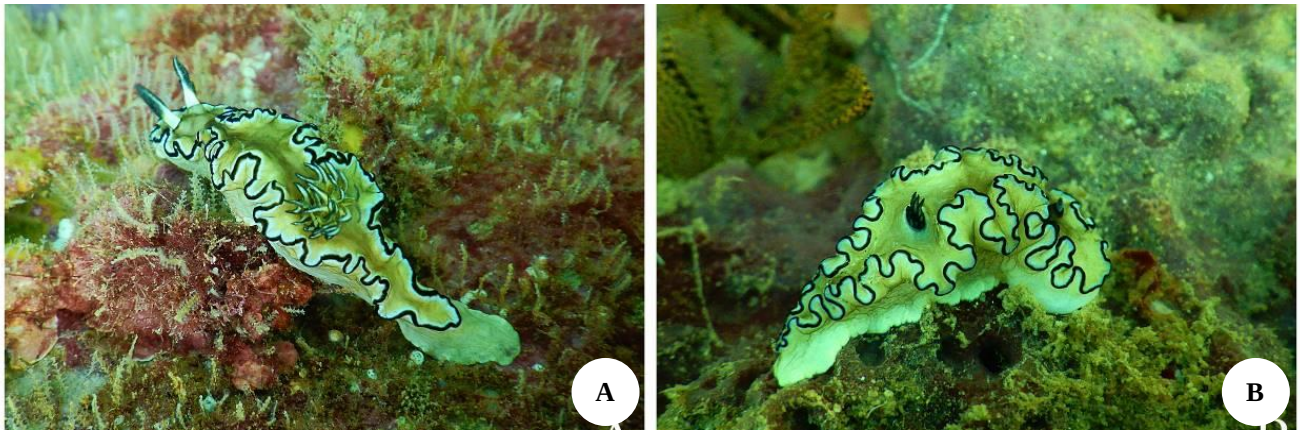

Figure 4. (A-B) *Doriprismatica atromarginata* (Cuvier, 1804)

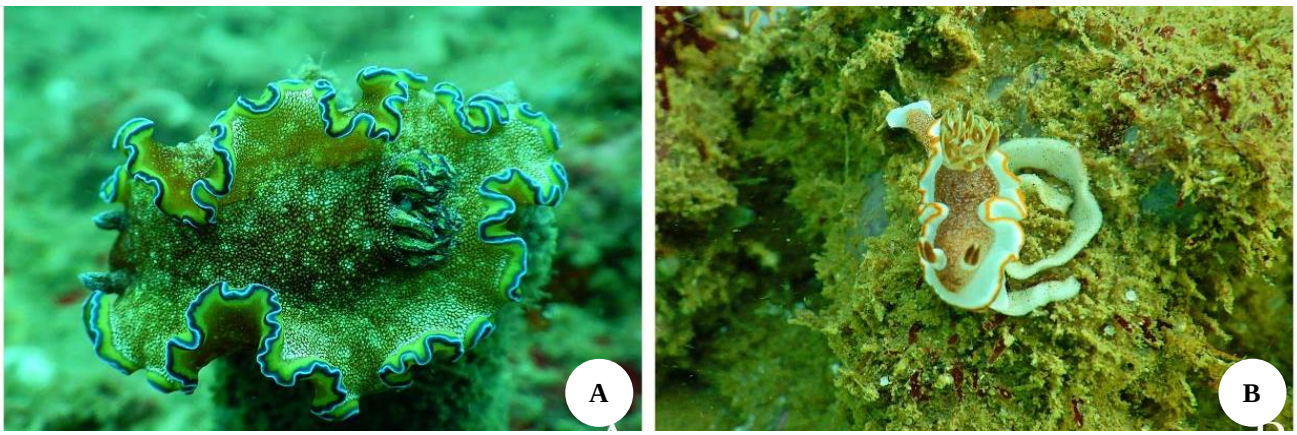

Figure 5. A. *Glossodoris* sp. cf. *cincta* (Bergh, 1888), B. *Glossodoris rufomarginata* (Bergh, 1890)

Diagnosis: The specimen exhibits red and yellow spots bordered by a blue margin. The mantle flaps display a vibrant yellow band at the edge, succeeded by a dark blue band and a light blue band along the outermost edge. The foot appears deep red or brown with a blue border. The rhinophores are ribbed and blue with a red base, while the gills are white with blue borders.

Size: 40 mm

Habitat: Artificial shipwreck ecosystem with rocky bottom covered in algae.

Distribution: The Red Sea to Tanzania, Japan, Fiji, Papua New Guinea, Australia, Maldives, Hong Kong, and India (Tamil Nadu, Lakshadweep, Andaman and Nicobar Islands).

Remarks: New distribution report to Andhra Pradesh State.

Glossodoris rufomarginata (Bergh, 1890) (Figure 5.B)

Synonyms: *Casella rufomarginata* Bergh, 1890; *Chromodoris rufomarginata* (Bergh, 1890); *Chromodoris youngbleuthi* Kay & Young, 1969; *Chromolaichma youngbleuthi* (Kay & Young, 1969); *Glossodoris youngbleuthi* (Kay & Young, 1969).

Material Examined: ZSI/MARC M6870, Off Rushikonda Beach (Lat. 17°46.868' N; Long. 83°23.426' E), Visakhapatnam coast, Andhra Pradesh, 15.12.2019.

Diagnosis: The specimens from the study site displayed a white coloration with an orange-brown speckled line pattern adorning the mantle, while the mantle's border exhibits an orange-brown hue. Typically, the margin appears white in most individuals, encircled by a delicate orange or tan line. As individuals mature, the mantle margin develops more intricate folds. The rhinophores and gills are light brown with white linings.

Size: 25 mm

Habitat: Rocky bottom covered in algae.

Distribution: Red Sea, Indonesia, Malaysia, Japan, Korea, Myanmar, Taiwan, Philippines, Tanzania, Aldabra, Papua New Guinea, Hawaii, Australia, Solomon Island, French Polynesia, India (Andaman and Nicobar Islands).

Remarks: New distribution reports to Andhra Pradesh State.

Genus *Goniobranchus* Pease, 1866

Goniobranchus alius (Rudman, 1987) (Figure 6.A)

Synonyms: *Chromodoris alius* Rudman, 1987

Material Examined: ZSI/MARC M7360, Off Vammivanipalem (Lat. 17°47.421' N; Long 83°23.618' E), Visakhapatnam coast, Andhra Pradesh, 14.12.2019.

Diagnosis: The body is creamy-white with dull brown and yellow spots all over the mantle surface. The mantle

border is decorated with a series of oblong violet spots. Rhinophores stalks are translucent white, and dark brown clubs and gills are white.

Size: 35 mm

Habitat: Rocky bottom covered in algae.

Distribution: South Africa, Madagascar, Tanzania, Reunion Island, Sri Lanka, India (Lakshadweep Islands, Andaman and Nicobar Islands).

Remarks: New distributional record for Andhra Pradesh State. This species displays a range of color variations, spanning from a white dorsum with a purple mantle edge to a brownish dorsum with light yellow spots within the purple margin. The latter pattern bears resemblance to *Goniobranchus aureopurpurus* found in the West Pacific. According to Rudman (2005), there is a suggestion that "*G. alius*, *G. aureopurpureus*, *G. rufomaculatus*, and *G. albopustulosus*" might represent the same species with extensive geographical distribution and color variations.

Goniobranchus setoensis (Baba, 1938) (Figure 6.B)

Synonyms: *Chromodoris decora* (Pease, 1860); *Chromodoris ndukuei* Risbec, 1928; *Doris decora* Pease, 1860; *Glossodoris (Chromodoris) ndukuei* (Risbec, 1928); *Glossodoris decora* (Pease, 1860); *Glossodoris ndukuei* (Risbec, 1928).

Material Examined: ZSI/MARC M7361, Off Vammivanipalem (Lat. N 17°47.421'; Long E 83°23.618'), Visakhapatnam coast, Andhra Pradesh, 14.12.2019.

Diagnosis: The species is translucent, with considerable variability in coloration. However, its most distinctive feature is an opaque white line running along the dorsal midline, branching into an inverted 'Y' shape. However, purple spots are absent in the midline (present incase of *G. decorus*). Along the mantle edge, there's a delicate, opaque white line, often fragmented into a series of white spots or patches, followed by a deep orange band and purple spots. A slender white line between the rhinophores extends along the dorsal midline towards the center, where it divides to form a loop encircling the gill pocket. The rhinophores have a translucent straw coloration with a solid white core. At the same time, the gills exhibit a similar hue, with their lamellae appearing creamy-brown straw-colored and their interior displaying an opaque white shade.

Size: 10 mm

Habitat: Rocky bottom covered in algae.

Distribution: Kenya, South Africa, Sri Lanka, Burma, Reunion Island, Maldives, Myanmar, Thailand, India (Lakshadweep Island, Andaman and Nicobar Islands, Kerala).

Remarks: New distributional record for Andhra Pradesh State.

Goniobranchus fidelis (Kelaart, 1858) (Figure 6.C)

Synonyms: *Chromodoris fidelis* (Kelaart, 1858); *Chromodoris flammulata* Bergh, 1905; *Chromodoris krishna* Rudman, 1973; *Chromodoris lactea* Bergh, 1905; *Doris fidelis* Kelaart, 1858; *Glossodoris fidelis* (Kelaart, 1858).

Material Examined: ZSI/MARC M6245, Off Chinthapalli (Lat. 18°00.265'N; Long 83°43.022' E), Vizianagaram, Andhra Pradesh, 27.02.2019.

Diagnosis: The specimens were creamy white, and the margin of the mantle was orange. Typically, along the inner boundary of the orange band, a succession of elongated patches resembling tongues that extend into the white area is observed. The rhinophores are greyish with white tips, and the gills are the same color.

Size: 20 mm

Habitat: Artificial shipwreck ecosystem with rocky bottom covered in algae.

Distribution: New Caledonia, Hong Kong, Japan, Red Sea, Australia, Seychelles, Indonesia, Malaysia, Papua New Guinea, India (Gujarat, Tamil Nadu, Andhra Pradesh, Lakshadweep, Andaman and Nicobar Island).

Remarks: Ramakrishna et al. (2010) documented the presence of *Chromodoris fidelis* along the Andhra Pradesh coast. Our current study reports on the same species after a nine-year interval, including underwater live photographs from Visakhapatnam, Andhra Pradesh.

Goniobranchus trimarginatus (Winckworth, 1946) (Figure 6.D)

Synonyms: *Chromodoris trimarginata* Winckworth, 1946); *Glossodoris trimarginata* Winckworth, 1946.

Material Examined: ZSI/MARC M6871, Off Vammivanipalem (Lat. N 17°47.421'; Long E 83°23.618'), Visakhapatnam coast, Andhra Pradesh, 14.12.2019.

Diagnosis: The specimen appears transparent with minor black or brown markings. A delicate purple line delineates the edge of the mantle, succeeded by black and yellow lines, each of the same breadth. The rhinophores exhibit lamellate structures, and both the gill leaves and rhinophores are white.

Size: 20 mm

Habitat: Rocky bottom covered in algae.

Distribution: Thailand, Malaysia, India (Tamil Nadu, Maharashtra).

Remarks: New distributional record for Andhra Pradesh State. The species was originally documented based on a group of 80 specimens from Bombay; Rudman (1985) provided a new description of its anatomy, while Valdes et al. (1999) presented a color photograph from southern India, aiding in clarifying its association with other species of similar coloration.

Genus *Hypselodoris* Stimpson, 1855

Hypselodoris bullockii (Collingwood, 1881) (Figure 7.A)

Synonyms: *Chromodoris bullockii* Collingwood, 1881; *Risbecia bullockii* (Collingwood, 1881)

Material Examined: ZSI/MARC M6247, Off Chinthapalli (Lat. 18°00.265'N; Long 83°43.022' E), Vizianagaram, Andhra Pradesh, 27.02.2019; ZSI/MARC M7362, Off Timmapuram (Lat. N 17°48.272'; Long E 83°24.869'), Visakhapatnam coast, Andhra Pradesh, 18.12.2019.

Diagnosis: The species displays a pale lavender hue, with the mantle featuring a slender border of white. Its rhinophores and gill leaves are yellow, adorned with bands of pink or purple. Size: 20 mm.

Habitat: Artificial shipwreck ecosystem, rocky bottom with algae.

Figure 6. A. *Goniobrachus alius* (Rudman, 1987), B. *Goniobranchus setoensis* (Baba, 1938), C. *Goniobranchus fidelis* (Kelaart, 1858), D. *Goniobranchus trimarginatus* (Winckworth, 1946)

Distribution: South China, Australia, Thailand, Malaysia, India (Tamil Nadu, Andaman and Nicobar Islands).

Remarks: New distribution reports to Andhra Pradesh State. Originally documented in the South China Sea, this species can be observed in the western Pacific, extending south of southern Queensland. Additionally, it inhabits regions of northwestern Australia and Thailand.

Hypselodoris nigrostriata (Eliot, 1904) (Figure 7.B)

Synonyms: *Chromodoris nigrostriata* Eliot, 1904

Material Examined: ZSI/MARC M6248, Off Chinthapalli (Lat. 18°00.265'N; Long 83°43.022' E), Vizianagaram, 27.02.20219; ZSI/MARC M7884, Off Rushikonda Beach (Lat. 17°46.715' N; Long. 83°23.319' E) Andhra Pradesh, 22.01.2021.

Diagnosis: The specimen exhibits a creamy white complexion dotted with yellow spots and black-streaked lines distributed across its entire body. A distinguishing feature of this species is the presence of diagonal black lines. Both the rhinophores and gill leaves display an orange-red hue.

Size: 15 mm

Habitat: Artificial shipwreck ecosystem, rocky bottom with algae.

Distribution: Red Sea, Tanzania, United Arab Emirates, India (Andhra Pradesh, Tamil Nadu, Maharashtra, Andaman and Nicobar Islands).

Remarks: In this study, specimens of this species were obtained from a shipwreck off the Chinthapalli coast in Visakhapatnam, Andhra Pradesh.

Hypselodoris sagamiensis (Baba, 1949) (Figure 7.C)

Synonyms: *Glossodoris sagamiensis* Baba, 1949

Material Examined: ZSI/MARC M7363, Off Mangamari Peta (Lat. 17°49.656'N; Long 83°27.096'E), Visakhapatnam coast, Andhra Pradesh, 19.12.2019.

Diagnosis: The live animal is translucent colored with a white mantle and black spots over it. There is a purple band in mantle edges with a yellow or orange broken band inside. Rhinophore stalks are white with a red tip, and gills are white with a red border. The distinct trait of this species is the presence of small pustules covering its mantle.

Size: 20 mm

Habitat: Rocky bottom with algae.

Distribution: Indonesia, Vanuatu, Japan, Australia, India (Andaman and Nicobar Island).

Remarks: New distributional report to Andhra Pradesh State.

Hypselodoris kanga Rudman, 1977 (Figure 7.D)

Material Examined: ZSI/MARC M6869, Off Rushikonda Beach (Lat. 17°46.868' N; Long. 83°23.426' E), Andhra Pradesh, 15.12.2019; ZSI/MARC M7883, Off Rushikonda Beach (Lat. 17°46.715' N; Long. 83°23.319' E), Visakhapatnam coast, Andhra Pradesh, 22.01.2021.

Figure 7. A. *Hypselodoris bullockii* (Collingwood, 1881), B. *Hypselodoris nigrostriata* (Eliot, 1904), C. *Hypselodoris sagamiensis* (Baba, 1949), D. *Hypselodoris* kanga (Rudman, 1977)

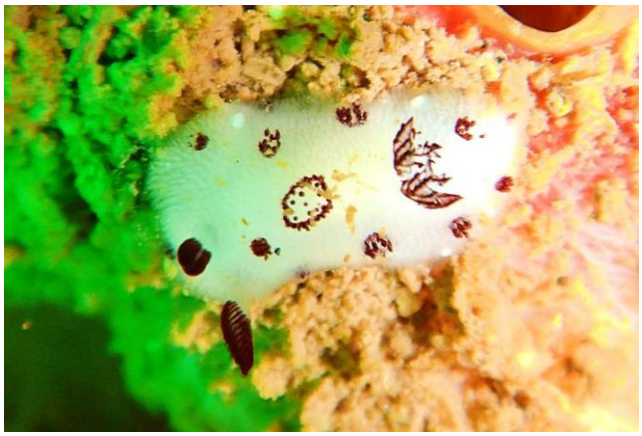

Figure 8. *Jorunna funebris* (Kelaart, 1859)

Diagnosis: The species are bluish-white with yellow or orange spots and dark blue lines. Rhinophores are reddish brown and have a blue ring on the bottom. Gills edges are also bluish-coloured with a series of red or yellow spots. One of the most noticeable external features is the triangular-shaped gills, bordered in blue and adorned with a row of yellow spots along the outer edge.

Size: 15 mm

Habitat: Rocky bottom with algae.

Distribution: Indonesia, Philippines, Thailand, Bali, Singapore, Sulawesi, Papua New Guinea, Hong Kong, Australia, India (Tamil Nadu, Kerala, Maharashtra, Andaman and Nicobar Islands).

Remarks: New distributional report to Andhra Pradesh State.

Family Discodorididae Bergh, 1891

Genus *Jorunna* Bergh, 1876

Jorunna funebris (Kelaart, 1859) (Figure 8)

Synonyms: *Discodoris wetleyi* Allan, 1932; *Doris funebris* Kelaart, 1859; *Jorunna zania* EV. Marcus, 1976; *Kentrodoris annuligera* Bergh, 1876; *Kentrodoris funebris* (Kelaart, 1859); *Kentrodoris gigas* Bergh, 1876; *Kentrodoris maculosa* Eliot, 1906

Material Examined: ZSI/MARC, M6249 Off Chinthapalli (Lat. 18°00.265'N; Long 83°43.022' E), Vizianagaram, Andhra Pradesh, 27.02.2019.

Diagnosis: The species showcases a waxen-white coloration embellished with black markings. Its mantle, possessing a leathery texture, showcases an ivory-white shade adorned with circular black spots and fragmented rings or incomplete spotted patterns. The dorsal tentacles are substantial and club-like, tipped with black, whereas the oral tentacles are slender, with white bodies and black tips. The foot is waxy-white, displaying irregular edges speckled with both small and large linear markings.

Size: 50 mm

Habitat: Artificial shipwreck ecosystem, rocky bottom with algae.

Distribution: Oman, Red Sea, Australia, Maldives, Papua New Guinea, Hong Kong, Singapore, Australia, Japan, India (Distribution in India: Gujarat, Tamil Nadu, Andhra Pradesh, Lakshadweep, Andaman and Nicobar Islands).

Remarks: Alder and Hancock (1864) documented the species along the Coromandel Coast. In this current study, specimens of this species were collected from Off Chinthapalli, Coromandel Coast, more than 155 years after the initial report.

Family Phyllidiidae Rafinesque, 1814

Genus *Phyllidia* Cuvier, 1797

Phyllidia ocellata Cuvier, 1804 (Figure 9.A)

Synonyms: *Phyllidia baccata* Pruvot-Fol, 1957; *Phyllidia japonica* Baba, 1937; *Phyllidia ocellata* subsp. *undula* Yonow, 1986; *Phyllidia tuberculata* Baba, 1930*; Phyllidiopsis carinata* Eliot, 1910

Material Examined: ZSI/MARC M7365, Off Mangamari Peta (Lat. 17°49.656'N; Long 83°27.096'E), Visakhapatnam coast, Andhra Pradesh, 19.12.2019.

Diagnosis: The live animal mantle, bearing yellow tubercles in different sizes and a jet-black color bordered with white, expands and meanders on both sides of the mantle, forming rings.

Size: 15 mm

Habitat: Rocky bottom covered in algae.

Distribution: Indonesia, Singapore, Philippines, Red Sae, Thailand, Solomon Island, Australia, Fiji, Egypt, Mauritius, Japan, Papua New Guinea, Hong Kong, South Africa, Mozambique, India (Tamil Nadu, Andaman and Nicobar Islands).

Remarks: New distributional report to Andhra Pradesh State. *P. ocellata* stands out among predominantly gold-yellow *Phyllidia* species. While it shares a similar coloration with *P. flava*, the latter lacks any black pigmentation. *P. varicosa*, *P. tula*, and *P. coelestis* feature yellow-capped tubercles, but they all exhibit blue-grey pigmentation, with the two former also displaying a black stripe on the sole of their foot.

Phyllidia polkadotsa Brunckhorst, 1993 (Figure 9.B)

Material Examined: ZSI/MARC M6252, Off Chinthapalli (Lat. 18°00.265'N; Long 83°43.022' E), Vizianagaram, Andhra Pradesh, 27.02.2019.

Diagnosis: The animal is yellow, and its typical dorsal pattern consists of eight black bands with a white margin from the mantle to the central part. Around four to five black spots are also present, with a white margin in the central portion.

Size: 20 mm

Habitat: Artificial shipwreck ecosystem, rocky bottom with algae.

Distribution: Hawaii, Japan, Indonesia, Thailand, Vanuatu, and India (Andaman and Nicobar Islands).

Remarks: New distributional report to Andhra Pradesh State.

Genus *Phyllidiopsis* Bergh, 1876

Phyllidiopsis phiphiensis Brunckhorst, 1993 (Figure 9.C)

Material Examined: ZSI/MARC M6250, Off Chinthapalli (Lat. 18°00.265'N; Long 83°43.022' E), Vizianagaram, Andhra Pradesh, 27.02.2019.

Diagnosis: The species presents a white body decorated with three black stripes running lengthwise and encircled by black spots along the mantle's periphery. Additionally, it showcases two subtle white ridges, each bordered by three black-outlined furrows. Both the rhinophores and the underside of the foot exhibit a white hue.

Size: 15 mm

Habitat: Reef ecosystem

Distribution: Thailand, Madagascar, India (Lakshadweep, Andaman and Nicobar Islands).

Remarks: A recent distributional report in Andhra Pradesh State. Small longitudinal stripes characterize three additional species of Phyllidiopsis. Among these, *P. annae* and *P. sphingis* are distinguishable from the current species by their blue coloring, grey gills, and either black (in *P. annae*) or pale yellow (in *P. sphingis*) rhinophores. While *P. striata* presents a somewhat greater challenge in differentiation, it can still be recognized. *P. striata* is identified by three low, white ridges and four black bands (in contrast to *P. phiphiensis*, which has two white ridges and three black bands), lemon yellow rhinophores, and ventral coloring in shades of grey and black.

Superorder Sacoglossa

Superfamily Plakobranchoidea, Gray, 1840

Family Plakobranchidae Gray, 1840

Genus *Elysia* Risso, 1818

Elysia marginata (Pease, 1871) (Figure 9.D)

Synonyms: *Thallepus ornata* Swainson, 1840

Material Examined: ZSI/MARC M6252, Off Chinthapalli (Lat. 18°00.265'N; Long 83°43.022' E), Vizianagaram, Andhra Pradesh, 27.02.2019.

Diagnosis: The species usually displays a semi-transparent green tone with a black outline along the parapodia. Within the margin, there's a yellow or orange strip. Occasionally, a white line may separate the orange and yellow bands. The rhinophore tips frequently mimic these color bands. Furthermore, the body is adorned with numerous black and white dots.

Size: 25 mm

Habitat: Reef ecosystem with algae

Distribution: New Caledonia, French Polynesia, Australia, Florida, Indonesia, Reunion Island, Dubai, South China, Red Sea, Bahamas, Malaysia, Singapore, Japan, Taiwan, Saudi Arabia, Papua New Guinea, Philippines, Hawaii, American Samoa, India (Gujarat, Maharashtra, Tamil Nadu, Karnataka, Goa, Lakshadweep, Andaman and Nicobar Islands).

Remarks: New distributional report to Andhra Pradesh Coast. The species was very commonly observed and photo-documented along the study sites. The species was previously identified as *E. ornata*, although *E. ornata* was originally described from the Caribbean and is part of the *E. marginata* species complex. *E. grandifolia*, *similar to E. marginata* from the Indo-West Pacific, can be distinguished by larger and thin parapodia (Jensen 1992).

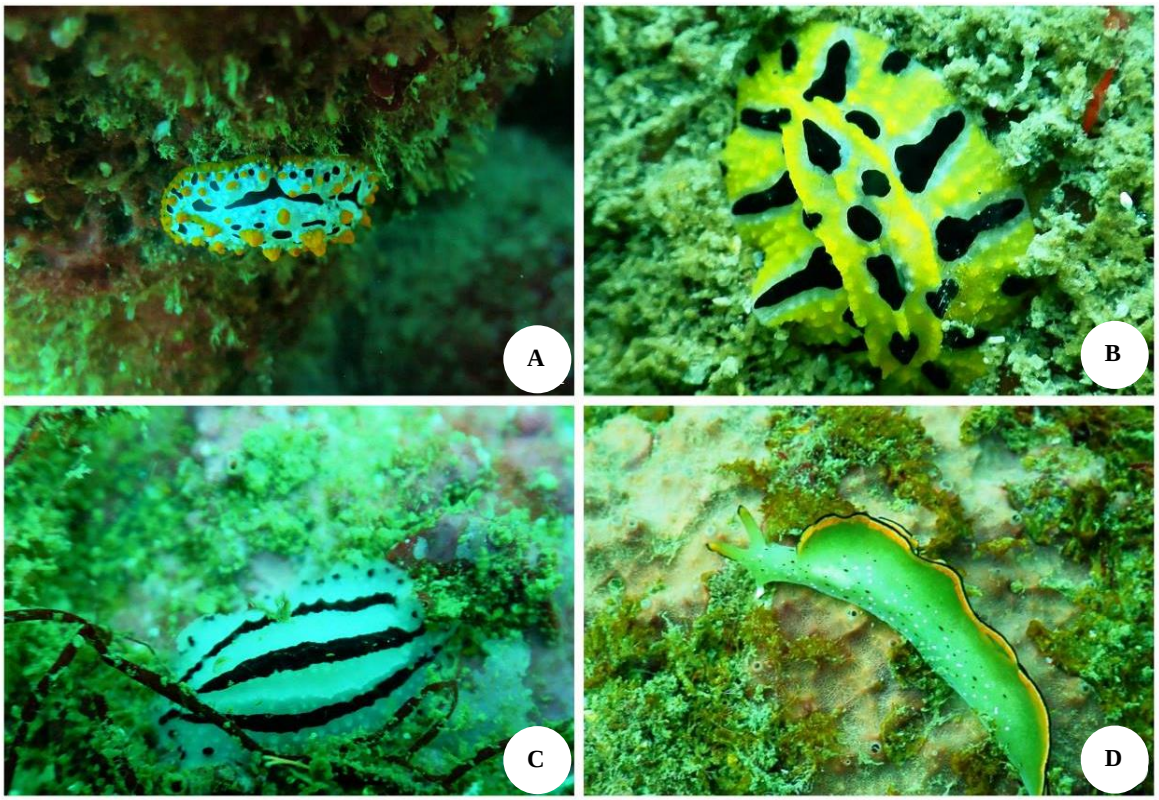

Figure 9. A. *Phyllidia ocellata* (Cuvier, 1804), B. *Phyllidia polkadotsa* (Brunckhorst, 1993), C. *Phyllidiopsis phiphiensis* (Brunckhorst, 1993), D. *Elysia marginata* (Pease, 1871)

Discussion

Andhra Pradesh, as a maritime state located on the east coast of India, boasts a coastline stretching 974 km and a continental shelf area of 33,227 km² across 12 coastal districts (Monolisha and Edward 2015). Regarding comprehensive studies on marine slug biodiversity, only a select few prominent researchers in the country have been involved (Thambi et al. 2023). Some researchers have studied the distribution of Heterobranchs along the coast of Andhra Pradesh, as documented by a few workers. However, in the current study, the underwater survey conducted using SCUBA equipment marks the first endeavor along the Visakhapatnam coast of Andhra Pradesh. The surveyed ecosystems, predominantly rocky reefs and sandy bottoms in intertidal and sub-tidal zones (Figure 1), are favorable habitats for heterobranch sea slugs (Kumar et al. 2011, 2019). The taxonomy of heterobranchs in India traces back to the efforts of Alder and Hancock, who initiated studies along the Visakhapatnam coast. Alder and Hancock (1864) described a new species based on collections made by Walter Elliot during surveys conducted in 1853 and 1854 aboard a survey ship along this coast. This study, 19 species were identified across the study sites (Figures 2-9), among which 13 were documented for the first time in Andhra Pradesh. Including these mollusks significantly enhances the marine faunal richness of the region. Notably, species such as *C. exoptata*, *G. rufomarginata*, *G. alius*, *H. sagamiensis*, *P. polkadotsa*, and *P. phiphiensis* were previously reported only in island ecosystems of India, such as the Lakshadweep Islands and Andaman and Nicobar Islands. However, the present study confirms that the range of these species extends to mainland reef ecosystems in India (Apte and Desai 2017). This study's findings indicate a significant underutilization of the diversity of heterobranchs in rocky reef and sandy bottom ecosystems.

According to the literature review and the additional 13 species identified in the present study, the total number of species documented from the Andhra Pradesh coast now stands at 103 (Table 3). Alder and Hancock (1864) reported 40 species during their survey of the Coromandel Coast study sites. Sarma (1974) documented algae-associated faunal density and listed mollusks from the Visakhapatnam coast, reporting 26 species of heterobranchs. Meanwhile, six species were identified solely at the generic level. Therefore, species such as *Smaragdinella* sp., *Berthelinia* (Tamanovalva) sp. 1, *Berthelinia* (Tamanovalva) sp. 2, *Glossodoris* sp., *Melibe* sp., and *Madrella* sp. were excluded from this work (Table 2). Ramakrishna et al. (2007) reported only five species from collections at landing centers along the Visakhapatnam coast. Venkataraman et al. (2015) and Raghunathan et al. (2016) updated the checklist of sea slugs from India, listing 45 species from the Andhra Pradesh coast. Apte and Desai (2017) recently published a study on sea slugs from the Indian coast, identifying 26 species from the Andhra Pradesh coast. This updated list confirms 103 species available from Andhra Pradesh, making it the second most diverse area in terms of Indian sea slugs.

According to the existing literature, the Andaman and Nicobar Islands boast the highest number of reported species, while the Goa coast has the lowest number (Venkataraman et al. 2015; Raghunathan et al. 2016). The variation in reported species numbers can be attributed to differences in research efforts and publication outputs. Regions with more extensive research tend to report higher species counts, whereas areas with limited research face species identification and collection challenges, resulting in fewer reported species. More detailed underwater surveys are essential to explore these fascinating mollusks further and uncover their ecology, reproductive biology, feeding habits, and potential pharmacological compounds. Such surveys would not only contribute to a better understanding of these organisms but also shed light on their ecological roles and potential applications in various fields.

In conclusion, compared to other regions where marine biodiversity has been extensively documented, the knowledge regarding the diversity of heterobranchs in the Indian subcontinent is notably lacking. Since 1864, there has been insufficient research on heterobranchs along the coast of Andhra Pradesh, with only limited studies conducted on this group of animals. Recent and abrupt changes in coastal ecology are attributed to pressures from both natural phenomena and human activities. Coastal ecosystems, particularly rocky reefs, are experiencing a gradual loss of biodiversity, raising concerns about the potential extinction of numerous species that may be disappearing unnoticed. Sea slugs, being benthic organisms, have a strong connection to the seabed, and the possible use of bottom trawling in Andhra Pradesh, a significant hub for marine fish production in India, poses a grave threat to these sea slugs' diversity. While these slugs play a vital role in the lower levels of the food chain, the impacts of pollution, fishing activities, and climate change on their diversity have not been thoroughly documented. This underscores the need for targeted conservation efforts in the future. It is important to note that these organisms are highly sensitive to environmental changes. Rising sea temperatures and ocean acidification could potentially disrupt their food sources and alter their reproductive cycles, ultimately leading to a decline in their populations. In addition to climate change, other human activities, such as pollution and coastal development, can significantly impact sea slug populations. Polluted waters can lead to the death of these delicate creatures, while development along coastlines can destroy their natural habitats, leaving them nowhere to go. Additionally, it's important to consider that this study was conducted at specific diving sites along the Andhra Pradesh coast, which introduces sampling bias in population analysis. However, regarding diversity study, it can be confirmed that these species are indeed present in the study area. Conducting future population estimations will provide a clearer understanding of the distribution patterns of these species.

Despite not being consumed as food in India, sea slugs are recognized for possessing anti-cancer, anti-tumor, and anti-viral compounds, which are valuable in the pharmaceutical industry. Compounds such as Dolastatin-10 (ILX651, Cemadotin, and Kahalalide F, derived from sea slugs (*Dolabella auricularia*, *Symploca* sp.), are currently undergoing various stages of clinical trials (Sethi and Pattnaik 2012). However, in India, sea slugs are considered low-value bycatch and are often discarded or used for manure and fish feed production. Nonetheless, the ecological significance of these organisms, including their feeding habits, nutrient recycling, chemical defense mechanisms, and role as indicator species, cannot be ignored for the overall health of ecosystems (Andrimida 2022). To those who argue that the economic value of sea slugs is not significant enough to warrant conservation efforts, it is important to remember that all species play a crucial role in maintaining the balance of our ecosystem. Furthermore, sea slugs have been found to have potential medicinal properties that could be beneficial for humans. Ultimately, the conservation of sea slugs and other marine species is not only important for their survival but also for the health and well-being of our planet as a whole. The recent underwater exploration report has expanded our understanding of the distribution of heterobranchs along the Visakhapatnam coast in Andhra Pradesh. However, it is crucial to conduct additional thorough surveys and in-depth taxonomic research to fully investigate the variety of these fascinating sea slugs along the coast of Andhra Pradesh, India. It's conceivable that not all sea slug diversity in the region has been documented so far. Consequently, future conservation strategies may need to be developed, as these organisms have largely been overlooked in many coastal areas of India. As of now, there has been no conservation planning specifically focused on these organisms.

ACKNOWLEDGMENTS

The authors express their gratitude to the Director of the Zoological Survey of India, Kolkata, and the Ministry of Environment, Forest, and Climate Change, Government of India, for providing the necessary facilities and financial support. Additionally, the authors extend their thanks to the Principal Chief Conservator of Forest (Andhra Pradesh), Chief Conservator of Forest (Visakhapatnam), and Divisional Forest Officer (Vizianagaram) for their support and permission for this study. Special thanks are also due to Dr. Deepak Apte (Bombay Natural History Society, Bombay), Sudhanshu Dixit (Centre for Marine Living Resources and Ecology, Cochin), and Dr. Sreeraj C.R. from ZSI, ANRC, Port Blair, for their assistance in identifying sea slug species. The authors are grateful for the SCUBA assistance Mr. Balaram Naidu, PADI SCUBA diving Instructor, Live in Adventures, Rushikonda, and Visakhapatnam provided.

REFERENCES

Alder J, Hancock A. 1864. Notice on the collection of Nudibranchiate mollusca made in India by Walter Eliot Esq. with descriptions of several new genera and species. Tran Zoo Soc London 5: 117-147. DOI: 10.1111/j.1096-3642.1864.tb00643.x.

Andrimida A. 2022. New records of nudibranchs and a sacoglossan (Gastropoda: Heterobranchia) from Sempu Strait, Indonesia. Indo Pac J Ocean Life 6 (1): 1-9. DOI: 10.13057/oceanlife/o060101.

Apte D, Desai D. 2017. Field Guide to the sea slugs of India. Bombay Natural History Society, Mumbai, Inda.

Bhave V, Apte D. 2013. Current status of Indian Opisthobranch fauna. In: Venkataraman K, Sivaperuman C, Raghunathan C (eds). Ecology and Conservation of Tropical Marine faunal communities. Springer, India. DOI: 10.1007/978-3-642-38200-0_5.

Eliot C. 1906. On the nudibranchs from southern India and Ceylon with special reference to the drawings by Kelaart and the collections belonging to Alder and Hancock preserved in the Hancock Museum at Newcastle-on-Tyne. Proc Zoo Soc London 1906: 636-691.

Gobbeler K, Klussmann-Kolb A. 2011. Molecular phylogeny of the Euthyneura (Mollusca, Gastropoda) with special focus on Opisthobranchia as a framework for reconstruction of evolution of diet. Thalassas 27 (2): 121-153.

Gosliner TM, Behrens DW, Valdes A. 2008. Indo-Pacific Nudibranchs and Seaslugs - A field Guide to the World's Most Diverse Fauna. Sea Challengers Natural History Books, Washington.

Gosliner TM. 1995. The genus *Thuridilla* (Opisthobranchia: Elysiidae) from the tropical Indo-Pacific, with a revision of the phylogeny and systematic of the Elysiidae. Proc Calif Acad Sci 49: 1-54.

Gosliner VA, Behrens DW. 2015. Nudibranch and Sea Slug Identification: Indo-Pacific. New world Publication, Jacksonville, Florida, USA.

Jensen KR. 1992. Anatomy of some Indo-Pacific Elysiidae (Opisthobranchia: Sacoglossa (=Ascoglossa), with a discussion of the generic division and phylogeny. J Molluscan Stud 58 (3): 257-296. DOI: 10.1093/mollus/58.3.257.

Kumar JSY, Sreeraj CR, Sornaraj R. 2011. Opisthobranchs of the Gulf of Mannar Biosphere Reserve, Tamil Nadu, India. Indian J Fish 58 (4): 105-114.

Kumar JSY, Venkatraman C, Shrinivaasu S, Raghunathan C. 2019. New records of Opisthobranchs (Mollusca: Gastropoda) from Gulf of Mannar, India. Indian J Mar Geo-Sci 48(10): 1508-1515.

Monolisha S, Edward JK. 2015. Biodiversity of marine mollusc from selected locations of Andhra Pradesh coast, South eastern India. Indian J Geo-Mar Sci 44 (6): 842-855.

Nimbs MJ, Larkin M, Davis TR, Harasti D, Willan R, Smith SDA. 2016. Southern range extensions for twelve heterobranch sea slugs (Gastropoda: Heterobranchia) on the eastern coast of Australia. Mar Bio Rec 9: 27. DOI: 10.1186/s41200-016-0027-4.

Nimbs MJ, Willan RC, Smith SDA. 2015. Range extensions for heterobranch sea slugs (formerly opisthobranch) belonging to the families Diaphanidae, Plakobranchidae and Facelinidae on the eastern coast of Australia. Mar Bio Rec 8: e76. DOI: 10.1017/S1755267215000524.

Raghunathan C, Sudhanshu D, Chandra K. 2016. Diversity of Opisthobranchs in coastal water of India. In: Chandra K, Raghunathan C, Mondal T, Dash S (eds). Current Status of Marine Faunal Diversity of India. Zoological Survey of India, Kolkata.

Ramakrishna, Dey A, Barua S, Mukhopadhya A. 2007. Marine Molluscs: Polyplacophora and Gastropoda - Fauna of Andhra Pradesh, State Fauna Series. Zoological Survey of India, Kolkata.

Ramakrishna, Sreeraj CR, Raghunathan C, Sivaperuman C, Kumar JSY, Raghuraman R, Immanuel T, Rajan PT. 2010. Guide to Opisthobranchs of Andaman and Nicobar Islands. Zoological Survey of India, Kolkata.

Rudman WB. 1985. The Chromodorididae (Opisthobranchia: Mollusca) of the Indo-West Pacific: *Chromodoris aureomarginata*, *C. verrieri* and *C. fidelis* colour groups. Zool J Linn Soc 83: 241-299. DOI: 10.1111/j.1096-3642.1985.tb00875.x.

Rudman WB. 2005. White and Yellow-Spotted Hawaiian Chromodorids. Sea Slug Forum. Australian Museum, Sydney. http://www.seaslugforum. net/find/13260.

Sarma ALN. 1974. Phytal fauna of *Caulerpa taxifolia* & *C. racemosa* off Visakhapatnam coast. Indian J Mar Sci3: 155-164.

Sethi SN, Pattnaik P. 2012. Record of the sea slug, *Kalinga ornata* Alder & Hancock, 1864 from the inshore waters of Bay of Bengal along Chennai coast. Indian J Fish 59 (1): 151-154.

Srinivasulu B, Srinivasulu C, Chethan Kumar G. 2012. First record of the blue sea slug (*Glaucus atlanticus*) from Andhra Pradesh, India. Taprobanica 4 (1): 52-53. DOI: 10.4038/tapro.v4i1.4386.

Thambi BP, Prabhakaran MP, Miraj CA, Kiran J, Pereira FB. 2023. Opisthobranch (Mollusca: Gastropoda) fauna of rocky reef ecosystems of kerala coast, India. Braz J Aqua Sci Tech 27 (1): 18-25. DOI: 10.14210/bjast.v27n1.17676.

Valdes A, Mollo E, Ortea J. 1999. Two new species of *Chromodoris* (Mollusca, Nudibranchia, Chromodorididae) from southern India, with a redescription of *Chromodoris trimarginata* (Winckworth, 1946). Proc Cal Acad Sci 51 (13): 461-472.

Venkataraman K, Raghunathan C, Raghuraman R, Dixit S. 2015. Fascinating Seaslugs and Flatworms of Indian Seas. Zoological Survey of India, Kolkata.

NUSANTARA BIOSCIENCE
Vol. 16, No. 2, pp. 169-184
November 2024

ISSN: 2087-3948
E-ISSN: 2087-3956
DOI: 10.13057/nusbiosci/n160203

Review: Phytochemistry and ethnopharmacology of *Dracaena trifasciata*

WHIKA FEBRIA DEWATISARI[1,♥], NELSIANI TO'BUNGAN[2]

[1]Department of Biology, Faculty of Science and Technology, Universitas Terbuka. Jl. Cabe Raya, Pondok Cabe, Pamulang, South Tangerang 15418, Banten, Indonesia. Tel.: +62-21-7490941, ♥email: whika@ecampus.ut.ac.id

[2]Faculty of Biotechnology, Universitas Atma Jaya Yogyakarta. Jl. Babarsari No. 44, Tambak Bayan, Caturtunggal, Depok, Sleman 55281, Yogyakarta, Indonesia

Manuscript received: 8 February 2024. Revision accepted: 2 June 2024.

Abstract. *Dewatisari WF, To'bungan N. 2024. Review: Phytochemistry and ethnopharmacology of* Dracaena trifasciata. *Nusantara Bioscience 16: 169-184. Dracaena trifasciata* (Prain) Mabb. (syn. *Sansevieria trifasciata* Prain.) or mother-in-law's tongue, is a species belonging to the genus *Dracaena*, widely cultivated and used by various communities. This plant is recognized as an ornamental, pollutant-absorbing, and textile material. Its leaves and roots have also been used as traditional remedies across Asia and Africa for cough, flu, respiratory tract inflammation, diarrhea, wound healing, and snakebites. Bioactive compounds found in the roots and leaves include alkaloids, tannins, terpenoids, saponins, steroids, phenols, methyl glucuronate acid, glycosides, cardenolides, polyphenols, carbohydrates, and abamagenin. Therefore, this review aims to provide insights into the phytochemical constituents and pharmacological potential of *D. trifasciata*. It also explores its use in traditional medicine and prospects for further advancement to promote the broader application. Comprehensive literature studies showed that the attributes of *D. trifasciata* can be applied as an antibacterial, antioxidant, and anticancer agent, having a promising source of natural compounds for novel drug development. Further investigations are needed to assess the long-term and short-term toxicity associated with the use of this plant material, thereby making it a potential source for the development of modern drugs from natural sources. Considering the extensive application of *D. trifasciata* as a natural remedy, further investigations are crucial to assess the pharmacological potential and safety.

Keywords: Anti-toxic, antibacterial, anticancer, antioxidant, *Sansevieria*

INTRODUCTION

Dracaena trifasciata (Prain) Mabb. (syn. *Sansevieria trifasciata* Prain.) or mother-in-law's tongue, is categorized under the Genus *Dracaena*, featuring sword-shaped leaves with attractive patterns and colors (Figure 1). The *D. trifasciata* has been cultivated since the 16th century. It later became popular for cultivation as an ornamental plant in Indonesia starting from the 19th century.This plant is known as the snakeplant or mother-in-law's tounge among international ornamental plant traders. This ornamental plant is extensively cultivated in gardens or pots and widely used for decorative purposes in gardens and homes (Tinggi 2018; Aref et al. 2023; Dewatisari and Nuryandani 2024). The cultivation is driven by its high economic value, primarily due to the abundant fiber content, which serves as a natural textile raw material (Adeniyi et al. 2020; Papaj 2022; Raj et al. 2023). The elastic, white, and strong fibers derived from *D. trifasciata* are used in the production of ropes, clothing, fishing lines, bowstrings, fine weaves, and binding cords due to their high strength (Sathishkumar 2016; Widyasanti et al. 2020).

The *D. trifasciata* is recognized for its capability to absorb pollutants both indoors and outdoors, functioning as an air purifier, effectively absorbing harmful gases including formaldehyde, xylene, and total volatile organic compounds (Ullah et al. 2021; Guo et al. 2023; Sutrisno et al. 2023; Weerasinghe et al. 2023). The well-established knowledge regarding *D. trifasciata* plants is their ability to effectively remove toluene within confined indoor setting. Furthermore, these plants exhibit toluene (Gunasinghe et al. 2023). Additionally, this plant shows the ability to accumulate heavy metals (Gabriel et al. 2023; Pandiyarajan et al. 2024). In addition, *D. trifasciata* can improve indoor air quality and is very effective in reducing computer radiation (Dewatisari and Lyndiani 2015; Mardiyati et al. 2016; Yu et al. 2020; Panduwinata et al. 2021; Permana et al. 2023).

The *D. trifasciata* has also been used as a traditional medicine across various communities in Asia and Africa by consuming the juice or decoction from its leaves for the treatment of gonorrhea, earaches, toothaches, respiratory tract inflammation, flu, diarrhea, coughs, hemorrhoids, and influenza. The leaf latex of this plant is applied externally to treat bruises, sprains, wounds, abscesses, scabs, itchiness, and ear diseases, alongside being used as a natural antibiotic, hair tonic, and pain reliever (Sunilson et al. 2009; Andhare et al. 2012; Berame et al. 2017; Aseptianova 2019; Hijrah et al. 2019; Nahdi and Kurniawan 2019; Sun et al. 2019; Hartanti and Budipramana 2020; Thu et al. 2020; Pathy et al. 2021). In Africa, the latex from this plant can be used as a snake and insect repellent (Umoh et al. 2020; Sharma et al. 2023). Antibacterial agents are also derived from *D. trifasciata*. In tropical countries, *D. trifasciata* is used for treating inflammatory diseases and is sold in markets as a crude oil

for treating snake bites, earaches, swelling, boils, and fever (Aliero et al. 2008; Anbu et al. 2009).

The medicinal properties of *D. trifasciata* are attributed to the diverse bioactive compounds including alkaloids, tannins, terpenoids, cardenolides, polyphenols, methyl glucuronate acid, glycosides, saponins, steroids, phenols, carbohydrates, and abamagenin, found in the roots, rhizomes, and leaves (Aliero et al. 2008; Narendhiran et al. 2014; Dewatisari et al. 2018; Megantika et al. 2020). The ethanolic extract phytochemical content of *D. trifasciata* includes compounds from the group of fatty acids, sugars, cyclic ketones, alkaloids, aliphatic nitro compounds, and citric acid. Flavonoids are one of the abundant compounds found in *D. trifasciata* leaves, which act as antioxidants (Adhityaxena et al. 2020; Van Kleinwee et al. 2022; Marjoni et al. 2023). Several studies have shown that the leaves and rhizomes of *D. trifasciata* contain saponins, cardenolins, polyphenols, methyl glucuronate acid, and abamagenin. Gas chromatography-mass spectrometry (GC-MS) data from the leaves of various *Sansevieria* species indicate the presence of antioxidant and antibacterial compounds such as 3,4-Dimethoxybenzoic anhydride, 2,5-Dimethoxybenzhydrazide, Diallyl Acetal, 1,2-Benzenedicaboxylic Acid, BIS (2-Ethylhexyl) ester, 1-Butyl 2-(8-Methylnonyl) Phthalate, Palmitaldehyde, Delta-Undecalactone, n-Hexadecanoic acid, Dodecanoic acid, and 6,10,14-trimethyl-2-Pentadecanone. These phytochemical compounds have the potential to treat various diseases such as wounds, antiseptic applications, hemorrhoids, chickenpox, parasitic infections, eye and ear diseases, cough, snake bites, and as a refreshing beverage (Baldwin and Webb 2016; Saxena et al. 2022).

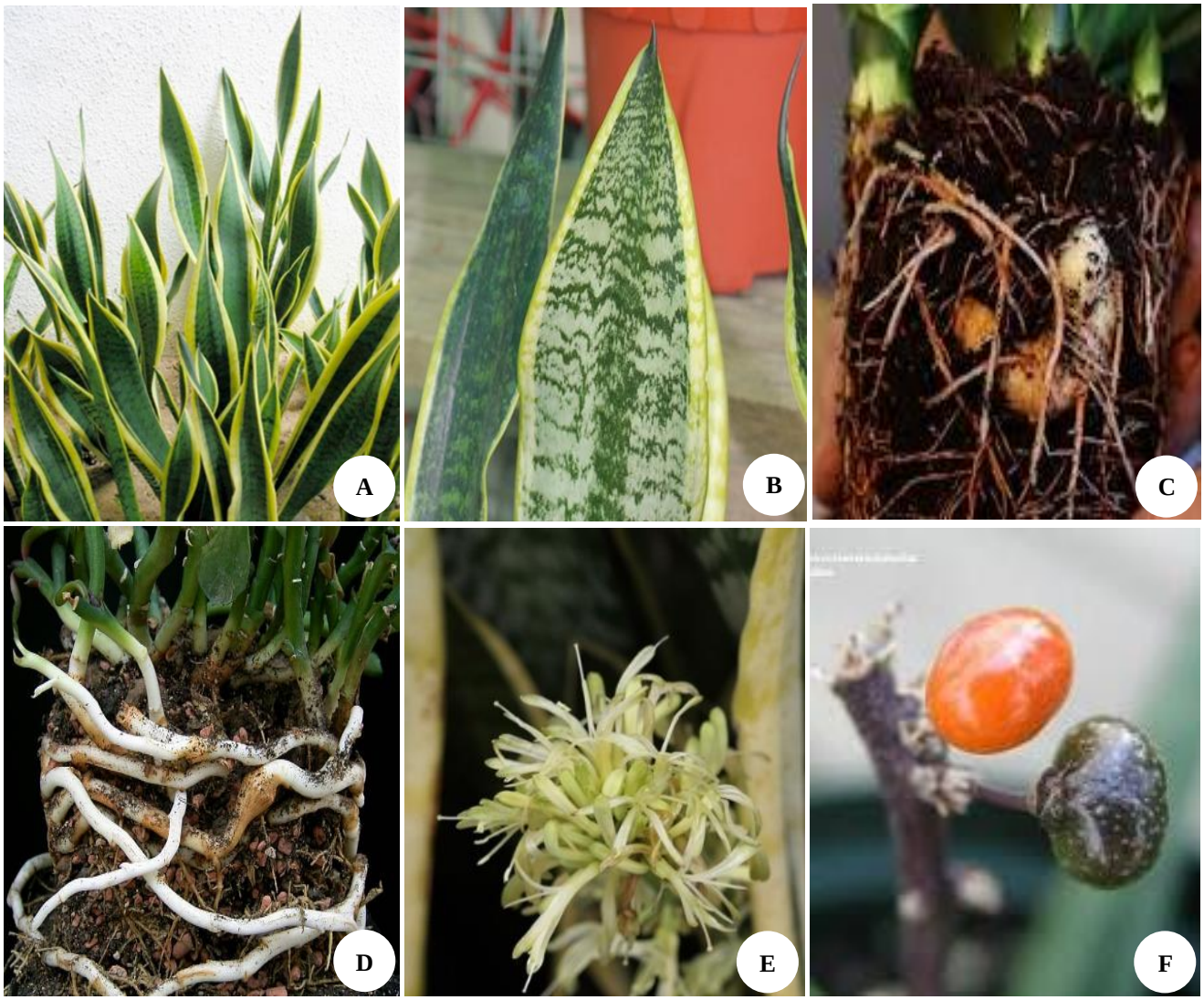

Figure 1. *Dracaena trifasciata* (Prain) Mabb.: A. Plants, B. Leaf, C-D. Roots, E. Flowers, F. Fruits (Source: lucidcentral.org & NParks | *Dracaena trifasciata* 'Prain')

Information from the literature shows, *D. trifasciata* has numerous benefits for medicinal purposes and contains active compounds that benefit the environment and health. The pharmacological activities of *D. trifasciata* have been investigated, including its antioxidant, anticancer, antidiabetic, antianaphylaxis, and antibacterial properties (Bhattacharjee et al. 2016; Damen et al. 2018). Nevertheless, research is rare on the ethnopharmacological aspects of this plant in the existing literature. Consequently, conducting a comprehensive investigation in this ethnopharmacological domain provides valuable insights into the potential compounds derived from this plant, and identifies subject for further natural medicine development (Figure 2). Therefore, a systematic review of its traditional uses in various countries is needed. Furthermore, information from the literature regarding the pharmacological properties of *D. trifasciata* should be studied and analyzed.

DISTRIBUTION AND HABITAT

The Genus *Dracaena* originates from Africa and partly from Asia, with cultivars reaching over 600 globally, of which approximately 100 are identified in Indonesia (Stover 1983). These cultivars exhibit leaf shape, size, color, and texture variations. Moreover, *Dracaena* is widely naturalized in South Asia (India) to Southeast Asia (Indonesia, Malaysia, Thailand, Vietnam), Australia, America, and several Pacific islands. The extensively commercialized species in the nursery trade include *D. trifasciata* and *D. cylindrica* (Dewatisari et al. 2008).

The *D. trifasciata*, commonly found in wild tropical and subtropical regions, is also cultivated as an ornamental plant in many places in Indonesia. Due to invasive and aggresive nature, it can survive in various habitats (Tallei et al. 2016). This plant's ability to grow under full sunlight or in shaded areas facilitates its global thriving in moist, fertile soil with high organic content and minimal care (Appell 2001). The *D. trifasciata* exhibits high salt tolerance and low nutrient requirements (Brown 2011).

The distribution and habitat of *D. trifasciata* reflect its wide adaptation and species' success in various environments. Its primary origin in Africa and parts of Asia, with extensive spread to South Asia, Southeast Asia, Australia, America, and some Pacific islands, demonstrates its adaptability to diverse ecological conditions. Its presence in varying conditions, from tropical and subtropical regions to naturalized lands, confirms its resilience to different light intensities, soil types, and water availability. The success of *D. trifasciata* in adapting to different habitats, both under full sunlight and in shaded areas, as well as in moist and organically rich soils with minimal care, indicates great potential for further dispersal and naturalization. Its high tolerance to salt levels and low nutrient requirements also support its ability to survive in less-than-ideal conditions, making it an intriguing species from both ecological and horticultural perspectives (Stover 1983; Swinbourne and Robert 2007; Dewatisari et al. 2008).

The interpretation regarding the distribution of *D. trifasciata's* habitat reveals how this species exemplifies adaptation success and survival in various geographic and ecological environments. With origins spanning from Africa to Asia and naturalization in diverse regions such as South Asia, Southeast Asia, Australia, America, and the Pacific islands, *D. trifasciata* demonstrates exceptional flexibility in adapting to different habitats. Its ability to thrive under varying light conditions, and in moist and nutrient-rich soils, reaffirms its resilience as a species. Tolerance to diverse soil conditions and resistance to high salt levels prove its adaptability. This phenomenon not only showcases the genetic and ecological diversity that enables *D. trifasciata* to thrive outside its native habitat but also its potential invasiveness in new habitats, where it can impact local ecosystems (Damen et al. 2018; Adeniyi et al. 2020; Witthayaphirom and Nuansawan 2023).

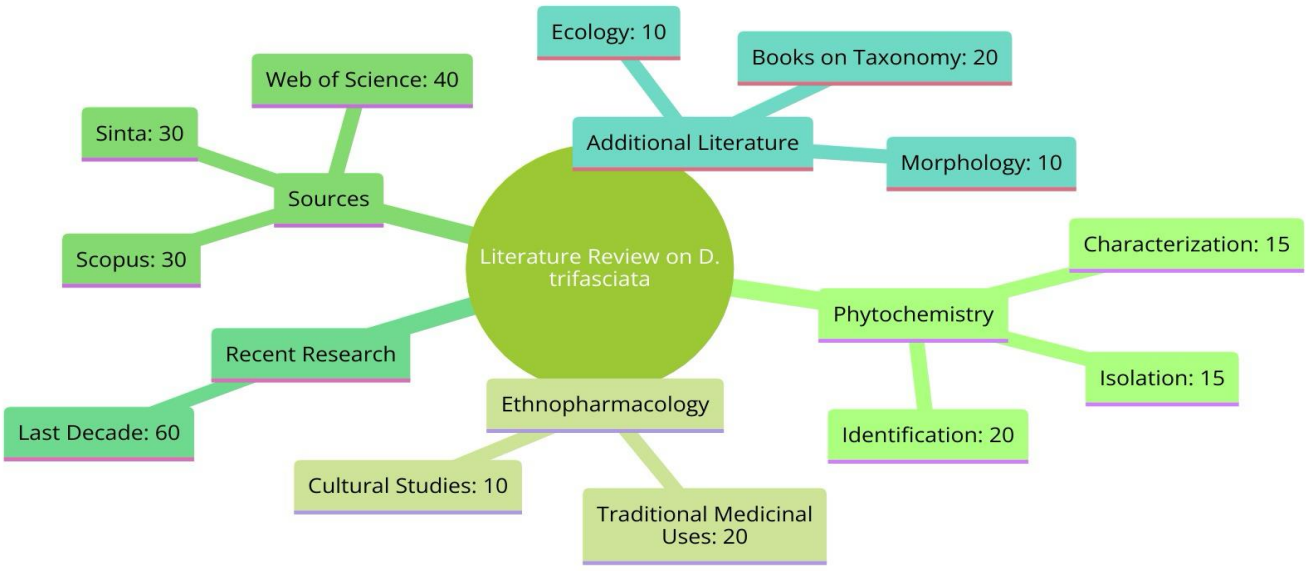

Figure 2. Systematical review diagram of phytochemistry and ethnopharmacology of *Dracaena trifasciata*

Comparing the distribution of *D. trifasciata's* habitat with other plant species reveals unique characteristics that distinguish it as a highly adaptive and widely distributed species. The *D. trifasciata* has spread to various parts of the world, showcasing its remarkable adaptability compared to other species that may have more limited or specific habitat distributions. For example, many endemic plant species can only be found in specific locations and are unable to adapt to diverse environments like *D. trifasciata*. The *D. trifasciata* is a hardy and low-maintenance plant that can be easily cultivated both indoors and outdoors. It prefers well-drained soil and moderate sunlight. It can be propagated through division, leaf cuttings, or rhizome cuttings. The ease of cultivation makes it a popular choice for indoor greenery and landscaping (Tallei et al. 2016; Tungmunnithum et al. 2018).

The *D. trifasciata*, a perennial plant with erect growth habit and broad evergreen leaves, is commonly cultivated as a popular indoor houseplant. It thrives in partially shaded areas that receive 2 to 6 hours of daily direct sunlight, although it can tolerate low light conditions (Denk et al. 2014; El Mokni and Verloove 2022). Providing well-drained soil and practicing careful watering is crucial to prevent root rot. During the spring to autumn seasons, it is advisable to allow the soil to dry between waterings, while in winter, watering once every one to two months is sufficient. With its ability to tolerate low humidity and cool temperatures around 50 degrees Fahrenheit, *D. trifasciata* demonstrates resilience and remains undamaged under various conditions (Freiberg et al. 2020; Ghaderi 2023). Although it naturally produces blooms during winter in its native habitat, flowering is rare when grown as a houseplant. One notable feature of this plant is its capacity to enhance air quality, making it a suitable choice for indoor environments. In the 1970s, NASA discovered that certain common houseplants, including *D. trifasciata*, effectively remove pollutants like formaldehyde, benzene, and ammonia from indoor spaces. Subsequent studies have corroborated these findings. As a result, *D. trifasciata* is often cultivated in containers and utilized as a ground cover filler in interior landscape designs (Husti et al. 2016; Pamonpol et al. 2020).

MORPHOLOGICAL CHARACTERS

The *D. trifasciata* is a species of evergreen perennial plant in the family Asparagaceae. The genus *Dracaena* encompasses various species of evergreen plants known for their ornamental foliage. The specific epithet "trifasciata" refers to the three longitudinal stripes or bands often present on this species's leaves. The *D. trifasciata* is commonly known by various names, including Snake Plant, Mother-in-Law's Tongue, Saint George's Sword, Viper's Bowstring Hemp, and more. These names are inspired by their appearance and the shape of their leaves (Rwawiire and Tomkova 2015). Numerous cultivars and varieties of *D. trifasciata* have been developed, featuring variations in leaf color, size, and pattern. Some popular cultivars include 'Golden Hahnii' with yellow-edged leaves, 'Laurentii' with yellow bands along the leaf edges, and 'Bantel's Sensation' with narrow white stripes running through the leaves (Wetterer and Wetterer 2022).

The *D. trifasciata* consist of two to six linear-oblanceolate leaves from fleshy underground rhizomes with pointed tips. They are often arranged in artistic clusters due to their striped, erect, and stiff nature. The 40-90 cm long and 5-7 cm wide sword-shaped leaves, resembling zebra skin, exhibit dark to light green coloration with yellow margins. Furthermore, they appear in ribbons ranging from 0.3 to 1 m in length, featuring whitish-green or grayish-white flowers attached to upright stalks, which are shorter than the leaves and approximately 30-75 cm long. The plant blooms during the spring and summer seasons (from September to February). The rhizomatous or creeping and relatively thick stem commonly grows underground. The rhizomes, which usually have a bright orange external part and a whitish inner portion, often grow horizontally on the soil surface or underground (Swinbourne and Robert 2007; Stover 1983). The wild roots are fibrous in shape and known to originate from the stem base, while normal roots possess a white pattern and appear full. The small round fruits, with a 7-9 mm diameter and two seed components, often turn bright orange once ripe. The seeds are pale brown and elongated, measuring around 6-7 mm in length and approximately 5 mm in width (Stover 1983; Acevedo-Rodríguez and Strong 2005; Dewatisari 2009).

ECOLOGICAL ASPECT

This species is known for its capacity to withstand various environmental conditions (Papaj 2022). It can adjust to various lighting situations, from dim indirect to strong light, and may additionally withstand periods of dry soil and be fairly drought-resistant. Therefore, the plan tis an increasingly common indoor landscaping and gardening choice. With a clumping growth style, this plant produces several rosettes of leaves that branch off a single base. The plant may eventually form dense colonies or clusters (Indirasetyo and Kusmono 2022).

The *D. trifasciata* plants are used as phytoremediation (Iswoyo et al. 2023). This plant can be a solution to environmental problems, one of which is reducing the bad effects of acid rain on the environment (Papaj 2022). Apart from being beneficial in reducing soil pollution, placing *D. trifasciata* in a closed room also contributes to improving indoor air quality, by reducing carbon dioxide concentrations by 10.47-19.29% (Pamonpol et al. 2020).

TRADITIONAL MEDICAL USES

Traditional medicinal use of *D. trifasciata* includes its application in wound healing. The plant extracts have been reported to promote wound closure, reduce inflammation, and accelerate tissue regeneration. These effects may be beneficial in managing various types of wounds (Yuniarsih et al. 2023). In traditional medicinal systems such as

traditional Chinese medicine (TCM) and Ayurveda, *D. trifasciata* has been used to alleviate bronchitis, coughs, colds, and cold. The plant's mucilaginous properties help soothe throat irritation and promote expectoration. In traditional African medicine, various parts of the plant, including the leaves and rhizomes, have been used to treat skin infections, gastrointestinal disorders, and respiratory conditions. The *D. trifasciata* has been used as a traditional medicinal for treating influenza, cough, respiratory problems, inflammation, earaches, stomach ulcers, jaundice, pharyngitis, skin itching, and urinary diseases in India, Nigeria, Ghana, Congo, Indonesia, the Philippines, Myanmar, Yemen, China, Vietnam, Cambodia, Thailand, and Malaysia (Andhare et al. 2012; Berame et al. 2017; Abdullah et al. 2018; Dewatisari 2019). Additionally, it functions as an analgesic and antipyretic, and all the traditional uses in various countries can be seen in Table 1.

Table 1. The use of *Dracaena trifasciata* as traditional medicine in various countries

Continent & Country	Etnomedicinal Use/Ethnopharmacological Significance/Potential	Plant Part Used	Form Usage	References
Africa				
West Africa, Nigeria	Hemorrhage, dysentery, diarrhea, stomach and external ulcers, wounds, leucorrhea, fractures, piles, diabetes, and even tumors	Leaves and rhizomes	Brewed, decoction, pasted	Wambugu and Waweru (2016); Thu et al. (2020)
Congo	Rheumatism and gynecological problems	Leaves	Brewed	Machala et al. (2001); Sun et al. (2019); Sunilson et al. (2009); Thu et al. (2020)
Asia				
Indonesia	Snake bite, cough, cold, diarrhea, and treat wound	Leaves and rhizomes	Crushed, infusion, decoction	Aseptianova 2019); Wakhidah and Sari (2019); Hartanti and Budipramana 2020); Gita and Danuji 2021); Dewatisari 2022); Dewatisari and To'bungan 2023); Lestari et al. (2023); Dewatisari and Nuryandani (2024)
Philipines	Asthma, abdominal pains, colic, diarrhea, hemorrhoids, hypertension, menorrhagia, piles, sexual weakness, wounds of the foot, cough, leprosy, rheumatism, glandular Enlargement, nutritional deficiencies and treatment of snake bite	Leaves and rhizomes	No remark	Berame et al. (2017
India	Bronchitis, asthma, food poisoning, toxemia, cough, snake bite, insect bite	Leaves and rhizomes	Brewed, decoction, pasted	Machala et al. (2001); Sun et al. (2019); Thu et al. (2020)
Myanmar	Blood Forming Organs and Immune Mechanism Cancerous tumour 1 Digestive Constipation 1 Skin	Leaves and rhizomes	No remark	Machala et al. (2001); Andhare et al. (2012); Myint and Swe (2019); Sun et al. (2019); Thu et al. (2020); Kyaw et al. (2021); Nguyen et al. (2023)
Yemen	Hemorrhage, dysentery, diarrhea, stomach and external ulcers, wounds, leucorrhea, fractures, piles, diabetes, and even tumors	Leaves and rhizomes	Brewed, decoction, pasted	Machala et al. (2001); Sun et al. (2019); Thu et al. (2020)
China	Treating pain and stopping hemorrhages, and used as the substitute for the traditionally imported dragon's blood, called Long-Xue-Jie	Leaves and rhizomes	Brewed, decoction	Bratu et al. (2006); Thu et al. (2020)
Vietnam, Cambodia, Thailand	Cough, leprosy, rheumatism, glandular Enlargement, nutritional deficiencies and treatment of snake bite	Leaves and rhizomes	Brewed, decoction, pasted	Luu-Dam et al. (2016)
Malaysia	Ear pain, swellings, boils and fever	Leaves and rhizomes	Pasted, brewed, decoction	Anbu et al. (2009); Sunilson et al. (2009); Afrasiabian et al. (2017); Kee et al. (2020)
Yemen	Enhance immune function, promote skin repair, stop bleeding, and enhance blood circulation	Leaves and rhizomes	Pasted, brewed, decoction	Thu et al. (2020)

In Ghana, the roots are reportedly used for abortion and are often applied during childbirth. In Nigeria, the leaves and roots serve as traditional medicinal including asthma, stomach aches, colic, diarrhea, eczema, gonorrhea, hypertension, hemorrhoids, menorrhagia, snake bites, sexual weakness, and foot wounds (Okunlola et al. 2018; Tamanna et al. 2021; Permana et al. 2023). In Bangladesh, the whole plant is a tonic for treating alopecia, malaria, and snake bites. The leaves and rhizomes also treat bronchitis, asthma, cough, snake bites, and insect bites. The roots and leaves contain secondary metabolites such as saponins, which are applied as a cough medicine for snake bites, sprains, bruises, boils, abscesses, respiratory inflammation, and hair tonic. The plant also has antidiabetic, anti-allergic, anti-anaphylactic, and thrombolytic properties. The leaf extracts exhibit antibacterial activity against *Escherichia coli* and *Staphylococcus aureus* bacteria. Recent studies have shown the anti-alopecia activity of the leaves (Babu and Prabhu 2023; Dewatisari et al. 2023). In Indonesia, the roots and leaves are boiled to treat diarrhea, cough, and flu among the Buton, Lampung, Purwakarta, and Yogyakarta communities (Hamidu 2009; Wakhidah and Sari 2019; Hartanti and Budipramana 2020; Gita and Danuji 2021). In Central Sulawesi, the roots and leaves are ground to treat snake bites and wounds (Aseptianova 2019; Hijrah et al. 2019; Nahdi and Kurniawan 2019; Hartanti and Budipramana 2020).

These findings highlight the extensive traditional uses of *D. trifasciata* in various countries to treat various ailments. The plant's bioactive compounds and medicinal properties became a subject of interest for further research and exploration of its potential applications in modern medicine. The *D. trifasciata* has a long history of traditional medicinal use in multiple countries. Its utilization in various regions for treating different ailments suggests that it possesses diverse medicinal properties (Maheshwari et al. 2017; Maroyi 2019). The plant is commonly employed to address respiratory issues like cough, bronchitis, and influenza, indicating its potential as a respiratory remedy. Additionally, its use in treating gastrointestinal problems such as stomach ulcers, diarrhea, and colic suggests its effectiveness in soothing digestive ailments. The *D. trifasciata* is also utilized for managing inflammatory conditions, including respiratory inflammation and skin itching. Its application as a traditional remedy for urinary diseases and jaundice indicates its potential diuretic and hepatoprotective properties. Furthermore, the plant's use in treating conditions like earaches, pharyngitis, and snake bites indicates its analgesic and anti-inflammatory characteristics. The secondary metabolites, such as saponins, in the roots and leaves of *D. trifasciata* may contribute to its medicinal properties. These metabolites are known for their expectorant, anti-inflammatory, and antimicrobial activities. The antibacterial activity against *E. coli* and *S. aureus* bacteria exhibited by leaf extracts highlights its potential as an antimicrobial agent (Bratu et al. 2006; Dewatisari et al. 2021). The findings also suggest that *D. trifasciata* holds promise in the management of certain chronic conditions. Its reported antidiabetic, anti-allergic, and anti-alopecia activities indicate potential therapeutic applications in diabetes, allergies, and hair loss (Aseptianova 2019; Hijrah et al. 2019; Nahdi and Kurniawan 2019; Hartanti and Budipramana 2020).

The integration of traditional knowledge and modern analytical methods offers a promising approach to uncover the medicinal properties of plants, including *D. trifasciata* (Walker et al. 2014; Krishna et al. 2020). By combining these resources, researchers can effectively identify and isolate bioactive compound for the plant's therapeutic effects. However, it is crucial to acknowledge the potential safety concerns associated with *D. trifasciata*. While the plant has a long history of traditional medicinal use, certain parts, contain toxic compounds if consumed in large quantities, particulary the leaves (Krishna et al. 2020). Therefore, it an imperative to exercise caution when utilizing *D. trifasciata* for medicinal or therapeutic purposes. It is advisable to seek guidance from healthcare professionals or subject matter experts before incorporating it into any treatment regimen.

Traditional preparations of *D. trifasciata* vary among different cultures and regions. Common preparation methods include decoctions, infusions, poultices, and topical applications. The traditional use of *D. trifasciata* is passed down through generations often based on empirical. Indigenous communities have developed specific knowledge and practices related to the plant, including its identification, collection, preparation, and administration. This knowledge is often deeply intertwined with local cultural beliefs, rituals, and healing systems. Many traditional uses of *D. trifasciata* have been documented, it is important to note that not all traditional claims have been scientifically validated. Modern scientific research aims to explore the plant's bioactive compounds and pharmacological properties to verify its traditional uses and identify potential new therapeutic applications (Takawira-Nyenya et al. 2018; Rezgui et al. 2015). These studies can help bridge the gap between traditional and modern medicine and contribute to developing evidence-based healthcare practices.

ANTIOXIDANT ACTIVITY

The *D. trifasciata* extracts have been found to possess antioxidant properties. These properties are attributed polyphenols, flavonoids, and other bioactive compounds (Huang et al. 2024). As presented in Table 2, the 2,2-diphenyl-1-picrylhydrazyl (DPPH) method was commonly used to assess the antioxidant activity of *D. trifasciata*. The use of the DPPH method to assess antioxidant activity is a common approach in research. This method involves measuring the ability of a sample to neutralize or reduce the DPPH radical, which is a stable free radical. A lower IC_{50} value indicates a stronger antioxidant activity, as it represents the sample required concentration to scavenge 50% of the DPPH radicals (Baliyan et al. 2022).

Despite limited studies related to this, preliminary investigations have revealed high antioxidant activity, with an IC_{50} value <100 µg/mL, influenced by the

phytochemical compounds in the plant (Lontoc et al. 2018; Pinky and Hossain 2020; Sarjani et al. 2021). Phenolic compounds are a group of phytochemicals known for their antioxidant attributes. These compounds are likely responsible for scavenging free radicals and protecting against oxidative stress (Tungmunnithum et al. 2018; Yu et al. 2020; Dohre and Yadav 2021). The leaf extracts have been reported to contain phenolic compounds, including flavonoids such as pyrano-isoflavones, which possess antioxidant potential (Swinbourne and Robert 2007; Abdullah et al. 2018; Lontoc et al. 2018; Yumna et al. 2018; Pinky and Hossain 2020). While the research results provide preliminary evidence of the antioxidant activity of *D. trifasciata*, further studies are crucial to explore the specific phenolic compounds and their mechanisms of action. Other methods and assay could also be employed to evaluate the plant's antioxidant activity and validate its potential as a natural antioxidant source. The *D. trifasciata* extracts may help protect cells from oxidative damage caused by free radicals. By reducing oxidative stress, the extracts may prevent DNA mutations and damage leading to cancer development (Maheshwari et al. 2017; Dewatisari et al. 2023).

ANTICANCER ACTIVITY

The cytotoxic or anticancer effects of *D. trifasciata* may be attributed to its phytochemical composition. Studies have identified various bioactive compounds in *D. trifasciata* extracts, including saponins, flavonoids, phenolic compounds, and alkaloids, known for their potential anticancer properties.The anticancer potential exploration of *D. trifasciata* is currently limited. As depicted in Table 3, investigations into the cytotoxic attributes of this plant focused on breast (T47D), liver (HepG2), and cervical cancer cells (HeLa). Based on the classification criteria of the US National Cancer Institute (Abdel-Hameed et al. 2012; Srisawat et al. 2013), the ethanol leaf extract of *D. trifasciata* induced weak cytotoxic activity in T47D cells (IC_{50} 537 µg/mL), while it stimulated moderate cytotoxicity in HepG-2 cells (IC_{50} 81±18.8 µg/mL). This is consistent with Trifasciatosides which exhibited moderate cytotoxicity against HeLa cells (Indrayanto et al. 2021). Although limited, some studies have explored the potential anticancer effects of *D. trifasciata* extracts. The plant extracts have shown cytotoxic activity against certain cancer cell lines in vitro. Overall, while the initial findings suggest some cytotoxic activity of *D. trifasciata* against certain cancer cell lines, further research is required to comprehensively evaluate its anticancer potential, optimize extraction methods, and elucidate the underlying mechanisms of action. The *D. trifasciata* extracts may induce apoptosis in cancer cells by activating signaling pathways that lead to cell death. This mechanism helps eliminate cancer cells without causing damage to healthy cells. The *D. trifasciata* extracts may interfere with the cell cycle progression of cancer cells, leading to cell cycle arrest. By halting cell division at specific checkpoints, the plant extracts prevent cancer cells from proliferating uncontrollably, inhibiting tumor growth. The bioactive compounds in *D. trifasciata* extracts may modulate various signaling pathways involved in cancer progression. These compounds have the potential to impede cellular pathways involved in processes such as cell proliferation, cell survival, angiogenesis (the formation of new blood vessels to supply tumors), and metastasis (the spread of cancer to other parts of the body) (Baldwin and Webb 2016; Krishna et al. 2022).

Further studies must be conducted on anticancer properties, specifically concerning the solvent type, extraction methods, and specific plant parts such as rhizomes, roots, and flowers. The anticancer mechanisms of the ethanol leaf extract of *D. trifasciata* and Trifasciatosides should be examined to understand their effects on the hallmarks of cancer. Future studies should focus on elucidating the bioactive compounds responsible for the anticancer effects, investigating their mechanisms of action, assessing their efficacy in animal models and clinical trials, and evaluating potential side effects and safety profiles.

Table 2. Antioxidant activity of *Dracaena trifasciata*

Sample	IC_{50} value	Method	References
Ethanolic extract of *D. trifasciata* leaves	93.15 and 50.84 mg/mL,	DPPH	Onah et al. (1994)
Ethanolic extract of *D. trifasciata* leaves	9.44 ppm	DPPH	Sarjani et al. (2021)
Ethanolic extract of *D. trifasciata* leaves	2.19 µg/mL	DPPH	Pinky and Hossain (2020)
Aqueous extract of *D. trifasciata* leaves	94.84 µg/mL	DPPH	Lontoc et al. (2018)

Table 3. Anticancer activity of *Dracaena trifasciata* in various cell models using in vitro methods

Sample	Cell model	IC_{50} (µg/mL) value	References
Ethanolic extract of *D. trifasciata* leaves	T47D	537 µg/mL	Saribanon et al. (2021)
Ethanolic extract of *D. trifasciata* aerial part nonflowering	HepG-2	81 ± 18.8 µg/mL	El-Hawary et al. (2021)
Trifasciatosides isolated from metanol extract aerial part of *D. trifasciata*	HeLa	26.5 µM	Teponno et al. (2017)

ANTIBACTERIAL ACTIVITY

The antibacterial potential of *D. trifasciata* is presented in Table 4. Bioactive compounds responsible for antibacterial activity include saponins, polyphenols, triterpenoids, alkaloids, and flavonoids (Hartono 2009; Oomariyah and Van Dijk 2022). Alkaloids, tannins, anthraquinones, terpenoids, saponins, flavonoids, steroids, and phenols found in the roots and leaves exhibit antiseptic and antibacterial properties by inhibiting the growth of *S. aureus*, *E. coli*, and *Pseudomonas aeruginosa* (Ahamad et al. 2017; Berame et al. 2017; Halyna et al. 2017; Buyun 2018).

Methanol, ethyl acetate, and ethanol extracts of *D. trifasciata* leaves can restrain pathogenic bacteria such as *S. aureus*, *P. aeruginosa*, *Bacillus cereus*, *Klebsiella pneumoniae*, *E. coli*, and *Salmonella* sp. (Table 4). According to Dewatisari et al. (2022), the active fraction of the leaves inhibits biofilm formation and virulence-related genes of *P. aeruginosa*. Biofilms are complex communities of bacteria enclosed in a self-produced extracellular matrix. They can enhance bacterial resistance to antibiotics and contribute to chronic infections. The active fraction derived from *D. trifasciata* leaves has been found to inhibit biofilm formation in *P. aeruginosa*, a bacterium commonly associated with biofilm-related infections (Dewatisari et al. 2021). Although research suggests the antibacterial potential of *D. trifasciata* and its bioactive compounds, additional investigations are warranted extraction techniques must be optimized and stable, and effifacy and safety in clinical setting must be evaluated. These further studies are essential for a comprehensive understanding of the therapeutic potential of *D. trifasciata* and its bioactive constituents in combating bacterial infections.

Review analysis has demonstrated the antibacterial efficacy of *D. trifasciata* extracts against specific bacterial strains. The study reported the inhibitory effects of the plant's methanol extract on the growth of *S. aureus*, *E. coli*, *P. aeruginosa*, *B. cereus*, *K. pneumoniae*, and *Salmonella* species. Another study found that the ethanol leaf extract of *D. trifasciata* exhibited antibacterial activity against *S. aureus*, *E. coli*, *P. aeruginosa*, and *Bacillus subtilis*. The *D. trifasciata* extracts have shown promise in combating multi-drug resistant bacteria, which are strains that have developed resistance to multiple antibiotics. A study reported that the ethanol extract of *D. trifasciata* leaves exhibited antibacterial activity against Methicillin-Resistant *S. aureus* (MRSA), a notorious multi-drug resistant pathogen. In some cases, combining *D. trifasciata* extracts with conventional antibiotics has demonstrated synergistic effects, enhancing the antibacterial activity (Kulkarni et al. 2023). This suggests that the plant extracts may augment existing antibacterial treatsments' efficacy.

The *D. trifasciata* has been traditionally used for wound healing purposes. Its antibacterial properties may contribute to its effectiveness in treating wounds by preventing or inhibiting bacterial growth at the injury site. While *D. trifasciata* extracts have shown antibacterial potential, it is important to consider safety aspects. Therefore, further research is needed to evaluate these extracts' toxicity, dosage, and potential side effect to ensure their safety in therapeutic applications. Future studies can focus on exploring the specific bioactive compounds inhibiting the antibacterial activity of *D. trifasciata* and understanding their action mechanisms (Huang et al. 2024). Additionally, investigations can be conducted to assess the extracts' efficacy in animal models and clinical trials to determine their potential use as antimicrobial agents. It is important to note that while the antibacterial potential of *D. rifasciata* extracts is promising, more research is needed to fully understand their mechanisms of action, optimize their extraction methods, evaluate their safety, and determine their efficacy in various bacterial infections.

TOXICITY

The toxicity of *D. trifasciata* has been extensively evaluated as indicated in Table 5. Several animal subjects previously used for this assessment included *Artemia salina*, Guinea pigs, Female Wistar Rats, Male Wistar Rats, and Swiss mice. The brine shrimp lethality test conducted using *A. salina* showed the toxic effects of various plant extracts with an LC_{50} value <1000 µg/ml (Meyer et al. 2018; El-Hawary et al. 2021).

Table 4. Antibacterial activity of *Dracaena trifasciata*

Sample	Tested Microorganism	MIC	References
Methanolic extract of *D. trifasciata* leaves	*S. aureus* *P. aeruginosa* *B. cereus* *K. pneumoniae* *E. coli*	50 µg/mL	Kingsley et al. (2013)
Ethyl acetate extract of *D. trifasciata* leaves	*E. coli*	12.5 mg/mL	Febriani et al. (2019)
Methanolic extract of *D. trifasciata* leaves	*S. aureus*	25 mg/mL	Febriani et al. (2019)
Ethanolic extract *D. trifasciata* leaves	*P. aeruginosa*	8 mg/mL	Dewatisari et al. (2021, 2023)
Potential fraction of ethanolic extract *D. trifasciata* leaves	*P. aeruginosa*	4 mg/mL	Dewatisari et al. (2021)

Table 5. Toxicity of *Dracaena trifasciata*

Sample	Toxicity	Value	References
Chloroform extract of *D. trifasciata* leaves	Toxic effect on female Wistar rats (*Rattus norvegicus* Berkenhout, 1769)	2000 mg/kg	Fitria et al. (2022)
Fresh leaves of *D. trifasciata*	Toxic effect on Brine shrimp (*A. salina*)	10 mg/mL	Berame et al. (2017)
Fresh roots of *D. trifasciata*	Toxic effect on Brine shrimp (*A. salina*)	44.49 µg/mL	Berame et al. (2017)
Ethanolic extract of *D. trifasciata* leaves	Toxic effect on Swiss mice (18-20 g) and Wistar rats (150-200 g)	1513.5±21.5 mg/kg; 1426± 43.6 mg/kg	Sunilson et al. (2009)
Ethanolic extract of *D. trifasciata* leaves	Toxic effect on Brine Shrimp (*A. salina)*	29.646 ppm	Mawardi and Siregar (2021)
Ethanolic extract of *D. trifasciata* leaves	Toxic effect on Brine Srimp (*A. salina)*	58.67 µg/mL	Pinky and Hossain (2020)
Ethanolic extract of *D. trifasciata* leaves	Toxic effect on Male rats of the Wistar strain	774.60 mg/kg	Ighodaro et al. (2017)

However, during testing with vertebrates comprising Female Wistar Rats, Male Wistar Rats, and Swiss mice, different results were obtained, as evidenced by higher LC_{50} values compared to *A. salina*. This indicated the lower toxicity effects experienced in vertebrate laboratory animals upon exposure to *D. trifasciata* preparations. Previous studies on Female Wistar Rats categorized the effect of the ethanol extract as the lowest hazardous (Fitria et al. 2022). The lower toxicity in the vertebrate test animals suggested its safety as a potential medicinal ingredient for human consumption, and further safety investigations are a must to consider the impacts on the kidneys, liver, and reproductive organs. Therefore, further dedicated studies are needed to comprehensively understand the impact of *D. trifasciata* extracts on these organs. These studies would involve rigorous toxicological evaluations, including histopathological examinations of organ tissues, assessment of organ function, and investigation of potential biochemical and molecular changes. Natural products, including plant extracts, can exhibit varying effects on different organs and individuals. Factors such as the dosage, exposure duration administration route, and individual susceptibility can influence the potential impacts on specific organs. These investigations are crucial to fully understand the safety and potential side effects of using *D. trifasciata* extracts as medicinal ingredients.

PHYTOCHEMISTRY

The *D. trifasciata* contains phytoconstituents such as flavonoids, sapogenin steroids including 25S-ruscogenin and sansevierigenin, pregnane glycosides, steroid saponins, methyl pyropheophorbide A, oliveramine, (2S)-3´,4´-methylenedioxy-5,7-dimethoxyflavane, 1-acetyl-β-carboline, digiprolactone, trichosanic acid, and methyl gallate (Tchegnitegni et al. 2017; Kasmawati et al. 2022; Dewatisari et al. 2023; Nguyen et al. 2023). Two known saponins, namely (24S,25R)-1b-[(β-D-fucopyranosyl)oxy]-3b -hydroxyspirost- 5-en-24-yl β-D-glucopyranoside (1) and 26- [(β-D-glucopyranosyl) oxy] -3 β, 22α -dihydroxyfurosta -5, 2 5(27)-dien-1β-yl-O-α-L-rhamnopyranosyl-(1→2)-α-L arabinopyranoside (2), were isolated and structurally characterized through an examination of the roots of *D. trifasciata* (Tchegnitegni et al. 2017; Nguyen et al. 2023). Phytochemical analysis of the whole plant revealed the presence of 1β,3β-dihydroxypregna-5,16-dien-20-one glycoside (Mimaki et al. 1997). These results provide insights into the diverse chemical composition of *D. trifasciata* and the geographical variations in the identified compounds. It highlights the potential for further exploration of the plant's phytochemical properties and potential applications in various fields such as medicine, agriculture, and industry.

The *D. trifasciata* leaves contain active ingredients, such as pregnane glycosides, alongside other compounds, including carotenoids, phytates, saponins, and tannins (Ikewuchi et al. 2011). A previous study reported high vitamin C content in Snake Plants (El-Hawary et al. 2021). A mature Snake Plant, comprising four to five leaves, can effectively purify the air within a $20m^2$ room area (Li and Yang 2020; Dewatisari and Nuryandani 2024).

The phytochemical constituents presented in Table 6 indicated the presence of tannins, glucogallin, gallic acid, corilagin, ellagic acid, terchebin, chebulagic acid, chebulinic acid, mucic acid, phyllembic acid, emblicol in leaves and rhizomes of *D. trifasciata* (Hariana 2013). A particular study identified several compounds from the ethanol leaf extract using GC-MS analysis. The results showed linoleic acid, palmitic acid (fatty acids), quinolone, steroid (campesterol), alkaloid (pyridine), terpenoid (phytol and cycloeucalenol), tocopherol (vitamin E), and flavonoid (pyrano-isoflavone). Additionally, squalene, L-(+)-ascorbic acid 2,6-dihexadecanoate, 1-heptacosanol, hexadecanoic acid 2-hydroxy-1-(hydroxymethyl)ethyl ester, p-cymene, Z-13-docosenamide, pentadecanoic acid, 1-iodo-2-methylundecane, 1-iodotridecane, isosorbide, Z-9-octadecenamide, 3,4-dimethoxybenzoic acid, palmitaldehyde, 1,2-benzene-dicarboxylic acid, delta-undecalactone, n-hexadecanoic acid, 6,10,14-trimethyl-2-pentadecanone, and dodecanoic acid were observed (Abdullah et al. 2018; Yumna et al. 2018). The obtained active compounds belonging to the fatty acid group included Cyclopropanebutanoic acid, 2-\[\[2-\[\[2-\ [(2-pentyl cyclopropyl) methyl\] cyclopropyl\] methyl\] cyclopropyl\] methyl\]-, methyl ester, n-hexadecanoic acid, hexadecanoic acid, ethyl ester, 11-octadecenoic acid,

methyl ester, vitamin B5 (2-myristoyl pantetheine), strigol (2H-Indeno\[1,2-b\]furan-2-one, 3,3a,4,5,6,7,8,8b-octahydro-8,8-dimethyl), and diterpenoid (neophytadiene) (Dewatisari et al. 2021; Dewatisari and To'bungan 2023). These compounds have shown inhibitory effects on biofilm growth and gene expression in *P. aeruginosa*, reducing its pathogenecity (Dewatisari et al. 2023). Squalene, campesterol, neophytadiene, palmitic acid, and linoleic acid were also reported to possess anticancer properties (To'bungan et al. 2022a,b,c; Zhu et al. 2022). Furthermore 6,10,14-trimethyl-2-pentadecanone is predicted to act as a natural larvicidal against *Culex quinquefasciatus* larvae (To'bungan and Jati 2022).

The composition of phytochemicals can vary between different plants and within the same plant species. In the case of *D. trifasciata*, genetic variations, environmental conditions, and cultivation practices can influence the specific phytochemical composition. Phytochemicals are molecules that give plants their odor, color, and flavor while also being an important part of their defense system. Plants naturally manufacture these chemicals to protect themselves from external threats such as pathogenic microorganisms. This benefit can be extended to humans and is the foundation for plant-based medicine. There are over 6,000 phytochemical substances that have been isolated and identified.

Table 6. Phytochemical component of *Dracaena trifasciata*

Isolated/Detected Chemical Compound	Plant Part	Solvent	Analysis Methods	Plant Sources	Reference
Fatty acid (Cyclopropanebutanoic acid, 2-[[2-[[2-[(2-pentylcyclopropyl) methyl] cyclopropyl] methyl] cyclopropyl]methyl]-, methyl ester, n-Hexadecanoic acid, hexadecanoic acid, ethyl ester, 11-Octadecenoic acid, methyl ester), vitamin B5 (2-myristynoyl pantetheine), strigol (2H-Indeno [1,2-b] furan-2-one, 3,3a, 4,5,6,7,8, 8b-octahydro-8,8-dimethyl) dan diterpenoid (neophytadiene)	Leaves	Ethanol	GC-MS	Indonesia	Dewatisari (2022)
Alkaloids, tannins and cardiac glycosides	Leaves	Methanol	Observation on qualitative phytochemical screening	Nigeria	Umoh et al. (2020)
Steroidal saponins/Trifasciatune: 1,2-(dipalmitoyl)-3-*O*-*β*-D-galactopyranosylglycerol (6), aconitic acid (7), and 1-methyl aconitic acid	Leaves	Ethanol	NMR	Germany	Tchegnitegni et al. (2017); Teponno et al. (2017)
Sappanin-type homoisoflavonoids, named trifasciatine A and (-)-(3*R*)-trifasciatine B Dihydrochalcone (+)-(8*S*)-trifasciatine C	Whole plant	Methanol &Ethanol	NMR	Myanmar	Thu et al. (2020)
Alkaloids (1-Acetyl-β carboline, methyl pyrophaeophorbide A and oliveramine, flavonoids such as (2S)-3′, 4′-methylenedioxy-5, 7-dimethoxyflavane, monoterpenes digiprolactone, phenolic methyl gallate, and fatty acid trichosanic acid) 1,2-(dipalmitoyl)-3-O-β-D-galactopyranosylglycerol, Sansevierigenin, and Spirosta-5,25(27)dien-1b,3b-diol-1-O-a-L-rhamnopyranosyl-(1,2)-a-L-arabinopyranoside steroids or terpenoids	Leaves	Ethanol	LC-MS/MS	Indonesia	Kasmawati et al. (2022)
Phytol, stigmasterol, linoleic acid, oleic acid, stearic acid, palmitic acid, methyl linoleate, phytol, linoleic acid, oleic acid, stearic acid, stigmasterol, 2,3-Dyhidro-3,5-dihydroxy-6methyl-4H-pyran-4-one, Methyl14methylpentadecanoate and (23S)-ethylcholest-5-en3.beta.-ol	Leaves	Methanol	GC-MS	Indonesia	Oomariyah and Van Dijk (2022)
Tanin, glukogalin, gallic acid, korilagin, ellagic acid, terchebin, chebulagic acid, chebulinic acid, mucid acid, phyllembic acid, and emblicol	Leaves	Methanol and Ethanol	GC-MS	Russia	Karamova et al. (2016); Yumna et al. (2018)
Alkaloid, tannin, terpenoid, saponin, steroid, fenol, kardenolin, polifenol, asam metil glukoronat, glikosida, karbohidrat dan abamagenin	Leaves and rhizomes	Methanol	GC-MS	India	Philip (2011)
Alkaloids, tannins, antraquinnons, saponins, flavonoids, glycosides, sterols and triterpenes	Leaves and roots	Ethanol	GC-MS	Philippines	Bañez and Castor (2013); Berame et al. (2017)
Lignin, fatty material, cellulose	Leaves	Ethanol	LC-MS	Bangladesh	Abdullah et al. (2018)

These chemicals are used as medicinal agents and in manufacturing pharmaceuticals. Alkaloids can interfere with DNA and protein synthesis, causing cell death. They are utilized to kill cancer cells, and their antimicrobial activity is attributed to their capacity to block ATP-binding cassette (ABC) transporters. Anthraquinones stimulate the release of gastrointestinal hormones and the creation of histamine, serotonin, and prostaglandin PGE2. They also reduce water absorption and enhance intestinal peristalsis. Plants with these chemicals are used as purgatives (Klimko et al. 2018). Some carotenoids have the ability to block ABC transporters, which are typically overexpressed in drug-resistant tumor cells (Martin et al. 2019). Isoflavones are phytoestrogens that prevent some malignancies in menopausal women by blocking tyrosine kinases and expressing antioxidant and estrogenic activities. Furanocoumarins crosslink with proteins and DNA bases when exposed to UV light (Sreenivasan et al. 2015).

As a result, those phytochemicals play a crucial role in treating vitiligo and psoriasis by helping to eliminate growing keratinocytes in the skin. Lignins and lignans have cytotoxic and immunomodulatory properties that impede cell division by inhibiting microtubule formation. Saponins are amphiphilic chemicals that interact with cholesterol in the biomembrane, causing leakage and cell death. As a result, they play an important role in traditional medicine for infection treatment. Terpenes have antibacterial activity against various human diseases, including fungi and bacteria. Sansevieria is classified into the Nolinoideae subfamily of the Asparagales order and has approximately 70 species. These plants are primarily found in Africa but grow in subtropical and tropical regions around the world. *Dracaena* species can grow in locations with low rainfall due to the plants's ability to store a large amount of water in their leaves. The roots and leaves of Sansevieria plants are used to treat ear infections, diarrhea, viral hepatitis, jaundice, asthma, and other conditions (Sriprapat et al. 2014; Wei et al. 2021).

Therefore, it is important to consider these factors when studying or utilizing the plant for its potential health benefits, extracting phytochemicals from *D. trifasciata* requires appropriate extraction methods. Various techniques, such as maceration, Soxhlet extraction, and solid-phase extraction, can isolate and concentrate the desired compounds. The choice of extraction method can impact the extract's efficiency, selectivity, and overall phytochemical profile. The phytochemical-rich extracts of *D. trifasciata* have been explored for their potential applications in different fields. For instance, the antimicrobial properties of the plant extracts have been investigated for use in natural preservatives or disinfectants. The antioxidant and anti-inflammatory properties of the phytochemicals may have implications for the development of dietary supplements or skincare products. Additionally, the plant's traditional medicinal uses in certain cultures have sparked interest in further exploring its potential therapeutic applications (Dewatisari et al. 2018; Dewatisari 2019).

The *D. trifasciata* contains alkaloids, flavonoids, saponins, steroids, terpenoids, and tannins. At the same time, the linoleic acid component can interact with 5α-reductase receptors to prevent alopecia by prolonging the anagen phase of hair growth (Kasmawati et al. 2022), while steroid can affect the ability to eat *A. salina* larvae, so they are called as antifeedant (To'bungan et al. 2021). Alkaloids are nitrogen-containing compounds found in *D. trifasciata*. Some alkaloids present in the plant may have pharmacological activities, such as antimicrobial or analgesic effects. However, specific alkaloids identified in *D. trifasciata* and their exact biological activities are less well-studied than other phytochemical groups. Flavonoids are a group of polyphenolic compounds found in *D. trifasciata*. These compounds are known for their antioxidant and anti-inflammatory properties. They have been studied for their potential protective effects against chronic diseases, including cardiovascular diseases, certain types of cancer, and neurodegenerative disorders. Flavonoids are also been associated with immune-modulating effects and may contribute to the plant's therapeutic potential. Saponins are bioactive compounds found in *D. trifasciata*. These compounds have been associated with various biological activities, including antimicrobial, anti-inflammatory, and antioxidant effects. Saponins are known for their ability to form a foamy lather when shaken with water, and they are often responsible for the bitter taste of plants. They have been studied for their potential benefits in cardiovascular health, immune modulation, and cancer prevention. The *D. trifasciata* contains various phenolic compounds, including phenolic acids and tannins. These compounds possess antioxidant properties and have been shown to scavenge free radicals, reduce oxidative stress, and protect against cellular damage. Phenolic compounds have been studied for their potential role in preventing chronic diseases, like cardiovascular diseases, cancer, and neurodegenerative disorders. Terpenoids, including terpenes and sterols, are present in *D. trifasciata*. These compounds have diverse biological activities, including antimicrobial, anti-inflammatory, and antioxidant effects. Terpenoids have been investigated for their potential therapeutic applications, such as cancer treatment, infectious diseases, and inflammatory conditions (Maheshwari et al. 2017; Maroyi 2019).

The extract from *D. trifasciata* leaves shows promise as a herbal remedy for wound healing and could be formulated into hydrogel preparations to create a medicinal drug (Ahmed et al. 2022; Yuniarsih et al. 2023). The *D. trifasciata* also has therapeutic prospects in liver fibrosis (Raslan et al. 2021). These phytochemical compounds strengthens the potential of *D. trifasciata* as a medicinal plant, capable of providing antibacterial, antioxidant, and anticancer effects. The *D. trifasciata* has been investigated for potential hepatoprotective (liver-protective) and neuroprotective effects. Some studies have suggested that the plant's phytochemicals may help protect liver cells from damage and support liver function. Additionally, certain compounds may possess neuroprotective properties, which could have implications for managing neurodegenerative diseases. The *D. trifasciata* has a promising antiulcerative potential, and is safe for use in folk medicine. This valuable

medicinal property is probably due to the array of important phytochemicals contained in the plant (Ighodaro et al. 2017).

The chemical compounds in different parts of *D. trifasciata* exhibit various properties and bioactive potential. Some of the compounds identified include fatty acids like cyclopropane butanoic acid, hexadecanoic acid, and 11-octadecenoic acid, which are known to have various biological activities. These fatty acids can affect inflammation, cell signaling, and lipid metabolism. Other compounds detected in *D. trifasciata* include alkaloids, tannins, cardiac glycosides, steroidal saponins, homoisoflavonoids, terpenoids, and flavonoids. These compounds have been studied for their potential pharmacological properties, such as antimicrobial, antioxidant, anti-inflammatory, antitumor, and immunomodulatory effects. The presence of these chemical compounds in different parts of the plant, such as leaves, roots, and rhizomes, suggests that *D. trifasciata* possesses a diverse array of bioactive constituents. This diversity may contribute to its traditional uses in various cultures for medicinal purposes. The abundance of compounds within natural sources provides excellent drug discovery and development opportunities, specifically serving as a guide for modern medicine. Natural compounds possess unique chemical structures and various pharmacological properties (Atanasov et al. 2015; Dewatisari 2015, et al. 2017; Mathur et al. 2022). The *D. trifasciata* has the potential to be applied as an antioxidant, antibacterial, and anticancer agent.

It is important to note that the specific composition and concentration of phytochemicals in *D. trifasciata* can vary. Several factors influence this variability, including plant age, growing conditions, and extraction methods, plant age can affect the accumulation of phytochemicals. Younger plants may have lower concentrations of certain compounds compared to mature plants. Similarly, the growing conditions, such as the availability of nutrients, light exposure, temperature, and humidity, can influence the plant's synthesis and accumulation of phytochemicals. Extraction methods also play a significant role in determining the composition and concentration of phytochemicals in *D. trifasciata*. Different extraction techniques, such as solvent extraction, steam distillation, or supercritical fluid extraction, can yield different results regarding the phytochemical profile. Factors like the choice of solvent, extraction time, temperature, and pressure can impact the efficiency and selectivity of the extraction process. Therefore, when studying the phytochemical profile of *D. trifasciata* or utilizing its extracts for various applications, it is crucial to consider these factors and account for the potential variations in composition and concentration. This understanding can contribute to more accurate and reliable research outcomes and effectively ensure the utilization of *D. trifasciata* in various fields, including medicine, cosmetics, and agriculture.

The chemical composition of *D. trifasciata* highlights its potential as a source of bioactive compounds with possible applications in medicine, cosmetics, and other industries. The effectiveness and safety of using *D. trifasciata* or its extracts for medicinal purposes should be evaluated through rigorous scientific investigations. Further safety investigations are needed to assess the long-term and short-term toxicity associated with using this plant material, making it a potential source for the development of modern drugs from natural sources. It's important to note that while *D. trifasciata* shows promise in various traditional uses and preliminary studies, more scientific research is necessary to understand and validate its potential health benefits fully.

ACKNOWLEDGMENTS

The Institute of Research and Community Service Universitas Terbuka, South Tangerang, Banten, Indonesia, facilitated this publication.

REFERENCES

Abdel-Hameed ESS, Bazaid SA, Shohayeb MM, El-Sayed MM, El-Wakil EA. 2012. Phytochemical studies and evaluation of antioxidant, anticancer and antimicrobial properties of *Conocarpus erectus* L. growing in Taif, Saudi Arabia. Eur J Med Plants 2 (2): 93-112. DOI: 10.9734/EJMP/2012/1040.

Abdullah, Angelina, Yumna M, Arbianti R, Utami TS, Hermansyah H, Ningsih S. 2018. Flavonoid isolation and identification of mother-in-law's tongue leaves (*Sansevieria trifasciata*) and the inhibitory activities to xanthine oxidase enzyme. E3S Web Conf 67 (1): 03011. DOI: 10.1051/e3sconf/20186703011.

Acevedo-Rodríguez P, Strong MT. 2005. Monocotyledons and Gymnosperms of Puerto Rico and the Virgin Islands. Department of Botany National Museum of Natural History, Washington, DC

Adeniyi AG, Adeoye SA, Ighalo JO. 2020. *Sansevieria trifasciata* fibre and composites: A review of recent developments. Intl Polym Process 35 (4): 344-354. DOI: 10.3139/217.3914.

Adhityaxena AT, Megantika A, Arbianti R, Utami TS, Hermansyah H. 2020. Extraction of flavonoid from mother-in-law's tongue leaves (*Sansevieria trifasciata*) by ultrasound assisted enzymatic extraction and its inhibition test. AIP Conf Proc 2255: 040008. DOI: 10.1063/5.0014728.

Afrasiabian S, Hajibagheri K, Roshani D, Zandsalimi S, Barari M, Mohsenpour B. 2017. Investigation of the knowledge, attitude and performance of the physicians in regard to rational antibiotic prescription. Sci J Kurdistan Univ Med Sci 22 (1): 25-35. DOI: 10.22102/22.1.25.

Ahamad T, Negi DS, Khan MF. 2017. Phytochemical analysis, total phenolic content, antioxidant and antidiabetic activity of *Sansevieria cylindrica* leaves extract. J Nat Prod Resour 3 (2): 134-136. DOI: 10.21767/2472-0151.100026.

Ahmed S, John P, Paracha RZ, Bhatti A, Guma M. 2022. Docking and molecular dynamics study to identify novel phytobiologics from *Dracaena trifasciata* against metabolic reprogramming in rheumatoid arthritis. Life 12 (8): 1148. DOI: 10.3390/life12081148.

Aliero AA, Jimoh F, Afolayan AJ. 2008. Antioxidant and antibacterial properties of *Sansevieria hyacinthoides*. Intl J Pure Appl Sci 2: 103-110.

Anbu JSJ, Jayaraj P, Varatharajan R, Thomas J, Jisha J, Muthappan M. 2009. Analgesic and antipyretic effects of *Sansevieria trifasciata* leaves. Afr J Tradit Complement Altern Med 6 (4): 529-533. DOI: 10.4314/ajtcam.v6i4.57191.

Andhare RN, Raut MK, Naik SR. 2012. Evaluation of antiallergic and anti-anaphylactic activity of ethanolic extract of *Sanseveiria trifasciata leaves* (EEST) in rodents. J Ethnopharmacol 142 (3): 627-633. DOI: 10.1016/j.jep.2012.05.007.

Appell SD. 2001. The Potted Garden: New Plants and New Approaches for Container Gardens (Vol. 168). Brooklyn Botanic Garden, Brooklyn, NY.

Aref YM, Othaman R, Anuar FH, Ku Ahmad KZ, Baharum A. 2023. Superhydrophobic modification of *Sansevieria trifasciata* natural fibres: A promising reinforcement for wood plastic composites. Polymers 15 (3): 594. DOI: 10.3390/polym15030594.

Aseptianova A. 2019. Utilization of family medicinal plants for family medicine in Kebun Bunga Village, Sukarami District, Palembang City. Batoboh 3 (1): 1-25. DOI: 10.26887/bt.v3i1.680. [Indonesian]

Atanasov AG, Waltenberger B, Pferschy-Wenzig EM, Linder T, Wawrosch C, Uhrin P, Temml V, Wang L, Schwaiger S, Heiss EH, Rollinger JM, Schuster D, Breuss JM, Bochkov V, Mihovilovic MD, Kopp B, Bauer R, Dirsch VM, Stuppner H. 2015. Discovery and resupply of pharmacologically active plant-derived natural products: A review. Biotechnol Adv 33 (8): 1582-1614. DOI: 10.1016/j.biotechadv.2015.08.001.

Babu K, Prabhu DKS. 2023. Studies on anatomy, physico-chemical and thin-layer chromatography of rhizome, root and leaf of *Dracaena trifasciata* (Prain) Mabb. J Pharmacogn Phytochem 12 (1): 668-671. DOI: 10.22271/phyto.2023.v12.i1f.14611.

Baldwin AS, Webb RH. 2016. The genus *Sansevieria*: An introduction to molecular (DNA) analysis and preliminary insights to intrageneric relationships. Sansevieria 34: 14-26.

Baliyan S, Mukherjee R, Priyadarshini A, Vibhuti A, Gupta A, Pandey RP, Chang CM. 2022. Determination of antioxidants by DPPH radical scavenging activity and quantitative phytochemical analysis of *Ficus religiosa*. Molecules 27 (4): 1326. DOI: 10.3390/molecules27041326.

Bañez SES, Castor LA. 2013. Phytochemical screening and insecticidal testing of mother in law's tongue (*Sansevieria trifasciata*). IAMURE Intl J Sci Clin Lab 3 (1): 1.

Berame J, Cuenca S, Cabilin D, Manaban M. 2017. Preliminary phytochemical screening and toxicity test of leaf and root parts of the snake plant (*Sansevieria trifasciata*). J Phylogenet Evol Biol 5: 3. DOI: 10.4172/2329-9002.1000187.

Bhattacharjee N, Khanra R, Dua TK, Das S, De B, Zia-Ul-Haq M, De Feo V, Dewanjee S. 2016. *Sansevieria roxburghiana* Schult. & Schult. F. (Family: Asparagaceae) attenuates type 2 diabetes and its associated cardiomyopathy. PloS ONE 11 (11): e0167131. DOI: 10.1371/journal.pone.0167131.

Bratu S, Gupta J, Quale J. 2006. Expression of the las and rhl quorum-sensing systems in clinical isolates of *Pseudomonas aeruginosa* does not correlate with efflux pump expression or antimicrobial resistance. J Antimicrob Chemother 58 (6): 1250-1253. DOI: 10.1093/jac/dkl407.

Brown SH. 2011. *Scyphophorus acupunctatus* in *Sansevieria*. University of Florida Extension, Florida.

Buyun L. 2018. A Promising alternative for treatment of bacterial infections by *Sansevieria cylindrica* Bojer ex Hook leaf extract. Agrobiodivers Improv Nutr Health Life Qual 2: 82-93. DOI: 10.15414/agrobiodiversity.2018.2585-8246.082-93.

Damen TH, Van der Burg WJ, Wiland-Szymańska J, Sosef MS. 2018. Taxonomic novelties in African *Dracaena* (Dracaenaceae). Blumea 63 (1): 31-53. DOI: 10.3767/blumea.2018.63.01.05.

Denk T, Güner HT, Grimm GW. 2014. From mesic to arid: Leaf epidermal features suggest preadaptation in Miocene dragon trees *(Dracaena*). Rev Palaeobot Palynol 200: 211-228. DOI: 10.1016/j.revpalbo.2013.09.009.

Dewatisari W, Nugroho LH, Retnaningrum E, Purwestri YA. 2023. Inhibition of protease activity and anti-quorum sensing of the potential fraction of ethanolic extract from *Sansevieria trifasciata* Prain leaves against *Pseudomonas aeruginosa*. Indones J Biotechnol 28 (1): 23-30. DOI: 10.22146/ijbiotech.73649.

Dewatisari W. 2022. Antibacterial and anti-biofilm- forming activity of secondary metabolites from *Sansevieria trifasciata*- leaves against *Pseudomonas aeruginosa*. Indones J Pharm 33 (1): 100-109. DOI: 10.22146/ijp.2815.

Dewatisari WF, Lyndiani M. 2015. Kemampuan kultivar *Sansevieria trifasciata* dalam menyerap gas karbon monoksida (CO) dari asap rokok. Ekosains 7 (3): 99-106. [Indonesian]

Dewatisari WF, Nugroho LH, Retnaningrum E, Purwestri YA. 2021. The potency of *Sansevieria trifasciata* and *S. cylindrica* leaves extracts as an antibacterial against *Pseudomonas aeruginosa*. Biodiversitas 22 (1): 408-415. DOI: 10.13057/biodiv/d220150.

Dewatisari WF, Nuryandani E. 2024. A review: The potency of *Dracaena liberica* (Gerome & Labroy) Christenh. as etnomedicine dan treaupetic. E3S Web Conf 483: 01005. DOI: 10.1051/e3sconf/202448301005.

Dewatisari WF, Rumiyanti L, Rakhmawati I. 2018. Rendemen dan skrining fitokimia pada ekstrak daun *Sanseviera* sp. Jurnal Penelitian Pertanian Terapan 17 (3): 197-202. DOI: 10.25181/jppt.v17i3.336.

Dewatisari WF, Subandi, Desmawati. 2017. Antibacterial activity of saponins from *Sanseviera trifasciata* prain cv. Golden Hahnii roots on *Escherichia coli* and *Staphylococcus aureus*. Afr J Biochem Res 11 (5): 22-27. DOI: 10.5897/AJBR2016.0914.

Dewatisari WF, Suranto, Setyono P. 2008. Keanekaragaman beberapa varietas *Sansevieria trifasciata* berdasarkan karakter anatomi, isozim, dan kandungan saponin. Bioteknologi 5 (2): 56-62. DOI: 10.13057/biotek/c050203. [Indonesian]

Dewatisari WF, To'bungan N. 2023. Biological activity and phytochemistry of *Dracaena angolensis* Welw. ex Carrière. Plant Sci Today 10 (4): 206-214. DOI: 10.14719/pst.2498.

Dewatisari WF. 2009. Anatomical, Secondary and Molecular Metabolite Analysis of *Sansevieria trifasciata*. [Thesis]. Universitas Sebelas Maret, Surakarta. [Indonesian]

Dewatisari WF. 2015. Antimicrobial activity of the saponin extract of *Sansevieria trifasciata* var. Golden Hahnii. J Bacteriol Parasitol 6 (4): 9597.

Dewatisari WF. 2019. Comparison of solvent variations from mother in law tongue (*Sansevieria trifasciata*) leaf extract on yield and antibacterial activity. Proceeding Biologi Seminar 4. Universitas Muhammadiyah Surakarta, Surakarta. [Indonesian]

Dohre V, Yadav S. 2021. Impact of two different methods of extraction on total antioxidant activity and phenolic content in an uncommon plant (*Sansevieria trifasciata*) and commonly consumed fruits. Flora Fauna 27 (1): 35-41. DOI: 10.33451/florafauna.v27i1pp35-41.

El Mokni R, Verloove F. 2022. Further records of non-native succulents within Asparagaceae sensu lato as casual or naturalising aliens in Tunisia and North Africa. Bradleya 40 (40): 119-129. DOI: 10.25223/brad.n40.2022.a10.

El-Hawary SSED, Rabeh M, Ali ZY, Albohy A, Fawaz NE. 2021. *Sansevieria*: An evaluation of potential cytotoxic activity in reference to metabolomic and molecular docking studies. Egypt J Chem 64 (2): 835-849. DOI: 10.21608/ejchem.2020.43384.2877.

Febriani Y, Mierza V, Handayani NP, Surismayanti S, Ginting I. 2019. Antibacterial activity of *lidah mertua* (*Sansevieria trifasciata* Prain.) leaves extract on *Escherichia coli* and *Staphylococcus aureus*. Open Access Maced J Med Sci 7 (22): 3882-3886. DOI: 10.3889/oamjms.2019.525.

Fitria L, Gunawan ICP, Sanjaya WBT, Meidianing MI. 2022. Single-dose acute oral toxicity study of chloroform extract of snake plant (*Sansevieria trifasciata* Prain.) leaf in Wistar rats (*Rattus norvegicus* Berkenhout, 1769). J Trop Biodivers Biotechnol 7 (1): 69389. DOI 10.22146/jtbb.69389.

Freiberg M, Winter M, Gentile A, Zizka A, Muellner-Riehl AN, Weigelt A, Wirth C. 2020. LCVP, The Leipzig catalogue of vascular plants, a new taxonomic reference list for all known vascular plants. Sci Data 7 (1): 416. DOI: 10.1038/s41597-020-00702-z.

Gabriel M, Betim F, de Oliveira C, Bianchini A, Moura P, Dalarmi L, Montrucchio D, Fernandes I, Dias J, Miguel O. 2023. Bioactive metabolites and biological, toxic and pharmacological activities of ornamental plants: A review of the species *Hydrangea macrophylla*, *Euphorbia milii*, *Dieffenbachia seguine* and *Dracaena trifasciata*. Arquivos de Ciências da Saúde da UNIPAR 27 (6): 2623-2640. DOI: 10.25110/arqsaude.v27i6.2023-032.

Ghaderi F. 2023. New report of Phytophthora occultans associated with root and crown rot on *Sansevieria*. Mycol Iran 10 (1): 45-54. DOI: 10.22043/MI.2023.361284.1250.

Gita RSD, Danuji S. 2021. Studi keanekaragaman tumbuhan obat yang digunakan dalam pengobatan tradisional masyarakat Kabupaten Pamekasan. Bioma 6 (1): 11-23. DOI: 10.32528/bioma.v6i1.4817. [Indonesian]

Gunasinghe YK, Rathnayake IV, Deeyamulla MP. 2023. The entophytic and potting soil bacteria of the *Sansevieria trifasciata* plant have a purifying impact on indoor toluene. Intl J Environ Res 17 (4): 48. DOI: 10.1007/s41742-023-00538-6.

Guo K, Yan L, He Y, Li H, Lam SS, Peng W, Sonne C. 2023. Phytoremediation as a potential technique for vehicle hazardous pollutants around highways. Environ Pollut 322: 121130. DOI: 10.1016/j.envpol.2023.121130.

Halyna T, Buyun L, Osadowski Z, Maryniuk M. 2017. The antibacterial activity of certain *Sansevieria* Thunb. species against *Escherichia coli*. Agrobiodivers Improv Nutr Health Life Qual 1: 446-453. DOI: 10.15414/agrobiodiversity.2017.2585-8246.446-453.

Hamidu H. 2009. Kajian Etnobotani Suku Buton (Kasus Masyarakat Sekitar Hutan Lambusango, Kabupaten Buton, Provinsi Sulawesi Tenggara). [Undergraduate Thesis]. Institut Pertanian Bogor, Bogor. [Indonesian]

Hariana HA. 2013. 262 Tumbuhan Obat dan Khasiatnya. Penebar Swadaya Grup, Jakarta. [Indonesian]

Hartanti D, Budipramana K. 2020. Traditional antidiabetic plants from Indonesia. Ethnobot Res Appl 19: 1-24. DOI: 10.32859/era.19.34.1-24.

Hartono T. 2009. Saponin Phytochemical Natural Ingredients. Farmasi, DIKTI. [Indonesian]

Hijrah H, Nugrahani AW, Ramadanil R. 2019. Studi etnobotani tumbuhan berkhasiat obat pada Suku Tau Taa Wana di Desa Bulan Jaya Kecamatan Ampana Tete, Kabupaten Tojo Una Una, Provinsi Sulawesi Tengah. Biocelebes 13 (1): 76-86. [Indonesian]

Huang X, Arjsri P, Srisawad K, Yodkeeree S, Dejkriengkraikul P. 2024. Exploring the anticancer potential of traditional Thai medicinal plants: A focus on *Dracaena loureiri* and its effects on non-small-cell lung cancer. Plants 13 (2): 290. DOI: 10.3390/plants13020290.

Husti A, Cantor M, Stefan R, Miclean M, Roman M, Neacsu I, Contiu I, Magyari K, Baia M. 2016. Assessing the indoor pollutants effect on ornamental plants leaves by FT-IR spectroscopy. Acta Phys Pol A 129 (1): 142-149. DOI: 10.12693/APhysPolA.129.142.

Ighodaro OM, Adeosun AM, Ojiko BF, Akorede AT, Fuyi-Williams O. 2017. Toxicity status and antiulcerative potential of *Sansevieria trifasciata* leaf extract in Wistar rats. J Intercult Ethnopharmacol 6 (2): 234-239. DOI: 10.5455/jice.20170421103553.

Ikewuchi J, Ikewuchi C, Igboh N, Mark-Balm T. 2011. Protective effect of aqueous extract of the rhizomes of *Sansevieria liberica* Gérôme and Labroy on carbon tetrachloride induced hepatotoxicity in rats. EXCLI J 10: 312-321. DOI: 10.17877/DE290R-5133.

Indirasetyo NL, Kusmono. 2022. Isolation and properties of cellulose nanocrystals fabricated by ammonium persulfate oxidation from *Sansevieria trifasciata* fibers. Fibers 10 (7): 61. DOI: 10.3390/fib10070061.

Indrayanto G, Putra GS, Suhud F. 2021. Validation of in-vitro bioassay methods: Application in herbal drug research. Profiles Drug Subst Excip Relat Methodol 46: 273-307. DOI: 10.1016/bs.podrm.2020.07.005.

Iswoyo H, Bahrun HA, Ganing W. 2023. Phytoremidation by *Sansevieria* sp. through absorption of Carbon Monoxide (CO). Jurnal Agroekoteknologi 16 (1): 46-52. DOI: 10.21107/agrovigor.v16i1.18258.

Karamova N, Gumerova S, Hassan GO, Abdul-Hafeez EY, Ibrahim OHM, Orabi MAA, Ilinskaya O. 2016. Antioxidant and antimutagenic potential of extracts of some Agavaceae family plants. BioNanoScience 6: 591-593. DOI: 10.1007/s12668-016-0286-x.

Kasmawati H, Mustarichie R, Halimah E, Ruslin R, A Sida N. 2022. Antialopecia activity and IR-Spectrometry characterization of bioactive compounds from *Sansevieria trifasciata* P. Egypt J Chem 65 (13): 19-24. DOI: 10.21608/ejchem.2022.104463.4825.

Kee YJ, Zakaria L, Mohd MH. 2020 Identification, pathogenicity and histopathology of *Colletotrichum sansevieriae* causing anthracnose of *Sansevieria trifasciata* in Malaysia. J Appl Microbiol 129 (3): 626-636. DOI: 10.1111/jam.14640.

Kingsley J, Chauhan R, Sinha P, Abraham J. 2013. Screening and characterization of antimicrobial agents from *Sanseveria roxburghiana* and *Sanseveria trifasiata*. Asian J Plant Sci 12: 224-227. DOI: 10.3923/ajps.2013.224.227

Klimko M, Nowińska R, Jura-Morawiec J, Wiland-Szymańska J, Wilkin P. 2018. Pollen morphology of selected species of the genera Chrysodracon and *Dracaena* (Asparagaceae, subfamily Nolinoideae) and its systematic implications. Plant Syst Evol 304: 431-443. DOI: 10.1007/s00606-017-1486-8.

Kulkarni V, Dhruthi KS, Suresh D, Murali P, Kumar KA, Ravi L. 2023. *Veratrum viride* as a potential therapeutic source for the treatment of *Bovine babesiosis*. Med Plants-Intl J Phytomed Related Ind 15 (3): 446-454. DOI: 10.5958/0975-6892.2023.00045.X.

Krishna AGR, Espenti CS, Rami Reddy YV, Obbu A, Satyanarayana MV. 2020. Green synthesis of silver nanoparticles by using *Sansevieria roxburghiana*, their characterization and antibacterial activity. J Inorg Organomet Polym Mat 30: 4155-4159. DOI: 10.1007/s10904-020-01567-w.

Krishna MG, Kailasanathan C, nagarajaganesh B. 2022. Physico-chemical and morphological characterization of cellulose fibers extracted from *Sansevieria roxburghiana* Schult. & Schult. F leaves. J Nat Fibers 19 (9): 3300-3316. DOI: 10.1080/15440478.2020.1843102.

Kyaw YMM, Bi Y, Oo TN, Yang X. 2021. Traditional medicinal plants used by the Mon people in Myanmar. J Ethnopharmacol 265: 113253. DOI: 10.1016/j.jep.2020.113253.

Lestari E, Setyaningrum E, Wahyuningsih S, Rosa E, Nurcahyani N, Kanedi M. 2023. Antimalarial activity test and GC-MS analysis of ethanol and ethyl acetate extract of snake plant (*Sansevieria trifasciata* Prain). World J Biol Pharm Health Sci 15 (02): 091-097. DOI: 10.30574/wjbphs.2023.15.2.0337.

Li X, Yang Y. 2020. Preliminary study on Cd accumulation characteristics in *Sansevieria trifasciata* Prain. Plant Divers 42 (5): 351-355. DOI: 10.1016/j.pld.2020.05.001.

Lontoc SMH., Soriano CF, Comia SAMM, Hernandez AFR, Dumaoal OSR. 2018. In vitro antioxidant activity and total phenolic content of *Sansevieria trifasciata* (Snake plant) crude ethanolic and aqueous leaf extracts. Asia Pac J Allied Health Sci 1: 35-58. DOI: 10.1016/j.fct.2009.06.024.

Luu-Dam NA, Ninh BK, Sumimura Y. 2016. Ethnobotany of colorant plants in ethnic communities in Northern Vietnam. Anthropology 4 (158): 2332-2915. DOI: 10.4172/2332-0915.1000158.

Machala M, Kubínová R, Hořavová P, Suchý V. 2001. Chemoprotective potentials of homoisoflavonoids and chalcones of *Dracaena cinnabari*: Modulations of drug-metabolizing enzymes and antioxidant activity. Phytother Res 15 (2): 114-118. DOI: 10.1002/ptr.697.

Maheshwari R, Shreedhara CS, Polu PR, Managuli RS, Xavier SK, Lobo R, Setty M, Mutalik S. 2017. Characterization of the phenolic compound, gallic acid from *Sansevieria roxburghiana* Schult and Schult. f. rhizomes and antioxidant and cytotoxic activities evaluation. Pharmacogn Mag 13 (Suppl 3): S693-S699. DOI: 10.4103/pm.pm_497_16.

Mardiyati M, Steven S, Rizkiansyah RR, Senoaji A, Suratman R. 2016. Effects of alkali treatment on the mechanical and thermal properties of *Sansevieria trifasciata* fiber. AIP Conf Proc 1725: 020043. DOI: 10.1063/1.4945497.

Marjoni RM, Naim A, Zubaidah, Fajri Y, Nadia R. 2023. The effect of different extraction solvents on total phenolic and flavonoid total of snake plant (*Sansevieria trifasciata* var. Laurentii). J Pharm Negat Results 14 (1): 38-43. DOI: 10.47750/pnr.2023.14.01.008.

Maroyi A. 2019. *Sansevieria hyacinthoides* (L.) Druce: A review of its botany, medicinal uses, phytochemistry, and biological activities. Asian J Pharm Clin Res 12 (9): 21-26. DOI: 10.22159/ajpcr.2019.v12i9.34721.

Martin CE, Herppich WB, Roscher Y, Burkart M. 2019. Relationships between leaf succulence and Crassulacean acid metabolism in the genus *Sansevieria* (Asparagaceae). Flora 261: 151489. DOI: 10.1016/j.flora.2019.151489.

Mathur S, Pareek S, Verma R, Shrivastava D, Bisen PS. 2022. Therapeutic potential of ginger bio-active compounds in gastrointestinal cancer therapy: the molecular mechanism. Nutrire 47 (2): 15. DOI: 10.1186/s41110-022-00170-y.

Mawardi AL, Siregar ARS. 2021. Anticancer pre-screening of *Sansevieria masoniana* C. using brine shrimp lethality assay. Proc 2nd Intl Conf Sci Technol Modern Soc 2021: 6-9. DOI: 10.2991/assehr.k.210909.002.

Megantika A, Adhityaxena AT, Arbianti R, Utami TS, Hermansyah H. 2020. Production of flavonoid compounds from mother in law's tongue leaves (*Sansevieria trifasciata*) using microwave-assisted enzymatic extraction as anti-inflammatory. AIP Conf Proc 2255: 040009. DOI: 10.1063/5.0021017.

Meyer CA, Hall H, Heise N, Kaminski K, Ivie KR, Clapp TR. 2018. A systematic approach to teaching case studies and solving novel problems. J Microbiol Biol Educ 19 (3): 19.3.95. DOI: 10.1128/jmbe.v19i3.1593.

Mimaki Y, Inoue T, Kuroda M, Sashida Y. 1997. Pregnane glycosides from *Sansevieria trifasciata*. Phytochemistry 44 (1): 107-111. DOI: 10.1016/s0031-9422(96)00477-3.

Myint HH, Swe TT. 2019. Study on morphological, physicochemical investigation and antimicrobial activities of *Sansevieria trifasciata* hort. Ex prain.(na-gar-set-gamon). Myanmar Acad Arts Sci 17 (4): 483-500.

Nahdi MS, Kurniawan AP. 2019. The diversity and ethnobotanical study of medicinal plants in the southern slope of Mount Merapi, Yogyakarta, Indonesia. Biodiversitas 20 (8): 2279-2287. DOI: 10.13057/biodiv/d200824.

Narendhiran S, Mohanasundaram S, Arun J, Rannjith RV, Saravanan L, Catherine L, Subathra M. 2014. Phytochemical screening and antimicrobial activity of Thespesiapopulnealinn. Intl J Pharmacogn Phytochem Res 6 (1): 7-10.

Nguyen DH, Tu QT, Chu HM. 2023. Isolation and structural characterization of two saponins from the roots of *Sansevieria trifasciata* 'Laurentii'. Dalat Univ J Sci 15: 76-92. DOI: 10.37569/DalatUniversity.13.2.1136(2023).

Okunlola AI, Arije DN, Nnodim OC. 2018. Rooting development of *Sansevieria trifasciata* (Mother-In-Law Tongue) as influenced by different propagation substrates. Intl J Environ Agric Biotechnol 3 (3): 264371. DOI: 10.22161/ijeab/3.3.42.

Onah JO, Ntiejumokun S, Ayanbimpe G. 1994. Antifungal properties of an aqueous extract of *Sansevieria zeylanica*. Med Sci Res 22 (2): 147-148.

Oomariyah N, van Dijk G. 2022. The bioavailability prediction and screening phytochemicals of *Sansevieria trifasciata* leaves extract. MATEC Web Conf 372: 02003. DOI: 10.1051/matecconf/202237202003.

Pamonpol K, Areerob T, Prueksakorn K. 2020. Indoor air quality improvement by simple ventilated practice and *Sansevieria trifasciata*. Atmosphere 11 (3): 271. DOI: 10.3390/atmos11030271.

Pandiyarajan S, Manickaraj SS, Liao AH, Baskaran G, Selvaraj M, Assiri MA, Zhou H, Chuang HC. 2024. Supercritical CO_2 mediated construction of aluminium waste recovered γ-Al2O3 impregnated *Dracaena trifasciata* biomass-derived carbon composite: A robust electrocatalyst for mutagenic pollutant detection. J Colloid Interface Sci 659: 71-81. DOI: 10.1016/j.jcis.2023.12.117.

Panduwinata RA, Yamtana Y, Suyanto A. 2021. Use of *Sansevieria trifasciata* to reduce computer radiation in internet cafe operators. InJoint Intl Conf 8th Ann Conf Ind Syst Eng 2021 1st Intl Conf Ergonom Saf Health 2021: 13-14.

Papaj N. 2022. The phytoremediation properties of *Sansevieria trifasciata*: A solution to acid rain. Can Sci Fair J 5 (1): 1-9.

Pathy KK, Flavien NB, Honoré BK, Vanhove W, Van Damme P. 2021. Ethnobotanical characterization of medicinal plants used in Kisantu and Mbanza-Ngungu territories, Kongo-Central Province in DR Congo. J Ethnobiol Ethnomed 17: 5. DOI: 10.1186/s13002-020-00428-7.

Permana BH, Krobthong S, Yingchutrakul Y, Saithong T, Thiravetyan P, Treesubsuntorn C. 2023. Evidence of brassinosteroid signalling and alternate carbon metabolism pathway in the particulate matter and volatile organic compound stress response of *Sansevieria trifasciata*. Environ Exp Bot 205: 105116. DOI: 10.1016/j.envexpbot.2022.105116.

Philip DC. 2011. Antimicrobial, Antioxidant and Anticancer Activity of a Hemp Plant, *Sansevieria roxburghiana* Schult and Schult f. [Thesis]. St Peters University, Chennai, India.

Pinky S, Hossain A. 2020. Antioxidant, anti-inflammatory, cytotoxic and analgesic activities of *Sensevieria trifasciata*. Bangladesh Pharm J 23 (2): 195-200. DOI: 10.3329/bpj.v23i1.48341.

Raj FI, Appadurai, Pushparaj L, Thanu C. 2023. Mechanical characterization of randomly oriented short. natural fibre composites. Intl Polym Process 38 (5): 564-581. DOI: 10.1515/ipp-2023-4377.

Raslan M, Abdel Rahman R, Fayed H, Ogaly H, Fikry R. 2021. Metabolomic profiling of *Sansevieria trifasciata* hort ex. Prain leaves and roots by HPLC-PAD-ESI/MS and its hepatoprotective effect via activation of the NRF2/ARE signaling pathway in an experimentally induced liver fibrosis rat model. Egypt J Chem 64 (11): 6647-6671. DOI: 10.21608/ejchem.2021.78970.3877.

Rezgui A, Mitaine-Offer AC, Miyamoto T, Tanaka C, Lacaille-Dubois MA. 2015. Spirostane-type saponins from *Dracaena fragrans* "Yellow Coast". Nat Prod Commun 10 (1): 37-38. DOI: 10.1177/1934578X1501000111.

Rwawiire S, Tomkova B. 2015. Morphological, thermal, and mechanical characterization of *Sansevieria trifasciata* fibers. J Nat Fibers 12 (3): 201-210. DOI: 10.1080/15440478.2014.914006.

Saribanon N, Utami KP, Rahayu SE. 2021. Exploration of ethno-medicinal knowledge among periurban community of Hurip Jaya Village, Babelan, District Bekasi, West Java. J Trop Biodivers 1 (2): 103-113. DOI: 10.59689/bio.v1i2.49.

Sarjani TM, Mawardi AL, Pandia ES, Siregar ARS. 2021. Antioxidant activity and phytochemical screening of some *Sansevieria* plants. 2nd Intl Conf Sci Technol Modern Soc 2020: 381-384. DOI: 10.2991/assehr.k.210909.084.

Sathishkumar TP. 2016. Influence of cellulose water absorption on the tensile properties of polyester composites reinforced with *Sansevieria ehrenbergii* fibers. J Ind Text 45 (6): 1674-1688. DOI: 10.1177/1528083715569374.

Saxena R, Sharma V, Udavat U. 2022. Review paper some medicinal plants used for depression. Intl J Innov Sci Res Technol 7 (8): 1582-1584.

Sharma A, Kirti, Kumari A, Srivastava DN, Paul P. 2023. Fluorescent carbon dots from snake plant for applications as probe for optical and electrochemical sensing of Hg2+ and Fe3+ and bio-imaging agent. ChemistrySelect 8 (42): e202301249. DOI: 10.1002/slct.202301249.

Sreenivasan VS, Rajini N, Alavudeen A, Arumugaprabu V. 2015. Dynamic mechanical and thermo-gravimetric analysis of *Sansevieria cylindrica*/polyester composite: Effect of fiber length, fiber loading and chemical treatment. Compos B: Eng 69: 76-86. DOI: 10.1016/j.compositesb.2014.09.025.

Sriprapat W, Suksabye P, Areephak S, Klantup P, Waraha A, Sawattan A, Thiravetyan P. 2014. Uptake of toluene and ethylbenzene by plants: Removal of volatile indoor air contaminants. Ecotoxicol Environ Saf 102: 147-151. DOI: 10.1016/j.ecoenv.2014.01.032.

Srisawat T, Chumkaew P, Heed-Chim W, Sukpondma Y, Kanokwiroon K. 2013. Phytochemical screening and cytotoxicity of crude extracts of *Vatica diospyroides* Symington type LS. Trop J Pharm Res 12(1): 71-76. DOI: 10.4314/tjpr.v12i1.12.

Stover H. 1983. The Sansevieria Book. Endangered Species Press, California.

Sun J, Liu, JN, Fan B, Chen XN, Pang DR, Zheng J, Zhang Q, Zhao YF, Xiao W, Tu PF, Song YL, Li J. 2019. Phenolic constituents, pharmacological activities, quality control, and metabolism of *Dracaena* species: A review. J Ethnopharmacol 244: 112138. DOI: 10.1016/j.jep.2019.112138.

Sunilson J A, Jayaraj P, Varatharajan R, Thomas J, James J, Muthappan M. 2009. Analgesic and antipyretic effects of *Sansevieria trifasciata* leaves. Afr J Tradit Complement Altern Med 6 (4): 529-533. DOI: 10.4314/ajtcam.v6i4.57191.

Sutrisno S, Wiwaha G, Sofiatin Y. 2023. The effect of *Sansevieria* plant on Particulate Matter 2.5 levels in classroom. Jurnal Kesehatan Masyarakat 18 (3): 397-407. DOI: 10.15294/kemas.v18i3.39642.

Swinbourne, Robert FG. 2007. *Sansevieria* in Cultivation in Australia. Adelaide Botanic Gardens, Adelaide.

Takawira-Nyenya R, Mucina L, Cardinal-Mcteague WM, Thiele KR. 2018. *Sansevieria* (Asparagaceae, Nolinoideae) is a herbaceous clade within *Dracaena*: inference from non-coding plastid and nuclear DNA sequence data. Phytotaxa 76 (6): 254-276. DOI: 10.11646/phytotaxa.376.6.2.

Tallei TE, Rembet RE, Pelealu JJ, Kolondam BJ. 2016. Sequence variation and phylogenetic analysis of *Sansevieria trifasciata* (Asparagaceae). Biosci Res 13 (1): 1-7.

Tamanna MR, Kaur R, Kaur A, Gill NS, Kaur N. 2021. Phytoflavonoids: Contribution in anciexty management. World J Pharm Res 10 (4): 1572-1586.

Tchegnitegni BT, Teponno RB, Jenett-Siems K, Melzig MF, Miyamoto T, Tapondjou LA. 2017. A dihydrochalcone derivative and further steroidal saponins from *Sansevieria trifasciata* Prain. Z Naturforsch C J Biosci 72 (11-12): 477-482. DOI: 10.1515/znc-2017-0027.

Teponno RB, Dzoyem JP, Nono RN, Kauhl U, Sandjo LP, Tapondjou LA, Bakowsky U, Opatz T. 2017. Cytotoxicity of secondary metabolites from *Dracaena viridiflora* Engl & Krause and their semisynthetic analogues. Rec Nat Prod 11 (5): 421-430. DOI: 10.25135/rnp.54.17.03.050.

Thu ZM, Myo KK, Aung HT, Armijos C, Vidari G. 2020. Flavonoids and stilbenoids of the genera *Dracaena* and *Sansevieria*: Structures and bioactivities. Molecules 25 (11): 260. DOI: 10.3390/molecules25112608.

Tinggi B. 2018. Effects of fibre size on *Sansevieria trifasciata*/natural rubber/high-density polyethylene biocomposites. Malays J Anal Sci 22 (6): 1057-1064. DOI: 10.17576/mjas-2018-2206-16.

To'bungan N, Jati WN, Zahida F. 2021. Toksisitas akut ekstrak etanol batang rumput knop (*Hyptis capitata* Jacq.) dengan Metode Brine Shrimp Lethality Test (BSLT). Biota 6 (1): 52-57. DOI: 10.24002/biota.v6i1.3577. [Indonesian]

To'bungan N, Jati WN, Zahida F. 2022b. Acute toxicity and anticancer potential of knobweed (*Hyptis capitata*) ethanolic leaf extract and fraction. Plant Sci Today 9 (4): 955-962. DOI: 10.14719/pst.1847.

To'bungan N, Pratiwi R, Widyarini S, Nugroho LH. 2022c. Cytotoxicity extract and fraction of knobweed (*Hyptis capitata*) and its effect on

migration and apoptosis of T47D cells. Biodiversitas 23 (1): 572-580. DOI: 10.13057/biodiv/d230162.

To'bungan N, Jati WN. 2022. Larvicidal activity of Knobweed (*Hyptis capitata*) leaves ethanolic extract and fraction against Culex quinquefasciatus. Biogenesis 10 (2): 236-243. DOI: 10.24252/bio.v10i2.31825.

To'bungan N, Widyarini S, Nugroho LH, Pratiwi R. 2022a. Ethnopharmacology of *Hyptis capitata*. Plant Sci Today 9 (3): 593-600. DOI: 10.14719/pst.1602.

Tungmunnithum D, Thongboonyou A, Pholboon A, Yangsabai A. 2018. Flavonoids and other phenolic compounds from medicinal plants for pharmaceutical and medical aspects: An overview. Medicines 5 (3): 93. DOI: 10.3390/medicines5030093.

Umoh O, Edet V, Uyoh, V. 2020. Comparative analysis of the phytochemical contents of dry and fresh leaves of *Sansevieria trifasciata* Prain. Asian J Res Bot 3 (1): 41-47.

Ullah H, Treesubsuntorn C, Thiravetyan P. 2021. Enhancing mixed toluene and formaldehyde pollutant removal by *Zamioculcas zamiifolia* combined with *Sansevieria trifasciata* and its CO_2 emission. Environ Sci Pollut Res 28: 538-546. DOI: 10.1007/s11356-020-10342-w.

Van Kleinwee I, Larridon I, Shah T, Bauters K, Asselman P, Goetghebeur P, Leliaert F, Veltjen E. 2022. Plastid phylogenomics of the *Sansevieria* Clade of *Dracaena* (*Asparagaceae*) resolves a recent radiation. Mol Phylogenet Evol 169: 107404. DOI: 10.1016/j.ympev.2022.107404.

Wakhidah ZA, Sari I. 2019. Etnobotani pekarangan di Dusun Kaliurang Barat, Kecamatan Pakem, Sleman-Yogyakarta. Jurnal EduMatSains 4 (1): 1-28. DOI: 10.33541/edumatsains.v4i1.1041. [Indonesian]

Walker C. 2014. All change in *Dracaena* and *Sansevieria*. Cactus World 32 (2): 140-141.

Wambugu FK, Waweru WR. 2016. In vitro anthelmintic activity of *Sansevieria trifasciata* leaves extract against *Fasciola hepatica*. World J Pharm Sci 4 (11): 136-139.

Weerasinghe NH, Silva PK, Jayasinghe RR, Abeyrathna WP, John GK, Halwatura RU. 2023. Reducing CO_2 level in the indoor urban built environment: Analysing indoor plants under different light levels. Clean Eng Technol 14:100645. DOI: 10.1016/j.clet.2023.100645.

Wei N, Mwachala G, Hu GW, Wang QF. 2021. *Dracaena neobella* Nom. Nov., a replacement name for *D. bella* (LE Newton) Byng & Christenh. (Asparagaceae). Phytotaxa 514 (1): 85-87. DOI: 10.11646/phytotaxa.514.1.6.

Wetterer SK, Wetterer JK. 2022. Spread of the African spotted orchid *Oeceoclades maculata* in the New World. Lankesteriana 11: 215-224. DOI: 10.15517/lank.v22i3.53113.

Widyasanti A, Napitupulu LO, Thoriq A. 2020. Physical and mechanical properties of natural fiber from *Sansevieria trifasciata* and *Agave sisalana*. IOP Conf Ser: Earth Environ Sci 462 (1): 012032. DOI: 10.1088/1755-1315/462/1/012032.

Witthayaphirom C, Nuansawan N. 2023. Improving indoor air quality: Utilizing tropical ornamental plants for carbon dioxide reduction. Thai Environ Eng J 37 (3): 55-64.

Yu T, Yao H, Qi S, Wang J. 2020. GC-MS analysis of volatiles in cinnamon essential oil extracted by different methods. Grasas y Aceites 71 (3): e372. DOI: 10.3989/gya.0462191.

Yumna M, Angelina, Abdullah, Arbianti R, Utami TS, Hermansyah H. 2018. Effect of mother-in-law's tongue leaves (*Sansevieria trifasciata*) extract's solvent polarity on anti-diabetic activity through in vitro α-glucosidase enzyme inhibition test. E3S Web Conf 67: 3003. DOI: 10.1051/e3sconf/20186703003.

Yuniarsih N, Hidayah H, Gunarti NS, Kusumawati AH, Farhamzah F, Sadino A, Alkandahri MY. 2023. Evaluation of wound-healing activity of hydrogel extract of *Sansevieria trifasciata* leaves (Asparagaceae). Adv Pharmacol Pharm Sci 2023: 7680518. DOI: 10.1155/2023/7680518.

Zhu Y, Xie N, Chai Y, Nie Y, Liu K, Liu Y, Yang Y, Su J, Zhang C. 2022. Apoptosis induction, a sharp edge of berberine to exert anti-cancer effects, focus on breast, lung, and liver cancer. Front Pharmacol 13: 803717. DOI: 10.3389/fphar.2022.803717.

NUSANTARA BIOSCIENCE
Vol. 16, No. 2, pp. 185-191
November 2024

ISSN: 2087-3948
E-ISSN: 2087-3956
DOI: 10.13057/nusbiosci/n160204

Comparative assessment of carbon dioxide (CO_2) absorption capacities in *Koompassia malaccensis* and *Hopea nervosa* in Tekam Forest Reserve, Pahang, Malaysia

HASYA HANNANI RUZIMAN[1], AZIAN MOHTI[2], NURUL EMYLIANA SYAFIKA CHE YO[1], FAEZAH PARDI[1,3,♥]

[1]Faculty of Applied Sciences, Universiti Teknologi MARA. 40450 Shah Alam, Selangor Darul Ehsan, Malaysia
[2]Forestry and Environment Division, Forest Research Institute Malaysia. 52109 Kepong, Selangor Darul Ehsan, Malaysia
[3]Institute for Biodiversity and Sustainable Development, Universiti Teknologi MARA. 40450 Shah Alam, Selangor Darul Ehsan, Malaysia.
Tel.: +603-55444486, ♥email: faezahpardi@uitm.edu.my

Manuscript received: 29 February 2024. Revision accepted: 2 June 2024.

Abstract. *Ruziman HH, Mohti A, Yo NESC, Pardi F. 2024. Comparative assessment of carbon dioxide (CO_2) absorption capacities in* Koompassia malaccensis *and* Hopea nervosa *in Tekam Forest Reserve, Pahang, Malaysia. Nusantara Bioscience 16: 185-191.* Trees, the dominant life form in forests, are essential in the functioning of the terrestrial biosphere, especially for the carbon cycle of the ecosystem. This study aims to assess CO_2 absorption by two forest production species: *Koompassia malaccensis* Maingay and *Hopea nervosa* King. The experiment was carried out in an acrylic box, and the variation of carbon dioxide concentration, humidity, light, and temperature was measured using a Carbon Dioxide, Light, Temperature, and Humidity (CLTM) sensor. The experiment was conducted in an open area from 7:30 am to 6:30 am the next day (23 hours). The results showed that *H. nervosa* absorbed more CO_2 (71.13 ppm/hour) than *K. malaccensis* (51.54 ppm/hour), thus promoting its ability to address climate change in the microenvironment. As for the relationship between carbon dioxide absorption and photosynthesis variables, both species show a positive correlation between CO_2 absorption and humidity. In contrast, light and temperature were very weakly correlated to CO_2. Therefore, it was identified that *H. nervosa* (Dipterocarpaceae) and *K. malaccensis* (Fabaceae) are tree species with high CO_2 absorption capacity and thus can be considered suitable trees for replanting, especially in light of carbon mitigation initiatives.

Keywords: Carbon dioxide absorption, climate change, forest, trees

INTRODUCTION

Carbon dioxide is necessary for the biochemical process of photosynthesis, such that all plants require CO_2 to thrive. However, excessive CO_2 emissions harm the environment because they are mostly greenhouse gases released at the highest rate. This has led to an environment where greenhouse gases, mainly carbon dioxide, have increased significantly, and the Earth's climate is changing due to rising temperatures. According to the Malaysian Meteorological Department Scientific Report 2018, higher temperatures have been recorded in Peninsular Malaysia due to global climate change, with the western Peninsular Malaysia region having seen the highest increase in temperature (Rahman 2018). Because these emissions increase the greenhouse effect and contribute to global climate change, they affect the health of people, crops, forest species, numerous ecosystems, and the environment. Based on recent reports from the International Panel on Climate Change (IPCC), the global mean concentration of carbon dioxide is almost 400 parts per million (ppm). However, the most thorough studies indicate that the safe level of carbon dioxide concentration is below 350 ppm.

Malaysia is also not exceptional in being affected by climate change. This country is recorded as the fourth largest emitter of greenhouse gases in ASEAN, contributing to 0.52% of the total carbon emissions in the world (Rahman 2018). The importance of forest resources in providing valuable natural resources and ecological services contributed to the development of socioeconomic, forest biodiversity, conservation of land and water resources, and ecosystem stability (Ministry of Energy and Natural Resources 2022). However, the industrial revolution in the agricultural sector has become a contributing factor to the changing climate in addition to CO_2 emissions from deforestation and forest degradation (Pearson et al. 2017; Wadanambi et al. 2020).

The inevitable consequences may include temperature increase and other devastating impacts such as increasing frequency and intensity of heat waves, coastal adaptation, and extremity of flood events. The role of forests in mitigating and adapting to climate change is essential. Forests are capable of effectively sequestering and storing of atmospheric carbon in above-ground and below-ground biomass through photosynthesis and tree growth. According to Kanniah et al. (2014), trees from family of Dipterocarpaceae have high potential to absorb a

significant amount of CO_2 from the atmosphere thereby contributing to mitigating the localized effects of global warming. Fabaceae family is found to be the most popularly grown plants in the urban forest due to their rapid growth and good absorber of air pollution. According to Daud et al. (2019), *Pterocarpus indicus* from family of Fabaceae absorbed the most carbon dioxide per tree per year with 16,608,610.88 kg/tree/year compared to other families. In comparison of carbon dioxide absorption among several tree species, a study in Indonesia's tropical lowland forests found that CO_2 absorption rate ranged from 3.42 to 20 µmol m^{-2} s^{-1}. *Dadap merah* (*Erythrina crista-galli*) from Fabaceaea's family was the third highest absorption of CO_2 (15.49 µmol m^{-2} s^{-1}) after *entabuloh* tree (*Teijsmanniodendron bogoriense*) and *jati* (*Tectona grandis*) (Davis and Hidayati 2020). Based on a study by Suwanmontr et al. (2013), *Peltophorum pterocarpus* and *Samanea saman* from Fabaceae's family reach their maximum CO_2 uptake rates of 24.5 and 20.9 CO_2 µmol m^{-2} s^{-1} and are good carbon sink and they should be planted in the city for optimal CO_2 absorption. Dipterocarpaceae are known as economical timber trees and ecologically important because of their abundance can contribute to the total biodiversity of forests and function in absorbing CO_2 to the forest ecosystems (Zafriakma et al. 2020). Based on a study conducted by Trisurat et al. (2011) in Peninsular Thailand showed that *Dipterocarpus* species are more vulnerable to future climate change than species in other families such as *Parkia timorina* from Fabaceae family and *Callophylum calaba* from Guttiferae family. Dipterocarps, including *Hopea* sp. are dominant in Southeast Asian tropical rainforests. Meanwhile, *Koompassia malaccensis* is a leguminous tree, which forms a symbiotic relationship with nitrogen-fixing bacteria, enhancing the microbial diversity within tropical peat swamp forests (Too et al. 2018). Both species are highly valued for timber wood's quality and durability. Thus, they are equally crucial to Malaysia's ecology and economy (Asanok et al. 2020). However, due to the increasing demand for timber and greenhouse gas emissions leading to global climate change, these species are expected to be at risk of endangerment if adequate protective measures are not implemented. Much research on CO_2 absorption rate was conducted mainly on the wayside trees in urban areas (Misni et al. 2015; Daud et al. 2019, 2021), but fewer studies focus on timber trees in tropical forests.

Thus, the study aims to assess CO_2 absorption by forest tree species namely *K. malaccensis* (Fabaceae) and *H. nervosa* (Dipterocarpaceae) and to determine the relationship between CO_2 absorption of tree species and environmental variables. This study may be beneficial in providing information on the carbon sequestration capacity of these timber trees, and those with higher CO_2 uptake will be advantageous as the trees can reduce environmental pollution and CO_2 emission in the environment. The importance of fully understanding the rate of CO_2 absorption and their possible responses is needed so that a comprehensive management and conservation action plan can be carried out to maintain the sustainability of the forest under changing climate in the future.

MATERIALS AND METHODS

Materials

The materials used in this study were *K. malaccensis* and *Hopea nervosa* that categorized as production forest species. They are sampled from Tekam Forest Reserve, Pahang. The average age of the saplings used in this study is between 3 to 4 months.

Apparatus

Four units of acrylic transparent box shape as a medium for sampling with size of 40 cm width x 60 cm height x 40 cm length were used as a medium for sampling. Acrylic box was used to place the seedlings and the Carbon Dioxide, Light, Temperature and Moisture (CLTM) sensor to undergo photosynthesis. The acrylic box is shown in Figure 1. CLTM sensor was used as a source of electrical. The sensor was used to measure and store the amount of carbon dioxide that will capture the saplings, the temperature and light intensity. The CLTM sensor is shown in Figure 2.

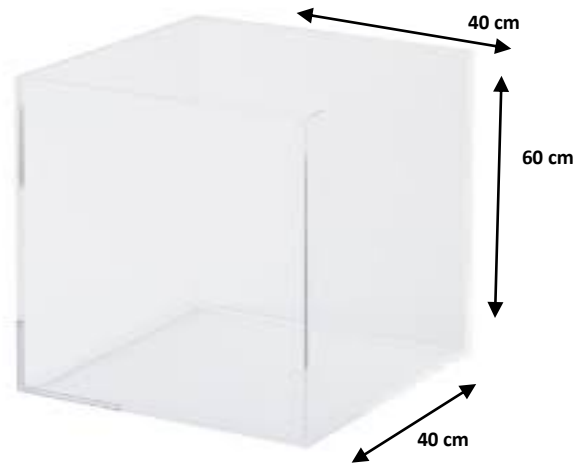

Figure 1. Two dimensional geometric model of the acrylic box

Figure 2. CLTM sensor used in the experiment

Procedures

Each sapling was located in an acrylic box, then stand under a completely clear sky for 23 hours to undergo the photosynthesis and respiration process. One acrylic box was used as a control by recording the carbon dioxide levels with no plant inside. The measurement of environmental variables including daily CO_2 concentration, temperature, light and humidity was conducted from May 8th to 9th starting from 7:30 am to 6:30 am on the next day. Carbon dioxide, Light, Temperature and Moisture (CLTM) sensor was inserted into each acrylic box to measure each environmental variable. The door of the acrylic box was closed to prevent the carbon dioxide (CO_2) from going in and out during the experiment. Any cracks in the plastic door were insulated so that the CO_2 inside the box did not escape. After the experiment was completed, all the saplings and the sensors were removed from the acrylic box to transfer the data of the environmental variables to computer. The data collected throughout the experiment was used to calculate the average of carbon dioxide concentration, humidity, light and temperature. The level of absorption of CO_2 by the saplings under different initial concentrations was calculated by using the following formula (Fathurrahman 2023):

Total absorption of CO_2 = CO_2 first reading – CO_2 next reading

Data analysis

Statistical analysis was performed using PAST Statistical Software to perform T-test (Hammer 2001). It is used to compare the means between the production forest species and determine whether any of those means are statistically significantly different from each other. Relationship between environmental variables of light, temperature, humidity and their influence on carbon dioxide absorption was determined using linear regression analysis.

RESULTS AND DISCUSSION

Carbon dioxide concentration and absorption level of *Hopea nervosa* and *Koompassia malaccensis*

Quantification of carbon dioxide concentration and absorption level by both species of *H. nervosa* and *K. malaccensis* are presented in Table 1. The study of variation of CO_2 concentration is separated into daytime period (08:30 am to 18:30 pm) and night-time period (19:30 pm to 05.30 am). For daytime, the concentration of carbon dioxide for *H. nervosa* decreases from 626.61 ppm to 446.54 ppm and for *K. malaccensis* decreases from 637.50 ppm to 475.58 ppm. Average values at night for *K. malaccensis* rises from 486.80 ppm to 548.09 ppm and for *H. nervosa* rises from 454.02 ppm to 601.48 ppm. The CO_2 concentration inside the box at night-time gradually increases because of the atmosphere is relatively calm when the sun is no longer heating the surface, the ground losses heat and cools down and photosynthesis do not occur at night. In contrast, the concentration gradually decreases during the day due to the plants' involvement in photosynthesis (Yarn et al. 2013).

Carbon dioxide absorption rate

Figure 3 shows the carbon dioxide absorption rate monitored between May 8th and 9th 2023, from 7:30 am until 12:30 pm for *H. nervosa* and *K. malaccensis*. For *H. nervosa*, the carbon dioxide absorption rate ranges from 3.04 ppm to 71.13 ppm, while for *K. malaccensis*, ranges from 10.85 ppm to 51.54 ppm. This study found that the highest carbon dioxide absorption was found in *H. nervosa* from family of Dipterocarpaceae compared to *K. malaccensis*. At 7:30 am, *H. nervosa* absorbs carbon dioxide at a value of -10.54 ppm and *K. malaccensis* at a value of -10. -10.63 ppm. This negative value of carbon dioxide absorption during this time due to the saplings consuming and breaking down carbohydrates and using them in other metabolic processes (Daud et al. 2021). Thus, there is a temporary negative carbon dioxide absorption during this time because plants typically release more carbon dioxide. In addition, at 7:30 am, there is no photosynthesis because plants have not received sufficient light intensity of sunlight. At this time, the light intensity for *K. malaccensis* is 251.31 lux and *H. nervosa* only absorbs 207.51 of light. Photosynthesis cannot occur if one of the required factors (sunlight) does not exist (Daud et al. 2019).

The rate of carbon dioxide absorption value for *H. nervosa* in the afternoon from 13:30 pm until 18:30 pm ranges from 7.95 ppm to 27.30 ppm and the value of carbon dioxide absorption rate for *K. malaccensis* ranges from 6.28 ppm to 13.78 ppm. This study found that carbon dioxide absorption by *H. nervosa* was higher compared *to K. malaccensis*. According to the result, from 8:30 am until 14:30 pm, the carbon absorption by *K. malaccensis* decreased. Throughout the day, the temperature may rise and possibly go above the range that is optimal for photosynthesis. High temperatures can cause photosynthesis to be less effective, which in turn causes less CO_2 to be absorbed. One of the other potential causes of the decreased carbon dioxide absorption value in this study is that the stomata, or tiny pores on plant leaves that regulate gas exchange, may partially close in order to reduce water loss through transpiration, which would then reduce the amount of CO_2 that plants can absorb (Wahidah et al. 2017).

At night or in the absence of light, photosynthesis stops and respiration is the dominant process. The dark respiration rate, which is the rate at which leaves take in oxygen and give out carbon dioxide is represented by the negative (-ve) value in the graph. The amount of CO_2 released through respiration is typically less than the amount of CO_2 absorbed throughout the day during photosynthesis (Yacob 2021). On 8th May 2023, the rate of carbon dioxide absorption for both species was observed between 21:30 pm and 00:30 am. For *H. nervosa*, the carbon dioxide ranges from -2.53 ppm to -131.93 ppm while for *K. malaccensis* ranges from -3.15 ppm to -32.67 ppm. On 9th May 2023, the rate of carbon dioxide absorption was observed from 01:30 am until 06:30 am at a

value of -3.67 ppm to -4.00 ppm for *H. nervosa* and *K. malaccensis* at a value of - 3.70 ppm to -75.11 ppm. Therefore, the carbon dioxide absorption during the night is a result of respiration and is generally negative, indicating a release of carbon dioxide rather than absorption.

The finding shows that both species undergo carbon dioxide absorption in the morning and evening. However, it can be seen that there is also active carbon dioxide absorption in both species at night, which is around at 22:30 pm until 23:30 pm. It also demonstrates that photosynthesis works best between at 8:30 am (for *H. nervosa*), at 09:30 (for *K. malaccensis*) and at 15:30 pm. for both species during the day. Then, as the light faded, it started to gradually decrease (Yacob 2021). Photosynthesis stops or slows down in the absence of light, lowering plants ability to absorb carbon dioxide. In the absence of light, photosynthesis ceases or slows down, reducing the carbon dioxide absorption capacity of plants.

Table 1. Variation of carbon dioxide concentration and carbon dioxide absorption level of *Hopea nervosa* and *Koompassia malaccensis*

Time (h)	*Hopea nervosa*		*Koompassia malaccensis*	
	Mean of Carbon Dioxide Level in Acrylic Box	Carbon Dioxide Absorption (ppm/hour)	Mean of Carbon Dioxide Level in Acrylic Box	Carbon Dioxide Absorption (ppm/hour)
07:30 am	616.07	-10.54	626.87	-10.63
08:30 am	626.61	48.62	637.50	51.54
09:30 am	577.99	71.13	585.96	39.03
10:30 am	506.86	7.33	546.93	15.39
11:30 am	499.53	19.48	531.54	14.03
12:30 pm	480.05	3.04	517.51	10.85
13:30 pm	477.01	7.95	506.66	9.45
14:30 pm	469.06	8.17	497.21	9.13
15:30 pm	460.89	27.3	488.08	13.78
16:30 pm	433.59	-7.94	474.30	6.28
17:30 pm	441.53	-5.01	468.02	-7.56
18:30 pm	446.54	-7.48	475.58	-11.22
19:30 pm	454.02	-3.79	486.80	-12.92
20:30 pm	457.81	-4.29	499.72	-9.57
21:30 pm	462.10	-131.93	509.29	-32.67
22:30 pm	594.03	15.38	541.96	5.77
23:30 pm	578.65	3.87	536.19	1.42
00:30 am	574.78	-2.53	534.77	-3.15
01:30 am	577.31	-3.67	537.92	-3.70
02:30 am	580.98	-6.41	541.62	-3.09
03:30 am	587.39	-6.72	544.71	-1.41
04:30 am	594.11	-7.37	546.12	-1.97
05:30 am	601.48	-10.59	548.09	-3.67
06:30 am	612.07	-4.00	551.76	-75.11

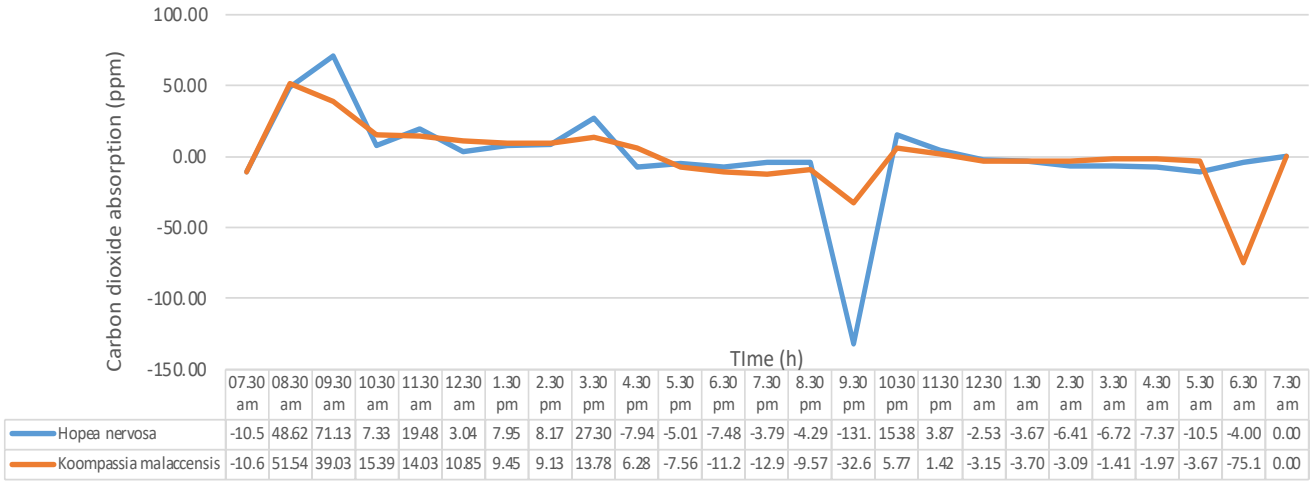

Figure 3. Carbon dioxide absorption level of *Hopea nervosa* and *Koompassia malaccensis*

Different rate of CO_2 absorption by tree species

This result demonstrates that the two types of forest tree species can absorb different amounts of carbon dioxide through photosynthesis. The data collected show that *H. nervosa* was the higher CO_2 absorber plant at 71.13 ppm/hour compared to *K. malaccensis*. At a value of 51.54 ppm/hour (Table 2). Kanniah et al. (2014) stated that the dipterocarp forest typically has a wide variety of valuable tree species, with the majority belonging to the genera *Hopea*, *Dryobalanops*, *Dipterocarpus*, *Shorea*, and *Parashorea*. The *H. odorata*, a member of the same family as *H. nervosa*, can absorb and store the most carbon dioxide among the other tree species studied at Linear Park, with a value of 274.06 kgCO2 e. In comparison, *Evatamia divaricata* had the lowest carbon dioxide absorption (35.59 kg CO_2 e) (Othman et al. 2019). Thus, this indicated that *Hopea* trees have a high rate of carbon absorption, which is mainly related to their rapid growth. In tropical climate zones, fast-growing trees frequently exhibit comparatively more excellent rates of CO_2 absorption, indicating that CO_2 assimilation rates may serve as indicators for assessing fast-growing characteristics.

Meanwhile, *K. malaccensis* from Fabaceae family recorded slightly lower carbon dioxide absorption at 51.54 ppm/hour, similarly in another study conducted by Yunusa and Linatoc (2018) which reported that *K. malaccensis* absorbs the second highest carbon dioxide at a value of 14.03 µmol m^{-2} s^{-1}. Among Fabaceae family, *P. indicus* Willd is commonly reported to have the highest capacity to absorb CO_2 per tree per hour with a capacity of up to 4624.29 grams (Daud et al. 2019). Similarly, *P. indicus* was identified with higher capacity to absorb carbon dioxide according to the findings of studies by Misni et al. (2015) and Pane et al. (2016).

Environmental variables and carbon dioxide absorption

Environmental variables are categorized as external factors that might influence absorption capacity such as light, humidity and temperature. In assessing the influence of these factors towards carbon dioxide absorption, linear correlation analysis was conducted among the environmental variables of light, temperature and humidity with the carbon dioxide absorption capacity. The analysis showed that only humidity factor was positively correlated with the carbon dioxide absorption, while other factors of light and temperature had negative correlation. According to Rawson et al. (2004), humidity affects photosynthesis, transpiration and water use efficiency in leaves of various plant species. Figure 4 shows positive correlation between humidity and carbon dioxide absorption for both species. From the allometric equation, the R^2 value for *H. nervosa* was 0.30 or in percentage, in other words, 30% of the differences in humidity were explained by carbon dioxide absorption of plants, while the R^2 value for *K. malaccensis* was 0.78 or 78%. The R^2 value of this sapling was higher than the R^2 value for *H. nervosa*. This implied that the decreased humidity would have less carbon dioxide absorption by plants. Based on the collected data, *K. malaccensis*'s humidity decreased from 91.56% to 83.98% and at the same time, carbon dioxide absorption also decreased from 51.54 ppm to 6.28 ppm. Besides, *H. nervosa*'s humidity also decreased from 59.38 % to 62.03 % and CO_2 absorption decreased from 71.13 ppm to 27.30 ppm.

Meanwhile, other factors, such as temperature and light, negatively correlated with the carbon dioxide absorption for both species. A negative correlation describes a situation where one of the variables sees an increase in value while the other one experiences a decrease. For *H. nervosa*, a simple linear regression that predicts temperature from carbon dioxide absorption has an R^2 value of 0.70. From this R^2 value, 70% of the changes in carbon dioxide absorption are attributed to changes in temperature, and 30% are unexplained by the model. The R^2 value for *K. malacenssis* was 0.90 or, in percentage, 90%. Both R2 values indicated that they have a strong negative correlation with carbon dioxide absorption. This means that carbon dioxide absorption appears to decrease when temperature increases. According to some research by Suwanmontr et al. (2013), air temperature has no direct impact on the activities of the photosynthetic enzymes.

Table 2. Carbon dioxide absorption level by two different saplings

Type of saplings	CO_2 absorption level (ppm/hour)
Hopea nervosa (Dipterocarpaceae)	71.13
Koompasia malaccensis (Fabaceae)	51.54

Table 3. Carbon dioxide absorption rate for *Hopea nervosa* and *Koompassia malaccensis* and the record of environmental variables of temperature, light and humidity

CO_2 absorption (ppm)	Environmental variables		
	Temp. (°C)	Light (lux)	Humidity (%RH)
Hopea nervosa			
48.62	28.00	1061.94	88.92
71.13	40.93	2185.45	59.38
7.33	64.41	2509.65	52.52
19.48	65.07	2256.76	52.49
3.04	62.82	2143.17	57.92
7.95	64.94	2412.21	52.66
8.17	64.53	2397.34	52.00
27.30	61.37	1337.51	62.03
48.62	28.00	1061.94	88.92
Koompassia malaccensis			
51.54	52.51	566.43	91.56
39.03	54.00	1076.96	86.82
15.39	55.95	1397.75	83.55
14.03	56.98	1229.26	82.06
10.85	56.57	888.82	84.39
9.45	56.88	917.29	83.85
9.13	57.26	1214.68	84.37
13.78	58.39	1032.57	82.15
6.28	57.87	764.82	83.98

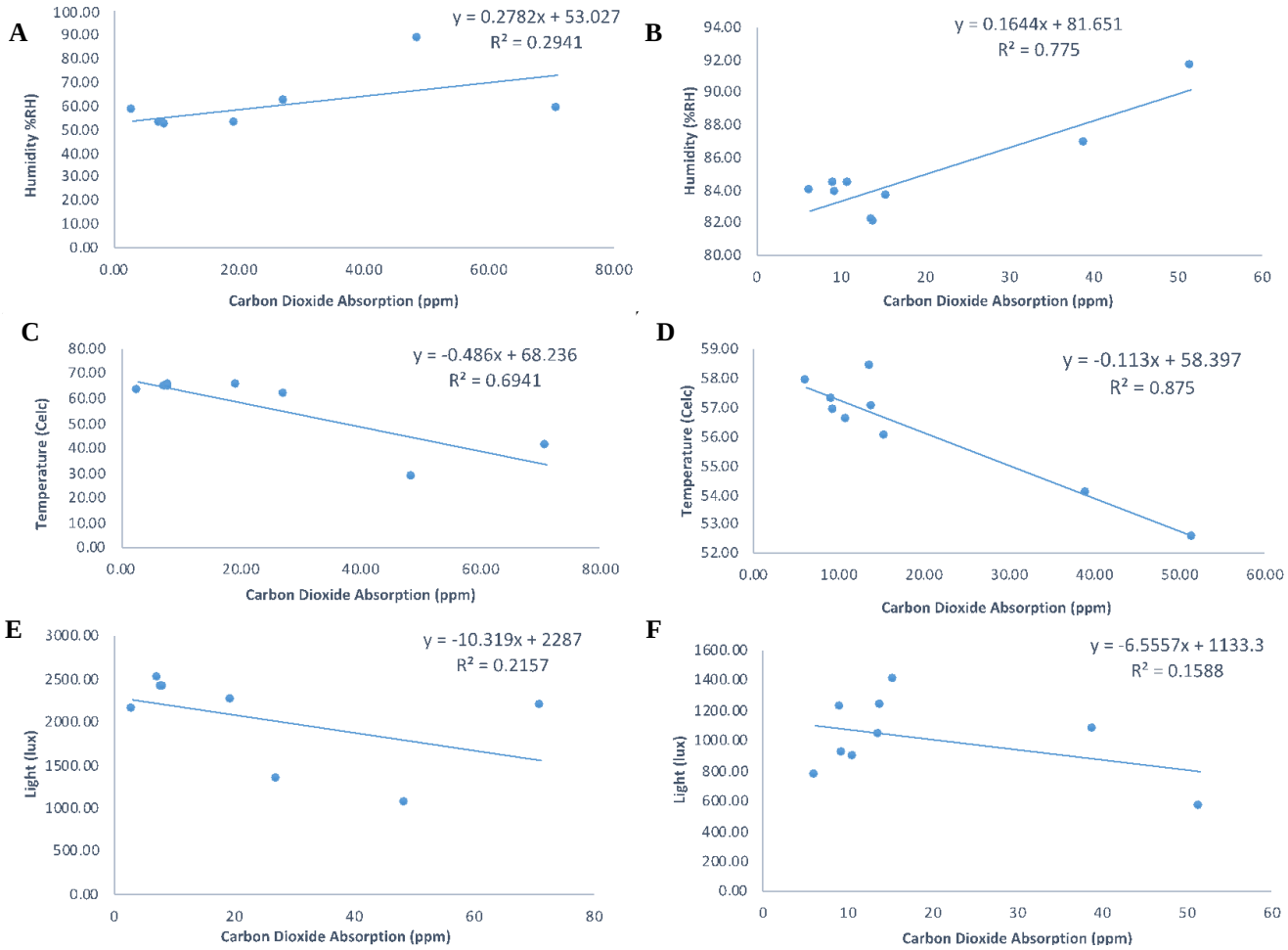

Figure 4. Relationship between carbon dioxide absorption and other environmental variables (humidity, temperature, light) for both species. Note: A, C, E. for *H. nervosa*, B, D, F. for *Koompassia malaccensis*

Light factor is also reported to have less influence on the carbon dioxide absorption capacity, as indicated by the downward slope of the graph in Figure 4. The equations show that R^2 value for *H. nervosa* was 0.22 and *K. malaccensis* with lower R^2 value of 0.16 or 16%. A lower R^2 value did not necessarily imply that plants would absorb more carbon dioxide at higher light intensities. When light intensity was 2185.45 lux, *H. nervosa* absorbed 71.33 ppm. When the light intensity was 2509.65 lux, the carbon dioxide absorption was only 7.33 ppm. For *K. malaccensis*, when light intensity was 1079.96 lux, the carbon dioxide absorption was 39.03 ppm, and at 1397.75 lux, it only absorbed 15.39 ppm of carbon dioxide (Table 3). According to Sari et al. (2005), the light intensity rises and falls based on cloud conditions in the atmosphere, affecting the carbon dioxide absorption rate (Daud et al. 2019). During the day, plants experience many changes in the type and amount of radiation they receive. Light is necessary for photosynthesis in plants, but too much light can cause harm. When there are frequent changes in light or plants cannot adapt to the prevailing light conditions, there may be a surplus of stimulation in the photosynthetic apparatus. This can lead to photoinhibition, where the excess energy from light damages the plant's photosynthetic pigments and proteins (Alves et al. 2002). As a result, this may hinder the plant's capacity to perform photosynthesis and absorb carbon dioxide. A 2000 µmol m^{-2} s^{-1} (full sunlight) exposure to algal cells in an experiment revealed that photosynthesis was quickly inhibited (Powles 1984).

In conclusion, trees in forests may give advantages in mitigating greenhouse gas emissions, mainly CO_2, and reducing the impact of global warming. In this study, a semi-closed technique to measure the concentration of CO_2 was used to determine the type of saplings with a high potential of absorbing CO_2. The study results concluded that the variation in CO_2 absorption ranged from 1.42 ppm to 71.13 ppm for both species. The highest rate was observed in *H. nervosa*, followed by *K. malaccensis*. Therefore, both *H. nervosa* and *K. malaccensis* could be suggested to stakeholders in planning or developing urban forests to reduce air pollution and, consequently, reduce the carbon emissions from various urban sources like power plants, discharge of industrial gases, and from passing vehicles on the roadsides. Other than that, both environmental variables, namely light and temperature, negatively correlate with carbon dioxide absorption, while humidity positively correlates with carbon dioxide absorption by plants.

ACKNOWLEDGEMENTS

This research was funded by the Ministry of Higher Education, Malaysia, under the Fundamental Research Grant Scheme (FRGS)-FRGS/1/2021/WAB03/ UITM/02/1.

REFERENCES

Alves PL, Magalhães AN, Barja PR. 2002. The phenomenon of photoinhibition of photosynthesis and its importance in reforestation. Bot Rev 68 (2): 193-208. DOI: 10.1663/0006-8101(2002)068[0193:TPOPOP]2.0.CO;2.

Asanok L, Kamyo T, Marod D. 2020. Maximum entropy modeling for the conservation of *Hopea odorata* in riparian forests, central Thailand. Biodiversitas 21 (10): 4663-4670. DOI: 10.13057/biodiv/d211027.

Daud M, Bustam B, Harnelly E, Dharma, W. 2021. Carbon absorption capability of single-leaf and compound-leaf plants in the BNI Urban Forest, Banda Aceh. IOP Conf Ser: Earth Environ Sci 918 (1): 012027. DOI: 10.1088/1755-1315/918/1/012027.

Daud M, Bustam BM, Arifin B. 2019. A comparative study of carbon dioxide absorption capacity of seven urban forest plant species of Banda Aceh, Indonesia. Biodiversitas 20 (11): 3372-3379. DOI: 10.13057/biodiv/d201134.

Davis LA, Hidayati N. 2020. Carbon dioxide absorption and physiological characteristics of selected tropical lowland tree species for revegetation. IOP Conf Ser: Earth Environ Sci 591 (1): 012039. DOI: 10.1088/1755-1315/591/1/012039.

Fathurrahman F. 2023. Effects of carbon dioxide concentration on the growth and physiology of *Albizia saman* (Jacq.) Merr. J Ecol Eng 24 (9): 302-311. DOI: 10.12911/22998993/169145.

Hammer Ø, Harper DAT, Ryan PD. 2001. PAST: Paleontological Statistics Software Package for education and data analysis. Palaeontol Electron 4 (1): 1-9.

Kanniah KD, Muhamad N, Kang C. 2014. Remote sensing assessment of carbon storage by urban forest. IOP Conf Ser: Earth Environ Sci 18: 012151. DOI: 10.1088/1755-1315/18/1/012151.

Ministry of Energy and Natural Resources 2022. Malaysia Policy on Forestry. Koyak Kreatif Venture, Selangor.

Misni A, Jamaluddin S, Kamaruddin SM. 2015. Carbon sequestration through urban green reserve and open space. J Malays Inst Plan 8: 101-122. DOI: 10.21837/pm.v13i5.142.

Othman R, Suid S, Noor NSM, Baharuddin ZMH, Hashim KSH, Mahamod LH. 2019. Estimation of carbon sequestration rate of urban park with linear and curvilinear design landscape setting. Appl Ecol Environ Res 17 (4): 8089-8101. DOI: 10.15666/aeer/1704_80898101.

Pane MS, Yoza D, Sulaeman R. 2016. Potensi serapan karbon dioksida (CO_2) pada pohon peneduh di Jalan Soekarno Hatta Kota Pekan Baru. Jom Faperta 3 (2): 1-8. [Indonesian]

Pearson TR, Brown S, Murray L, Sidman, G. 2017. Greenhouse gas emissions from tropical forest degradation: An underestimated source. Carbon Balance Manag 12: 3. DOI: 10.1186/s13021-017-0072-2.

Powles SB 1984. Photoinhibition of photosynthesis induced by visible light. Ann Rev Plant Physiol 35 (1): 15-44. DOI: 10.1146/annurev.pp.35.060184.000311.

Rahman HA. 2018. Climate change scenarios in Malaysia: Engaging the public. Intl J Malays-Nusantara Stud 1 (2): 55-77.

Rawson H, Begg J, Woodward R. 2004. The effect of atmospheric humidity on photosynthesis, transpiration and water use efficiency of leaves of several plant species. Planta 134: 5-10. DOI: 10.1007/BF00390086.

Sari MB, Yulkifli, Kamus Z. 2015. Sistem pengukuran intensitas dan durasi penyinaran matahari Realtime PC berbasis LDR dan motor stepper. Jurnal Otomasi, Kontrol & Instrumentasi 7 (1): 37-52. DOI: 10.5614/joki.2015.7.1.5. [Indonesian]

Suwanmontr C, Kositanont C, Panich N. 2013. Carbon dioxide absorption of common trees in Chulalongkorn University. Modern Appl Sci 7 (3): 1-7. DOI: 10.5539/mas.v7n3p1.

Too CC, Keller A, Sickel W, Lee SM, Yule CM. 2018. Microbial community structure in a Malaysian tropical peat swamp forest: The influence of tree species and depth. Front Microbiol 9: 02859. DOI: 10.3389/fmicb.2018.02859.

Trisurat Y, Shrestha RP, Kjelgren R. 2011. Plant species vulnerability to climate change in Peninsular Thailand. Appl Geogr 31 (3): 1106-1114. DOI: 10.1016/j.apgeog.2011.02.007.

Wadanambi RT, Wandana LS, Chatumini KKGL, Dassanayake NP, Preethika DDP, Arachchige USPR. 2020. The effects of industrialization on climate change. J Res Technol Eng 1 (4): 86-94.

Wahidah MNL, Ahmad WFW, Nizam, Zain CRCM. 2017. Effects of elevated atmospheric CO_2 on photosynthesis, growth and biomass in *Shorea platycarpa* F. Heim (Meranti Paya). Sains Malays 46 (9): 1421-1428. DOI: 10.17576/jsm-2017-4609-10.

Yacob MNM. 2021. Estimating carbon sequestration of green roof plants in tropical climate. Intl J Integr Eng 13 3: 200-206. DOI: 10.30880/ijie.2021.13.03.024.

Yarn KF, Yu KC, Huang JM, Luo WJ, Wu PC. 2013. Utilizing a vertical garden to reduce indoor carbon dioxide in an indoor environment. Wulfenia 20 (10): 180-194.

Yunusa A, Linatoc AC. 2018. Inventory of vegetation and assessment of carbon storage capacity towards a low carbon campus: A case study of Universiti Tun Husein Onn Malaysia, Johor Malaysia. Path Sci 4 (12): 3001-3006. DOI: 10.22178/pos.41-3.

Zafriakma N, Masran MN, Ahmad DD, Nazli MW, Zakaria R, Karim MKA, Amaludin NA. 2020. Preliminary study on tree species composition, diversity and biomass of *Dipterocarpus* and *Hopea* genera of Bukit Bakar Forest Eco Park, Machang, Kelantan. IOP Conf Ser: Earth Environ Sci 549 (1): 012037. DOI: 10.1088/1755-1315/549/1/012037.

NUSANTARA BIOSCIENCE
Vol. 16, No. 2, pp. 192-200
November 2024

ISSN: 2087-3948
E-ISSN: 2087-3956
DOI: 10.13057/nusbiosci/n160205

Seed morphology and germination type of some species of dipterocarps

INDRIANI EKASARI[1,♥], LUSI OKTAVIANI[2]

[1]Seed Conservation Research Group, Research Centre for Plant Conservation Botanical Garden and Forestry, National Research and Innovation Agency. Kawasan Sains dan Teknologi Dr. (H.C.) Ir. Soekarno, Jl. Raya Jakarta-Bogor Km. 46, Cibinong, Bogor 16911, West Java, Indonesia.
Tel.: +62-21-87907604, ♥email: indriani.ekasari@brin.go.id; indriani.ekasari@gmail.com

[2]Department of Agrotechnology, Faculty of Agriculture, Universitas Sultan Ageng Tirtayasa. Jl. Raya Jakarta-Serang Km 4, Panancangan, Serang 42163, Banten, Indonesia

Manuscript received: 24 December 2023. Revision accepted: 4 June 2024.

Abstract. *Ekasari I, Oktaviani L. 2024. Seed morphology and germination type of some species of dipterocarps. Nusantara Bioscience 16: 192-200.* The dipterocarps seed conservation and effective seedling management of threatened plants required basic information on morphology and germination type to provide information on biological, ecological, and characteristics with taxonomic relevance. Seeds and seedlings characters can provide useful data in the delimitation and identification of species, including wings, sizes, shapes, germination type, and stages. The study aims to investigate the morphology and germination type of the seeds of some species of dipterocarps to contextualize and understand their ecological implications because the seed was the fundamental stage for the propagation and perpetuation of the species. This study was conducted for three months from seed collection, seed morphology measurement, seed sowing, and observation for germination type. The seeds from five species of dipterocarps (*Shorea selanica*, *S. pinanga*, *S. stenoptera*, *Hopea gregaria*, and *Vatica pauciflora*) were collected from the Forest Research and Development, Ministry of Forestry (FORDA), Dramaga, Bogor, Indonesia and they were brought to seed conservation laboratory in Bogor Botanical Gardens. The results showed six characters to describe each species seed (seed shape, the dimensions of longer wings, the dimensions of shorter wings, seed weight, seed length, and seed width). The *S. pinanga* showed the longest wings among others (152.25±9.93 mm), and *H. gregaria* showed the lightest weight (0.49±0.06 g). All species showed the same germination type (epigeal) with cotyledons that rise above ground. There were five stages of seed germination from radicle growth until cotyledon was removed or perfectly germinated for 90 days. The plantings and pathogens management were required to increase the Dipterocarpaceae seedlings' growth success. This finding was crucial for developing methods for seed conservation and tropical rainforest restoration.

Keywords: Dipterocarps, germination type, seed, seed conservation, seed morphology

INTRODUCTION

Tropical rainforests in Southeast Asia are suitable habitats for dipterocarp trees, and these tree canopies provide ecological services. This taxon comprises many tree species (approximately 500 species in Southeast Asia) closely related, but the growth has environmental stress tolerance (Aoyagi et al. 2013; Ediriweera et al. 2020; Kenzo et al. 2023). In recent decades, many of the dipterocarp species in this region have been threatened by logging and other human activities that have critically reduced the numbers of their individuals and populations. The main threat to the dipterocarp species were habitat conversion into pine (*Pinus merkusii*) and coffee (*Coffea canephora*) plantations and degradation due to timber and fuel wood harvesting (Zulkarnaen et al. 2023). Accordingly, the sustainable management of remnant dipterocarp populations has become increasingly important for their sustainable use and species conservation (Naito et al. 2008). Their prevalence and broad geographical distribution means that different species, or groups of species from the Dipterocarpaceae family, are well-adapted to cope with diverse climatic and disturbance regimes (Hamilton et al. 2019).

The heavier seeds performed better than lighter seeds at germination and seedling establishment in the same species; in particular, only seed mass significantly affected seedling establishment. Since the seed mass of selfed progeny is lighter overall than that of the outcrossed progeny, the failure to germinate or establish may be more likely among lighter, selfed seeds than heavier, outcrossed seeds (Naito et al. 2008). Morphological studies of this family have typically analyzed small sample numbers and/or are locally focused (Hamilton et al. 2019). In tropical rain forests, many species, often within the same genus, can be differentiated regarding dispersal strategies. The inherent ability of seeds to resist deterioration and decay is also crucial from an ecological perspective. Some plant species might conduct strategies by producing seeds with different depths of dormancy to maintain the species presence in soil seed banks and thereby contribute to ecological diversity and species persistence over extended periods (Rehmani et al. 2023).

Therefore, seed characteristics can provide useful species delimitation and identification data. The morphologic features of different seed structures provide a wide range of characters that can play an important role in the identification of taxa and have traditionally been used to solve systematic and phylogenetic problems (Gabr 2014). The seed features of the dipterocarps family include wings, sizes, and colors. Thus, the study of seeds provides biological and ecological information on the species and

characters with taxonomic relevance, and it offers eco-physiological information on the species; in this manner, the seed morpho-anatomical characteristics indicate the strategies of the species in response to a loss or increase of precipitation, and other factors (i.e. temperature); as a result, the findings of these studies can help establish which species are ecologically suited for planting in restoration (Montaño-Arias et al. 2022). Upon germination, the seed may normally grow, halt at various stages of development, or give rise to seedlings with abnormal morphology that fail to survive. Seed germination was a tightly regulated process ensuring that germination occurs under conditions that ultimately lead to the completion of the plant life cycle. As a result, seed or timber production companies must be able to create high-quality vigor seeds to produce high-quality timber as a final product. Therefore, commercial seed testing routines did not include abnormal seedlings in final germination percentages. These seedlings would likely fail, leading to discrepancies between percentage germination and viability (Rehmani et al. 2023). The study aims to investigate the morphology and germination type of the seeds of some species of dipterocarps to contextualize and understand their ecological implications because the seed was the fundamental stage for the propagation and perpetuation of the species.

MATERIALS AND METHODS

Study area

The study was carried out from September to December 2023 in Dramaga Experimental Forest of the Forest Research and Development Agency (S6º33'7" E106º45'11"), Ministry of Forestry and Environment, Indonesia for dipterocarps seed collection and Bogor Botanic Gardens Laboratory, for seed morphology and anatomy investigations and nursery for seed germination in West Jawa, Indonesia (Figure 1). Dramaga Experimental Forest's total area was about 60 ha, and the elevation was 244 m asl. Annual rainfall was about 350 mm, and the soil type was reddish latosol. The minimum temperature was 20.1°C and 30.1°C at the maximum.

Procedures

Seed sample and collection

Seed samples from stands of *Shorea selanica*, *S. pinanga*, *S. stenoptera*, *Hopea gregaria*, and *Vatica pauciflora* after natural dispersal in the Dramaga Experimental Forest were carefully chosen and randomly collected. The quantity of seeds produced by these five species varies; roughly 300 seeds were gathered for each species. From 20 to 25-year-old trees that were flourishing in the forest, about 2 kg of seeds were gathered. The collected seeds were placed in cloth bags to prevent heat and preserve freshness. The seeds were brought to the laboratory the same day for additional processing. After the seeds had dropped to the ground, a cutting test was done to determine how fresh the seeds were. The seeds selected were those with brownish fruit wings, and the fallen seeds were collected from the ground (Masano 1991). Then, the seeds were immediately taken to the laboratory and greenhouse for analysis

Seed morphology observation

This study analyzed the morphology of seeds from five species belonging to the dipterocarps family. Each species contains ten seeds, and the wings and the seed's length and width were photographed using a Galaxy Samsung 22 Ultra camera. At least 10 seeds for each species had their morphology measured. They were split longitudinally and transversely using a scalpel to determine their morphological characteristics and photographed using a Dino lite digital microscope MS35B.

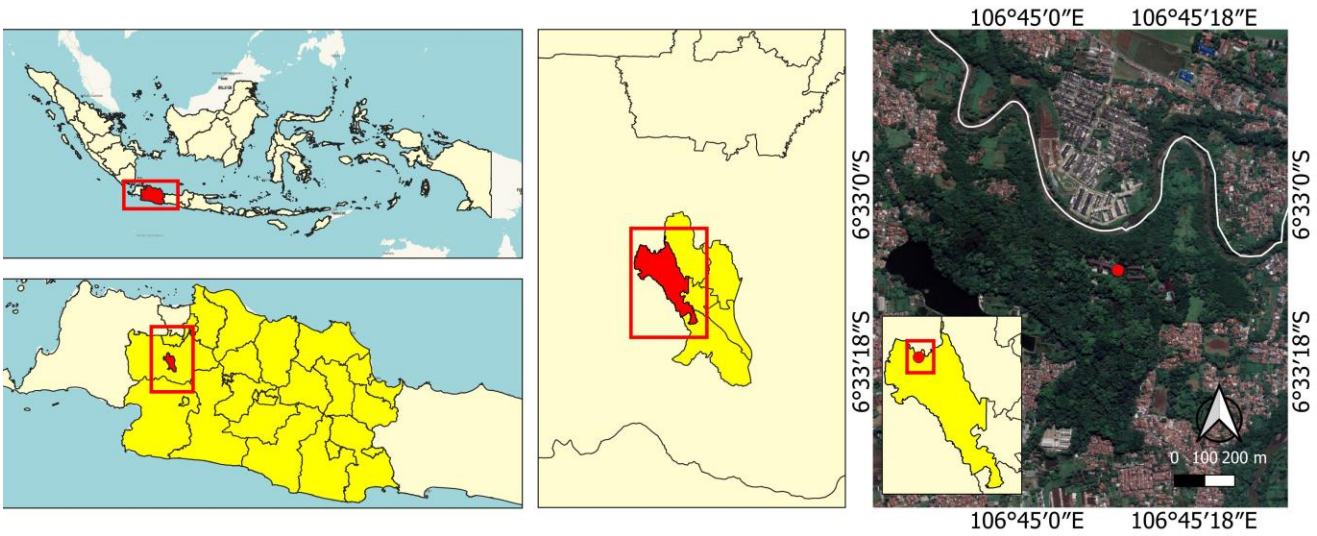

Figure 1. Study site in Dramaga Experimental Forest of the Forest Research and Development Agency, Bogor District, West Java, Indonesia

Germination types observation

Approximately 100 dipterocarp seeds were sown in the sand and germinated within 24 hours in the nursery after being collected from the field. The wings of each seed were removed before sowing. The seeds were selected to be as uniform as possible with large size and brown color, indicating the seeds maturity (Otsamo et al 1996); the already germinated seeds were excluded. The seeds in portray were watered every day, and the observations were conducted once a week.

Data analysis

The description analysis was applied based on observations and examined with a camera and a microscope. The obtained data were presented in tables and graphs, and the color brightness and fish blood profile data were analyzed descriptively.

RESULTS AND DISCUSSION

Seed morphology

The seeds morphological characteristics enable us to distinguish between some species of dipterocarps. The dipterocarps were characterized by their winged fruits or nuts with zero to five wings and were generally poorly dispersed by gravity or gyration. Secondary seed dispersal was unlikely to play a significant role in species dispersal as dipterocarp seeds are highly recalcitrant and germinate rapidly after reaching the forest floor (de Morais et al. 2015). In this study, species *S. selanica, S. pinanga, S. stenoptera, H. gregaria,* and *V. pauciflora* showed similar fruiting times, but *H. gregaria* was the first to fruiting. The mature fruits, indicating the dark reddish brown on the wings, were heavier than the immature ones. Ripe fruit was distinguished by color, weight, and the seeds' flawless form. Fruits of the *S. pinanga* and *S. stenoptera* species were asymmetrically shaped when they were young, but when they ripened, they became perfectly round and were comparatively larger than unripe fruits.

Examination of available specimens yielded a wealth of information concerning seed morphology and sculpture of seed surface. Variation in these aspects among the species is listed in Table 1 and recorded comparatively illustrated for individual species in Figure 2. In this study, six characteristics describe the seeds, they were seed shape, the dimensions of longer wings, the dimensions of shorter wings, seed weight, seed length, and seed width (Table 1). The results of seed shape were round with tapered ends (*S. selanica, S. pinanga*, and *S. stenoptera*), round (*H. gregaria*), and round with wavy curves (*V. pauciflora*). The seed shape would support an interesting pattern to be observed in the cotyledons during the germination process (Maharani et al. 2013). Species *S. selanica* showed the longest wing lengths among others. Furthermore, the seed weight of *S. selanica* was heavier than other species. Species *S. stenoptera* had the longest wing length (64.63±1.87 mm) and seed width (36.63±1.87 mm) than other species' seed lengths.

Three genera of *Shorea*, one genus of *Hopea*, and one genus of *Vatica* were observed in this study (Figure 2). The uniqueness of the *Shorea* spp. seed was the overlapping petals, clearly thickened in the middle and swollen at the base. Species *S. pinanga* and *S. stenoptera* were well-known as Tengkawang with large seeds. The seed shape of *S. pinanga is* usually ovate to round and relatively has the same size in length and width. The seed surface of *S. stenoptera* was short hairy. Species *S. selanica* seeds surface was glabrous, smooth, and punctuate, and they can be either opaque or shiny, but those of *S. pinanga* were dark reddish brown or yellowish red. The *S. stenoptera* seeds were black or reddish brown. The color was determined using Munsell soil color charts. The seed surface of both *S. pinanga* and *S. stenoptera* species showed fracture lines; however, in *S. selanica*, they gave an exfoliated appearance. Seeds coat surfaces in *S. stenoptera* were reticulate, and each space enclosed by the reticulation was densely rugose, while in *S. pinanga* only an irregularly rugose pattern was observed.

Species *H. gregaria* showed round with short same length wings, but species *V. pauciflora* showed an interesting curvy shape in their surface seed coat. The seed wings of *V. pauciflora* have the same length and almost disappeared. The seed surfaces in both species, *H. gregaria* and *V. pauciflora*, were glabrous, smooth, and opaque. The seed coat colors were dark brown, reddish brown, or black. It was also determined that the seeds of both species were hard since they were necessary to exert force to break the seed coats. Therefore, seed characters can provide useful data in the delimitation and identification of species. The morphologic features of different seed structures provide a wide range of characteristics that are important in identifying taxa and have traditionally been used to solve systematic and phylogenetic problems (Gabr 2014).

Table 1. Mean characters of *Shorea selanica, S. pinanga, S. stenoptera, Hopea gregoria* and *Vatica pauciflora*

Characters	*Shorea selanica*	*Shorea pinanga*	*Shorea stenoptera*	*Hopea gregaria*	*Vatica pauciflora*
Seed shape	Round with tapered ends	Round with tapered ends	Round with tapered ends	Round	Round with wavy curves
Longer wing length (mm)	73.01±7.97	152.25±9.93	101.15±7.44	4.83±0.68	2.84±0.39
Shorter wing length (mm)	40.54±5.51	96.9±10.29	79.26±7.15		
Seed weight (g)	0.88±0.09	20.88±0.08	17.89±3.43	0.49±0.06	6.06±1.65
Seed length (mm)	19.11±0.83	43.15±3.58	64.63±1.87	12.86±1.29	24.71±2.05
Seed width (mm)	10.56±0.39	25.36±1.15	36.63±1.87	8.85±0.44	23.78±2.81

Note: Wings of *Hopea gregoria* and *Vatica pauciflora* seeds have the same length (no longer and no shorter)

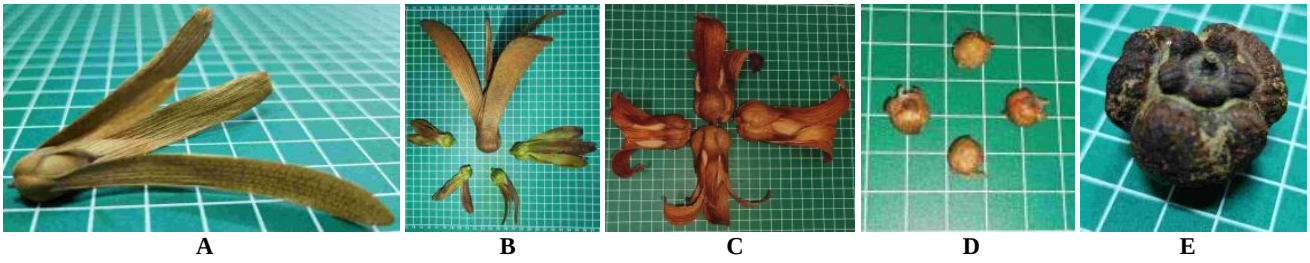

Figure 2. Seed shape of five species of dipterocarps. A. Round with tapered ends for *Shorea selanica*, B. Round with tapered ends for *Shorea pinanga*, C. Round with tapered ends for *Shorea stenoptera*, D. Round for *Hopea gregaria*, E. Round with wavy curves for *Vatica pauciflora*

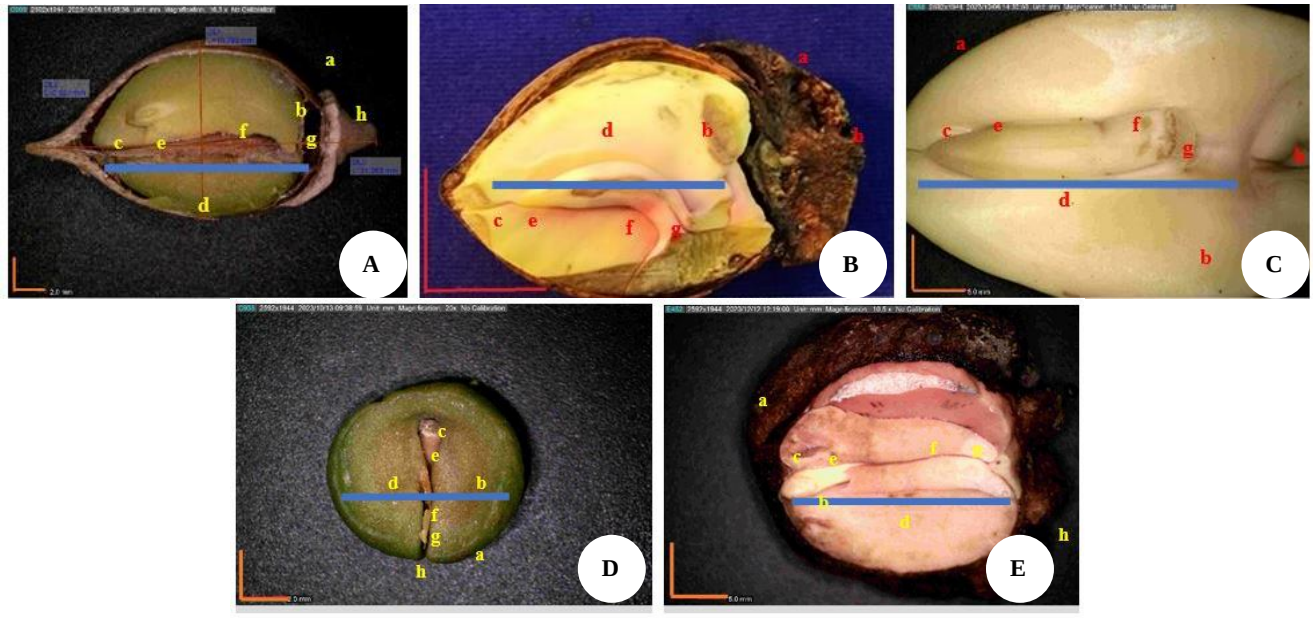

Figure 3. Seed transversely morphology of five species of dipterocarps A. *Shorea selanica*, B. *Shorea pinanga*, C. *Shorea stenoptera*, D. *Hopea gregaria*, E. *Vatica pauciflora*. Note: a. Testa; b. Cotyledon; c. Radicle; d. Embryo; e. Hypocotyl; f. Epicotyl; g. Plumule; h. Hilum. Scale: 1:2.0 mm (*S. selanica*, *S. pinanga*, and *H. gregaria*). Scale: 1:5.0 mm (*Shorea stenoptera* and *Vatica pauciflora*).

Dipterocarps seeds were dicotyledonous and share many morphological features with other dicotyledonous species. Their external anatomy consists of an aril attached around the hilum, but there was no visible lens or micropyle on any of the seed samples investigated. However, it was possible that the micropyle could be observed at greater magnifications or that it existed beneath the cuticle layer and was thus hidden from view. The seed morphology was investigated using light microscopy and was found to consist of a seed coat layer and a substantial endosperm surrounding the unattached embryo. The hilum was a scar that remains on the seed at the point where the funiculus attaches to the body of the ovule, connecting the ovule to the placenta (Koen et al. 2017). The pointier side of the seed, rather than the hilum side, is where the root or radicle emerges in all seeds belonging to the dipterocarp species. The hilar slit (or hilar fissure) serves as a natural opening for water and gas exchange for many species, and so do for these five dipterocarps seeds. The seed coat or testa was the protective outer covering of a mature seed. The seed coat consists of layers called integuments that develop from maternal tissue (sacs of the ovule) and are, therefore, determined by maternal genotype. The seed coat protects the seed parts' integrity against injury by mechanical damage and/or attack by pests and disease. The seed coat also modulated seed–environment relationships, regulating gaseous exchange and imbibition.

The embryo includes the region proximal to the cotyledon and extends to the region occupied by the embryonic axis (Figures 3 and 4). The cotyledon shapes were very similar in these five species of dipterocarps since they were constituted by a sheath, varying from fleshy to foliaceous. Five species had auriculate cotyledons. The cotyledon is attached to the seed coat of the seeds. Like dicotyl seed, plumules, and radicles were not covered in dipterocarp seed. Every seed's embryonic axis was straight. In this study, *S. stenoptera* and *S. pinanga* seeds had longer radicle sizes than other dipterocarps seeds; this was directly correlated with the size of their seeds. On the epicotyls, there was no growth of leaf primordia or plumules. The pointier side of the seed emerges, rather than the hilum side, where the root or radicle emerges in all seeds

belonging to the dipterocarp species. While the study's seed species were compared, no discernible changes in their morphological structures were discovered. Examining the cellular structure of the seeds could explain variations in their form. These variations might be biological; however, this study provided an overview and did not explore these possibilities.

Germination types

All dipterocarps seeds were germinated under the paranet (55%) with a microclimate state at an average daily temperature of 33.8°C, 48.9% relative humidity of 48.9%, the light intensity of 11,186.67 lux, and wind speed of 0.87 m/sec. Following germination, seedlings' development, morphology, and seedlings' growth habits were important characteristics to study. Some characteristics often used to study the morphology of seedlings of woody plant species are the emergence of seedlings, the position and development of the cotyledons, and the function of the cotyledons (Handayani 2017). Therefore, for each species under investigation, the seeds employed in this study were comparatively similar in size and weight. According to Rachman and Sunaryo (1999), this was because larger seeds will germinate more quickly than smaller ones. The protrusion of the growing radicle to create the primary root and the base of the cotyledonary sheath signals the onset of germination in representatives of *Shorea*, *Hopea*, and *Vatica*. Plant reproductive success was determined by seedling development patterns, including structures adapted to environmental circumstances, access to seed reserves, and germination control factors (Silva et al 2014). In this study, five seeds of dipterocarps showed an epigeal pattern of seed germination types (Figure 5). A previous study showed that seed germination of *Hopea ponga* in the Dipterocarpaceae family occurs in epigeal (Muralikrishna and Chandrashekar 1997).

All seeds are germinated without any treatment, meaning that after the seeds are collected from the field, the seeds are spread in a sowing tank to germinate (Figures 5 and 6). This study was conducted for approximately 90 days, starting from collecting seeds, spreading seeds, and observing seed germination until the growth of leaves and the shedding of the cotyledon from the stems of dipterocarps seedlings. In the germination, this study described six stages with at least one or more stages of growth and development that can be observed and followed, namely:

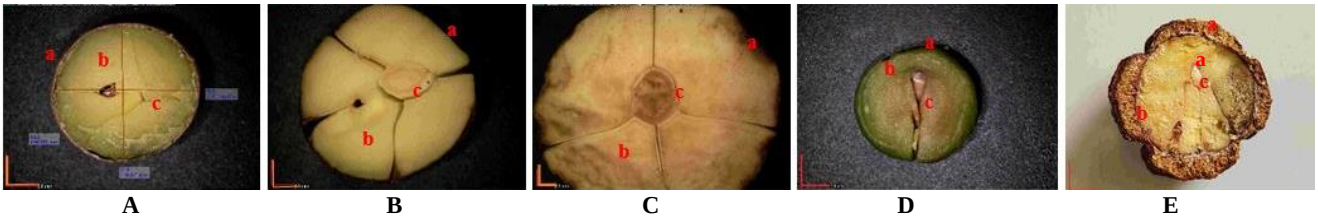

Figure 4. Seed longitudinally morphology of five species of dipterocarps. A. *Shorea selanica*, B. *Shorea pinanga*, C. *Shorea stenoptera*, D. *Hopea gregaria*, E. *Vatica pauciflora*. Note: a. Testa; b. Cotyledon; c. Embryo. Scale: 1:2.0 mm

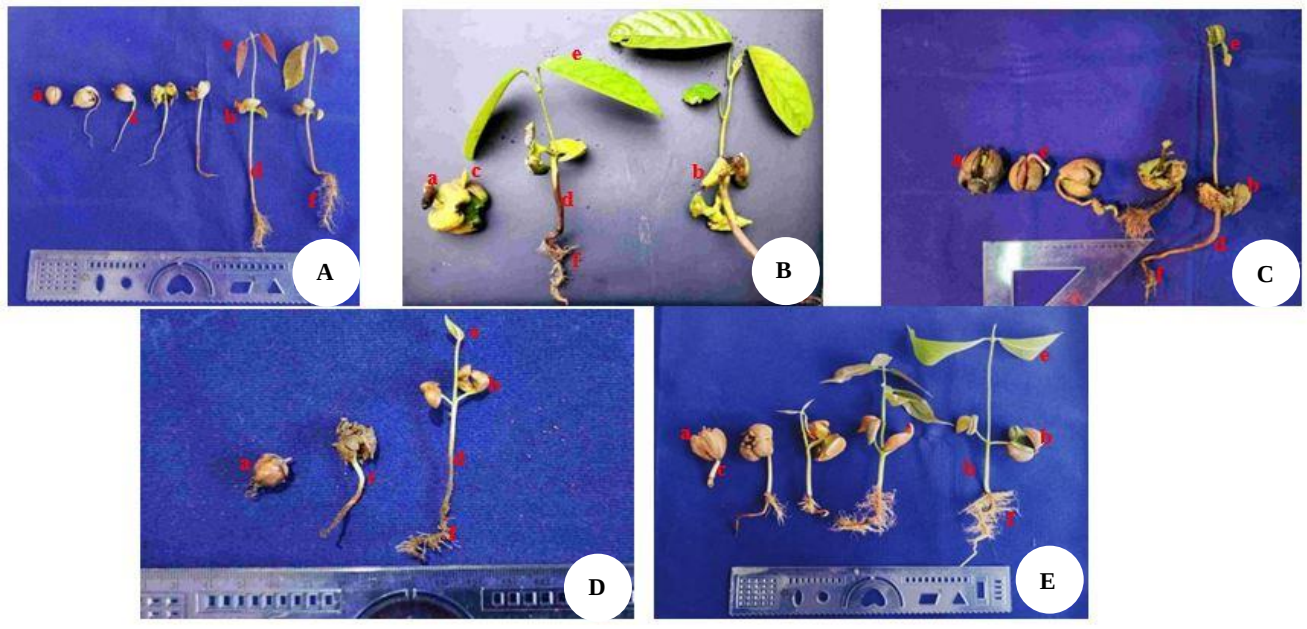

Figure 5. Germination stages of five species of dipterocarps. A. *Shorea selanica*, B. *Shorea pinanga*, C. *Shorea stenoptera*, D. *Hopea gregaria*, E. *Vatica pauciflora*. Note: a. Testa seed coat; b. Cotyledon; c. Radicle; d. Hypocotyl; e. Epicotyl (first leaf); f. Root

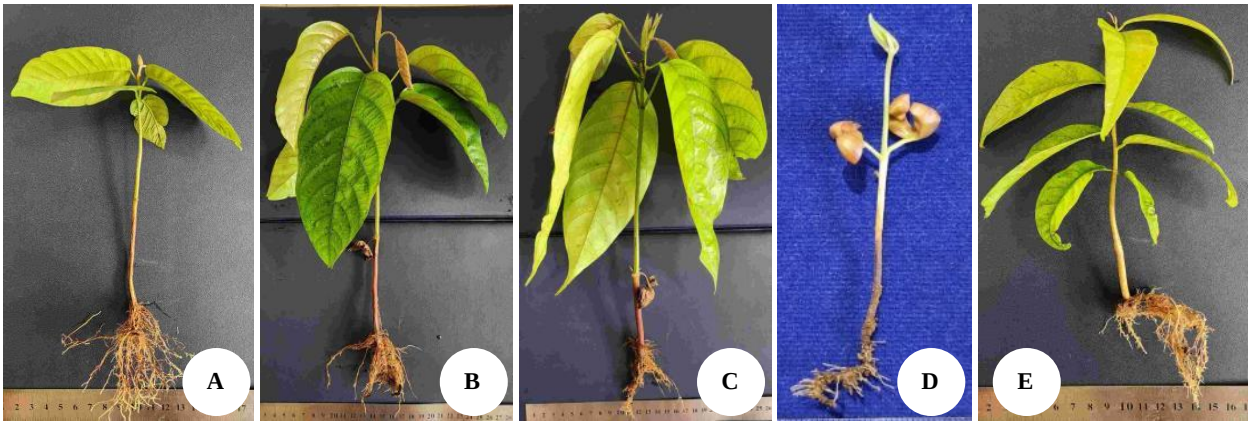

Figure 6. The final stages of five species of dipterocarps. A. *Shorea selanica*, B. *Shorea pinanga*, C. *Shorea stenoptera*, D. *Hopea gregaria*, E. *Vatica pauciflora*

(1) The first stage was the radicle growth stage. There were the initial steps within 14 days for *S. selanica*, *H. gregaria*, and *V. pauciflora* and within 35 days for *S. stenoptera* and *S. pinanga*. The emerged radicles, pale pinkish, which initially grew vertically upwards, turned positively geotrophic the next day. It continues with the growth of additional roots around the main root.

(2) The second stage was the primary root growth stage. It showed that the emergence of the hypocotyl followed root sprouting. The process of photosynthetic assimilation starts at this point. A green color, assumed a chlorophyll, with increasing concentration appears on the entire cotyledon stalk, except the section nearest the major root, and indicates that the primary roots start to actively transport nutrients from the soil to aid in the assimilation process. A yellowish hypocotyl stem emerges with continued growth and extends through the cotyledon, gradually growing longitudinally to form an arch under the ground. The hypocotyl stem grew longer and longer until, at last, both the tip of the stem and the seed pod were above the soil in the next 7-12 days after the first stage for all dipterocarps seeds.

(3) The third stage was the opening process of the cotyledon bulb. The cotyledon bulbs fully split into two equal sections in dipterocarp seeds. The cotyledon bulbs were opened as the epicotyl emerged from the surface towards sunlight. The growths of the hypocotyl, which penetrates the soil, were directly correlated with the epicotyl's rise to the above ground in the next 14 days after the complete second stage for all dipterocarps seeds.

(4) The fourth stage was the epicotyl growth stage. The first leaves began to grow with yellowish-to-green-colored, slowly growing shoots with pointy tips emerging at the tip of the epicotyl stem. The shoot enlarges until it breaks into two sections, eventually giving rise to the first two opposing leaves. The initial leaf was shaped somewhat like an adult leaf but with a slight roundness in the next 10-14 days after the third stage for all dipterocarps seeds was completed.

(5) The fifth stage was the cotyledon removal from dipterocarps seedlings. When the first leaf fully emerges, the cotyledons stay in place, and when the second leaf starts to develop, they decompose. The cotyledons' color changes from green to brown to black, and eventually, they break off on their own, signifying the process of cotyledon shedding. This demonstrates that within 10 to 15 days following the completion of the fourth stage, the seeds have perfectly germinated.

Discussion

These findings generally encouraged using dipterocarps species in restoration, provided that the species' geographic distribution ranges were maintained. The morphology and seed germination type of the five dipterocarps examined here unequivocally demonstrate that the seeds embody every distinguishing trait that three genera (*Shorea*, *Hopea*, and *Vatica*) share. Distinct morphological features that were only developed in three genera of dipterocarps were observed in their wings. The longer wings of the *Shorea* seeds under investigation possessed structural similarities to those of Hopea and *Vatica*. The two additional *Shorea* species, Tengkawang, *S. stenoptera*, and *S. pinanga*, had shorter wings than *S. selanica* (*Meranti*). In addition to being known to aid in seed dissemination, wings were a component of dipterocarps seeds. Moreover, an ecological report was regarding the clumped formations of *S. pinanga* in recently exploited open areas, which were thought to be the result of wind-dispersed seeds (Muralikrishna and Chandrashekar 1997; Smith et all 2015). Based on seed morphological data, only the wings length arguments were found to separate *Shorea* spp. from other genera of dipterocarps.

Therefore, to investigate the methods by which dipterocarps seeds adapt to their environment and the relationship between dormancy and recalcitrance in terms of reproductive success, this study examined the structural characteristics of the seeds. Comprehending the germination and seedling growth ecology is crucial for developing methods for seed conservation and tropical rainforest restoration, in addition to providing insights into plant community processes and succession. It was possible to apply knowledge of how dipterocarps germinate in

nature to industrial forest and agroforestry plantings. Human activity was not the only cause of decreased dipterocarps seed development behavior factors (Primananda et al. 2023), but also, irregular flowering patterns may have occurred due to El Niño in 2023. The other causes of seed resistance were short-lived viability (recalcitrant seeds) and seed predators (post-dispersal predation and pre-dispersal predation). Additionally, after escaping seed predation and successfully germinating, seedlings must survive or resist pathogens, herbivory, and mechanical damage, limiting their growth and development (Chong et al. 2016).

Figure 5 illustrates how pathogen infections cause the cotyledons of *S. pinanga* seedlings to decay more quickly in the early development stages, disrupting the seedlings' normal development. A previous study revealed that dipterocarp seedlings are dying at a rate that is rising annually in their natural habitat (Ediriweera et al. 2020). Supposing this species was perpetuated and protected, more pathogens management is required to increase the success of the plantation. When planted in a shallow media, the roots of the *S. stenoptera* species also fold easily. Treatment for this kind of root growth involves maintaining the planting media loose and ensuring the soil is not compacted, particularly when propagating in nurseries. Furthermore, a loose, porous medium was easily penetrated by roots growing from the seed and this kind of media had enough pores for water and air to circulate. A planting media that is too dense will make it difficult for roots to penetrate and cause water stagnation so that the conditions become too humid and the seedlings become decayed (Susanto et al. 2016). Although potrays can be used in nurseries to encourage root growth, it is more advisable to utilize square-shaped containers as they are more effective than round-shaped ones (Rachmat et al. 2018). Dipterocarpaceae, including *S. stenoptera*, had limited seed viability, which raises concerns about forest regeneration in their natural habitat. This was frequently followed by significant levels of vertebrate predation after the seeds fell to the ground or before they disseminated. This, in turn, can differ between forests with different levels of disturbance (Blackham et al. 2013). There may also be interactions between the various stages from seed to seedling establishment; previous processes depend on positive density in avoiding seed predation by insects or vertebrates or attack by herbivores or fungi (Chong et al. 2016).

Moreover, to understand how the adaptive mechanisms of mass flowering can be disrupted by human disturbance, we must study each step of the related process, from seed morphology to seedling establishment. Seeds of certain species damaged by drying below critical levels cannot be stored for long periods (Molina et al. 2017) and are called recalcitrant seeds. The findings of this study showed that the dipterocarp seeds germinated in 14–30 days, allowing them to be classified as recalcitrant seeds. More preservation must be conducted to keep seeds viable, especially for some species with no yearly fruiting. The reason for the complicated loss of viability is the sequential loss of water content that damages the cells with loss of semipermeable character, as evidenced by leaches, and it is thought that the damage to the membrane cannot be repaired by further hydration. Dipterocarps seeds produced in humid environments are usually stubborn because they are not resistant to dehydration and low temperatures, causing loss of viability during storage. Recalcitrant is associated with certain structural and physiological characteristics associated with short dormancy (Silva et al. 2014). Excessive moisture in planting media in the nursery also should be avoided since this can lead to root rot. There was an obvious interaction between the media and methods of breaking seed dormancy at the initial seedling height (Rivai et al. 2015).

Furthermore, very little information is available regarding the eco-physiological aspects of dipterocarps, such as detailed descriptions and no detailed study on the germination process of recalcitrant seeds. The association between dormancy and recalcitrance is crucial to the reproductive success of dipterocarps seeds. Dormancy is an adaptive characteristic of great importance in many species, as it spreads germination over time, making germination under many environmental conditions favourable to seedling establishment more probable, diminishes competition between seedlings, and even contributes to forming a seed bank. As dipterocarps have seasonably variable fruiting, occur in constantly humid environments, and produce recalcitrant seeds with low potential for seed bank formation, it is possible to propose that short dormancy in these species takes on a different but equally relevant role, favouring species dispersal by rapid germination. These study findings can be applied to promote the implementation of dipterocarp restoration in low-impact logging systems and the sustainable and extended growth of high-conservation value forests. Nevertheless, even previous studies mentioned the distance from tourist attractions of at least 50 m must closed to avoid a massive landslide in the dipterocarps restoration location (Fambayun et al. 2020). Policymakers should prioritize the conservation gaps found in this study when creating new protected areas to fulfil the 2030 target. This includes lowland areas of in-situ conservation areas that are preferable for dipterocarps, as earlier studies have shown (Luo et al. 2022). It should be highlighted that the distribution patterns of dipterocarp species are clustered in their natural habitat (Irni 2022). Therefore, it is important to ensure that dipterocarp seed collection occurs closely to the mother tree and that restoration efforts match the distribution patterns found in their native habitat.

Regarding the germination type, the species analyzed in this study have epigeal germination, with cotyledons that rise above the ground. Cotyledons are the first leaves that appear on a plant, playing an important role in seedling development, especially in the early stages. Cotyledons can serve as a food store and/or photosynthetic organs (Handayani 2017). The hypocotyl was long in size in the species analyzed, and the cotyledonary sheath's presence caused the seed elevation. Consequently, it is partially above and, at the same time, partially below the soil. This author suggests that these terms should be used to frame the plant regarding the position of the seed concerning the

soil, in which the term epigeal is used for plants that have seeds above ground, and hypogeal is for seeds that remain below ground; this study used the term epigeal since the seed is elevated through the cotyledonary sheath. The final germination rate was observed when no more seeds germinated three months after planting.

In conclusion, this study showed three winged seeds (*S. selanica*, *S. pinanga*, and *S. stenoptera*) and two winged-less seeds (*H. gregaria* and *V. pauciflora*). Species *S. pinanga* had the longest wings (152.25±9.93 mm) among the five species, while species *V. pauciflora* showed the shortest wings (2.84±0.39 mm). Species *H. gregaria* had the first fruiting time, followed by others, and it had the lightest weight (0.49±0.06 g). Dipterocarps seeds were dicotyledonous and contained the complete and easy-to-identify seed parts (testa, cotyledon, radicle, hypocotyl, epicotyl, plumule, and hilum). It takes around 90 days for all dipterocarps seeds to reach the final stage of germination, indicated by the cotyledons falling off the epicotyl stem. Further research is required to determine the function of wings in dipterocarps seeds for germination, as well as the seeds' resistance to mechanical harm after falling to the ground.

ACKNOWLEDGEMENTS

We thank the Ministry of Environment and Forestry, Indonesia, for providing every necessary support for the field study in Dramaga Research Forest, Bogor, Indonesia. Thanks to Dr. Andes Hamuraby Rozak (National Research and Innovation Agency), and Dr. Wening Sri Wulandari (Ministry of Environment and Forestry) for their permission and support during our research. Rinto Nurman and Sugianto for their kindness during field investigations.

REFERENCES

Aoyagi R, Imai N, Kitayama K. 2013. Ecological significance of the patches dominated by pioneer trees for the regeneration of dipterocarps in a Bornean logged-over secondary forest. For Ecol Manag 289: 378-384. DOI: 10.1016/j.foreco.2012.10.037.

Blackham GV, Thomas A, Webb EL, Corlett RT. 2013. Seed rain into a degraded tropical peatland in Central Kalimantan, Indonesia. Biol Conserv 167: 215-223. DOI: 10.1016/j.biocon.2013.08.015.

Chong KY, Chong R, Tan LWA, Yee ATK, Chua MAH, Wong KM, Tan HTW. 2016. Seed production and survival of four dipterocarp species in degraded forests in Singapore. Plant Ecol Divers 9(5-6): 483-490. DOI: 10.1080/17550874.2016.1266404.

de Morais CT, Ghazoul J, Maycock CR, Bagchi R, Burslem DRFP, Khoo E, Itoh A, Nanami S, Matsuyama S, Finger A, Ismail SA, Kettle CJ. 2015. Understanding local patterns of genetic diversity in dipterocarps using a multi-site, multi-species approach: Implications for forest management and restoration. For Ecol Manag 356: 153-165. DOI: 10.1016/j.foreco.2015.07.023.

Ediriweera S, Bandara C, Woodbury DJ, Mi X, Gunatilleke IAUN, Gunatilleke CVS, Ashton MS. 2020. Changes in tree structure, composition, and diversity of a mixed-dipterocarp rainforest over a 40-year period. For Ecol Manag 458: 117764. DOI: 10.1016/j.foreco.2019.117764.

Fambayun RA, Kalima T, Rachmat HH. 2020. Species diversity and threats on the habitat of *Vatica javanica* in the Ciangir Forest, Indonesia. IOP Conf Ser: Earth Environ Sci 533 (1): 012013. DOI: 10.1088/1755-1315/533/1/012013.

Gabr DG. 2014. Seed morphology and seed coat anatomy of some species of Apocynaceae and Asclepiadaceae. Ann Agric Sci 59 (2): 229-238. DOI: 10.1016/j.aoas.2014.11.010.

Hamilton R, Hall T, Stevenson J, Penny D. 2019. Distinguishing the pollen of Dipterocarpaceae from the seasonally dry and moist tropics of Southeast Asia using light microscopy. Rev Palaeobot Palynol 263: 117-133. DOI: 10.1016/j.revpalbo.2019.01.012.

Handayani T. 2017. Seed germination and seedling morphology of *Artabotrys hexapetalus*. Nusantara Biosci 9 (1): 23-30. DOI: 10.13057/nusbiosci/n090105.

Irni J. 2022. Analisis pola sebaran spasial beberapa jenis pohon di Hutan Penelitian Dramaga. Agrotristek 1 (1): 18-27. [Indonesian]

Kenzo T, Ichie T, Norichika Y. Kamiya K, Inoue Y, Ngo KM, Lum SKY. 2023. Drought tolerance in dipterocarp species improved through interspecific hybridization in a tropical rainforest. For Ecol Manag 548: 121388. DOI: 10.1016/j.foreco.2023.121388.

Koen J, Slabbert MM, Bester C, Bierman F. 2017. Germination characteristics of dimorphic honeybush (*Cyclopia* spp.) seed. S Afr J Bot 110: 68-74. DOI: 10.1016/j.sajb.2016.03.006.

Luo W, Strijk JS, Barstow M, Wee AKS. 2022. The role of protected areas in tropical tree conservation post-2020: A case study using threatened Dipterocarpaceae. Biol Conserv 272: 109634. DOI: 10.1016/j.biocon.2022.109634.

Maharani R, Handayani P, Hardjana AK. 2013. Panduan identifikasi jenis pohon tengkawang (Sidiyasa, K.). Balai Besar Penelitian Dipterokarpa, Balai Penelitian dan Pengembangan Kehutanan, Departemen Kehutanan bekerjasama dengan ITTO Project PD 586/10 Rev.1(F). [Indonesian]

Masano. 1991. Planting trial of *Shorea johorensis* with strips of different width at Haurbentes Experimental Garden, West Java. Buletin Penelitian Hutan 540: 25-33.

Molina JR, Moreno N, Moreno R. 2017. Influence of fire regime on forest structure and restoration of a native forest type in the southern Andean Range. Ecol Eng 102: 390-396. DOI: 10.1016/j.ecoleng.2017.02.059.

Montaño-Arias SA, Camargo-Ricalde SL, Grether R, Díaz-Pontones D. 2022. Seed morphology, anatomy and histochemistry in two Mexican species of Mimosa (Leguminosae, mimosoid clade). Flora 286: 151970. DOI: 10.1016/j.flora.2021.151970.

Muralikrishna H, Chandrashekar KR. 1997. Regeneration of *Hopea ponga*: influence of wing loading and viability of seeds. J Trop For Sci 10(1): 58-65.

Naito Y, Kanzaki M, Iwata H, Obayashi K, Lee SL, Muhammad N, Okuda T, Tsumura Y. 2008. Density-dependent selfing and its effects on seed performance in a tropical canopy tree species, *Shorea acuminata* (Dipterocarpaceae). For Ecol Manag 256 (3): 375-383. DOI: 10.1016/j.foreco.2008.04.031.

Otsamo R, Adjers G, Kuusipalo J, Otsamo A, Susilo N, Tuomela K. 1996. Effect of nursery practices on seed germination of selected dipterocarps species. J Trop For Sci 9 (1): 23-34.

Primananda E, Sunardi, Fefirenta AD, Rahmawati K, Mira FR, Budi SW, Robiansyah I. 2023. Survey for threatened plants in riparian fragmented forests: A case study on three Vatica (Dipterocarpaceae) species in Kapuas Hulu, West Kalimantan. J Nat Conserv 72: 126367. DOI: 10.1016/j.jnc.2023.126367.

Rachman E, Sunaryo S. 1999. Karakter morfologi dan perkecambahan biji *Strombosia javanica* Bl. (Olacaceae) dalam kaitannya dengan sifat-sifat parasitisme. Berita Biologi 4 (5): 235-240. [Indonesian]

Rachmat HH, Subiakto A, Susilowati A. 2018. Mass vegetative propagation of rare and endangered tree species of Indonesia by shoot cuttings by KOFFCO method and effect of container type on nursery storage of rooted cuttings. Biodiversitas 19 (6): 2353-2358. DOI: 10.13057/biodiv/d190645.

Rehmani MS, Xian BS, Wei S, He J, Feng Z, Huang H, Shu K. 2023. Seedling establishment: The neglected trait in the seed longevity field. Plant Physiol Biochem 200: 107765. DOI: 10.1016/j.plaphy.2023.107765.

Rivai RR, Wardani FF, Devi MG. 2015. Germination and breaking seed dormancy of *Alpinia malaccensis*. Nusantara Biosci 7 (2): 67-72. DOI: 10.13057/nusbiosci/n070202.

Silva RS, Ribeiro LM, Mercadante-Simões MO, Nunes YRF, Lopes PSN. 2014. Seed structure and germination in buriti (*Mauritia flexuosa*), the swamp palm. Flora 209 (11): 674-685. DOI: 10.1016/j.flora.2014.08.012.

Smith JR, Bagchi R, Ellens J, Kettle CJ, Burslem DFRP, Maycock CR, Khoo E, Ghazoul J. 2015. Predicting dispersal of auto-gyrating fruit

in tropical trees: A case study from the Dipterocarpaceae. Ecol Evol 5 (9): 1794-1801. DOI: 10.1002/ece3.1469.

Susanto D, Ruchiyat D, Sutisna M, Amirta R. 2016. Flowering, fruiting, seed germination and seedling growth of *Macaranga gigantea*. Biodiversitas 17 (1): 192-199. DOI: 10.13057/biodiv/d170128.

Zulkarnaen RN, Helmanto H, Primananda E, Kusuma YWC, Robiansyah I. 2023. Population status and conservation of the threatened and endemic tree *Vatica javanica* subsp. *javanica* (Dipterocarpaceae). J Asia-Pac Biodivers 16(4): 653-657. DOI: 10.1016/j.japb.2023.08.008.

NUSANTARA BIOSCIENCE
Vol. 16, No. 2, pp. 201-209
November 2024

ISSN: 2087-3948
E-ISSN: 2087-3956
DOI: 10.13057/nusbiosci/n160206

Optimization design of tetra-primer ARMS-PCR using SNP lectin gene and in silico characterization of lectin protein in rodent tuber (*Typhonium flagelliforme*) mutant of Bogor accessions

NESTI F. SIANIPAR[1,2,♥], ZIDNI MUFLIKHATI[3], KHOIRUNNISA ASSIDQI[1,2]

[1]Department of Biotechnology, Faculty of Engineering, Universitas Bina Nusantara. Jl. K. H. Syahdan No. 9, Kemanggisan, Palmerah, Jakarta 11480, Indonesia. Tel.: +62-21-534-5830, ♥email: nsianipar@binus.edu

[2]Food Biotechnology Research Center, Universitas Bina Nusantara. Jl. K. H. Syahdan No. 9, Kemanggisan, Palmerah, Jakarta 11480, Indonesia

[3] Program of Biotechnology, Graduate School, Universitas Padjadjaran. Jl. Dipati Ukur No.35, Bandung 40132, Indonesia

Manuscript received: 26 February 2024. Revision accepted: 5 June 2024.

Abstract. *Sianipar NF, Muflikhati Z, Assidqi K. 2024. Optimization design of tetra-primer ARMS-PCR using SNP lectin gene and in silico characterization of lectin protein in rodent tuber (*Typhonium flagelliforme*) mutant* of Bogor accessions. *Nusantara Bioscience 16: 201-209.* Rodent tuber plant (*Typhonium flagelliforme* (G.Lodd.) Blume) contains several anticancer compounds. Mutant plants have a higher cytotoxic effect than wild-type plants. This study aimed to devise a tetra-primer ARMS PCR using lectin gene SNPs to differentiate *T. flagelliforme* mutants and wild-type of Bogor accessions. A protein modeling study was also conducted to investigate the impact of point mutations on the structure of protein. The tetra-primer ARMS design and in silico protein modeling analysis were based on mutation points from previously sequenced lectin genes. A pair of primers was successfully designed using the missense mutation type specific to the SNP site that causes amino acid variation. The ARMS lec183 tetra-primer focuses on a 183 bp mutation in the lectin gene that converts threonine to arginine to provide a successful lec183 primer. The ARMS lec183 primer pair did not differentiate *T. flagelliforme* mutant plants from wild-type of Bogor accessions. The tetra-primer ARMS lec183 could be amplified successfully in all *T. flagelliforme* samples at a size of 278 bp outer primer and 193 bp inner primer, as determined by primer size. In the mutant protein structure, the 183 bp mutation results in amino acid changes that closely match those in wild-type proteins.

Keywords: In silico lectin protein, lectin gene, specific primer design, tetra-primer ARMS PCR, *Typhonium flagelliforme*

Abbreviation: ARMS: Amplification Refractory Mutation System, SNPs: Single Nucleotide Polymorphisms

INTRODUCTION

The rodent tuber plant (*Typhonium flagelliforme* (G.Lodd.) Blume) contains anticancer compounds among the Indonesian herbs. The gamma irradiation of plants has been biotechnology studied to produce mutant plants (Sianipar et al. 2017). A *T. flagelliforme* mutant plant contains higher levels of anticancer compounds, such as palmitic acid, sitosterol, and stigmasterol than the wild-type plant (Sianipar et al. 2021, 2022). Sianipar et al. (2021) reported that stigmasterol from *T. flagelliforme* mutant plants has an IC_{50} value of 0.1623 M, which means it inhibits the proliferation of MCF-7 cancer cells. The Indonesian Ministry of Agriculture granted Plant Variety Protection to two stable mutants of these plants in 2020 (Sianipar et al. 2020b). Specific molecular markers are still being identified to distinguish *T. flagelliforme* mutant plants from wild-type ones (Sianipar et al. 2023).

The plant cell wall contains carbohydrates recognized by lectins (Petrova et al. 2021) and several proteins have a LecRLK architecture, forming LecRLK-type receptor-like kinases with kinases and transmembrane domains (Bellande et al. 2017). Proteins without kinase domains are LecRLPs, while soluble proteins without kinase and transmembrane domains are LecPs. Sianipar et al. (2015, 2016, 2020a) and Sianipar and Purnamaningsih (2018) demonstrate that gamma irradiation can produce superior *T. flagelliforme* mutant plants with higher cytotoxicity than the wild-type (control). There is an increase in stigmasterol content in *T. flagelliforme* mutant plants with the development of lectin genes linked to increased anticancer compounds. At a dosage of 20 g/mL, the compound inhibits the proliferation of uterine cancer cells by 50% (Alfarabi et al. 2015). These findings can be a basic reference to explain lectin gene function in superior *T. flagelliforme* mutant of Bogor accession.

Single Nucleotide Polymorphisms (SNPs) are highly polymorphic and can identify diversity with just one base variation (Islam et al. 2015). A unique SNP marker developed was the tetra-primer Amplification Refractory Mutation System (ARMS). The tetra-primer ARMS-PCR method is a high-efficiency, fast, and economical technique to find mutations or SNPs in a genome (Ye et al. 2001). ARMS-PCR uses tetra-primer primers containing a 3' end at the polymorphism and an additional variance at -2 bp to the 3' end of the primer. This design promotes greater amplification and reduces false positive results due to mismatch the primers (Garcés-Claver et al. 2007).

The ARMS-PCR method has been successfully used to *Schisandra chinensis* (Turcz.) Baill. (Kim et al. 2012) and

sweet potato (Meng et al. 2017). It is possible to generate mutant and wild-type alleles simultaneously with ARMS-PCR by using two sets of primers in single PCR tube. several studies have been conducted using internal DNA controls to investigate various mutations, such as Hou et al. (2013), Wang et al. (2014), Cai et al. (2019), and Park et al. 2020). Ye et al. (1992) developed tetra-primer PCR using four primers (two outer and two inner primers) for allele-specific amplification. Tetra-primer ARMS-PCR was created by merging this technique with ARMS in 2001. Regardless of gene genotype, outer primers significantly amplify target genes in one reaction step.

Sianipar et al. (2022) reported a sequence for lectin gene with a base length of about 500 bp in mutant and wild-type *T. flagelliforme* plants show numerous mutation points. The structure of proteins can be altered by point mutations that change amino acids (Kimball and Jefferson 2006). The tetra-primer ARMS analyzes sequence diversity through the gene point mutations, and successful ARMS-PCR requires well-designed primers. This study aimed to devise tetra-primer ARMS-PCR based on SNPs in lectin gene regions, and characterize lectin proteins in silico to identify specific allele differences and amino acid arrangement structures of *T. flagelliforme* mutants and wild-type plants.

MATERIALS AND METHODS

Plant materials

DNA samples were collected at Bina Nusantara (Binus) University, Jakarta, Indonesia in 2021. In the analysis of *T. flagelliforme* sequences, four mutant clones with sequence lengths of approximately 500 bp were compared to the wild-type ones (KB-control_61F). It was found that two mutant clones were classified as being high anticancer (KB-6-2-5-3_61F and BM-8-2_61) and low anticancer (KB-6-1-1-2_61F and KB-6-2-6-3_61F) (Sianipar et al. 2022). Therefore, a tetra-primer ARMS was built on top of these sequences, and a lectin protein model was developed. The study use DNA template samples of fresh leaf tissue from wild-type and 12 mutants of *T. flagelliforme* (Table 1).

Procedures

Genomic DNA extraction and quality test

Genomic DNA was extracted using Cetyltrimethylammonium Bromide (CTAB) method described by Calderón-Cortés et al. (2010). Samples were collected from *T. flagelliforme* mutants and wild-type of Bogor accessions. After mixing liquid nitrogen and mortar, a 1,000 mL extract buffer was combined with fresh leaf tissue. The mixture was incubated in 2 mL microtubes for 45 minutes and homogenized every 15 minutes. An 800 mL of isoamyl alcohol chloroform was added to 1.5 mL of the tube 0.01% sodium acetate supernatant. During the DNA strand examination, the tubes were kept closed. The supernatant was removed from the sample with a micropipette after 10 minutes of incubation at room temperature.

TE buffer was combined with the leftover DNA pellet at room temperature. Then, RNase was added and the solution was gently mixed and incubated at 37°C for 30 minutes. The sodium acetate solution was diluted to one-tenth by adding the DNA solution and stirring carefully, and the DNA was precipitated by processing samples in 600 mL of 95% ethanol. These samples were gently combined after incubation for 45 minutes at 20°C. The supernatant was removed from the solution by centrifugation for 10 minutes at 13,500 rpm with a MiniSpin plus (EU-IVD) (Eppendorf, UK). DNA was dried before being rehydrated with 200 μL of TE buffer. The instrument was calibrated at room temperature using TE buffer solution. A260/A280 ratios were determined using a Nanodrop Spectrophotometer 2000 manufactured by ThermoScientific™USA. Moreover, to test the quality including purity and concentration of the isolated DNA, Thermo Scientific™ USA's NanoDrop 2000 was utilized. DNA samples were stored at -20°C after diluting to a total concentration of 10-15 ng/μL for further use.

Table 1. Rodent tuber (*Typhonium flagelliforme*) mutant plants used in the study

No.	Accession numbers	Accession name	Types	Source
1.	B1	KB Control (wild-type)	Bogor accession	Binus collection
2.	B2	BM 8-2	Bogor accession	Binus collection
3.	B3	KB 6-2-6-3	Bogor accession	Binus collection
4.	B4	KB 6-2-5-3	Bogor accession	Binus collection
5.	B5	KB 6-1-1-2	Bogor accession	Binus collection
6.	B6	KB 6-1-3-4	Bogor accession	Binus collection
7.	B7	BM 8-8	Bogor accession	Binus collection
8.	B8	BM 8-4	Bogor accession	Binus collection
9.	B9	BM 8-9	Bogor accession	Binus collection
10.	B10	KB 6-2-8-2	Bogor accession	Binus collection
11.	B11	KB 6-9-3	Bogor accession	Binus collection
12.	B12	KB 6-9-5	Bogor accession	Binus collection
13.	B13	KB 6-3-3-6	Bogor accession	Binus collection

Design of tetra-primer ARMS

Gene-specific tetra-primer ARMS were developed based on SNP sites previously identified by Sianipar et al. (2022). SNP sites that caused amino acid changes were recorded as missense mutations. SNP sites that could be developed into tetra-primer ARMS and identified as having bi-allelic alternative alleles were then analyzed for primer design. Using the online tool Primer1 (http://primer1.soton.ac.uk/primer1.html) (Ye et al. 2001), a set of outer and inner PCR primers was created. The specificity of these outer primers, intended for detecting the lectin gene, was verified using NCBI BLAST primers. Next, a 183 bp position tetra-primer ARMS design was carried out with the following parameters: a PCR product range of 100-300 bp, a primer concentration of 5µM, a primer size range of 20-24 bp, and a primer melting temperature range of 62-70°C.

Tetra-primer ARMS PCR

Tetra-primer ARMS were designed and *T. flagelliforme* template DNA was used in the PCR machine for amplification. Next, 12 µL was used for the reaction mixture in the PCR reaction. This PCR mixture included 1x MyTaqTMHS Red Mix (Bioline, UK) (containing dNTPs, $MgCl_2$, MyTaq HS DNA polymerase, and reaction buffer) of 5 µL, 2-5 µL genomic DNA (3-5 ng template DNA), primers with a concentration of 10 µM each 0.5 µL, and added ddH_2O. Palm-Cycler Thermal Cycler PCR machine (Corbett, USA) with CG1-96 plates was applied to conduct the PCR procedures. The cycle parameters were set up: 4 minutes of initial denaturation at 94°C, followed by 30 seconds of denaturation at the same temperature, 30 seconds of annealing at 65°C, and 30 seconds of extension at 72°C. A last extension cycle lasting 5 minutes at 72°C made the reaction close. The PCR products were subsequently run on a 2% agarose gel (Vivantis.Sdn.Bhd.) in Tris Borate EDTA buffer and stained with a Florosafe DNA stain (1st BASE). Electrophoresis was run at 75 V for 85 minutes. DNA ladders (Geneaid Biotech Ltd.) were used as standards for estimating the size of the PCR product. An Agarose gel was illuminated with UV light using a UV transilluminator (Syngene, USA).

The amplification results were visualized by showing the DNA bands of internal control and alleles in mutant and wild-type *T. flagelliforme*. Tetra-primer ARMS are designed based on lectin gene mutation points that cause amino acid changes. Point mutations that cause amino acid changes can affect protein structure (Kimball and Jefferson 2006). Therefore, protein characterization and protein modeling can be done to determine the difference in protein structure due to missense mutation points.

Data analysis

Lectin genes with approximately 500 bp were used to characterize the proteins (Sianipar et al. 2022). Using the NCBI database, the CDS lectin gene sequence was adjusted based on the start codon by Multiple Sequence Alignment (MSA). Expasy translate (https://web.expasy.org/translate/) was used for translating gene sequences into proteins. This stage revealed differences in amino acids. For the identification of differences in protein types caused by point mutations, we used the Uniprot website (https://www.uniprot.org/blast). A manual comparison of *T. flagelliforme* mutant plants with wild-type revealed differences and similarities in the lectin proteins.

The amino acid arrangement was used for protein structure modeling through SWISS MODEL (https://swissmodel.expasy.org/). Protein data bank (PDB) files were downloaded based on the best-selected protein templates and further visualized with PyMol 2.0 software. Molecular weights and isoelectric points (pl) of mature proteins were estimated using the Compute pI/Mw tool (https://web.expansy.org/compute_pi/). An alteration in the isoelectric point can affect a protein's functional state (Kimball and Jefferson 2006).

RESULTS AND DISCUSSION

DNA quality

The test results indicated that the DNA concentration varied between 10 and 106.8 ng/µL, and the purity of A260/A280 was 1.4 to 2.0. Piskata et al. (2019) suggested that the optimal range for a pure DNA sample is from 1.7 to 2.0. Residual protein may produce higher values, whereas lower values represent extremely low DNA contents (Ke-xin et al. 2023). The DNA bands obtained in this study were reproducible and very clearly performed. The results of the DNA quality test showed that all samples of *T. flagelliforme* DNA were suitable for additional PCR analysis (Servusova and Piskata 2021).

Design of tetra-primer ARMS

The tetra-primer ARMS was successfully designed following the point mutation of the lectin gene sequence by Sianipar et al. (2022) (Table 2). The 183 bp mutation point has a G/C sequence mutation. The tetra-primer ARMS pair was constructed using the Primer1 software. ARMS PCR pairs with mismatches were designed to improve the specificity of alleles (Ye et al. 2001). Several mismatch bases were selected based on Little's (1997) guidelines. It was most effective to couple mismatches scored as "strong" at the 3' end (such as G/A or T/C mismatches) with a second mismatch rated as "weak" (such as A/C or T/G). A/A, T/T, C/C, or G/G are examples of "medium or intermediate" strength pairings that could be employed.

The ARMS method of detecting small deletions or point mutations has quick and accurate results. ARMS-PCR allows genotype-specific identification in a single PCR step, eliminating expensive post-PCR manipulations (Ye et al. 2001). ARMS method success largely depends on the primer's design and several criteria found to design ARMS primers. These criteria include primer base length, complementary primers, and the number of percent of GC or Tm (Bates 1995). This study calculated primer Tm with the web-based program OligoAnalyzer™Tool (https://sg.idtdna.com/calc/analyzer). Generally, the Tm values of all primer sequences designed in this study are fairly significant.

Table 2. A tetra-primer ARMS of lectin genes was used for this study

SNP position (bp)	SNP variation	Type of mutation in amino acid residues	Primer Id	Primer sequences (5'-3')	Tm (ºC)	Product Size (bp)
183	C/G	Missense (Threonine-Arginine)	Lec183_F_In_G	GAGCAGCGGCTCCCAGTCGGACAG	67.5	193
			Lec183_R_In_C	ACGGCGGCGTACTTGCCGGG	67.9	129
			Lec183_F_Out	ACGGCGAACAGAGGACGGGACTGC	67.0	278
			Lec183_R_Out	TGCCGTCGGCGTAGAGGACCTGG	67.0	

Note: Lec183: Primer designed based on the lectin gene with the 183 bp SNP, F: Forward, R: Reverse, In: Inner, Out: Outer

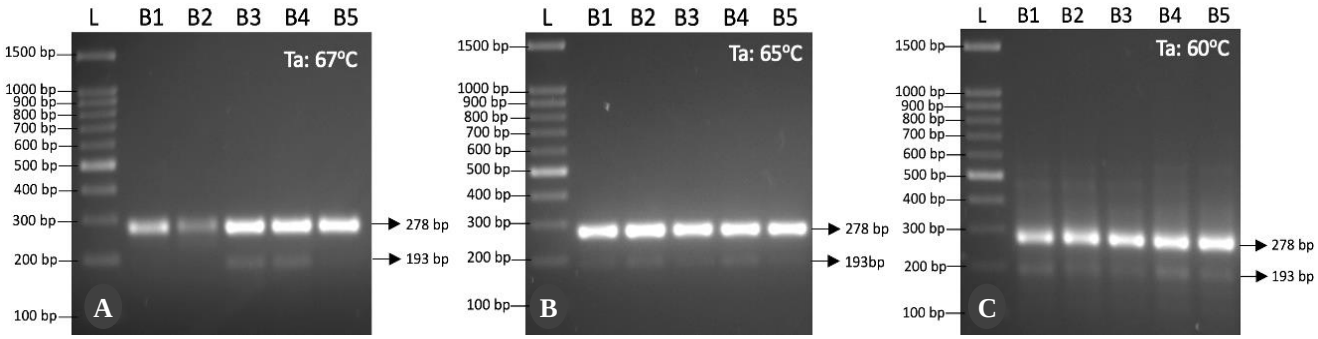

Figure 1. Electrophoresis outcomes of tetra-primer ARMS-PCR with different annealing temperatures in 5 *T. flagelliforme* mutant clones: A. 67°C, B. 65°C, C. 60°C. L: 100 bp DNA ladder, B1: KB Control, B2: BM 8-2, B3: KB 6-2-6-3, B4: KB 6-2-5-3, B5: KB 6-1-1-2, Ta: Annealing temperature

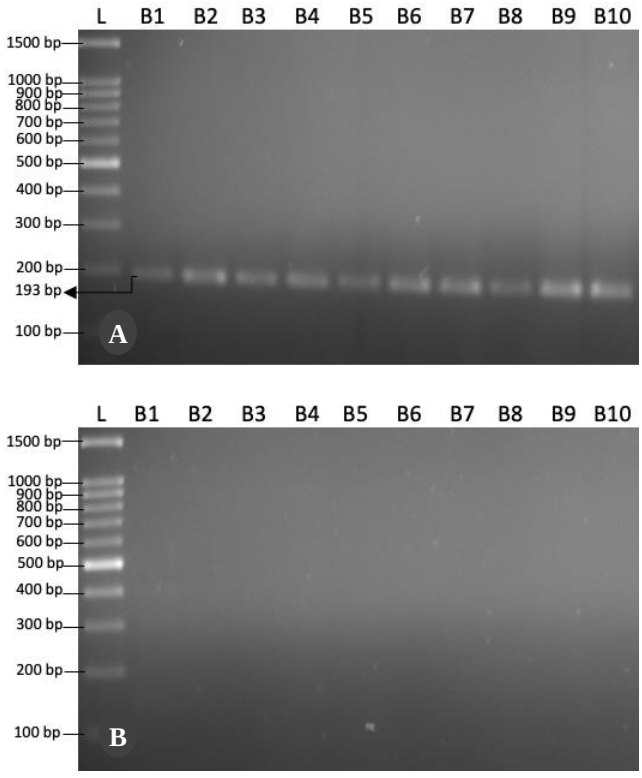

Figure 2. Electrophoresis results of inner primer ARMS separation in *T. flagelliforme* clones: A. G allele-specific reaction, B. C allele-specific reaction. L: 100 bp DNA ladder, B1: KB Control, B2: BM 8-2, B3: KB 6-2-6-3, B4: KB 6-2-5-3, B5: KB 6-1-1-2, B6: KB 6- 1-3-4, B7: BM 8-8, B8: BM 8-4, B9: BM 8-9, B10: KB 6-2-8-2

Tetra-primer ARMS-PCR

The ARMS tetra-primer was successfully designed in this study. ARMS primer lec183 was used to amplify *T. flagelliforme* mutants and wild-type based on the fragment size of the tetra-primer ARMS-PCR product (Lec183_F_In_G: GAGCAGCGGCTCCCAGTCGGACAG; Lec183_R_In_C: ACGGCGGCGTACTTGCCGGG; Lec183_F_Out: ACGGCGAACAGAGGACGGGACTGC; Lec183_R_Out: TGCCGTCGGCGTAGAGGACCTGG). The tetra-primer ARMS-PCR product was specific for the 183 bp lectin gene SNP containing 278 bp as internal control and 193 bp as the G/Guanin allele.

Three annealing temperatures were used to obtain optimum conditions and detect specific inner alleles (Figure 1). An internal control band at 278 bp was produced in five samples by the forward outer and reverse outer primer pairs. There were only a few samples that amplified the inner allele at 67°C. Only five samples successfully amplified the inner allele at 65°C and 60°C; all samples annealed at 60°C produced smears. The results indicate that too high annealing temperatures can cause the *T. flagelliforme* DNA to not adhere to the inner primer, while too low annealing temperatures can cause smears (Suhda et al. 2016). Different annealing temperatures affect the appearance of allele-specific bands in some samples (Zabala et al. 2017). Tanha et al. (2015) notes the ARMS-PCR method's strength is its ability to find the optimal PCR program (annealing temperature). According to this study, the ideal annealing temperature was 65°C.

Separating inner forward and inner reverse primers was performed to confirm the bands that appeared clearly (Figure 2). The inner forward/allelic G primer (Lec183_F_In_G:

GAGCAGCGGCTCCCAGTCGGACAG; Lec183_R_Out: TGCCGTCGGCGTAGAGGACCTGG) was successfully amplified in all samples at 193 bp according to the product size during primer construction (Figure 2.A). In contrast, the inner reverse/allele C primer (Lec183_R_In_C: ACGGCGGCGTACTTGCCGGG; Lec183_F_Out: ACGGCGAACAGAGGACGGGACTGC) was not amplified in all samples (Figure 2.B). This is because primers designed specifically for the G allele can attach to *T. flagelliforme* DNA, while primers specifically for the C allele cannot attach to *T. flagelliforme* DNA. Medrano and de Oliveira (2014) reported that inner reverse primers are used to recognize that they have a C sequence near the 3' end, which allows non-specific binding to DNA despite intentional mismatches.

DNA fragments of wild-type *T. flagelliforme* with three mutants were produced in the same reaction [all outer and inner primers (G/C)] and two specific alleles [inner primer of allele G (G) and inner primer of allele C (C)] were amplified separately to obtain the specific allele (Figure 3). The three mutant samples represent the results of amplifying all samples on the outer and inner primers of allele G. The outer primer pair (Lec183_F_Out: ACGGCGAACAGAGGACGGGACTGC; Lec183_R_Out: TGCCGTCGGCGTAGAGGACCTGG) was successfully produced in all samples at 278 bp according to the primer preparation. All samples with the inner forward primer or allele G (G) amplified separately showed bands at 193 bp.

Both *T. flagelliforme* wild-type (control) and mutant were successfully amplified and showed clear DNA bands in all samples. Three standalone PCR reactions were performed to examine reproducibility: one with an outer/internal control primer, one with an inner primer specific for the G allele, and one with an inner primer for the C allele. When amplified separately, the C allele (C) showed no bands (Figure 3). It has been suggested by Garcés-Claver et al. (2007) that the high variability in the 3' end UTR region may result in the absence of specific fragments from the inner allele primer. G allele data showed a 193-bp band when the inner forward primer is amplified separately. This G allele band is clearer than the mixing reaction (G/C). Zabala et al. (2017) reported that DNA fragments between two specific alleles can be separated if the amplicons have a minimum size of 50 bp.

Two outer primers can produce DNA fragments of different sizes, serving as a non-specific internal control band for allele detection. Combining the fragments with two allele-specific inner primers allows simultaneous amplification. The inner primers are asymmetrically located around the common primer, designed to anneal in opposite orientations, enabling the separation of wild-type and mutant amplicons by standard gel electrophoresis (Zabala et al. 2017). In this study, the designed tetra-primer ARMS lec183 was unable to differentiate the wild-type from the mutant. However, the ARMS lec183 tetra-primer was successfully amplified in all *T. flagelliforme* samples. Tóth et al. (2023) suggested that not all SNPs may be compatible with allele-specific methods due to limitations in primer design or challenging optimization.

Tetra-primer ARMS-PCR is used for genotyping SNPs. This method is considered more convenient than other techniques like PCR-RFLP (Restriction Fragment Length Polymorphism) because it does not require restriction enzyme incubation (Alvarez et al. 2016). In addition, tetra-primer ARMS only requires a small DNA concentration of 10-15 ng/μL. Tetra-primer ARMS-PCR comes with its own set of benefits and drawbacks. It is not suggested to use this method for SNP present in DNA sections that are abundant in guanine and cytosine. Also, it is not recommended to use it for unpurified DNA samples. However, this method has been successfully utilized in several applications, such as diagnosing human spinal muscular atrophy when SMN1 and SMN2 deletions were simultaneously identified (Baris et al. 2010). A similar approach has also been used to evaluate the diversity of *Panax* species (Yang et al. 2023), assess pork quality (Chai et al. 2010), and design cultivar markers for *Capsicum* species (Rubio et al. 2008). Tetra-primer ARMS are designed based on point mutations that cause amino acid changes (missense mutations). Additionally, Kimball and Jefferson (2006) associate missense mutation points in the genome with the protein structure associated with the change.

Lectin characterization and protein modeling

Lectins were characterized by translating DNA bases into protein amino acids and amino acid alignment by translating DNA bases into protein amino acids and aligning amino acids based on sequences of the lectin genes presented by Sianipar et al. (2022). The results of the alignment of lectin amino acids showed changes in amino acids due to point mutations (Figure 4). The amino acid change occurred from threonine (T) to arginine (R) (red box). Threonine is an amino acid with an uncharged closed R group, while arginine is a basic amino acid. BLAST results of the *T. flagelliforme* protein show that the *T. flagelliforme* mutant and wild-type lectins are highly similar to the bulb-type lectin domain-containing protein in *Colocasia esculenta* (red box) (Figure 5). This indicates that although there are differences in amino acids due to the mutation point, there is no change in the type of lectin protein in *T. flagelliforme* mutant and wild-type ones.

Protein modeling was performed to calculate the effect of mutations in the *T. flagelliforme* lectin sequence on the tertiary structure of the mature protein. Protein modeling showed no change in the tertiary structure of the wild-type lectin protein with the mutant despite the amino acid changes (Figure 6). The residue of amino acid in the wild-type lectin is threonine (T) and in the mutant lectin protein is arginine (R) at the 61st amino acid (red box). This indicates that lectin point mutations can change amino acids even though protein structure remains unchanged. The wild-type and mutant lectin proteins have the same estimated isoelectric value of 5.16 and molecular weight of 31.5 kDa. This study's results are similar to those of Alfarabi et al. (2015) which states that the molecular weight of lectins in *T. flagelliforme* is around 10-30 kDa. A similar claim was made by Luo et al. (2007), stating that lectins in *T. divaricatum* have a molecular weight of 12-48

kDa. This study's lectins of *T. flagelliforme* mutants are similar to those of *T. flagelliforme* (Alfarabi et al. 2015).

Proteins known as lectins have at least a single non-catalyzed domain that reversibly binds to particular carbohydrate molecules, and structurally, lectins consist of 4 types, namely merolectin, hololectin, chimerolectin, and superlectin (Peumans and van Damme 1995). Each type of lectin is distinguished by the number of domains that bind to carbohydrates. Mutant and wild-type *T. flagelliforme* have bulb-type lectin domain-containing protein. This type of lectin can bind specifically to mannose, a simple sugar C-2 epimer of glucose (Peumans and van Damme 1995). Through protein structure modeling, it is possible to determine an individual's protein type (Holle et al. 2017). Modeling of lectin proteins has also been carried out on *Acacia farnesiana* (L.) Willd. (AFAL) (Abrantes et al. 2013) and potatoes (van Damme et al. 2004).

Point mutation of the 183 bp lectin gene reported by Sianipar et al. (2022) affects amino acid translation. The in silico protein modeling analysis is based on the arrangement of amino acids that have changed due to point mutations. From this analysis, we can model the protein structure, molecular weight, and isoelectric point prediction due to point mutation changes that cause amino acid changes. Point mutations that cause changes in amino acids can affect protein structure (Kimball and Jefferson 2006). Protein structures that are naturally from wild-type sequences can be altered due to mutations in the protein sequence (Taverna and Goldstein 2002; Kimball and Jefferson 2006). the location of the mutation differs from the location of function, however, Yang et al. (2016) and Mitternacht and Berezovsky (2011) also found an impairment of function or changes at the level of functionality. These studies suggest that while the structure of the mutant protein closely resembles the structure of the wild-type protein, the topology of the mutant protein may be altered at locations far from the mutation site (Rajasekaran et al. 2017).

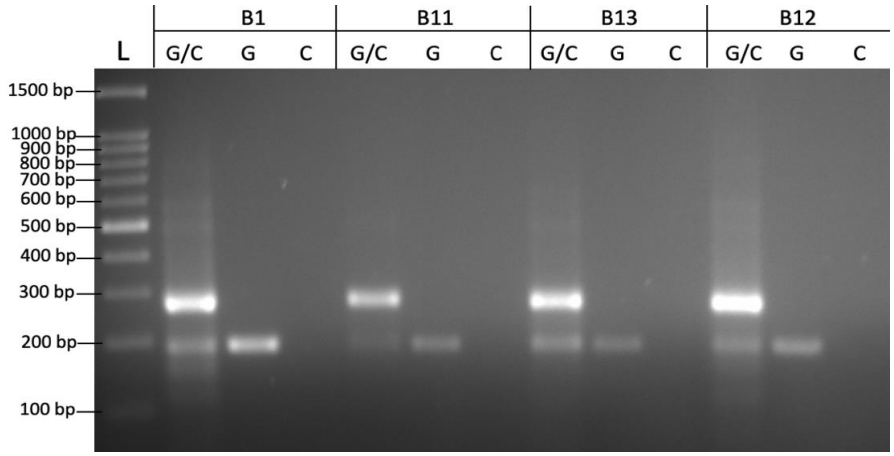

Figure 3. Electrophoresis results with mixing and separation ratio of outer primer and inner primer reactions in *T. flagelliforme* clones: G/C: All four primers in the same reaction, G: Guanine allele reaction, C: Cytosine allele reaction, L: 100 bp DNA ladder, B1: KB Control, B11: 6-9-3 KB, B12: 6-9-5 KB, B13: 6-3-3-6 KB

```
CLUSTAL O(1.2.4) multiple sequence alignment

KB-6-2-5-3_61F      NGDFDLVMQDDCNLVLYNGNWQSNTANRGRDCKLTLTDRGELIIQDGDGSNVWSSGSQSE       60
KB-Kontrol_61F      NGDFDLVMQDDCNLVLYNGNWQSNTANRGRDCKLTLTDRGELIIQDGDGSNVWSSGSQSE       60
KB-6-1-1-2_61F      NGDFDLVMQDDCNLVLYNGGWQSNTANRGRDCKLTLTDRGELIIQDGDGSNVWSSGSQSE       60
KB-6-2-6-3_61F      NGDFDLVMQDDCNLVLYNGGWQSNTANRGRDCKLTLTDRGELIIQDGDGSNVWSSGSQSE       60
BM-8-2_61F          NGDFDLVMQDDCNLVLYNGGWQSNTANRGRDCKLTLTDRGELIIQDGDGSNVWSSGSQSE       60
                    ******************.*****************************************

KB-6-2-5-3_61F      RGNYAAVVHPEGKLVIYGPSVFKINPWVPGLNSLRLGNIPSTSNMLFSGQVLYADGKLTA       120
KB-Kontrol_61F      TGNYAAVVHPEGKLVIYGPSVFKINPWVPGLNSLRLGNIPSTSNMLFSGQVLYADGKLTA       120
KB-6-1-1-2_61F      TGNYAAVVHPEGKLVIYGPSVFKINPWVPGLNSLRLGNIPSTSNMLFSGQVLYADGKLTA       120
KB-6-2-6-3_61F      TGNYAAVVHPEGKLVIYGPSVFKINPWVPGLNSLRLGNIPSTSNMLFSGQVLYADGKLTA       120
BM-8-2_61F          TGNYAAVVHPEGKLVIYGPSVFKINPWVPGLNSLRLGNIPSTSNMLFSGQVLYADGKLTA       120
                     ************************************************************

KB-6-2-5-3_61F      RNHML       125
KB-Kontrol_61F      RNHML       125
KB-6-1-1-2_61F      RNHML       125
KB-6-2-6-3_61F      RNHML       125
BM-8-2_61F          RNHML       125
                    *****
```

Figure 4. Alignment of lectin amino acids in wild-type ones and *T. flagelliforme* mutant. Amino acid residue substitutions in *T. flagelliforme* mutant (red box); the "*" mark indicates the position of a highly conserved residue; the "." mark indicates one of the conserved weak groups

Entry	Entry Name	Protein Names	Gene Names	Organism	Length
A0A843WNH9	A0A843WNH9_COLES	Bulb-type lectin domain-containing protein	Taro_044356	Colocasia esculenta (Wild taro) (Arum esculentum)	264 AA
R9RL27	CEA_COLES	Mannose-specific lectin CEA[...]	CEA	Colocasia esculenta (Wild taro) (Arum esculentum)	264 AA
B5LYJ9	LEC1_REMVI	Mannose-specific lectin 1[...]	L1, RVL	Remusatia vivipara (Hitchhiker elephant ear) (Arum viviparum)	256 AA

A

Entry	Entry Name	Protein Names	Gene Names	Organism	Length
A0A843WNH9	A0A843WNH9_COLES	Bulb-type lectin domain-containing protein	Taro_044356	Colocasia esculenta (Wild taro) (Arum esculentum)	264 AA
R9RL27	CEA_COLES	Mannose-specific lectin CEA[...]	CEA	Colocasia esculenta (Wild taro) (Arum esculentum)	264 AA
B5LYJ9	LEC1_REMVI	Mannose-specific lectin 1[...]	L1, RVL	Remusatia vivipara (Hitchhiker elephant ear) (Arum viviparum)	256 AA

B

Figure 5. BLAST results of *T. flagelliforme* lectin protein. A. Lectin protein of *T. flagelliforme* wild-type, B. Lectin protein of *T. flagelliforme* mutant

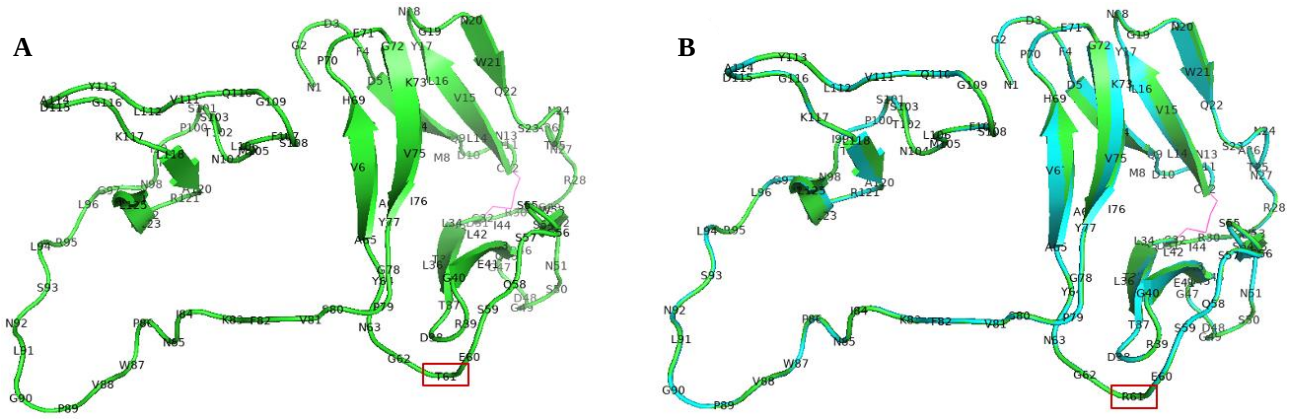

Figure 6. Predicted stereo structure models of lectin proteins. A. Superimposition of wild-type lectin protein (green) on the model protein of Mannose-specific lectin 2 (A5HMM7.1.A), B. Superimposition of mutant lectin protein (green) against the Mannose-specific lectin 2 protein model (A5HMM7.1.A; blue). Amino acid residue differences in mutant and wild-type lectins and (red squares) disulfide bonds (magenta)

Overall, the mutation point-based design of the tetra-primer ARMS lectin gene led to its effective amplification in both mutant and wild-type *T. flagelliforme* plants. The difference in mutation points in the 183 bp lectin gene is due to gamma irradiation treatment at six Gy doses (Sianipar et al. 2016, 2017; Sianipar and Purnamaningsih 2018). The lectin gene can impact environmental factors, such as temperature, light, and soil composition. These factors can influence the expression of the lectin gene, potentially affecting the plant's growth, development, and production of bioactive compounds (Mishra et al. 2019). The expression of lectin genes in *T. flagelliforme* mutants has not been directly studied. Protein structure modeling studies with similarities with the wild-type show the possibility of the same gene expression as the wild-type. Changes in point mutations that cause changes in protein structure can affect gene expression (Kim et al. 2004). This study's mutant protein structure is very similar

to the wild-type. The significance of lectin genes in producing *T. flagelliforme* plants has been reported by Alfarabi et al. (2015). The study stated that lectin isolates were successfully obtained and could inhibit breast cancer cells. The difference between *T. flagelliforme* mutants and wild-types in this study could not be obtained through the lectin gene approach. This allows the expression of the wild-type lectin gene to be very similar to the mutant, but the approach to genes controlling other anticancer compounds may differ.

In conclusion, tetra-primer ARMS lec183 (Lec183_F_In_G: GAGCAGCGGCTCCCAGTCGGACAG; Lec183_R_In_C: ACGGCGGCGTACTTGCCGGG; Lec183_F_Out: ACGGCGAACAGAGGACGGGACTGC; Lec183_R_Out: TGCCGTCGGCGTAGAGGACCTGG) was successfully designed based on the 183 bp point mutation of the lectin gene. Although the tetra-primer ARMS lec183 could not distinguish *T. flagelliforme* mutants from wild-type, the primer pair was successfully amplified in all *T. flagelliforme* samples at 278 bp outer primer and 193 bp inner primer G allele according to the product size during primer preparation. Amino acid variations based on the 183 bp mutation point of the lectin gene show that the mutant protein structure is very similar to the structure of the wild-type protein, which is a bulb-type lectin domain-containing protein. Therefore, research on primer design through genes encoding other anticancer compounds can be carried out to obtain molecular markers that differentiate *T. flagelliforme* mutants from wild-type plants.

ACKNOWLEDGMENTS

The Ministry of Education, Culture, Research, and Technology, Republic of Indonesia funded this study under project number 095/VRRTT/V/2023. The authors declare no conflicts of interest.

REFERENCES

Abrantes VE, Matias da Rocha BA, Batista Da Nóbrega R, Silva-Filho JC, Teixeira CS, Cavada BS, Gadelha CA, Ferreira SH, Figueiredo JG, Santi-Gadelha T, Delatorre P. 2013. Molecular modeling of lectin-like protein from *Acacia farnesiana* reveals a possible anti-inflammatory mechanism in carrageenan-induced inflammation. Biomed Res Intl 2013: 253483. DOI: 10.1155/2013/253483.

Alfarabi M, Rosmalawati S, Bintang M, Miftahudin, Rofa'ani E, Chaidir. 2015. Antip roliferation activity of tuber protein from *Typhonium flagelliforme* (Lodd.) Blume on MCF-7 cell line. Intl J Biosci 6 (12): 52-60. DOI: 10.12692/ijb/6.12.52-60.

Alvarez MF, Gomez MEV, Siewert S. 2016. Designing, optimization, and validation of tetra primer ARMS-PCR protocol for genotyping Single Nucleotide Polymorphism rs4731702 (C/T) of KLF14 gene associated with type 2 diabetes mellitus: A study in San Luis, Argentina. Open Access Libr J 3: e3270. DOI: 10.4236/oalib.1103270.

Baris I, Etlik O, Koksal V, Arican-Baris ST. 2010. Rapid diagnosis of spinal muscular atrophy using tetra-primer ARMS PCR assay: Simultaneous detection of SMN1 and SMN2 deletion. Mol Cell Probes 24 (3): 138-141. DOI: 10.1016/j.mcp.2009.12.001.

Bates G. 1995. Book Review: Current Protocols in Human Genetics. Edited by Dracopoli NC et al. Current Protocols, 1994. $295.00 loose leaf (750 pages) ISBN 0 471 03420 7. Trends Genet 11 (11): 458-459. DOI: 10.1016/s0168-9525(00)89147-7.

Bellande K, Bono JJ, Savelli B, Jamet E, Canut H. 2017. Plant lectins and lectin receptor-like kinases: how do they sense the outside? Intl J Mol Sci 18 (6): 1164. DOI: 10.3390/ijms18061164.

Cai L, Wang W, Wang F, Zhang R, Zhang L, Qi H, Gu W, Zhou N. 2019. A comparison of MASS-PCR and ARMS-PCR for the detection of lung cancer gene mutation. Transl Cancer Res 8 (7): 2564-2569. DOI: 10.21037/tcr.2019.10.37.

Calderón-Cortés N, Quesada M, Cano-Camacho H, Zavala-Páramo G. 2010. A simple and rapid method for DNA isolation from xylophagous insects. Intl J Mol Sci 11 (12): 5056–5064. DOI: 10.3390/ijms11125056.

Chai J, Xiong Q, Zhang PP, Shang YY, Zheng R, Peng J, Jiang SW. 2010. Evidence for a new allele at the SERCA1 locus affecting pork meat quality in part through the imbalance of Ca^{2+} homeostasis. Mol Biol Rep 37 (1): 613-619. DOI: 10.1007/s11033-009-9872-0.

Garcés-Claver A, Fellman SM, Gil-Ortega R, Jahn M, Arnedo-Andrés MS. 2007. Identification, validation, and survey of A Single Nucleotide Polymorphism (SNP) associated with pungency in *Capsicum* spp. Theor Appl Genet 115 (7): 907-916. DOI: 10.1007/s00122- 007-0617-y.

Holle S, de Schutter K, Eggermont L, Tsaneva M, Dang L, van Damme EJM. 2017. Comparative study of lectin domains in model species: New insights into evolutionary dynamics. Intl J Mol Sci 18 (6): 1136. DOI: 10.3390/ijms18061136.

Hou Y, Luo Q, Chen C, Zhou M. 2013. Application of tetra primer ARMS-PCR approach for detection of *Fusarium graminearum* genotypes with resistance to carbendazim. Australas Plant Pathol 42 (1): 73-78. DOI: 10.1007/s13313-012-0162-2.

Islam MS, Thyssen GN, Jenkins JN, Fang DD. 2015. Detection, validation, and application of genotyping-by-Sequencing Based Single Nucleotide Polymorphisms in upland cotton. Plant Genome 8 (1): plantgenome2014.07.0034. DOI: 10.3835/plantgenome2014.07.0034.

Ke-xin Y, Xiang C, Qing-qing H, Yi-an Y, Xiao-ming W, Ai-chun X, Jian G, Feng G. 2023. Development of a tetra-primer ARMS-PCR for identification of sika and red deer and their hybrids. Anal Sci 39: 1947-1956. DOI: 10.1007/s44211-023-00405-6.

Kim JS, Jang HW, Kim JS, Kim HJ, Kim JH. 2012. Molecular identification of *Schisandra chinensis* and its allied species using multiplex PCR based on SNPs. Genes Genom 34 (3): 283-290. DOI: 10.1007/s13258-011-0201-3.

Kim S, Binzel ML, Yoo KS, Park S, Pike LM. 2004. Pink (P), a new locus responsible for a pink trait in onions (*Allium cepa*) resulting from natural mutations of anthocyanidin synthase. Mol Genet Genom 272 (1): 18-27. DOI: 10.1007/s00438-004-1041-5.

Kimball SR, Jefferson LS. 2006. New functions for amino acids: Effects on gene transcription and translation. Am J Clin Nutr 83 (2): 500S-507S. DOI: 10.1093/ajcn/83.2.500s.

Little S. 1997. ARMS analysis of point mutations. In: Taylor GR (Ed.) Laboratory Methods for the Detection of Mutations and Polymorphisms in DNA. CRC Press, Boca Raton.

Luo Y, Xu X, Liu J, Li J, Sun Y, Liu Z, Liu J, van Damme E, Balzarini J, Bao J. 2007. A novel mannose-binding tuber lectin from *Typhonium divaricatum* (L.) Decne (family Araceae) with antiviral activity against HSV-II and anti-proliferative effect on human cancer cell lines. J Biochem Mol Biol 40 (3): 358-367. DOI: 10.5483/bmbrep.2007.40.3.358.

Medrano RFV, de Oliveira CA. 2014. Guidelines for the tetra-primer ARMS-PCR technique development. Mol Biotechnol 56 (7): 599-608. DOI: 10.1007/s12033-014-9734-4.

Meng K, Xu JL, Li Q, Liu YJ, Wang X, Tang W, Yan H, Zhang YG, Fu MD. 2017. Development of SNP markers using RNA-seq technology and tetra-primer ARMS-PCR in sweet potato. J Integr Agric 16 (2): 464-470. DOI: 10.1016/S2095-3119(16)61405-3.

Mishra A, Behura A, Mawatwal S, Kumar A, Naik L, Mohanty SS, Manna D, Dokania P, Mishra A, Patra SK, Dhiman R. 2019. Structure-function and application of plant lectins in disease biology and immunity. Food Chem Toxicol 134: 110827. DOI: 10.1016/j.fct.2019.110827.

Mitternacht S, Berezovsky IN. 2011. Binding leverage as a molecular basis for allosteric regulation. PloS Comput Biol 7 (9): e1002148. DOI: 10.1371/journal.pcbi.1002148.

Park H, Kim S, Nie H, Kim J, Lee J, Kim S. 2020. Molecular identification of sweet potato accessions using ARMS-PCR based on

SNPs. J Plant Biotechnol 47 (2): 124-130. DOI: 10.5010/JPB.2020.47.2.124.

Petrova N, Nazipova A, Gorshkov O, Mokshina N, Patova O, Gorshkova T. 2021. Gene expression patterns for proteins with lectin domains in flax stem tissues are related to deposition of distinct cell wall types. Front Plant Sci 12: 634594. DOI: 10.3389/fpls.2021.634594.

Peumans WJ, van Damme EJM. 1995. Lectins as plant defense proteins. Plant Physiol 109 (2): 347-352. DOI: 10.1104/pp.109.2.347.

Piskata Z, Servusova E, Babak V, Nesvadbova M, Borilova G. 2019. The quality of DNA isolated from processed food and feed via different extraction procedures. Molecules 24 (6): 1186. DOI: 10.3390/molecules24061188.

Rajasekaran N, Suresh S, Gopi S, Raman K, Naganathan AN. 2017. A general mechanism for the propagation of mutational effects in proteins. Biochemistry 5 6(1): 294-305. DOI: 10.1021/acs.biochem.6b00798.

Rubio M, Caranta C, Palloix A. 2008. Functional markers for selection of potyvirus resistance alleles at the pvr2-eIF4E locus in pepper using tetra-primer ARMS-PCR. Genome 51 (9): 767-771. DOI: 10.1139/G08-056.

Servusova E, Piskata Z. 2021. Identification of selected tuna species in commercial products. Molecules 26 (4): 1137. DOI: 10.3390/molecules26041137.

Sianipar NF, Assidqi K, Abbas BS. 2020a. The effects of subculture on the mutant plant regeneration of rodent tuber (*Typhonium flagelliforme*) in vitro mutagenesis using gamma-ray irradiation. IOP Conf Ser: Earth Environ Sci 426: 012180. DOI: 10.1088/1755-1315/426/1/012180.

Sianipar NF, Assidqi K, Hadisaputri YE, Salam S. 2023. Mutant plant tipobio variety of rodent tuber (*Typhonium flagelliforme*): Fatty acids compounds and in vitro anticancer activity. E3S Web Conf 01032: 4-8. DOI: 10.1051/e3sconf/202338801032.

Sianipar NF, Hadisaputri YE, Assidqi K, Salam S, Yusuf M, Destiarani W, Purnamaningsih R, Gautama So I. 2021. Characterization and investigation of stigmasterol isolated from rodent tuber mutant plant (*Typhonium flagelliforme*), its molecular docking as anticancer on MF-7. Preprints 2021: 2021070278. DOI: 10.20944/preprints202107.0278.v1.

Sianipar NF, Purnamaningsih R, Chelen C. 2016. Effect of gamma irradiation on protein profile of rodent tuber (*Typhonium flagelliforme* Lodd.) in vitro mutant based on 1D and 2D-page analyses. Jurnal Teknologi 78 (10-4): 35-40. DOI: 10.11113/jt.v78.9888.

Sianipar NF, Purnamaningsih R, Darwati I, Laurent DC. 2015. The effects of gamma irradiation and somaclonal variation on morphology variation of rodent tuber mutant (*Typhonium flagelliforme* Lodd.) lines. KnE Life Sci 2 (1): 637. DOI: 10.18502/kls.v2i1.236.

Sianipar NF, Purnamaningsih R, Darwati I. 2020b. Binus University. Plant Variety Protection (PVP) Rights. Tipobio. No. HKI: 00490/PPVT/S/2020. Center for Plant Variety Protection and Agricultural Licensing, Ministry of Agriculture of the Republic of Indonesia.

Sianipar NF, Purnamaningsih R, Gumanti DL, Rosaria, Vidianty M. 2017. Analysis of gamma irradiated-third generation mutants of rodent tuber (*Typhonium flagelliforme* Lodd.) based on morphology, RAPD, and GC-MS Markers. Pertanika J Trop Agric Sci 40 (1): 185-202.

Sianipar NF, Purnamaningsih R. 2018. Enhancement of the contents of anticancer bioactive compounds in mutant clones of rodent tuber (*Typhonium flagelliforme* Lodd.) based on GC-MS analysis. Pertanika J Trop Agric Sci 41 (1): 305-320.

Sianipar NF, Reflinur R, Ashan MD, Assidqi K, Widyaningrum D, Purnamaningsih R. 2022. Determination of lectin genes in superior mutant of rodent tuber bogor accession (*Typhonium flagelliforme*) based on PCR amplification. Proc 7th Intl Conf Biol Sci (ICBS 2021) 2022: 278-283. DOI: 10.2991/absr.k.220406.039.

Suhda S, Paramita DK, Fachiroh J. 2016. Tetra primer ARMS PCR optimization to detect single nucleotide polymorphisms of the CYP2E1 gene. Asian Pac J Cancer Prev 17 (7): 3065-3069. DOI: 10.4236/oalib.1104145.

Tanha HM, Naeini MM, Rahgozar S, Rasa SMM, Vallian S. 2015. Modified tetra-primer ARMS PCR as a single-nucleotide polymorphism genotyping tool. Genet Test Mol Biomarkers 19 (3): 156-161. DOI: 10.1089/gtmb.2014.0289.

Taverna DM, Goldstein RA. 2002. Why are proteins so robust to site mutations? J Mol Biol 315 (3): 479-484. DOI: 10.1006/jmbi.2001.5226.

Tóth T, Csaba Á, Bokor A, Ács N. 2023. Variable Fragment Length Allele-Specific Polymerase Chain Reaction (VFLASP), a method for simple and reliable genotyping. Mol Cell Probes 69: 101910. DOI: 10.1016/j.mcp.2023.101910.

van Damme EJM, Barre A, Rougé P, Peumans WJ. 2004. Potato lectin: An updated model of a unique chimeric plant protein. Plant J 37 (1): 34-45. DOI: 10.1046/j.1365-313X.2003.01929.x.

Wang YZ, Zhu Z, Zhang HY, Zhu MZ, Xu X, Chen CH, Liu LG. 2014. Detection of hepatitis B virus A1762T/G1764A mutant by amplification refractory mutation system. Braz J Infect Dis 18 (3): 261-265. DOI: 10.1016/j.bjid.2013.09.005.

Yang G, Hong N, Baier F, Jackson CJ, Tokuriki N. 2016. Conformational tinkering drives evolution of a promiscuous activity through indirect mutational effects. Biochemistry 55 (32): 4583-4593. DOI: 10.1021/acs.biochem.6b00561.

Yang Z, Lo YT, Quan Z, He J, Chen Y, Faller A, Chua T, Wu HY, Zhang Y, Zou Q, et al. 2023. Application of a modified tetra-primer ARMS-PCR assay for rapid *Panax* species identity authentication in ginseng products. Sci Rep 13: 14396. DOI: 10.1038/s41598-023- 39940-7.

Ye S, Dhillon S, Ke X, Collins AR, Day INM. 2001. An efficient procedure for genotyping single nucleotide polymorphisms. Nucleic Acids Res 29 (17): 88. DOI: 10.1093/nar/29.17.e88.

Ye S, Humphries S, Green F. 1992. Allele specific amplification by tetra-primer PCR. Nucleic Acids Res 20 (5): 1152. DOI: 10.1093/nar/20.5.1152.

Zabala AS, Gomez MEV, Álvarez MF, Siewert S. 2017. Tetra primer ARMS PCR optimization to detect Single Nucleotide Polymorphism of the KLF14 gene. Open Access Libr J 4: e4145. DOI: 10.4236/oalib.1104145.

NUSANTARA BIOSCIENCE
Vol. 16, No. 2, pp. 210-218
November 2024

ISSN: 2087-3948
E-ISSN: 2087-3956
DOI: 10.13057/nusbiosci/n160207

The effects of *Jebisa* on nutrient intake and hematology profile in adolescent girls with anemia

MARTHA ARUM NUGRAHENI[1,2], DONO INDARTO[1,3,4,♥], ETI PONCORINI PAMUNGKASARI[1,5], TRI NUGRAHA SUSILAWATI[6], SINU ANDHI JUSUP[4], NINIEK PURWANINGTYAS[7], SETYO SRI RAHARDJO[8], SRI WULANDARI[4], KEZIA ELIAN DEVINA[1]

[1]Postgraduate Program of Nutrition Sciences, Universitas Sebelas Maret. Jl. Ir. Sutami 36A Surakarta 57126, Central Java, Indonesia
[2]Department of Food Technology, Faculty of Agriculture, Universitas Tidar. Jl. Barito 1 Magelang 56114, Central Java, Indonesia
[3]Biomedical Laboratory, Faculty of Medicine, Universitas Sebelas Maret. Jl. Ir. Sutami 36A Surakarta 57126, Central Java, Indonesia. Tel./fax.: +62-271- 664178/637400 , ♥email: dono@staff.uns.ac.id
[4]Department of Physiology, Faculty of Medicine, Universitas Sebelas Maret. Jl. Ir. Sutami 36A Surakarta 57126, Central Java, Indonesia
[5]Department of Public Health, Faculty of Medicine, Universitas Sebelas Maret. Jl. Ir. Sutami 36A Surakarta 57126, Central Java, Indonesia
[6]Department of Microbiology, Faculty of Medicine, Universitas Sebelas Maret. Jl. Ir. Sutami 36A Surakarta 5 126, Central Java, Indonesia
[7]Department of Cardiology and Blood Circulation, General Hospital Dr. Moewardi Surakarta/Faculty of Medicine, Universitas Sebelas Maret. Jl. Ir. Sutami 36A Surakarta 57126, Central Java, Indonesia
[8]Department of Pharmacology, Faculty of Medicine, Universitas Sebelas Maret. Jl. Ir. Sutami 36A Surakarta 57126, Central Java, Indonesia

Manuscript received: 30 March 2024. Revision accepted: 28 June 2024.

Abstract. *Nugraheni MA, Indarto D, Pamungkasari EP, Susilawati TN, Jusup SA, Purwaningtyas N, Rahardjo SS, Wulandari S, Devina KE. 2024. The effects of* Jebisa *on nutrient intake and hematology profile in adolescent girls with anemia. Nusantara Bioscience 16: 210-218.* Anemia is a public health problem that often occurs in adolescent girls in developing countries, including Indonesia, mainly due to iron deficiency. Iron supplementation has been implemented for anemia treatment, but there are some side effects for long-term use. The Indonesian Government also fortified wheat flour with iron and folic acid, but the efficacy of fortification remains unclear. Snake fruit seeds contain high iron (Fe) and vitamin C levels but they are usually thrown away. Therefore, this study aimed to analyze the effects of jelly-containing snake fruit seed flour (SSF) and sugar, now called *Jebisa*, on macro and micronutrient intake and hematological profile in adolescent girls with anemia. Thirty tree adolescent girls from five public high schools in Sukoharjo Regency, Central Java, Indonesia, were randomly grouped into three categories: Control group (C) was given plain jelly with Fe tablets, and Treatment groups (T1-T2) were given jelly-containing 18.52 g and 37.04 g SSF, respectively, for 60 days. Data were analyzed using the one-way and repeated measures ANOVA tests followed by the Post Hoc Tukey and the Kruskal-Wallis test for non-parametric data. A significant value was set to $p<0.05$. The results suggested that the average daily energy intake, carbohydrates, and fibers significantly increased in the T1 and T2 groups compared to the C group ($p<0.05$). The average Fe intake in the T2 (19.59±1.70 mg/day) was significantly higher than that of T1 (10.74±2.40 mg/day) and C group (4.74±3.43 mg/day) with $p<0.001$. The T1 group had higher hemoglobin (Hb) levels (11.44±2.01 g/dL) than the C (11.04±1.92 g/dL) and T2 groups (10.89±0.67 g/dL) but were not significantly different. In conclusion, regular consumption of jelly-containing SSF increased the daily intake of energy, carbohydrates, fibers, Fe, and Hb levels in adolescent girls with anemia.

Keywords: Adolescent girl, anemia, hematological profile, nutrient intake, snake fruit seed

Abbreviations: Fe: Iron; SSF: Snake fruit Seeds Flour; *Jebisa*: Plain jelly, SSF, and sugar; C: Control group; T1: Treatment group 1; T2: Treatment group 2; HSD: Honestly Significant Difference; SD: Standard Deviation; BW: Body Weight; Hb: Hemoglobin; BMI: Body Mass Index; MCH: Mean Corpuscular Hemoglobin; MCV: Mean Corpuscular Volume; MCHC: Mean Corpuscular Hemoglobin Concentration; Zn: Zinc; RDA: Recommended Dietary Allowances; CYBRD1: Duodenal Cytochrome B

INTRODUCTION

Anemia is a public health problem affecting the world's population in both developed and developing countries (Petry et al. 2016). A study conducted by the Indonesia Basic Health Research (Kemenkes RI, Riskesdas) in 2018 revealed that adolescent girls represent one of the highest-risk age groups with a prevalence of 32% of suffering anemia. In addition, the national coverage of adolescent girls receiving iron supplementation reaches 80.9%, but 98.6% of them take iron supplementation less than 52 tablets per year (Kemenkes RI 2017). Furthermore, Sukoharjo is a Regency in Central Java Province, Indonesia, with a high prevalence of anemia in adolescent girls (22%) (Rahayu et al. 2017).

Generally, anemia in adolescent girls is mainly caused by iron deficiency due to increased iron needs for growth, regular blood loss (menstruation), and an inappropriate diet for weight management (Engidaw et al. 2018). The Indonesian Government has established two national programs to overcome iron deficiency anemia: iron supplementation and fortification. However, iron supplementation in adolescent girls is not evenly distributed in all Indonesian areas, with 26.5% not receiving it. In addition, some adolescent girls reported side

effects after taking iron supplementation (Kemenkes RI 2023).

Wheat flour fortified with iron, zinc, thiamine, riboflavin, and folic acid has been used to treat anemia in Indonesia since 2002 (Kendrick et al. 2015)However, the efficacy of iron fortification remains debatable. It is possible to make alternative iron fortifications using local ingredients from Indonesian natural products such as *Moringa* leaves flour and fermented buffalo milk (*dadih*). A previous study reported that consuming 4 g *Moringa* leaves flour in *cilok* (street food, ball-shaped dumping made from starch) for 15 days could increase Hb levels by 1 g/dL in female adolescents with anemia (Ariendha et al. 2022). In contrast, consumption of 100 g/day *dadih* for 14 days slightly decreased Hb levels by 0.6 g/dL and serum ferritin levels by 3.9 ng/mL in normal adolescent girls (Budiyatri et al. 2024). Administration of 60 mg iron supplements, combined with 200 mL of cava smoothie from ripe Cavendish bananas, buttery avocados, pure honey, and Sukkari dates, consumed every 2 days for 28 days could increase Hb levels by 2.54±1.24 g/dL, MCH by 1.61±0.99 pg, MCHC by 1.60±0.99 g/dL, and MCV by 1.97±1.19 fL in adolescent girls with moderate anemia (Aryani et al. 2023). Another study reported that consumption of jelly candy containing jelly, snake fruit, banana, and ferrous fumarate for 13 weeks can increase 0.65±0.39 mg/dL Hb levels in female adolescents with mild anemia (Megawati et al. 2023). However, the study does not state the daily dose of jelly candy given to female adolescents and which part of the snake fruits were used in the study.

Snake fruit (*Salacca edulis* Reinw) is a native Indonesian plant whose annual production has increased from 0.89 million in 2018 to 1.14 million in 2022 (Badan Pusat Statistik 2023). This fruit plant can be found in several regions in Indonesia, such as Central Java, North Sumatra, Bali, East Java, and North Sulawesi Provinces. However, the most popular snake fruit comes from the Sleman Regency of Yogyakarta Province, known as "*salak pondoh*," the center of snake fruit plantation and production in Indonesia. A previous study revealed that snake fruit seeds and peels have been utilized for food production with high nutritional values and health benefits (Mazumdar et al. 2019; Kumoro et al. 2020). In addition, snake fruit seeds contain secondary metabolites such as tannins, quinones, monoterpenes, sesquiterpenes, alkaloids, and polyphenolics (Febyawati et al. 2023). Based on our previous studies, 100 g of snake fruit seed flour (SSF) contains 7.5 g of protein, 19.9 mg of iron, 5.79 mf of Zn, and 152.21 mg of vitamin C. Administration of 3.72 g/100 g Body Weight (BW) SSF increases BW, Hb levels, erythrocyte and hematocrit account in female rats with anemia (Indarto et al. 2023). However, a higher amount of SSF is needed when given to adolescent girls with anemia. In addition, the improvement of SSF processing in our study could increase by 1.10 g of protein, 2.67 mg of iron, 0.04 mg of vitamin C, and 0.36 mg of zinc compared to the previous SSF.

The Indonesian Government also has a national program to overcome undernutrition in toddlers, school children, and pregnant women. For example, biscuits fortified with 18 micronutrients have been used as supplementary food for pregnant women (Kemenkes RI 2017). However, there is no supplementary food for anemia in children, adolescent girls, and pregnant women. Several studies have formulated supplementary foods by fortification with iron into cookies (Landim et al. 2016), candy (El-Tahan and Alfky 2016), and chocolate (Mostafa 2023). However, supplementary food for anemia in the form of jelly has not been established. Based on Sani's study (2014), we formulated jelly containing 6 g plain jelly, 29±5 g SSF, and 22.5±5 g sugar for anemia supplementary food (Indarto et al. 2022), hereinafter called *Jebisa* (Indonesian: *jeli biji salak*). This original formulation is granted a patent with IDS 000005116 by the General Directorate of Intellectual Properties, the Indonesian Ministry of Law and Human Rights. Therefore, this study aimed to analyze the effects of jelly-containing SSF (*Jebisa*) on macro and micronutrient intake and hematological profile in adolescent girls with anemia.

MATERIALS AND METHODS

Materials

Fresh snake fruit seeds were purchased from a farmer in Donokerto Village, Turi Sub-district, Sleman Regency, Yogyakarta Province, Indonesia, from which were processed into SSF using the existing method with IDS 000005116 patent number (Indarto et al. 2022). Plain jelly powder was purchased from PT. Satelit Sriti Pandaan, Surabaya, East Java, Indonesia (MD 818513068111). The main ingredients used to make *Jebisa* in this research study were SSF, plain jelly powder, sugar, and water, which were also reported in our previous study (Indarto et al. 2022).

Methods

Research design

This randomized control trial (RCT) study with a pre-posttest control group design was conducted in five public senior high schools (SMAN) 1 Weru, Nguter, Kartasura, Mojolaban, and SMAN 3 Sukoharjo, Central Java, Indonesia, which were determined using the stratified random sampling. The sample size was calculated using the formula of Charan et al. (2021). The final sample size for each group was at least 11 adolescent girls. The study included adolescent girls in senior high schools who were aged 16-18 years old and had <11 g/dL Hb levels, except for those with infectious diseases such as tuberculosis, dengue fever, malaria, typhoid, and helminthiasis, who were menstruation during the screening, taking Fe, and vitamin C supplements, and who were allergies to flour-based foods. Before the research intervention, ethical clearance was acquired from the Medical Research Ethics Committee, Faculty of Medicine, Universitas Sebelas Maret, Surakarta, Central Java, Indonesia Number 165/UN27.6/KEPK/2018.

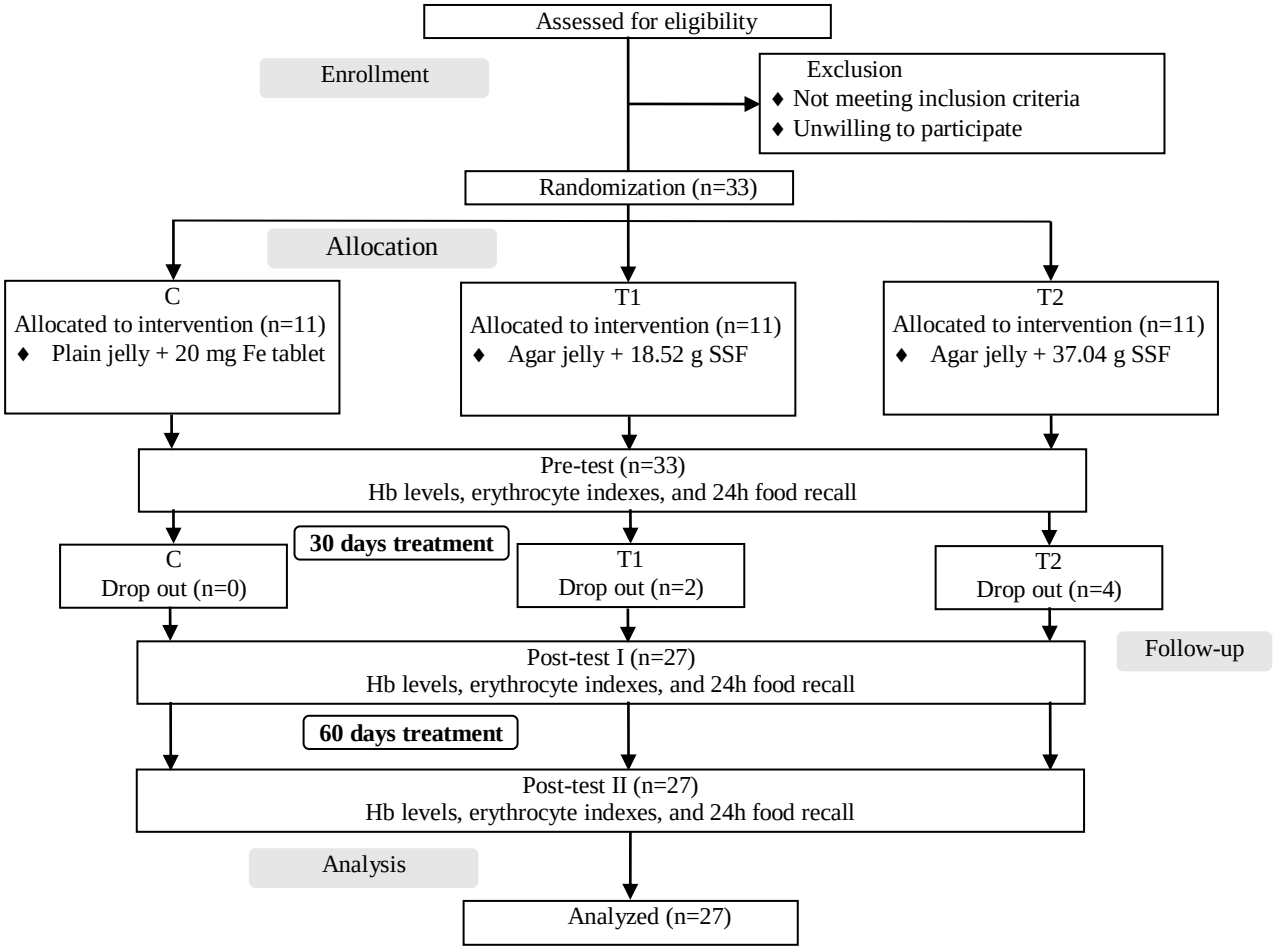

Figure 1. Consort flow diagram for selecting adolescent girls in five senior high schools in Sukoharjo Regency, Central Java, Indonesia.

Jebisa *treatment*

Before the study began, all adolescent girls in five senior high schools were educated about daily nutrition intake and asked to complete personal biodata. Following this, the selected adolescent girls and their parents were carefully guided through the informed consent process, ensuring full understanding and agreement. A venous blood sample was then taken from the upper left arm to determine the Hb level. Suppose the Hb level was less than 11 g/dL (WHO 2011). The research subjects should take 400 mg oral Albendazole in a single dose to treat worm infection, which results in chronic intestinal bleeding. Figure 1 summarizes the selection process of adolescent girls to get the final 27 research subjects. Initially, as mentioned above, we screened adolescent girls in five senior high schools in Sukoharjo Regency and got 33 research subjects that met the inclusion criteria. The selected adolescent girls were randomly allocated into three groups: Control (C), given plain jelly with 20 mg Fe tablets, and Treatment groups (T1 and T2), given jelly-containing 18.52 g and 37.04 g SSF, respectively. All research subjects in the three groups consumed their daily foods and drinks as usual while taking *Jebisa* thrice weekly for 60 days. At the day 30 intervention, however, two and four research subjects in the T1 and T2 groups dropped out of this study for several reasons. Finally, 27 research subjects completed this study and were used for further analysis.

Data collection of anthropometries, daily nutrition intake, and hematology status

Anthropometric data were collected by measuring BW and height before, during, and after interventions. The BW measurement used a Gea weight scale with 0.1 kg accuracy, while the height measurement utilized a stature meter with 0.1 cm accuracy. Body Mass Index for age (BMI/age) was determined using the z-score: subject's individual BMI – (BMI standard median/BMI standard deviation) and then classified into underweight, normal, overweight, and obese (Kemenkes RI 2020). Data on daily nutrition intake were also assessed three times (day 1, 30, and 60 of interventions) using the 24-hour food recall questionnaires and then converted into macro and micronutrient intake using free Nutrisurvey 2007 software (www.nutrisurvey.de). The venous blood samples collected at 1st, 30th, and 60th-day interventions were utilized to measure Hb levels and erythrocyte indexes: Mean Corpuscular Hemoglobin (MCH), Mean Corpuscular Volume (MCV), and Mean Corpuscular Hemoglobin Concentration (MCHC) ratio, performed at the Rahanu

Clinic Laboratory, Karanganyar Regency, Central Java, Indonesia.

Statistical analysis

The characteristics of research subjects were presented as mean ± standard deviation for numerical data, while numbers and percentages were used for categorical data. The following variables were analyzed using a one-way ANOVA test: height, BMI, egg allergy, seafood allergy, parental income, carbohydrate intake, and MCV. Post-hoc tests, including the reliable Tukey's Honestly Significant Difference (HSD) and repeated measures ANOVA, were used to ensure the validity of the results. The Kruskal-Wallis test analyzed age, BW, Hb levels, energy, protein, fat, fiber, Fe, Zn, Vitamin C, MCH, and MCHC. Mann-Whitney and Friedman tests were then applied to these variables. A p-value of <0.05 was considered statistically significant, further reinforcing the reliability of the statistical methods.

RESULTS AND DISCUSSION

Characteristics of research subjects

This study involved 33 adolescent girls from five senior high schools in Sukoharjo Regency. Table 1 shows that the characteristics of research subjects among the three groups were similar, except for the mothers' income with p=0.04. The mean BW in the T2 group (53.36±10.27 kg) was higher than that of the C (49.73±7.80 kg) and T1 groups (46.77±6.44 kg). The same pattern was also observed in height and BMI variables. However, the T1 group had slightly higher Hb levels (10.37±0.76 g/dL) than the C and T2 groups, and most research subjects had mild anemia. Egg and seafood allergies were found in all groups (less than 25%). Most parents in all groups had monthly incomes below the regional minimum salary. Regarding mothers' income, there were research subjects in the T2 group (28.5%) whose mothers earn a salary above the regional minimum. In contrast, the other groups had mothers' incomes below (100%) the regional minimum salary.

***Jebisa* consumption increased macronutrient and fiber intake**

Before *Jebisa* treatment, we evaluated macronutrient and fiber intake in all groups (Table 2). All research subjects among the three groups had low energy, fat, protein, and fiber intake and did not differ significantly (p>0.05) except for carbohydrate intake. The mean carbohydrate intake in T2 groups (165.37±40.37 g/day) was significantly higher than that of C (123.77±48.04 g/day; p=0.146) and T1 (109.36±41.33 g/day; p=0.047) groups. The T2 group also exhibited the highest energy and fat intake, though this was not a statistically significant difference (p=0.41). The highest protein and fat intake were observed in the C groups (34.98±11.19 g/day) and T1 groups (38.29±24.68 g/day).

After 30 days of treatment, the daily intake of energy, protein, and fat decreased, while the daily intake of carbohydrates and fiber increased in the T1 and T2 groups. The C group had a lower daily intake of macronutrients and fiber compared to the 0-day treatment. All mean differences were not significant (p>0.05). However, the mean carbohydrate intake in T2 group (205.30±97.64 g/day) was significantly higher than that of T1 (189.63±36.89 g/day; p=0.872) and C (96.73±49.38 g/day; p=0.004) groups. A slightly increased fat intake was found in the T2 group (31.37±22.29 g/day). In contrast to day 30 of treatment, all daily intake of macronutrients and fiber in the T1 and T2 groups increased; at the same time, energy, carbohydrate, and fiber intake increased significantly (p=0.004; p<0.001; p=0.01, respectively) for 60 days of treatment. The energy intake in the T2 group was 62.44% of the Recommended Dietary Allowances (RDA) for Indonesian female adolescents, which was significantly higher than the energy intake in the T1 (50.22%) and C (40.86%) groups. Meanwhile, the carbohydrate intake in T2 was 91.73%, significantly higher than in T1 (65.08%; p=0.034) and C (33.44%; p<0.001) groups. In comparison to the C group (3.98±3.66 g/day), the mean fiber intake in T1 (6.67±3.77 g/day) and T2 (8.88±3.23 g/day) groups also differed significantly (p=0.01). After 60 days of treatment, daily carbohydrate intake showed significant differences in T1 (p=0.005) and T2 (p=0.02) groups.

***Jebisa* consumption increased Fe, Zn, and Vitamin C intake**

We also evaluated micronutrient intake in all groups (Table 3). The T1 group had the highest Fe (9.82±1.45 mg/day) and Zn (5.00±2.55 mg/day) intake, but the C group (32.07±45.71 mg/day) had the highest vitamin C intake. All mean differences were not significant (p>0.05). After 30 days of treatment, the daily intake of Fe, Zn, and Vitamin C decreased in the C and T1 groups, but the daily intake of Fe and Zn increased in the T2 group. The mean Fe intake in the T2 group (10.90±3.60 mg/day) was significantly higher than that of the T1 and C groups (8.78±1.66 mg/day; 3.69±0.87 mg/day; p<0.001). A slightly increased Zn intake was found in the T2 group (4.44±1.37 mg/day), but it was higher than in the C group (3.79±1.45 mg/dL) and lower than the T1 group (4.72±1.80 mg/dL) The mean differences among groups were not statistically different (p>0.05). The mean vitamin C intake in the T2 group (10.90±3.60 mg/day) was significantly higher than in the T1 and C groups 8.78±1.66 mg/day; 3.69±0.87 mg/day; p<0.001).

After 60 days of treatment, all groups increased their daily intake of Fe, Zn, and vitamin C. Daily intake of Fe significantly increased in T1 (p=0.04) and T2 (p=0.03) groups, compared to the same groups before treatment. The mean Fe intake in the T2 group (19.59±1.70 mg/day) was significantly higher than that of the T1 (10.74±2.40 mg/day; p=0.003) and C (4.74±3.43 mg/day; p=0.001) groups. The higher mean of Zn intake was found in the T2 group (5.92±2.46 mg/day) compared to the C (4.55±2.95 mg/day) and T1 (5.65±1.65 mg/day) groups, but it did not differ significantly (p=0.14). In comparison to the C group (25.22±30.55 mg/day), the mean vitamin C intake in T1 (29.56±43.76 mg/day) and T2 (41.47±40.68 mg/day) groups also did not differ significantly (p=0.73).

Table 1. Characteristics of research subjects treated with or without *Jebisa* (n=27)

Variable	C	T1	T2	P
Age (old)[a]	15.91±0.83	15.89±0.60	15.86±0.69	0.99
BW (kg)[a]	49.73±7.80	46.77±6.44	53.36±10.27	0.28
Height (m)	1.53±0.06	1.53±0.05	1.56±0.05	0.51
BMI (kg/m^2)	21.25±3.15	20.00±2.49	22.04±4.62	0.48
Hb (g/dL) [a]	9.90±0.89	10.37±0.76	10.24±0.72	0.28
- mild (10-12 g/dL)	6 (54.55%)	7 (63.64%)	7 (63.64%)	0.37
- moderate (8-10 g/dL)	5 (45.45%)	4 (36.36%)	4 (36.36%)	
Egg allergy	1 (9.09%)	1 (11.11%)	0 (0%)	0.70
Seafood allergy	2 (18.18%)	2 (22.22%)	1 (14.29%)	0.93
Parent's Income (IDR)				
Father				
< regional minimum salary	7 (63.64%)	7 (77.78%)	3 (42.86%)	0.39
≥ regional minimum salary	4 (36.36%)	2 (22.22%)	4 (57.14%)	
Mother				
< regional minimum salary	11 (100%)	9 (100%)	5 (71.43%)	0.04*
≥ regional minimum salary	0 (0%)	0 (0%)	2 (28.57%)	

Note: [a] Statistical test with Kruskal-Wallis and the other variables with One-Way ANOVA. * Significant value of p<0.05. C: Control; T1: Treatment 1; T2: Treatment 2

Table 2. Effects of *Jebisa* on macronutrient and fiber intake in adolescent girls with anemia (n=27)

Macronutrient and fiber intake	Day	Mean ± SD (%RDA)			P
		C (n= 11)	T1 (n= 9)	T2 (n= 7)	
Energy (kcal/day) [a]	0	943.42±303.07 (44.92%)	921.07±383.33 (43.86%)	1066.77±185.95 (50.80%)	0.41
	30	728.55±328.28 (34.69%)	911.68±297.87 (43.41%)	927.50±562.40 (44.17%)	0.27
	60	858.04±480.55 (40.86%)	1054.63±330.12 (50.22%)	1311.25±323.15 (62.44%)	0.04*
	p	0.20	0.53	0.14	
Carbohydrate (g/day)	0	123.77±48.04 (41.26%)	109.36±41.33 (36.45%)	165.37±40.37 (55.12%)	0.05*
	30	96.73±49.38 (32.24%)	189.63±36.89 (63.21%)	205.30±97.64 (68.43%)	0.002*
	60	100.33±54.93 (33.44%)	195.24±70.71 (65.08%)	275.20±48.19 (91.73%)	<0.001**
	p	0.41	0.005*	0.02*	
Protein (g/day) [a]	0	34.98±11.19 (53.82%)	34.87±15.99 (53.65%)	31.63±12. 01 (48.66%)	0.72
	30	23.48±9.92 (36.12%)	28.65±12.89 (44.08%)	30.33±14.23 (46.66%)	0.67
	60	33.88±15.51 (52.12%)	37.68±11.84 (57.97%)	39.92±15.61 (61.42%)	0.54
	p	0.06	0.41	0.49	
Fat (g/day) [a]	0	34.28±11.05 (48.97%)	38.29±24.68 (54.70%)	31.20±11.95 (44.57%)	0.91
	30	27.51±17.56 (39.30%)	29.02±20.61 (41.46%)	31.37±22.29 (44.81%)	0.94
	60	35.85±30.05 (51.21%)	39.16±11.08 (55.94%)	39.78±18.74 (56.83%)	0.60
	p	0.36	0.25	0.53	
Fiber (g/day) [a]	0	5.53±3.19 (18.43%)	4.47±2.24 (14.90%)	7.86±1.76 (26.20%)	0.06
	30	4.57±2.16 (18.23%)	5.34±1.87 (17.80%)	6.13±2.11 (20.43%)	0.23
	60	3.98±3.66 (13.27%)	6.67±3.77 (22.23%)	8.88±3.23 (29.60%)	0.01*
	p	0.35	0.41	0.22	

Note: [a] Statistical test with Kruskal-Wallis and the other variables with One-Way ANOVA. * Significant value of p<0.05 and ** significant value of p<0.001. C: Control; T1: Treatment 1; T2: Treatment 2

***Jebisa* consumption increased Hb levels in adolescent girls with anemia.**

Hemoglobin (Hb) levels are a crucial indicator for the assessment of anemia (Figure 2 and Table 4). The mean Hb levels increased in all groups: C (10.59±1.61 g/dL), T1 (10.90±1.42 g/dL), and T2 (10.60±0.61 g/dL) groups after 30 days of treatment. However, the T1 group (11.44±2.01 g/dL) had higher mean Hb levels than that of the C (11.04±1.92 g/dL) and T2 (10.89±0.67 g/dL) groups after 60 days of treatment, which did not differ significantly (p>0.05). Table 4 indicated that some female adolescents in the C (36.36%) and T1 (55.56%) groups had normal Hb levels after 60 days of treatment. Only two female adolescents in the C group (18.18%) and one female adolescent in the T1 group (11.11%) showed increased Hb levels following 30 days of treatment. At the end of treatment, only female adolescents with mild anemia in both C and T1 groups showed improved anemia, resulting in normal Hb levels. One female adolescent in the C group, however, exhibited moderate anemia at the outset and subsequently transitioned to mild anemia. Notably, the T2 group did not demonstrate any improvement in anemia, yet the increased Hb levels among the groups did not differ significantly (p<0.05).

Table 3. Effects of *Jebisa* on micronutrient intake in adolescent girls with anemia (n=27)

Micronutrient intake	Day	Mean ± SD (%RDA)			P
		C (n=11)	T1 (n=9)	T2 (n=7)	
Fe (mg/day) [a]	0	5.11±1.82 (34.07%)	9.82±1.45 (65.47%)	4.94±2.08 (32.93%)	0.75
	30	3.69±0.87 (24.60%)	8.78±1.66 (58.53%)	10.90±3.60 (72.67%)	<0.001**
	60	4.74±3.43 (31.60%)	10.74±2.40 (71.60%)	19.59±1.70 (130.60%)	<0.001**
	p	0.22	0.04*	0.03*	
Zn (mg/day) [a]	0	4.44±1.67 (49.33%)	5.00±2.55 (55.56%)	4.07±1.04 (45.22%)	0.98
	30	3.79±1.45 (42.11%)	4.72±1.80 (52.44%)	4.44±1.37 (49.33%)	0.48
	60	4.55±2.95 (50.56%)	5.65±1.65 (62.78)	5.92±2.46 (65.78%)	0.14
	p	0.63	0.42	0.29	
Vitamin C	0	32.07±45.71 (42.76%)	21.72±24.37 (28.96%)	28.39±20.24 (37.85%)	0.59
(mg/day) [a]	30	3.69±0.87 (4.92%)	8.78±1.66 (11.71%)	10.90±3.60 (14.53%)	<0.001**
	60	25.22±30.55 (33.63%)	29.56±43.76 (39.41%)	41.47±40.68 (55.29%)	0.73
	p	0.09	0.68	0.12	

Note: [a] Statistical test with Kruskal-Wallis and others with One-Way ANOVA. * Significant value of p<0.05 and ** significant value of p<0.001. C: Control; T1: Treatment 1; T2: Treatment 2

Table 4. Effect of *Jebisa* on Hb levels in adolescent girls with anemia (n=27)

Day	Hb levels	C (n=11)	T1 (n=9)	T2 (n=7)	P
0	Moderate	5 (45.45%)	4 (36.36%)	4 (36.36%)	0.29
	Mild	6 (54.55%)	7 (63.64%)	7 (63.64%)	
30	Moderate	4 (36.36%)	3 (33.33%)	1 (14.29%)	0.52
	Mild	5 (45.45%)	5 (55.56%)	6 (85.74%)	
	Normal	2 (18.18%)	1 (11.11%)	-	
60	Moderate	3 (27.27%)	3 (33.33%)	1 (14.29%)	0.60
	Mild	4 (36.36%)	1 (11.11%)	6 (85.74%)	
	Normal	4 (36.36%)	5 (55.56%)	-	

Note: C: Control; T1: Treatment 1; T2: Treatment 2

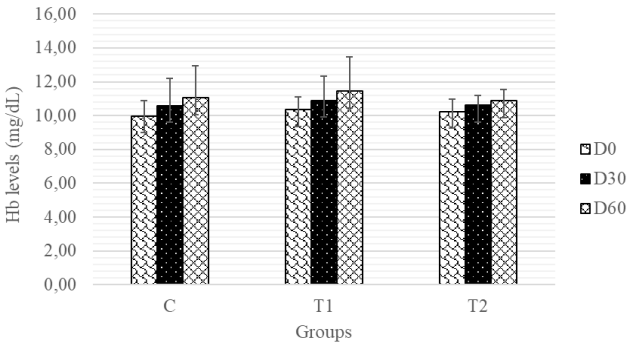

Figure 2. Effect of *Jebisa* on Hb levels in adolescent girls with anemia

***Jebisa* consumption increased the erythrocyte indexes in adolescent girls with anemia.**

Erythrocyte indexes (MCH, MCHC, and MCV ratio) were also evaluated in all groups (Table 5) to confirm anemia etiology. The mean MCV in the T2 group (76.43±5.22 fL) was lower than that of the C (77.45±8.89 fL) and T1 (77.56±8.60 fL) groups, but it did not differ significantly (p= 0.96). The highest MCH and MCHC were observed in the T1 group (24.61±3.82 pg; 31.60±1.65 g/dL) compared to the other groups before treatment, but all mean differences were not significant (p>0.05). The highest erythrocyte indexes were observed in the T1 group compared to the other groups, but it was not significantly different (p=0.66; p=0.76; p=0.48, respectively) following 30 days of treatment. After 60 days of treatment, erythrocyte indexes declined in all groups, returning to levels comparable to those observed before treatment. The decreased MCHC in all groups was significantly lower than 30 days of treatment (p=0.006; p=0.01; p=0.03, respectively).

Discussion

This study evaluated the effects of jelly consumption containing 18.52 g and 37.04 g SSF on dietary intake and hematological profile in adolescent girls with anemia. Consumption of both doses of *Jebisa* three times per week for 60 days significantly increased the daily intake of energy, carbohydrates, fibers, and Fe but did not increase the daily intake of proteins, fats, Zn, and vitamin C. Furthermore, the mean Hb levels increased, but it was not significant. Interestingly, a higher concentration of SSF increased Hb levels from moderate to mild anemia (6: 85.74%), and only one adolescent girl (14.29%) remained in the moderate anemia category. In contrast, 5 adolescent girls had normal Hb levels (55.56%), and 1 (11.11%) adolescent girl had mild anemia, while 3 (33.33%) adolescent girls remained in the moderate anemia category after consuming a lower concentration of SSF in the *Jebisa*. Surprisingly, *Jebisa* consumption had minor effects on MCV, MCH, and MCHC. These findings underscore the encouraging impact of *Jebisa* consumption on Hb levels, providing a strong motivation for further research and application that *Jebisa* consumption may become a supplementary food for anemia in adolescent girls.

Table 5. Effect of *Jebisa* on erythrocyte indexes in adolescent girls with anemia (n=27)

Erythrocyte indexes	Day	Mean ± SD			P
		C (n=11)	T1 (n=9)	T2 (n=7)	
MCV (fL)	0	77.45±8.89	77.56±8.60	76.43±5.22	0.96
Normal: 80-100 fL	30	77.91±9.89	80.33±8.52	76.57±5.16	0.66
	60	74.82±9.64	77.11±6.21	72.57±4.58	0.50
	p	0.71	0.65	0.26	
MCH (pg)[a]	0	23.87±3.63	24.61±3.82	23.27±1.79	0.77
Normal: 27-31 pg	30	26.70±5.19	27.83±4.15	26.73±3.91	0.76
	60	23.45±4.79	24.47±3.48	22.54±1.71	0.52
	p	0.18	0.17	0.01*	
MCHC (g/dL)[a]	0	30.73±1.74	31.60±1.65	30.44±0.54	0.17
Normal: 32-36 g/dL	30	33.98±2.62	34.57±2.08	32.99±2.45	0.48
	60	31.09±2.62	31.63±2.35	31.06±0.97	0.77
	p	0.006*	0.01*	0.03*	

Note: [a] Statistical test with Kruskal-Wallis and the other variables with One-Way ANOVA. * Significant value of $p<0.05$. C: Control; T1: Treatment 1; T2: Treatment 2

Based on the calculation of Fe ingredients in *Jebisa* with a higher concentration of SSF (37.04 g), it is adequate to support Hb synthesis in the human body. Our data showed that the mean Fe intake in adolescent girls with anemia increased approximately four-fold (19.59±1.70 mg/day) compared to the mean Fe intake before *Jebisa* consumption. The low intake of Fe in those adolescent girls is probably caused by the lack of a variety of foods rich in Fe because their monthly parents' income is lower than the regional minimum salary in Sukoharjo Regency (Table 1). Adding SSF into plain jelly will provide affordable supplementary food using natural ingredients from Indonesia. However, SSF dominantly contains ferric (Fe^{3+}) ions, which should be converted into ferrous (Fe^{2+}) ions in the presence of vitamin C and can be absorbed in the small intestine (Florez and Alborzinia 2021). In addition, the absorption rate of SSF is lower than Fe-rich foods derived from animals (35%) (Piskin et al. 2022).

Even though *Jebisa* has a beneficial effect on daily Fe intake, the daily intake of proteins (39.92±15.61 g/day) and vitamin C (41.47±40.68 mg/day) remained lower than the recommended dietary allowances (46 g/day and 75 mg/day, respectively) (Keats et al. 2018; National Institutes of Health 2021). This is most likely due to the low protein and vitamin C-rich foods such as meat, poultry products, fish, vegetables, and fruits since their parent's income is lower than the regional minimum salary in Sukoharjo Regency. This finding was similar to a recent study, indicating daily vegetable consumption is positively related to nutritional status and Hb levels in adolescent girls (Ilmiyati et al. 2023). This nutrient deficiency also plays a vital role in iron deficiency anemia, which can interfere with the heme formation process and the Hb formation (Adilah et al. 2023). Therefore, the Hb levels of adolescent girls slightly increased, and they continued to still suffer from anemia.

In community-based anemic evaluation, Hb levels represent the most crucial parameter. Our data indicated that jelly consumption containing 18.52 g and 37.04 g SSF could increase Hb levels by 1.1±1.6 g/dL and 0.64±0.78 g/dL in adolescent girls with anemia. The increased Hb levels in our findings were lower than the increased Hb levels in another study after the research subjects consumed 100 g jelly containing 14.9 g SSF and 5.7 g *Moringa* leaves flour (6.17±0.63 g/ dL) (Wijayanti et al. 2021). In addition, the increase of Hb levels in our study was slightly lower than in the previous study with the administration of 7 dates and Fe tablets for 30 days, which could increase Hb levels by 1.28±0.07 mg/dL (Sari et al. 2018). Thus, adding other food ingredients such as chocolate, milk, and eggs into the *Jebisa* is required to increase protein and vitamin C levels, and adolescent girls should take the iron tablet supplementation. The genetic factor may also contribute to the pathogenesis of anemia in adolescent girls with no improvement of Hb levels (moderate anemia). A recent study reported that the AA genotype of a duodenal Cytochrome B (CYBRD1) gene polymorphism, involving the conversion of Fe^{3+} to Fe^{2+} ions, increases the higher risk of anemia, compared to the GG and GA genotypes (Ilmiyati et al. 2023).

The most common anemia in developing countries is caused by iron deficiency, characterized by low erythrocyte indexes such as MCV, MCH, and MCHC (Helmyati et al. 2023). We found that *Jebisa* consumption did not affect the erythrocyte indexes in 30 or 60 days of treatment. In contrast, our results were different from another study that administration of 1.400 mg/day of *Moringa* leaves extract with 200 mg ferrous sulfate for 3 weeks in anemic women aged 16-49 years old increased the MCH by 1.31±4.94 pg and MCHC by 2.46±2.86 g/dL (Suzana et al. 2017). Administration of 100 g cookies containing 16 g sweet basil leaves powder for 4 months could also increase MCV by 1.34 fL, MCH by 1.14 pg, and MCHC by 1.67 g/dL in anemic adolescent girls (Akbar et al. 2024). Administration of fortified chocolate biscuits with iron sulfate for 10 weeks could increase MCV by 2.4±0.2 fL, MCH by 1.7±0.6 pg, and MCHC by 1.1±0.8 g/dL in Mexican schoolchildren with anemia (Quintero-Gutiérrez et al. 2016). Female adolescents with anemia who consumed 2×15 ml/day of date syrup and bee pollen for 14 days could increase MCV by 9.07±10.46 fL, MCH by 3.60±3.88 pg,

and MCHC by 1.25±1.66 g/dL (Mony et al. 2022). There were two reasons why *Jebisa* did not affect the erythrocyte indexes. The Fe ion in *Jebisa* from snake fruit seeds has lower Fe absorption than that from animal products (Shubham et al. 2020; Piskin et al. 2022). Secondly, the adolescent girls with moderate anemia were probably unresponsive to the oral Fe since the anemic adolescent girls in the control group who received oral iron tablets also had their erythrocyte indexes remain the same (Table 5).

This study recognizes several limitations because our main findings had limited beneficial effects on nutrient intake and hematology profiles. *Jebisa* in this study consisted of SSF and plain jelly but did not contain Fe^{2+} ions and proteins derived from milk, chocolate, and egg. Theoretically, Fe^{2+} ion absorption is easier than Fe3+ ion absorption, which requires vitamin C to convert into Fe^{2+} ions. The erythrocyte indexes remained unchanged after *Jebisa* consumption in adolescent girls with anemia. We speculated that the genetic factor also contributed to the pathogenesis of anemia in adolescent girls in Sukoharjo Regency because those in the control group also had minor increases in Hb levels and erythrocyte indexes.

In conclusion, regular consumption of *Jebisa* containing SSF increased daily intake of energy, carbohydrates, fibers, Fe, and Hb levels. This does not affect protein and vitamin C intake and the erythrocyte indexes in adolescent girls with anemia. In the future, it is hoped that *Jebisa* can be used as an additional food for anemia with other ingredients of iron sources, such as milk, chocolate, and egg. Therefore, to ascertain the efficacy of the food supplementation, it is essential to assess the hepcidin and matriptase 2 levels and genotype of the CYBRD1 gene. It is also important to know whether *Jebisa* consumption can enhance Hb levels and erythrocyte indexes.

ACKNOWLEDGEMENTS

The authors would like to express their gratitude to the principals and their staff of senior high schools (SMAN) of 1 Weru, Nguter, Kartasura, Mojolaban, and 3 Sukoharjo of Sukoharjo Regency, Central Java, Indonesia, for their kind permission to conduct this study. The authors would also like to thank the Rahanu Clinic Laboratory, Karanganyar Regency, for their assistance in examining Hb levels and erythrocyte indexes. We also gratefully acknowledge the support of Universitas Sebelas Maret, Central Java, which has provided us with a Research Group Grant Number 260/UN27.22/HK.07.00/2021.

REFERENCES

Adilah LH, Syafiq A, Sukoso S. 2023. Correlation of anemia in pregnant women with stunting incidence: A review. Indones J Multidiscip Sci 2: 3155-3169. DOI: 10.55324/ijoms.v2i9.545.

Akbar FN, Mahmood S, Mueen-ud-din G, Khalid W, Khalid MZ, Aziz Z, Alfarraj S, Ansari MJ, Madilo FK. 2024. A randomized controlled trial of sweet basil leaf powder-enriched cookies for anemia management in adolescent girls. Food Sci Nutr 12 (6): 4321-4329. DOI: 10.1002/fsn3.4098.

Ariendha DSR, Handayani S, Pratiwi YS. 2022. The effect of *Moringa* leaf *cilok* supply on hemoglobin levels of female adolescents with anemia. Glob Med Heal Commun 10: 63-68. DOI: 10.29313/gmhc.v10i1.8951.

Aryani VDK, Muthmainah M, Nuhriawangsa AMP. 2023. Cava smoothie as an adjuvant in iron supplementation can increase hemoglobin levels and erythrocyte indices in anemic adolescent girls. Media Gizi Indonesia 18: 188-200. DOI: 10.20473/mgi.v18i3.188-200.

Badan Pusat Statistik. 2023. Produksi Tanaman Buah-Buahan. www.bps.go.id/id/statistics-table/2/NjIjMg==/produksi-tanaman-buah-buahan.html. [Indonesian]

Budiyatri R, Anjani G, Legowo AM, Syauqy A, Limijadi EKS. 2024. The effect of *dadih* for the prevention of iron deficiency anemia in adolescent girls 12-15 years old. J AcTion 9: 91-99. DOI: 10.30867/action.v9i1.1527.

Charan J, Kaur R, Bhardwaj P, Singh K, Ambwani SR, Misra S. 2021. Sample size calculation in medical research: A primer. Ann Natl Acad Med Sci 57: 74-80. DOI: 10.1055/s-0040-1722104.

El-Tahan NR, Alfky NAA. 2016. Effect of iron and Vitamin C fortified candies on the iron status of early teenager. Intl J Adv Res 4: 6-11. DOI: 10.21474/IJAR01/100.

Engidaw MT, Wassie MM, Teferra AS. 2018. Anemia and associated factors among adolescent girls living in Aw-Barre refugee camp, Somali regional state, Southeast Ethiopia. PLoS One 13: 0205381. DOI: 10.1371/journal.pone.0205381.

Febyawati HFA, Indarto D, Handayani S. 2023. Nutritional analysis of aqueous extract of snake fruit seeds (*Salacca edulis* Reinw) for development of anemia treatment. Proc Intl Conf Nurs Heal Sci 4: 297-302. DOI: 10.37287/picnhs.v4i1.1818.

Florez AF, Alborzinia H. 2021. Ferroptosis: Mechanism and diseases. In: Dong H, Radeke HH, Rezaei N, Steinlein O, Xiao J, Rosenhouse-Dantsker A, Gerlai R (eds). Advances in Experimental Medicine and Biology. Springer Nature, Switzerland. DOI: 10.1007/978-3-030-62026-4.

Helmyati S, Syarifa CA, Rizana NA, Sitorus NL, Pratiwi D. 2023. Acceptance of Iron Supplementation Program Among Adolescent Girls in Indonesia: A Literature Review. Amerta Nutr. DOI: 10.20473/amnt.v7i3SP.2023.50-61.

Ilmiyati L, Indarto D, Wasita B. 2023. Anemia in female adolescents at Karanganyar regency: A cross-sectional study associated with polymorphism of duodenal cytochrome B gene and daily consumptions of fruits and vegetables. Nutr Health 13: 2601060231201891. DOI: 10.1177/02601060231201891.

Indarto D, Pramestiyani M, Natasia K. 2023. Proses Fraksinasi Ekstrak Biji Salak Pondoh (*Salacca edulis Reinw*). Paten Sederhana dengan IDS 000005559. https://pdki indonesia.dgip.go.id/detail/d62ec34a72b30af5bd41f07a126a9a5b769401841559731a511a4524df5b8dbc?nomor=S00202107. [Indonesian]

Indarto D, Susanti T, Nugraheni M, Melati D, Ristanti I. 2022. Metode Pembuatan Jeli Biji Salak Pondoh (*Salacca edulis* Reinw) sebagai Sumber Bahan Pangan untuk Anemia. Paten Sederhana Dengan IDS 000005116. https://pdki-indonesia.dgip.go.id/detail/243d76272193723639a910f0e0549580c6493ed52bc3d72527eab505eb24fcf5?nomor=SID201905891&type=patent&keyword=Metode%20pembuatan%20jeli%20biji%20salak%20pondoh%20(Salacca%20edulis%20reinw). [Indonesian]

Keats EC, Rappaport AI, Shah S, Oh C, Jain R, Bhutta ZA. 2018. The dietary intake and practices of adolescent girls in low-and middle-income countries: A systematic review. Nutrients 10: 1978. DOI: 10.3390/nu10121978.

Kementerian Kesehatan Republik Indonesia (Kemenkes RI). 2023. Survei Kesehatan Indonesia (SKI) dalam Angka. Kementerian Kesehatan RI, Jakarta. [Indonesian]

Kemenkes RI. 2020. Peraturan Menteri Kesehatan Republik Indonesia Nomor 2 Tahun 2020 Tentang Standar Antropometri Anak. Kementerian Kesehatan RI, Jakarta. [Indonesian]

Kemenkes RI. 2017. Petunjuk Teknis Pemberian Makanan Tambahan (Balita-Ibu Hamil-Anak Sekolah). Kementerian Kesehatan RI, Jakarta. [Indonesian]

Kemenkes RI, Riset Kesehatan Dasar (Riskesdas). 2018. Hasil Utama Riset Kesehatan Dasar 2018. Kementerian Kesehatan RI. Badan Penelitian dan Pengembangan. 2018. Available from: https://www.litbang.kemkes.go.id/laporan-riset-kesehatan-dasar-riskesdas/. [Indonesian]

Kendrick KL, Codling K, Muslimatun S, Pachon H. 2015. The contribution of wheat flour fortification to reducing anemia in

Indonesia. Eur J Nutr Food Saf 5: 446-447. DOI: 10.9734/EJNFS/2015/20904.

Kumoro AC, Alhanif M, Wardhani DH. 2020. A critical review on tropical fruits seeds as prospective sources of nutritional and bioactive compounds for functional foods development: A case of Indonesian exotic fruits. Intl J Food Sci 2020: 40511475. DOI: 10.1155/2020/4051475.

Landim LADSR, Pessoa MLDSB, Brandão ADCAS, Morgano MA, Araújo MADM, Rocha MDM, Arêas JAG, Moreira-Araújo RSDR. 2016. Impacto de dos galletas diferentes enriquecidas con hierro en el tratamiento de la anemia en niños en edad preescolar en Brasil. Nutr Hosp 33: 1142-1148. DOI: 10.20960/nh.579.

Mazumdar P, Pratama H, Lau SE, Teo CH, Harikrishna JA. 2019. Biology, phytochemical profile and prospects for snake fruit: An antioxidant-rich fruit of South East Asia. Trends Food Sci Technol 91: 147-158. DOI: 10.1016/j.tifs.2019.06.017.

Megawati M, Sudargo T, Susetyowati. 2023. The effect of jelly candy snake fruit and banana with ferrous fumarat fortified using nano technology in adolescent female at junior high school. Pharmacogn J 15: 1150-1155. DOI: 10.5530/pj.2023.15.209.

Mony B, Sartini S, Hadju V, Usman AN, Sinrang AW, Widaningsih Y. 2022. The effect of combination syrup of dates (*Phoenix dactilyfera*) and bee pollen on erythrocyte index in female adolescents with anemia. Intl J Health Sci 6: 454-464. DOI: 10.53730/ijhs.v6ns6.9472.

Mostafa HS. 2023. Formulation and evaluation of iron-rich chocolate spread from sugarcane syrup and sunflower seeds. J Food Qual 2023: 9531768. DOI: 10.1155/2023/9531768.

National Institutes of Health. 2021. Vitamin C: Fact Sheet for Health Professionals. https://ods.od.nih.gov/factsheets/VitaminC-HealthProfessional/.

Petry N, Olofin I, Hurrell RF, Boy E, Wirth JP, Moursi M, Angel MD, Rohner F. 2016. The proportion of anemia associated with iron deficiency in low, medium, and high human development index countries: A systematic analysis of national surveys. Nutrients 8: 693. DOI: 10.3390/nu8110693.

Piskin E, Cianciosi D, Gulec S, Tomas M, Capanoglu E. 2022. Iron absorption: Factors, limitations, and improvement methods. ACS Omega 7: 20441-20456. DOI: 10.1021/acsomega.2c01833.

Quintero-Gutiérrez AG, González-Rosendo G, Pozo JP, Villanueva-Sánchez J. 2016. Heme iron concentrate and iron sulfate added to chocolate biscuits: Effects on hematological indices of Mexican Schoolchildren. J Am Coll Nutr 35 (6): 544-551. DOI: 10.1080/07315724.2015.1060875.

Rahayu D, Indarto D, Yudhani RD, Kusumawati R. 2017. Iron deficiency is the main cause of anemia in female students of secondary schools in Sukoharjo Regency with no polymorphism of Transferrin Receptor 1. Adv Heal Sci Res 10: 161-164. DOI: 10.2991/ichlas-17.2017.41.

Sani. 2014. Pengembangan Puding Instan Tinggi Fe sebagai Makanan Selingan untuk Remaja Putri. [Thesis]. Institut Pertanian Bogor, Bogor. [Indonesian]

Sari A, Pamungkasari EP, Dewi YLR. 2018. The addition of dates palm (*Phoenix dactylifer*a) on iron supplementation (Fe) increases the hemoglobin level of adolescent girls with anemia. Bali Med J 7: 356-360. DOI: 10.15562/bmj.v7i2.987.

Shubham K, Anukiruthika T, Dutta S, Kashyap AV, Moses JA, Anandharamakrishnan C. 2020. Iron deficiency anemia: A comprehensive review on iron absorption, bioavailability and emerging food fortification approaches. Trends Food Sci Technol 99: 58-75. DOI: 10.1016/j.tifs.2020.02.021.

Suzana D, Suyatna FD, Azizahwati, Andrajati R, Sari SP, Mun'im A. 2017. Effect of *Moringa oleifera* leaves extract against hematology and blood biochemical value of patients with iron deficiency anemia. J Young Pharm 9: S79-S84. DOI: 10.5530/jyp.2017.1s.20.

WHO. 2011. Haemoglobin Concentrations for the Diagnosis of Anaemia and Assessment of Severity. www.who.int/publications/i/item/WHO-NMH-NHD-MNM-11.1.

Wijayanti P, Dewi YLR, Indarto D. 2021. Consumption of jelly combination of *Salacca* seed (*Salacca zalacca*) and *Moringa* leaves flour (*Moringa oleifera*) on hemoglobin level in female adolescents with moderate anemia. Indones J Med 6: 307-314. DOI: 10.26911/theijmed.2021.06.03.08.

NUSANTARA BIOSCIENCE
Vol. 16, No. 2, pp. 219-227
November 2024

ISSN: 2087-3948
E-ISSN: 2087-3956
DOI: 10.13057/nusbiosci/n160208

The role of ginseng extracts green nanoparticles as an antioxidant on physiological parameters and fertility in male rats exposed to potassium dichromate

MOHAMMED A. HAMZA, MAYADA S. HASSAN, RANA F. MOUSA♥
College of Veterinary Medicine, University of Kerbala. Kerbala 56001, Iraq. ♥email: rana.f@uokerbala.edu.iq

Manuscript received: 18 April 2024. Revision accepted: 28 June 2024.

Abstract. *Hamza MA, Hassan MS, Mousa RF. 2024. The role of ginseng extract green nanoparticles as an antioxidant on physiological parameters and fertility in male rats exposed to potassium dichromate. Nusantara Bioscience 16: 219-227.* The toxicity of chrome ions is prevalent due to their commonly used in the industry. Some plants are useful for treating toxicity, and ginseng is one of the most known medicinal herbs worldwide and possesses numerous health benefits. The present study aims to use ginseng extract and nano ginseng particles to treat toxicity by potassium dichromate PDC in a rat's model. Therefore, the PDC-toxified rats were treated with ginseng extract and ginseng-NPs at different concentrations, and ginseng-NPs were prepared using green biosynthesis. ELISA technique was used for serum estimation of GSH, SOD, MDA, LH, FSH, and testosterone in the animals' groups. Ginseng extract and ginseng nanoparticles could alleviate the toxic effects of PDC, as indicated by lower MDA, higher levels of antioxidants (SOD and catalase), FSH, and LH-Ab compared to the PDC intoxication group. The results display the lower toxicity of MDA and Catalase parameters compared to groups 2 and 5, whereas the other parameters indicate an increase. By buffering the concentrations of the tested biomarkers in a concentration-dependent way, the nanoparticles added to the protective effects of ginseng. For PDC, ginseng extract has antioxidant and antitoxic properties. Using ginseng nanoparticles led to a concentration-dependent increase in the activity of ginseng extract.

Keywords: Extraction, ginseng, nanoparticles, potassium dichromate, toxicity

INTRODUCTION

Ginseng is a plant that is part of the family Araliaceae, and it has been for several centuries because of its numerous active ingredients (Liu et al. 2020); ginseng's multiple health benefits are noted. Investigations revealed the exceptional role of ginseng in decreasing the frequency of diabetes, high triglycerides, high blood pressure, tumors, pain, and other psychological problems (Majid 2019). Ginseng is not just any herb; it has multiple pharmacological effects, making it unique among its peers (Park et al. 2019). Ginseng has been found effective in many diseases, not specific to any particular organ but those affecting the entire system, including issues related to the cardiovascular system, hormonal imbalances, immunity weaknesses, menopausal discomforts, and reproductive anomalies (Park et al. 2017); research indicates that ginseng has a visible impact on skin health, showing how an organ-specific benefit is manifested due to its use (Ahn et al. 2021). The active components of ginseng contribute significantly to its benefits; for instance, reductase degradation is one pathway at the endoplasmic reticulum (Dong et al. 2021). Ginseng modulates several intracellular pathways by acting on cells' genomic and non-genomic signals through surface interactions with receptors like estrogen or growth factor-induced receptors. Structurally similar to 17-β-estradiol, ginseng attaches itself to different nuclear receptors, facilitating cellular functions like PCNA expression or estrous behavior regulation (Seghinsara et al. 2019; Saadi et al. 2024). Therefore, acting as an anti-stress agent along with other properties like anti-aging and antioxidant capabilities, ginseng also modulates follicular development while affecting sex hormone levels, thus controlling inflammation plus oxidative stress in this time frame (Chen et al. 2022; Mohammed et al. 2023). Prooxidants and antioxidants coexist peacefully and unharmed in a constant state (Fan et al. 2022). Numerous investigations have indicated that SOD significantly delays Nitric Oxide (NO) chemical inactivation. This results in endothelial and mitochondrial dysfunction and inhibits the production of nitrates (Gaur et al. 2021). Due to its many toxicities, chromium risks human and animal health (Fukai and Ushio-Fukai 2011). Hexavalent chromium undergoes an intracellular conversion to trivalent chromium, which results in reactive oxygen species and their deleterious effects on tissue and a range of cellular processes (Kawanish et al. 2002). Hexavalent chromium is professionally exposed to around 500,000 persons globally, and hexavalent chromium-contaminated water is a global issue (Patlolla et al. 2009). Potassium dichromate ($K_2Cr_2O_7$) is a chemical widely used in many sectors and is soluble in hexavalent chromium. PDC is categorized as hexavalent chromium, a type of environmental pollution that may be linked to lower male rat fertility. PDC can be harmful to reproduction by lowering blood levels of LH, testosterone, and sperm motility, as well as the quantity of epididymal sperm. Furthermore, spermatogonial tissue was damaged by the PDC treatment; this was demonstrated by a

marked increase in cell layer thickness, the presence of vacuoles, and bleeding in the stromal cells (Arivarasu et al. 2008).

Therefore, combining the fields of nanotechnology with biotechnology, nanobiotechnology focuses on using nanoparticles to solve biological problems in new and creative ways. Furthermore, drug delivery, cancer treatment, and other biological uses depend heavily on nanoparticles. Recent developments in the design and manufacturing of nanomaterials have created new opportunities to manipulate the size of molecules to alter their effect, particularly in immunity and anticancer activity. The current work intends to alleviate PDC toxicity in a rat model using ginseng extract and nano ginseng particles. This study aimed to reduce the toxicity of PDC in a rat by using ginseng extract and tiny ginseng particles.

MATERIALS AND METHODS

Alcoholic extraction of ginseng

This study used air-dried and ground ginseng material (100 g as a sample) using the method described by (Sultana et al. 2009). An entirely different experiment used 500 mL of liquid methanol (methanol: water, 80% v/v) to remove impurities for 8 hours using Soxhlet extraction on a water bath. The extract was also made stronger with a rotating evaporator, and the solvent was taken away at 45°C under lowered pressure. To figure out the output, the dried, pure, concentrated extract was weighed out and put in the fridge at 4°C until further needed (Bashandy et al. 2019).

Biosynthesis of Se NPs

The ginseng plant extract was used for the green biosynthesis of Se-NPs (Salem et al. 2022).

Characterization of the nanoparticles

Various techniques, including UV and FTIR, characterized the prepared nanoparticle composite.

Measuring the oxidative stress biomarkers and the sex hormones

The ready-for-use kits were used for estimating serum GSH, SOD, MDA, LH, FSH, and testosterone in the animals by using the ELISA technique purchased from Sunlong Biotech Company, China.

Experiments design

Six groups of animals were used in the study, and six male rats were used in each group as follows: 1-In Group 1, the control negative group, animals were given normal water orally daily for six weeks. 2-Animals in Group 2 (potassium dichromate group) were given 2 mg/kg of body weight of potassium dichromate intraperitoneally every day for two weeks. 3—Group 3 (Ginseng positive group): Animals were given 200 mg/kg of body weight of ginseng every day for 4 weeks. 4—Group 4 (Nano ginseng) Nano ginseng was given to animals orally once a day at a 200 mg/kg body weight dose for four weeks (Al-Mukhtar et al. 2016). Animals in Group 5 were given potassium dichromate 2 mg/kg plus one oral dose of ginseng (200 mg/kg). Six animals in group 6 were given 200 mg/kg of body weight of PDC + ginseng nanoparticles every day for four weeks (0.3 mL); seven animals in group 7 were given 200 mg/kg of body weight of potassium dichromate + ginseng nanoparticles every day for four weeks (0.1 mL).

RESULTS AND DISCUSSION

Serum biomarkers levels

Table 1 compares the amounts of blood biomarkers in rats exposed to dichromate (Group 2), ginseng extract (Group 3), and ginseng nanoparticles (Group 4). The levels in the control group (Group 1) are shown next to each other. This study found that MDA levels increased in Group 2 compared to the control group, Group 1. Along with Group 2, Groups 3 and 4 we observed less MDA and a drop in Group 2. These are the differences between the levels of blood biomarkers in rats that were exposed to dichromate (Group 2), ginseng extract (Group 3), and ginseng nanoparticles (Group 4). The first group is the reference group. The levels of serum SOD are much higher in Groups 3 and 4 than in Group 2. It is found that Group 2 has a lower amount of serum catalase than Groups 1, 3, and 4. The amount of LH-Ab is higher in Groups 3 and 4 than in Group 2. The amount of DHT in the blood is lower in Group 2 than in Groups 1, 3, and 4. Groups 3 and 4 have more serum FSH than Groups 1 and 2.

Table 1. The amounts of blood biomarkers in rats exposed to dichromate, ginseng extract, and ginseng nanoparticles

Parameter	Group1[A] Mean±SD	Group 2 [B] Mean±SD	Group 3 [C] Mean±SD	Group 4 [D] Mean±SD	F	p
MDA mmol/mL	10.3±0.96 [B, C, D]	14.52±1.12 [A, C, D]	7.18±1.68 [A,B]	6.95±1.41 [A,B]	35.683	<0.001
SOD u/mL	380.4±39.83	254.77±67.46 [C]	436.4±134.39 [B]	447±47.24 [B]	5.890	0.007
Catalase u/mL	6.05±0.67 [B]	4.55±0.76 [A, C, D]	6.53±0.77 [B]	7±0.37 [B]	12.806	<0.001
LH-Ab Iu/l	4.14±0.56	2.88±0.67 [C, D]	5.78±1.51 [B]	5.91±1.17 [B]	9.487	0.001
DHT pg/mL	342±69.07 [B]	134.2±42.04 [A, C, D]	383±22.93 [B]	386.8±28.19 [B]	36.604	<0.001
FSH ng/mL	22.7±2.08 [B, C, D]	15.15±2.19 [A, C, D]	29.02±3.37 [A,B]	29±3.29 [A,B]	27.735	<0.001

Note: [A]: Comparison with control group, [B]: Comparison with the dichromate treated group, [C]: Comparison with ginseng treated group, [D]: Comparison with ginseng-nanoparticles treated group

The ginseng juice used to treat dichromate poisoning

Therefore, to evaluate how ginseng affects PDC's toxicity, the group that got PDC (Group 2) was compared to the group that got PDC and ginseng extract (Group 5), as shown in Table 2. The amount of SOD in the blood is higher in Group 5 than in Group 2. Also, there is a big difference between Group 5 and Group 2 in the levels of DHT. There are also significant differences between the groups in the levels of MDA, SOD, LH-Ab, and FSH.

Toxicity of dichromate, ginseng, and ginseng-NP

Table 3 shows the effect of ginseng nanoparticles at two concentrations, 0.3 mL (Group 6) and 0.15 mL (Group 7) of nanoparticle solution, on the toxicity of PDC compared with Group 2, which applied only by PDC. The results show that ginseng-NP, at two concentrations, has no significant effect on the levels of MDA, catalase, and LH-Ab. Serum SOD level was increased after using ginseng-NPs at a concentration of 0.3 mL. While the level of DHT and FSH are increased after adding ginseng-NPs at concentrations of 0.15 and 0.3 mL.

Histopathologic results

A control rat's epididymis (testes), which showed normal histopathological traits under a microscope (Figure 1), revealed important information about the basic properties of healthy testicular tissue. This finding shows how important it is to keep the structure of seminiferous tubules and Leydig cells intact for healthy spermatogenesis and testicular function, which is in line with earlier research by Adamczewska et al. (2022). These researchers stressed how important these normal histological features are for men's reproductive health. The microscope study of testicular and epididymal tissue slices from animals given potassium dichromate (Figure 2) showed clear histopathological changes that showed the testicles and epididymis were toxic. This study observed many changes, including tubules getting smaller, tubules becoming empty, interstitial blood vessels getting clogged, germinal epithelia dying, areas of epithelium necrosis, changes in tubular epithelia, dying spermatogonia, pyknotic nuclei, low spermatic density, and interstitial spaces getting bigger. According to the current research, there is no compelling evidence to support a significant influence of ginseng on tubular epithelial changes and pyknotic nuclei. Consequently, it is reasonable to conclude that ginseng does not exhibit a clear and direct effect on these cellular processes. Based on these results, potassium dichromate may have damaged the male reproductive organs greatly. Researchers have already evaluated how hexavalent chromium, which includes potassium dichromate, affects the function of ovaries and, by extension, men's sexual health. Multiple studies have shown that chromium compounds can change the process of spermatogenesis, which can damage the testicles and cause changes in the cells of the testicles and epididymis (Aruldhas et al. 2005; Aitken and Roman 2008). Because of this, oxidative stress has been put ahead of other possible causes, such as mitochondrial damage and changes in the normal function of the testicles, as a likely pathophysiologic process adding to chromium-induced testicular toxicity. So, these results align with what other experts said about the changes in the testicular and epididymal tissues after potassium dichromate treatment.

After examining the changes in the shape of the testicles and epididymis of male rats, the study concludes that the potassium dichromate effect should not be taken lightly. It also shows that herb amounts of nano ginseng particles are needed to lower the chance of exposure to potassium dichromate (Marouani et al. 2012).

Table 2. Treatment of toxicity of dichromate by ginseng

Parameter	Group 2 Mean±SD	Group 5 Mean±SD	F	p
MDA			1.370	0.275
mmol/mL	14.52±1.12	10.3±0.96		
SOD u/mL	254.37±66.07	380.4±39.83	<0.001	0.993
Catalase u/mL	6.05±0.67	6.37±0.7	15.504	0.004
LH-Ab Iu/l	4.14±0.56	3.32±0.76	0.965	0.355
DHT pg/mL	342±69.07	237.4±52.99	11.637	0.009
FSH ng/mL	22.7±2.08	18.04±2.74	3.387	0.103

Note: Group 2: Comparison with the dichromate-treated group, Group 5: Animals received potassium dichromate +ginseng extract

Table 3. Treatment of toxicity of dichromate by ginseng-NP

Parameter	Group 2 [A] Mean±SD	Group 6 [B] Mean±SD	Group 7 [C] Mean±SD	F	p
MDA mmol/mL	14.52±1.12	11.89±5.63	13.28±0.76	0.774	0.483
SOD u/mL	254.77±67.46 [B]	342.4±21.64 [A]	303.6±20.67	5.310	0.022
Catalase u/mL	4.55±0.76	6.17±2.47	5.37±1.66	1.039	0.384
LH-Ab Iu/l	2.88±0.67	3.6±0.48	3.25±0.78	1.517	0.259
DHT pg/mL	134.2±42.04 [B,C]	313.4±25.98 [A]	269.4±42.97 [A]	30.503	<0.001
FSH ng/mL	15.15±2.19 [B,C]	22.08±2.6 [A]	19.56±1.5 [A]	13.376	0.001

Note: [A]: Comparison with the dichromate treated group, [B]: Comparison with ginseng treated group, [C]: Comparison with ginseng-nanoparticles treated group

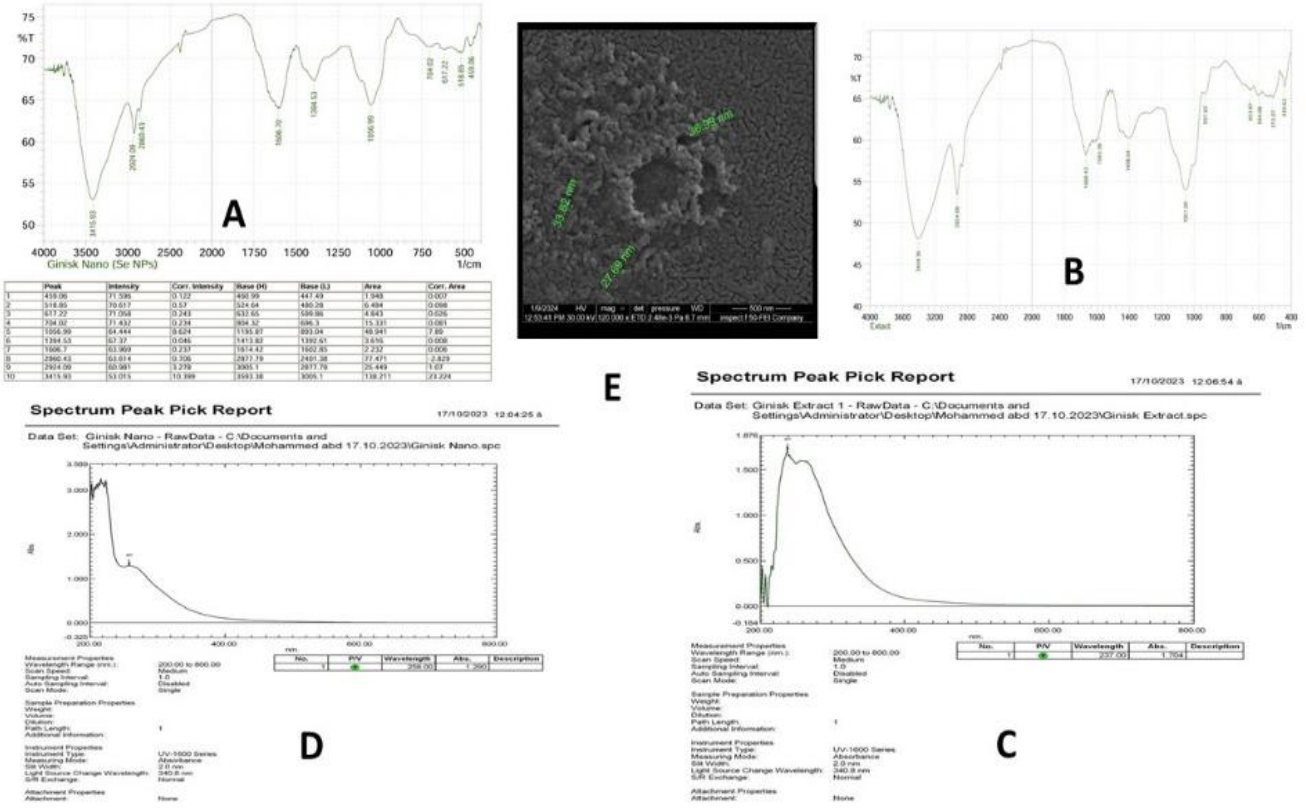

Figure 1. Characterization of ginseng nanoparticles (NPs). A. FT-IR spectrum showing functional groups of ginseng nanoparticles, B. FT-IR spectrum showing functional groups of ginseng extract, C. UV-visible spectroscope of ginseng extract, D. UV-visible spectroscope of ginseng nanoparticles, E. Scanning Electron Microscopy (SEM) shows the morphology and size of biogenic nanoparticles (NPs)

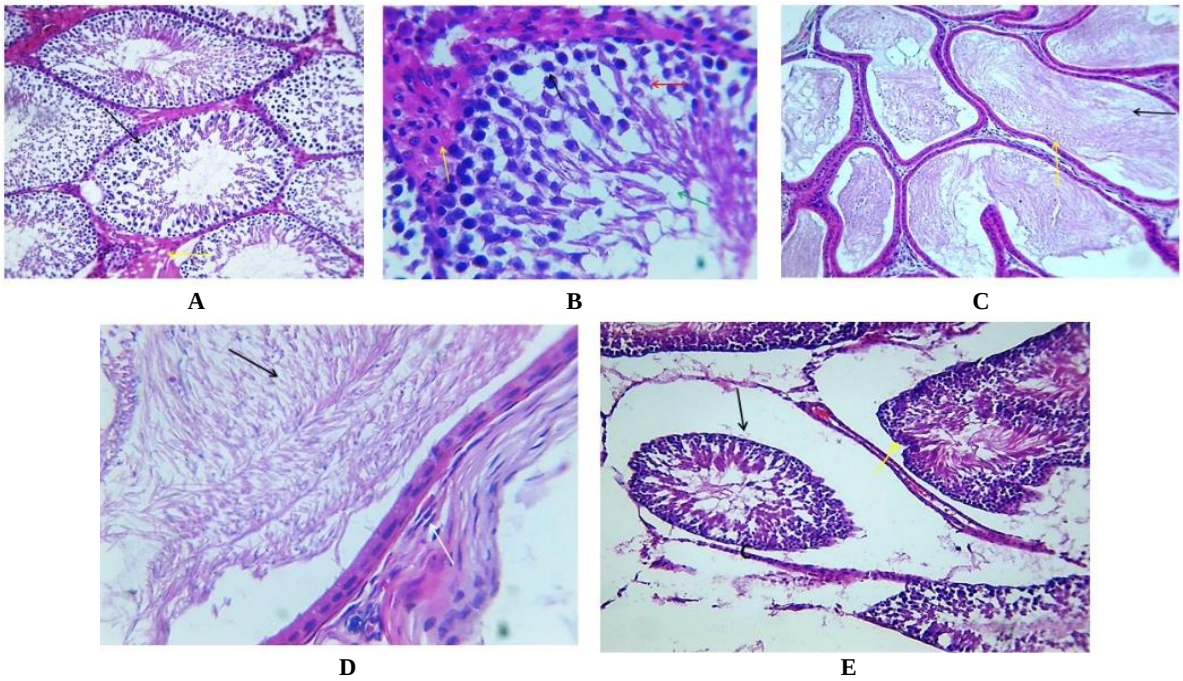

Figure 2. A-E Microscopical examination of a control rat testes and epididymis

Figure 3 shows that animals that were administered ginseng extract had good effects on the tissues in their testicles and epididymis. At 10X magnification, the testes showed normal testicular tissue shape with many blood vessels clustered between the cells. At 40X magnification, the seminiferous tubules looked normal, with wider interstitial areas and normal spermatogenesis. This shows that the ginseng extract treatment improved testicle health and the process of spermatogenesis. At 10X magnification, normal epididymal tubules with some lengthening were seen in the epididymis; there were also observed several sperms with good quality, and the spaces between the cells were getting bigger. The epididymal tubules looked normal at 40X magnification, with enough spermatic density and wider interstitial spaces. This suggests that treatment with ginseng extract may help keep the shape and quality of the epididymis normal. Previous research studies that supported the health benefits of ginseng extract on the testicles and epididymis have also been observed in this study. The study supports this result that animals' testes and epididymis looked better after treatment with ginseng (Jang et al. 2011).

The structural changes were observed in testicular and epididymal tissue sections (Figure 4). At 10X magnification, the testicular tissue showed some degradation and plenty of crowded blood vessels in the interstitial space. At 40X magnification, mild disorganization in the tube germinal epithelia and Leydig cell degeneration were seen. At 10X magnification, the epididymis changes were not too different, with some showing degeneration in the germinal epithelium and marked dilation in the interstitial spaces. These changes led to hyperplastic cellular epithelia, whereas at 40X magnification, sperm density was seen to be moderate. Much research on ginseng and its products has shown that it can affect a man's ability to reproduce, especially by observing the effects on the testicles and the epididymis (Won et al. 2014)

Moreover, some studies have shown that ginseng and its products can improve the testicles and epididymis parameters (Sawiress et al. 2011). It might be like looking into a mist to see the changes when rat testicular and epididymal tissues were treated with ginseng nanoparticles. There seems to be a mysterious combination between ginseng's bioactive parts and reproductive tissues, and more research is needed to figure out how it all works.

Figure 5 shows the changes seen under a light microscope in rats' seminiferous tubules and epididymis administered with potassium dichromate and ginseng extract. Some rats' had normal germinal epithelium, while the other tubules showed signs of degeneration and clogged interstitial blood vessels at both ends; therefore, other people had completely different situations. There were normal spermatogonia and normal spermatocytes found only in places where there was no sign of these cells' future development because they were between two areas of congestion. This information indicated an ongoing spermatogenesis process in the studied tissue sections, even though some parts did not support this activity. These results show that ginseng extract might protect testicular and epididymal cells, even with potassium dichromate. As a known poison, the fact that ginseng has positive effects when combined with other drugs (despite the negative effects of the individual drugs) may help us understand how ginseng might protect the male reproductive system.

Histological analysis of rat testes and epididymis following treatment with potassium dichromate and ginseng nanoparticles 0.3 mL (as used in Group 6) depicted marked enhancements and reversible changes in tissue morphology (Figure 6). At a magnification of 10X, the seminiferous tubules exhibited a typical structure characterized by normal interstitial spaces and Leydig cells. In comparison, at 40X magnification, the germinal epithelium appeared healthy, with spermatogonia, spermatocytes, and spermatids being normal. The findings in the epididymis also showed improvements; at 10X magnification, tubule morphology was near normalcy with a healthy spermatic population and spaces that were slightly dilated; observations with a higher magnification of 40X revealed that the epididymal tubules were indeed normal with appropriate spermatic population and orderly arrangement of tubular epithelium. These collective results point towards a positive impact of combining potassium dichromate and ginseng nanoparticles 0.3 on testicular and epididymal health, an effect which fosters development through enhancement of tissue morphology; thus, spermatogenesis occurred. Literature has previously highlighted ginseng's protective and therapeutic effects on testicular health, including protection against toxicants inducing testicular atrophy, such as TCDD (Elgharabawy and Emara 2014), corroborating our findings.

Histological examination reveals the testicular composition of potassium dichromate and ginseng nanoparticles 0.15 mL treated rat (see Figure 7), showing some tubular sloughing elements within a congested interstitial space, semi-normal. The findings from the seminiferous tubule indicate degeneration of germinal epithelia and necrosis of spermatids. At the same time, those in epididymis show significant alterations with moderate to normal populations of spermatic disarrangements plus epithelial cells' distribution along the tubules. These observations suggest that potassium dichromate and ginseng nanoparticles of 0.15 mL have a moderate protective effect on testicular and epididymal health, improving tissue morphology and spermatogenesis indices. Studies have previously demonstrated ginseng's protective and therapeutic effects on testicular health, including protection against atrophy induced by TCDD; thus, this study will evaluate WA's ameliorative effects on DM-induced male reproductive dysfunction in mice based on these positive outcomes. Results indicated WA treatment improved sperm population and motility among diabetic mice, implying potential protective roles toward testicular components, especially when considered alongside other related findings concerning alterations seen following the use of potassium dichromate coupled with ginseng nanoparticles 0.15 mL as it used in Group 7, indicating potency via protection against toxicant-induced damage: supportive literature notes high prospects for ginseng also (Al-Saadi 2017).

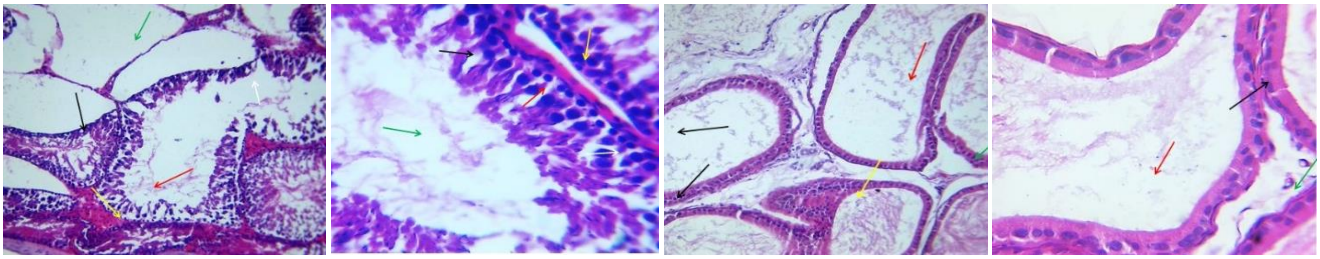

A B C D

Figure 3. A-D Microscopical examination of rat testes and epididymis after animals received potassium dichromate

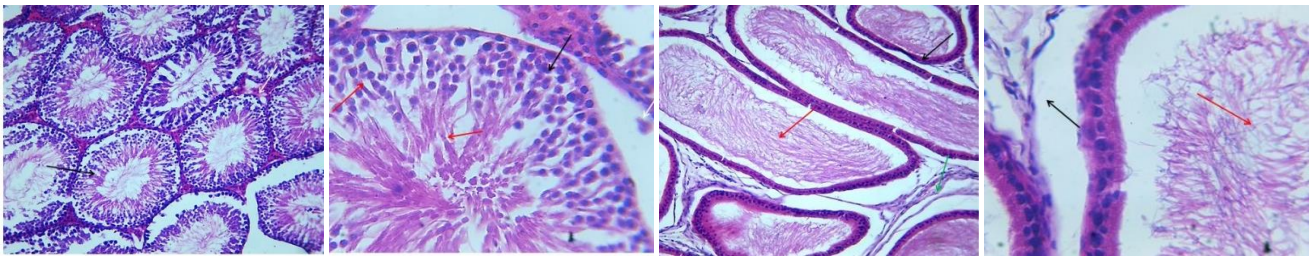

A B C D

Figure 4. A-D D Microscopical examination of rat testes and epididymis after Animals received ginseng orally.

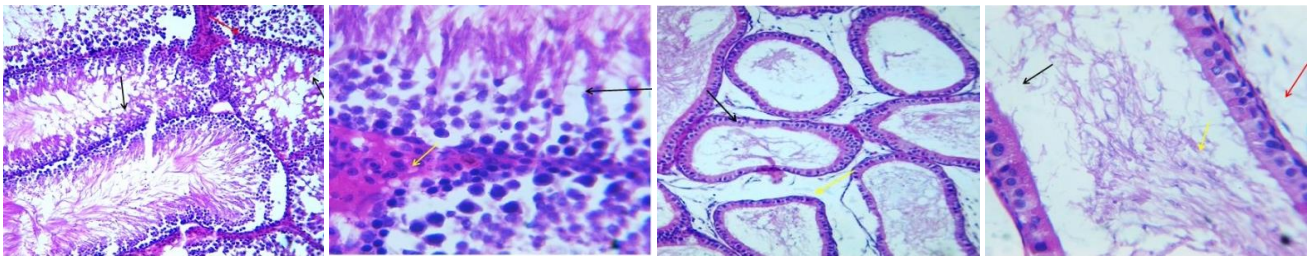

A B C D

Figure 5. A-D Microscopical examination of rat testes and epididymis after animals received nano-ginseng orally

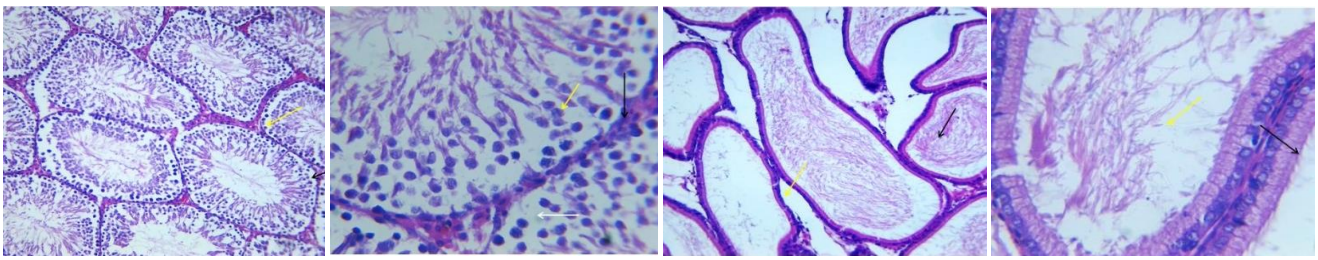

A B C D

Figure 6. A-D Microscopical examination of rat testes and epididymis after animals were administered a mixture of potassium dichromate and ginseng

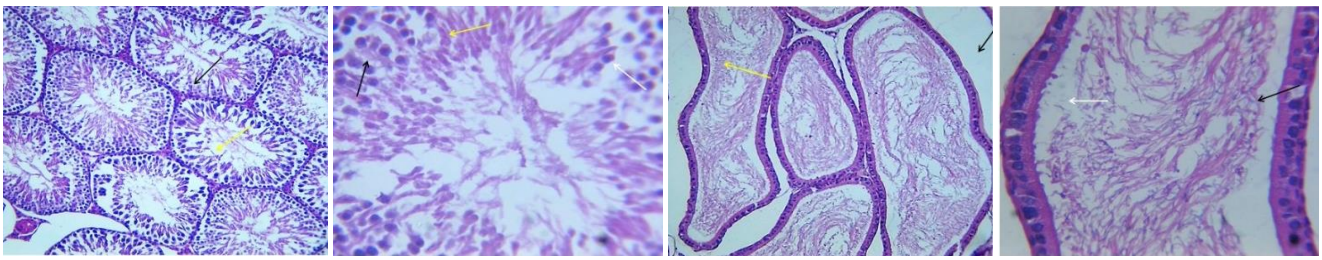

A B C D

Figure 7. A-D Microscopical examination of rat testes and epididymis after Animals received Potassium Dichromate + ginseng -NPs

Discussion

The first important result of this study is that the MDA level lowered after rats were exposed to PDC and remained low after being treated with ginseng extract and ginseng nanoparticles. This shows that these ginseng products protected the rats from the harmful effects of PDC. Some other parameters of ginseng preparation were raised amounts of LH-Ab, FSH, and DTH hormones, and SOD and catalase enzymes, which are antioxidants. These results are important for animal tests that use ginseng to protect against poisoning.

Studies in the past have shown that adding ginseng can help lower the harmful effects of tobacco. The amounts of FSH and LH were much higher after being treated with tobacco and ginseng (Faghani et al. 2022). In addition, the tissues of the group that received both nicotine and ginseng had lower levels of MDA and higher levels of SOD compared to the nicotine group; this is what Faghani et al. (2022) stated. Mekhoukhe et al. (2019) explain how carob's ability to raise testosterone levels affects Leydig cells and testosterone production. Many know PDC has a detrimental effect on testicles (Morsy et al. 2023). Researchers in a previous study found that administering rats PDC orally every day for 8 weeks caused oxidative stress in their testicles, as shown by a noticeable rise in MDA, NO, and GSSG levels. It was also seen that the PDC group had significantly lower amounts of SOD, CAT, GSH, and Car in their testicles compared to the control group. These results align with earlier research that showed how PDC-induced oxidative stress causes testes not to work properly (Marouani et al. 2017).

This study revealed that higher antioxidant levels will help eliminate free radicals that could be harmful due to potassium dichromate. These results follow the researcher found in 2018 (Ighodaro and Akinloye 2018). MDA is a steady byproduct of lipid peroxidation pathways and is generally known as an indirect sign of higher ROS production inside cells (Cherian et al. 2019). Therefore, ginseng protects folliculogenesis by changing several hormone levels in the body, encouraging cell growth, and hindering cell death through anti-oxidative effects in the ovary, such as by lowering apoptotic markers (Salem et al. 2022). Additionally, Ibrahima et al. (2018) say that ginseng keeps other endocrine glands, like the thyroid glands, from detrimental effects by PDC model rats. Previous research shows that administering ginseng to animals with benign prostatic hyperplasia lowers DHT levels in the prostate significantly. It also helps keep the balance between cell death and proliferation, which means that proliferation takes over and apoptosis is stopped (Shin et al. 2012).

The second important result was that ginseng extract made PDC less harmful. Its health benefits derive from the many useful chemicals in the plant juice. A new study shows ginseng has many useful parts, like ginsenosides, polypeptides, and carbohydrates. Ginsenosides are one of ginseng's most important active ingredients that affect the immune, circulatory, and nervous systems (Zheng et al. 2018). Furthermore, K substance derived from Panax ginseng can stop cell death, reduce inflammation, and fight free radicals. It can also protect the meiotic maturation of pig eggs from damage caused by benzo(a)pyrene (Luo et al. 2020). Additionally, ginsenoside Rb1 is another chemical found in ginseng, which has been shown to help keratinocytes move and speed up the healing of skin wounds (Shin et al. 2018).

Rb3 can also boost the antioxidant power of diabetic mice, raising the level of superoxide dismutase (SOD) in their blood and lowering the level of malondialdehyde (MDA), which is a lipid peroxidation product. This is very important to lower possible illness (Ridha and Al-Shawi 2017). Ginseng stops oxidative damage, boosts the benefits of antioxidants, and lowers the number of free radicals in rats administered by alloxan (Kim et al. 2011). Another ginseng substance, ginsenoside Rf, can help with intestinal conditions by stopping the MAPK/NF-κB signaling pathway (Ahn et al. 2016).

Table 3 shows the third important result: ginseng-NP can treat PDC poisoning by being antitoxic. The amount of ginseng-NPs has a direct relationship with this effect. NPs are very small, less than 100 nm, but have many interesting physical and chemical features. These nanoparticles are crucial because of their surface energy, that have a lot of surface atoms, few flaws, and are confined in space, which makes them nanostructures. Nanotechnology can be used in many biology studies because nanoparticles are very small and have great physicochemical qualities (Chaudhary et al. 2015). In the past few years, NPs have become very useful and hopefully promising tools in biology (McNamara and Tofail 2017). NPs merge biology, chemistry, physics, and materials science, which leads to new therapeutic materials based on nano-sized materials used in various biological settings. Because they are small, they can easily get into cells and do many useful things in biology and antioxidants without being put into other carrier systems. Since NPs are also good at transport systems, they can be used as anti-inflammatory drugs or for imaging-based diagnostics (Farhan et al. 2023) with drug carriers or bioconjugates administered using biological treatments. Additionally, NPs were widely used in drug compounds as bio-conjugate materials where they were needed for treatment.

ROS are said to be made when hexavalent chromium changes to trivalent chromium inside cells (Stohs et al. 2001). According to (El-Sakhawy et al. 2017), vasoconstriction could be caused by the breakdown of lipids. Potassium dichromate raises the amount of Nitric Oxide (NO) inside cells. This turns on nuclear factor kappa B (NF-KB), "a key activator of genes involved in inflammation, immunity, and apoptosis" that causes more apoptosis by damaging DNA and turning on p53 (Kawanishi et al. 2002). This study's oxidative stress biomarkers went down because ginseng did the same phenomenon as Jadhav and Saudagar (2014) observed. The current study demonstrated that ginseng significantly reduced MDA levels and enhanced the levels of both catalase and SOD in the treated rat groups, whether administered as an extract or a nanoformulation.

In conclusion, the activity of Ginseng extracts as an antitoxic agent for PDC combined with the antioxidant factor; when ginseng nanoparticles were used, ginseng extract increased concentration-dependent.

REFERENCES

Adamczewska D, Słowikowska-Hilczer J, Walczak-Jędrzejowska R. 2022. The fate of leydig cells in men with spermatogenic failure. Life 12 (4): 570. DOI: 10.3390/life12040570.

Ahn H, Han BC, Hong EJ, An BS, Lee E, Lee SH, Lee GS. 2021. Korean red ginseng attenuates ultraviolet-mediated inflammasome activation in keratinocytes. J Ginseng Res 45 (3): 456-463. DOI: 10.1016/j.jgr.2021.02.002.

Ahn S, Siddiqi MH, Aceituno VC, Simu SY, Yang DC. 2016. Suppression of MAPKs/NF-κB activation induces intestinal anti-inflammatory action of ginsenoside Rf in HT-29 and RAW264. 7 cells. Immunol Invest 45 (5): 439-449. DOI: 10.3109/08820139.2016.1168830.

Aitken RJ, Roman SD. 2008. Antioxidant systems and oxidative stress in the testes. Oxid Med Cell Longev 1 (1): 15-24. DOI: 10.4161/oxim.1.1.6843.

Al-Mukhtar N, Mohmmed A, Mahdi H. 2016. The effects of potassium dichromate on testes, accessory sex glands, liver and kidney in adult male rats treated with ascorbic acid. Austr J Basic Appl Sci 10 (4): 99-108.

Al-Saadi FAH. 2017. Histological study to the effect of potassium dichromate on the reproductive organs in mature rats. Tikrit J Pure Sci 22 (5): 93-97. DOI: 10.25130/tjps.v22i5.773.

Arivarasu NA, Fatima S, Mahmood R. 2008. Oral administration of potassium dichromate inhibits brush border membrane enzymes and alters antioxidant status of rat intestine. Arch Toxicol 82: 951-958. DOI: 10.1007/s00204-008-0311-0.

Aruldhas MM, Subramanian S, Sekar P, Vengatesh G, Chandrahasan G, Govindarajulu P, Akbarsha MA. 2005. Chronic chromium exposure-induced changes in testicular histoarchitecture are associated with oxidative stress: Study in a non-human primate (*Macaca radiata* Geoffroy). Hum Reprod 20 (10): 2801-2813. DOI: 10.1093/humrep/dei148.

Bashandy SAE, Ahmed-Farid OAH, Omara EA, El-Toumy SA, Salib JY. 2019. Protective effect of *Citrus reticulata* peel extract against potassium dichromate-induced reproductive toxicity in rats. Asian Pac J Reprod 8 (6): 267-275. DOI: 10.4103/2305-0500.270104.

Chaudhary RG, Tanna JA, Gandhare NV, Rai AR, Juneja HD. 2015. Synthesis of nickel nanoparticles: Microscopic investigation, an efficient catalyst and effective antibacterial activity. Adv Mater Lett 6 (11): 990-998. DOI: 10.5185/amLett.2015.5901.

Chen Z, Wang G, Xie X, Liu H, Liao J, Shi H, Chen M, Lai S, Wang Z, Wu X. 2022. Ginsenoside Rg5 allosterically interacts with P2RY12 and ameliorates deep venous thrombosis by counteracting neutrophil NETosis and inflammatory response. Front Immunol 13: 918476. DOI: 10.3389/fimmu.2022.918476.

Cherian DA, Peter T, Narayanan A, Madhavan SS, Achammada S, Vynat GP. 2019. Malondialdehyde as a marker of oxidative stress in periodontitis patients. J Pharm Bioallied Sci 11 (Suppl 2): S297-S300. DOI: 10.4103/JPBS.JPBS_17_19.

Dong J, Xia K, Liang W, Liu L, Yang F, Fang X, Xiong Y, Wang L, Zhou Z, Li C, Zhang W, Wang J, Chen D. 2021. Ginsenoside Rb1 alleviates colitis in mice via activation of endoplasmic reticulum-resident E3 ubiquitin ligase Hrd1 signaling pathway. Acta Pharmacol Sinica 42 (9): 1461-1471. DOI: 10.1038/s41401-020-00561-9.

Elgharabawy RM, Emara AM. 2014. The protective effect of *Panax ginseng* against chromium picolonate induced testicular changes. Afr J Pharm Pharmacol 8 (12): 346-355. DOI: 10.5897/AJPP2013.3822.

El-Sakhawy MA, Elyazeed GA, Mohamed MA. 2017. Histological and Immunohisto chemical studies on the submandibular salivary glands of male albino rats after hexavalent chromium and vitamin C exposure. Res J Pharm Biol Chem Sci 8 (4): 411-421.

Faghani M, Saedi S, Khanaki K, Mohammadghasemi F. 2022. Ginseng alleviates folliculogenesis disorders via induction of cell proliferation and downregulation of apoptotic markers in nicotine-treated mice. J Ovarian Res 15 (1): 14. DOI: 10.1186/s13048-022-00945-x.

Fan N, Zhang X, Zhao W, Zhao J, Luo D, Sun Y, Li D, Zhao C, Wang Y, Zhang H, Rong J.. 2022. Covalent inhibition of pyruvate kinase M2 reprograms metabolic and inflammatory pathways in hepatic macrophages against non-alcoholic fatty liver disease. Intl J Biol Sci 18 (14): 5260. DOI: 10.7150/ijbs.73890.

Farhan LO, Abed BA, Ghasaq J K, Salman IN. 2023. Insulin like growth factor binding Protein 7 as a novel diagnostic marker in Sera of Iraqi patients with acromegaly. Baghdad Sci J 20 (3(Suppl.)): 0979. DOI: 10.21123/bsj.2023.7797.

Fukai T, Ushio-Fukai M. 2011. Superoxide dismutases: Role in redox signaling, vascular function, and diseases. Antioxid Redox Signal 15 (6): 1583-1606. DOI: 10.1089/ars.2011.3999.

Gaur P, Prasad S, Kumar B, Sharma SK, Vats P. 2021. High-altitude hypoxia induced reactive oxygen species generation, signaling, and mitigation approaches. Intl J Biometeorol 65: 601-615. DOI: 10.1007/s00484-020-02037-1.

Ibrahima SS, Saidb AM, Aboubakrc M. 2018. Ameliorative effect of ascorbic acid and/or ginseng extract against thyroid gland toxicity induced by potassium dichromate in rats. J Pharmacol Clin Res 5 (1): 1-6. DOI: 10.19080/JPCR.2018.05.555655.

Ighodaro OM, Akinloye OA. 2018. First line defence antioxidants-superoxide dismutase (SOD), catalase (CAT) and glutathione peroxidase (GPX): Their fundamental role in the entire antioxidant defence grid. Alex J Med 54 (4): 287-293. DOI: 10.1016/j.ajme.2017.09.001.

Jadhav GB, Saudagar RB. 2014. Free radical scavenging and antioxidant activity of *Punica granatum* Linn. Asian J Res Pharm Sci 4 (2): 51-54. DOI: 10.52711/2231-5659.

Jang M, Min JW, In JG, Yang DC. 2011. Effects of red ginseng extract on the epididymal sperm motility of mice exposed to ethanol. Intl J Toxicol 30 (4): 435-442. DOI: 10.1177/1091581811405074.

Kawanishi S, Hiraku Y, Murata M, Oikawa S. 2002. The role of metals in site-specific DNA damage with reference to carcinogenesis. Free Radic Biol Med 32 (9): 822-832. DOI: 10.1016/S0891-5849(02)00779-7.

Kim HJ, Lee SG, Chae IG, Kim MJ, Im NK, Yu MH, Lee EJ, Lee IS. 2011. Antioxidant effects of fermented red ginseng extracts in streptozotocin-induced diabetic rats. J Ginseng Res 35 (2): 129-137. DOI: 10.5142/jgr.2011.35.2.129.

Liu H, Lu X, Hu Y, Fan X. 2020. Chemical constituents of *Panax ginseng* and *Panax notoginseng* explain why they differ in therapeutic efficacy. Pharmacol Res 161: 105263. DOI: 10.1016/j.phrs.2020.105263.

Luo ZB, Rahman SU, Xuan MF, Han SZ, Li ZY, Yin XJ, Kang JD. 2020. The protective role of ginsenoside compound K in porcine oocyte meiotic maturation failed caused by benzo (a) pyrene during in vitro maturation. Theriogenology 157: 96-109. DOI: 10.1016/j.theriogenology.2020.07.006.

Majid A. 2019. *Panax ginseng*–a review. Univ Thi-Qar J Sci 7 (1): 96-102.

Marouani N, Tebourbi O, Mahjoub S, Yacoubi MT, Sakly M, Benkhalifa M, Rhouma KB. 2012. Effects of hexavalent chromium on reproductive functions of male adult rats. Reprod Biol 12 (2): 119-133. DOI: 10.1016/S1642-431X(12)60081-3.

Marouani N, Tebourbi O, Hallègue D, Mokni M, Yacoubi MT, Sakly M, Benkhalifa M, Rhouma KB. 2017. Mechanisms of chromium hexavalent-induced apoptosis in rat testes. Toxicol Ind Health 33 (2): 97-106. DOI: 10.1177/0748233715600333.

McNamara K, Tofail SAM. 2017. Nanoparticles in biomedical applications. Adv Phys: X 2 (1): 54-88. DOI: 10.1080/23746149.2016.1254570.

Mekhoukhe A, Kicher H, Ladjouzi A, Medouni-Haroune L, Brahmi F, Medouni-Adrar S, Madani K. 2019. Antioxidant activity of carob seeds and chemical composition of their bean gum by–products. J Complement Integr Med 16 (1): 20170158. DOI: 10.1515/jcim-2017-0158.

Mohammed NUG, Gorial FI, Khaleel FM, Abed BA, Mutar SA, Farhan LO, Salman IN. 2023. Role of Human β-Defensin-3 in Rheumatoid Arthritis: An Observational Single-Center Study. Al-Rafidain J Med Sci 5 (1S): S71-S75. DOI: 10.54133/ajms.v5i1S.289.

Morsy MM, Hassan HA, Alabassery N, Ramadan RS. 2023. Selenium could alleviate potassium dichromate-induced epididymal, prostatic and seminal vesicle changes in adult rats: Potential role of inhibiting NF-κB pathway. Egypt Soc Clin Toxicol J 11 (1): 87-106. DOI: 10.21608/esctj.2023.184880.1025.

Park J, Song H, Kim SK, Lee MS, Rhee DK, Lee Y. 2017. Effects of ginseng on two main sex steroid hormone receptors: estrogen and androgen receptors. J Ginseng Res 41 (2): 215-221. DOI: 10.1016/j.jgr.2016.08.005.

Park SJ, Nam J, Ahn CW, Kim Y. 2019. Anti-diabetic properties of different fractions of Korean red ginseng. J Ethnopharmacol 236: 220-230. DOI: 10.1016/j.jep.2019.01.044.

Patlolla AK, Barnes C, Hackett D, Tchounwou PB. 2009. Potassium dichromate induced cytotoxicity, genotoxicity and oxidative stress in

human liver carcinoma (HepG2) cells. Intl J Environ Res Public Health 6 (2): 643-653. DOI: 10.3390/ijerph6020643.

Ridha DKA, Al-Shawi NN. 2017. The impacts of graded doses of pyridoxine on the biomarkers, aspartate aminotransferase, lactate dehydrogenase and total antioxidant capacity in doxorubicin-induced cardiotoxicity in female rats. Iraqi J Pharm Sci 26 (2): 12-21. DOI: 10.31351/vol26iss2pp12-21.

Saadi MT, Mohammed NUG, Abed BA, Farhan LO, Salman IN. 2024. Validity of galactin-3 in acromegaly: Comparison with traditional markers. Ir J Med Sci. DOI: 10.1007/s11845-024-03674-w.

Salem SS, Badawy MSEM, Al-Askar AA, Arishi AA, Elkady FM, Hashem AH. 2022. Green biosynthesis of selenium nanoparticles using orange peel waste: Characterization, antibacterial and antibiofilm activities against multidrug-resistant bacteria. Life 12 (6): 893. DOI: 10.3390/life12060893.

Sawiress FA, Ziada MS, Bebawy WS, Amer HA. 2011. Effect of ginseng extract supplementation on testicular functions in diabetic rats. Endocr Regul 45 (3): 139-148. DOI: 10.4149/endo_2011_03_139.

Seghinsara AM, Shoorei H, Taheri MMH, Khaki A, Shokoohi M, Tahmasebi M, Khaki AA, Eyni H, Ghorbani S, Rad KHR, Kalarestaghi H, Roshangar L. 2019. *Panax ginseng* extract improves follicular development after mouse preantral follicle 3D culture. Cell J 21 (2): 210. DOI: 10.22074/cellj.2019.5733.

Shin IS, Lee MY, Ha HK, Seo CS, Shin HK. 2012. Inhibitory effect of Yukmijihwang-tang, a traditional herbal formula against testosterone-induced benign prostatic hyperplasia in rats. BMC Complement Altern Med 12: 48. DOI: 10.1186/1472-6882-12-48.

Shin KO, Choe SJ, Uchida Y, Kim I, Jeong Y, Park K. 2018. Ginsenoside Rb1 enhances keratinocyte migration by a sphingosine-1-phosphate-dependent mechanism. J Med Food 21 (11): 1129-1136. DOI: 10.1089/jmf.2018.4246.

Stohs SJ, Bagchi D, Hassoun E, Bagchi M. 2001. Oxidative mechanisms in the toxicity of chromium and cadmium ions. J Environ Pathol Toxicol Oncol 20 (2): 201-213. DOI: 10.1615/JEnvironPatholToxicolOncol.v20.i2.10.

Sultana B, Anwar F, Ashraf M. 2009. Effect of extraction solvent/ technique on the antioxidant activity of selected medicinal plant extracts. Molecules 14: 2167-2180. DOI: 10.3390/molecules 14062167.

Won YJ, Kim BK, Shin YK, Jung SH, Yoo SK, Hwang SY, Sung JH, Kim SK. 2014. Pectinase-treated *Panax ginseng* extract (GINST) rescues testicular dysfunction in aged rats via redox-modulating proteins. Exp Gerontol 53: 57-66. DOI: 10.1016/j.exger.2014.02.012.

Zheng M, Xin Y, Li Y, Xu F, Xi X, Guo H, Cui X, Cao H, Zhang X, Han C. 2018. Ginsenosides: A potential neuroprotective agent. BioMed Res Intl 2018: 8174345. DOI: 10.1155/2018/8174345.

NUSANTARA BIOSCIENCE
Vol. 16, No. 2, pp. 228-236
November 2024

ISSN: 2087-3948
E-ISSN: 2087-3956
DOI: 10.13057/nusbiosci/n160209

Implementation of Floating Net Cages (FNC) cultivation and risks to sustainable fisheries in the Gajah Mungkur Reservoir, Wonogiri, Central Java, Indonesia

SANTI KURNIASIH[1,♥], SUNARTO[1,2], PRABANG SETYONO[1,2]

[1]Department of Environmental Science, Graduate School, Universitas Sebelas Maret. Jl. Ir. Sutami 36A Surakarta 57126, Central Java, Indonesia. Tel./fax.: +62-271-632450, ♥email: santi.kurniasih@student.uns.ac.id

[2]Department of Environmental Science, Faculty of Mathematics and Natural Sciences, Universitas Sebelas Maret. Jl. Ir. Sutami 36A Surakarta 57126, Central Java, Indonesia

Manuscript received: 2 May 2024. Revision accepted: 17 July 2024.

Abstract. *Kurniasih S, Sunarto, Setyono P. 2024. Implementation of Floating Net Cages (FNC) cultivation and risks to sustainable fisheries in the Gajah Mungkur Reservoir, Wonogiri, Central Java, Indonesia. Nusantara Bioscience 16: 228-236.* Floating Net Cages (FNC) is an effort to intensify fish production in the Gajah Mungkur Reservoir, Wonogiri, Central Java, Indonesia. The increase in the number of FNC is directly proportional to the production of FNC fish, so it can decrease water quality. The study aims to look into how FNC affects the water quality in the FNC area of the Gajah Mungkur Reservoir and how the threat of FNC water conditions affects the long-term viability of FNC aquaculture in the Gajah Mungkur Reservoir. The data collection technique was purposive sampling, which was analyzed using quality standard evaluation and plankton community structure analysis. The research results show that the water quality parameters measured are based on standards for fisheries activities, except for the COD and BOD parameters. Most plankton found are from the Bacillariophyceae class. The FNC area in the Gajah Mungkur Reservoir includes eutrophic waters with a low diversity and moderate pollution. The evenness exceeds 6 and the C value is less than 0.5. The saprobic indexes for the pollution level in the FNC area's waters is classified as very low to low, with few organic and inorganic compounds in the Oligo/β-Mesosaprobik to β-mesosaprobik phase. Six families of fish have been found in the Gajah Mungkur Reservoir, namely Cyprinidae, Pangasiidae, Eleotrididae, Cichlidae, Channidae, and Bagridae. Social conflict, mass fish deaths, and increasing water pollution are risks to floating net cages cultivation. Commitment, implementation, and supervision are crucial in executing FNC management through an ecosystem approach, ensuring the sustainability of FNC aquaculture and preserving food security.

Keywords: Floating net cages, FNC, Gajah Mungkur Reservoir, risks, sustainable fisheries, water quality

INTRODUCTION

Reservoirs are created by blocking rivers or streams. They serve various purposes such as flood control, hydropower generation, providing drinking water, and irrigation. Additionally, they significantly contribute to inland fish production (Sarkar et al. 2017). Reservoir ecosystems are sensitive to disturbances caused by human activities and climate change (Yang et al. 2017; Znachor et al. 2018). Climate change, eutrophication, and human impact lead to issues in lake and reservoir waters (Ismest'eva et al. 2015). Reservoirs and lakes are commonly used for fisheries and aquaculture. Floating Net Cages (FNC) are widely used for aquaculture in reservoirs as they are easy to monitor and harvest (Astuti et al. 2020, 2023).

FNC cultivation, an intensive aquaculture production system in net cages, has gained significant attention in recent years. The increase in fish production in net cages worldwide is helping to meet the growing demand for animal protein due to population growth (Sajina et al. 2021). There is encouragement to continue developing FNCs due to their economic benefits (Simangunsong and Hidayat 2017). In Sumatra and Java, Indonesia, several lakes and reservoirs have FNCs and fish production numbers that exceed their carrying capacity (Figure 1). If this situation is left unchecked, it is predicted that the frequency of mass fish deaths will increase (Sulaiman et al. 2020).

The Gajah Mungkur Reservoir, Wonogiri, Central Java, Indonesia, has great potential for fisheries. According to Wonogiri District Regional Regulation Number 2 of 2020, the FNC area in the Gajah Mungkur Reservoir covers approximately 25 hectares on the reservoir's edge. The FNC cultivation area is located in Wuryantoro and Wonogiri Sub-districts. Based on the marine, fisheries, and livestock services of Wonogiri District in 2023, the trend of increasing FNC numbers is accompanied by an increase in FNC production (Dislapernak Wonogiri 2023), as shown in Figure 1. In Wonogiri District, FNC fish production in the Gajah Mungkur Reservoir accounts for 90% of the aquaculture output. Cultivation of FNC can increase fish production (Astuti et al. 2023).

The main commodity for FNC cultivation in the Gajah Mungkur Reservoir is tilapia (*Oreochromis niloticus*). Tilapia is an aquaculture Species that can adapt, has high tolerance, fast growth, reproductive efficiency, high fillet yields, and is widely accepted by consumers (Brande et al.

2023). FNC cultivation also produces fish waste, feed waste, and metabolic products. The remaining waste from FNC cultivation will affect water quality through changes in macrobenthos structure, phytoplankton blooms, and fluctuations in physical parameter values (Nabirye et al. 2016).

According to the Direktorat Jenderal Perikanan Budidaya (2017), measuring water quality parameters for FNC cultivation includes water temperature, brightness, pH, dissolved oxygen, ammonia, and phytoplankton abundance. Plankton is a good bioindicator of aquatic change due to its sensitivity to fluctuating environmental conditions (Hemraj et al. 2017), including physico-chemical changes and anthropogenic pollution (Dembowska et al. 2015). Phytoplankton can be a bioindicator to assess the quality of aquatic ecosystems (Haroon and Hussian 2017). Bacillariophyceae (diatoms) communities react directly to environmental physical and chemical changes. They also the most found of algal communities in many freshwater systems (Heramza et al. 2021). On the other hand, the mass growth of Cyanobacteria not only worsens the aquatic environment but also harms the economy, health and human life because of its potential toxins (Chatterjee and More 2023).

This research aims to analyze the influence of FNC on water quality in the FNC area of the Gajah Mungkur Reservoir, and the risk of FNC waters conditions on the sustainability of FNC aquaculture in the Gajah Mungkur Reservoir Wonogiri. The overall analysis includes all environmental components (abiotic, biotic, and sociocultural). The research output is data that can be used as a consideration for managing sustainable FNC cultivation activities.

MATERIALS AND METHODS

Study area

The research was carried out in September 2023. The sampling location consisted of 5 points determined based on the aquaculture area in Gajah Mungkur Reservoir, Wonogiri, Central Java, Indonesia (Figure 2). The station I is at the reservoir inlet in Wuryantoro Sub-district (110° 53' 42.84" E and 07° 52' 56.66" S), station II in the FNC area in Wuryantoro Sub-district (110°53'53.12" E and 07°52'33.32" S), station III in the FNC area in Wonogiri Sub-district (110°54'31.84" E and 07°51'59.57" S), station IV at the reservoir inlet in Wonogiri Sub-district (110°54'33.34" E and 07°51'37.29" S), and station V in the reservoir outlet area (110°54'58.42" E and 07°51'23.27" S).

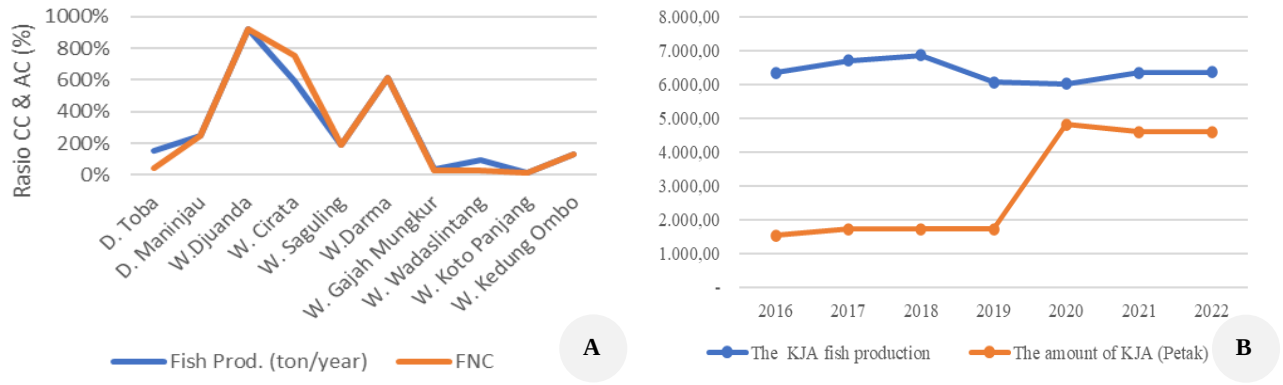

Figure 1. A. The trend of FNCs and fish production numbers that exceed their carrying capacity (Sulaiman et al. 2020) and B. Trend of FNC's fish production and amount of FNC in Gajah Mungkur Reservoir, Wonogiri, Indonesia (Dislapernak Wonogiri 2023) in left to right

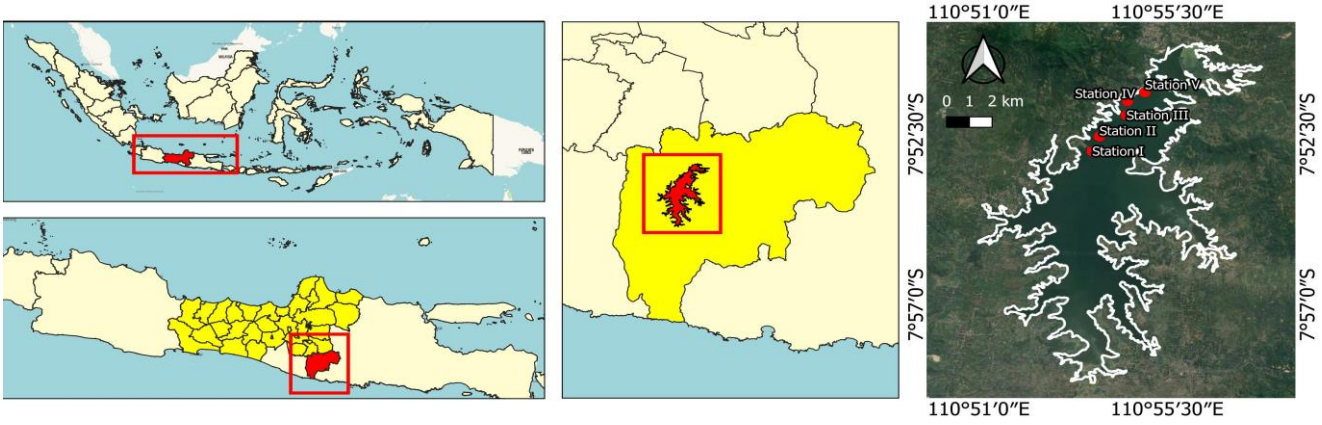

Figure 2. Maps of the research location in Gajah Mungkur Reservoir, Wonogiri, Indonesia

Procedures

Materials

Physical and chemical parameters were observed in the waters of the FNC cultivation area in the Gajah Mungkur Reservoir, Wonogiri, Indonesia (Table 1).

Data collection

Purposive sampling, with specific reasons and considerations, served as the data collection technique, yielding a representative sample that provided a comprehensive view of the research area. Water samples from the Gajah Mungkur Reservoir FNC cultivation fishery area, along with depth composites, served as the research material.

Data analysis

The data was analyzed both qualitatively and quantitatively. The objective parameters of the water quality that were studied were described, and these were then compared with the water quality standards for fishing activities set by Government Regulation Number 22 of 2021 on the Implementation of Environmental Protection and Management. The plankton data obtained is then analyzed to determine the abundance of plankton and phytoplankton, the Diversity Index (H'), Evenness Index (e), Dominance Index (C), and Saprobic Index (SI).

Plankton abundance

To calculate the number of phytoplankton per liter, use the APHA formula (1989), namely:

$$N = n \times (A/B) \times (C/D) \times (1/E)$$

Where:
N: Total number of plankton (ind/L)
n: Average number of individuals per field of view
A: Area of the cover glass (mm^2)
B: Area of one field of view (mm^2)
C: Volume of concentrated water (mL)
D: Volume of one drop (mL) under the cover glass
E: Volume of filtered water (L)

Diversity index

The diversity index is used to assess the level of Species diversity in a community (Odum and Barrett 2009):

$$H' = -\sum_{i=0}^{i} pi \ln pi$$

Where:
H' : Species diversity index
Pi : A probability function for each part as a whole (ni/N)
Ni : Number of individuals of type i
N : Total number of individuals

Evenness index

The evenness index is used to assess the amount of similarity in the distribution of several individuals from each clan at the community level. Evenness index based on equality (Odum and Barrett 2009):

$$e = H' / \ln S$$

Where:
e : Evenness index
H' : Species diversity index
S : Number of types

Dominance index

The dominance index is calculated using the Simpson index (Odum and Barrett 2009):

$$c = -\sum_{i=0}^{i} sn \, (ni/N)^2$$

Where:
C : Simpson's dominance index
ni : Number of individuals of type i
N : Total number of individuals

Saprobic index

The saprobic index is used to assess the level of organic pollution in waters using existing organisms.

Plankton Saprobic Index (X) (Dresscher and van der Mark 1976):

$$SI = (C + 3D + B - 3A) / (A + B + C + D)$$

Where:
A : the Ciliata group shows polysaprobity
B : Euglenophyta group, shows α mesosaprobity
C : Chlorococcales + Diatomae group, shows β mesosaprobity
D : Peridinae/Chrysophyceae/Conjugatae group, shows oligosaprobity

Table 1. Measurement of water quality parameters

Parameter	Units	Methods/tools
Water temperature	°C	SNI 06-6989.23-2005/ Thermometer
Total Suspended Solids (TSS)	mg/L	SNI 6989.3-2019/ Water tested
Brightness	m	Secchi disc
Current speed	cm/s	current meter
Depth	m	Scale Benchmark
pH	-	SNI 6989.11-2004/ pH meter
Free ammonia (NH_3-N)	mg/L	SNI 06-6989.30-2005/Water tested
PO4-P/phosphate	mg/L	APHA/AWWA/WEF 2017:4500-P D/Water tested
DO	mg/L	SNI 06-6989.14-2004/Water tested
COD	mg/L	SNI 6989.2-2019/Water tested
BOD	mg/L	SNI 6989.72.2009/ Water tested
Plankton	Ind/L	SNI 06-3963-1995/ Water tested

RESULTS AND DISCUSSION

The composition of bioindicators and the diversity index

Table 2 presents plankton as a bioindicator for water samples. The most commonly found phytoplankton are *Synedra* sp. from the Bacillariophyceae class and *Chroococcus* sp. from the Cyanophyceae class. *Cyclops* sp., a zooplankton belonging to the Monogononta class, is also present. Table 3 displays the Shanon-Weiner diversity index for each station. Figure 3 displays the number of individual plankton in relation to the class and composition of fish caught in the Gajah Mungkur Reservoir FNC area. Table 4 displays the fish composition based on the Dinas Kepemudaan dan Olahraga dan Pariwisata Kabupaten Wonogiri (2021) data from Wonogiri District.

Analyses of evaluation the results physicochemical parameters

The results of measuring physical-chemical (abiotic) parameters in Table 5 are evaluated using water quality standards stated in Government Regulation Number 22, 2022 to determine the suitability of water for fishing activities. Physico-chemical variables are evaluated based on Government Regulation Number 22, 2022, except turbidity and depth because there are no standards for these two parameters.

Analyses the risk of FNC's water conditions to the sustainability of the FNC aquaculture

Kartamihardja and Krismono (2016), and Sulaiman et al. (2020) found that the Gajah Mungkur Reservoir can hold a certain number of fish and FNC. This number was then compared to the most recent data from the Wonogiri District Maritime, Fisheries, and Livestock Service, which can be seen in Table 6. Figure 4 shows the trend of mass fish deaths, which is one of FNC activities' risks.

Table 2. Composition of plankton in the waters of the Gajah Mungkur Reservoir FNC area, Wonogiri District, Central Java, Indonesia

Genus	Class
Nitzschia sp.	Bacillariophyceae
Amphora sp.	Bacillariophyceae
Navicula sp.	Bacillariophyceae
Synedra sp.	Bacillariophyceae
Scenedesmus sp.	Chlorophyceae
Anabaena sp.	Cyanophyceae
Chroococcus sp.	Cyanophyceae
Microcystis sp.	Cyanophyceae
Phacus sp.	Euglenoidea
Trachelomonas sp.	Euglenoidea
Ulotrix sp.	Ulvophyceae
Closterium sp.	Zygnematophyceae
Mougeotia sp.	Zygnematophyceae
Spirogyra sp.	Zygnematophyceae
Staurastrum sp.	Charophyceae
Peridinium sp.	Dinophyceae
Difflugia sp.	Tubulinea
Cyclops sp.	Copepoda
Keratella sp.	Monogononta
Trichocerca sp.	Monogononta

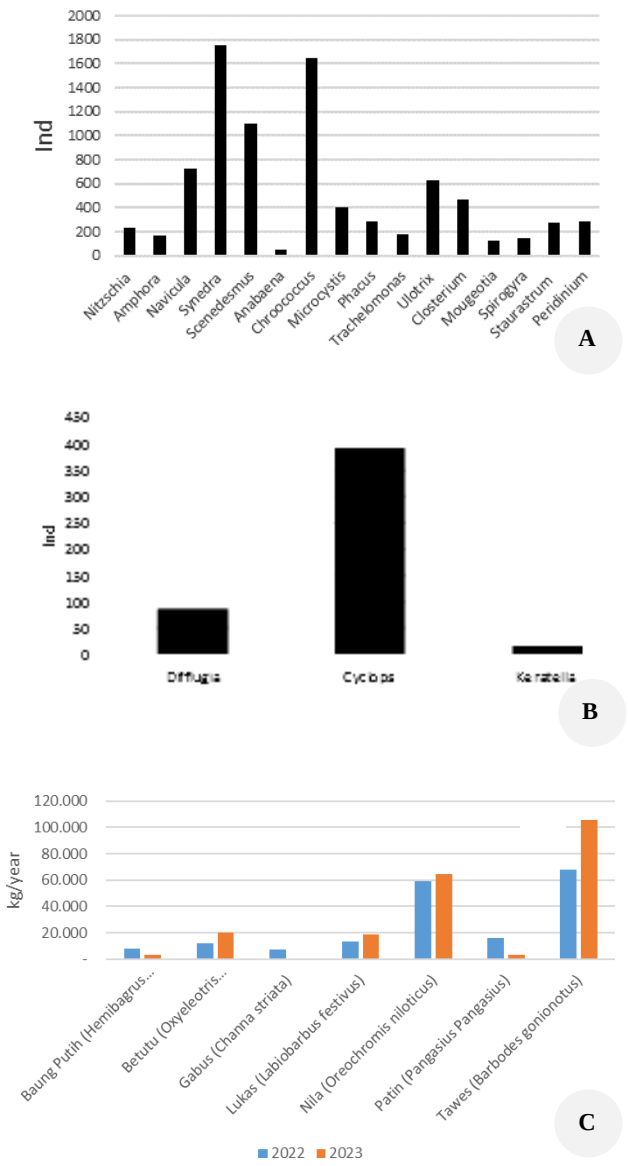

Figure 3. A. The number of in the group of phytoplankton, B. Zooplankton, and C. Composition of caught fish in the FNC's area of Gajah Mungkur Reservoir, Wonogiri District, Central Java, Indonesia

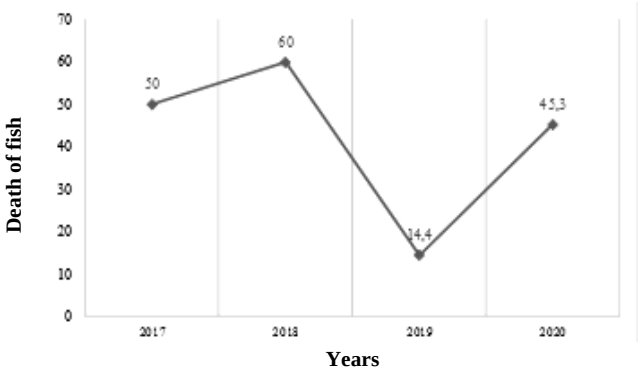

Figure 4. The trend of the mass death of fish in Gajah Mungkur Reservoir, Wonogiri District, Central Java, Indonesia

Table 3. Abundance of zooplankton, phytoplankton, Diversity Index (H'), Evenness Index (e), Dominance Index (C), and Saprobic index (X)

Location point	Zooplankton abundance (ind/L)	Phytoplankton abundance (ind/L)	H'	e	C	X
I	65,500	421,500	2.24	0.74	0.12	0.7
II	17,250	487,000	2.19	0.72	0.14	1.8
III	22,250	315,000	2.07	0.68	0.15	1
IV	23,000	543,250	2.25	0.74	0.12	1.6
V	74,250	350,000	2.04	0.67	0.16	1.3

Table 4. The fish composition in Gajah Mungkur Reservoir, Wonogiri District, Central Java, Indonesia

Scientific name	Local name	Family
Oreochromis niloticus (Linnaeus, 1758)	*Nila/ Nile tilapia*	Cichlidae
Pangasianodon hypophthalmus (Sauvage, 1878)	*Jambal siam/Patin*	Pangasiidae
Barbonymus gonionotus (Bleeker, 1849)	*Tawes*	Cyprinidae
Hemibagrus nemurus (Valenciennes, 1840)	*Saga*	Bagridae
Labiobarbus leptocheilus (Valenciennes, 1842)	*Lukas*	Cyprinidae
Barbodes balleroides (Valenciennes, 1842)	*Iro soka*	Cyprinidae
Hampala macrolepidota Kuhl & Van Hasselt, 1823	*Palung*	Cyprinidae
Osteochilus vittatus (Valenciennes, 1842)	*Salem*	Cyprinidae
Rasbora argyrotaenia (Bleeker, 1849)	*Lunjar/Wader pari*	Cyprinidae
Parachela oxygastroides (Bleeker, 1852)	*Lalang*	Cyprinidae
Oxyeleotris marmorata (Bleeker, 1852)	*Betutu*	Eleotridae
Channa striata (Bloch, 1793)	*Kutuk*	Channidae
Mystus singaringan (Bleeker, 1846)	*Nggaringan*	Bagridae

Source: Dinas Kepemudaan dan Olahraga dan Pariwisata Kabupaten Wonogiri (2021)

Table 5. Physicochemical parameters and comparison with a quality standard for the water utilization classification in FNC's area of Gajah Mungkur Reservoir, Wonogiri, Central Java, Indonesia

Parameter	Analysis results per location point					Quality standards (PP 22/2021)	
	I	II	III	IV	V	Class of II	Class of III
Water Temperature (°C)	27	28	28	28	28		Dev. 3
Total Suspended Solids (TSS) (mg/L)	45	52	50	48	39	50	100
Brightness (m)	0.36	0.38	0.39	0.35	0.4	4	2.5
Current speed (cm/s)	20	39	18	7	22	-	-
Depth (m)	11	5.5	9.5	3.5	12	-	-
pH	8.89	8.95	8.78	8.89	8.97	6-9	6-9
Ammonia Free (NH3-N) (mg/L)	0.139	0.198	0.18	0.159	0.154	0.2	0.5
PO_4-P/Phosphate (mg/L)	0.164	0.199	0.194	0.175	0.142	0.2	1
DO (mg/L)	4.9	3.51	3.4	2.58	4.74	4	3
COD (mg/L)	29.79	42.15	43.03	46.56	32	25	40
BOD (mg/L)	10.31	13.9	14.65	15.68	10.31	3	6

Note: Determination of the class of utilization was based on the standard quality of Government Regulation No. 22 the year 2021

Table 6. Carrying capacity and actual conditions of FNC in Gajah Mungkur Reservoir, Wonogiri District, Central Java, Indonesia

Gajah Mungkur Reservoir	Fish production (tons/year)	FNC (plot)	Source
Carrying Capacity (CC)	14,673	4,891	Kartamihardja and Krismono (2016), Sulaiman et al. (2020)
Actual Condition (AC)	6,358	4,591	Dislapernak Wonogiri (2023)
Rasio CC & AC	43%	94%	

Discussion

The FNC area in the Gajah Mungkur Reservoir has two inlets that affect the water condition: one in Gumiwang Village, Wuryantoro Sub-district, and the other in Sendang Village, Wonogiri Sub-district. The surrounding environment, including agriculture, residential areas, and tourism, also contributes to organic pollution in the FNC area, which can impact water quality. In 2016, there were approximately 1,530 FNC plots in the Gajah Mungkur Reservoir, which increased to 4,591 plots by 2022 (Dislapernak Wonogiri 2023). The cultivation of these FNCs results in the release of 30% of the remaining fish feed and 25-30% of fish waste. Since most FNCs lack waste filters, the waste easily sinks and accumulates into pollutants, posing a potential risk of eutrophication. Due to its significant contribution to the trophic level and pollution, the FNC requires significant attention (Kusen et al. 2014; Setyono and Himawan 2018).

In reservoirs, phytoplankton communities are mainly made up of Bacillariophyceae, Cyanophyceae, and Chlorophyceae (Henderson-Sellers and Markland 1987). According to Odum and Barrett (2005), Bacillariophyta are abundant in water due to their ability to easily adapt to the environment, withstand extreme conditions, and reproduce rapidly. For instance, they can double their population every 18-36 hours, which is twice as fast as other phytoplankton. *Synedra* is commonly found in freshwater bodies like lakes and rivers, as well as in marine environments such as estuaries. As a bioindicator, *Synedra* can evaluate water quality by its sensitivity to environmental factors like temperature, light, pH, and nutrients. The presence of *Synedra* in aquatic ecosystems can provide valuable information about water quality and environmental conditions, which can impact other organisms living in the ecosystem (Barinova and Mamanazarova 2021).

Chroococcus is a type of cyanobacterium that is commonly found in fresh waters, marine waters, and wet soil environments. It is highly tolerant of habitat pollution (Wood et al. 2017; Fitri et al. 2021). This bacterium is able to thrive in both acidic and alkaline water, as well as in extreme environments. *Chroococcus* plays a crucial role in the production of oxygen in biogeochemical cycles and can serve as a bioindicator of water quality. A significant decrease in the *Chroococcus* population could indicate poor water ecosystem health (Masithah and Islamy 2023). Additionally, *Chroococcus* has cyanoremediation properties and can absorb chromium (Cr) from a mixture of domestic and industrial waste (Singh et al. 2019). However, it is important to note that Cyanobacteria, including *Chroococcus*, can produce toxins that pose a threat to individuals using water bodies for drinking, irrigation, and recreational purposes (Chatterjee and More 2023).

The abundance of phytoplankton in the waters of the FNC area in the Gajah Mungkur Reservoir indicates eutrophication due to the high fertility level, with phytoplankton abundance exceeding 15,000 ind/L (Landner 1978). The low diversity index value of less than 2.3 suggests limited diversity and low community stability. According to Shanon Wiener's classification for aquatic environments, a water quality range of 2-3 corresponds to moderate quality (Balloch et al. 1976; Islam et al. 2022). With H' falling within the range of 1-3, the water can be categorized as moderately polluted (Wilhm and Dorris 1966; Islam et al. 2022). An Evenness Index (e) close to 1 indicates relatively even distribution of individuals among Species, with no Species dominating. A value of >0.5 for the evenness index suggests light pollution (Islam et al. 2022). This is evident in the relatively low Dominance Index (C) value (<0.5). When the Dominance Index (C) value is close to 0, there is no dominant Species (Odum 1998), and as C increases, the index of evenness decreases (Kumar and Mina 2018).

The plankton identification results revealed the presence of two types of α-mesosaprobic groups (*Phacus* sp. and *Trachelomonas* sp.), 5 types of β-mesosaprobic group (*Nitzschia* sp., *Amphora* sp., *Navicula* sp., *Synedra* sp., *Scenedesmus* sp.), and 4 types of oligosaprobic group (*Closterium* sp., *Mougeotia* sp., *Spirogyra* sp., *Peridinium* sp.). The saprobic indexes ranges from 0.7 to 1.8, indicating very low to low pollution levels in the waters of the FNC area, with a few organic and inorganic compounds in the Oligo/β-Mesosaprobic to β-mesosaprobic phase. These findings align with Wiryanto's research in 2016, which also classified the pollution level in the Gajah Mungkur Reservoir as low based on the pollution index value.

The diversity of fish in the Gajah Mungkur Reservoir is influenced by the inlet and outlet. According to data from the Dislapernak Wonogiri (2023), the types and numbers of fish living in the reservoir are detailed in Figure 3. Additionally, Dinas Kepemudaan dan Olahraga dan Pariwisata Kabupaten Wonogiri (2021) data from the District of Wonogiri indicates the presence of 13 types of fish from six families: Cyprinidae, Pangasiidae, Eleotrididae, Cichlidae, Channidae, and Bagridae. The most commonly found fish in the reservoir belong to the Cyprinidae family, which is the dominant family in the reservoir according to Sajina et al. (2021).

The Gajah Mungkur Reservoir supplies water to regional drinking water companies, which must meet class 1 quality standards. According to Government Regulation Number 22 of 2021, the Dissolved Oxygen (DO) value for class 1 water should be equal to or greater than 6 mg/L. The waters of the Gajah Mungkur Reservoir are classified as class 2 for activities such as irrigation, tourism, fisheries, hydropower, and others, which have the same quality standards. The quality standards for fisheries activities are class 2 and class 3. A low DO concentration can hinder the self-purification process of water (Wardhani and Sugiarti 2021). In stagnant waters like reservoirs or lakes, DO concentration decreases with increasing depth due to reduced oxygen supply from photosynthesis and diffusion processes (Leidonald et al. 2019). Additionally, the use of oxygen for organic matter decomposition, sediment, and rainfall also contributes to the depletion of DO concentrations (Noori et al. 2018).

The quality standards for fisheries activities refer to water quality standards Government Regulation Number 22 of 2021; the brightness value for fisheries activities is 2.5-4

m. The results of brightness measurements at locations in the waters of the Gajah Mungkur Reservoir FNC area are not much different from the Perum Jasa Tirta I year capacity study report (2018) that the transparency in the Gajah Mungkur Reservoir, which is around 20.5-49 cm. A good brightness value for fish cultivation is around 30-40 cm (Rahmayanti et al. 2021); if the brightness reaches less than 25 cm, DO will decrease drastically. According to Effendi (2003), the ability of sunlight to penetrate the river bed is influenced by the turbidity of the water. The water depth at the FNC location is at least 5 meters from the bottom of the net at the lowest low tide with a water flow range of 20-40 cm/s (Direktorat Jenderal Perikanan Budidaya 2017). The location of FNC activities is on the edge of the Gajah Mungkur Reservoir so that during the dry season, the waters recede, and the water depth varies at each point.

Human activities in the waters around aquaculture sites significantly increase BOD and decrease DO and PO_4-P (Ghazali et al. 2022). An increase in BOD concentration, such as water intake, indicates a high accumulation of organic matter (Ling et al. 2017). Wardhani and Sugiarti (2021) stated that the high concentration of BOD in the waters of the Jatiluhur Reservoir is caused by fish culture waste in FNC originating from feed and fish faeces. The high level of COD indicates a high level of water pollution caused by organic matter. Meanwhile, according to Wiryanto (2016), the high BOD value is influenced by FNC and reservoir tourism activities. COD concentrations in FNC areas have higher values and significantly differ from non-FNC (Ghazali et al. 2022).

The cultivation of FNC in the Gajah Mungkur Reservoir has had a positive impact on the socio-economic status of the surrounding community. However, intensive FNC cultivation, driven by profit, has led to negative effects on the reservoir's aquatic ecosystem. Excessive feeding to boost production has resulted in leftover feed entering the water, causing nutrient enrichment. As a result, the current condition of the reservoir is eutrophic, leading to mass fish deaths and increased water pollution. To maintain the reservoir and lake ecosystem, the amount of FNC should not exceed the carrying capacity of the reservoir/lake. Additionally, the management of FNC cultivation should implement fisheries management using an ecosystem approach, which will help maintain water and fish quality, and ensure sustainable FNC activities through effective monitoring.

The water quality in the FNC cultivation area of the Gajah Mungkur Reservoir meets the quality standards of Government Regulation Number 22 of 2021 physically and chemically. However, the COD and BOD parameters exceed the water quality standards for fisheries activities, class II and class III, even though the waters are classified as eutrophic. To control the amount of waste and prevent it from exceeding the reservoir's carrying capacity, the development of FNC cultivation should be regulated and limited. The number of FNCs should be controlled to allow time for water recovery (Setyono and Himawan 2018). Determining the reservoir's carrying capacity is the first step in estimating the optimal number of FNCs to avoid negative impacts from FNC activities. Cross-sector and agency coordination is necessary to monitor the reservoir environment. The coordination between the government/private sector and fisheries should be as equal partners (Simangunsong and Hidayat 2017). In the future, it is important for the government and relevant stakeholders to commit to implementing FNC management using an ecosystem approach to ensure sustainable FNC cultivation for maintaining food security.

ACKNOWLEDGEMENTS

The authors would like to thank the Ministry of Maritime Affairs and Fisheries, the Wonogiri District Maritime, Fisheries and Livestock Service, the Wonogiri District Bappeda, the Wonogiri District Environmental Service, Perum Jasa Tirta I, fish farmers in the Gajah Mungkur Reservoir, and Universitas Sebelas Maret, Indonesia for providing supports and assist in providing data and information related to this research.

REFERENCES

American Public Health Association (APHA), American Water Works Association (AWWA), Water Environment Federation (WEF). 2017. Standards Methods for the Examination of Water and Wastewater, 23rd Edition. American Public Health Association, American Water Works, Water Pollution Control Federation. Washington, D.C.

American Public Health Association (APHA). 1989. Standard Methods for the Examination of Waters and Wastewater. 17thed. American Public Health Association, American Water Works, Water Pollution Control Federation. Washington, D.C.

Astuti LP, Hendrawan AS, Warsa A. 2020. Controlling pollution from floating cage culture in reservoir and lake using SMART-FCC system. IOP Conf Ser: Earth Environ Sci 521 (1): 012013. DOI: 10.1088/1755-1315/521/1/012013.

Astuti LP, Warsa A, Tjahjo DWH, Sembiring T. 2023. Environment-friendly floating net cage culture research in Indonesia. BIO Web Conf 74: 01016. DOI: 10.1051/bioconf/20237401016.

Badan Standardisasi Nasional/ SNI 06-3963-1995. 1995. Metode Pengujian Jenis dan Jumlah Plankton dalam Air Badan. BSN, Jakarta. [Indonesian]

Badan Standardisasi Nasional/ SNI 06-6989.11-2004. 2004. Air dan Air limbah-Bagian 11: Cara Uji Derajat Keasaman (pH) dengan Menggunakan Alat pH Meter. BSN, Jakarta. [Indonesian]

Badan Standardisasi Nasional/ SNI 06-6989.14-2004. 2004. Air dan Air Limbah-Bagian 14: Cara Uji Oksigen Terlarut Secara Yodometri. BSN, Jakarta. [Indonesian]

Badan Standardisasi Nasional/ SNI 06-6989.23-2005. 2005. Air dan Limbah – Bagian 23: Cara Uji Suhu dengan Termometer. BSN, Jakarta. [Indonesian]

Badan Standardisasi Nasional/ SNI 06-6989.30-2005. 2005. Cara Uji Kadar Amonia dengan Spektrofotometer Secara Fenat. BSN, Jakarta. [Indonesian]

Badan Standardisasi Nasional/ SNI 6989.2-2019. 2019. Air dan Air Limbah – Bagian 2: Cara Uji Kebutuhan Oksigen Kimiawi (Chemical Oxygen Demand/COD) dengan Refluks Tertitip Secara Spektrofotometri. BSN, Jakarta. [Indonesian]

Badan Standardisasi Nasional/ SNI 6989.3:2019. 2019. Cara Uji Padatan Tersuspensi Total (TSS) Secara Gravimetri. BSN, Jakarta. [Indonesian]

Badan Standardisasi Nasional/ SNI 6989.72-2009. 2009. Air dan Air Limbah – Bagian 72: Cara Uji Kebutuhan Oksigen Biokimia (Biochemical Oxygen Demand/BOD). BSN, Jakarta. [Indonesian]

Balloch D, Davies CE, Jones FH. 1976. Biological Assessment of Water Quality in Three British Rivers: The North Esk (Scotland), The Ivel (England) and The Taff (Wales). Water Pollution Control, U.K.

Barinova S, Mamanazarova K. 2021. Diatom algae-indicators of water quality in the lower Zarafshan River, Uzbekistan. Water 13 (3): 358. DOI: 10.3390/w13030358.

Brande MR, Santos DFL, Fialho NS, Proença D C, Ojeda PG, Godói, FCM, Roubach R, Bueno GW. 2023. Economic and financial risks of commercial tilapia cage culture in a neotropical reservoir. Heliyon 9 (6): e16336. DOI: 10.1016/j.heliyon.2023.e16336.

Chatterjee S, More M. 2023. Cyanobacterial harmful algal bloom toxin microcystin and increased vibrio occurrence as climate-change-induced biological co-stressors: Exposure and disease outcomes via their interaction with gut–liver–brain axis. Toxins 15 (4): 289. DOI: 10.3390/toxins15040289.

Dembowska EA, Napiorkowski P, Mieszczankin T, Josefowitz S. 2015. Planktonic indices in the evaluation of the ecological status and the trophic state of the longest lake in Poland. Ecol Indic 56: 15-22. DOI: 10.1016/j.ecolind.2015.03.019.

Dinas Kelautan dan Perikanan dan Peternakan Kabupaten Wonogiri (Dislapernak Wonogiri). 2023. Laporan Singkat Produksi 2015-2020 Penyuluh Perikanan Kabupaten Wonogiri. Wonogiri. [Indonesian]

Dinas Kepemudaan dan Olahraga dan Pariwisata Kabupaten Wonogiri. 2021. Analisis Dampak Lingkungan Hidup: Rencana Pengembangan Obyek Wisata Waduk Gajah Mungkur. Wonogiri. [Indonesian]

Direktorat Jenderal Perikanan Budidaya. 2017. Petunjuk Teknis Klaster Pembesaran Ikan Nila di KJA. Kementerian Kelautan dan Perikanan. Jakarta. [Indonesian]

Dresscher TGN, van der Mark H. 1976. A Simplified method for the assessment of quality of fresh & Slightly Brakish Water. Hydrobiologia 48 (3): 199-201. DOI: 10.1007/BF00028691.

Effendi H. 2003. Telaah Kualitas Air bagi Pengelolaan Sumberdaya dan Lingkungan Perairan. Kanisius, Yogyakarta. [Indonesian]

Fitri SGS, Sutarno S, Sasongko H, Rosyadi H, Ratnasari M, Chairunisa S. 2021. Morphological diversity of culturable cyanobacteria from habitats in Segara Anakan, Java, Indonesia. Biodiversitas 22 (12): 5617-5626. DOI: 10.13057/biodiv/d221258.

Ghazali M, Widoretno W, Arumingtyas EL, Retnaningdyah C. 2022. Macroepiphyte biodiversity on *Kappaphycus alvarezii* surface and its interaction with environment in cultivation centers on Lombok Island, Indonesia. Biodiversitas 23 (12): 6284-6292. DOI: 10.13057/biodiv/d231224.

Government Regulation No. 22. 2021. Peraturan Pemerintah Nomor 22 Tahun 2021 tentang Penyelenggaraan Perlindungan dan Pengelolaan Lingkungan Hidup. [Indonesian]

Haroon AM, Hussian AEM. 2017. Ecological assessment of the macrophytes and phytoplankton in El-Rayah Al-Behery, River Nile, Egypt. Egypt J Aquat Res 43 (3): 195-203. DOI: 10.1016/j.ejar.2017.08.002.

Hemraj DA, Hossain MdA, Ye Q, Qin JQ, Leterme SC. 2017. Plankton Bioindicators of environmental conditions in coastal lagoons. Estuar Coast Shelf Sci 184: 102-114. DOI: 10.1016/j.ecss.2016.10.045.

Henderson-Sellers B, Markland HR. 1987. Decaying Lakes. The Origins and Control of Cultural Eutrophication. John Willey & Son, New York.

Heramza K, Barour C, Djabourabi A, Khati W, Bouallag C. 2021. Environmental parameters and diversity of diatoms in the Aïn Dalia dam, Northeast of Algeria. Biodiversitas 22 (9): 3633-3644. DOI: 10.13057/biodiv/d220901.

Islam MS, Azadi MA, Nasiruddin M, Sarker MM. 2022. Plankton Species composition, abundance and diversity indices in three ponds of Chittagong University Campus, Bangladesh. J Biol Pharm Chem Res 2: 1-14.

Ismest'eva LR, Moore MV, Hampton SE, Ferwerda CJ, Gray DK, Woo KH, Pislegina HV, Kraschuk RS, Shimaraeva SV, Silow EA. 2015. Lake-wide physical and biological trends associated with warming in Lake Baikal. J Great Lakes Res 42: 6-17.

Kartamihardja ES, Krismono. 2016. Fenomena, Penyebab dan Pengendalian Kematian Massal Ikan serta Pengembangan Budidaya Ikan dalam Floating Net Cages Berkelanjutan di Perairan Waduk dan Danau. Policy Brief. Pusat Riset Perikanan. Badan Penelitian dan Pengembangan Kelautan dan Perikanan. [Indonesian]

Kumar P, Mina U. 2018. Fundamentals of Ecology and Enviroment. 2th ed. Pathfinder Publication, New Delhi.

Kusen DJ, Marsoedi, Kusuma Z, Tamod Z. 2014. Environmental friendly foods in the cultivation of floated net cages at Tondano Lake in North Sulawesi Province. Sch Acad J Biosci 2 (12A): 877-881. DOI: 10.36347/sajb.2014.v02i12.006.

Landner. 1978. Eutrophication of Lakes. Analysis Water and Air Pollution. Research Laboratory Stockholm, Sweden.

Leidonald R, Muhtad A, Lesmana I, Harahap ZA, Rahmadya A. 2019. Profiles of temperature, salinity, dissolved oxygen, and pH in Tidal Lakes. IOP Conf Ser: Earth Environ Sci 260: 012075. DOI: 10.1088/1755-1315/260/1/012075.

Ling TY, Gerunsin N, Soo CL, Nyanti L, Sim SF, Grinang J. 2017. Seasonal changes and spatial variation in water quality of a large young tropical reservoir and its downstream river. J Chem 2017: 8153246. DOI: 10.1155/2017/8153246.

Masithah ED, Islamy RA. 2023. Checklist of freshwater periphytic diatoms in the midstream of Brantas River, East Java, Indonesia. Biodiversitas 24 (6): 3269-3281. DOI: 10.13057/biodiv/d240621.

Nabirye H, Mwebaza-Ndawula L, Bugenyi FWB, Muyodi FJ. 2016. The evaluation of cage fish farming effects om water quality using selected benthic macro-invertebrate community parameters in the Napoleon Gulf, Northern Lake Victoria. Intl J Fish Aquat Stud 4 (1): 42-50.

Noori R, Berndtsson R, Adamowski JF et al. 2018. Temporal and depth variation of water quality due to thermal stratification in Karkheh Reservoir, Iran. J Hydrol: Reg Stud 19: 279-286. DOI: 10.1016/j.ejrh.2018.10.003.

Odum EP, Barrett GW. 2005. Fundamental of Ecology. Thomson Brooks/Cole, Belmouth, CA.

Odum EP, Barrett GW. 2009. Fundamentals of Ecology, 5th ed. Cengage Learning, Melbourne.

Odum EP. 1998. Dasar-dasar Ekologi. Diterjemahkan dari Fundamental of Ecology oleh Samingan T. Universitas Gadjah Mada Press, Yogyakarta. [Indonesian]

Perum Jasa Tirta I. 2018. Laporan Akhir: Kajian Penetapan Daya Tampung Beban Pencemaran dan Zonasi Waduk Wonogiri. Perum Jasa Tirta I, Malang. [Indonesian]

Rahmayanti F, Najmi N, Islama, DD, Muliyana A. 2021. Studi kesesuaian parameter fisika-kimia perairan untuk pengembangan area budidaya ikan dengan media floating net cages di Danau IE Sayang. Jurnal Akuakultura 5 (1): 1-7. DOI: 10.35308/ja.v5i1.4146. [Indonesian]

Sajina AM, Sarkar UK, JC, Das BK, Saha A, Mishal P, PKJ, Ramteke M, Das AK. 2021. Influence of cage farming and environmental parameters on spatio-temporal variability of fish assemblage structure in a tropical reservoir of Peninsular India. Limnologica 91: 125925. DOI: 10.1016/j.limno/2021.125925.

Sarkar UK, Sandhya KM, Mishal P, Karnatak G, Lianthuamluaia, Kumari S, Panikkar P, Palaniswamy R, Karthikeyan M, Sibina MS, Paul TT, Ramya VL, Rao DSK, Feroz KM, Panda D, Das BK. 2017. Status, prospects, threats, and the way forward for sustainable management and enhancement of the tropical indian reservoir fisheries: An overview. Rev Fish Sci Aquac 26 (2): 155-175. DOI: 10.1080/23308249.2017.1373744.

Setyono P, Himawan W. 2018. Analyses of bioindicators and physicochemical parameters of water of Lake Tondano, North Sulawesi Province, Indonesia. Biodiversitas 19 (3): 817-824. DOI: 10.13057/biodiv/d190315.

Simangunsong NF, Hidayat A. 2017. Carrying capacity and institutional analysis of floating net cages in Jatiluhur Reservoir. Sustinere 1 (1): 37-47. DOI: 10.22515/sustinere.jes.v1i1.6.

Singh JS, Kumar A, Singh M. 2019. Cyanobacteria: A sustainable and commercial bio-resource in production of bio-fertilizer and bio-fuel from waste waters. Environ Sustain Indic (3-4): 100008. DOI: 10.1016/j.indic.2019.100008.

Sulaiman PS, Fitri Rachmawati P, Puspasari R, Wiadnyana, NN. 2020. Upaya pencegahan dan penanggulangan kematian massal ikan di danau dan waduk. Jurnal Kebijakan Perikanan Indonesia 12 (2): 59-73. DOI: 10.15578/jkpi.12.1.2020.59-73. [Indonesian]

Wardhani E, Sugiarti ZA. 2021. Jatiluhur Reservoir water quality analysis at various depths. Jurnal Presipitasi 18 (3): 400-411. DOI: 10.14710/presipitasi.v18i3.400-411.

Wilhm JL, Dorris TC. 1966. Species diversity of benthic macroinvertebrats in a stream receiving domestic and oil refinery effluents. Am Midl Nat 76: 427-449. DOI: 10.2307/2423096.

Wiryanto. 2016. Spatial and temporal description of water pollution status of Gadjah Mungkur Reservoir Wonogiri, central Java, Indonesia. Biodiversitas 17 (2): 888-893. DOI: 10.13057/biodiv/d170266.

Wonogiri District Regional Regulation Number 2. 2020. Peraturan Daerah Kabupaten Wonogiri Nomor 2 Tahun 2020 tentang Rencana Tata Ruang Wilayah Kabupaten Wonogiri Tahun 2020-2040. [Indonesian]

Wood SA, Rhodes LE, Smith KF, Lengline F, Ponikla K, Pochon X. 2017. Phylogenetic characterisation of marine *Chroococcus*-like

(Cyanobacteria) strains from the Pacific region. NZ J Bot 55 (1): 513. DOI: 10.1080/0028825x.2016.1205634.

Yang JR, Lv H, Isabwe A, Liu L, Yu X, Chen H, Yang J. 2017. Disturbance-induced phytoplankton regime shifts and recovery of cyanobacteria dominance in two subtropical reservoirs. Water Res 120: 52-63. DOI: 10.1016/j.watres.2017.04.062.

Znachor P, Nedoma J, Hejzlar J, Seďa J, Kopáček J, Boukal D, Mrkvička T. 2018. Multiple long-term trends and trend reversals dominate environmental conditions in a man-made freshwater reservoir. Sci Total Environ 624: 24-33. DOI: 10.1016/j.scitotenv.2017.12.061.

NUSANTARA BIOSCIENCE
Vol. 16, No. 2, pp. 237-244
November 2024

ISSN: 2087-3948
E-ISSN: 2087-3956
DOI: 10.13057/nusbiosci/n160210

Influence of media variations and growth regulators on in vitro propagation of *Dendrocalamus asper* bamboo

WAN NURFARZANA WAN MOHAMAD ZANI[1], NORRIZAH JAAFAR SIDIK[1,♥], NUR AFIQAH MOHD ISA[1], ASMAH AWAL[2], NURUL IZZATI OSMAN[3], NORALIZA ALIAS[4], MOHD KHAIRI NORDIN[5]

[1]Department of Biology, Faculty of Applied Science, Universiti Teknologi MARA Shah Alam. 40450 Shah Alam, Selangor, Malaysia. Tel.: +603-5560-5543, Fax.: +603-5543-4562, ♥email: norri536@uitm.edu.my

[2]Agricultural Biotechnology Research Group, Faculty of Plantation and Agrotechnology, Universiti Teknologi MARA Jasin Campus. 77300, Merlimau, Malacca, Malaysia

[3]Department of Pharmacology and Pharmaceutical Chemistry, Faculty of Pharmacy, Universiti Teknologi MARA Puncak Alam Campus. 42300 Bandar Puncak Alam, Selangor, Malaysia

[4]Forest Biotechnology Division, Forest Research Institute Malaysia. 52109 Kepong, Selangor, Malaysia

[5]School of Electrical Engineering, College of Engineering, Universiti Teknologi MARA Shah Alam. 40450 Shah Alam, Selangor, Malaysia

Manuscript received: 17 April 2024. Revision accepted: 29 July 2024.

Abstract. *Zani WNWM, Sidik NJ, Isa NAM, Awal A, Osman NI, Alias N, Nordin MK. 2024. Influence of media variations and growth regulators on in vitro propagation of* Dendrocalamus asper *bamboo. Nusantara Bioscience 16: 237-244.* This study reports the effects of different types of media and combinations of plant growth regulators on the in vitro propagation of *Dendrocalamus asper* (Schult.f.) Backer bamboo species, a species known for its economic significance and challenges in traditional cultivation. The experiment was initiated through the cultivation of in vitro nodal segments as explants in various strengths (half-strength and full-strength) of Murashige and Skoog's (MS) and Vacin & Went (VW) media, supplemented with 1.0 mg L^{-1} 6-benzylaminopurine (BAP) hormone. Optimal results were achieved in full-strength MS media with 1.0 mg L^{-1} BAP, with the highest shoot number (5.6 shoots) and length (2.14±0.18 cm), surpassing outcomes in VW media. Shoot multiplication in full-strength MS media, with varying BAP and indole-3-butyric acid (IBA) hormone combinations (0.5, 1.0, 2.0, and 4.0 mg L^{-1}), was conducted. The combination of 4.0 mg L^{-1} BAP and 0.5 mg L^{-1} IBA yielded the highest number of shoots (5.17±3.97), while supplementation with 4.0 mg L^{-1} IBA alone resulted in the longest shoot with 1.89±1.15 cm. These findings underscore the significance of tailored conditions for optimal in vitro propagation of this species. Further investigations could explore additional factors influencing the propagation process for better refinement of bamboo cultivation techniques.

Keywords: Bamboo, *Dendrocalamus asper*, micropropagation, plant growth regulators

Abbreviations: BAP: 6-benzylaminopurine, IBA: Indole-3-butyric acid, MS: Murashige and Skoog, VW: Vacin & Went

INTRODUCTION

Bamboo is a versatile plant that is widely used for reforestation and has economic significance in various regions of the world. This is mainly due to its fibers' mechanical and physical properties, which allow it to be used in different industries such as food, textile, construction, furniture, handicrafts, and household products (Gusmiaty et al. 2020; Hartono et al. 2022). Moreover, bamboo serves as an effective carbon sequestrator while aiding in soil and water conservation (Emamverdian et al. 2020).

One of the species that possesses the mentioned qualities is *Dendrocalamus asper* (Schult.) Back. ex. Hyne, a tropical bamboo species that is native to China and falls under the subfamily Bambusoideae (Souza et al. 2020). It has several common names, known as *betong* bamboo, sweet bamboo, black bamboo, giant bamboo, or rough bamboo (Charoenphun and Pakeechai 2021; Gonçalves et al. 2023). The shoots are rich in secondary metabolites and consumed by many as part of delicacies, making them one of the most important export commodities (Chandramouli et al. 2015; Kong et al. 2020). In Malaysia, this species holds economic prominence (Hossain et al. 2018), and its mature culms are extensively being used as raw materials to make paper, handicrafts, and floorboards for construction (Zang et al. 2019).

Rising demands for bamboo necessitate efficient propagation methods to ensure that there is a constant and sustainable supply of bamboo plants. Traditional propagation methods using seeds and culm cuttings face limitations in availability, transportation, and quantity (Sharothi et al. 2022). Additionally, the infrequent and season-dependent flowering that occurs between 25 to over 100 years poses challenges in obtaining seeds for propagation (Pasqualini et al. 2019; Zang et al. 2019). Therefore, to overcome these problems, micropropagation presents an alternative via in vitro techniques, enabling large-scale bamboo propagation. However, this method encounters challenges, particularly in optimizing growth through suitable media and Plant Growth Regulators (PGRs) to promote shoot proliferation and rooting of the explants.

The basal medium significantly impacts in vitro plant growth, with the majority of the species exhibiting preferences for MS (Murashige and Skoog 1962) medium. Although MS medium is commonly used, some plant species thrive better in alternative media formulations such as VW (Vacin and Went). This medium is known to be established for orchids, but previous studies have successfully utilized this medium to culture other plant species (Lestari et al. 2020; Menezes et al. 2016). The potential of this medium for bamboo growth, particularly for *D. asper*, remains unevaluated. In comparison, other types of media, such as B5 (Gamborg et al. 1968), SH (Schenk and Hildebrant 1972), and NN (Nitsch and Nitsch 1979) have been tested in the previous study (Singh et al. 2012). Apart from that, the salt strength in the media also impacts plant growth, in which reduced media strength resulted in superior growth compared to the full-strength media (Saad and Elshahed 2012). Hence, precise selection of medium type and concentration is vital to improve micropropagation efficiency in *D. asper* bamboo (Suwal et al. 2020).

Plant growth regulators (PGRs) like cytokinin (BAP, kinetin) and auxins (IAA, IBA) mimic natural hormones in micropropagation media, in which the former often promotes bud breaking and shoot multiplication while the latter induces rooting during bamboo micropropagation (Pratibha and Sarma 2014; Patel et al. 2015; Gantait et al. 2018; Lin et al. 2019). Previous studies recorded that the combination of auxin and cytokinin at specific concentrations could further enhance the explant's growth, in this case, *Bambusa bambos* (L.) Voss and *B. vulgaris* Schrad. ex J.C.Wendl. species, with the right ratio of auxin to cytokinin being crucial for optimal results (Desai et al. 2019). To our knowledge, no published studies have investigated the combination effects on *D. asper* species. Therefore, this study aims to evaluate the effectiveness of basal media formulations and the synergistic effects of BAP and IBA growth regulators on in vitro propagation, along with rooting and acclimatization, with the aim of optimizing protocols for enhanced propagation efficiency of *D. asper* species.

MATERIALS AND METHODS

Preparation of the culture medium

The media used in this study were MS (Murashige and Skoog 1962) (Duchefa Biochemies, The Netherlands) and VW (Vacin and Went) (Duchefa Biochemies, The Netherlands) media. Each medium was prepared either half-strength or full-strength, with the addition of 30 g/L sucrose (Systerm, Malaysia), 100 mg L^{-1} myo-inositol (Duchefa Biochemies, The Netherlands), 1 mg L^{-1} BAP hormone (Duchefa Biochemies, The Netherlands) and 3 g L^{-1} Gelrite (Sigma, St. Louis, USA). The media were adjusted to pH 5.7 prior to autoclaving at 121°C for 20 minutes. The autoclaved media were then poured into 100 mL sterile pill box containers at a volume of approximately 20 mL per container.

Culture in different types and strength of basal media

In this study, in vitro *D. asper* plantlets were utilized. The young, actively growing nodal segments were cut into 10-15 mm and cultured on different strengths of two different basal media, MS and VW media, with or without the addition of 1 mg L^{-1} BAP hormone, according to Table 1. The cultures were maintained in the culture room at 27±2°C under a 16 h light photoperiod of white cool fluorescent light (Philips, China). The observation for length and number of shoots were taken after the 8th week of culture.

Multiplication and shoot proliferation

The nodal explants were cultured in full-strength MS basal medium supplemented with a combination of BAP and IBA hormone to determine the most suitable hormone combination that supports the establishment of multiple shoots (Duchefa Biochemies, The Netherlands) at different concentrations from 0.5 to 4.0 mg L^{-1} in approximately 20 mL media. All media used in this study were supplemented with 3 g L^{-1} sucrose, 100 mg L^{-1} myo-inositol, and 0.3 g L^{-1} Gelrite as a gelling agent. The pH of the media was adjusted to 5.7 prior to autoclaving at 121°C for 20 min. All cultures were maintained in the culture room at 27±2°C under 16 h light photoperiod of white cool fluorescent light. The observation for length and number of shoots were taken after the 12th week of culture.

Rooting and acclimatization

During this stage, propagules consisting of 3 to 5 shoots were transferred in liquid MS media supplemented with different concentrations of IBA hormone (1.0-5.0 mg L^{-1}) for rooting induction. The culture was maintained in the culture room at 27±2°C under 16 h light photoperiod of white cool fluorescent light. After four weeks of culture, the rooted plantlets underwent pre-hardening, where they were transferred to seedling trays containing peat moss and maintained in the culture room for three weeks. The plants were then removed from the trays and transferred to bigger trays containing a mixture of soil, vermiculite, and vermicompost at (1:1:1) ratio. The trays were placed in the greenhouse, and the survival of the plantlets was observed after a month.

Table 1. Experimental treatments and corresponding media specifications

Treatment	Media type	Strength	BAP concentration (mg L^{-1})
1	MS	Half	0
2	MS	Half	1
3	MS	Full	0
4	MS	Full	1
5	VW	Half	0
6	VW	Half	1
7	VW	Full	0
8	VW	Full	1

Statistical analysis

Six replicates were utilized for each treatment, and the experiment was repeated twice. All collected data were analyzed and subjected to one-way ANOVA to test for statistical significance, followed by Tukey's post hoc test at $p<0.05$ if significant data was obtained. Correlations between the PGRs used and shoot data were evaluated using Pearson's correlation coefficient. All analyses were performed using IBM SPSS statistical software v.28.0.

RESULTS AND DISCUSSION

Effect of different types and strength of basal media

Number of shoots

The highest average number of shoots was observed in full-strength MS with BAP hormone (5.6 shoots), followed by full-strength VW with added BAP hormone (4.57 shoots) (Figure 1). Half-strength VW without hormone resulted in the lowest shoot number with an average of 1 shoot per explant. The findings from ANOVA analysis indicated that the treatments had no significant effect (at $p<0.05$) on the overall average number of shoots of *D. asper* as compared to the length of shoots.

The result obtained was in line with a previous study in which *D. asper* nodal explants responded better in MS media, producing an average of 5.33 shoots per explant compared to other media tested such as SH (Schenk and Hildebrandt 1972), NN (Nitsch and Nitsch 1969) and B5 (Gamborg et al. 1968) media (Singh et al. 2012). However, another study conducted on the same bamboo species reported that MS media with the strength of three-fourths (¾) supplemented with 3 ppm TDZ resulted in the highest number of shoots (Gusmiaty et al. 2020). Another study conducted on *D. strictus* (Roxb.) Nees had shown the maximum shoot with the incorporation of 0.5 mg L^{-1} TDZ into the half-strength MS liquid media (Singh et al. 2001).

The comparison between MS and VW media showed that the length of shoots in full-strength MS media with or without 1.0 mg L^{-1} BAP was higher compared to the full-strength VW media with and without the hormone. The presence of 1 mg L^{-1} BAP hormone in the media played a vital role in improving the growth of explants, and all media with this hormone showed better responses than those without it. The effect of BAP in improving shoot proliferation has been observed in previous studies on the same species (Ojha et al. 2009).

While VW medium is prominently used in orchid culture, this medium is not limited exclusively to orchids. In fact, many previous studies have utilized this medium in culturing different plant species. Suryaningsih et al. (2018) cultured sorghum, a plant from the grass family in VW media to induce callus formation. Pal et al. (2022) remarked that VW medium promoted indirect organogenesis of *Eleusine coracana* (L.) Gaertn. seeds by formation of callus compared to other media. In our study, however, the observed outcomes suggested that the growth and development of bamboo were less favorable in the VW medium compared to the MS medium (Figure 2). This underscores the importance of selecting an appropriate culture medium tailored to the specific needs of bamboo species, and our finding recommends MS medium as a more effective choice for successful tissue culture.

Length of shoots

From the result, it was found that the highest shoot length was obtained from explants in full-strength MS media with the addition of 1.0 mg L^{-1} BAP hormone (Treatment 4) with 2.14±0.18 cm (Figure 3). This treatment was significantly different ($p<0.05$) from others except for full-strength MS without BAP (Treatment 3), suggesting that full-strength MS resulted in a distinct impact on shoot length compared to other treatments. ANOVA analysis revealed that treatments of different media types and strengths significantly affected the length of shoots of the *D. asper* explants. The length of shoots observed in all VW media was overall relatively lower compared to the one cultured in MS media.

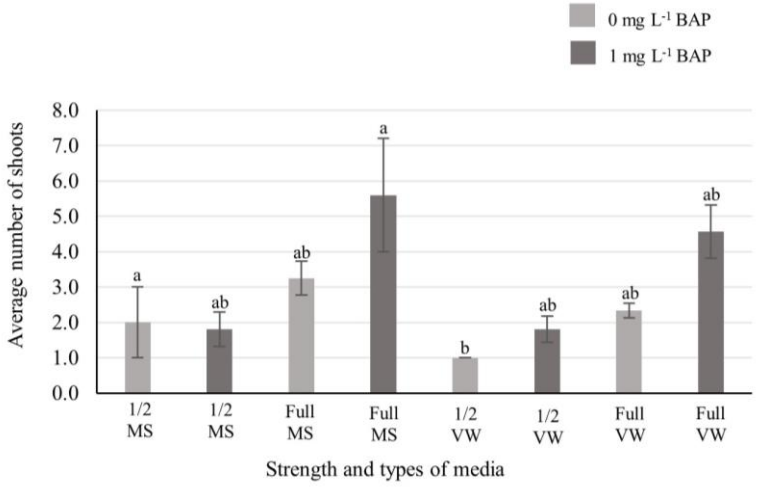

Figure 1. Effects of different treatments (types and strength of media) on shoot number of *Dendrocalamus asper*

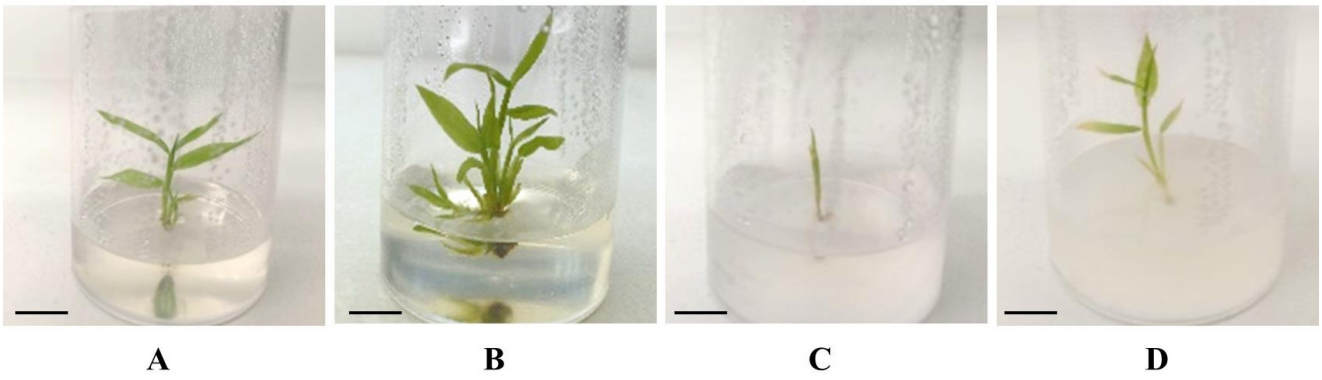

Figure 2. Observation for culture initiation of *Dendrocalamus asper* in different types of media after 8 weeks of culture. A. Culture in full-strength MS without BAP, B. Culture in full-strength MS with 1 mg L^{-1} BAP, C. Culture in full-strength VW media without BAP, D. Culture in full-strength VW media with 1 mg L^{-1} BAP. Bar = 1 cm

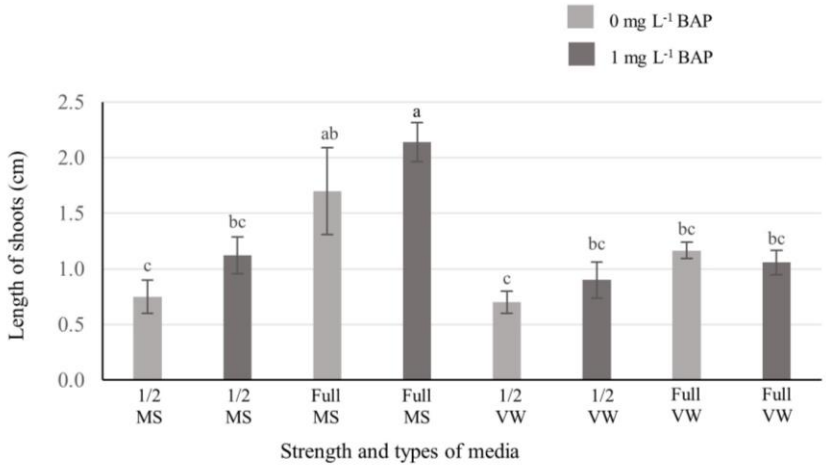

Figure 3. Effects of different treatments (types and strength of media) on shoot length of *Dendrocalamus asper*

A previous study conducted on *Phyllostachys meyeri* McClure nodes revealed that cultivation in half-strength liquid MS without the addition of phytohormone improved the elongation of shoots (Ogita et al. 2008). Another study conducted by Patel et al. (2015) using *B. balcooa* Roxb. species showed that the highest shoot elongation was recorded in half-strength MS with an additional 3 mg L^{-1} BAP during the pre-hardening stage. In the present experiment, full-strength MS showed better performance than half-strength MS in terms of shoot length. The strength of media refers to the concentration of nutrients and salts present in the media. A higher strength of MS media possessed high levels of macro elements, especially nitrogen content (KNO3 and NH4NO3) in the form of ammonium and nitrate that helps to improve the regeneration of explants compared to other basal media (Arab et al. 2014; Phillips and Garda 2019). Nucleic acids, proteins, and secondary metabolites were also highly influenced by nitrogen concentration during plant development (Sidek et al. 2018). This difference in results emphasized the need for tailored approaches considering species-specific requirements in tissue culture studies.

Effect of different combinations of hormones during shoot multiplication

Number of shoots

The results of ANOVA analysis showed that the different treatments of hormones significantly affected ($p<0.05$) the number of shoots produced per explant. Concentration of 4.0 mg L^{-1} BAP combined with 0.5 mg L^{-1} IBA was shown to produce the highest number of shoots compared to other treatments with 5.17±3.97 (Table 2). Other combinations of BAP and IBA also displayed a high number of shoots in vitro, such as the combination of 4.0 mg L^{-1} BAP with 1.0 mg L^{-1} IBA and 4.0 mg L^{-1} IBA, resulting in 4.75±1.91 and 4.8±2.95 shoot number respectively. The lowest shoot number was obtained in the treatment of 0.5 mg L^{-1} BAP and 1.0 mg L^{-1} IBA.

Table 2. Effect of different BAP and IBA hormone concentrations in MS medium on length and number of shoots of *Dendrocalamus asper* after 12 weeks

Concentration (mg L^{-1})		Length of shoots (cm)	No of shoots
BAP	IBA		
0	0	1.59±1.20^{abcde}	2.00±1.00^{ab}
0.5	0	1.25±0.44^{ab}	3.43±1.81^{ab}
1.0	0	1.11±0.65^{efg}	3.56±2.35^{ab}
2.0	0	0.82±0.32^{fg}	2.86±1.35^{ab}
4.0	0	0.93±0.55^{cdefg}	3.00±2.16^{ab}
0	0.5	1.13±0.84^{efg}	2.14±1.35^{ab}
0	1.0	1.27±0.50^{efg}	1.89±1.05^{ab}
0	2.0	1.77±1.33^{abcd}	2.29±1.50^{ab}
0	4.0	1.89±1.15^{a}	1.75±0.89^{ab}
0.5	0.5	1.47±0.93^{abcd}	2.14±0.70^{ab}
0.5	1.0	1.75±0.10^{abcdef}	1.56±0.73^{b}
0.5	2.0	1.26±0.65^{abc}	2.33±0.87^{ab}
0.5	4.0	0.87±0.31^{efg}	3.00±0.82^{ab}
1.0	0.5	0.78±0.45^{defg}	2.25±1.75^{ab}
1.0	1.0	1.13±0.55^{bcdefg}	2.43±1.62^{ab}
1.0	2.0	1.03±0.76^{bcdefg}	1.90±1.29^{ab}
1.0	4.0	1.07±0.49^{bcdefg}	3.71±1.98^{ab}
2.0	0.5	1.35±1.01^{bcdefg}	2.33±1.75^{ab}
2.0	1.0	0.65±0.32^{efg}	3.50±2.67^{ab}
2.0	2.0	1.02±0.81^{defg}	4.09±2.26^{ab}
2.0	4.0	0.80±0.31^{efg}	2.67±1.22^{ab}
4.0	0.5	1.01±0.33^{cdefg}	5.17±3.97^{a}
4.0	1.0	0.62±0.27^{g}	4.75±1.91^{ab}
4.0	2.0	0.85±0.71^{fg}	2.71±1.60^{ab}
4.0	4.0	1.06±0.91^{fg}	4.80±2.95^{ab}

Note: Data shown as mean ± SE followed by the same letter are not significantly different according to Tukey's post hoc test at $p<0.05$

Table 3. Pearson correlation between BAP concentration on shoot length and shoot number of *Dendrocalamus asper*

Variables	BAP Concentration	Shoot length	Shoot number
BAP concentration	1	-0.562**	0.103
Shoot length	-0.562**	1	-0.417**
Shoot number	0.103	-0.417**	1

Note: Correlation was significant at the 0.05 level (2-tailed)

Table 4. Pearson correlation between IBA concentration on shoot length and shoot number of *Dendrocalamus asper*

Variables	IBA Concentration	Shoot length	Shoot number
IBA concentration	1	-.030	.147
Shoot length	-.030	1	-.388**
Shoot number	.147	-.388**	1

Note: Correlation was significant at the 0.05 level (2-tailed)

Our finding was closely aligned with Devi and Sharma (2009), in which a concentration of 13.3 µM BAP and 1.0 µM IBA used together in the media resulted in an enhanced multiplication rate in *Arundinaria callosa* Munro bamboo species. A previous study has reported the combination of 4.0 mg L^{-1} BAP, and 1.0 mg L^{-1} 1-Naphthaleneacetic acid (NAA) resulted in an average of 62 shoots per explants in *B. balcooa* Roxb. culture (Rajput et al. 2020). In another study, instead of increasing shoot multiplication, media enriched 8.0 µM BAP and 1.0 µM NAA led to an expanded rhizomatous section of the explants of *D. hamiltonii* Nees & Arn. Ex. Munro (Agnihotri and Nandi 2009). Other studies have also documented impressive outcomes when utilizing the combined influence of cytokinin and auxin together (Venkatachalam et al. 2015; Rajput et al. 2019; Huang et al. 2024). Apart from that, a combination of two cytokinins has been reported to enhance the proliferation of shoots in certain bamboo species. Utilizing 2 mg L^{-1} kinetin (Kn) and 3 mg L^{-1} BAP together led to the highest average shoots per explant in two different bamboo species, *Melocanna baccifera* (Roxb.) Kurz and *B. tulda* Roxb. (Waikhom and Louis 2014).

Apart from the combination of BAP and IBA hormone, explants cultured in single hormone BAP produced a relatively higher number of shoots compared to single hormone IBA. The role of BAP as a shoot-inducing hormone can be observed from this, and among all treatments with single hormone BAP, a concentration of 1.0 mg L^{-1} resulted in the highest number of shoots. A previous study by Arya et al. (1999) showed that 3.0 mg L-1 BAP added in MS medium produced up to a 16-fold multiplication rate of *D. asper* nodal explants. Favorable responses from single BAP treatments have also been observed in *B. balcooa* (Gantait et al. 2018; Pratibha and Sarma 2014), in which a maximum number of shoots were obtained in their study.

Length of shoots

The highest length of shoots was observed in MS with 4.0 mg L^{-1} IBA with 1.89±1.15 cm, followed by 2.0 mg L^{-1} IBA with 1.77±1.33 cm (Table 2). The shortest shoot length was recorded in treatment combining 4.0 mg L^{-1} BAP and 1.0 mg L^{-1} IBA with an average of 0.62±0.27 cm. Based on the statistical analysis conducted, the hormone concentration also significantly affected ($p<0.05$) the length of shoots.

IBA is a type of hormone that is commonly used as a rooting hormone in woody plants (Zhao et al. 2022) and is responsible for enhancing cell elongation, especially in root cells (Pacheco-Villalobos et al. 2016). The result of this study was slightly different from most previous publications, reported a significant increase in shoot length in media with a combination of BAP and IBA compared to individual hormone treatments in different bamboo species (Venkatachalam et al. 2015; Desai et al. 2019; Rajput et al. 2019). Plus, compared to IBA, most of the bamboo explants produced higher lengths of shoots when treated with a single BAP hormone or other cytokinin only, such as Kn and thidiazurone (TDZ) (Ornellas et al. 2017; Gusmiaty et al. 2020; Choudhary et al. 2022; Gonçalves et al. 2023) instead of IBA alone.

Correlation between BAP and IBA hormone concentrations on the length and number of shoots

Pearson's correlation coefficients were calculated for the length and number of shoots in relation to BAP and IBA hormones to assess the relationship between PGR concentration and shoot morphology. Our results indicated a significant, strong negative correlation between BAP

concentration and shoot length (-0.562) (Table 3), suggesting that elevated BAP levels promote shorter shoot development. This finding is consistent with a previous study, where an increased concentration of BAP also resulted in an overall downward increment in the mean shoot length of this species, as reported by Gunasena et al. (2024).

Meanwhile, IBA concentration exhibited a weak, non-significant negative correlation with shoot length (-0.030) (Table 4), implying a minimal influence on shoot elongation under the experimental conditions, though the highest mean shoot length was observed in cultures supplemented with the maximum IBA concentration (4.0 mg/L). This somehow indicated that, under the specific conditions of this study, IBA either minimally influenced or potentially inhibited cell elongation shoots; however, the effect was very minimal and not significant. This apparent contradiction might be attributed to several factors, such as species-specific response by this plant species and other experimental conditions, such as light and nutrient availability in the media (Long et al. 2022).

Both BAP and IBA hormones displayed a very weak, positive correlation with the number of shoots formed (0.103 and 0.147, respectively). These results contrast with previous findings in *Guadua angustifolia* Kunth bamboo, where a modest positive correlation between BAP concentration and shoot formation was reported (Jiménez et al. 2006). The discrepancy might be attributed to the same factors, such as species-specific responses to PGRs or variations in experimental conditions.

Rooting and acclimatization

The effect of different concentrations of IBA hormone on *D. asper* plantlet rooting was evaluated after 4 weeks of culture. All IBA concentrations (1, 2, 3, 4, and 5 mg L^{-1}) resulted in some degree of rooting. The concentration of 5 mg L^{-1} IBA resulted in the highest percentage of rooting success (60%), while the concentration of 1 mg L^{-1} IBA resulted in the lowest rooting success (20%). Despite varying rooting performance across treatments, all replicates in nearly all treatments had over 10 roots, and the average length of roots exceeded 7 cm for most of the roots.

The observed positive correlation between IBA concentration and rooting success aligns with established knowledge regarding auxin's role in root initiation (Mustafa et al. 2021). Furthermore, the optimal concentration for rooting in our study (5 mg L^{-1} IBA) was consistent with the findings of a previous study that reported successful rooting in another bamboo species, *Oxytenanthera abyssinica* (A.Rich.) Munro uses the same IBA concentration (Admas 2024).

Following successful rooting, plantlets were subjected to a pre-hardening stage to facilitate acclimatization to ex-vitro conditions. This transfer occurred within the controlled environment of the culture room, where key parameters like humidity, light intensity, and temperature were maintained for an additional three weeks. This stage allowed the plantlets to gradually adjust to a slightly less humid environment and develop a more robust root system suited for independent growth in the greenhouse. The formation of new white secondary roots was observed (Figure 4.C) after this stage. The formation of these roots is vital to ensure the highest survival frequency during the acclimatization stage (Patel et al. 2015). All plantlets displayed healthy morphology and 100% successfully established themselves within the chosen substrate mixture (soil, vermiculite, and vermicompost).

In conclusion, the results of this study demonstrated that MS media at full strength is the best media for the initiation of culture in *D. asper* bamboo plants. Shoot multiplication was most successful on full-strength MS media supplemented with 4 mg L^{-1} BAP and 0.5 mg L^{-1} IBA, resulting in the highest number of shoots with satisfactory lengths. This finding suggests that the combination of these hormones has a positive impact on the growth and development of *D. asper* bamboo plants. For rooting, liquid MS media containing 5 mg L^{-1} IBA achieved the highest percentage of rooting success, and all rooted plantlets survived during the acclimatization stage. The findings of this study are of utmost importance for the successful in-vitro propagation of *D. asper* bamboo species, which can contribute to the development of efficient and sustainable bamboo cultivation practices for this economically important species.

Figure 4. Rooting and acclimatization of *Dendrocalamus asper* plantlets. A. Rooted plantlets cultured in liquid MS media supplemented with 5 mg L^{-1} IBA, B. Plantlets during pre-hardening stage after three weeks in the culture room, C. Rooted plantlets after pre-hardening, ready for transfer to new substrate mixture, D. Plantlets established in the chosen substrate mixture (soil, vermiculite and vermicompost) and maintained in the greenhouse

ACKNOWLEDGEMENTS

The authors are grateful for the research grant from the Ministry of Higher Education Malaysia through the Fundamental Research Grant Scheme (FRGS) with code FRGS/1/2021/WAB04/UITM/02/12 and Universiti Teknologi MARA (UiTM) Shah Alam, Malaysia.

REFERENCES

Admas A. 2024. Microclonal propagation protocol for lowland bamboo (*Oxytenanthera abyssinica*) and adapted the propagated seedling in the dryland areas of Abay Valley, Ethiopia. J Adv Biol Biotechnol 27 (5): 490-497. DOI: 10.9734/JABB/2024/v27i5810.

Agnihotri RK, Nandi SK. 2009. In vitro shoot cut: A high-frequency multiplication and rooting method in the bamboo *Dendrocalamus hamiltonii*. Biotechnology 8 (2): 259-263. DOI: 10.3923/biotech.2009.259.263.

Arab MM, Yadollahi A, Shojaeiyan A, Shokri S, Ghojah SM. 2014. Effects of nutrient media, different cytokinin types and their concentrations on *in vitro* multiplication of G × N15 (hybrid of almond × peach) vegetative rootstock. J Genet Eng Biotechnol 12 (2): 81-87. DOI: 10.1016/j.jgeb.2014.10.001.

Arya S, Sharma S, Kaur R, Dev Arya I. 1999. Micropropagation of *Dendrocalamus asper* by shoot proliferation using seeds. Plant Cell Rep 18 (10): 879-882. DOI: 10.1007/s002990050678.

Chandramouli S, Jagadish MR, Viswanath S. 2015. Cultivation prospects of *Dendrocalamus asper* Backer for edible shoots in semiarid and humid tropics of Peninsular India. Intl J Plant Anim Environ Sci 5: 95-101.

Charoenphun N, Pakeechai K. 2021. Effect of thickness on qualities of dried sweet bamboo shoots (*Dendrocalamus asper* Backer) products. J Food Health Bioenvironm Sci 14 (1): 1-8.

Choudhary AK, Kumari P, Kumari S. 2022. In vitro propagation of two commercially important bamboo species (*Bambusa tulda* Roxb. and *Dendrocalamus stocksii* Munro.). Afr J Biotechnol 21: 83-94. DOI: 10.5897/AJB2021.17437.

Desai P, Desai S, Patel A, Mankad M, Gajera B, Patil G, Narayanan S. 2019. Development of efficient micropropagation protocol through axillary shoot proliferation for *Bambusa vulgaris* 'wamin' and *Bambusa bambos* and assessment of clonal fidelity of the micropropagated plants through Random Amplified Polymorphic DNA markers. Agric Nat Resour 53 (1): 26-32. DOI: 10.34044/j.anres.2019.53.1.04.

Devi WS, Sharma GJ. 2009. In vitro propagation of *Arundinaria callosa* Munro - an edible bamboo from nodal explants of mature plants. Open Plant Sci J 3: 35-39. DOI: 10.2174/1874294700903010035.

Emamverdian A, Ding Y, Ranaei F, Ahmad Z. 2020. Application of bamboo plants in nine aspects. Sci World J 2020: 7284203. DOI: 10.1155/2020/7284203.

Gantait S, Pramanik BR, Banerjee M. 2018. Optimization of planting materials for large scale plantation of *Bambusa balcooa* Roxb.: Influence of propagation methods. J Saudi Soc Agric Sci 17 (1): 79-87. DOI: 10.1016/j.jssas.2015.11.008.

Gonçalves DS, Souza DMSC, Molinari LV, Avelar MLM, De Carvalho D, Teixeira GL, Brondani GE. 2023. Clonal microplant production, morphological evaluation and genetic stability of *Dendrocalamus asper* (Schult. & Schult.) Backer ex. K. Heyneke. Nativa 11 (1): 1-9. DOI: 10.31413/nativa.v11i1.14394.

Gunasena MDKM, Chandrasena PH, Senarath WTPSK. 2024. *In vitro* mass propagation of *Dendrocalamus asper* (Giant bamboo) through direct organogenesis. Adv Bamboo Sci 8: 100090. DOI: 10.1016/j.bamboo.2024.100090.

Gusmiaty, Restu M, Larekeng SH, Setiawan E. 2020. The optimization of in vitro micropropagation of betung bamboo (*Dendrocalamus asper* backer) by medium concentrations and plant growth regulators. IOP Conf Ser: Earth Environ Sci 575: 012024. DOI: 10.1088/1755-1315/575/1/012024.

Hartono R, Iswanto AH, Priadi T, Herawati E, Farizky F, Sutiawan J, Sumardi I. 2022. Physical, chemical, and mechanical properties of six bamboo from Sumatera Island Indonesia and its potential applications for composite material. Polymers 14 (22): 4868. DOI: 10.3390/polym14224868.

Hossain M, Kumar S, Seca G, Maheran A, Nor-Aini A. 2018. Mass propagation of *Dendrocalamus asper* by branch cutting. J Trop For Sci 30 (1): 82-88. DOI: 10.26525/jtfs2018.30.1.8288.

Huang L, Zhang Y, Zhou C, Zhu F, Lv Z, Wang S. 2024. Establishment of micropropagation system of *Dendrocalamus brandisii*. Braz J Bot 47 (1): 1-11. DOI: 10.1007/s40415-023-00978-6.

Jiménez VM, Castillo J, Tavares E, Guevara E, Montiel M. 2006. In vitro propagation of the neotropical giant bamboo, *Guadua angustifolia* Kunth, through axillary shoot proliferation. Plant Cell Tiss Organ Cult 86: 389-395. DOI: 10.1007/s11240-006-9120-4.

Kong CK, Tan YN, Chye FY, Sit NW. 2020. Nutritional compositions, biological activities, and phytochemical contents of the edible bamboo shoot, *Dendrocalamus asper*, from Malaysia. Intl Food Res J 27 (3): 546-556.

Lestari NKD, Deswiyanti NW, Astarini IA, Arpiwi LM. 2020. Morphogenesis in vitro flower pedicel of *Lilium longiflorum* with NAA and BAP. KnE Life Sci 5 (2). DOI: 10.18502/kls.v5i2.6436.

Lin S, Liu G, Guo T, Zhang L, Wang S, Ding Y. 2019. Shoot proliferation and callus regeneration from nodular buds of *Drepanostachyum luodianense*. J For Res 30: 1997-2005. DOI: 10.1007/s11676-018-0772-9.

Long Y, Yang Y, Pan G, Shen Y. 2022. New insights into tissue culture plant-regeneration mechanisms. Front Plant Sci 13: 926752. DOI: 10.3389/fpls.2022.926752.

Menezes AP, Almeida JCC, Mergener RA, Gerber T, Schneeberger AH. 2016. In vitro callogenesis from *Cedrela fissilis* leaves. Sci Electron Arch 9 (4): 44-47. DOI: 10.36560/942016248.

Mustafa AA, Derise MR, Yong WTL, Rodrigues KF. 2021. A concise review of *Dendrocalamus asper* and related bamboos: Germplasm conservation, propagation and molecular biology. Plants 10 (9): 1897. DOI: 10.3390/plants10091897.

Ogita S, Kashiwagi H, Kato Y. 2008. In vitro node culture of seedlings in bamboo plant, *Phyllostachys meyeri* McClure. Plant Biotechnol 25 (4): 381-385. DOI: 10.5511/plantbiotechnology.25.381.

Ojha A, Verma N, Kumar A. 2009. In vitro micropropagation of economically important edible bamboo (*Dendrocalamus asper*) through somatic embryos from root, leaves and nodal segments explants. Res Crop 10 (2): 430-436.

Ornellas TS, Werner D, Holderbaum DF, Scherer RF, Guerra MP. 2017. Effects of vitrofural, BAP and meta-topolin in the in vitro culture of *Dendrocalamus asper*. Acta Hortic 1155: 285-292. DOI: 10.17660/ActaHortic.2017.1155.41.

Pacheco-Villalobos D, Díaz-Moreno SM, van der Schuren A, Tamaki T, Kang YH, Gujas B, Novak O, Jaspert N, Li Z, Wolf S, Oecking C, Ljung K, Bulone V, Hardtke CS. 2016. The effects of high steady state auxin levels on root cell elongation in brachypodium. Plant Cell 28 (5): 1009-1024. DOI: 10.1105/tpc.15.01057.

Pal N, Prajna S, Ramesh BS, Reddy J. 2022. Assessing the growth of *Eleusine coracana* seeds in artificial medium under in-vitro conditions. Intl J Bot Stud 7 (2): 123-126.

Pasqualini APDA, Schneider GX, Fraga HPDF, Biasi LA, Quoirin M. 2019. In vitro establishment of *Bambusa oldhamii* Munro from field-grown matrices and molecular identification of endophytic bacteria. Pesqui Agropecu Trop 49: e53673. DOI: 10.1590/1983-40632019v4953673.

Patel B, Gami B, Patel N, Baria V. 2015. One step pre-hardening micro propagation of *Bambusa balcooa* Roxb. J Phytol 7: 1-9. DOI: 10.5455/jp.2015-06-02.

Phillips GC, Garda M. 2019. Plant tissue culture media and practices: an overview. In vitro Cell Dev Biol Plant 55 (3): 242-257. DOI: 10.1007/s11627-019-09983-5.

Pratibha S, Sarma KP. 2014. In vitro propagation of *Bambusa nutan* in commercial scale in Assam, India. J Environ Res Dev 9 (2): 348-355.

Rajput BS, Jani M, Ramesh K, Manokari M, Jogam P, Allini VR, Kher MM, Shekhawat MS. 2020. Large-scale clonal propagation of *Bambusa balcooa* Roxb.: An industrially important bamboo species. Ind Crops Prod 157: 112905. DOI: 10.1016/j.indcrop.2020.112905.

Rajput BS, Jani MD, Sasikumar K, Manokari M, Shekhawat MS. 2019. An improved micropropagation protocol for Manga bamboo - *Pseudoxytenanthera stocksii* (Munro). World News Nat Sci 25: 141-154.

Saad AIM, Elshahed AM. 2012. Plant tissue culture media. In: Leva A, Rinaldi LMR (eds). Recent Advances in Plant in vitro Culture. IntechOpen, London, UK. DOI: 10.5772/50569.

Sharothi P, Raju RI, Hossain MT. 2022. In vitro propagation of an ornamental bamboo (*Bambusa tuldoides* Munro). Plant Tissue Cult Biotechnol 32 (2): 157-166. DOI: 10.3329/ptcb.v32i2.63550.

Sidek N, Mohd Anuar NS, Naher L, Abdul Rahman KAM. 2018. The effect of different nutrient media on *in vitro* shoot and root proliferation of *Vanilla planifolia* Jacks. ex Andrews. Afr J Biotechnol 17 (39): 1241-1246. DOI: 10.5897/AJB2018.16610.

Singh M, Jaiswal U, Jaiswal VS. 2001. Thidiazuron-induced shoot multiplication and plant regeneration in bamboo (*Dendrocalamus strictus* Nees). J Plant Biochem Biotechnol 10 (2): 133-137. DOI: 10.1007/BF03263122.

Singh SR, Dalal S, Singh R, Dhawan AK, Kalia RK. 2012. Micropropagation of *Dendrocalamus asper* {Schult. & Schult. F.} Backer ex k. Heyne): An exotic edible bamboo. J Plant Biochem Biotechnol 21 (2): 220-228. DOI: 10.1007/s13562-011-0095-9.

Souza PFD, Santos CMRD, Ree J, Guerra MP, Pescador R. 2020. Flowering and morphological characterization of *Dendrocalamus asper* androecium and pollen grains. Grana 60 (1): 20-34. DOI: 10.1080/00173134.2020.1736148.

Suryaningsih DR, Prakeswa SA, Me M. 2018. Propagation *in vitro* of sorghum in MS, VW and NT mediums. J Agric Sci Agric 2 (1): 1-8.

Suwal MM, Lamichhane J, Gauchan DP. 2020. Regeneration technique of bamboo species through nodal segments: A review. Nepal J Biotechnol 8 (1): 54-68. DOI: 10.3126/njb.v8i1.30209.

Venkatachalam P, Kalaiarasi K, Sreeramanan S. 2015. Influence of plant growth regulators (PGRs) and various additives on *in vitro* plant propagation of *Bambusa arundinacea* (Retz.) Wild: A recalcitrant bamboo species. J Genet Eng Biotechnol 13 (2): 193-200. DOI: 10.1016/j.jgeb.2015.09.006.

Waikhom SD, Louis B. 2014. An effective protocol for micropropagation of edible bamboo species (*Bambusa tulda* and *Melocanna baccifera*) through nodal culture. Sci World J 2014: 345794. DOI: 10.1155/2014/345794.

Zang Q, Liu Q, Zhuge F, Wang X, Lin X. 2019. In vitro regeneration via callus induction in *Dendrocalamus asper* (Schult.) backer. Propag Ornam Plants 19 (3): 66-71.

Zhao Y, Chen Y, Jiang C, Lu M, Zhang J. 2022. Exogenous hormones supplementation improve adventitious root formation in woody plants. Front Bioeng Biotechnol 10: 1009531. DOI: 10.3389/fbioe.2022.1009531.

NUSANTARA BIOSCIENCE
Vol. 16, No. 2, pp. 245-250
November 2024

ISSN: 2087-3948
E-ISSN: 2087-3956
DOI: 10.13057/nusbiosci/n160211

Anti-inflammatory effects of *Eucheuma denticulatum* and *Padina minor* crude extracts in an egg albumin-induced paw edema of ICR mice

ALITA S. LABIAGA[1,2,♥], MICHAEL B. PLES[1], MARCO NEMESIO E. MONTAÑO[3]

[1]Department of Biology, College of Science, De La Salle University. 2401 Taft Avenue, 0922 Manila, Philippines. Tel.: +63-2-536-0228, [♥]email: alita.labiaga@ctu.edu.ph

[2]Cebu Technological University. Corner M.J. Cuenco and R. Palma Street, Cebu City 6000, Philippines

[3]The Marine Sciences CS Institute, University of the Philippines. Velasquez Street University of the Philippines Diliman, Quezon City 1101, Philippines

Manuscript received: 17 February 2024. Revision accepted: 31 August 2024.

Abstract. *Labiaga AS, Ples MB, Montaño MNE. 2024. Anti-inflammatory effects* of Eucheuma denticulatum *and* Padina minor *crude extracts in an egg albumin-induced paw edema of ICR mice. Nusantara Bioscience 16: 245-250.* Inflammation indicates that the body is unhealthy and exposed to harmful stimuli. Hence, it is important to study natural compounds with anti-inflammatory activities. This study assessed the anti-inflammatory effects of the aqueous and ethanolic crude extracts of *Eucheuma denticulatum* (N.L. Burman) F.S. Collins & Hervey and *Padina minor* (Yamada, 1925) in an egg albumin-induced paw edema of male Institute for Cancer Research (ICR) mice. This in vivo study investigated the anti-inflammatory activity of the aqueous and ethanolic crude extracts from *E. denticulatum* and *P. minor* at a dose of 100 mg/kg and compared it with a commercial anti-inflammatory drug (mefenamic). The study showed a significant decrease in the paw size, body temperature, neutrophil count, and white blood cell count in mice treated with seaweed crude extracts. The results of the first hour showed that the *Eucheuma* ethanolic extract treatment had the highest decrease in paw size, and the highest temperature reduction was found in the treatment of *Padina* ethanolic extract. There are significant differences in paw size, temperature, and leukocytes between the control and treatment groups, as well as between the aqueous and ethanolic extracts. The extracts from *E. denticulatum* significantly decrease the temperature, paw size, and leukocytes, which are the inflammation markers of egg albumin-induced paw edema. The diverse seaweed in the country has various pharmacological potential that should be studied further to maximize utilization.

Keywords: Bioactive compounds, brown algae, ethanolic extracts, red algae, seaweeds

Abbreviations: CBC: Complete Blood Count, EAE: *Eucheuma* Aqueous Extract, EAIPE: egg-albumin-induced paw edema, EDTA: Ethylenediaminetetraacetic Acid, EEE: *Eucheuma* Ethanolic Extract, IACUC: Institutional Animal Care and Use Committee, IBMC: Institutional Biorisk Management Committee, ICR: Institute for Cancer Research, PAE: *Padina* Aqueous Extract, PC: Positive Control, PEE: *Padina* Ethanolic Extract, NC: Negative Control, SC: Sham control, WBC: White Blood Cells

INTRODUCTION

Health and safety are important and concerning matters for everyone. Utilizing natural resources to develop pharmacological and biomedical products still plays an important role in overcoming various diseases. Traditional medicines have low side effects, and natural products remain valuable in the age of traditional and modern medicines.

Marine algae are abundant in the Philippines, and it is famous for its good seaweed cultivation. There are various seaweed species in the country, but most of them remain underexplored. People benefit from abundant seaweeds as food, for export, and as growth promoters or fertilizers, but there are very few studies on the benefits of bioactive products and organic compounds. The red seaweed *Eucheuma denticulatum* (N.L. Burman) F.S. Collins & Hervey is one of the Philippines' four main farmed red seaweed species (Dumilag et al. 2023). However, there are more important benefits of seaweed, namely drug development. Many people consider seaweeds for food; therefore, it is essential to explore information on their utilization for nutraceuticals and pharmaceuticals (Masoumi et al. 2021). Abundant marine algae can also source seaweed-derived bioactive products with high potential for different bioactivities. Only less than half of the species in the country have an economic value, with less than 5% of these species having significant economic value (Magdugo 2020) because many seaweeds are underutilized, and their pharmacological potentials remain unexplored. Ordinary people on the coast have even less notice for the brown seaweed *Padina minor* (Yamada, 1925). Resort owners and swimmers want these brown seaweeds removed because they can add dirt to the beach with the tides.

The phytochemical content of seaweed provides a wealth of potential health benefits, offering a promising avenue for natural medicine against diseases. Various brown, red, and green seaweeds provide sulfated polysaccharides and other bio-active constituents, namely, fucoidan, laminarin, carrageenan, agar, ulvan, tannins, phlorotannin, polyphenols, folic and folinic acids, tocopherols, terpenoids, fucoxanthin, lipids, fatty acids, proteins, and their derivatives (Saraswati et al. 2019; Lomartire and Gonçalves 2022). Seaweeds are

a reservoir of essential bioactivities with the potential as anti-inflammatory, antibacterial, anticancer, antiviral, anti-thrombocytopenia, analgesic, antioxidant, anticoagulant, and antihyperglycemic, cardio- and neuroprotective, and have anti-obesity properties.

Inflammation indicates the body is unhealthy and exposed to harmful stimuli like infections, injuries, and toxins. Acute inflammation displays fever, redness, warmth, swelling, and pain around tissues and joints as a response to injury or disease. It may also progress to chronic degenerative diseases like rheumatoid arthritis, multiple sclerosis, cancer, arthritis, atherosclerosis, heart disease, obesity, diabetes, asthma, dermatitis, migraine, irritable bowel disease, insulin resistance, autoimmune, and other diseases (Barbu et al. 2022). The anti-inflammatory activity of natural compounds is vital in treating the health conditions mentioned above. Some of the seaweed species in the country that are included in the summary of their utilization with an emerging interest in their anti-inflammatory bioactivity are *Asparagopsis taxiformis*, *Porphyra yezoensis*, and *Kappaphycus alvarezii* (Hurtado et al. 2020). The majority of the anti-inflammatory activities of *Eucheuma* species are used in food and industry. Despite the tremendous biodiversity of seaweeds in the Philippines, to the best of the author's knowledge, there are still limited published studies on seaweed utilization for biomedical and pharmacological potential in the country. This study on the anti-inflammatory activities of *E. denticulatum* and *P. minor* in an egg albumin-induced paw edema was aimed at assessing the pharmacological potential of red and brown seaweed extracts and utilizing seaweed bioactive compounds to impact public health and to prevent and overcome diseases.

MATERIALS AND METHODS

Ethical consideration

IACUC certification

The Cebu Technological University-Institutional Animal Care and Use Committee (IACUC) approved laboratory animal safety and proper handling as a protocol under certificate IACUC2020-MA-A03. The study followed the IACUC guidelines, the principles of animal welfare, the Animal Welfare Act of the Philippines (RA 8485), and AO 45 of the Bureau of the Animal Industry.

Biosafety/biorisk clearance

The Institutional Biorisk Management Committee of Cebu Technological University provided the ethical certificate IBMC-2020-MA-004-LAB. The proper procedure for the safety and security of any valuable biological materials was followed throughout the experimentation. Approved safety protocols with necessary precautionary measures to avoid harming humans handling the experiment and providing animal biosafety were observed when dealing with chemicals (e.g., Zoletil).

Research procedure

Seaweed collection and extract preparation

Fresh samples of red seaweed *E. denticulatum* and brown seaweed *P. minor* (25 kg of each) were collected from the shallow coast of Olango Island, Visayas, Philippines, with geographical coordinates at 10°21' 37" North, 124°04'58" East Pangan-an, Lapu-Lapu City, Cebu, Philippines. The samples were naturally air-dried and cut into smaller sizes. The study carried out the phenolic extraction and seaweed bioactive compound preparation techniques of Cotas et al. (2020) with minor modifications. Some seaweeds were preserved as representative samples and submitted for identification to the herbarium curator at the University of San Carlos. The seaweed samples were identified as *P. minor* Yamada (1925) and *E. denticulatum* (N.L. Burman) F.S. Collins & Hervey. The accession number of the herbarium specimen is USCBM2678.

The study used the modified decoction aqueous-extraction method of Godlewska et al. (2016). The red seaweed crude extracts were obtained using a 1:3 seaweed: water ratio. For every 0.5 kg of seaweed powder, 1.5 L of water was used. The extract was heated at 333.15 Kelvin (60°C) and filtered to collect the supernatant. The *Eucheuma* Aqueous Extract (EAE) was stored at 4°C until used. The same procedure was performed to obtain the *Padina* Aqueous Extract (PAE). Air-dried and powdered seaweed samples were used to generate the ethanolic extracts of *E. denticulatum*. The samples were macerated in 95% ethanol (at a 1:3 sample: solvent ratio) for at least 72 hours and then filtered. The *Eucheuma* Ethanolic Extract (EEE) was then collected. The excess alcohol was removed using a rotary evaporator at 100 rpm at 40 to 60°C, with an extract yield of 20-30%. The same method was used to conduct the *P. minor* Ethanolic Extract (PEE). All collected samples were stored in 10-50 mL amber bottles at 4°C until used.

Test animal preparation

The study used 49 male albino Institute for Cancer Research (ICR) mice, 6-8 weeks old, weighing 25-35 g, obtained from the Animal Laboratory in Fil-Scientia Research and Consultancy Services in Cebu City, Philippines. The mice were grouped into seven groups (with seven individuals each) before the 7 days of acclimatization. Three control groups were sham, negative, and positive (SC, NC, and PC), and four treatment groups, PAE, EAE, PEE, and EEE, were closely monitored and observed for their behavior, body score, and attitude. The mice were provided with a regular pellet diet and reverse osmosis water ad libitum from acclimatization until the end of the experiment. The animals were housed in a room with a 12-hour cycle of light and dark at 18-26°C. During the experiment, the animal's paw size was measured using a Vernier caliper (mm), and the temperature (°C) was taken using a digital ear scanner for mice. The temperatures and the paw sizes after induction and post-treatment (first hour, 3 h, 6 h, and 24 h) were then compared. The extracts were given to the treatment groups via oral gavage, 1 h after the egg albumin induction and every 6 h afterward. The animals were weighed before treatment.

Egg albumin inflammation induction and monitoring

After acclimatization, egg albumin was injected into the sub-plantar region of the right hind paw to induce paw edema. The egg albumin-induced paw edema is an animal model for developing rheumatoid arthritis. Next, 0.1 mL of egg albumin in 20% normal saline was induced in all groups except the sham control. This induction procedure followed the method of Akinloye et al. (2020). A digital Vernier caliper and a digital ear scanner thermometer were used to measure the paw size and the temperature, respectively, during pre- and post-induction and -treatments (after the first hour, 3 h, 6 h, and 24 h). The blood samples were collected post-induction and -treatment to compare blood parameters and analyzed for White Blood Cell count (WBC), especially the neutrophil count.

Experimental design and administration of treatments

The study used a randomized experimental design with 49 male albino ICR mice (seven mice for each of the seven groups). The mice had 7 days of acclimatization and 2 days of treatment. Baseline data of uninduced, untreated sham control groups and the groups with egg albumin-induced paw edema were taken. The anti-inflammatory activity of mice treated with seaweed extract was compared to the Sham Control (SC) and the negative and positive control groups. The Negative Control (NC) group was only given after induction, and the Positive Control group (PC) was assigned a dose of 250 mg/kg of mefenamic acid in 0.9% saline (Feng and Wang 2018). Through oral gavage, the treatment groups were given four different seaweed extracts, i.e., EAE, PAE, EEE, and PEE, at a dose of 100 mg/kg (Tumang and Ples 2017; Lomartire and Gonçalves 2022). The experimental extracts were administered an hour after induction and every 6 hours afterward.

Blood collection and analysis

A total of 49 tubes of blood samples were collected using the tail–vein method an hour after induction and 24 hours after treatment. Blood was collected in purple-top ethylenediaminetetraacetic acid (EDTA) vacutainers between 0.25 and 0.5 mL. The WBC and neutrophil counts were compared across the control and the remaining treatment groups. The anesthetic, Zoletil, was used before extraction at 0.2 mL per 0.30 g bodyweight via the intraperitoneal route. The second blood extraction was performed via the orbital sinus method to obtain a blood sample 24 hours after the first treatment, followed by termination. During the terminal blood collection, the capillary tube was placed into the orbital sinus of the mice, and 0.25–0.5 mL of blood was collected and sent to a laboratory for complete blood count, which includes WBC and neutrophil counts. The data of six induced groups (i.e., NC, PC, EAE, PAE, EEE, and PEE) were compared to the uninduced group SC and the data before induction. The anti-inflammatory activity of all treatments was compared to the positive control using a commercial anti-inflammatory drug.

Data analysis

The mean and the standard deviation of the paw size, temperature, WBC, and neutrophil count were presented and compared. The measured parameters were analyzed using one-way Analysis of Variance (ANOVA) with a statistical significance level of 0.05α.

RESULTS AND DISCUSSION

Evaluating the anti-inflammatory effects of bioactive seaweed compounds included markers of inflammation and indicators: paw size, temperature, WBC, and neutrophil count, pre- and post-induction, and post-treatment. Table 1 shows the relative difference between the pre-induction and every succeeding hour until the end of the treatment period. One hour after applying 0.1 mL egg albumin for paw edema induction, a significant increase in the paw sizes of the induced group of mice (NC, PC, EAE, PAE, EEE, and PEE) was recorded as 1.16, 1.19, 1.27, 1.26, 1.67, and 1.38 cm, respectively. The induced groups' temperature increases (in degrees Celsius) were 0.9, 0.8, 1.0, 1.0, 1.4, and 1.5, respectively. It indicates the success of egg albumin-induced paw edema in mice. The paw size significantly decreased 3 h after the animals were treated with seaweed extracts, and the extracts were continuously provided every 6 h for 24 h.

After the EAIPA induction, the results showed an increase in paw size in all of the induced groups, from the negative control to the experimental groups (compared to the baseline data). However, decreased paw size was evident after treatment from the paw size in 1 hour to the 3rd hour or 2 hours after treatment, except for NC. The negative control group (treated with water only) did not decrease after 1 h (instead, it increased from 1.68 to 1.71) and showed the lowest decrease in the following hours, with the decrease range from 0.3 to 0.11 mm. The highest decrease in the paw size was obtained in the EEE between 1 and 3 h post-treatment with a 0.76 mm decrease (2.18 to 1.42), while the PEE ranked second with a 0.69 mm decrease (from 1.88 to 1.19). In all the induced groups, the recorded range of decrease in paw size after treatment was from 0.01 to 0.76 mm. After treatment, the experimental groups showed a significant decrease in paw size 24 hours after the increase in post-induction. The negative control has the least decrease of 0.13 (from 1.68 to 1.55), PC has 0.37 difference, both aqueous extracts (EAE decreased from 1.73 to 1.07 and PAE from 1.76 to 1.10) have 0.66 difference, 1.08 difference from 1.88 to 1.08 in PEE, and the EEE has the highest difference of 1.23 mm for the size dropped from 2.18 to 0.98. The effectiveness of the extracts on mice paw size was higher in the two ethanolic extracts, which might be due to polyphenolic compounds, such as phenols and tannins.

Changes in body temperature are a sign of inflammation and the effectiveness of anti-inflammatory treatments. In this study, the body temperature of the mice control group, housed at 18–26°C, ranged from 35.1°C to 35.4°C. The highest increase in baseline body temperature before induction was recorded as 1.5°C. It is important to note that a significant difference of approximately 1°C can significantly affect the mice (Guo et al. 2012). The normal surface temperature of mice may vary. The temperature induced by diseases may also fall within the normal limits

but show a slight increase or decrease.

Table 2 presented a noticeable increase in mice's body temperature at 1st hour in induced groups (not in Sham) and decreased temperature after treatment (3, 6, and 24 hours) except for the little increase on 3rd hour of NC and 6th hour of PC. The highest temperature difference from the pre-and post-treatments was obtained in the treatment group PEE with a 2.1°C difference, from 37.5°C post-induction temperature to 35.4°C body temperature after 24 hours or after treatment. However, the temperature of mice after treatment ranged from 35.1 °C to 36.2 °C in all groups. The PEE treatment potentially reduced the temperature faster and showed an anti-inflammatory effect. Both aqueous extracts (EAE and PAE) decreased the temperature 3 h after treatment, while the standard drug had a temperature difference of 0.5 at most. There is a significant difference in the temperature of the three control and treatment groups. The temperature change in *P. minor* significantly differed from that in *E. denticulatum*. The temperature of the aqueous extracts also statistically varied in the ethanolic extracts.

The WBC range was within the typical WBC count in mice, which ranged from 2,000 to 10,000 (Table 3). The decreased WBC count in the treatment of seaweed extract indicated the positive effects of the seaweed extracts. In the results of the leukocyte level of the induced groups, the PAE group has the lowest decrease of 1.3, while the decrease in EEE (2.6 difference) is almost the same as the decrease in PC, which is 2.7. The EEE in the treatment group, which is the group treated with ethanolic extract of seaweed, has almost the same effect as the positive control group, which used the commercial anti-inflammatory drug. Polyphenols, such as flavonoids, are bioactive compounds that can inhibit regulatory enzymes or transcription factors to control mediators (Maleki et al. 2019) and reduce the WBC and neutrophil count, important indicators of inflammation. Neutrophil counts are approximately 20 to 30% of the WBC count of laboratory animals with lymphocytic hemograms, like rodents (Tizard 2017). The average neutrophil count decreased post-induction and post-treatment, except in SC (Table 3). The neutrophil count showed no statistical difference between the control and treatment groups an hour after induction and before treatment. Table 3 shows a significant decrease from pre- to post-treatments.

Table 1. The paw size in egg albumin-induced mouse

Group baseline		Paw size (mm)				
		1st hour	3rd hour	4th hour	6th hour	24 hours
SC	0.54±0.04	0.54±0.04	0.55±0.03	0.56±0.03	0.57±0.03	0.57±0.02
NC	0.52±0.09	1.68±0.25	1.71±0.17	1.62±0.17	1.58±0.16	1.55±0.17
PC	0.50±0.06	1.69±0.12	1.65±0.09	1.48±0.16	1.58±0.16	1.32±0.06
EAE	0.46±0.13	1.73±0.16	1.42±0.11	1.27±0.12	1.26±0.08	1.07±0.10
PAE	0.50±0.07	1.76±0.08	1.41±0.07	1.30±0.11	1.26±0.08	1.10±0.06
EEE	0.51±0.09	2.18±0.30	1.42±0.05	1.24±0.10	1.15±0.09	0.98±0.13
PEE	0.50±0.09	1.88±0.18	1.19±0.19	0.94±0.10	0.86±0.06	0.80±0.08
F-computed value	0.293	30.738	43.860	34.219	45.457	40.803
P-value	0.9367667080 39595	0.00000000000007 389494 (**)	0.00000000000000 015629 (**)	0.00000000000001 200810 (**)	0.000000000000 00008242 (**)	0.0000000000 0000056337 (**)

Note: p>0.05: No significant difference, *p<0.05: Significant difference, **p<0.01: Highly significant difference. SC: Sham Control, NC: Negative Control, PC: Positive Control, EAE: *Eucheuma* Aqueous Extract, PAE: *Padina* Aqueous Extract, EEE: *Eucheuma* Ethanolic Extract, PEE: *Padina* Ethanolic Extract (PEE)

Table 2. The temperature and the results of ANOVA of mice after paw edema induction

	Pre-induction (Baseline Data) in °C	1st-hour post-induction (°C)	*3rd hour* Post-treatment (°C)	4th hour Post-treatment (°C)	6th Hours Post-treatment (°C)	24 hours Post-treatment (°C)
SC	35.4	35.4	35.3	35.2	35.2	35.1
NC	35.5	36.4	36.5	36.2	36.2	36.2
PC	35.5	36.3	36.8	36.5	36.3	36.0
EAE	35.2	36.2	36.7	36.2	35.8	35.4
PAE	35.5	36.5	36.5	36.2	35.8	35.6
EEE	35.5	36.9	36.5	36.1	36.0	35.5
PEE	36.0	37.5	35.4	34.8	35.0	35.4
F-computed value	1.902	9.622	16.659	22.499	23.645	10.205
P-value	0.1030810 9061643	0.0000011 74328656 (**)	0.000000001 018497 (**)	0.00000000 0011515 (**)	0.00000000 0005286 (**)	0.0000 00595550103 (**)

Note: p>0.05: No significant difference, *p<0.05: Significant difference, **p<0.01: Highly significant difference. SC: Sham Control, NC: Negative Control, PC: Positive Control, EAE: *Eucheuma* Aqueous Extract, PAE: *Padina* Aqueous Extract, EEE: *Eucheuma* Ethanolic Extract, PEE: *Padina* Ethanolic Extract (PEE)

Table 3. The leukocyte and neutrophil count and results of ANOVA in mice pre- and post-treatment

	Leukocyte count		Neutrophil Count	
	One hour pre-treatment	**24-hour pre-treatment**	**One hour pre-treatment**	**24-hour pre-treatment**
SC	2.7	3.0	2.7	3.0
NC	5.1	2.7	5.1	2.7
PC	4.6	1.9	4.6	1.9
EAE	3.8	2.4	3.8	2.4
PAE	3.6	2.3	3.6	2.3
EEE	5.1	2.5	5.1	2.5
PEE	3.9	2.2	3.9	2.2
F-computed value	7.04	2.47	0.70	2.33
P-value	0.0000314901075156512 (**)	0.04 (**)	0.66	0.05 (*)

Note: p>0.05: No significant difference, *p<0.05: Significant difference, **p<0.01: Highly significant difference. SC: Sham Control, NC: Negative Control, PC: Positive Control, EAE: *Eucheuma* Aqueous Extract, PAE: *Padina* Aqueous Extract, EEE: *Eucheuma* Ethanolic Extract, PEE: *Padina* Ethanolic Extract (PEE)

The extracts and the commercial drug significantly reduced the neutrophil count. There was a considerable decrease in neutrophils between pre- and post-treatments, but no significant difference existed between the control and treatment groups. Several studies on inflammation mediators supported these findings. Bioactive compounds normalize the body's WBC and neutrophil counts. These compounds are associated with anti-inflammatory activity, such as carotenoids, phytosterols, alkaloids, and sulfated polysaccharides from *Caulerpa cupressoides* (Khursheed et al. 2023). Labiaga et al. (2021) showed that the phytochemical analysis results on *E. denticulatum* and *P. minor* contained high alkaloids and carbohydrates. The *E. denticulatum* had a low phenol and sterols, but *P. minor* had paw sizes that were much higher than the critical value of 2.32. Both the aqueous and ethanolic extracts showed a potential anti-inflammatory effect, decreasing neutrophil count and reducing paw edema.

The egg albumin significantly induced paw edema in mice as the paw size increased from pre- to post-induction. The paw size from post-induction treatment was much higher than the critical value of 2.32. The seaweed extracts decreased the paw size in the post-treatment and showed considerable difference in the paw edema of mice in all treatment groups. The highest increase after induction and the highest decrease in paw size post-treatment was evident in the EEE group. The fastest decrease in body temperature was in PEE. The highest reduction of WBC and neutrophil was traced in the positive control group, with only 0.1 difference from the EEE treatment group. A significant difference was also observed between the control group and the groups with seaweed extract treatment and between the aqueous and ethanolic extracts. Extracts of *E. denticulatum* and *P. minor* positively reduced mice's paw size and body temperature.

The brown seaweed *P. minor* significantly decreased the paw size, temperature, WBC, and neutrophil count among the induced mice. The bioactive constituents of these species, which are not well known but are abundant in temperate countries like the Philippines, have a high potential for anti-inflammatory. Previous studies showed that a phlorotannin-rich fraction of brown seaweed, *Cystoseira sedoides*, had great anti-inflammatory effectivity (Lomartire and Gonçalves 2022). Its lectin promotes the reduction of inflammatory hypernociception and inhibits plasma extravasation, cytokine levels, cyclooxygenase-2, and intercellular adhesion molecules (Rivanor et al. 2018). A study in Thailand showed that the aqueous extract of *P. minor* lessened rat ear edema (Peerapornpisal et al. 2010). The strong suppression of edema in the methanolic extract of *Ulva linza* and *Undaria pinnatifida* indicated its anti-inflammatory significance (Lomartire et al. 2021).

Seaweeds, such as *Eucheuma* and *Kappaphycus*, have the potential as anti-inflammatory in solid edema suppression, decreased neutrophil migration, and are potential sources of effective functional metabolites that are potential in inhibiting α-amylase, leukocyte recruitment, and reduced leukocyte influx in the peritoneal cavity (Balasubramaniam et al. 2016). The compounds associated with the anti-inflammatory activity are phenolics, carotenoids, phytosterols, alkaloids, flavonoids, tannins, and sulfated polysaccharides like fucans, flavonoids, tannins, fucoidan, and fucoxanthin (Cotas et al. 2020). Flavonoid is a polyphenol-based bioactive compound that can inhibit regulatory enzymes or transcription factors to control mediators involved in inflammation (Maleki et al. 2019).

Other inflammation mediators are nitric oxide, prostaglandins, and cytokines. Polysaccharides from *Sargassum horneri* showed the highest nitric oxide inhibition and effectively reduced the production of inflammatory cytokines (Jayawardena et al. 2020). *Padina australis* was also assessed to suppress nitric oxide production in lps-induced macrophages and potential as an anti-inflammatory agent (Pechroj et al. 2020). The seaweeds used in previous studies were *C. sedoides*, *Cladostephus spongiosis*, *Padina pavonica*, *Padina gymnospora*, *P. australis*, methanol extracts of *U. linza*, *Ulva pinnatifida*, *Ulva prolifera*, *Chaetomorpha linum*, and *C. cupressoides* (Marques et al. 2012; Ripol et al. 2018; Lomartire et al. 2021; Khursheed et al. 2023). These are just a few, and vast seaweed potentials remain for biomedical and pharmaceutical utilization.

In conclusion, as egg albumin successfully induced paw edema in male ICR mice, the aqueous and ethanolic seaweed extracts from *E. denticulatum* and *P. minor* showed significant anti-inflammatory effects. The seaweed extracts substantially reduced the induced mice's paw size, temperature, WBC, and neutrophil count. The decrease in the paw size and temperature from post-induction to post-treatment indicated the anti-inflammatory effects of the crude extracts. The difference between the WBC and the neutrophil count from post-induction to post-treatment supports the claim that the extracts from the two seaweed species effectively treat inflammation. The bioactive compounds of *E. denticulatum* and *P. minor* potentially affect the inflammation after seaweed extract treatment. This result showed that seaweed extracts have health benefits; therefore, the abundance of seaweeds in the Philippines can have high pharmacological and biomedical potential. Besides being a food and functional food ingredient, seaweed may also be used to fight diseases.

ACKNOWLEDGEMENTS

The authors thank Cebu Technological University, Philippines, for allowing the researchers to experiment in the laboratory and the seaweed farm owners for sharing their resources during sample collection.

REFERENCES

Akinloye OA, Alagbe OA, Ugbaja RN, Omotainse SO. 2020. Evaluation of the modulatory effects of *Piper guineense* leaves and seeds on egg albumin-induced inflammation in experimental rat models. J Ethnopharmacol 255: 112762. DOI: 10.1016/j.jep.2020.112762.

Balasubramaniam V, Lee JC, Noh MFM, Ahmad S, Brownlee IA, Ismail A. 2016. Alpha-amylase, antioxidant, and anti-inflammatory activities of *Eucheuma denticulatum* (NL Burman) FS Collins and Hervey. J Appl Phycol 28: 1965-1974. DOI: 10.1007/s10811-015-0690-6.

Barbu E, Popescu MR, Popescu AC, Balanescu SM. 2022. Inflammation as a precursor of atherothrombosis, diabetes and early vascular aging. Intl J Mol Sci 23 (2): 963. DOI: 10.3390/ijms23020963.

Cotas J, Leandro A, Monteiro P, Pacheco D, Figueirinha A, Gonçalves AM, da Silva GJ, Pereira L. 2020. Seaweed phenolics: From extraction to applications. Mar Drugs 18 (8): 384. DOI: 10.3390/md18080384.

Dumilag RV, Crisostomo BA, Aguinaldo ZZA, Hinaloc LAR, Liao LM, Roa-Quiaoit HA, Dangan-Galon F, Zuccarello GC, Guillemin ML, Brodie J, Cottier-Cook EJ, Roleda MY. 2023. The diversity of eucheumatoid seaweed cultivars in the Philippines. Rev Fish Sci Aquac 31 (1): 47-65. DOI: 10.1080/23308249.2022.2060038.

Feng X, Wang X. 2018. Comparison of the efficacy and safety of non-steroidal anti-inflammatory drugs for patients with primary dysmenorrhea: a network meta-analysis. Mol Pain 14: 1744806918770320. DOI: 10.1177/1744806918770320.

Godlewska K, Michalak I, Tuhy Ł, Chojnacka K. 2016. Plant growth biostimulants based on different methods of seaweed extraction with water. BioMed Res Intl 2016: 5973760. DOI: 10.1155/2016/5973760.

Guo Y, Flaherty MP, Wu WJ, Tan W, Zhu X, Li Q, Bolli R. 2012. Genetic background, gender, age, body temperature, and arterial blood pH have a major impact on myocardial infarct size in the mouse and need to be carefully measured and/or taken into account: Results of a comprehensive analysis of determinants of infarct size in 1,074 mice. Basic Res Cardiol 107: 288. DOI: 10.1007/s00395-012-0288-y.

Hurtado AQ, Magdugo R, Critchley AT. 2020. Harvesting and potential uses of selected red seaweeds in the Philippines with emerging high-value applications. Adv Bot Res 95: 19-56. DOI: 10.1016/bs.abr.2019.12.004.

Jayawardena TU, Sanjeewa KA, Nagahawatta DP, Lee HG, Lu YA, Vaas APJP, Abeytunga DTU, Nanayakkara CM, Lee DS, Jeon YJ. 2020. Anti-inflammatory effects of sulfated polysaccharide from *Sargassum swartzii* in macrophages via blocking TLR/NF-Kb signal transduction. Mar Drugs 18 (12): 601. DOI: 10.3390/md18120601.

Khursheed M, Ghelani H, Jan RK, Adrian TE. 2023. Anti-inflammatory effects of bioactive compounds from seaweeds, bryozoans, jellyfish, shellfish and peanut worms. Mar Drugs 21 (10): 524. DOI: 10.3390/md21100524.

Labiaga AS, Montaño MNE, Ybañez AP, Ples MB. 2021. Phytochemical Profiling of *Eucheuma denticulatum* (NL Burman) Collins and Hervey, 1917 and Padina minor (Yamada, 1925) Seaweeds for Compounds of Potential Biomedical and Pharmaceutical Applications. DLSU Research Congress. De La Salle University, Manila, Philippines.

Lomartire S, Gonçalves AM. 2022. An overview of potential seaweed-derived bioactive compounds for pharmaceutical applications. Mar Drugs 20 (2): 141. DOI: 10.3390/md20020141.

Lomartire S, Marques JC, Gonçalves AM. 2021. An overview to the health benefits of seaweeds consumption. Mar Drugs 19 (6): 341. DOI: 10.3390/md19060341.

Magdugo R. 2020. Marine Seaweeds with Economic Importance in the Philippines: Valuation of Six Species *Caulerpa racemosa* (Forsskål), *Ulva fasciata* (Delile), *Sargassum polycystum* (C. Agardh), *Sargassum ilicifolium* (Turner) C. Agardh, *Halymenia durvillei* (Bory de Saint-Vincent), and *Halymenia dilatata* (Zanardini) from the Philippines. [Doctoral Dissertation]. Université de Bretagne Sud, Lorient, France.

Maleki SJ, Crespo JF, Cabanillas B. 2019. Anti-inflammatory effects of flavonoids. Food Chem 299: 125124. DOI: 10.1016/j.foodchem.2019.125124.

Marques CT, de Azevedo TC, Nascimento MS, Medeiros VP, Alves LG, Benevides N, Rocha HAO, Leite EL. 2012. Sulfated fucans extracted from the algae Padina gymnospora have anti-inflammatory effects. Rev Bras Farmacogn 22 (1): 115-122. DOI: 10.1590/S0102-695X2011005000206.

Masoumi S, Borugadda VB, Dalai AK. 2021. Techno-economic analysis of algal biorefineries. In: Dalai AK, Goud VV, Nanda S, Borugadda VB (eds). Algal Biorefinery: Developments, Challenges, and Opportunities. Routledge, London. DOI: 10.4324/9781003100317-11.

Pechroj S, Potiparsat K, Nangam O, Athipornchai A, Suriyaphan J, Muangham S, Srisook K. 2020. Comparative evaluation of antioxidant and anti-inflammatory activities of four seaweed species from the east coast of the Gulf of Thailand. Health Sci Technol Rev 13 (3): 11-21.

Peerapornpisal Y, Amornlerdpison D, Jamjai U, Taesotikul T, Pongpaibul Y, Nualchareon M, Kanjanapothi D. 2010. Antioxidant and anti-inflammatory activities of a brown marine alga, *Padina minor* Yamada. Chiang Mai J Sci 37(3): 507-516.

Ripol A, Cardoso C, Afonso C, Varela J, Quental-Ferreira H, Pousão-Ferreira P, Bandarra NM. 2018. Composition, anti-inflammatory activity, and bioaccessibility of green seaweeds from fish pond aquaculture. Nat Prod Commun 13 (5): 1934578X1801300521. DOI: 10.1177/1934578X1801300521.

Rivanor RLdC, Do Val DR, Ribeiro NA, Silveira FD, de Assis EL, Franco ÁX, Vieira LV, de Queiroz INL, Chaves HV, Bezerra MM, Benevides NMB. 2018. A lectin fraction from green seaweed *Caulerpa cupressoides* inhibits inflammatory nociception in the temporomandibular joint of rats dependent from peripheral mechanisms. Intl J Biol Macromol 115: 331-340. DOI: 10.1016/j.ijbiomac.2018.04.065.

Saraswati, Giriwono PE, Iskandriati D, Tan CP, Andarwulan N. 2019. *Sargassum* seaweed as a source of anti-inflammatory substances and the potential insight of the tropical species: A review. Mar Drugs 17 (10): 590. DOI: 10.3390/md17100590.

Tizard IR. 2017. Veterinary Immunology-E-Book: Veterinary Immunology-E-Book. Elsevier, Missouri.

Tumang VMC, Ples MB. 2017. Evaluating the anti-inflammatory activity of aqueous extract of Philippine *Morinda citrifolia* (Noni) juice on Albino rats (*Rattus norvegicus*) using carrageenan-induced paw edema. DLSU Research Congress. De La Salle University, Manila, Philippines.

NUSANTARA BIOSCIENCE
Vol. 16, No. 2, pp. 251-262
November 2024

ISSN: 2087-3948
E-ISSN: 2087-3956
DOI: 10.13057/nusbiosci/n160212

Macroplastic pollution in mangrove forests of Tangub City, Panguil Bay, Philippines

LESLIE SAM L. PACULBA, RIALONA CHRISTINE AN C. MABIDA, GENECA CLAIRE M. PERICO, EDUARDO D. MAGDAYO JR.♥, FRANK T. ACOT JR.

Department of Environmental Science, College of Agriculture and Environmental Studies, Northwestern Mindanao State College of Science and Technology. Tangub City, Philippines. Tel.: +63-88-586-0173, ♥email: eduardo.magdayo@nmsc.edu.ph

Manuscript received: 16 July 2024. Revision accepted: 19 September 2024.

Abstract. *Paculba LSL, Mabida RCAC, Perico GCM, Magdayo Jr ED, Acot Jr FT. 2024. Macroplastic pollution in mangrove forests of Tangub City, Panguil Bay, Philippines. Nusantara Bioscience 16: 251-262.* Plastic pollution poses a growing threat to coastal ecosystems. In the Philippines, studies on macroplastic pollution in mangrove forests are limited. This study was therefore conceptualized to assess the extent of macroplastic litter in the mangrove forests of Tangub City, Misamis Occidental, Philippines. The objectives encompassed on determining the count, composition, weight, and polymer type of collected macroplastics, quantifying and comparing the density of macroplastic litter, assessing the clean-coast index, and investigating the impacts of macroplastic litter in mangrove forests. A 50-meter transect line perpendicular to the shore with three 10m×10m quadrats was delineated in the sampling areas. Macroplastic litter collection was done during eight non-consecutive days in in September-October 2023. Results found that *Sonneratia alba* Sm. with its aerial root structure dominated in San Apolinario trapped more plastics. Food packaging accounted for 48.7% of the composition, with Low-Density Polyethylene (LDPE) being the most common polymer type at 44%. The highest macroplastic density was 0.20 items/m² for San Apolinario. While plastic density varied across sites despite similar cleanliness ratings, the distribution remained consistent throughout the mangrove forests indicating no significant differences in areas (p=.45). Moreover, findings showed that plastic litter harmed the mangrove forests as the pneumatophores were smothered, the branches were twisted, and the stems were damaged disrupting the mangroves' structure. This study highlights the importance of understanding plastic pollution in mangroves to develop effective waste management and conservation strategies.

Keywords: Food packaging, macroplastic litter, mangrove forest, plastic pollution

INTRODUCTION

Plastics have become versatile materials with a wide range of applications across various sectors (Baynes et al. 2021). The widespread use of single-use plastics (trash bags, shopping bags, etc.) unfortunately fuels plastic pollution due to improper disposal (Khoaele et al. 2023). This surge in plastic waste has severe consequences, leading to plastic pollution as a global environmental catastrophe and a rising environmental problem (Rochman et al. 2013). Plastic pollution is particularly concerning due to the persistence of plastic in the marine environment (Landrigan et al. 2020). These materials can linger for extended periods, with varying persistence depending on factors like size, polymer type, shape, and density (Hidalgo-Ruz et al. 2012; Eriksen et al. 2014; Sajorne et al. 2021; Inocente and Bacosa 2022; Requiron and Bacosa 2022). This extended presence, combined with transport by currents, and wind, and its presence in various land- and sea-based sources, ultimately leads to the widespread occurrence of plastic residues throughout the world's oceans (Lebreton et al. 2012; Van Sebille et al. 2012; Do Sul et al. 2014; Dris et al. 2016).

The Philippines is responsible for over one-third (36%) of plastic inputs worldwide (Ritchie and Roser 2018). It ranked third globally in plastic waste emissions, contributing approximately 0.28 to 0.75 million tons of plastic waste annually. This was part of a larger issue where over 466 of the 1,656 rivers worldwide collectively deposited more than 0.36 million tons of plastic waste each year into the environment (Jambeck et al. 2015; Braganza 2017). The increased prevalence of disposable plastic waste in the environment is caused by multiple factors, include inadequate recycling rates, challenges in waste collection, and the lack of consistent separation of plastic packaging in Local Government Units (LGUs) (Manas 2023). Also, the tropical country of the Philippines experiences significant annual precipitation (PAGASA 2021), which leads to the transportation of plastic debris from land to rivers through surface run-off, stormwater, and sewage, and eventually, the plastics are carried from the rivers to the seas and oceans (Li et al. 2020).

Plastic waste problem affects various ecosystems (Alava et al. 2023) including mangroves which are high risk of being polluted (Koop 2021). According to Garcia et al. (2014), the Philippines is renowned for having one of the largest coastlines in the world, stretching approximately 36,289 kilometers, which is particularly significant in tropical areas due to the abundance of mangroves. The country hosts at least half of the world's 65 mangrove species (Kathiresan and Bingham 2001; Goloran et al. 2020), which provide food for many fishes, invertebrates,

and birds, as well as protection from coastal disasters (Alongi 2008). With their abundant prop roots, pneumatophores, and robust tree trunks, they provide great wave protection while simultaneously acting as natural traps for floating plastic garbage carried by tidal currents (Horstman et al. 2014; Norris et al. 2017; Martin et al. 2019; Duan et al. 2021). Plastics can get buried in the sediment or become hooked by mangrove branches, stunting their growth, and potentially harming the mangrove trees (Ali et al. 2021). In certain cases, it reduces oxygen penetration into the rhizosphere, causing mangrove suffocation (Smith 2012), which results in pneumatophore distortion or poor growth (Van Bijsterveldt et al. 2021). Furthermore, in a study conducted by Manullang (2020), macroscopic plastic waste has also been shown to directly hinder photosynthesis and entangle plant seedlings having a significant influence on plant survival in littered ecosystems.

Concerning these threats, there are several studies conducted to document the impacts of plastic wastes (Ryan 2015). However, the potential impact of plastic litter in the mangrove forests in the Philippines is far less studied. Plastic litter has been found in many mangrove areas in Tangub City and there is no data on the density, composition, classification, and possible impacts of macroplastics in mangrove ecosystem. Thus, this research was conceptualized to determine the count, composition, weight, and polymer type of collected macroplastics, quantify the density of macroplastic litter, assess the clean-coast index, compare the density of macroplastics litter found in three sampling sites, and investigate the impacts of macroplastic litter in mangrove forests. This study provides a baseline data on macroplastic contamination in the mangrove forests of Tangub City and to furnish policy recommendations to the concerned agencies to combat plastic litter in mangrove ecosystems.

MATERIALS AND METHODS

Study area

The study was conducted in Panguil Bay, specifically in Tangub City, Misamis Occidental (Figure 1). This bay is bordered by the provinces of Lanao del Norte to the east and Zamboanga del Sur and Misamis Occidental to the west (Israel et al. 2004). Covering approximately 18,000 hectares, it features a coastline that stretches 112 kilometers (70 miles). Tangub City, situated in the province of Misamis Occidental, is a coastal city spanning an area of 162.78 square kilometers and has a population of 68,389 residents. The coastal fringes of Tangub City are home to rich mangrove forests, comprising both naturally occurring and replanted mangroves. Despite ongoing restoration efforts, there are noticeable differences in the density and composition of these mangrove forests; some areas thrive while others are more sparse due to encroachment from informal settlements. For this study, three barangays—Lorenzo Tan, San Apolinario, and Mantic—were selected as sampling sites based on criteria such as accessibility, mangrove cover, and proximity to human habitation to minimize biases.

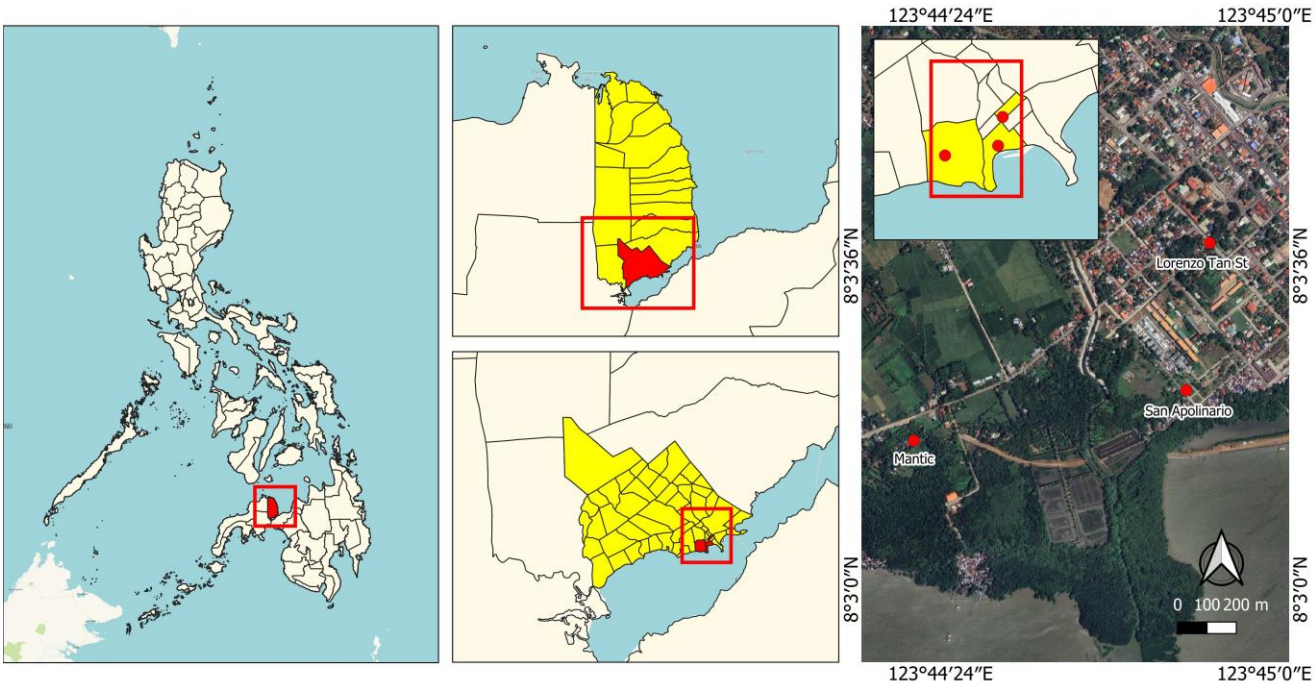

Figure 1. Map of Tangub City, Misamis Occidental, Philippines showing the three sampling areas

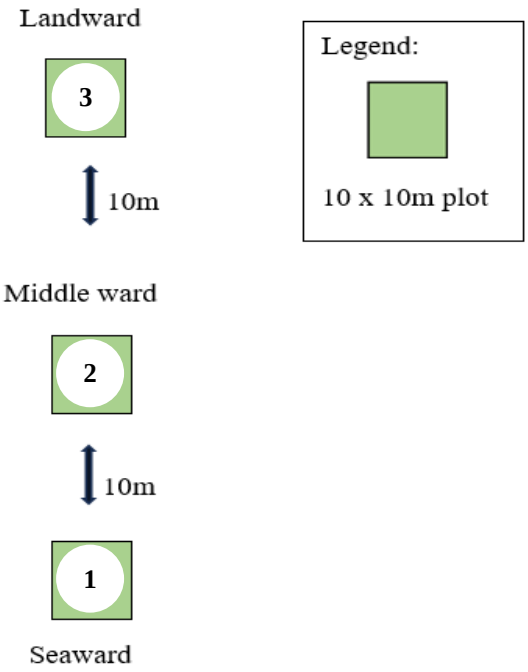

Figure 2. A schematic diagram for macroplastic litter sampling subplot in a 10x10 m^2 transect quadrat for the study of three mangrove forests in Tangub City, Philippines (zone 1. facing seaward side, zone 3. facing the landward side).

Data collection procedure

Identification of mangrove composition

The inventory of mangrove species composition was made in every study site before the collection of macroplastic litter. The basic mangrove identification survey was conducted during low tide to be able to identify the different species found in the three study sites (Abreo et al. 2020). All mangrove species found in all quadrats were counted, documented, and identified. The mangrove species were determined using the field guide manual to Philippine Mangroves Identification of Primavera et al. (2019) along with other online literature and researchers (Primavera et al. 2004).

Transect line and sampling station establishment

A 50-meter transect line perpendicular to the shore was employed in this study to collect samples of macroplastic litter. This method was based on the study by Suyadi and Manullang (2020) with modifications. On each transect, three 10 m×10 m (100 m^2) quadrats were laid out following the methods conducted by Yin et al. (2019). The subplots were 10 meters away making them not independent from each other. This method was modified from the study of Do Sul et al. (2014) (Figure 2).

Mangrove plastic litter collection

Plastic litter were collected at the lowest tide of the day. Plastic litter (macroplastics) found in the quadrat were manually collected by hand and placed in a labeled bag. The collected plastics were classified based on their plastic category following Syakti et al. (2017) and Kalnasa et al. (2019). The study employed a simultaneous collection of eight non-consecutive days to assess the accumulation of macroplastics in each area. Sampling collection was undertaken from the 20th day of September to the 14th day of October 2023. The collection specifically took place on Wednesdays to represent weekdays and Saturdays to represent weekends (Acot et al. 2022).

Plastic litter category and classification

The litter collected from each quadrat was properly washed and air-dried before its dry weight was measured with a digital top pan balance. Then, the items were manually counted and sorted into specific categories based on the study of Syakti et al. (2017) and Kalnasa et al. (2019) with some minor modifications: (a) food packaging, (b) disposable utensils (c) food containers (d) cloth, (e) napkin and diapers, (f) ropes, (g) cigarette, (h) plastic fragments, (i) plastic bags, (j) styrofoam, (k) medical waste, (l) sack, and (m) nylon fishing line, (n) footwear, (o) plastic bottle, (p) plastic caps, (q) fishing nets, (r) other bottle containers, (s) disposable lighters, (t) plastic cups (u) straws, (v) toiletries, (w) rubbers, (x) tetra packs, (y) metals, (z) glass, (aa) aluminum, (ab) electronics.

Macroplastic identification based on polymer type

The polymer types were identified according to the application. This method was based on the study of Andrady and Neal (2009), Namazi et al. (2017), and PlasticsEurope (2018). Most plastics were considered "hard-to-degrade" materials because of their corrosion resistance (Cole et al. 2011; Porta 2021).

Examining the impacts of plastic litter in mangrove forests

Direct observation with the aid of mobile cameras was employed to assess the visible impact of macroplastic litter in mangrove forests. The effects on mangroves were categorized into four categories (Damaged stem, Twisted Branches, Damaged pneumatophores and Smothering pneumatophores).

Data analysis

Composition of macroplastic litter prevalent in mangrove forests.

For the composition of plastic litter, the use of percent composition was calculated based on the study of Abreo et al. (2019) as shown in the equation below:

$$Composition\ analysis = \frac{Number\ of\ items\ in\ category}{total\ number\ of\ items\ in\ all\ categories} \times 100$$

Abundance and density of plastic litter

The density of the plastic litter collected was computed from the total number of items collected divided by the total sampled area which was expressed in no. of items/m^2 as shown in the equation below following the study of Abreo et al. (2019).

$$Density\ analysis = \frac{Number\ of\ plastic\ litter}{m^2}$$

Table 1. The classification of Clean Coast Index (CCI)

Clean Coast Index	Cleanliness rating	Visual assessment
0-2	Very clean	Very little debris is seen
2-5	Clean	Little debris is seen over a large area
5-10	Moderate	A few pieces of debris can be detected
10-20	Dirty	A lot of debris in the mangrove area
20+	Extremely dirty	Most of the mangrove area is covered with plastics

Clean Coast Index (CCI)

The Clean-Coast Index (CCI) was first proposed by Alkalay et al. (2007) as a tool to estimate the level of dirtiness or cleanliness of the coastal areas. It considered a range of factors, including the amount and type of litter present, as well as the level of public awareness and participation in clean-up efforts. This mathematical instrument was an easy way to avoid bias conducted by the assessor (Alkalay et al. 2007). Using the CCI evaluation, the total amount of plastic litter collected in the study was analyzed to qualitatively assess the cleanliness of each mangrove area. To ensure that the resulting value from the CCI equation did not fall between zero and one, a coefficient of k=20 was included in the equation as a multiplier. This was suggested by Alkalay et al. (2007) to ensure that the values generated do not fall between 0 and 1. The CCI was calculated as follow:

$$CCI = \frac{Total\ number\ of\ plastic\ items\ on\ transect}{Total\ area\ of\ transect} \times K$$

The final CCI numbers were used to determine the corresponding cost grade index. In accordance with the CCI scale, Table 1 shows the assessment of coastal beach cleanliness which is classified as follows: values ranging from 0 to 2 represent a state of being very clean, 2 to 5 indicate a clean condition, 5 to 10 suggest a moderately clean state, 10 to 20 denote a dirty condition, and values exceeding 20 indicate an extremely dirty state, where the majority of the beach is covered in plastic debris (Vlachogianni et al. 2018).

Statistical analysis

The collected data were analyzed using Jamovi statistical software version 2.4.11. To identify the significant difference between sites, a one-way Analysis of Variance (ANOVA) test was used. The density (items/m^2) ± SD was calculated, and values were evaluated as significantly different at $p<0.05$.

RESULTS AND DISCUSSION

Mangrove species composition

Mangroves are salt-tolerant trees that thrive along tropical and subtropical coastlines (Kesavan et al. 2021). It flourishes amid the tides, forming an intricate network of roots and branches that act as a natural barrier, effectively trapping objects carried by currents, such as floating plastic (Horstman et al. 2014; Norris et al. 2017). However, due to the differences in the physical structure of mangrove species, some species are more able than others to capture plastic litter (Luo et al. 2022). Among mangrove species, *bungalon* (*Avicennia marina* (Forssk.) Vierh.) can trap more plastics due to its distinct aerial root system, which includes sieve-like pneumatophores able to capture floating plastic debris (Martin and Duarte 2019). Conversely, the White mangrove (*Laguncularia racemose* (L.) C.F.Gaertn.) has no visible aerial roots that may not be able to retain plastic litter.

In this study, there were eight (8) mangrove species identified in the sampling areas: *pagatpat* (*Sonneratia alba* Sm.), *api-api puti* (*Avicennia alba* Blume), *bakauan-lalaki* (*Rhizophora apiculata* Blume), *saging-saging* (*Aegiceras corniculatum* (L.) Blanco), *lagiwliw* (*Acanthus ilicifolius* L.), *palaypay* (*Acrostichum aureum* L.), *tambigi* (*Xylocarpus granatum* J.Koenig) and *nipa* (*Nypa fruticans* Wurmb) (Table 2). Among the identified mangrove species, *pagatpat* (*S. alba*) was more apparent in Brgy. Lorenzo Tan and Brgy. San Apolinario. This species has an aerial root that grows upward (Costa et al. 2019) and can trap garbage (Siddiqui and Pandey 2013). Moreover, *A. alba* has pneumatophores with a knobby protrusion on their roots that effectively capture plastic waste. Understanding the plastic capture capabilities exhibited by various mangrove species is crucial in developing strategic actions to safeguard vital mangrove ecosystems from the detrimental effects of plastic pollution.

Table 2. Mangrove species composition and number of individuals in all sampling sites

Mangrove species	Lorenzo Tan	San Apolinario	Mantic
Pagatpat (*Sonneratia alba*)	13 (49%)	16 (100%)	0
Api-api puti (*Avicennia alba*)	2 (7%)	0	27 (71%)
Bakauan-lalaki (*Rhizophora apiculata*)	1 (4%)	0	0
Saging-saging (*Aegiceras corniculatum*)	2 (7%)	0	0
Lagiwliw (*Acanthus ilicifolius*)	0	0	6 (16%)
Palaypay (*Acrostichum aureum*)	3 (11%)	0	3 (8%)
Tambigi (*Xylocarpus granatum*)	3 (11%)	0	0
Nipa (*Nypa fruticans*)	3 (11%)	0	2 (5%)
Total number of species	7	1	4
Total strands	27	16	38

Table 3. Count of macroplastic litter collected in all sampling sites

Plastic category	Number of pieces	Composition (%)	Weight (g)
Food packaging	609	48.7	3320.86
Plastic bags	278	22.24	4071.28
Napkin/diapers	66	5.28	1754.98
Plastic cups	44	3.52	226.48
Plastic bottle	32	2.56	722.05
Sacks	30	2.40	3238.79
Glass	25	2.00	5284.25
Footwear	19	1.52	2929.59
Clothes	17	1.36	4067.65
Plastic fragments	16	1.28	396.56
Ropes	15	1.20	255.38
Nylon fishing line	14	1.12	259.2
Plastic caps	13	1.04	41.51
Fishing nets	12	0.96	673.45
Medical waste	9	0.72	73.35
Styrofoam	7	0.56	145.82
Aluminum	6	0.48	220.31
Food containers	4	0.32	183.49
Straws	4	0.32	23.22
Electronic	4	0.32	98.29
Disposable utensils	4	0.32	12.89
Toiletries	3	0.24	20.73
Disposable lighters	2	0.16	27.08
Metals	2	0.16	70.56
Rubbers	1	0.08	51.28
Others	14	1.12	260.07
Total	1250	100	28,419.39

Count, composition, and weight of collected macroplastics in all sampling sites

Macroplastic can be easily transported by natural forces throughout the environment, particularly in vulnerable ecosystems like mangrove forests. The findings from this study exemplify this concern, revealing a significant amount of plastic litter collected within just eight non-consecutive days across various mangrove sampling sites (Table 3). Out of 27 different types of plastic waste in all sampling sites, a total count of 1250 plastic items and a total weight of 28,429.11 g were collected. Out of the accounted macroplastics, 609 pieces (48.7%) of which were single-use plastics such as food packaging (e.g. sachet of shampoo, junk foods, candies, etc.). It was recorded to be the most abundant in terms of count, composition, and weight. According to the studies of Kalnasa et al. (2019), Paler et al. (2019), Esquinas et al. (2020), and Sajorne et al. (2021), in developing countries like the Philippines, readily available and affordable single-use food, products packaging, such as sachets, is the most common plastic waste and the primary contributor to the increasing adverse effects of plastic garbage.

Meanwhile, plastic bags were the second most abundant item collected, accounting for 278 pieces (22.2%) of all plastic waste items collected. While their affordability and lightweight nature make plastic bags a convenient choice for carrying groceries and other goods, they pose a significant threat to marine life, particularly species like seabirds and sea turtles. These animals, which feed exclusively at sea and exhibit non-selective surface foraging behavior, are especially vulnerable to plastic pollution, as evidenced by the high prevalence of plastic debris found in their stomachs (Besseling et al. 2015; Hardesty et al. 2015; Wilcox et al. 2015; Kumartasli and Avinc 2020).

Moreover, the results also highlight site-specific variations in waste composition. Each site exhibits its waste profile, with variations in the relative combination of factors that influence consumption patterns and waste generation in each area. Understanding these factors is essential for developing effective waste management strategies tailored to the specific challenges of each site. For instance, as shown in Figure 3, Lorenzo Tan (A) recorded numerous categories of plastic types (26), dominated by food packaging (30%). The presence of a fish port, tourist spot, and numerous variety stores likely contributes to this, as they rely heavily on single-use plastics. Additionally, the high proportion of disposable personal care products (napkins and diapers, 11%) suggests potential cultural influences or convenience-driven choices. On the other hand, in San Apolinario (B), with 24 types of plastics, food packaging emerges as the dominant waste component, making up 59% of the total waste. This high contribution can be attributed to factors like the concentration of food establishments, variety stores, and street food vendors and the lack of sustainable waste management practices, such as limited waste collection further exacerbating the issue. The significant contribution of plastic bags at 21% can be attributed to their availability and widespread use indicating a need for targeted interventions to reduce their usage and promote reusable alternatives. However, in Mantic (C), despite having the lowest plastic composition of 17, food packaging still emerges as the primary composition of waste, accounting for a substantial 61% of the total waste generated. Notably, the significant contributions of plastic bags (14%) and plastic cups (8%) can be linked to the popularity of take-out beverages and the consumption of beverages on the go.

Overall, the study suggests a general similarity in plastic waste composition likely influenced by factors like the local businesses which contributed to the prevalent usage of single-use plastic packaging in the areas and the flow of water that significantly connects the coastal areas in Tangub City. The data obtained underscore the need for comprehensive waste management strategies that address the entire waste stream, considering not only the highest contributors but also the smaller categories. A holistic approach should involve the potential for behavior change and the adoption of more sustainable practices, reducing plastic consumption, promoting recycling and reuse, implementing proper waste disposal systems, and fostering a circular economy.

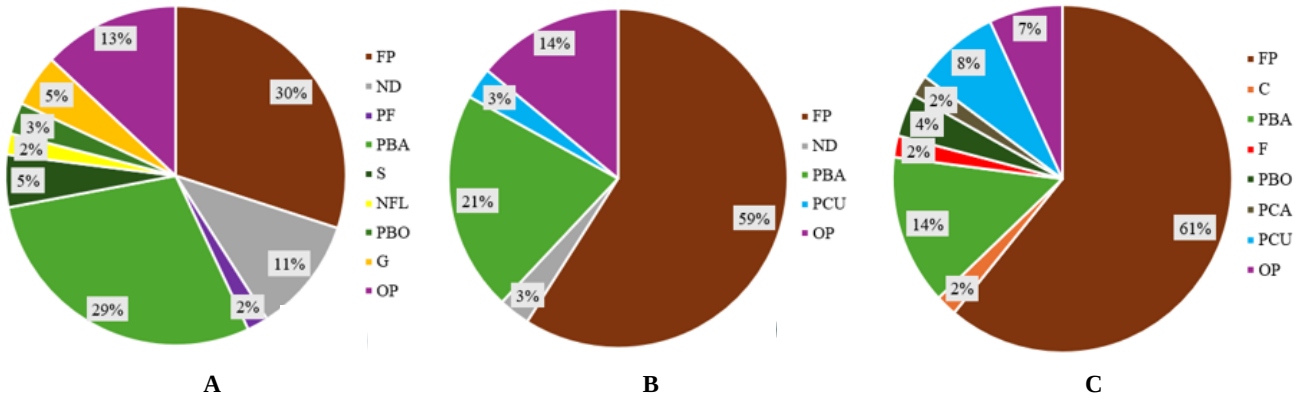

Figure 3. Composition of macroplastic litter of each site in Tangub City, Misamis Occidental, Philippines, i.e. A. Lorenzo Tan, B. San Apolinario, C. Mantic. Note: FP: Food Packaging, NP: Napkins and Diapers, PF: Plastic Fragments, PBA: Plastic Bags, S: Sacks, NFL: Nylon Fishing Lines, F: Footwears, PBO: Plastic Bottles, PCA: Plastic Caps, PCU: Plastic Cups, G: Glasses, OT: Other Plastics

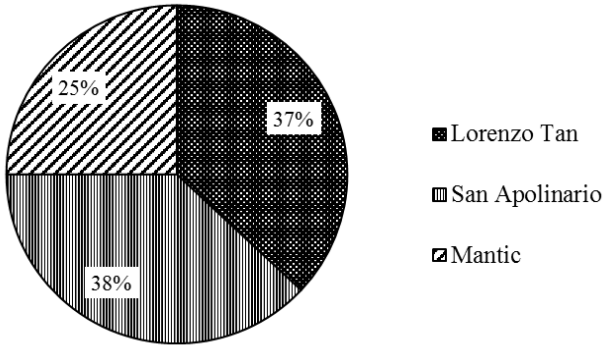

Figure 4. Overall total waste count in three sampling sites with corresponding percentage

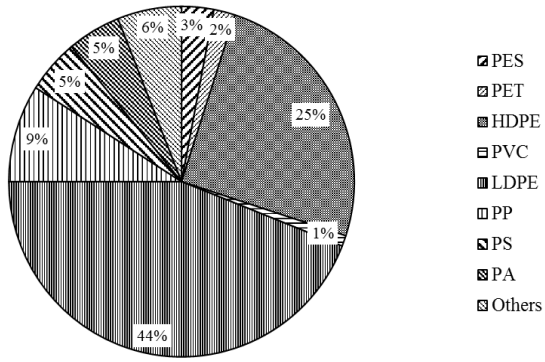

Figure 5. Polymer composition of macroplastics collected from all sampling sites

The total count of macroplastics from each sampling site (Figure 4) reveals the extent of plastic litter pollution across these environments. Among the three sampling sites, San Apolinario had the highest macroplastic litter collected with 480 items, accounting for 38% of the total waste. Following San Apolinario is Lorenzo Tan with 459 (37%) total waste, and Mantic had the lowest waste counts of 311 (25%). Some factors could explain the high waste counts in these sampling sites. In San Apolinario, due to its extensive mangrove cover, is predominantly dominated by the *S. alba* species, known for its aerial roots that effectively trap and retain plastic debris within the intricate structures of the mangrove habitat and the presence of numerous small convenience stores and mooring areas likely contributes to waste accumulation. Additionally, Barangay Lorenzo Tan exhibited a significant amount of plastic litter, characterized by the presence of stack macroplastics in the quadrat facing the landward side, along with the existence of a fish port and a scenic spot, which collectively contributed to the considerable volume of waste collected.

Meanwhile in Barangay Mantic, near the sampling area, an ongoing seawall construction serves as a barrier against debris, potentially reducing the likelihood of plastics reaching the mangrove area where they could accumulate. Additionally, Barangay Mantic is influenced by the plastic ban implemented by the city of Tangub, particularly on specific days. This ban has led to reduced plastic usage in the area.

Polymer classification of collected macroplastics

In this study (Figure 5), the plastics collected were further classified into 13 polymer types, which include Polyester (PES), Polyethylene terephthalate (PET), Polyethylene (PE), High-density polyethylene (HDPE), Polyvinyl chloride (PVC), Low-density polyethylene (LDPE), Polypropylene (PP), Polystyrene (PS), High-impact polystyrene (HIPS), Polyamides (PA) (nylons), Acrylonitrile butadiene styrene (ABS), Polycarbonate (PC), and Polytetrafluoroethylene (PTFE) (Shah et al. 2008; Halden 2010; Andrady 2011; Ghosh et al. 2013;). Findings presented in Figure 5, show that collected plastic wastes consist of PES, PET, PVC, LDPE, HDPE, PP, PA, PS, and others. The sampling areas were dominated by LDPE plastic waste, having 44%, which is attributed to its widespread usage in everyday items such as plastic bags, packaging materials, and disposable products. The convenience and versatility of LDPE contribute to its extensive presence in the waste stream. The other significant type of plastic dominated also in the areas was HDPE accounting for 25%. This polymer is known for its

high strength-to-density ratio, chemical resistance, and impact strength (Wang et al. 2019). The high percentage of HDPE in the waste collected can be attributed to its widespread usage in packaging and durable goods. The durability and versatility of HDPE make it a preferred choice for many industries, leading to its significant presence in the waste stream (Kumar et al. 2021). The findings suggest that most of the plastics collected came from household or community settlements. While these plastics are useful to humans, they have also created an emerging environmental threat (Thompson et al. 2009; Olanrewaju and Oyebade 2019; Dumbili and Henderson 2020). According to the study of Lebreton et al. (2018), polyethylene-based plastics have been discovered in the marine environment since the early days of production, resulting in a global plastic crisis. The flexible and thin structure of plastic LDPE causes it to decompose quickly into microplastics (Devi et al. 2016), which can cause physical damage and harm to the environment and organisms in the water (Adithama et al. 2023). Furthermore, in a study by Shimao (2001) and Barnes et al. (2009), the widespread use of LDPE and HDPE has significant negative impacts on terrestrial and marine ecosystems, such as the obstruction of fish, birds, and marine mammals' intestines by plastic litter. Moving on to the other polymer types, PET (2%), PP (9%), PS (5%), PA (5%), and others (6%) make up the remaining percentages of the waste collected. The category of "Others" encompasses polymer types that may not be as prevalent but still contribute to the overall waste composition. This category includes various polymers that can be found in applications in different industries.

Understanding the composition of these polymer types in the waste stream is crucial for developing effective waste management strategies. It allows for targeted efforts in recycling, promoting sustainable alternatives, and reducing the environmental impact of plastic waste. By focusing on the highest contributors, such as LDPE and HDPE, and considering the characteristics and applications of other polymer types, it becomes possible to develop comprehensive waste management approaches that address the specific challenges posed by each polymer type.

Macroplastics density and Clean-Coast Index (CCI) analysis for cleanliness assessment

Table 4 shows the macroplastic litter density and Clean-Coast Index level across different locations. Among the three sites, San Apolinario had the highest density of 0.2 items/m^2, while Mantic, on the other hand, had the lowest overall macroplastic litter count of 311 pieces with a density of 0.13 items/m^2. Moreover, the results were further analyzed using the Clean-Coast Index to assess the level of cleanliness in the mangrove areas (Alkalay et al. 2007). The findings indicated that Lorenzo Tan, San Apolinario, and Mantic were comparatively clean, in which CCI ranging from 2 to 5.

However, it is important to note that the analysis focuses solely on macroplastics and does not consider other types of litter. To sustain the cleanliness and minimize the impact of plastic pollution, monitoring and waste management strategies should be continued in the areas. This includes not only addressing macroplastics but also considering other types of litter. By implementing comprehensive waste management practices and raising awareness about the importance of reducing plastic waste to maintain the cleanliness and contribute to a healthier coastal environment.

As illustrated in Figure 6, a detailed summary of every collection is presented. It depicts the quantity of plastic litter collected from three distinct mangrove areas across eight non-consecutive days. The results indicated that during the initial collection on Day 1, all sites exhibited a higher accumulation of plastics. This outcome was expected, as it represents the buildup of plastics over time in each respective area. Meanwhile, as observed there is considerable variation in the amount of litter collected, indicating fluctuations in collection over time. After the collection of stack macroplastic on Day 1, it was shown that Day 3 of the collection was found to have the highest total count with 187 items while the lowest count with 83 items was recorded on Day 6 of the collection.

Moreover, in comparing the three sites, the highest collection of plastic waste appears in San Apolinario on Day 2 which coincided with heavy rain and high tide in San Apolinario. The amount of plastic litter collection was affected with the transport of waste from river and canals along with heavy rains and high tide, also entanglement of waste in pneumatophores and branches in mangroves which likely the factors contributed to the accumulation of plastic debris in the coastal environment (Galgani et al. 2013; Veerasingam et al. 2016; Requiron and Bacosa 2022; Garcés-Ordóñez et al. 2023). During the low tide period in the afternoon, as the tide receded, a significant amount of plastic waste, including sachets and plastic bags, which had been washed ashore or carried by water currents, was observed caught in the pneumatophores of *S. alba* and was entangled in its branches especially the tree near in the seaward side.

Further research and analysis to gain a more comprehensive understanding of the specific factors contributing to the higher plastic collection in all areas is important. This knowledge can inform targeted interventions and strategies to mitigate plastic pollution in the areas and promote sustainable waste management practices.

Comparison of macroplastic litter density found in three sampling sites

The data presented in Table 5 reveals a comparison of macroplastic litter density across all sampling sites. Inferential statistics results show that there is no significant difference in plastic waste density across three sites, $F(2,12) = 0.82$, $p = 0.45$. This suggests that the distribution of macroplastic pollution is relatively consistent across the sampling sites. It could further imply that factors influencing macroplastic pollution such as anthropogenic activities and waste management practices are similar in the areas.

Impacts of macroplastic litter in mangrove forest

The impacts of macroplastic litter on mangrove forests are extensive and complex, posing a serious threat to these vital ecosystems (Cordova 2021; Luo et al. 2022; Wang et al. 2023). Figure 7 illustrates the damage caused by plastic pollution on mangroves. Pneumatophores are crucial for mangrove tree respiration (Pallardy 2008), and plastic suffocating the root system that is smothered with plastic bags, bottles, and debris (Figures 7.A and 7.B) may significantly hinder their ability to exchange gases and acquire nutrients (Reef et al. 2010; Sundaramanickam et al. 2021; Moniuszko et al. 2023). Plastics in mangroves can also interfere with the respiratory function of mangrove roots, leading to reduced tree health and overall degradation of the mangrove ecosystem (Chai et al. 2023; Gunawardana et al. 2023). It can cause local scale anoxia in mangrove sediment, limit the growth of pneumatophores and propagules, and limit the growth of new saplings (Smith 2012; Selvam and Thamizoli 2021; Van Bijsterveldt et al. 2021). Moreover, the entanglement of plastic bags and fishing line around mangrove branches causes them to twist (Figure 7.C), and the resultant damage to the stem (Figure 7.D) disrupts the structure of the mangrove habitat that can cause physical damage leading to deterioration (Van Bijsterveldt et al. 2021; Liu et al. 2023).

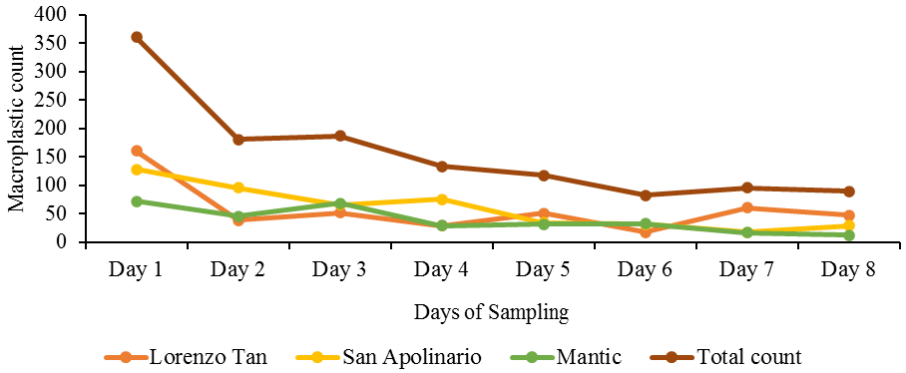

Figure 6. Quantity of plastic litter collected from three mangrove areas for eight non-consecutive days

Figure 7. Evidence of macroplastic litter found in all sampling sites in Tangub City, Philippines: smothering pneumatophores at A-B. Lorenzo Tan and San Apolinario, C. Twisted branches found at Lorenzo Tan, D. Damaged stem found at San Apolinario

Table 4. Macroplastic litter collected from different sites with density, Standard Deviation (SD) CCI analysis, and cleanliness rating

Site	Total litter count	Total area	Density	CCI	Cleanliness rating
Lorenzo Tan	459	2400	0.19±0.15	3.8	Clean
San Apolinario	480	2400	0.20±0.13	4	Clean
Mantic	311	2400	0.13±0.07	2.6	Clean

Table 5. One-way analysis of variance results for density between sites

Sampling sites	N	Mean	Sd	F-Value	Df	P-Value
San Apolinario	8	0.20	0.13	0.82	2, 21	0.45
Lorenzo Tan	8	0.19	0.14			
Mantic	8	0.13	0.07			

Several scientific studies support these findings, emphasizing the detrimental impact of macroplastic litter on mangrove ecosystems. The presence of plastics in the mangrove environment can cause prolonged anoxic conditions in the sediment, compromising the mangrove's overall health (Deng et al. 2023). A further investigation found that the constant entry of marine litter into mangroves can disrupt their natural conditions and harm the ecosystem, organisms, and humans (Vélez-Mendoza et al. 2022). These findings highlight the urgent need for waste reduction actions, such as education promotion, community involvement, and supportive policies (Paler et al. 2022), while emphasizing the significance of conducting studies on mangrove pollution to protect these vulnerable coastal ecosystems (Luo et al. 2021).

This study assessed the extent of macroplastic litter present in the mangrove forests across three barangays in Tangub City, Misamis Occidental, Philippines. The findings revealed that mangrove ecosystems act as natural filters, trapping plastic litter with varying efficiency depending on the mangrove species' composition. Food packaging, particularly those made of Low-Density Polyethylene (LDPE) polymer type, was the dominant type of litter collected, highlighting the influence of human activities on plastic pollution. Despite the cleanliness assessment rating all sites as "clean", the amount of plastic litter collected varied across sites. This suggests that both anthropogenic activities and waste management practices play significant roles in plastic distribution within the mangroves. Statistical analysis showed consistent plastic distribution across the studied areas and zones, indicating no significant differences across the mangrove forests. The study also emphasized the detrimental effects of macroplastic litter on mangrove forests, potentially disrupting vital ecological processes and leading to degradation. Understanding the extent and nature of plastic pollution in these critical coastal habitats is crucial for implementing effective management strategies and conservation efforts.

The study identified plastic pollution as a significant threat to mangrove ecosystems. Based on these findings, here are comprehensive recommendations for various stakeholders: (i) The findings of the study would like to recommend targeted educational campaigns as these are crucial to raising awareness about the negative impacts of plastic pollution on mangroves. These campaigns should be directed towards people living near these areas, such as coastal communities, fishermen, and tourists. Local media channels and educational materials can be used to spread information about responsible waste disposal practices and the importance of a healthy mangrove ecosystem. For instance, campaigns could utilize slogans and infographics in local languages to effectively communicate the dangers of plastic pollution. School programs and workshops can educate younger generations about responsible waste management and mangrove conservation, fostering a sense of environmental stewardship. Additionally, community outreach events can provide information and encourage participation in clean-up activities. (ii) To the community, the findings of this study would like to recommend organizing regular clean-up events in collaboration with local communities, academe, and environmental organizations. This fosters a sense of ownership for the health of the mangrove ecosystem while removing existing plastic debris. Partnering with schools can provide educational opportunities for students to understand the impact of plastic pollution. Citizen science initiatives can be incorporated into these events, allowing participants to collect valuable data on plastic pollution levels in mangroves. This data can be used for research and advocacy efforts to protect these vital ecosystems. (iii) This study also recommends improved waste management infrastructure as it is crucial to prevent further plastic pollution. Advocacy efforts should focus on implementing effective waste collection and disposal systems in areas surrounding mangroves. This could involve improved infrastructure for waste collection, establishment of recycling facilities, and development of composting programs. Policy changes that incentivize waste reduction and responsible waste management practices are also important. Pushing for bans on single-use plastics, extended producer responsibility programs, and increased funding for waste management initiatives can significantly contribute to a solution. (iv) Promoting the use of eco-friendly alternatives to single-use plastics is another key strategy. Encouraging the use of reusable bags, containers,

and utensils can significantly reduce the amount of plastic entering the environment in the first place. Collaboration with businesses near mangroves can promote the availability and use of these sustainable options. (v) Lastly, the Barangay Local Government Unit (BLGU) in partnership with the DENR, should formulate localized policies and programs that address plastic pollution and protect the health of mangrove ecosystems.

REFERENCES

Abreo, N.A.S., Siblos, S.K., Macusi, D., 2019. Anthropogenic marine debris (AMD) in mangrove forests of Pujada Bay, Davao Oriental, Philippines. Journal of Marine and Island Cultures. doi: 10.21463/jmic.2020.09.1.03. Page 44-53.

Abreo NAS, Siblos SKV, Macusi ED. 2020. Anthropogenic Marine Debris (AMD) in mangrove forests of Pujada Bay, Davao Oriental, Philippines. J Mar Island Cult 9 (1): 34. DOI: 10.21463/jmic.2020.09.1.03.

Acot Jr FT, Sajorne RE, Omar NAK, Suson PD, Rallos LEE, Bacosa HP. 2022. Unraveling macroplastic pollution in rural and urban beaches in Sarangani Bay Protected Seascape, Mindanao, Philippines. J Mar Sci Eng 10 (10): 1532. DOI: 10.3390/jmse10101532.

Adithama RM, Munifah I, Yanto DHY, Meryandini A. 2023. Biodegradation of low-density polyethylene microplastic by new halotolerant bacteria isolated from saline mud in Bledug Kuwu, Indonesia. Bioresour Technol Rep 22: 101466. DOI: 10.1016/j.biteb.2023.101466.

Alava JJ, McMullen K, Jones J et al. 2023. Multiple anthropogenic stressors in the Galápagos Islands' complex social–ecological system: Interactions of marine pollution, fishing pressure, and climate change with management recommendations. Integr Environ Assess Manag 19 (4): 870-895. DOI: 10.1002/ieam.4661.

Ali MR, Islam MA, Hossain MF, Hossain SM, Khan R, Naher K, Tamim U, Nahid F. 2021. Depth-wise elemental contamination trend in sediment cores of the Sundarbans mangrove forest, Bangladesh. J Radioanal Nucl Chem 328 (3): 1349-1359. DOI: 10.1007/s10967-021-07739-3.

Alkalay R, Pasternak G, Zask A. 2007. Clean-coast index; a new approach for beach cleanliness assessment. Ocean Coast Manag 50: 352-362. DOI: 10.1016/j.ocecoaman.2006.10.002.

Alongi DM. 2008. Mangrove forests: resilience, protection from tsunamis, and responses to global climate change. Estuar Coast Shelf Sci 76 (1): 1-13. DOI: 10.1016/j.ecss.2007.08.024.

Andrady AL, Neal MA. 2009. Applications and societal benefits of plastics. Philos Trans R Soc Lond B Biol Sci 364 (1526): 1977-1984. DOI: 10.1098/rstb.2008.0304.

Andrady AL. 2011. Microplastics in the marine environment. Mar Pollut Bull 62 (8): 1596-1605. DOI: 10.1016/j.marpolbul.2011.05.030.

Barnes DK, Galgani F, Thompson RC, Barlaz M. 2009. Accumulation and fragmentation of plastic debris in global environments. Philos Trans R Soc Lond B Biol Sci 364 (1526): 1985-1998. DOI: 10.1098/rstb.2008.0205.

Baynes TM, Kapur-Bakshi S, Emami N, Bhattacharja S, Tapsuwan S Joseph S, Locock K, Kaur M, Sinha R, Bajpai N, Talwar S. 2021. A Material Flow Analysis of Polymers and Plastics in India (No. 2021-1). Report. CSIRO, Australia.

Besseling E, Foekema EM, Van Franeker JA, Leopold MF, Kühn S, Rebolledo EB, Heße E, Mielke L, IJzer J, Kamminga P, Koelmans AA. 2015. Microplastic in a macro filter feeder: Humpback whale *Megaptera novaeangliae*. Mar Pollut Bull 95 (1): 248-252. DOI: 10.1016/j.marpolbul.2015.04.007.

Braganza PAT. 2017. Assessment of the implementation of the plastic bag reduction ordinance in Quezon City (2012-2016). Philipp J Public Adm 61 (1-2): 20-42.

Chai M, Li R, Li B, Wu H, Yu L. 2023. Responses of mangrove (*Kandelia obovata*) growth, photosynthesis, and rhizosphere soil properties to microplastic pollution. Mar Pollut Bull 189: 114827. DOI: 10.1016/j.marpolbul.2023.114827.

Cole M, Lindeque P, Halsband C, Galloway TS. 2011. Microplastics as contaminants in the marine environment: A review. Mar Pollut Bull 62 (12): 2588-2597. DOI: 10.1016/j.marpolbul.2011.09.025.

Cordova MR. 2021. Study on Macro and Microplastics Debris in Indonesian Water: Current Condition and Problem. [Dissertation]. Tokyo University of Agriculture, Tokyo.

Costa LD, Budiastuti MTHS, Sutrisno J, Sunarto. 2019. The diversity of plant species in a mangrove forest in the Coast of Metinaro, Timor-Leste. IOP Conf Ser: Earth Environ Sci 256 (1): 012026. DOI: 10.1088/1755-1315/256/1/012026.

Deng H, Zhang Y, Li D, Fu Q, He J, Zhao Y, Feng D, Yu H, Ge C. 2023. Mangrove degradation retarded microplastics weathering and affected metabolic activities of microplastics-associated microbes. J Hazard Mater 445: 130535. DOI: 10.1016/j.jhazmat.2022.130535.

Devi RS, Kannan VR, Natarajan K, Nivas D, Kannan K, Chandru S, Antony AR. 2016. The role of microbes in plastic degradation. In: Candra R (eds). Environmental Waste Management. CRC Press, Boca Raton. DOI: 10.1201/b19243-16.

Do Sul JAI, Costa MF, Fillmann G. 2014. Microplastics in the pelagic environment around oceanic islands of the Western Tropical Atlantic Ocean. Water Air Soil Pollut 225: 2004. DOI: 10.1007/s11270-014-2004-z.

Do Sul JAI, Costa MF. 2014. The present and future of microplastic pollution in the marine environment. Environ Pollut 185: 352-364. DOI: 10.1016/j.envpol.2013.10.036.

Dris R, Gasperi J, Saad M, Mirande C, Tassin B. 2016. Synthetic fibers in atmospheric fallout: A source of microplastics in the environment? Mar Pollut Bull 104 (1-2): 290-293. DOI: 10.1016/j.marpolbul.2016.01.006.

Duan J, Han J, Cheung SG, Chong RKY, Lo CM, Lee FWF, Xu SJL, Yang Y, Tam NFY, Zhou HC. 2021. How mangrove plants affect microplastic distribution in sediments of coastal wetlands: Case study in Shenzhen Bay, South China. Sci Total Environ 767: 144695. DOI: 10.1016/j.scitotenv.2020.144695.

Dumbili E, Henderson L. 2020. The challenge of plastic pollution in Nigeria. In: Letcher TM (eds). Plastic Waste and Recycling. Academic Press, London. DOI: 10.1016/B978-0-12-817880-5.00022-0.

Eriksen M, Lebreton LC, Carson HS, Thiel M, Moore CJ, Borerro JC, Galgani F, Ryan PG, Reisser J. 2014. Plastic pollution in the world's oceans: more than 5 trillion plastic pieces weighing over 250,000 tons afloat at sea. PloS one 9 (12): e111913. DOI: 10.1371/journal.pone.0111913.

Esquinas GGMS, Mantala AP, Atilano MG, Apugan RP, Galarpe VRKR. 2020. Physical characterization of litter and microplastic along the urban coast of Cagayan de Oro in Macajalar Bay, Philippines. Mar Pollut Bull 154: 111083. DOI: 10.1016/j.marpolbul.2020.111083.

Galgani F, Hanke G, Werner S, Oosterbaan L, Nilsson P, Fleet D, Liebezeit G. 2013. Guidance on monitoring of marine litter in European seas. MSFD Technical Subgroup on Marine Litter (TSG-ML). In JRC Technical Report. European Commission, Joint Research Centre, Ispra (VA), Italy.

Garcés-Ordóñez O, Castillo-Olaya V, Espinosa-Díaz LF, Canals M. 2023. Seasonal variation in plastic litter pollution in mangroves from two remote tropical estuaries of the Colombian Pacific. Mar Pollut Bull 193: 115210. DOI: 10.1016/j.marpolbul.2023.115210.

Garcia KB, Malabrigo PL, Gevaña DT. 2014. Philippines' mangrove ecosystem: status, threats, and conservation. In: Hanum IF, Latiff A, Hakeem KR, Ozturk M (eds). Mangrove ecosystems of Asia: Status, challenges, and management strategies. Springer, New York. DOI: 10.1007/978-1-4614-8582-7_5.

Ghosh SK, Pal S, Ray S. 2013. Study of microbes having potentiality for biodegradation of plastics. Environ Sci Pollut Res 20: 4339-4355. DOI: 10.1007/s11356-013-1706-x.

Goloran A, Demetillo M, Betco G. 2020. Mangroves assessment and diversity in coastal area of Barangay Cagdianao, Claver, Surigao Del Norte, Philippines. Intl J Environ Sci Nat Res 26 (3): 556188. DOI: 10.19080/IJESNR.2020.26.556188.

Gunawardana D, Abeysiri S, Manage P. 2023. Legacy of "New Normal" plastics and "New Nitrogen" in the cyanotoxin footprint in mangrove ecosystems. Phycology 3 (1): 106-126. DOI: 10.3390/phycology3010007.

Halden RU. 2010. Plastics and health risks. Ann Rev Public Health 31: 179-194. DOI: 10.1146/annurev.publhealth.012809.103714.

Hardesty BD, Good TP, Wilcox C. 2015. Novel methods, new results and science-based solutions to tackle marine debris impacts on wildlife.

Ocean Coast Manag 115: 4-9. DOI: 10.1016/j.ocecoaman.2015.04.004.
Hidalgo-Ruz V, Gutow L, Thompson RC, Thiel M. 2012. Microplastics in the marine environment: A review of the methods used for identification and quantification. Environ Sci Technol 46 (6): 3060-3075. DOI: 10.1021/es2031505.
Horstman EM, Dohmen-Janssen CM, Narra PMF, Van den Berg NJF, Siemerink M, Hulscher SJ. 2014. Wave attenuation in mangroves: A quantitative approach to field observations. Coast Eng 94: 47-62. DOI: 10.1016/j.coastaleng.2014.08.005.
Inocente SAT, Bacosa HP. 2022. Assessment of macroplastic pollution on selected tourism beaches of Barobo, Surigao Del Sur, Philippines. J Mar Island Cult 11 (1): 203-214. DOI: 10.21463/jmic.2022.11.1.14.
Israel DC, Adan EY, Lopez NF, De Castro JC. 2004. Perceptions of fishermen households on the long-term impact of coastal resources management in Panguil Bay. Philippine J Dev 31 (1): 107-134.
Jambeck JR, Geyer R, Wilcox C, Siegler TR, Perryman M, Andrady A, Narayan R, Law KL. 2015. Plastic waste inputs from land into the ocean. Science 347 (6223): 768-771. DOI: 10.1126/science.1260352.
Kalnasa ML, Lantaca SMO, Boter LC, Flores GHT, Galarpe VRKR. 2019. Occurrence of surface sand microplastic and litter in Macajalar Bay, Philippines. Mar Pollut Bull 149: 110521. DOI: 10.1016/j.marpolbul.2019.110 21.
Kathiresan K, Bingham BL. 2001. Biology of mangroves and mangrove ecosystems. Adv Mar Biol 40: 81-251. DOI: 10.1016/S0065-2881(01)40003-4.
Kesavan S, Xavier KM, Deshmukhe G, Jaiswar AK, Bhusan S, Shukla SP. 2021. Anthropogenic pressure on mangrove ecosystems: Quantification and source identification of surficial and trapped debris. Sci Total Environ 794: 148677. DOI: 10.1016/j.scitotenv.2021.148677.
Khoaele KK, Gbadeyan OJ, Chunilall V, Sithole B. 2023. The devastation of waste plastic on the environment and remediation processes: A critical review. Sustainability 15 (6): 5233. DOI: 10.3390/su15065233.
Koop F. 2021. Mangroves are particularly at risk from plastic pollution from rivers, a study finds. ZME Science. https://www.zmescience.com/science/mangroves-at-risk- pollution 28012021/
Kumar M, Chen H, Sarsaiya S, Qin S, Liu H, Awasthi MK, Kumar S, Singh L, Zhang Z, Bolan NS, Pandey A, Varjani S, Taherzadeh MJ. 2021. Current research trends on micro-and nano-plastics as an emerging threat to global environment: A review. J Hazard Mater 409: 124967. DOI: 10.1016/j.jhazmat.2020.124967.
Kumartasli S, Avinc O. 2020. Recycling of marine litter and ocean plastics: A vital sustainable solution for increasing ecology and health problem. In: Muthu SS, Gardetti MA (eds). Sustainability in the Textile and Apparel Industries: Sourcing Synthetic and Novel Alternative Raw Materials. Springer, Cham. DOI: 10.1007/978-3-030-38013-7_6.
Landrigan PJ, Stegeman JJ, Fleming LE et al. 2020. Human health and ocean pollution. Ann Glob Health 86: 151. DOI: 10.5334/aogh.2831.
Lebreton L, Slat B, Ferrari F, Sainte-Rose B, Aitken J, Marthouse R, Hajbane S, Cunsolo S, Schwarz A, Levivier A, Noble K, Debeljak P, Maral H, Schoeneich-Argent R, Brambini R, Reisser J. 2018. Evidence that the Great Pacific Garbage Patch is rapidly accumulating plastic. Sci Rep 8 (1): 4666. DOI: 10.1038/s41598-018-22939-w.
Lebreton LM, Greer SD, Borrero JC. 2012. Numerical modelling of floating debris in the world's oceans. Mar Pollut Bull 64 (3): 653-661. DOI: 10.1016/j.marpolbul.2011.10.027.
Li Y, Zhang H, Tang C. 2020. A review of possible pathways of marine microplastics transport in the ocean. Anthr Coast 3: 6-13. DOI: 10.1139/anc-2018-0030.
Liu R, Zhao S, Zhang B, Li G, Fu X, Yan P, Shao Z. 2023. Biodegradation of polystyrene (PS) by marine bacteria in the mangrove ecosystem. J Hazard Mater 442: 130056. DOI: 10.1016/j.jhazmat.2022.130056.
Lovelock CE, Krauss KW, Osland MJ, Reef R, Ball MC. 2016. The physiology of mangrove trees with changing climate. In: Goldstein G, Santiago LS (eds). Tropical Tree Physiology. Springer, Cham. DOI: 10.1007/978-3-319-27422-5_7.
Luo YY, Not C, Cannicci S. 2021. Mangroves as unique but understudied traps for anthropogenic marine debris: A review of present information and the way forward. Environ Pollut 271: 116291. DOI: 10.1016/j.envpol.2020.116291.
Luo YY, Vorsatz LD, Not C, Cannicci S. 2022. Landward zones of mangroves are sinks for both land and water borne anthropogenic debris. Sci Total Environ 818: 151809. DOI: 10.1016/j.scitotenv.2021.151809.
Manas JJI. 2023. Top 5 waste management challenges in the Philippines and how to solve them. https://plasticbank.com/blog/top-5-waste-management-challenges-in-the-philippines-and-how-to-solve-them/
Manullang CY. 2020. Distribution of plastic debris pollution and it is implications on mangrove vegetation. Mar Pollut Bull 160: 111642. DOI: 10.1016/j.marpolbul.2020.111642.
Martin C, Almahasheer H, Duarte CM. 2019. Mangrove forests as traps for marine litter. Environ Pollut 247: 499-508. DOI: 10.1016/j.envpol.2019.01.067.
Moniuszko H, Malonga WAM, Koczoń P, Thijs S, Popek R, Przybysz A. 2023. Accumulation of plastics and trace elements in the mangrove forests of Bima City Bay, Indonesia. Plants 12 (3): 462. DOI: 10.3390/plants12030462.
Namazi H, Baghershiroudi M, Kabiri R. 2017. Preparation of electrically conductive biocompatible nanocomposites of natural polymer nanocrystals with polyaniline via in situ chemical oxidative polymerization. Polym Compos 38: E49-E56. DOI: 10.1002/pc.23943.
Norris BK, Mullarney JC, Bryan KR, Henderson SM. 2017. The effect of pneumatophore density on turbulence: A field study in a *Sonneratia*-dominated mangrove forest, Vietnam. Cont Shelf Res 147: 114-127. DOI: 10.1016/j.csr.2017.06.002.
Olanrewaju OO, Oyebade D. 2019. Environmental Menace of plastic waste in Nigeria: Challenges, policies and technological efforts. World Environ Conserv Conf 2019: 322-333.
Paler MKO, Malenab MCT, Maralit JR, Nacorda HM. 2019. Plastic waste occurrence on a beach off southwestern Luzon, Philippines. Mar Pollut Bull 141: 416-419. DOI: 10.1016/j.marpolbul.2019.02.006.
Paler MKO, Tabañag IDF, Siacor FDC, Geraldino PJL, Walton MEM, Dunn C, Skov MW, Hiddink JG, Taboada EB. 2022. Elucidating the surface macroplastic load, types and distribution in mangrove areas around Cebu Island, Philippines and its policy implications. Sci Total Environ 838: 156408.
Pallardy SG. 2008. Enzymes, energetics, and respiration. In: Pallardy SG (eds). Physiology of Woody Plants. Academic Press, London. DOI: 10.1016/B978-012088765-1.50007-5.
Philippine Atmospheric, Geophysical and Astronomical Services Administration (PAGASA). 2021. https://pubfiles.pagasa.dost.gov.ph/pagasaweb/files/tamss/weather/tcsummary/
PlasticsEurope. 2018. Annual review 2017–2018. https://www.plasticseurope.org/download_file/force/1830/181.
Porta R. 2021. Anthropocene, the plastic age and future perspectives. FEBS Open Bio 11 (4): 948-953. DOI: 10.1002/2211-5463.13122.
Primavera J, Sadaba R, Lebata MJHL, Altamirano J. 2004. Handbook of Mangroves in the Philippines-Panay. Aquaculture Department, Southeast Asian Fisheries Development Center, Iloilo, Philippines.
Primavera JH, Friess DA, Van Lavieren H, Lee SY. 2019. In: Sheppard C (eds). World Seas: An Environmental Evaluation. Academic Press, London. DOI: 10.1016/B978-0-12-805052-1.00001-2.
Reef R, Feller IC, Lovelock CE. 2010. Nutrition of mangroves. Tree Physiol 30 (9): 1148-1160. DOI: 10.1093/treephys/tpq048.
Requiron JCM, Bacosa HP. 2022. Macroplastic transport and deposition in the environs of Pulauan River, Dapitan City, Philippines. Philipp J Sci 151 (3): 1211-1220.
Ritchie H, Roser M. 2018. Plastic Pollution. Our World Data. https://ourworldindata.org/plastic-pollution
Rochman CM, Browne MA, Halpern BS, Hentschel BT, Hoh E, Karapanagioti HK, Rios-Mendoza LM, Takada H, Teh S, Thompson RC. 2013. Classify plastic waste as hazardous. Nature 494 (7436): 169-171. DOI: 10.1038/494169a.
Ryan PG. 2015. A brief history of marine litter research. In: Bergmann M, Gutow L, Klages M (eds). Marine Anthropogenic Litter. Springer, Cham. DOI: 10.1007/978-3-319-16510-3_1.
Sajorne RE, Bacosa HP, Cayabo GDB, Ardines Jr LB, Sumeldan JD, Omar JM, Creencia LA. 2021. Plastic litter pollution along sandy beaches in Puerto Princesa, Palawan Island, Philippines. Mar Pollut Bull 169: 112520. DOI: 10.1016/j.marpolbul.2021.112520.
Selvam V, Thamizoli P. 2021. Science-based and community-centered approach to restore and sustain mangrove wetlands of India. Curr Sci 1288-1296. DOI: 10.18520/cs/v121/i10/1288-1296.

Shah AA, Hasan F, Hameed A, Ahmed S. 2008. Biological degradation of plastics: A comprehensive review. Biotechnol Adv 26 (3): 246-265. DOI: 10.1016/j.biotechadv.2007.12.005.

Shimao M. 2001. Biodegradation of plastics. Curr Opin Biotechnol 12 (3): 242-247. DOI: 10.1016/s0958-1669(00)00206-8.

Siddiqui J, Pandey G. 2013. A review of plastic waste management strategies. Intl Res J Environ Sci 2 (12): 84-88.

Smith SD. 2012. Marine debris: A proximate threat to marine sustainability in Bootless Bay, Papua New Guinea. Mar Pollut Bull 64 (9): 1880-1883. DOI: 10.1016/j.marpolbul.2012.06.013.

Sundaramanickam A, Nithin A, Balasubramanian T. 2021. Role of mangroves in pollution abatement. In: Rastogi RP, Phulwaria M, Gupta DK (eds). Mangroves: Ecology, Biodiversity and Management. Springer, Singapore. DOI: 10.1007/978-981-16-2494-0_11.

Suyadi, Manullang CY. 2020. Distribution of plastic debris pollution and it is implications on mangrove vegetation. Mar Pollut Bull 160: 111642. DOI: 10.1016/j.marpolbul.2020.111642.

Syakti AD, Bouhroum R, Hidayati NV, Koenawan CJ, Boulkamh A, Sulisyo I, Lebarillier S, Akhulus S, Doumeq P, Wong-Wah-Chung P. 2017. Beach macrolitter monitoring and oating microplastic in a coastal area of Indonesia. Mar Pollut Bull 122 (1-2): 217-225. DOI: 10.1016/j.marpolbul.2017.06.046.

Thompson RC, Swan SH, Moore CJ, Vom Saal FS. 2009. Our plastic age. Philos Trans R Soc Lond B Biol Sci 364 (1526): 1973-1976. DOI: 10.1098/rstb.2009.0054.

Van Bijsterveldt CE, van Wesenbeeck BK, Ramadhani S, Raven OV, van Gool FE, Pribadi R, Bouma TJ. 2021. Does plastic waste kill mangroves? A field experiment to assess the impact of macro plastics on mangrove growth, stress response, and survival. Sci Total Environ 756: 143826. DOI: 10.1016/j.scitotenv.2020.143826.

Van Sebille E, England MH, Froyland G. 2012. Origin, dynamics and evolution of ocean garbage patches from observed surface drifters. Environ Res Lett 7 (4): 044040. DOI: 10.1088/1748-9326/7/4/044040.

Veerasingam S, Saha M, Suneel V, Vethamony P, Rodrigues AC, Bhattacharyya S, Naik BG. 2016. Characteristics, seasonal distribution and surface degradation features of microplastic pellets along the Goa coast, India. Chemosphere 159: 496-505. DOI: 10.1016/j.chemosphere.2016.06.056.

Vélez-Mendoza A. 2022. Marine litter in mangroves: composition, magnitude, and impacts. Boletín De Ciencias De La Tierra 51: 50-60. DOI: 10.15446/rbct.101510.

Vlachogianni T, Fortibuoni T, Ronchi F et al. 2018. Marine litter on the beaches of the Adriatic and Ionian Seas: An assessment of their abundance, composition and sources. Mar Pollut Bull 131: 745-756. DOI: 10.1016/j.marpolbul.2018.05.006.

Wang MH, He Y, Sen B. 2019. Research and management of plastic pollution in coastal environments of China. Environ Pollut 248: 898-905. DOI: 10.1016/j.envpol.2019.02.098.

Wang Y, Jiao M, Li T, Li R, Liu B. 2023. Role of mangrove forest in interception of microplastics (MPs): challenges, progress, and prospects. J Hazard Mater 445: 130636. DOI: 10.1016/j.jhazmat.2022.130636.

Wilcox C, Van Sebille E, Hardesty BD. 2015. Threat of plastic pollution to seabirds is global, pervasive, and increasing. Proc Natl Acad Sci 112 (38): 11899-11904. DOI: 10.1073/pnas.1502108112.

Yin CS, Chai YJ, Carey D, Yusup Y, Gallagher JB. 2019. Anthropogenic marine debris and its dynamics across peri-urban and urban mangroves on Penang Island, Malaysia. BioRxiv 756106. DOI: 10.1101/756106.

NUSANTARA BIOSCIENCE
Vol. 16, No. 2, pp. 263-276
November 2024

ISSN: 2087-3948
E-ISSN: 2087-3956
DOI: 10.13057/nusbiosci/n160213

Enhancing the production of phycocyanin biopigment from microalga *Arthrospira maxima* through medium manipulation utilizing Box-Behnken Design

MUHAMMAD SYAWALUDDIN HILMI YAHYA[1], MURNI HALIM[1,2], FADZLIE WONG FAIZAL WONG[1,2], HELMI WASOH[1,2], JOO SHUN TAN[3], MOHD SHAMZI MOHAMED[1,2,♥]

[1]Department of Bioprocess Technology, Faculty of Biotechnology and Biomolecular Sciences, Universiti Putra Malaysia. 43400 UPM Serdang, Selangor, Malaysia. Tel.: +60-9769-4545, Fax.: +60-38946-7510, ♥email: m_shamzi@upm.edu.my

[2]Bioprocessing and Biomanufacturing Research Complex, Faculty of Biotechnology and Biomolecular Sciences, Universiti Putra Malaysia. 43400 UPM Serdang, Selangor, Malaysia

[3]School of Industrial Technology, Universiti Sains Malaysia. 11800 Gelugor, Pulau Pinang, Malaysia

Manuscript received: 21 March 2024. Revision accepted: 15 September 2024.

Abstract. *Yahya MSH, Halim M, Wong FWF, Wasoh H, Tan JS, Mohamed MS. 2024. Enhancing the production of phycocyanin biopigment from microalga* Arthrospira maxima *through medium manipulation utilizing Box Behnken Design. Nusantara Bioscience 16: 263-276.* Phycocyanin is among the valuable pigments produced by microalgae *Arthrospira* spp. possessing significant nutritional and coloring properties. It is widely used in food, nutraceutical, and biotechnology applications. Presently, *Arthrospira platensis* is a species very much established for producing phycocyanin commercially. Given the extensive research works and understanding of *A. platensis*, there exists a significant opportunity to explore lesser-studied but potentially valuable strains, such as *A. maxima*, specifically for pigment production capabilities. This study aims to optimize the phycocyanin production from the *A. maxima* by first considering vital media components for phycocyanin secretion by the microalgal cells, namely sodium nitrate, sodium bicarbonate, dipotassium phosphate, sodium chloride and a number of precursors. Upon identifying the most significant factors, their composition in the NRC production medium was manipulated using Response Surface Methodology (RSM). Initial screening using the Plackett-Burman Design revealed two macronutrients and a precursor that significantly affected the target response ($\rho>0.05$): sodium nitrate, dipotassium phosphate and glutamic acid. The three factors were further refined using the Box-Behnken Design (BBD), a variation of the RSM technique. In one BBD run, the highest phycocyanin yield was 224.86 mg/L, achieved using a recipe comprising 0.0125 M sodium nitrate, 0.375 mM dipotassium phosphate and 0.625 mM L-glutamic acid. This resulted in an increase of 37.85% improvement over the basal medium. BBD's validating recipe comprising 0.0125 M sodium nitrate, 0.375 mM dipotassium phosphate and 0.625 mM L-glutamic acid then produced 235.98 g/L of phycocyanin, which in turn has a 44.67% improvement of phycocyanin yield compared with an unoptimized NRC medium. This significant increase in phycocyanin yield demonstrates the potential of this research to enhance phycocyanin production for commercial use and further research. In conclusion, optimizing the composition of a medium can significantly increase phycocyanin production.

Keywords: *Arthrospira maxima*, Box-Behnken Design, medium formulation, phycocyanin, Plackett-Burman Design

INTRODUCTION

Arthrospira spp., a filamentous and multicellular cyanobacterium commonly referred to as blue-green algae, is a member of the Microcoleaceae family. *Arthrospira* spp. typically comprises unbranched filaments of cylindrical cells arranged in a spiral pattern when viewed under a light microscope and thrives in alkaline, brackish, saline waters within tropical and subtropical regions, favored by its optimal growth temperature at 35°C (Furmaniak et al. 2017). The *Arthrospira* genus encompasses more than 30 species, notably including the industrially important *A. platensis* (Fujisawa et al. 2010) with widespread applications in the food, feed and pharmaceutical industries. Recognized as a Generally Recognized As Safe (GRAS) microorganism, *Arthrospira* spp. has been acknowledged for its absence of known toxic effects, a designation endorsed by the FDA and ANISVA (Fleurence and Levine 2018). Notably, *Arthrospira* spp. has a distinctive pigment group called phycobiliproteins.

Phycobiliprotein is a highly fluorescent and brightly colored pigment made up of water-soluble protein and can usually be found in many types of cyanobacteria and red algae. They mainly act as antennae responsible for light harvesting. Owing to its water-soluble characteristic, phycobiliprotein is not located in the same place as other accessory pigments at the thylakoid membrane. Instead, it is usually located at the phycobilisome, with protein microbodies anchored at the thylakoid membrane (Stadnichuk and Tropin 2017). Among the phycobiliproteins derived from microalgae, phycoerythrin (PE) and allophycocyanin (AP) are present in small amounts, while phycocyanin (PC) stands out as the most abundant. PC, characterized by its intense blue, non-toxic, water-soluble pigment-protein complex, possesses great potential across various important applications (Cuellar-Bermudez et al. 2015; Pagels et al. 2019). Functioning as a blue fluorescent protein pigment, PC finds utility in

industries like colorant production, medicine and fluorescent markers. The single visible absorption for this strongly fluorescent pigment is between 615 and 620 nm, while the maximum fluorescence emission is around 650 nm. Notably, PC has a large Stokes shift and high quantum efficiency. Furthermore, the properties of PC, namely antioxidants, brightening, wound healing and antiacne, can be applied in the cosmetic industry (Ragusa et al. 2021). It also serves as a key ingredient in the development of "Lina blue" by Dainippon Ink & Chemicals (Sakura, Japan), widely employed as a colorant in chewing gum, ice sherbets, popsicles, candies, soft drinks, dairy products and wasabi (Roda-serrat et al. 2018). The global market value of phycocyanin nearly reached USD 112.3 million in 2018, with value projections expected to escalate to USD 409.8 million by 2030 (Thevarajah et al. 2022).

Cultivating *Arthrospira* spp. is an essential step in obtaining a variety of biochemical compounds, especially phycocyanin. Culturing conditions, duration of growth cycles, and environmental ability can influence the change in biochemical compound content (Manirafasha et al. 2018). The culturing conditions, particularly the medium composition, wield decisive influence over the growth phases of microalgae, thereby inducing changes in their composition and modulating the proportion of phycobiliproteins, including phycocyanin. Several studies revealed that macronutrients, especially nitrogen, phosphorous and carbon, have a significant impact on growth and biomass accumulation, thereby influencing phycocyanin production (Shanthi et al. 2018; Hao et al. 2019; Mirhosseini et al. 2022; Magwell et al. 2023). Additionally, nitrogen can influence the formation of phycobiliprotein and cell reserve in cyanobacteria (Liotenberg et al. 1996). Besides, salinity and trace metal can negatively impact phycocyanin content if the concentration exceeds the threshold limit (Zhou et al. 2018; Akbarnezhad et al. 2020; Markou et al. 2023). Furthermore, incorporating metabolic stressors into the medium components has demonstrated a potential to optimize phycocyanin production. Manipulating metabolites like Monosodium Glutamate (MSG), aspartate, succinic acid, and glycine significantly boosts phycocyanin yields, with MSG and glycine enhancing production by up to 30% and 22.5%, respectively (Kotinskyi et al. 2018; Manirafasha et al. 2018; Fekrat et al. 2021). These metabolites act as precursors or metabolic enhancers facilitating the biosynthetic pathways involved in phycocyanin production. Heme synthesis begins with the formation of the core molecule, aminolaevulinic acid (ALA), using either glutamate or succinyl coenzyme A as an immediate precursor, while heme itself is a precursor for phycocyanin (Manirafasha et al. 2016).

Design of Experiments (DOE) is a systematic approach using statistical methods to explore relationships between manipulated and response variables, incorporating designs such as Plackett-Burman and Box-Behnken (Jankovic et al. 2021; Lee et al. 2022). The Plackett-Burman Design (PBD) employs an orthogonal array to screen and identify the significant factors affecting response variables. PBD is considered to be a very rugged test featuring $4 \cdot n$ number of experiment runs, where n is an integer and in each case, the maximum number of factors that can be studied is $4 \cdot n - 1$ (Das and Dewanjee 2018; Jankovic et al. 2021). On the other hand, the Box-Behnken Design (BBD), a component of Response Surface Methodology (RSM), optimizes conditions and examines variable interaction with efficiency and precision, albeit this can be obtained with lesser run number compared to other RSM composite designs (Gujral et al. 2018; Ait-Amir et al. 2020).

This study aims to enhance phycocyanin production from *Arthrospira maxima* through the innovative screening of medium components and precursors using a statistical design-of-experiment technique. Unlike previous research, this study employs a comprehensive approach to identify and optimize the critical factors influencing phycocyanin production. The novelty lies in the systematic application of the PBD to identify vital factors, followed by fine-tuning using the BBD design for optimization. This methodological advancement offers a more precise and efficient pathway to maximizing phycocyanin yields. The integration of metabolic stressors and innovative medium compositions highlights the unique approach of this study, paving the way for enhanced industrial applications of phycocyanin.

MATERIALS AND METHODS

The overall experimental design flow is outlined in Figure 1, which presents a step-by-step illustration of the methodological framework used in this study. The figure begins with inoculum preparation, followed by screening the significant macronutrients using Plackett-Burman Design, a steepest ascent experiment for finding coarse optimal region, Box-Behnken optimization, and concludes with a validation run. Each step highlights key processes and critical factors that contribute to the optimization of phycocyanin and biomass yield of *A. maxima*.

Cultivation of *Arthrospira maxima*

The *A. maxima* used in this study were sourced from the International Institute of Aquaculture and Aquatic Sciences (I-AQUAS), Universiti Putra Malaysia, Port Dickson, located in the state of Negeri Sembilan, Malaysia, and maintained in Zarrouk's medium (Zarrouk 1966) at pH 9, with slight modifications to the sodium chloride and sodium bicarbonate content. The composition of Zarrouk's medium (gram) per litres included: 16.8 g $NaHCO_3$, 2.5 g $NaNO_3$, 0.5 g K_2HPO_4, 23.0 g NaCl, 1.0 g K_2SO_4, 0.2 g $MgSO_4.7H_2O$, 0.08 g NaEDTA, 0.04 g $CaCl.2H_2O$, 0.01 g $FeSO_4.7H_2O$ and 1 mL trace elements solution containing of 2.86 g H_3BO_3, 1.81 g $MnCl_2.4H_2O$, 0.222 g $ZnSO_4.7H_2O$, 0.39 g $Na_2MoO_4.2H_2O$, 0.079 g $CuSO_4.5H_2O$, 0.049 g $Co(NO_3)_2.6H_2O$. The culture was incubated at room temperature (26±2°C) under 16:8-hour light : dark cycles for 21 days, with manual agitation by hand shaking performed two or three times a day.

Screening of macronutrients and precursors

Nine variables were selected to ascertain the significant factor affecting phycocyanin production by *A. maxima*. They comprised six medium components (sodium nitrate, sodium bicarbonate, dipotassium phosphate, sodium chloride, potassium sulphate, and magnesium sulphate) alongside three precursors acting as metabolic stress (glutamic acid, succinic acid, and glycine). The screening was conducted to evaluate the significance of various nutrients on the biomass and phycocyanin yield of *A. maxima* using Nallayam Research Centre Media (NRCM) at pH 9, developed by the Nallayam Research Centre for cultivating Arthrospira species. (AlFadhly et al. 2022). This study utilized the 14-run Plackett-Burman Design for preliminary screening to identify key factors influencing phycocyanin formation among the nine factors.

Within the Plackett-Burman Design, each variable was assigned -1 for denoting the low level and +1 for the high level. A center point indicated as 0 was also incorporated to estimate for pure error and curvature. Table 1 shows the variable levels for each factor. The response functions under scrutiny included the dried cell weight of *A. maxima* (g/L) and the phycocyanin yield (mg/L). Design matrices for the screening experiment using the Placket-Burman design were generated from Design Expert version 11 (Stat-Ease Inc, USA). The outcomes derived from the Plackett-Burman Design were fitted to a first-order model represented by Equation 1. Subsequently, an Analysis of Variance (ANOVA) was applied to assess the significance of the fitted model for each response. Following the identification of significant factors, they were earmarked for further optimization.

$$Y = B_o + \sum_{i=1}^{n} B_i X_i$$

where Y signifies the predicted response, B_0 represents the model constant, X_i denotes the independent variable, and B_i illustrates the variable's linear coefficient.

Steepest ascent

The steepest ascent method, on the other hand, follows suit by attempting to guide the variables along the trajectory toward the optimal region, either by increasing or decreasing their effects. In this experiment, three factors (sodium nitrate, dipotassium phosphate, and glutamic acid) with the direction of perceived increasing/decreasing levels obtained from prior Plackett-Burman Design were further refined by varying their concentration. The phycocyanin yield and biomass of *A. maxima* gained at 21 days were compared for each run. Table 2 displays the design experiment of the steepest ascents.

Optimization using box Behnken Design

Based on the rough estimate of the possible optimal region of the three significant factors contributing to the maximum phycocyanin yield uncovered from the steepest ascent method, design levels were further fine-tuned with the Box-Behnken Design. The Box-Behnken Design also contains three levels: -1 denotes the low level, 0 for the center point and +1 for the high level. For this stage, 17 runs were generated by Box-Behnken Design using the design experiment software Design Expert version 11 (Stat-Ease Inc, USA). Table 3 illustrates the design matrix for each factor in the Box-Behnken Design. The obtained results following the cultivation experiments would be usually fitted to the second polynomial equation as follows:

$$Y = \alpha_0 + \beta_1 A + \beta_2 B + \beta_3 C + \gamma_1 AB + \gamma_2 AC + \gamma_3 BC + \omega_1 A^2 + \omega_2 B^2 + \omega_3 C^2$$

Where Y is the predicted response, α_0 is constant, β1, β2, and β3 are the linear coefficients, γ1, γ2, and γ3 represent the interaction coefficient between variables, ω1, ω2, and ω3 are the quadratic coefficients, whereas A, B, and *C* are the symbols for variables. ANOVA was used to analyze the statistically significant model, while contour and response surface plots were used to determine the interaction between variables.

Model validation run

The optimal medium formulation, as forecasted by the Box-Behnken Design, was validated in triplicate experiments. Here, *A. maxima* was cultivated in a modified NRC medium with three additional precursors (glutamic acid, succinic acid and glycine). The composition of optimum medium (gram) per liter contained the following components: 10.5 g $NaHCO_3$, 1.06 g $NaNO_3$, 0.065 g K_2HPO_4, 7.31 g NaCl, 0.523 g K_2SO_4, 1.11 g $MgSO_4.7H_2O$, 0.11 g L-glutamic acid, 0.531 g succinic acid, 0.075 g glycine and 0.01 g $FeSO_4.7H_2O$. The growth condition was retained by using a 500 mL conical flask at room temperature (26±2°C) under 16:8-hour light: dark cycles for 21 days. The culture was manually shaken two or three times a day. The final actual biomass and phycocyanin concentration responses were then compared with the regression model's predicted response.

Table 1. Assigned levels for each factor in the Plackett-Burman Design

Factors	Symbol	Actual level of coded factors	
		-1 (M)	+1(M)
Sodium bicarbonate	A	0.05	0.2
Sodium nitrate	B	0.02	0.05
Sodium chloride	C	0.05	0.2
Dipotassium phosphate	D	0.001	0.01
Potassium sulphate	E	0.00	0.006
Magnesium sulphate	F	0.001	0.008
Glutamic acid	G	0.001	0.005
Glycine	H	0.001	0.003
Succinic acid	I	0.001	0.008

Table 2. Experimental design for the steepest ascent to uncover optimal region of phycocyanin production

Run	Factors		
	Sodium nitrate (M)	Dipotassium phosphate (mM)	L-glutamic acid (mM)
1	0.030	2.00	2.00
2	0.025	1.50	1.50
3	0.020	1.00	1.00
4	0.015	0.75	0.75
5	0.010	0.50	0.50
6	0.005	0.25	0.25

Table 3. Assigned levels for each factor in Box-Behnken Design

Factors	Actual level of coded factors		
	-1 (mM)	0 (mM)	+1 (mM)
Sodium nitrate	7.5	10	12.5
Dipotassium phosphate	0.375	0.5	0.625
L-glutamic acid	0.375	0.5	0.625

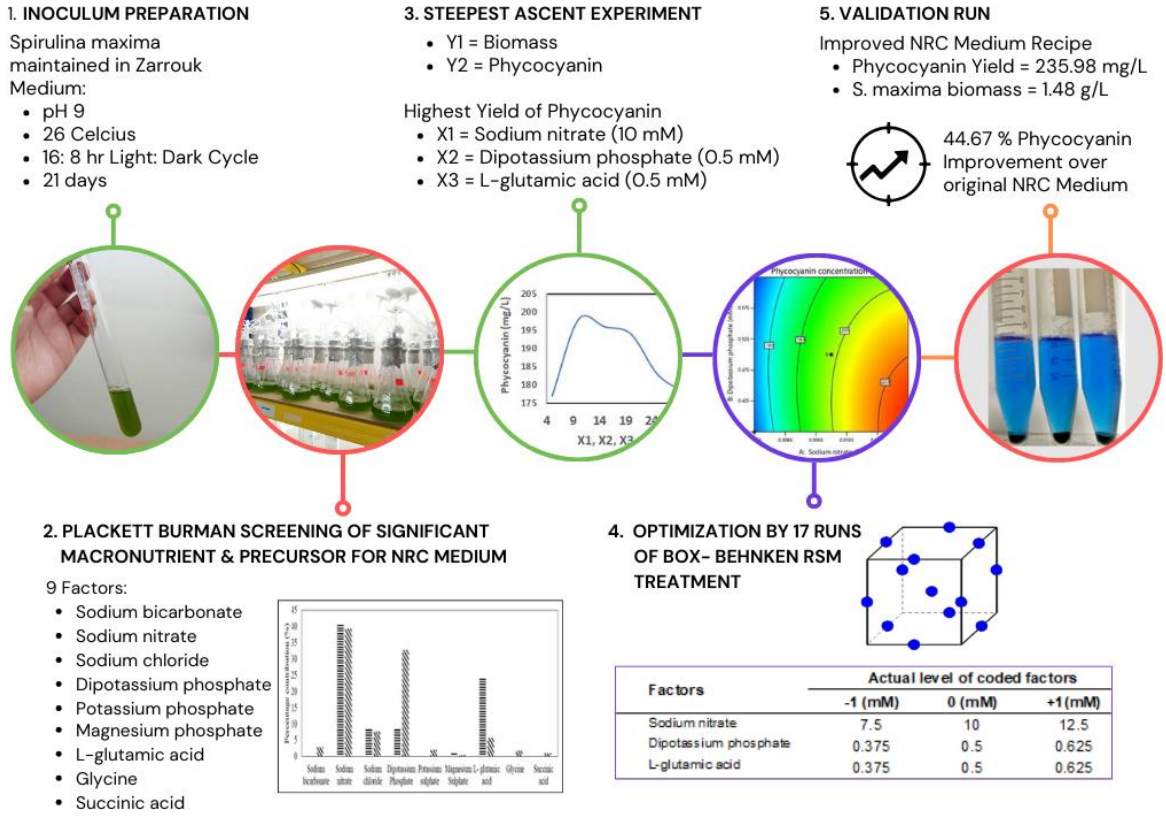

Figure 1. Overview of experimental design

Biomass density

Cell density was determined by the gravimetric method involving repeated weighing and oven drying of filter paper that entrapped the microalgal biomass until constant weight was achieved (Moheimani et al. 2013). Specifically, a 10 mL sample of *A. maxima* was filtered using pre-weighed glass microfiber filter paper with the aid of a vacuum pump. The filter paper containing *A. maxima* cells was then dried for 48 hours in an oven at 70°C until it reached a constant weight. The filter was weighed using an electronic balance (Ohaus PA413, China).

Extraction and detection of phycocyanin concentration

The extraction of phycocyanin was based on a particular method with a slight modification (Moraes et al. 2011). Next, 10 mL of samples were centrifuged at 3,500 RPM for 15 minutes (Kubota 2010, Japan) to separate the supernatant (spent medium) and settled pellet (microalgal cells). The pellet was washed with distilled water to remove any excess medium and dissolved salt. Then, 1 mL of 0.1 M phosphate buffer containing 0.1 M EDTA was added and left overnight at 5 ºC in the freezer. After that, 2 mL 0.1 M of phosphate buffer containing 0.1 M EDTA and 100 µg/mL of lysozyme was added, and the sample was left for four days at room temperature. The solution was measured using a spectrophotometer at 620 nm and 652 nm. The estimated concentration of phycocyanin was calculated based on the following equation:

$$\text{Phycocyanin (mg/L)} = \frac{OD_{620} - 0.474\,OD_{650}\,x1000}{5.34}\ x\ \frac{V_{ext}}{V_{cul}}$$

Where V_{ext} and V_{cul} denote the volume of extraction and volume of culture, respectively.

RESULTS AND DISCUSSION

Screening of macronutrients and precursors via Plackett-Burman Design

Screening plays an important role in any optimization process, which is primarily aimed at identifying significant factors influencing the response while discarding variables that prove to be trivial. This study employed a screening approach utilizing the Plackett-Burman Design (PBD) to pinpoint the key variables that create favorable conditions for enhancing phycocyanin production in *A. maxima*. The PBD was chosen owing to its saturated design, which led to a simple and reduced run (Lee et al. 2022). From the nine variables considered, six were typically found as part of media components: A) Sodium bicarbonate, B) Sodium nitrate, C) Sodium chloride, D) dipotassium phosphate, E) Potassium sulphate, and F) Magnesium sulphate, while the other three variables were those presenting metabolic stress affecting phycocyanin production: G) L-glutamic acid, H) Glycine and I) Succinic acid. Table 4 shows the PBD matrix comprising 14 experimental runs, including two added center points (Run 13 and 14), with the corresponding resulting biomass and phycocyanin yields meticulously documented.

From Table 4, the biomass of *A. maxima* for each run ranges from 0.55 g/L to 1.10 g/L, with the highest observed in Run 5 (1.10 g/L), followed by Run 12 (1.0 g/L) and Run 11 (0.95 g/L). The highest biomass in Run 5 is a notable improvement compared to the original NRC media, which yielded biomass levels between 0.5 g/L and 0.7 g/L, as reported by AlFadhly et al. (2022). A study by de Castro et al. (2015) also demonstrated that manipulating sodium bicarbonate, sodium nitrate, and irradiance using a central composite rotational design can achieve biomass levels ranging from 1.0 g/L to 3.2 g/L. Meanwhile, the highest phycocyanin concentrations were observed in Run 12 (160.3 ± 10.8 mg/L), Run 7 (105.4 ± 4.33 mg/L), and Run 5 (99.1 ± 4.71 mg/L). The phycocyanin concentration obtained in Run 12 exceeds the original NRC media, which yielded around 50 mg/g (AlFadhly et al. 2022). Furthermore, the study by Manirafasha et al. (2018) showed that adding a precursor can increase phycocyanin concentration by 13% to 24%.

Table 4. Plackett-Burman Design matrix of nine variables with observed and predicted biomass and phycocyanin yield by *Arthrospira maxima*

Run	A	B	C	D	E	F	G	H	I	Biomass (g/L)		Phycocyanin @ Day 21 (mg/L)	
										Obs	Pred	Obs	Pred
1	+1 (0.2)	+1 (0.05)	-1 (0.05)	+1 (0.01)	+1 (0.006)	+1 (0.008)	-1 (0.001)	-1 (0.001)	-1 (0.001)	0.65±0.05	0.71	29.8±0.61	44.9
2	-1 (0.05)	+1 (0.05)	+1 (0.2)	-1 (0.001)	+1 (0.006)	+1 (0.008)	+1 (0.005)	-1 (0.001)	-1 (0.001)	0.70±0.12	0.64	74.8±2.02	49.2
3	+1 (0.2)	-1 (0.02)	+1 (0.2)	+1 (0.01)	-1 (0)	+1 (0.008)	+1 (0.005)	+1 (0.003)	-1 (0.001)	0.85±0.1	0.76	51.9±2.21	53.6
4	-1 (0.05)	+1 (0.05)	-1 (0.05)	+1 (0.01)	+1 (0.006)	-1 (0.001)	+1 (0.005)	+1 (0.003)	+1 (0.008)	0.55±0.03	0.54	13.0±3.82	25.4
5	-1 (0.05)	-1 (0.02)	+1 (0.2)	-1 (0.001)	+1 (0.006)	+1 (0.008)	-1 (0.001)	+1 (0.003)	+1 (0.008)	1.10±0.14	1.03	99.1±4.71	119.5
6	-1 (0.05)	-1 (0.02)	-1 (0.05)	+1 (0.01)	-1 (0)	+1 (0.008)	+1 (0.005)	-1 (0.001)	+1 (0.008)	0.65±0.06	0.76	92.5±2.52	76.3
7	+1 (0.2)	-1 (0.02)	- (0.05)	-1 (0.001)	+1 (0.006)	-1 (0.001)	+1 (0.005)	+1 (0.003)	-1 (0.001)	0.70±0	0.86	105.4±4.33	122.6
8	+1 (0.2)	+1 (0.05)	-1 (0.05)	-1 (0.001)	-1 (0)	+1 (0.008)	-1 (0.001)	+1 (0.003)	+1 (0.008)	0.75±0.08	0.81	95.6±2.96	91.3
9	+1 (0.2)	+1 (0.05)	+1 (0.2)	-1 (0.001)	-1 (0)	-1 (0.001)	+1 (0.005)	-1 (0.001)	+1 (0.008)	0.65±0.09	0.64	32.6±3.85	49.2
10	-1 (0.05)	+1 (0.05)	+1 (0.2)	+1 (0.01)	-1 (0)	-1 (0.001)	-1 (0.001)	+1 (0.003)	-1 (0.001)	0.65±0.03	0.71	30.6±4.72	22.3
11	+1 (0.2)	-1 (0.02)	+1 (0.2)	+1 (0.01)	+1 (0.006)	-1 (0.001)	-1 (0.001)	-1 (0.001)	+1 (0.008)	0.95±0.05	0.93	71.9±1.93	73.2
12	-1 (0.05)	-1 (0.02)	-1 (0.05)	-1 (0.001)	-1 (0)	-1 (0.001)	-1 (0.001)	-1 (0.001)	-1 (0.001)	1.00±0.06	1.03	160.3±10.8	142.1
13	0 (0.125)	0 (0.035)	0 (0.125)	0 (0.0055)	0 (0.003)	0 (0.0045)	0 (0.003)	0 (0.002)	0 (0.0045)	0.90±0.13	0.77	80.9±9.21	72.5
14	0 (0.125)	0 (0.035)	0 (0.125)	0 (0.0055)	0 (0.003)	0 (0.0045)	0 (0.003)	0 (0.002)	0 (0.0045)	0.90±0.09	0.77	76.1±5.51	72.5

Note: Medium constituents expressed in unit molar (M): (A) Sodium bicarbonate; B. Sodium nitrate; C. Sodium chloride; D. dipotassium phosphate; E. Potassium sulphate; F. Magnesium sulphate; G. L-glutamic acid; H. Glycine and I. Succinic acid. Only real variables are shown; dummy variables in PBD were excluded

The full regression model ANOVA results of each factor affecting dried biomass, as well as phycocyanin yield in *A. maxima*, are recorded in Table 5. In the case of biomass, this table unequivocally illustrates that only sodium nitrate was deemed a significant medium factor where a crucial criterion necessitated a p-value of less than 0.05 ($p<0.05$) for significance. Notwithstanding, the entire model for biomass was considered insignificant, as indicated by a p-value of 0.2251. Meanwhile, in the case of variables influencing phycocyanin, the whole model, in turn, demonstrated a statistical significance, as indicated by a p-value of less than 0.05 (0.0389). Within this model, two variables stood out as statistically significant: sodium nitrate (0.0069) and dipotassium phosphate (0.0095), highlighting their pronounced influence on phycocyanin yield. However, it is important to note that despite the model's overall significance in terms of p-value and a favorable R^2 value (0.9398), the predicted R^2 (pred-R^2) value was shown as negative (-0.7596). This negative value could signify an overfitting of the model, suggesting that it may struggle to predict outcomes for new observations effectively. Thus, the backward elimination technique was systematically employed to address this issue. The backward elimination technique begins by selecting all variables and removing those with the highest insignificance. This technique was repeated until updated ANOVA produced an insignificant lack of fit, as well as the model p-value turned significant and improved the predicted R^2.

Employing the backward elimination technique resulted in revised regression models, with the new ANOVA outlined in Table 6 for both experimental responses. The updated table for dry biomass reflected the model's newfound significance, characterized by a p-value of 0.0022 with a 0.22% likelihood that the F-value (10.15) was attributable to random noise. Notably, two variables now emerged as statistically significant: A) sodium nitrate ($p=0.015$) and G) L-glutamic acid ($p=0.073$), signifying their notable influence on the dried cell weight of *A. maxima*. Besides, this model has an R^2 of 0.8186, which indicates its ability to explain around 81.86% of its variability. On the other hand, the model for phycocyanin yield has a significant p-value (0.0007) and a 0.07% chance that the F-value (13.58) occurs due to noise. This model also retained two significant variables: sodium nitrate (0.0007) and dipotassium phosphate (0.0014). Furthermore, this model has 0.8579 of R^2, which indicates that this model can explain 85.79% of the variation. In addition, the revision also has a well-adjusted R^2 (0.7947) and predicted R^2 (0.6059). The ANOVA result generated a first-order equation in terms of coded variables shown in the following equations for modelling biomass and phycocyanin yield.

$$Y_{biomass} = +1.14 - 7.22 * B + 0.67 * C - 11.11 * D - 41.67 * G$$

$$Y_{phycocyanin} = + 193.53 - 1693.65 * B - 150.7 * C - 5149.43 * D - 4876.14 * G$$

In the screening step, significant variables were determined based on statistically significant ($p\text{-value}<0.05$) and percentage contribution. The percentage contribution for each variable is tabulated in Figure 2. Four variables, sodium nitrate, sodium chloride, dipotassium phosphate, and L-glutamic acid, were found to have the potential to impact the models significantly. In contrast, other variables were disregarded due to their negligible influence on enhancing the regression models and their minimal contributions. The first variable chosen was sodium nitrate, which has a significant p-value (0.0015 and 0.0007) and high percentage contribution, around 37% to 40% for biomass and phycocyanin yield, respectively. Both models described that lower concentrations of sodium nitrate can produce high biomass and phycocyanin yields. Next, to be included was sodium chloride, which has almost the same percentage contribution of biomass and phycocyanin, around 8.6% concentration, but was statistically barely insignificant in both models.

Additionally, dipotassium phosphate exhibited a substantial percentage contribution, contributing significantly, particularly in phycocyanin yield (31.4%) and moderately for biomass (8.64%). However, this variable was only statistically significant to the phycocyanin yield model. Notably, a reduction in the concentration of dipotassium phosphate appeared to enhance biomass and phycocyanin yield. The final factor selected was that of L-glutamic acid which contributed a high percentage in biomass (24.05%) but was moderate in phycocyanin yield (5.79%). The model showed that low-concentration L-glutamic acid increased phycocyanin yield and biomass. As for the ANOVA table, this variable was only significant in the biomass model since it registered a p-value of 0.0874 for phycocyanin production.

To summarise the findings, three out of nine factors were chosen for the following Box-Behnken optimization: sodium nitrate, dipotassium phosphate, and L-glutamic acid. This decision was driven by their high to moderate percentage contributions in both models and their statistical significance in at least one of the ANOVA models.

Approaching the coarse optimal region via the steepest ascent experiment

The three NRC medium constituents that were deemed significant from the Plackett-Burman (PBD) exercise would first be subjected to the steepest ascent experiment. This experiment aimed to pinpoint the near-optimal concentration region for each variable. Based on the factors effect graph (Figure 3), the trending profile indicated that all variables should be decreased in concentration, aligning perfectly with the design of the steepest ascent experiment. This process was done until no further improvement was met. The obtained optimum concentration would then serve as the center point for a more fine-tuned optimization utilizing Box-Behnken Design (BBD). The result of this experiment is tabulated in Table 7. Upon inspection, the result showed that Run 5 has the highest phycocyanin yield (198.062±7.874 mg/L). The biomass yield remained relatively consistent across all runs, hovering around 0.9 g/L to 1.0 g/L. Consequently, Run 5 was chosen as the center point for BBD.

Table 5. ANOVA of the full regression model for A. Biomass density and B. Phycocyanin yield by *Arthrospira maxima*

Sources	Sum of Squares	df	Mean Square	F-value	p-value
Model A	0.2900	9	0.0322	2.26	0.2251
A-Sodium bicarbonate	0.0008	1	0.0008	0.0583	0.8210
B-Sodium nitrate	0.1408	1	0.1408	9.86	0.0349
C-Sodium chloride	0.0300	1	0.0300	2.10	0.2209
D-Dipotassium Phosphate	0.0300	1	0.0300	2.10	0.2209
E-Potassium sulphate	0.0008	1	0.0008	0.0583	0.8210
F-Magnesium Sulphate	0.0033	1	0.0033	0.2333	0.6543
G-L-glutamic acid	0.0833	1	0.0833	5.83	0.0731
H- Glycine	0.0000	1	0.0000	0.0000	1.0000
J- Succinic acid	0.0008	1	0.0008	0.0583	0.8210
Residual	0.0571	4	0.0143		
Lack of Fit	0.0571	3	0.0190		
Pure Error	0.0000	1	0.0000		
Cor Total	0.3471	13			
Model Summary: R^2 = 0.8354; C.V.% = 15.21; Adj-R^2 =0.465; Pred-R^2 = -1.8896					
Model B	18473.11	9	2052.57	6.94	0.0389
A-Sodium bicarbonate	573.39	1	573.39	1.94	0.2362
B-Sodium nitrate	7744.82	1	7744.82	26.19	0.0069
C-Sodium chloride	1532.87	1	1532.87	5.18	0.0851
D-Dipotassium phosphate	6443.53	1	6443.53	21.79	0.0095
E-Potassium sulphate	401.98	1	401.98	1.36	0.3084
F-Magnesium Sulphate	74.56	1	74.56	0.2521	0.6420
G-L-glutamic acid	1141.28	1	1141.28	3.86	0.1209
H- Glycine	367.13	1	367.13	1.24	0.3276
J- Succinic acid	193.54	1	193.54	0.6544	0.4639
Residual	1182.97	4	295.74		
Lack of Fit	1171.92	3	390.64	35.35	0.1229
Pure Error	11.05	1	11.05		
Cor Total	19656.08	13			
Model Summary: R^2 = 0.9398; C.V.% = 23.73; Adj-R^2 =0.8044; Pred-R^2 = -0.7596					

Table 6. ANOVA of a reduced regression model for A. Biomass density and B. Phycocyanin yield by *Arthrospira maxima*

Sources	Sum of Squares	df	Mean Square	F-value	p-value
Model A	0.2842	4	0.0710	10.15	0.0022
B-Sodium nitrate	0.1408	1	0.1408	20.13	0.0015
C-Sodium chloride	0.0300	1	0.0300	4.29	0.0683
D-Dipotassium phosphate	0.0300	1	0.0300	4.29	0.0683
G-L-glutamic acid	0.0833	1	0.0833	11.91	0.0073
Residual	0.0630	9	0.0070		
Lack of Fit	0.0630	8	0.0079		
Pure Error	0.0000	1	0.0000		
Cor Total	0.3471	13			
Model Summary: R^2 = 0.8186; C.V.% = 10.65; Adj-R^2 =0.7380; Pred-R^2 = 0.6131					
Model B	16862.51	4	4215.63	13.58	0.0007
B-Sodium nitrate	7744.82	1	7744.82	24.95	0.0007
C-Sodium chloride	1532.87	1	1532.87	4.94	0.0534
D-Dipotassium phosphate	6443.53	1	6443.53	20.76	0.0014
G-L-glutamic acid	1141.28	1	1141.28	3.68	0.0874
Residual	2793.57	9	310.40		
Lack of Fit	2782.52	8	347.81	31.47	0.1370
Pure Error	11.05	1	11.05		
Cor Total	19656.08	13			
Model Summary: R^2 = 0.8579; C.V.% = 24.31; Adj-R^2 =0.7947; Pred-R^2 = 0.6059					

Table 7. Steepest ascent experimental design with recorded biomass density and phycocyanin yield

Run	Variable level			Final biomass density (g/L)	Phycocyanin yield (mg/L)
	Sodium nitrate (mM)	Dipotassium phosphate (mM)	L-glutamic acid (mM)		
1	30	2.0	2.0	1.05	178.927 ± 4.683
2	25	1.5	1.5	0.9	183.798 ± 0.931
3	20	1.0	1.0	0.95	193.872 ± 0.391
4	15	0.75	0.75	0.9	195.962 ± 0.27
5	10	0.5	0.5	1.0	198.062 ± 7.874
6	5	0.25	0.25	1.0	77.125 ± 1.183

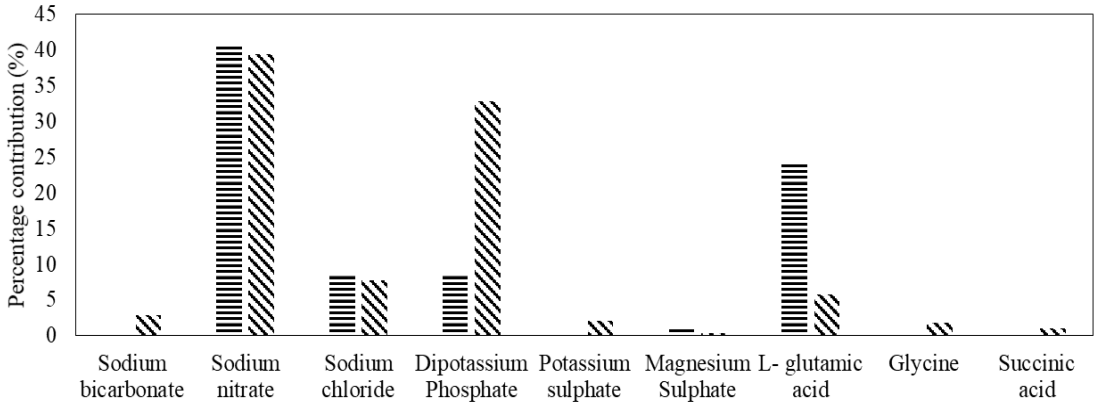

Figure 2. Percentage contribution for each medium variable for (▤) biomass and (▨) phycocyanin yield

Optimization of medium components and precursors using Box-Behnken Design

Table 8 documents the 17 runs from Box Behnken Design; the midpoint values used in this BBD were based on Run 5, as previously determined through the steepest ascent experiment. Meanwhile, the -1 and +1 BBD levels were subsequently adjusted accordingly by the Design Expert software, as shown in Table 3. Table 8 indicates the updated BBD's design matrix, including the observed and predicted biomass and phycocyanin yield.

From this dataset, the fitness to a second-order polynomial by Design Expert software resulted in two sets of second-order polynomial equations, as expressed in terms of coded value for biomass density and phycocyanin yield as follows.

$$\text{Biomass (g/L)} = 11.08 - 1031*A - 10.22*B - 8.92*C + 320*AB + 320*AC + 2.67*10^{-15}*BC + 36800*A^2 + 6.72*B^2 + 5.12*C^2$$

$$\text{Phycocyanin yield (mg/L)} = -16.57 + 48213.69*A + 478.84*B - 784.01*C - 22675.12*AB + 38342.17*AC + 247.88*BC - 2.09*10^6*A^2 - 445.05*B^2 + 259.17*C^2 \quad \text{Equation (7)}$$

In these equations, A represents sodium nitrate, B signifies dipotassium phosphate, and C stands for L-glutamic acid. The first equation illustratred that the interaction terms AB and AC, alongside all quadratic terms, contributed synergistically to biomass accumulation. Conversely, the linear terms in A, B, and C negatively influenced biomass accumulation. Non-existent BC's interaction term can be translated to the term that does not exhibit any discernible positive or negative effect on biomass accumulation. In the next equation describing phycocyanin yield, antagonistic effects are evident in the linear term of C, with a coefficient of -784.01, the interaction term AB (-22,675.12), and the quadratic terms A^2 ($-2.09*10^6$) and B^2 (-445.05). Conversely, other terms such as the linear terms of A (48,213.69) and B (478.84), as well as the interaction terms AC (38,342.17) and BC (247.88), demonstrated a synergistic effect on phycocyanin yield.

Graphical explanations of the mutual effect between interacting terms are represented by the contour plots and response surface plots shown in Figure 4, which first display the terms that influence biomass. Subsequent Figure 5 shows the terms affecting phycocyanin yield. All figures describing biomass interestingly indicated that an inverted relationship existed between factors and biomass density, with the optimal region lying somewhere at the corners of the surface plot, particularly highlighted in Figures 4.A and B with yellow to reddish heatmap. On the other hand, figures describing the phycocyanin yield eventually revealed the interaction that existed between terms with the projection of elliptical contours, with only Figure 4.C showing a somewhat nearly flat surface with no discernible optimum.

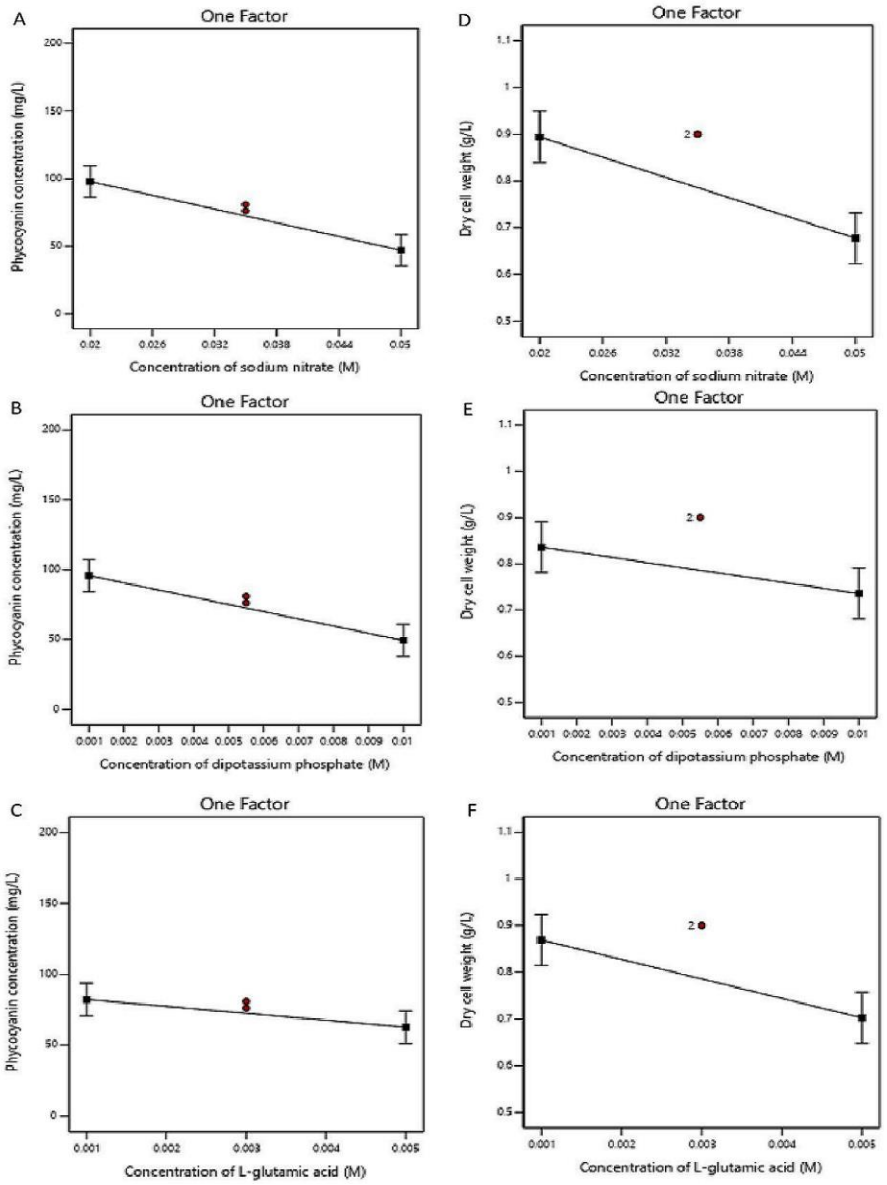

Figure 3. One-factor effect graph on A-C. The *A. maxima* phycocyanin yield and D-F. Biomass density

Table 8. BBD design matrix with observed and predicted values of biomass density and phycocyanin yield by *Arthrospira maxima*

Run	A: $NaNO_3$ (M)	B: K_2HPO_4 (mM)	C: L-Glu (mM)	Biomass (g/L)		Phycocyanin Yield (mg/L)	
				Obs	Pred	Obs	Pred
1	-1 (0.0075)	-1 (0.375)	0 (0.5)	1.45±0.1	1.44	148.81±3.87	150.85
2	+1 (0.0125)	-1 (0.375)	0 (0.5)	1.35±0.09	1.40	224.86±7.4	220.34
3	-1 (0.0075)	+1 (0.625)	0 (0.5)	1.20±0.14	1.15	138.00±1.7	142.53
4	+1 (0.0125)	+1 (0.625)	0 (0.5)	1.55±0.13	1.56	200.65±11.84	198.61
5	-1 (0.0075)	0 (0.5)	-1 (0.375)	1.45±0.06	1.46	169.87±3.4	163.36
6	+1 (0.0125)	0 (0.5)	-1 (0.375)	1.40±0.08	1.34	206.85±3.93	206.90
7	-1 (0.0075)	0 (0.5)	+1 (0.625)	0.90±0.12	0.956	139.23±4.49	139.17
8	+1 (0.0125)	0 (0.5)	+1 (0.625)	1.45±0.13	1.44	214.69±13.42	221.20
9	0 (0.01)	-1 (0.375)	-1 (0.375)	1.35±0.13	1.36	201.09±8.14	205.55
10	0 (0.01)	+1 (0.625)	-1 (0.375)	1.25±0.11	1.29	172.81±3.73	174.80
11	0 (0.01)	-1 (0.375)	+1 (0.625)	1.20±0.11	1.16	186.86±4.53	184.87
12	0 (0.01)	+1 (0.625)	+1 (0.625)	1.10±0.12	1.09	190.05±3.89	185.58
13	0 (0.01)	0 (0.5)	0 (0.5)	1.10±0.17	1.04	197.63±3.17	197.14
14	0 (0.01)	0 (0.5)	0 (0.5)	1.00±0.1	1.04	203.68±0.88	197.14
15	0 (0.01)	0 (0.5)	0 (0.5)	1.00±0.1	1.04	194.28±7.22	197.14
16	0 (0.01)	0 (0.5)	0 (0.5)	1.10±0.2	1.04	196.79±1.99	197.14
17	0 (0.01)	0 (0.5)	0 (0.5)	1.00±0.26	1.04	193.31±9.79	197.14

The first mutual effect between sodium nitrate and dipotassium phosphate is illustrated in Figures 4.A and 5.A. From these figures, the highest biomass was obtained by increasing sodium nitrate concentration from 0.01 M to 0.0125 M and increasing the concentration of dipotassium phosphate to 0.625 M while maintaining L-glutamic acid at 0.5 mM. However, this trend did not hold for phycocyanin yield, as the highest levels were reached when the concentration of dipotassium phosphate was decreased from 0.5 mM to 0.375 mM, coupled with an increase in sodium nitrate concentration from 0.01 M to 0.0125 M while maintaining L-glutamic acid at 0.5 mM. This figure showed that the interaction between sodium nitrate and dipotassium was different for biomass and phycocyanin yield. This phenomenon can be related to the dependence of phycocyanin and biomass on nitrogen available in the medium, where nitrogen starvation can cause stalemate or reduction in phycocyanin due to nitrogen uptake being prioritized in microalgae growth (Markou et al. 2014; Nur et al. 2019). In contrast, increasing phosphorus concentrations can promote biomass accumulation up to a certain point, but phosphorus limitation can lead to alterations in biochemical composition, particularly in photosynthetic pigments (Benavente-Valdés et al. 2016; Fattore et al. 2021).

Next, the interaction between sodium nitrate and L-glutamic acid while keeping dipotassium phosphate constant is depicted in Figures 4.B and 5.B. It was evident that adjusting the sodium nitrate concentration from 0.01 M to 0.0125 M and simultaneously altering the L-glutamic acid concentration from 0.5 mM to 0.625 mM, with dipotassium phosphate held at a constant 0.5 mM resulted in the highest biomass and phycocyanin yield. The interdependency between sodium nitrate and L-glutamic acid concerning biomass and phycocyanin production was shown throughout this interaction. This dependency was attributed to the microalgae's capacity to convert organic nitrogen sources, such as L-glutamic acid, into a nitrogen source through deamination facilitated by periplasmic amino acid oxidase (Kumar and Bera 2020).

Lastly, the combined effect of dipotassium phosphate and L-glutamic acid is illustrated in Figures 4.C and 5.C. The highest biomass and phycocyanin yield were achieved when L-glutamic acid and dipotassium phosphate concentrations were reduced from 0.5 mM to 0.375 mM, while sodium nitrate was maintained at 0.01 M. However, no significant interaction between dipotassium phosphate and L-glutamic acid was observed, especially when the concentration of sodium nitrate was altered, either by means of increasing or decreasing. Statistical analysis further supported this observation, where the p-value for the interaction between dipotassium phosphate and L-glutamic acid was insignificant.

Validation of predicted best outcome simulated from regression model

The BBD result was run through the software's optimization module, which predicted that the maximum phycocyanin yield and biomass by *A. maxima* could be achieved using concentration as follows: 0.0125 M of sodium nitrate, 0.375 mM of dipotassium phosphate, and 0.625 mM of L-glutamic acid. Other essential nutrients included 0.125 M of sodium bicarbonate, 0.125 M of sodium chloride, 0.003 M of potassium sulphate, 0.0045 M of magnesium sulphate, 0.001 M of glycine, and 0.0045 M of succinic acid. This model has a desirability of 0.992 and was predicted to obtain 1.48 g/L of biomass and 238.342 mg/L of phycocyanin yield. Meanwhile, the actual observed result produced 1.45 g/L of biomass and 235.976 mg/L of phycocyanin yield. A 95% confidence interval was employed to compare the observed and predicted values to validate the model's reliability and accuracy. As detailed in Table 9, the results affirmed the model's trustworthiness, showcasing a remarkable proximity between the observed and predicted outcomes. Since the aim of this study placed more emphasis on biopigment phycocyanin than the final biomass, by comparing the pre-and post-optimization conditions, a separate cultivation of *A. maxima* that employed the unoptimized basal NRC medium yielded about 163.26 mg/L of phycocyanin, which effectively put this new formulation to affect a 44.67% improvement over the original medium.

Nitrogen plays a crucial role in the growth and metabolite production. It is also an important building block for the protein backbone of phycobiliproteins, including phycocyanin. Numerous previous studies have emphasized the significant impact of nitrogen concentration, especially when sodium nitrate is employed, on both biomass and phycocyanin yield (de Castro et al. 2015; Mirhosseini et al. 2021). This assertion is reinforced by the findings from the Plackett-Burman Design (PBD), which highlight the substantial contribution of nitrogen to biomass (40.57%) and phycocyanin yield (39.4%). Banayan et al. (2022) also found that nitrogen sources play a vital role in phycocyanin production in PBD. Although earlier research has suggested an optimal sodium nitrate concentration of 0.03 M, L-glutamic acid as a secondary nitrogen and carbon source may alter this concentration (Shanthi et al. 2018). The inclusion of L-glutamic acid in the medium, serving as a source of glutamate, a precursor in various essential pathways such as the phycobilin cycle and Tricarboxylic Acid (TA) cycle, has the potential to enhance biomass and phycocyanin yield (Fekrat et al. 2021; Musifa et al. 2023). This statement is backed by the finding in this experiment where the use of L-glutamic acid influenced biomass especially. In addition, a study showed that using 0.05g/L of L-glutamic acid can enhance biomass (Shanthi et al. 2018).

Table 9. Statistical analysis using a 95% confidence interval of the validation experiment

Response	Predict	Observed	Std Dev	SE Pred	95% PI Low	95% PI High
Phycocyanin yield	238.34 mg/L	235.98 mg/L	1.6575	1.172	252.04	222.256
Biomass	1.48 g/L	1.4 g/L	0.0566	0.04	1.948	0.932

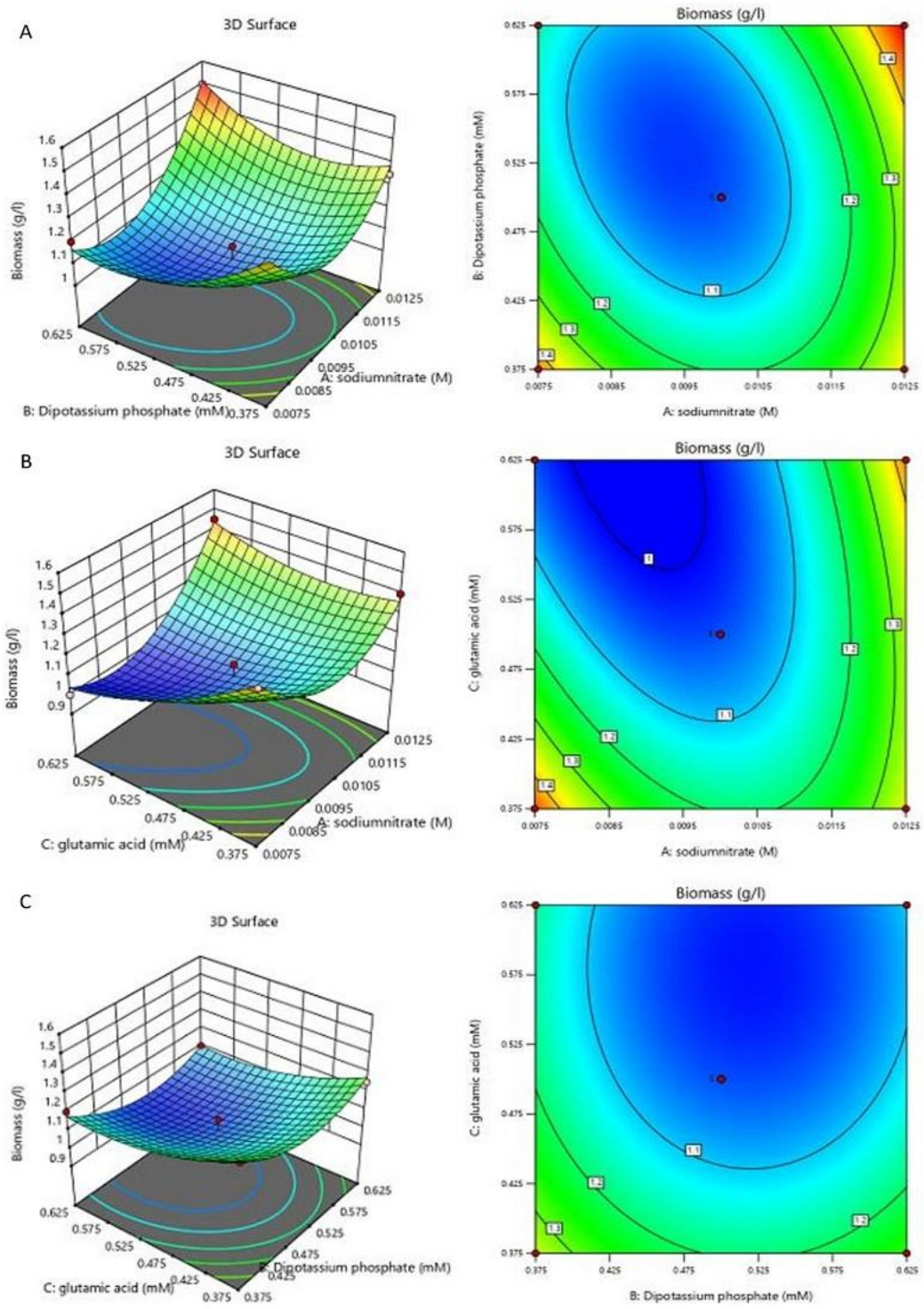

Figure 4. The mutual effect of A. Sodium nitrate and dipotassium phosphate, B. Sodium nitrate and L-glutamic acid, C. Dipotassium phosphate and L-glutamic acid on biomass by *Arthrospira maxima* as represented by contour and response surface plots

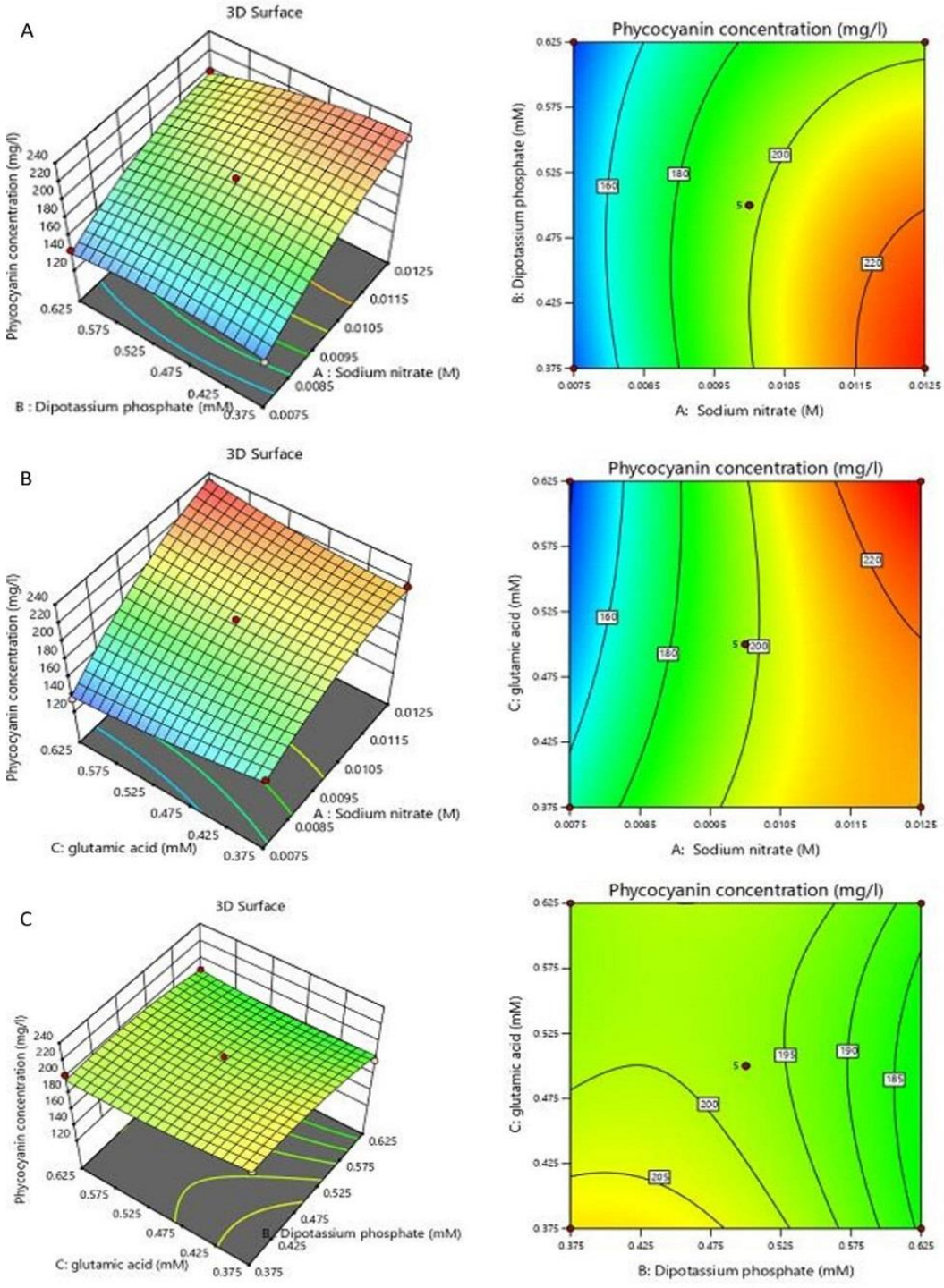

Figure 5. Mutual effect of A. Sodium nitrate and dipotassium phosphate, B. Sodium nitrate and L-glutamic acid, C. Dipotassium phosphate and L-glutamic acid on phycocyanin yield by *Arthrospira maxima* as represented by contour and response surface plots

Finally, phosphorus is a vital macronutrient that supports photosynthesis in producing various biological molecules such as phospholipids, Adenosine Triphosphate (ATP), and nucleic acids. Typically, phosphorus is sourced from dipotassium phosphate, which is frequently employed in culture media. While alterations in dipotassium phosphate concentration may not significantly impact biomass, it can induce changes in the biochemical composition. This statement is supported by Markou et al. (2012a, b), stating that altering phosphate concentration has little or no effect on biomass production. In addition, both studies discovered that a low concentration of dipotassium

phosphate (0.04 g/L to 0.05 g/L) can maintain optimal biomass production without loss. This finding is consistent with the results of this research, where dipotassium phosphate was significant for phycocyanin production but not for biomass production in the PBD experiments. Meanwhile, the use of low concentrations of dipotassium phosphate in this study exhibited high phycocyanin concentrations. The study by Hao et al. (2019) presented similar results when using low concentrations of dipotassium phosphate. This phenomenon is likely due to a resource allocation shift toward photosynthesis to generate essential nutrients (Senatore et al. 2023). However, there is a lack of studies on how dipotassium phosphate affects phycocyanin production, especially by *Arthrospira* sp. nutrients.

This study revealed that, out of nine screening media compositions investigated through the Plackett-Burman Design, only three, namely sodium nitrate, potassium dihydrogen phosphate, and L-glutamic acid, exerted significant influence on either biomass or phycocyanin yield. Through optimization using the steepest ascents followed by the Box-Behnken Design, the highest phycocyanin yield was achieved at 235.976 mg/L and biomass at 1.45 g/L. This was accomplished by employing the formulated NRC medium, which contained 0.0125 M of sodium nitrate, 0.375 mM of potassium dihydrogen phosphate, and 0.625 mM of L-glutamic acid. In conclusion, this study emphasizes the vital role of media composition in maintaining biomass and enhancing phycocyanin yield.

REFERENCES

Ait-Amir B, Pougnet P, El Hami A. 2020. 6 - Meta-Model Development. In: Pougnet E (eds.). Embedded Mechatronic Systems 2. ISTE. DOI: 10.1016/B978-1-78548-190-1.50006-2.

Akbarnezhad M, Mehrgan MS, Kamali A, Baboli MJ. 2020. Effects of microelements (Fe Cu Zn) on growth and pigment contents of *Arthrospira (Spirulina) platensis*. Iranian J Fisher Sci 19 (2): 653-668. DOI: 10.22092/ijfs.2019.120614.

AlFadhly NKZ, Alhelfi N, Altemimi AB, Verma DK, Cacciola F. 2022. Tendencies affecting the growth and cultivation of genus *Spirulina*: An investigative review on current trends. Plants 11 (22): 1-21. DOI: 10.3390/plants11223063.

Banayan S, Jahadi M, Khosravi-Darani K. 2022. Pigment productions by *Spirulina platensis* as a renewable resource. J Appl Biotechnol Rep 9 (2): 614-621. DOI: 10.30491/jabr.2021.292076.1406.

Benavente-Valdés JR, Aguilar C, Contreras-Esquivel JC, Méndez-Zavala A, Montañez J. 2016. Strategies to enhance the production of photosynthetic pigments and lipids in chlorophycae species. Biotechnol Rep 10: 117-125. DOI: 10.1016/j.btre.2016.04.001.

de Castro GFPDS, Rizzo RF, Passos TS, dos Santos BNC, Dias DDS, Domingues JR, Araújo KGDL. 2015. Biomass production by *Arthrospira platensis* under different culture conditions. Food Sci Technol 35 (1): 18-24. DOI: 10.1590/1678-457X.6421.

Cuellar-Bermudez SP, Aguilar-Hernandez I, Cardenas-Chavez DL, Ornelas-Soto N, Romero-Ogawa MA, Parra-Saldivar R. 2015. Extraction and purification of high-value metabolites from microalgae: Essential lipids, astaxanthin and phycobiliproteins. Microbial Biotechnol 8 (2): 190-209. DOI: 10.1111/1751-7915.12167.

Das AK, Dewanjee S. 2018. Optimization of extraction using mathematical models and computation. In: Sarker SD, Nahar L (eds). Computational Phytochemistry. Elsevier, Amsterdam. DOI: 10.1016/B978-0-12-812364-5.00003-1.

Fattore N, Bellan A, Pedroletti L, Vitulo N, Morosinotto T. 2021. Acclimation of photosynthesis and lipids biosynthesis to prolonged nitrogen and phosphorus limitation in *Nannochloropsis gaditana*. Algal Res 58: 102368. DOI: 10.1016/j.algal.2021.102368.

Fekrat F, Shahbazi M, Nami B, Amin Hejazi M, Ghaffari MR. 2021. Nitrogen-containing metabolic stressors stimulate high-value compounds accumulation in *Arthrospira platensis*. Authorea DOI: 10.22541/au.161555554.40888746/v1.

Fleurence J, Levine IA. 2018. Antiallergic and allergic properties. In: Levine IA, Fleurence (eds). Microalgae in Health and Disease Prevention. Academic Press, London. DOI: 10.1016/B978-0-12-811405-6.00014-1.

Fujisawa T, Narikawa R, Okamoto S et al. 2010. Genomic structure of an economically important cyanobacterium, *Arthrospira* (*Spirulina*) *platensis* NIES-39. DNA Res 17 (2): 85-103. DOI: 10.1093/dnares/dsq004.

Furmaniak MA, Misztak AE, Franczuk MD, Wilmotte A, Waleron M, Waleron KF. 2017. Edible cyanobacterial genus *Arthrospira*: Actual state of the art in cultivation methods, genetics, and application in medicine. Front Microbiol 8: 02541. DOI: 10.3389/fmicb.2017.02541.

Gujral G, Kapoor D, Jaimini M. 2018. An updated review on Design of Experiment (Doe) in pharmaceuticals. J Drug Deliv Ther 8 (3): 147-152. DOI: 10.22270/jddt.v8i3.1713.

Hao C, Bing-jie Y, Tao L, Hua-lian W, Hou-bo W, Wen-zhou X. 2019. Effects of phosphorus concentrations on growth and metabolism of seawater *Spirulina platensis*. Biotechnol Bull 35 (8): 103-110. DOI: 10.13560/j.cnki.biotech.bull.1985.2019-0181.

Jankovic A, Chaudhary G, Goia F. 2021. Designing the Design of Experiments (DOE) – An investigation on the influence of different factorial designs on the characterization of complex systems. Energy Build 250: 111298. DOI: 10.1016/j.enbuild.2021.111298.

Kotinskyi AV, Zhadan S, Salyuk AI. 2018. The influence of exogenous glycine on growth and intensity of cyanobacteria *Spirulina platensis* (Gom.) Geitl photosynthetic processes. Biotechnol Acta 11 (6): 39-46. DOI: 10.15407/biotech11.06.039.

Kumar A, Bera S. 2020. Revisiting nitrogen utilization in algae: A review on the process of regulation and assimilation. Bioresour Technol Rep 12: 100584.

Lee BCY, Mahtab MS, Neo TH, Farooqi IH, Khursheed A. 2022. A comprehensive review of Design of Experiment (DOE) for water and wastewater treatment application - Key concepts, methodology and contextualized application. J Water Process Eng 47: 102673. DOI: 10.1016/j.jwpe.2022.102673.

Liotenberg S, Campbell D, Rippka R, Houmard J, Tandeau De Marsac N. 1996. Effect of the nitrogen source on phycobiliprotein synthesis and cell reserves in a chromatically adapting filamentous Cyanobacterium. Microbiology 142 (3): 611-622. DOI: 10.1099/13500872-142-3-611.

Magwell PFR, Djoudjeu KT, Minyaka E, Tavea MF, Fotsop OW, Tagnikeu RF, Fofou AM, Darelle CKV, Dzoyem CUD, Lehman LG. 2023. Sodium bicarbonate ($NaHCO_3$) increases growth, protein and photosynthetic pigments production and alters carbohydrate production of *Spirulina platensis*. Curr Microbiol 80 (2): 63. DOI: 10.1007/s00284-022-03165-0.

Manirafasha E, Murwanashyaka T, Ndikubwimana T, Rashid Ahmed N, Liu J, Lu Y, Zeng X, Ling X, Jing K. 2018. Enhancement of cell growth and phycocyanin production in *Arthrospira* (*Spirulina*) *platensis* by metabolic stress and nitrate fed-batch. Bioresour Technol 255: 293-301. DOI: 10.1016/j.biortech.2017.12.068.

Manirafasha E, Ndikubwimana T, Zeng X, Lu Y, Jing K. 2016. Phycobiliprotein: Potential microalgae derived pharmaceutical and biological reagent. Biochem Eng J 109: 282-296. DOI: 10.1016/j.bej.2016.01.025.

Markou G, Chatzipavlidis I, Georgakakis D. 2012a. Carbohydrates production and bio-flocculation characteristics in cultures of *Arthrospira* (*Spirulina*) *platensis*: Improvements through phosphorus limitation process. Bioenergy Res 5 (4): 915-925. DOI: 10.1007/s12155-012-9205-3.

Markou G, Chatzipavlidis I, Georgakakis D. 2012b. Effects of phosphorus concentration and light intensity on the biomass composition of *Arthrospira* (*Spirulina*) *platensis*. World J Microbiol Biotechnol 28 (8): 2661-2670. DOI: 10.1007/s11274-012-1076-4.

Markou G, Kougia E, Arapoglou D, Chentir I, Andreou V, Tzovenis I. 2023. Production of *Arthrospira platensis*: Effects on growth and biochemical composition of long-term acclimatization at different

salinities. Bioengineering 10 (2): 233. DOI: 10.3390/bioengineering10020233.
Markou G, Vandamme D, Muylaert K. 2014. Microalgal and cyanobacterial cultivation: The supply of nutrients. Water Res 65: 186-202. DOI: 10.1016/j.watres.2014.07.025.
Mirhosseini N, Davarnejad R, Hallajisani A, Cano-Europa E, Tavakoli O. 2022. Sugarcane molasses as a cost-effective carbon Source on *Arthrospira maxima* growth by Taguchi technique. Intl J Eng 35 (3): 510-516. DOI: 10.5829/IJE.2022.35.03C.03.
Mirhosseini N, Davarnejad R, Hallajisani A, Cano-Europa E, Tavakoli O, Franco-Colín M, Blas-Valdivia V. 2021. Cultivations of *Arthrospira maxima* (*Spirulina*) using ammonium sulfate and sodium nitrate as an alternative nitrogen sources. Iran J Fish Sci 20 (2): 475-489. DOI: 10.22092/ijfs.2021.351071.0.
Moheimani NR, Borowitzka MA, Isdepsky A, Sing SF. 2013. Standard methods for measuring growth of algae and their composition. In: Borowitzka MA, Moheimani NR (eds). Algae for Biofuels and Energy. Springer, Dordrecht. DOI: 10.1007/978-94-007-5479-9_16.
Moraes CC, Sala L, Cerveira GP, Kalil SJ. 2011. C-Phycocyanin extraction from *Spirulina platensis* wet biomass. Braz J Chem Eng 28 (1): 45-49. DOI: 10.1590/S0104-66322011000100006.
Musifa E, Kusnanda AJ, Dharma A, Armaini. 2023. Monosodium Glutamate (MSG) as metabolic stressors stimulate the production of valuable compounds in *Spirulina platensis*. Egypt J Aquat Biol Fish 27 (2): 731-743. DOI: 10.21608/ejabf.2023.297611.
Nur MMA, Garcia GM, Boelen P, Buma AGJ. 2019. Enhancement of C-phycocyanin productivity by *Arthrospira platensis* when growing on palm oil mill effluent in a two-stage semi-continuous cultivation mode. J Appl Phycol 31 (5): 2855-2867. DOI: 10.1007/s10811-019-01806-9.
Pagels F, Guedes AC, Amaro HM, Kijjoa A, Vasconcelos V. 2019. Phycobiliproteins from cyanobacteria: Chemistry and biotechnological applications. Biotechnol Adv 37 (3): 422-443. DOI: 10.1016/j.biotechadv.2019.02.010.
Ragusa I, Nardone GN, Zanatta S, Bertin W, Amadio E. 2021. *Spirulina* for skin care: A bright blue future. Cosmetics 8 (1): 7. DOI: 10.3390/cosmetics8010007.
Roda-serrat MC, Christensen KV, El-houri RB, Fretté X, Christensen LP. 2018. Fast cleavage of phycocyanobilin from phycocyanin for use in food colouring. Food Chem 240: 655-661. DOI: 10.1016/j.foodchem.2017.07.149.
Senatore V, Rueda E, Bellver M, Díez-Montero R, Ferrer I, Zarra T, Naddeo V, García J. 2023. Production of phycobiliproteins, bioplastics and lipids by the cyanobacteria *Synechocystis* sp. treating secondary effluent in a biorefinery approach. Sci Total Environ 857: 159343. DOI: 10.1016/j.scitotenv.2022.159343.
Shanthi G, Premalatha M, Anantharaman N. 2018. Effects of L-amino acids as organic nitrogen source on the growth rate, biochemical composition and polyphenol content of *Spirulina platensis*. Algal Res 35: 471-478. DOI: 10.1016/j.algal.2018.09.014.
Stadnichuk IN, Tropin IV. 2017. Phycobiliproteins: Structure, functions and biotechnological applications. Appl Biochem Microbiol 53 (1): 1-10. DOI: 10.1134/S0003683817010185.
Thevarajah B, Nishshanka GKSH, Premaratne M, Nimarshana PHV, Nagarajan D, Chang JS, Ariyadasa TU. 2022. Large-scale production of *Spirulina*-based proteins and c-phycocyanin: A biorefinery approach. Biochem Eng J 185: 108541. DOI: 10.1016/j.bej.2022.108541.
Zarrouk C. 1966. Contribution a l'etude d'une Cyanophycee. Influence de Divers Facteurs Physiques et Chimiques sur la croissance et la photosynthese de *Spirulina mixima*. [Thesis]. University of Paris, Paris, France.
Zhou T, Wang J, Zheng H, Wu X, Wang Y, Liu M, Xiang S, Cao L, Ruan R, Liu Y. 2018. Characterization of additional zinc ions on the growth, biochemical composition and photosynthetic performance from *Spirulina platensis*. Bioresour Technol 269: 285-291. DOI: 10.1016/j.biortech.2018.08.131.

NUSANTARA BIOSCIENCE
Vol. 16, No. 2, pp. 277-283
November 2024

ISSN: 2087-3948
E-ISSN: 2087-3956
DOI: 10.13057/nusbiosci/n160214

Effect of dietary *atung* seed flour (*Parinarium glaberrimum*) on small intestine characteristics of broiler chickens

INSUN SANGADJI[1,♥], SYLVIA C. H. HEHANUSSA[1], RONY MARSYAL KUNDA[2]

[1]Program of Animal Husbandry, Faculty of Agriculture, Universitas Pattimura. Jl. Ir. Putuhena, Poka, Ambon 97233, Maluku, Indonesia. Tel./fax.: +62-911-322626, ♥email: insunsangadji@gmail.com

[2]Program of Biotechnology, Faculty of Science and Technology, Universitas Pattimura. Jl. Ir. Putuhena, Poka, Ambon 97233, Maluku, Indonesia

Manuscript received: 14 August 2024. Revision accepted: 14 October 2024.

Abstract. *Sangadji I, Hehanussa SCH, Kunda RM. 2024. Effect of dietary* atung *seed flour (Parinarium glaberrimum) on small intestine characteristics of broiler chickens. Nusantara Bioscience 16: 277-283.* This study was conducted to investigate the effect of feeding *atung* (*Parinarium glaberrimum* Hassk.) seed meal on intestinal microflora, pH, and micro-morphology in broiler chickens. A total of 168-day-old male New Lohmann broiler chickens were randomly assigned to six treatment groups with four replicates and seven birds in each replicate pen. The dietary treatments consisted of feeding the same corn-soybean meal basal diet with *P. glaberrimum* seed meal inclusions at levels of 0, 0.5, 1.0, 2.0, and 4.0%, respectively. Basal diet inclusion with 50 ppm of tetracycline was also used as a positive control treatment. The data was statistically analyzed using ANOVA in a completely randomized design, a robust methodology, and continued subsequently with Duncan's test for data with significant differences. Results showed that the number of lactic acid bacteria, duodenal and ileal villus height, villus width, and villus height to crypt depth ratio was increased ($p<0.05$) with the inclusion of 0.5-1.0% *P. glaberrimum* seed meal. Coliform numbers and intestinal pH were decreased ($p<0.01$) with 1.0% *P. glaberrimum* seed meal inclusion. With respect to the results of some response variables of intestinal pH and micro-morphology, additions of *P. glaberrimum* seed meal showed better results than the addition of 50 ppm tetracycline. It can be concluded that *P. glaberrimum* seed can be recommended as a green feed additive for replacing antibiotic growth promoters in the poultry diet based on the ability to improve gut microflora and micro-morphology.

Keywords: *Atung* seed, broiler chickens, intestinal microflora and morphology, phytobiotic

INTRODUCTION

The health of the digestive tract is important for supporting optimal animal production as it is related to the function of digestion and nutrient absorption and plays an essential role in the animal's defense system against disease infections. The intestinal microbiota has been known to play a crucial function in feed nutrient metabolism and animal intestinal health (Carrasco et al. 2019; Lee et al. 2019; Haberecht et al. 2020). Haberecht et al. (2020) suggested that a stable intestinal microflora has a significant effect on resisting pathogen infection. A healthy gut leads to efficiency in micronutrient digestibility and transportation. Colonization of non-pathogenic bacteria, such as *Lactobacillus* sp., in the gut of poultry is beneficial to inhibiting pathogen growth by producing lactic acid and short-chain fatty acid (Yadav and Jha 2019) and improving intestinal morphology and health (Li et al. 2018). Therefore, manipulation of animal's gut microbiota would be an important tool to maintain animal health and to enhance growth performance. Gut microflora can be influenced by diet (Ndotono et al. 2022), including additives such as antibiotics, prebiotics, probiotics, enzymes, synbiotics, and phytobiotics (Stanley et al. 2014; Yadav and Jha 2019).

Antibiotic Growth Promoters (AGPs) have been used in poultry production to improve growth performance for more than 60 years (Bajagai et al. 2020). AGP has a direct effect on the microflora in the digestive tract, which leads to reducing the nutrient competition between pathogenic bacteria and the host, reducing subclinical infections and toxic metabolites, and increasing feed efficiency due to the intestinal wall thinning (Bajagai et al. 2020; Tran et al. 2023).

Since AGP is no longer used as a feed additive in many countries due to the possible negative effects on the growing number of antibiotic-resistant bacteria (Tran et al. 2023), many studies have been conducted to find safer alternatives for AGP; among these are phytobiotics. Phytobiotics or phytogenic feed additives are a class of non-antibiotic growth promoters consisting of herbs, spices, or essential oils that are given to animals to improve growth performance and health (Wang et al. 2024). Contreras-López et al. (2024) reviewed the important properties of phytobiotics to improve growth performance in animals by improving gut microflora, nutrient digestibility, and morphology structure of the digestive tract. Some studies have shown that the inclusion of phytobiotics in poultry diets improved the balance of gut microflora (Abdelli et al. (2021) and intestinal morphology (Ndotono et al. 2022).

In this study, we supplemented diet of broiler chickens with a seed meal of *atung* (*Parinarium glaberrimum* Hassk.) to determine the probable positive effects on

the digestive tract profile, particularly the pH, microflora, and morphology of the small intestine. *P. glaberrimum* is a forest plant widespread in Maluku-Indonesia (Figure 1), whose seeds have historically been used to treat diarrhea and bleeding in pregnant women, as well as seafood preservatives (Hehanussa et al. 2022). In vitro studies have revealed that *P. glaberrimum* seed has antimicrobial properties (Pacana and Galarpe 2017b; Hehanussa et al. 2019) and antioxidant activities (Sarastani et al. 2002). To our knowledge, no studies have been published on the effect of *P. glaberrimum* seed meal supplementation on the pH, microflora, and morphology of the small intestine in broiler chickens.

MATERIALS AND METHODS

Experimental design and diet

This experiment was conducted at the Department of Animal Nutrition and Feed Science, Faculty of Animal Science, Universitas Gadjah Mada, Yogyakarta, Indonesia. A total of 168 one-day-old male New Lohmann broiler chickens were reared in litter-floor pens of 85×100 cm^2 for 35 days. The chicks were randomly placed into six treatment groups, with four replicates and seven chicks in each replicate pen. The temperature was initially set at 32°C for four days before gradually decreasing in accordance with the New Lohmann MB 202 broiler maintenance standard. In the lighting program, the birds received continuous light for the first week, and then the lighting was set at 23 h light: 1 h dark until slaughtered. The temperature, humidity, light, and ventilation settings were consistent across all treatment groups.

Figure 1. *Atung* (*Parinarium glaberrimum* Hassk.) tree and seed (Hehanussa et al. 2022)

Table 1. Ingredients and nutrient composition of dietary treatments for broiler chickens (0-35 d of age)

Ingredients (%)	Dietary treatments[1]					
	NC	PC	T-0.5	T-1	T-2	T-4
Yellow corn	58.50	58.50	58.50	58.50	58.50	58.50
Soybean meal	24.25	24.25	24.25	24.25	24.25	24.25
Meat bone meal	6.75	6.75	6.75	6.75	6.75	6.75
Rice bran	2.00	2.00	2.00	2.00	2.00	3.00
Palm oil	3.00	3.00	3.00	3.00	3.00	2.00
DL-Methionine 99%	0.20	0.20	0.20	0.20	0.20	0.20
L-Lysine 78%	0.10	0.10	0.10	0.10	0.10	0.10
L-Threonine 78%	0.05	0.05	0.05	0.05	0.05	0.05
NaCl	0.30	0.30	0.30	0.30	0.30	0.30
Vitamin-mineral premix[2]	0.20	0.20	0.20	0.20	0.20	0.20
Dicalcium phosphate	0.15	0.15	0.15	0.15	0.15	0.15
Calcium carbonate	0.50	0.50	0.50	0.50	0.50	0.50
Tetracycline (50 ppm)	-	+	-	-	-	-
P. glaberrimum seed meal	0.00	0.00	0.50	1.00	2.00	4.00
Filler (sand)	4.00	4.00	3.50	3.00	2.00	0.00
Total	100.00	100.00	100.00	100.00	100.00	100.00
Nutrient composition						
ME[3] (kcal/kg)	3017	3017	3035	3053	3088	3101
Crude protein (%)	21.01	21.01	21.04	21.07	21.13	21.35
Crude fat (%)	6.54	6.54	6.55	6.56	6.58	5.70
Crude fiber (%)	3.04	3.04	3.05	3.07	3.10	3.42
Calcium (%)	1.01	1.01	1.02	1.03	1.05	1.09
Available Phosphorus (%)	0.47	0.47	0.47	0.47	0.47	0.48
Methionine (%)	0.52	0.52	0.52	0.52	0.52	0.52
Lysine (%)	1.15	1.15	1.15	1.15	1.15	1.16
Threonine (%)	0.84	0.84	0.84	0.84	0.84	0.84

Note: [1]NC: Basal diet without additive (Negative Control), PC: Basal diet + 50 ppm of tetracycline (Positive Control), T-0.5: Basal diet + 0.5% *Parinarium glaberrimum* seed meal, T-1: Basal diet + 1.0% *P. glaberrimum* seed meal, T-2: Basal diet + 2.0% *P. glaberrimum* seed meal, T-4: Basal diet + 4.0% *P. glaberrimum* seed meal; [2]Vitamin-mineral premix composed of vitamin A 1.250.000 IU, vitamin D 250.000 IU, vitamin E 750 IU, vitamin K3 200 mg, vitamin C 5.000 mg, vitamin B1 250 mg, vitamin B2 400 mg, vitamin B6 100 mg, vitamin B12 1.2 mg, biotin 20 mg, folic acid 50 mg, nicotinic acid 3.000 mg, Ca-d pantothenate 400 mg, choline chloride 1.500 mg, copper 500 mg, iron 2.500 mg, iodine 20 mg, manganese 6.000mg, selenium 20 mg, zinc 7.000 mg, cobalt 20 mg, Lysine 16.000 mg, DL-methionine 5.000 mg; [3]ME: metabolizable energy

The first Newcastle Disease (ND) vaccine (Medivac ND La Sota, PT. Medion Farma, Bandung, Indonesia) was administered at 4 days of age via eye drop, and the second ND vaccine (Medivac ND La Sota, Bandung, Indonesia) was administered at 21 days of age via drinking water. Vaccination against infectious bursal disease (Medivac Gumboro A, PT. Medion Farma, Bandung, Indonesia) was carried out at the age of 18 days through drinking water. Birds in all groups were likely to consume feed and water on an ad libitum basis. All of the diets for the experiments were provided in mash form.

The diets were formulated to meet the nutrient requirements of broilers according to the National Research Council US (1984) provision. The ingredients composition and nutrient content of the experimental diets are shown in Table 1. The Negative Control (NC) group was a corn-soybean meal basal diet without any additive supplementation, while the Positive Control (PC) group was a basal diet with 50 ppm of tetracycline supplementation. The T-0.5, T-1, T-2, and T-4 were the basal diet with 0.5%, 1.0%, 2.0%, and 4.0% *P. glaberrimum* seed meal supplementations, respectively. On day 35, one male chicken with a body weight close to the median of each replicate group was chosen and was slaughtered by cutting the trachea, esophagus, as well as jugular vein, and carotid artery on both sides. After the birds had completely died, small intestines were eviscerated immediately to obtain data on intestinal pH, microbial population, and histomorphology.

***Parinarium glaberrimum* seed meal preparation**

Parinarium glaberrimum fruits were obtained from Soya Village, Maluku Province, Indonesia. *P. glaberrimum* seeds were collected from the ripe fruit that had already fallen on the ground. The seeds were removed, air-dried, and ground to pass a 40-mesh screen for use in mixed diet treatments.

Bacterial enumeration

Samples content of the small intestine (ileum) were immediately removed after being slaughtered, collected into sterile tubes, tightly sealed, and stored in ice before the enumeration of total bacteria. The total bacteria enumeration was performed immediately after the sample was collected using the method described by Manafi et al. (2016). In each replication, one gram of ileum digesta was diluted with 9 mL of phosphate buffer saline (Sigma-Aldrich Chemie GmbH, Schnelldorf, Germany). Initial dilution was used as a starting point for subsequent serial dilutions. Serial dilutions were made for *Lactobacillus* from 10^{-1} to 10^{-9} and 10^{-1} to 10^{-7} for coliforms. A 0.1 mL sample from each serial dilution was inoculated into the selective agar plate and spread with a sterile swab. *Lactobacillus* was grown anaerobically on MRS agar (Merck GmbH, Darmstadt, Germany) for 48 hours. Coliform was grown aerobically on Brilliance *Escherichia coli* coliform selective agar (Merck GmbH, Darmstadt, Germany) for 24 hours. After incubation, the colony of intestinal bacteria in every plate of each serial dilution was counted using a bacterial colony counter. The intestinal bacterial population was expressed in Log 10 CFU/g.

The pH of small intestine

The small intestine's acidity was measured immediately after the birds were slaughtered. The digestive tract was removed from the body, and the pH of each small intestinal segment was measured immediately using a digital pH meter (Hanna-HI 99121, Hanna Instruments, Woonsocket, USA) at three points in each section.

Intestinal micromorphology

Intestinal sample preparation and measurement of villus morphology were conducted following Popescu et al. (2021) and Alagbe et al. (2024). After the chicken was killed, the digestive tract was immediately removed from the body, followed by the separation of each part of the small intestine. Samples of the small intestine were collected from the endpoint gizzard to the ileocecal junction. Intestinal samples were taken approximately 6 cm from the middle of each section, flushed with phosphate-buffered saline (pH 7.4) gently, cut into 3 similar pieces, and fixed in 10% neutral buffered formalin solution (Sigma-Aldrich Chemie GmbH, Schnelldorf, Germany) for about 48 hours. Samples of the intestines tissue were dehydrated with increasing concentrations (70, 80, 95, and 100%) of alcohol. The samples were then infiltrated with xylene and embedded into paraffin. The tissue samples were cut in 5 µm using a microtome (S35, CellPath Ltd, Newtown, Powys, UK), attached to slides, and stained with hematoxylin (Sigma-Aldrich Chemie GmbH, Schnelldorf, Germany) and eosin (Sigma-Aldrich Chemie GmbH, Schnelldorf, Germany). Histomorphology slide of the villi was performed using an optical microscope (Olympus CX23, Olympus Corporation, Tokyo, Japan) coupled with a digital camera software (optical viewer 3.3, PT. Miconos, Yogyakarta, Indonesia) to capture images of the villi. The morphology of the villi was then measured using a computer-integrated image program software (Image raster, Version 3.0, PT. Miconos, Yogyakarta, Indonesia). Villus height was measured from the villus tip to the villus crypt junction and measurement of crypt depth following the depth of the invagination between adjacent villi. Villus width was measured at its middle part (Kavoi et al. 2016).

Statistical analysis

Data were statistically analyzed using Oneway ANOVA in a completely randomized design with six treatments and four replications. Data from different statistical analysis results between treatments were tested further using Duncan's new multiple-range test. Data were expressed in means, and were statistically analyzed with SPSS for Windows tools (SPSS, version 25, IBM, New York, USA).

RESULTS AND DISCUSSION

Ileal microflora

Table 2 shows that dietary supplementation of *P. glaberrimum* seed meal has positive effects on the gut microfloral population, which increases lactic acid bacteria and reduces the coliform numbers in the gut. The reduction in coliform numbers in *P. glaberrimum* seed meal groups confirmed the antibacterial properties of *P. glaberrimum* seed against intestinal pathogens. Phytochemical compounds contained in *P. glaberrimum* seeds, such as phenols, tannins, flavonoids, alkaloids, and saponins (Pacana and Galarpe 2017a; Hehanussa et al. 2019) were reported to have antibacterial activity against pathogenic bacteria. In vitro studies have previously demonstrated that *P. glaberrimum* seed inhibited the growth of *E. coli*, *Salmonella* sp., and *Staphylococcus aureus* (Pacana and Galarpe 2017b; Hehanussa et al. 2019).

Improvement of the *Lactobacillus* and reduction of the coliform bacteria numbers in the intestine could be attributed to the presence of phenolic compounds in *P. glaberrimum* seed. Polyphenols are absorbed in small amounts in the intestine (that was approximately 5-10%). Unabsorbed polyphenols, on the other hand, have a significant impact on the intestinal environment by suppressing or stimulating the growth of certain intestinal microbes. Phenolics that were unabsorbed and their metabolites may play an essential role in maintaining the intestinal environment by modulating microbiota growth and population.

A decrease in pathogenic bacteria in the intestine confirmed by dietary supplementation with *P. glaberrimum* seed leads to a decrease of toxic metabolites, which might result in a favorable condition of the intestine for beneficial bacteria growth. The results of this study were supported by Gheisar and Kim (2017), who suggested that a reduction in the number of pathogenic (e.g., *E. coli*) may lead to positive effects in the digestive tract by increasing the population of beneficial bacteria (e.g., *Lactobacillus* sp.). On the other hand, *Lactobacillus* produces Short-Chain Fatty Acids (SCFA), among these acetate, propionic, and butyrate, as well as lactic acid, that also have anti-microbial activities. Organic acids produced by *Lactobacillus* might inhibit the growth of pathogenic bacteria in the intestine (Yadav and Jha 2019). The result of the current study was similar to other researchers (Aleman and Yadav 2024), which reported that phytobiotic inclusions reduced the population of pathogenic bacteria in the gut and increased the population of beneficial bacteria, such as *Lactobacillus*. Wang et al. (2018) stated that increased *Lactobacillus* spp. and decreased coliform numbers lead to a favorable intestinal environment which may improve gastrointestinal function, nutrient digestibility, and growth performance.

The pH of small intestine

Statistical analysis (Table 3) showed that feeding broiler chickens with a diet supplemented with *P. glaberrimum* seed meal reduced intestinal pH, particularly in the treatments of 1-2% supplementations, 1-4% supplementation, and 0.5-1% supplementation which were significantly decreased ($p<0.01$) in the duodenum, jejunum, and ileum compared to that of in the negative control. A lower pH environment of the intestine is necessary for maintaining gut health because it inhibits the growth of harmful bacteria (Lee et al. 2019; Haberecht et al. 2020), and it can reduce metabolic requirements and increase the availability of nutrients for the host.

The decreased pH in the intestine of broiler chickens fed a diet with *P. glaberrimum* seed meal inclusions was probably linked to an elevated *Lactobacillus* population in the gut. *Lactobacillus* sp. produced SCFA that had the possibility to lower pH in the intestine of broiler chickens (Haberecht et al. 2020). Dono et al. (2014) stated that lower intestinal pH is associated with beneficial microbial colonization and may also be related to better energy and nutrient utilization efficiency. As a result, feeding *P. glaberrimum* seed meal might have the potency to improve energy utilization efficiency and nutrient utilization by lowering intestinal pH and suppressing the growth of pathogenic microbiota.

The findings were consistent with other studies that found supplementing broiler chicken diet with phytobiotics lowered the intestinal pH. Ferdous et al. (2019) showed that feeding phytobiotic additives decreased the intestinal pH of broiler chickens when compared to that of the negative control, positive control, or probiotic treatments. Administration of phytobiotic *Artemisia annua* L. has been shown to lower the ileal and cecal pH of broiler chickens (Lee et al. 2014). Similarly, Anugom and Ofongo (2019) discovered a decrease in ileal and cecal pH in 28-day-old broiler chickens fed a diet supplemented with *Ocimum gratissimum* L. leaf extract.

Intestinal micromorphology

Results in Table 4 showed that *P. glaberrimum* seed meal supplementations improved duodenal and ileal villus height but had no effect on jejunal villus height. When 0.5 and 4% *P. glaberrimum* seed meal were added to the diet, villus height in the duodenal section increased ($p<0.05$) when compared to that of the negative control group. The diet of 1-4% *P. glaberrimum* seed meal increased villus height in the ileum ($p<0.05$) when compared to that of the negative control group. The inclusion of 0.5-2% and 0.5-4% *P. glaberrimum* seed meal increased ($p<0.05$) both the duodenal and ileal villus width, respectively, when compared to those of the negative control group. Likewise, the inclusion of 0.5, 1.0, and 4.0% *P. glaberrimum* seed meal increased ($p<0.05$) villus width of the jejunal wall when compared to that of the negative control group.

Increased villus height in treated birds might correspond to the increased digestive and nutrient absorption surface area, intestinal enzyme expression, and transport nutrient system (Yadav and Jha 2019). Nurhayati et al. (2021) reported that a larger villus correlated with a larger surface area for nutrient absorption. Improvement in villus height due to the *P. glaberrimum* seed meal inclusion in the present study might have beneficial properties to improve micro-nutrients uptake for better growth performance.

Table 2. The effects of *Parinarium glaberrimum* seed supplementation on gut microflora in ileal digesta of 35-day-old broiler chickens

Bacteria (Log10 CFU/g)	Dietary treatments[1]						SEM[2]	*p*
	NC	PC	T-0.5	T-1	T-2	T-4		
Lactobacillus	6.92^{a}	7.95^{abc}	8.46^{c}	7.28^{ab}	7.74^{abc}	8.05^{bc}	0.158	0.044
Coliform	3.83^{b}	2.70^{a}	2.84^{a}	2.66^{a}	3.19^{a}	3.22^{a}	0.112	0.007

Note: ^{a,b,c}Mean in the same row without common letter are different at p<0.05; [1]NC: Basal diet without additive (Negative Control), PC: Basal diet + 50 ppm of tetracycline (Positive Control), T-0.5: Basal diet + 0.5% *P. glaberrimum* seed meal, T-1: Basal diet + 1.0% *P. glaberrimum* seed meal, T-2: Basal diet + 2.0% *P. glaberrimum* seed meal, T-4: Basal diet + 4.0% *P. glaberrimum* seed meal; SEM[2]: Standard Error of Mean

Table 3. The effect of *Parinarium glaberrimum* seed supplementation on the intestinal pH of 35-day-old broiler chickens

Intestinal segments	Dietary treatments[1]						SEM[2]	*p*
	NC	PC	T-0.5	T-1	T-2	T-4		
Duodenum	5.70^{bc}	5.49^{ab}	5.90^{c}	5.2^{a}	5.3^{a}	5.4^{ab}	0.676	0.002
Jejunum	5.72^{c}	5.97^{c}	5.43^{bc}	4.7^{a}	5^{ab}	5.4^{ab}	0.117	0.003
Ileum	6.09^{bc}	6.57^{c}	5.18^{a}	5.3^{a}	5.5^{ab}	5.8^{ab}	0.128	0.002

Note: ^{a,b,c}Mean in the same row without common letter are different at p<0.05; [1]NC: Basal diet without additive (Negative Control), PC: Basal diet + 50 ppm of tetracycline (Positive Control), T-0.5: Basal diet + 0.5% *P. glaberrimum* seed meal, T-1: Basal diet + 1.0% *P. glaberrimum* seed meal, T-2: Basal diet + 2.0% *P. glaberrimum* seed meal, T-4: Basal diet + 4.0% *P. glaberrimum* seed meal; SEM[2]: Standard Error of Mean

Table 4. The effect of antibiotic and *Parinarium glaberrimum* seed supplementation on the intestinal morphology of 35-day-old broiler chickens

Attribute	Dietary treatments[1]						SEM[2]	*p*
	NC	PC	T-0.5	T-1	T-2	T-4		
Villus height (µm):								
Duodenum	1762^{a}	1946^{ab}	2147^{b}	1989^{ab}	1914^{ab}	2098^{b}	38.458	0.033
Jejunum	1398	1437	1459	1487	1655	1523	32.647	0.281
Ileum	634^{a}	712^{ab}	698^{ab}	713^{b}	799^{bc}	861^{c}	21.255	0.013
Villus width (µm):								
Duodenum	170^{a}	179^{ab}	218^{c}	212^{bc}	211^{bc}	171^{a}	6.116	0.023
Jejunum	139^{a}	213^{b}	208^{b}	175^{ab}	219^{b}	198^{b}	8.158	0.022
Ileum	133^{a}	184^{b}	180^{b}	193^{b}	203^{b}	203^{b}	6.786	0.011
Crypt depth (µm):								
Duodenum	297	305	233	250	256	258	10.242	0.282
Jejunum	236	186	212	205	214	206	6.049	0.293
Ileum	155	137	122	123	130	130	4.715	0.389
VH/CD ratio:								
Duodenum	6.10^{a}	6.61^{ab}	9.37^{d}	8.05^{bcd}	7.61^{abc}	8.51^{cd}	0.292	0.002
Jejunum	6.06^{a}	7.88^{b}	7.03^{b}	7.31^{b}	7.73^{b}	7.20^{b}	0.170	0.013
Ileum	4.29^{a}	5.24^{b}	5.75^{bc}	5.86^{bc}	6.24^{bc}	6.53^{c}	0.190	<0.01

Note: ^{a,b,c}Mean in the same row without common letter are different at p<0.05; [1]NC: Basal diet without additive (Negative Control), PC: Basal diet + 50 ppm of tetracycline (Positive Control), T-0.5: Basal diet + 0.5% *P. glaberrimum* seed meal, T-1: Basal diet + 1.0% *P. glaberrimum* seed meal, T-2: Basal diet + 2.0% *P. glaberrimum* seed meal, T-4: Basal diet + 4.0% *P. glaberrimum* seed meal; SEM[2]: Standard Error of Mean

The result of the histo-morphology examination showed that *P. glaberrimum* seed meal inclusions had no effect on the villus crypt depth of the small intestine. The crypts are villus factories, and deeper crypts have faster tissue turnover, allowing for villus renewal as needed in response to normal shedding or inflammation caused by pathogens or their toxins. Deeper crypts indicate a greater need for new tissue regeneration, resulting in higher energy and protein requirements for intestinal maintenance (Mfoundou et al. 2022). However, no response in crypt depth with the dietary *P. glaberrimum* seed meal inclusion groups might indicate that chickens in all treatments were repairing or renewing villi at the same rate.

From the results obtained, there was a significant difference in the negative control treatment with the administration of *P. glaberrimum* seeds. It can be seen that the administration of 0.5-4% *P. glaberrimum* seed meal increased the ratio of villus height to crypt depth of the duodenum (p<0.05), jejunum (p<0.05), and ileum (p<0.01). Improvement of the villus height to crypt depth ratio in the duodenum, jejunum, and ileum could be attributed to the increased villus height with no alteration in crypt depth at the same time. Ali et al. (2018) stated that the increase in villus height to crypt depth ratio is associated with

improved host growth performance. The findings in the current experiment suggested that *P. glaberrimum* seed meal may promote a healthier intestinal environment with improved nutrient absorption capacity, allowing for improved growth performance in broiler chickens.

In general, *P. glaberrimum* seed meal inclusion improved the villus structure in the intestinal wall of broiler chicken, which is linked to better intestinal microflora balance in the digestive tract (Table 1). An increased number of *Lactobacillus* in groups with *P. glaberrimum* seed meal inclusion may also promote the improvement of intestinal structure. Li et al. (2018) reported that *Lactobacillus* inclusion improved intestinal morphology and gut health. Nurhayati et al. (2021) also stated that colonization of beneficial bacteria, such as *Lactobacillus*, in the digestive tract might improve intestinal villus structure. *Lactobacillus* sp. produced SCFA, which has been known as an essential energy source in stimulating intestinal epithelial cell proliferation, particularly butyric acid (Ali et al. 2018; Yadav and Jha 2019; Nurhayati et al. 2021). Improvement of the morphology structure of the small intestine in the current study, on the other hand, could be linked to the presence of polyphenols, particularly flavonoids, in the *P. glaberrimum* seed. Wang et al. (2020) stated that the health-promoting properties of flavonoids for intestinal health were related to the ability to modulate barrier permeability, protect the mucus layer, regulate the intestinal immune system, fight against oxidative stress, and positively shape the intestinal microbiome.

It has been reported in some research that diet inclusion with several green feed additives, or plant origins feed additives, improved the intestinal morphology of poultry, which was consistently found in the current experiment. For instance, 1.0-2.0% garlic meal inclusion or inclusion of 1.2% *Moringa oleifera* Lam. leaf meal (Khan et al. 2017) increased villus height in all small intestine segments of broiler chickens. Furthermore, dietary inclusion of *M. oleifera* leaf meal also increased villus height to crypt depth ratio on the wall of ileum. Boka et al. (2014) showed that 2.0 and 3.0% dietary inclusion of black cumin increased villus height, villus height to crypt depth ratio, and crypt depth. Kiczorowska et al. (2016) reported that incorporating a diet with 3-4% *Boswellia serrata* Roxb. ex Colebr. resin increased villus height to crypt depth ratio in the wall of duodenum.

In conclusion, based on the ability to improve gut microflora and morphology, *P. glaberrimum* seed meal can be recommended as a green feed additive to replace AGP in the poultry diet.

ACKNOWLEDGEMENTS

The authors are grateful to the Ministry of Research, Technology, and Higher Education, Indonesia, for funding support through the Domestic Education Scholarship (BPDN) and the Research Directorate of Universitas Gadjah Mada, Indonesia, for funding support through the Final Assignment Recognition Program (RTA) 2019.

REFERENCES

Abdelli N, Solà-Oriol D, Pérez JF. 2021. Phytogenic feed additives in poultry: Achievements, prospective and challenges. Animals 11: 3471. DOI: 10.3390/ani11123471.

Alagbe EO, Sung JY, Lindsey K, Pasternak JA, Adeola O. 2024. PSI-21 Optimizing sample size for accurate measurements and prediction equations for intestinal morphology in broiler chickens. J Anim Sci 102 (2): 281-282. DOI: 10.1093/jas/skae102.320.

Aleman RS, Yadav A. 2024. Systematic review of probiotics and their potential for developing functional nondairy foods. Appl Microbiol 4: 47-69. DOI: 10.3390/applmicrobiol4010004.

Ali N, Alkassar S, Alkassar A. 2018. The effect of using organic acid as an alternative to antibiotics drugs on productive and physiological performance of broilers ross – 308. Adv Anim Vet Sci 6 (9): 359-365 DOI: 10.17582/journal.aavs/2018/6.9.359.365.

Anugom YO, Ofongo RTS. 2019. Impact of aqueous *Ocimum gratissimum* (Lyn) leaf extract on growth performance, gut pH and bacterial counts in broiler chickens. Intl J Poult Sci 18 (7): 309-316. DOI: 10.3923/ijps.2019.309.316.

Bajagai YS, Alsemgeest J, Moore RJ, Van TT, Stanley D. 2020. Phytogenic products, used as alternatives to antibiotic growth promoters, modify the intestinal microbiota derived from a range of production systems: An in vitro model. Appl Microbiol Biotechnol 104: 10631-10640. DOI: 10.1007/s00253-020-10998-x.

Boka J, Mahdavi AH, SamieAH, Jahanian R. 2014. Effect of different levels of black cumin (*Nigella sativa* L.) on performance, intestinal *Escherichia coli* colonization dan jejunal morphology in laying hens. J Physiol Anim Nutr 98: 373-383. DOI: 10.1111/jpn.12109.

Carrasco JMD, Casanova NA, Miyakawa MEF. 2019. Microbiota, gut health and chicken productivity: what is the connection? Microorganisms 7: 374. DOI: 10.3390/microorganisms7100374.

Contreras-López G, Carrillo-Lopez LM, Vargas-Bello-Pérez E, García-Galicia IA. 2024. Microencapsulation of feed additives with potential in livestock and poultry production: A systematic review. Chil J Agric Anim Sci 40 (1): 229-249. DOI: 10.29393/chjaas40-21mfgi40021.

Dono ND, Sparks NH, Olukosi OA. 2014. Association between digesta pH, body weight, and nutrient utilization in chickens of different body weights and at different ages. J Poult Sci 51: 180-184. DOI: 10.2141/jpsa.0120151.

Ferdous FM, Arefin SM, Rahman MM, Ripon MMR, Rashid MH, Sultana RM, Hossain MT, Ahammad MU, Rafiq K. 2019. Beneficial effects of probiotic and phytobiotic as growth promoter alternative to antibiotic for safe broiler production. J Adv Vet Anim Res 6 (3): 409-415. DOI: 10.5455/javar.2019.f361.

Gheisar MM, Kim IH. 2017. Phytobiotics in poultry and swine nutrition. Italian J Anim Sci 10 (1): 1350120. DOI: 10.1080/1828051X.2017.1350120.

Haberecht S, Bajagai YS, Moore RJ, Moore RJ, Van TT, Stanley D. 2020. Poultry feeds carry diverse microbial communities that influence chicken intestinal microbiota colonisation and maturation. AMB Express 10: 143. DOI: 10.1186/s13568-020-01077-5.

Hehanussa SC, Zuprizal Z, Hanim C, Dono ND. 2022. Performance and haematological profile of broiler chickens fed diet containing *atung* (*Parinarium glaberrimum* Hassk.) seed powder. Buletin Peternakan 46 (2): 104. DOI: 10.21059/buletinpeternak.v46i2.73251.

Hehanussa SCH, Zuprizal, Dono ND, Hanim C. 2019. Potential of *atung* seeds (*Parinarium glaberrimum* Hassk.) as a phytobiotic candidate in poultry ration based on nutrient composition, phytochemical and antibacterial properties. IOP Conf Ser: Earth Environ Sci 387: 012072. DOI: 10.1088/1755-1315/387/1/012072.

Kavoi BM, Gakuya DW, Mbugua PN, Kiama SG. 2016. Effects of dietary *Moringa oleifera* leaf meal supplementation on chicken intestinal structure and growth performance. J Morphol Sci 33: 186-192. DOI: 10.4322/jms.095915.

Khan I, Zaneb H, Masood S, Yousaf MS, Rehman HF, Rehman H. 2017. Effect of *Moringa oleifera* leaf meal supplementation on growth performance and intestinal morphology in broiler chickens. J Anim Physiol Anim Nutr 101: 114-121. DOI: 10.1111/jpn.12634.

Kiczorowska B, Al-Yasiry ARM, Samolinska W, Marek A, Pyzik E. 2016. The effect of dietary supplementation of the broiler chicken diet with *Boswellia serrata* resin on growth performance, digestibility, and gastrointestinal characteristics, morphology, and microbiota. Livest Sci 191: 117-124. DOI: 10.1016/j.livsci.2016.07.019.

Lee H, Lee S, Kim IS, Oh S, Kim J, Sung NJ. 2014. Effect of dietary supplementation of *gaeddongssuk* (*Artemisia annua* L.) on the meat quality in the chicken (Woorimatdag). J Agric Life Sci 48: 235-250. DOI: 10.14397/jals.2014.48.3.235.

Lee S, La T, Lee H, Choi I, Song CS, Park S, Lee J, Lee S. 2019. Characterization of microbial communities in the chicken oviduct and the origin of chicken embryo gut microbiota. Sci Rep 9: 6838. DOI: 10.1038/s41598-019-43280-w.

Li W, Wang W, Liu D, Guo Y. 2018. Effects of *Lactobacillus acidophilus* on the growth performance and intestinal health of broilers challenged with *Clostridium perfringens*. J Anim Sci Biotechnol 9: 25. DOI: 10.1186/s40104-018-0243-3.

Manafi M, Hedayati M, Khalaji S. 2016. Effectiveness of phytogenic feed additive as alternative to bacitracin methylene disalicylate on hematological parameters, intestinal histomorphology and microbial population and production performance of Japanese quails. Asian-Australas J Anim Sci 29 (9): 1300-1308. DOI: 10.5713/ajas.16.0108.

Mfoundou JDL, Guo Y, Yan Z, Wang X. 2022. Morpho-histology and morphometry of chicken testes and seminiferous tubules among yellow-feathered broilers of different ages. Vet Sci 9: 485. DOI: 10.3390/vetsci9090485.

National Research Council (US). Subcommittee on Poultry Nutrition. 1984. Nutrient Requirements of Poultry: Eighth Revised Edition, 1984. The National Academy of Sciences Press, Washington DC. DOI: 10.17226/19397.

Ndotono EW, Khamis FM, Bargul JL, Tanga CM. 2022. Gut microbiota shift in layer pullets fed on black soldier fly larvae-based feeds towards enhancing healthy gut microbial community. Sci Rep 12: 16714. DOI: 10.1038/s41598-022-20736-0.

Nurhayati, Hartutik, Sjofjan O, Widodo E. 2021. The effect of using mannan oligosaccharides extracted from fermented palm kernel cake and cassava by-product mixture in ration on broiler gut profile. Livest Res Rural Dev 33: 39.

Pacana JM, Galarpe Van RKR. 2017a. Phytochemical screening and toxicity of *Atuna racemosa* Rafin. chrysobalanaceae shell and seed extracts. Intl J Adv Appl Sci 4 (11): 110-115. DOI: 10.21833/ijaas.2017.011.017.

Pacana JM, Galarpe Van RKR. 2017b. Antibacterial property *of Atuna racemosa* Rafin. chrysobalanaceae shell and kernel extracts (aqueous, methanol, ethyl acetate, and decoction). Intl J Biosci 11 (1): 443-448. DOI: 10.12692/ijb/11.1.443-448.

Popescu RG, Voicu SN, Grădișteanu Pîrcălăbioru G, Gharbia SA, Hermenean AO, Georgescu SE, Panaite TD, Turcu RP, Dinischiotu A. 2021. Impact of dietary supplementation of flaxseed meal on intestinal morphology, specific enzymatic activity, and cecal microbiome in broiler chickens. Appl Sci 11 (15): 6714. DOI: 10.3390/app11156714.

Sarastani D, Soekarto ST, Muchtadi TR, Fardiaz D, Apriyantono A. 2002. Aktivitas antioksidan ekstrak dan fraksi ekstrak biji Atung (*Parinarium glaberrimum* Hassk.) [Antioxidant Activities of *Parinarium glaberrimum* Hassk. Extracts and their Fractions]. Jurnal Teknologi dan Industri Pangan 13: 149-149. [Indonesian]

Stanley D, Hughes RJ, Moore RJ. 2014. Microbiota of the chicken gastrointestinal tract: Influence on health, productivity and disease. Appl Microbiol Biotechnol 98: 4301 - 4310. DOI: 10.1007/s00253-014-5646-2.

Tran C, Horyanto D, Stanley D, Cock IE, Chen X, Feng, Y. 2023. Antimicrobial properties of *Bacillus* probiotics as animal growth promoters. Antibiotics 12 (2): 407. DOI: 10.3390/antibiotics12020407.

Wang J, Deng L, Chen M, Che Y, Li L, Zhu L, Chen G, Feng T. 2024. Phytogenic feed additives as natural antibiotic alternatives in animal health and production: A review of the literature of the last decade. Anim Nutr 17: 244-264. DOI: 10.1016/j.aninu.2024.01.012.

Wang J, Ji H, Wang S, Liu H, Zhang W, Zhang D, Wang Y. 2018. Probiotic *Lactobacillus plantarum* promotes intestinal barrier function by strengthening the epithelium and modulating gut microbiota. Front Microbiol 9: 1953. DOI: 10.3389/fmicb.2018.01953.

Wang M, Zhao H, Wen X, Ho CT, Li S. 2020. Citrus flavonoids and the intestinal barrier: Interactions and effects. Compr Rev Food Sci Food Saf 20: 225-251. DOI: 10.1111/1541-4337.12652.

Yadav S, Jha R. 2019. Strategies to modulate the intestinal microbiota and their effects on nutrient utilization, performance, and health of poultry. J Anim Sci Biotechnol 10: 2. DOI: 10.1186/s40104-018-0310-9.

NUSANTARA BIOSCIENCE
Vol. 16, No. 2, pp. 284-291
November 2024

ISSN: 2087-3948
E-ISSN: 2087-3956
DOI: 10.13057/nusbiosci/n160215

Imidacloprid degradation by potential soil bacteria isolated from rice fields in Grobogan, Central Java, Indonesia

MUHAMMAD ALFIYAN HERMAWAN, ARTINI PANGASTUTI♥, RATNA SETYANINGSIH
Faculty of Mathematics and Natural Sciences, Graduate Program of Bioscience, Universitas Sebelas Maret. Jl. Ir. Sutami 36A Surakarta 57126, Central Java, Indonesia. Tel./fax.: +62-271-663375, ♥email: artini_p@staff.uns.ac.id

Manuscript received: 31 July 2024. Revision accepted: 16 October 2024.

Abstract. *Hermawan MA, Pangastuti A, Setyaningsih R. 2024. Imidacloprid degradation by potential soil bacteria isolated from rice fields in Grobogan, Central Java, Indonesia. Nusantara Bioscience 16: 284-291.* Imidacloprid a widely used pesticide is known for its polar nature, resistance to evaporation, and persistence in soil. When concentrations exceed environmental thresholds, imidacloprid can act as a pollutant, disrupting ecosystems, altering soil pH, and decreasing soil fertility. This study aimed to isolate and identify soil bacteria from rice fields capable of degrading imidacloprid and to highlight their potential role in bioremediation. Isolated bacteria are identified based on morphological characteristics, their ability to degrade imidacloprid and through molecular tests using 16S rRNA. Four bacterial colonies were obtained from the isolation results with different morphological variations. The degradation test results showed that the isolates were able to grow in media containing imidacloprid and were able to reduce imidacloprid by 26.66-31.75%. Based on 16S rRNA gene analysis, isolate IT1 was identified as *Enterobacterales*, IT2 was identified as the Enterobacteriaceae, IT3 as *Pectobacterium aroidearum* strain CCRMPA670, and IT4 was identified as *Bacillus thuringiensis* strain FDAARGOS_791.

Keywords: *Bacillus thuringiensis*, Bacteria, biodegradation, imidacloprid, *Pectobacterium aroidearum*, rice field

INTRODUCTION

The effective use of pesticides in controlling pests is a short-term solution. Pesticides create a dependency among farmers to consistently use them as a determinant factor for high yields and quality agricultural products (Putri et al. 2021). Imidacloprid is a type of pesticide that is widely used and its effect lasts about 156 days (Zamule et al. 2021). Previous studies have reported varying half-life values for imidacloprid in different soil types, namely 455-518 days on sandy clay soils in Australia and 233-366 days on muddy clay soil in India (Bhattacherjee et al. 2020).

Imidacloprid exceeding the environmental threshold becomes a pollutant and can disrupt the natural balance. Its uncontrolled use of imidacloprid can lead to various problems (Erguven and Demirci 2021). Approximately 20% of imidacloprid pesticides hit the target, while the remaining 80% falls into the soil, causing soil acidification and reducing soil fertility (Sabourmoghaddam et al. 2015). Continuous use of imidacloprid leads to environmental accumulation, resulting in soil and water pollution, potentially accumulating in the food chain (Bhattacherjee et al. 2020). Its residues in the soil affect the decline in the diversity of soil fauna (Bandeira et al. 2020). This occurs because imidacloprid can influence the growth and reproduction of soil fauna, reducing the quantity and variety of existing fauna. Additionally, imidacloprid can disrupt interactions among soil fauna, disturbing the balance of the soil ecosystem. The low quantity of soil fauna will reduce their contribution to soil quality and productivity.

Grobogan District has a rice harvest area of 179,124 hectares, with the highest rice production in Central Java, Indonesia, with a production of 787,275 tons-GKG in 2022. Grobogan District is indeed the largest among other districts in Central Java, so it has become an essential factor in Indonesia's rice production. Considering that it is the largest rice harvest area in Central Java, it is essential to maintain the soil condition of the area so as not to experience an increase in soil acidity due to the residue of the imidacloprid pesticide which in terms affects the rice crop productivity level. Imidacloprid can cause the accumulation of pesticide residues in the soil, potentially killing the diversity of soil fauna, increasing plant pest resistance and reducing soil fertility (Bandeira et al. 2020).

Imidacloprid can undergo natural environmental processes, including hydrolysis, photodegradation and biodegradation. Biodegradation is a promising process for reducing residues due to its relatively easy, selective, effective, safe, and cost-efficient operation (Hu et al. 2013). Cycoń and Seget (2015) demonstrated that various bacterial isolates can degrade imidacloprid residues as the sole carbon or nitrogen source or through metabolic transformation. Bhattacherjee et al. (2020) reported that *Burkholderia cepacia* from agricultural land can degrade 50 µg/mL of imidacloprid by 69% within 20 days. Gupta et al. (2016) used *Pseudomonas* sp. RPT 52 with a 0.5 mM imidacloprid solution, achieving approximately 46.5% degradation within 40 hours.

This study aimed to isolate and identify soil bacteria from rice fields capable of degrading imidacloprid and to highlight their potential role in bioremediation. The urgency of research is getting bacterial isolates that have

a high ability to grow in rice fields that are applied by imidacloprid and the ability to degrade the residue of the imidacloprid pesticide and know the level of efficiency of the isolates selected to re-feminist the imidacloprid residue in the soil.

MATERIALS AND METHODS

Study area

The sampling was conducted in the Godong, Wirosari, and Ngaringan Sub-districts of Grobogan, Central Java, Indonesia (Figure 1). Grobogan is located at an altitude of 100-500 meters above sea level with coordinates 7° 1' 18.188" S 110° 57' 45.306" E. The land in Grobogan is mostly used for the agricultural sector, such as rice fields and plantations.

Sample collection

The samples used were collected from the Grobogan region, consisting of soil exposed to imidacloprid pesticides based on a long history of using the pest-repellent pesticide for brown planthopper, namely Avidor 25 WP brand (imidacloprid 25%). The sampling locations were at three points in the Sub-districts of Godong, Wirosari, and Ngaringan, with soil samples taken from the central area due to the likelihood of containing a significant amount of pesticide residues and being the main rice cultivation area. Using a scoop, 500 grams of soil samples were taken from the top layer of soil (depth of 0–15 cm) (Gautam and Dubey 2022). The collected soil was then placed in an ice box (filled with ice bags to maintain a temperature of ±4°C) to preserve the soil conditions (Alwi et al. 2023).

Isolation and purification of potential pesticide imidacloprid degrading bacterial isolates

The soil was dried and ground with a mortar and then sieved through a 0.2 mM mesh to remove physical impurities. Each soil sample was weighed and 5 grams were taken using an analytical balance. Vortex was used to homogenize the soil samples after they were put in bottles with 45 mL of distilled water. Subsequently, centrifugation was carried out at 10,000 x g for 20 minutes (Irfan et al. 2021), referred to as a 10^{-1} dilution. One millilitre of the liquid was pipetted from the 10^{-1} dilution and added to a reaction tube holding nine millilitres of distilled water to make a 10^{-2} dilution. This process was repeated sequentially up to a 10^{-7} dilution using the serial dilution technique. Serial dilution was performed to reduce the density of microorganisms in the soil samples, facilitating the isolation of purer bacterial colonies on culture media (Bhattacherjee et al. 2020).

All the dilutions (10^{-1} to 10^{-7}) were spread using the pour plate method on 15 mL of MSM agar media supplemented with 2 ppm of imidacloprid as the sole carbon source in petri dishes. The minimal salts medium (MSM, g/L) consisted of K_2HPO_4 2.27 g, KH_2PO_4 0.95 g, and $(NH_4)_2SO_4$ 0.67 g per 1 L of deionized water, adjusted to pH 7.0 (Coleman 2002). The inoculated plates were then incubated for 48 hours at 28°C (Yadav et al. 2021). Bacteria obtained from the mixed culture were purified using the quadrant streaking method with four streaks until no other bacterial mixtures were present. Pure isolates were also inoculated into glycerol stocks and stored in the freezer.

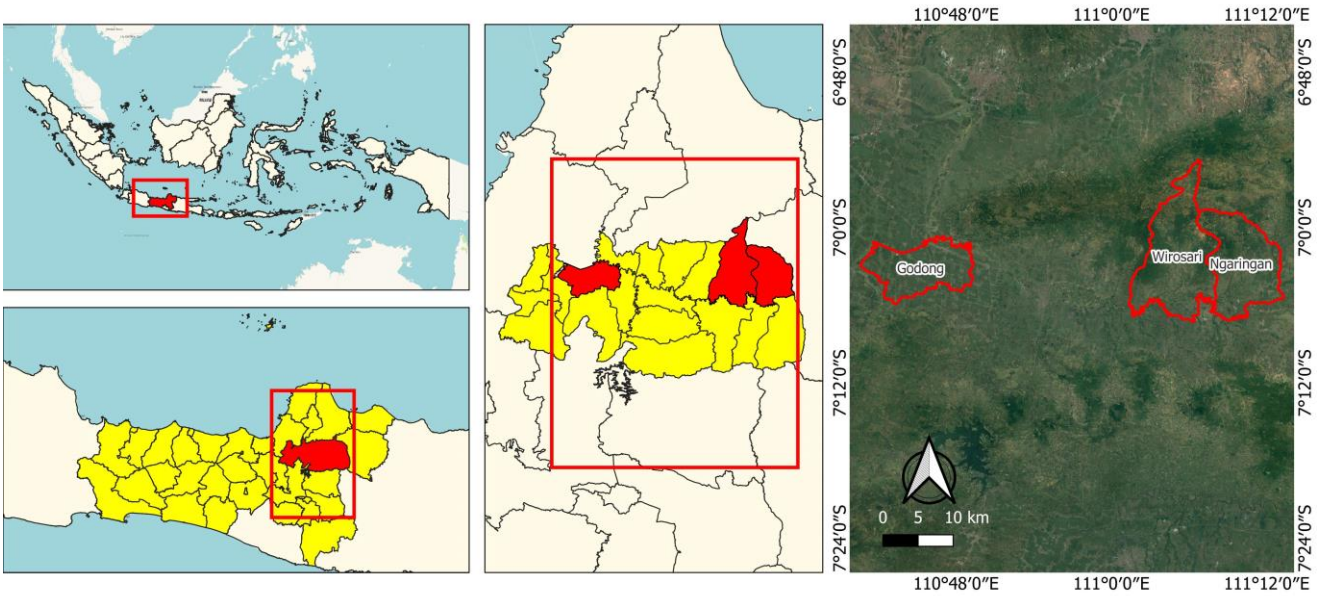

Figure 1. Locations of soil sampling sites: Wirosari, Godong, and Ngaringan Sub-districts of Grobogan, Central Java, Indonesia (7° 1' 18.188" S 110° 57'45.306" E)

Growth of bacterial isolates

Bacterial isolates were cultured in erlenmeyer flasks containing 250 mL of Minimal Salts Medium (MSM) supplemented with two ppm imidacloprid. Subsequently, the cultures were placed on a shaker incubator at 28°C and 150 rpm for 24 hours, allowing them to reach the exponential growth phase. A 10 mL sample was extracted and centrifuged at 8000 x g for 15 minutes, the supernatant was then discarded and replaced with 10 mL of sterile distilled water, followed by vortex. The Optical Density (OD) values were measured using a UV-Vis spectrophotometer at a wavelength of 600 nm (Mishra et al. 2014). Absorbance values were recorded every three hours until the bacterial culture entered the stationary phase.

Imidacloprid pesticide degradation test

The isolates cultured were transferred in a volume of 10 mL into a reaction tube containing 250 mL of liquid MSM with two ppm imidacloprid. The reaction tube was incubated at 170 rpm and 28°C. Samples were detected and measured on days 0, 3, 5, 7, 10, 12, 14, 17, 19, and 21. Pesticide imidacloprid degradation was assessed using High-Performance Liquid Chromatography (HPLC) (Hu et al. 2013).

Identification of selected bacterial isolates

The bacterial DNA genome from the isolate was extracted using the Quick-DNA™ Kit from Zymo Research, following the manufacturer's protocol. DNA obtained was then used as a template for the Amplification of DNA 16S rRNA. Amplification using a pair of 67F (5′-CCTACGGGNGGCWGCAG-3′) and Primer 1387R (5′-ACTACHV GGGTATCTAATCC-3′) and for sequencing using a primary 785F (5′-GGATTAGATACCCTGGTA-3′) and 907R (5′-CCGTCAATTCMTTTRAGTTT-3′) to target the partial region of the 16S rRNA gene. PCR reactions were performed in a thermocycler with 7.5 µL My Taq Red Mix buffer (2x), 0.5 µL forward primer, 0.5 µL reverse primer, 0.5 µL DNA template, and 19.8 µL ddH_2O. The denaturation, amplification, and annealing processes each had 30 cycles. The cycle parameters were as follows: initial primer denaturation at 95°C for 5 minutes, 30 cycles of denaturation at 95°C for 45 seconds, annealing at 62°C for 45 seconds, extension at 72°C for 2 minutes, and a final extension at 72 °C for 72 minutes (McCabe et al. 1999). The PCR products were then kept at 4°C for subsequent analysis by electrophoresis. The amplified products were electrophoresed on a 1% agarose gel. Electrophoresis was carried out for 45 minutes at an electric voltage of 84 V in 1x TAE buffer. The DNA amplicons in the agarose gel were stained with gel red dye. DNA visualization was performed using a UV transilluminator (Gao et al. 2021). The amplified DNA was then subjected to DNA sequencing. The 16S rDNA amplicon was subsequently sent to a third party for sequencing processing.

Data analysis

The growth curve of imidacloprid degrading bacteria was constructed, and the findings were obtained by incubating the bacteria with a UV-Vis spectrophotometer to measure Optical Density (OD) at 600 nm. The bacterial growth curve was generated based on the OD values obtained over time. Following the construction of the bacterial growth curve, a test for bacterial resistance to imidacloprid was conducted by observing the OD values at 600 nm under various concentrations of imidacloprid. Subsequently, a test of imidacloprid pesticide degradation by bacteria was performed using High-Performance Liquid Chromatography (HPLC). The data obtained consisted of residual imidacloprid concentrations after incubation with bacteria. The acquired data were then analyzed descriptively and qualitatively. The sequences obtained from the sequencing process underwent a similarity test using BLASTn features on NCBI, utilizing the 'nr/nt' or 'Bacteria' database.

RESULTS AND DISCUSSION

Imidacloprid residue

The soil sample from Wirosari exhibited the highest residue levels compared to the soil samples from Godong and Ngaringan (Table 1). According to the Indonesian Minister of Health and Minister of Agriculture Decree No. 881/MENKES/SKB/VIII/1996 and No. 711/Kpts/TP.270/8/1996 Regarding the Maximum Residue Limits of Pesticides in Agricultural Products, the maximum residue limit for imidacloprid in soil should be 0.5 ppm. The soil in Ngaringan and Godong has imidacloprid residues approaching the maximum allowable limit, while the Wirosari soil exceeds the imidacloprid residue limit permitted by the Department of Agriculture.

Isolation of indigenous bacteria

The isolates capable of growing on MSM + imidacloprid media were coded as IT1, IT2, IT3, and IT4. Color dissimilarity was the most noticeable aspect of isolates characterization. According to Table 2 and Figure 2, The color of isolates IT1, IT2, IT3, and IT4 were light pink color, brick-red color, whitish-yellow color, and white color, respectively.

Bacterial growth

All bacterial isolates experienced an exponential growth phase from hour 3 to 51, except for isolate IT1, which that it ended its exponential phase at hour 54 (Figure 3). The bacterial growth results from the unique capabilities of each bacterial isolate in utilizing nutrients present in the media, ultimately leading to variations in metabolic efficiency.

Table 1. The content of imidacloprid residue Grobogan, Central Java, Indonesia, soil sample

Soil samples	Residue (ppm)
Ngaringan	0.47
Godong	0.45
Wirosari	0.50

Imidacloprid pesticide degradation test

Bacterial isolates can grow in MSM + imidacloprid media. Isolates IT1, IT2, IT3, and IT4 can reduce the concentration of imidacloprid in MSM+imidacloprid 2 ppm media. The highest (31.75%) percentage of decreased imidacloprid was recorded in the IT1 isolate (Figure 4), and the percentage of decreased imidacloprid IT3 isolates was lower than the other three isolates. The percentage of reduced imidacloprid was consistently increased from day 0 to the 21st day; this shows the potential for the isolate's degradation or reduction of imidacloprid.

Identification of bacterial isolates

The results of BLAST-n analysis (Table 3) showed that identified bacterial isolates had a similarity of 16S rRNA gene sequences with bacteria from the genus *Pectobacterium* and *Bacillus*. IT 1 and IT 2 had a percentage of similarity <95% with a low category after comparing species data in Genbank. Based on the 16S rRNA enclosure gene, the results revealed that isolates IT1 and IT2 were not identified because the similarity was only 86.83% and 89.51% with *Serratia nevei* and *S. marcescens*, respectively. Isolates IT3 and IT4 showed 99.83% and 98.57% similarities with *Pectobacterium aroidearum* strain CCRMPA670 and *Bacillus thuringiensis* strain FDAARGOS_791. With this percentage, IT1 and IT2 were identified into Enterobacterales and Enterobacteriaceae, respectively.

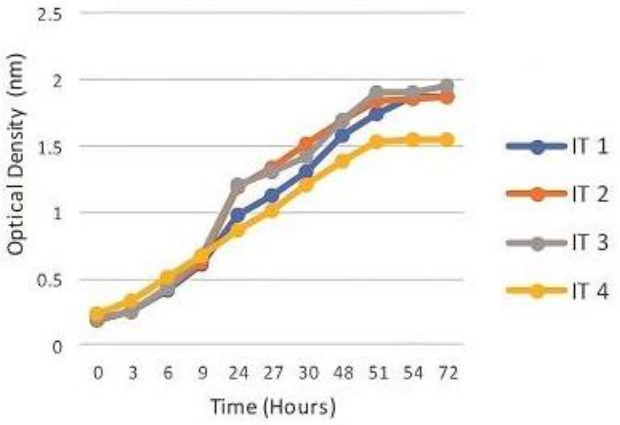

Figure 3. Growth of bacterial isolates on MSM with imidacloprid media

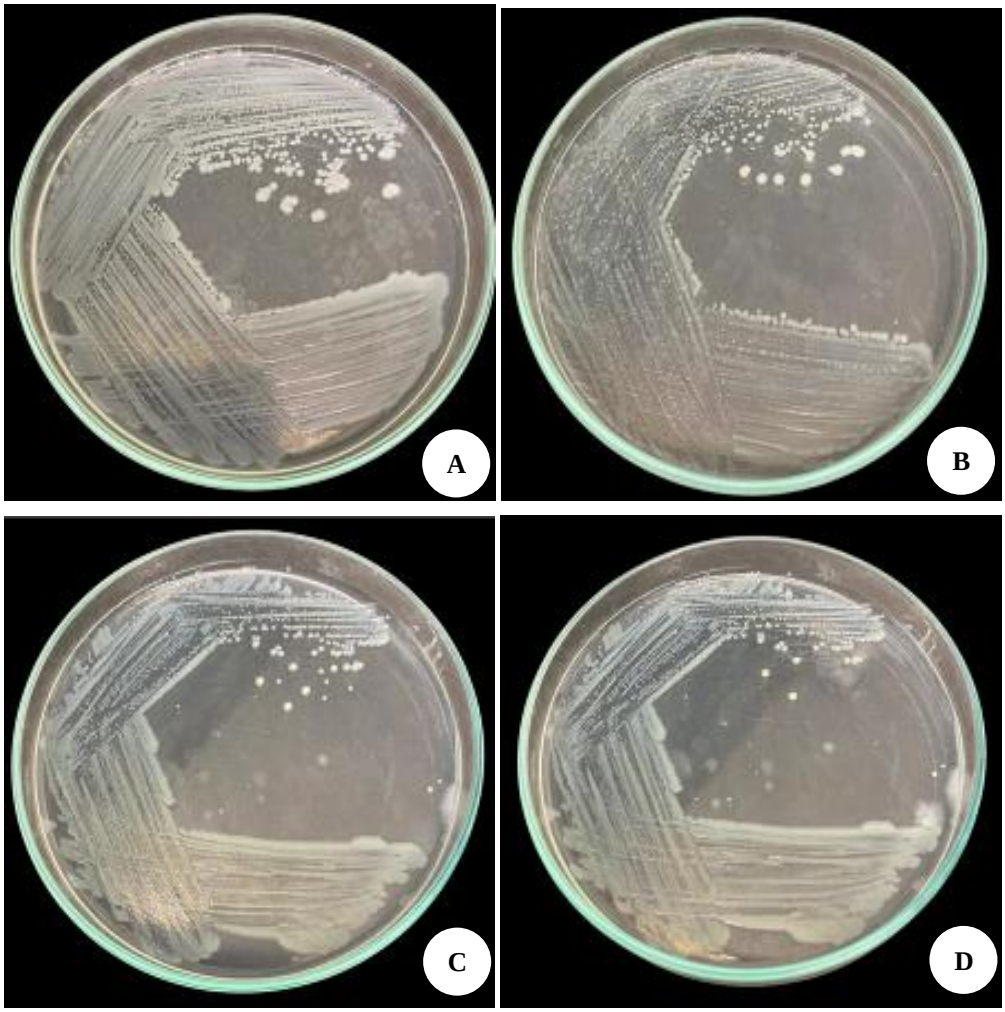

Figure 2. Bacterial colonies. A. IT1, B. IT2, C. IT3, D. IT4

Table 2. The characteristics of bacterial isolates from the rice fields in Grobogan, Central Java, Indonesia

Isolates code	Elevation	Margin	Colony color	Shape of colony	Shape of cell
IT1	Convex	Entire	Light pink	Circular	Bacilli
IT2	Convex	Entire	Brick red	Circular	Bacilli
IT3	Convex	Entire	Whitish yellow	Circular	Bacilli
IT4	Convex	Entire	White	Circular	Bacilli

Table 3. Similarity of 16S rRNA gene sequences of bacterial isolates using the BLAST-n program

Isolates code	Related species	Query cover (%)	Similarity (%)	ACC Numbers
IT1	*Serratia nevei* strain 2017-45-174	76	86.83	CP109739.1
IT2	*Serratia marcescens* strain JW-CZ2	100	89.51	CP055161.1
IT3	*Pectobacterium aroidearum* strain CCRMPA670	90	99.83	MN883868.1
IT4	*Bacillus thuringiensis* strain FDAARGOS_791	100	98.57	CP054568.1

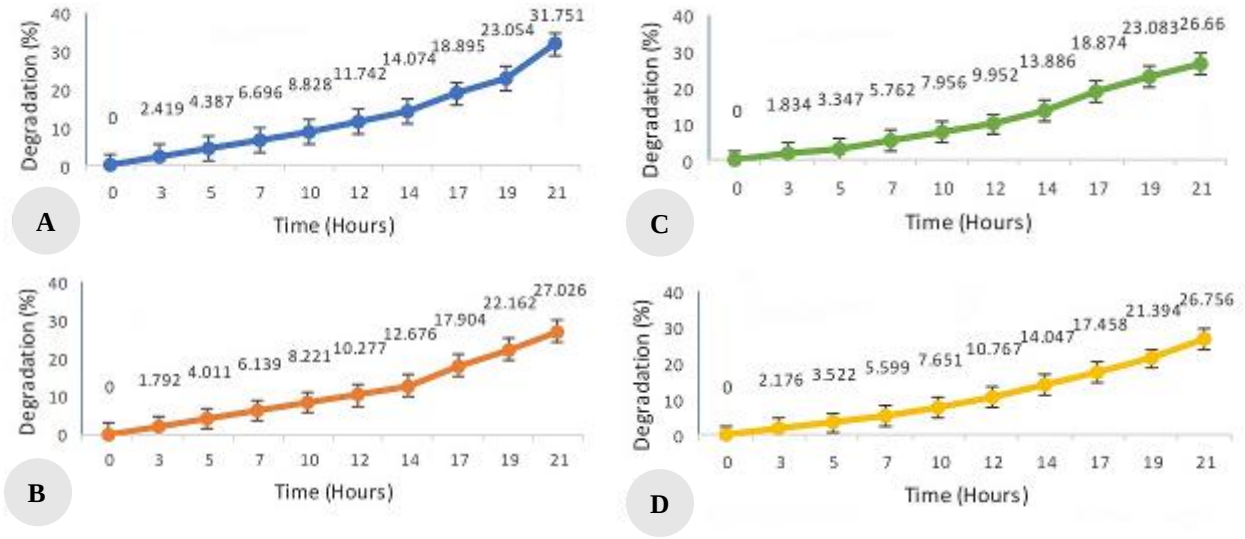

Figure 4. Growth of bacterial isolates on MSM + imidacloprid media: A. IT1, B. IT2, C. IT3, D. IT4

Discussion

Imidacloprid residue can affect the presence of soil bacteria through various mechanisms, both directly and indirectly. The impact of imidacloprid on soil bacteria depends on several factors such as bacterial types, imidacloprid concentrations, environmental conditions, and degradation of microorganisms. Excessive use of imidacloprid can interfere with the balance of soil microbes and decrease soil ecological function. Several studies have shown that imidacloprid residues can affect the composition of bacterial communities in the soil. Akter et al. (2023) reported that high imidacloprid concentrations could reduce the abundance of *Actinobacteria*, *Bacteroidetes*, and *Proteobacteria* in the soil. Astaykina et al. (2020) noted that imidacloprid changed the relative abundance of several eukaryotic and prokaryotic genera, such as *Apiotrichum*, *Gamicola*, *Humicola*, *Kitasatospora*, *Solicoccozyma*, *Sphingomonas*, *Streptomyces* and *Terrabacter*, respectively. He also stated that imidacloprid also reduces the relative abundance of Methylophilaceae, Coribacteraceae, Coxiellaceae, and Rhodospirillaceae in the soil, but imidacloprid increases the abundance of Nitrospirae bacteria in soil. Nitrospirae bacteria play a role in the nitrogen cycle, which is the conversion of ammonia into nitrate, a source of nitrogen that is important for plants (Yu et al. 2020).

All growth of bacterial isolates undergoes an exponential phase at a vulnerable time of 3 to 51 hours, except IT1 isolates, which ended the exponential phase at 54 hours. The growth of these bacteria arises due to the unique capabilities of each bacterial isolate in taking advantage of the nutrients contained in the media, which ultimately impacts variations in metabolic efficiency. The death of bacteria sensitive to imidacloprid can provide an opportunity for bacteria that are resistant to breed. Mohammed and Badawy (2017) reported that soil bacteria can quickly degrade imidacloprid through various metabolic pathways. Gonzalez and Aranda (2023) reported that growth in the exponential phase is influenced by the nature and shape of microbes in the environment, using

nutrients in the growth medium, temperature conditions, and media pH. Then, enter the stationary phase until 72 hours. The stationary phase occurs if the number of bacterial cells stops increases (Jõers et al. 2020). Although there is no growth in the stationary phase, cells can still grow and divide themselves. In this phase, the number of growing bacteria is balanced with the number of dead bacteria (Risna et al. 2022). Bacterial isolates demonstrate the ability to thrive in MSM+imidaclopridmedia due to their utilization of carbon and nitrogen sources in the media. This aligns with the findings of Zamule et al. (2021), who reported that various bacterial strains, including *Pseudomonas fluorescens, Pseudomonas putida, Pseudomonas aeruginosa, Alcaligenes faecalis, Escherichia coli* and *Streptococcus lactis* can flourish in imidacloprid-containing media.

The highest percentage of decreased imidacloprid in test was 31.75%, in IT1 isolates, while the percentage of reduction in IT3 isolates was lower than in the other three isolates. The percentage of decreased imidacloprid was increased from day 0 to 21st day, this shows the potential for degradation or reduction of imidacloprid by the isolates. Bacteria that can grow in MSM+imidacloprid media are bacteria that have enzymes that can break the chemical structure of imidacloprid into simpler molecules, which bacteria can then use as a source of carbon and nitrogen. Other bacteria that are unable to grow in MSM+imidacloprid media do not have the enzymes needed to utilize the carbon imidacloprid content. These bacteria have enzymes that can break imidacloprid, but these enzymes are not efficient enough to produce enough energy for bacterial growth. Cycoń and Seget (2015) reported that the activity of the enzyme dehydrogenase, hexaphosphatase, and urease in soil bacteria given imidacloprid has decreased performance. Every pesticide application that affects the microbial community and its biochemical activity in the soil can be estimated to produce changes in the level of soil enzyme activity. Akoijam and Singh (2015) observed that *Bacillus aerophilus* and *B. alkalinitrilicus* are capable of degrading over 90% of imidacloprid in clay loam within 56 days. The degradation produces metabolites, such as 6-chloronicotinic acid, nitrosimine, and imidacloprid-NTG, which remain unaffected by sterilization. In another study, *B. cepacia* strain CH 9 was able to degrade 69% of the 50 ppm imidacloprid in 20 days after inoculation in MSM media (Bhattacherjee et al. 2020). *Ochrobacterium* sp. strain BCL-1 can degrade 67.67% from 50 ppm imidacloprid in 48 hours after the application as mentioned in the literature (Hu et al. 2013). Akoijam and Singh (2015) have observed that the loss of imidacloprid follows the first pseudo-order kinetics when applied at levels of 50, 100, and 150 ppm in sandy clay enriched with *B. aerophilus* with a part-time value of 14.33, 15, 15, 05, and 18.81 days. A strain of *B. thuringiensis* isolated from polluted marine sediments has been shown to degrade 71% of imidacloprid within 11 days (Obayori et al. 2024). *Trichoderma*, one of the most promising biological control agents, is found across various agricultural climates and is prevalent in soil and root ecosystems, it has the ability to serve as both a biological control and a plant growth promoter. In another study, *Tepidibacillus decaturensis* strain ST1 was able to degrade imidacloprid effectively in liquid media, slurry, and soil microcosms (Tiwari et al. 2023).

The results of molecular analysis revealed that IT1 was identified at the level of the order Enterobacterales and IT2 isolates identified at the level of the Enterobacteriaceae family. Isolates IT3 and IT4 were identified as *Pectobacterium proidearum* strain CCRMPA670 and *B. thuringiensis* strain FDAARGOS_791. The similarity of the 16S rRNA gene is one of the characteristics of a close-related bacterium. The 16S rRNA gene is very conservative, so changes that occur in this gene usually occur slowly and gradually. This causes closely related bacteria to have a similar similarity to the 16S rRNA gene (Sharma et al. 2014). Determination of potential bacterial identity is based on the criteria for the percentage of similarities ≥99% shows the similarity of species, the percentage of similarity ≥95%-<99% shows the similarity of the genus, and the percentage of similarity <95% shows the similarity of the family (Collins et al. 1994). Church et al. (2020) reported that comparing sequences of the 16S rRNA gene can help distinguish organisms at the genus level across key bacterial phyla and classify strains at various levels. *Pectobacterium* is included in the gram-negative bacteria Enterobacteriaceae found in rice fields' soil (Rossmann et al. 2018). *Bacillus* is generally used as a plant growth booster agent found in plantations and rice fields (Akinrinlola et al. 2018). Pang et al. (2020) state that *Pectobacterium* can grow and survive under high levels of imidacloprid. According to Vu et al. (2022), *Pectobacterium* can resist imidacloprid pesticides, and the bacteria have developed mechanisms to protect themselves. Ferreira et al. (2016) research states that *B. thuringiensis* is able to degradate imidacloprid. Other members of the genus *Bacillus* who also showed the ability to degrade imidacloprid compounds such as *Bacillus cereus* (Talpur et al. 2023), and *Bacillus wehenstephanensis* (Shetti et al. 2021). *Bacillus striatum*, which contains CYP353D1v2 genes exhibits strong resistance to imidacloprid (Pang et al. 2020). Soil-dwelling bacteria from the genus *Bacillus* have the ability to break down pesticides into simpler residues. *B. cereus* was identified as an efficient catalyst for degrading imidacloprid, metabolizing 92% of it within 11 days at a neutral pH. Through optimization using the Box-Behnken design, the bacteria transformed imidacloprid into 6-CNA via the intermediate's guanidine and 5-hydroxy imidacloprid (Talpur et al. 2023). The *B. cereus* is considered a promising tool for removing imidacloprid from contaminated water and soil (Gangola et al. 2021). Isolating the enzyme responsible for this degradation could provide a pathway for commercial use of purified enzymes.

In conclusion, 4 colonies obtained with different morphological variations namely IT1, IT2, IT3, and IT4. Analysis of degradation activity using the HPLC method showed that all isolates have the ability to grow in MSM, which contains imidacloprid and succeed in reducing the imidacloprid content by 26.66-31.75%. Based on 16S rRNA gene analysis, isolate IT1 was identified as *Enterobacterales*, IT2 was identified into the

Enterobacteriaceae, IT3 as *P. aroidearum* strain CCRMPA670 and IT4 were identified as *B. thuringiensis* strain FDAARGOS_791.

ACKNOWLEDGEMENTS

We want to express our gratitude to the Laboratory in Universitas Sebelas Maret (UNS) Surakarta, Indonesia and the government of Grobogan District, Ministry of Research, Technology, Indonesia.

REFERENCES

Akinrinlola RJ, Yuen GY, Drijber RA, Adesemoye AO. 2018. Evaluation of *Bacillus* strains for plant growth promotion and predictability of efficacy by in vitro physiological traits. Intl J Microbiol 2018: 5686874. DOI: 10.1155/2018/5686874.

Akoijam R, Singh B. 2015. Biodegradation of imidacloprid in sandy loam soil by *Bacillus aerophilus*. Intl J Environ Anal Chem 95: 730-743. DOI: 10.1080/03067319. 2015.1055470.

Akter S, Hulugalle NR, Jasonsmith J, Strong CL. 2023. Changes in soil microbial communities after exposure to neonicotinoids: A systematic review. Environ Microbiol Rep 15: 431-444. DOI: 10.1111/1758-2229.13193.

Alwi MK, Razie F, Kurnain A. 2023. Hubungan ketersediaan fosfor dan kelarutan Fe pada tanah sawah sulfat masam. Acta Solum 1: 61-67. DOI: 10.20527/actasolum.v1i2.1839. [Indonesian]

Astaykina AA, Streletskii RA, Maslov MN, Belov AA, Gorbatov VS, Stepanov AL. 2020. The impact of pesticides on the microbial community of Agrosoddy-Podzolic soil. Eur Soil Sci 53: 696-706. DOI: 10.1134/S1064229320050038.

Bandeira FO, Lopes APR, Hennig TB, Toniolo T, Natal-da-Luz T, Baretta D. 2020. Effect of temperature on the toxicity of imidacloprid to *Eisenia andrei* and *Folsomia candida* in tropical soils. Environ Pollut 267: 115565. DOI: 10.1016/j.envpol.2020.115565.

Bhattacherjee AK, Garg N, Shukla PK, Singh B, Vaish S, Dikshit A. 2020. Bacterial bioremediation of imidacloprid in mango orchard soil by *Pseudomonas mosselii* Strain NG1. Intl J Curr Microbiol Appl Sci 9: 1150-1159. DOI: 10.20546/ijcmas.2020.910.138.

Church DL, Cerutti L, Gürtler A, Griener T, Zelazny A, Emler S. 2020. Performance and application of 16S rRNA gene cycle sequencing for routine identification of bacteria in the clinical microbiology laboratory. Clin Microbiol Rev 33: e00053-19. DOI: 10.1128/CMR.00053-19.

Coleman NV, Mattes TE, Gossett JM, Spain JC. 2002. Biodegradation of cis-dichloroethene as the sole carbon source by a β-proteobacterium. Appl Environ Microbiol 6: 2726-2730. DOI: 10.1128/AEM.68.6.2726-2730.2002.

Collins MD, Lawson PA, Willems A, Cordoba JJ, Fernandez-Garayzabal J, Garcia P, Farrow JAE. 1994. The phylogeny of the genus *Clostridium*: proposal of five new genera and eleven new species combinations. Intl J Syst Evol Microbiol 44: 812-826. DOI: 10.1099/00207713-44-4-812.

Cycoń M, Seget PZ. 2015. Biochemical and microbial soil functioning after application of the insecticide imidacloprid. J Environ Sci 27: 147-158. DOI: 10.1016/j.jes.2014.05.034.

Erguven GO, Demirci U. 2021. Using *Ochrobactrum thiophenivorans* and *Sphingomonas melonis* for bioremediation of imidacloprid. Environ Technol Innov 21: 101236. DOI: 10.1016/j.eti.2020.101236.

Ferreira L, Rosales E, Danko AS, Sanromán MA, Pazos MM. 2016. *Bacillus thuringiensis* a promising bacterium for degrading emerging pollutants. Process Saf Environ Prot 101: 19-26. DOI: 10.1016/j.psep.2015.05.003.

Gangola S, Joshi S, Kumar S, Sharma B, Sharma A. 2021. Differential proteomic analysis under pesticides stress and normal conditions in *Bacillus cereus* 2D. PLoS One 16 (8): e0253106. DOI: 10.1371/journal.pone.0253106.

Gao Y, Liu M, Zhao X, Zhang X, Zhou F. 2021. *Paracoccus* and *Achromobacter* bacteria contribute to rapid biodegradation of imidacloprid in soils. Ecotoxicol Environ Saf 225: 112785. DOI: 10.1016/j.ecoenv.2021.112785.

Gautam P, Dubey KS. 2022. Biodegradation of imidacloprid: Molecular and kinetic analysis. Bioresour Technol 350: 126915. DOI: 10.1016/j.biortech.2022.126915.

Gonzalez JM, Aranda B. 2023. Microbial growth under limiting conditions-future perspectives. Microorganisms 11: 1641. DOI: 10.3390/microorganisms11071641.

Gupta M, Mathur S, Sharma TK, Rana M, Gairola A, Navani NK. 2016. A study on metabolic prowess of *Pseudomonas* sp. RPT 52 to degrade imidacloprid, endosulfan and coragen. J Hazard Mater 301: 250-258. DOI: 10.1016/j.jhazmat.2015.08.055.

Hu G, Zhao Y, Liu B, Song F, You M. 2013. Isolation of an indigenous imidacloprid-degrading bacterium and imidacloprid bioremediation under simulated in situ and ex situ conditions. J Microbiol Biotechnol 23: 1617-1626. DOI: 10.4014/jmb.1305.05048.

Irfan M, Munir H, Ismail H. 2021. *Moringa oleifera* gum based silver and zinc oxide nanoparticles: Green synthesis, characterization and their antibacterial potential against MRSA. Biomater Res 25: 17. DOI:10.1186/s40824-021-00219-5.

Jõers A, Liske E, Tenson T. 2020. Dividing subpopulation of *Escherichia coli* in stationary phase. Res Microbiol 171: 153-157. DOI: 10.1016/j.resmic.2020.02.002.

McCabe KM, Zhang YH, Huang BL, Wagar EA, McCabe ER. 1999. Bacterial species identification after DNA amplification with a universal primer pair. Mol Genet Metab 66 (3): 205-211. DOI: 10.1006/mgme.1998.2795.

Mishra S, Singh SN, Pande V. 2014. Bacteria induced degradation of fluoranthene in minimal salt medium mediated by catabolic enzymes in vitro condition. Bioresour Technol 164: 299-308. DOI: 10.1016/j.biortech.2014.04.076.

Mohammed YM, Badawy MEI. 2017. Biodegradation of imidacloprid in liquid media by an isolated wastewater fungus *Aspergillus terreus* YESM3. J Environ Sci Health 52: 752-761. DOI: 10.1080/03601234.2017.1356666.

Obayori OS, Ashade AO, Salam LB, Adeyemo AC, Oladejo SO, Abanikannda ON, Oyebade AE. 2024. Heavily polluted mechanic workshop soil and its phenanthrene-degrading *Bacillus thuringiensis*. The Microbe 4: 100104. DOI: 10.1016/j.microb.2024.100104.

Pang S, Lin Z, Zhang Y, Zhang W, Alansary N, Mishra S, Bhatt P, Chen S. 2020. Insights into the toxicity and degradation mechanisms of imidacloprid via physicochemical and microbial approaches. Toxic 8 (3): 65. DOI: 10.3390/toxics8030065.

Putri SNS, Bari IN, Wilar G, Ridho A. 2021. Imidakloprid dalam formulasi insektisida. Gunung Djati Conf Ser 6: 298-307. [Indonesian]

Risna YK, Harimurti SSH, Wihandoyo W, Widodo W. 2022. Kurva pertumbuhan isolat bakteri asam laktat dari saluran pencernaan itik lokal asal Aceh. Indones J Anim Sci 24: 1-7. DOI:10.25077/jpi.24.1.1-7.2022. [Indonesian]

Rossmann S, Dees MW, Perminow J, Meadow R, Brurberg MB. 2018. Soft rot Enterobacteriaceae are carried by a large range of insect species in potato fields. Appl Environ Microbiol 84: e00281-18. DOI: 10.1128/AEM.00281-18.

Sabourmoghaddam N, Zakaria MP, Omar D. 2015. Evidence for the microbial degradation of imidacloprid in soils of Cameron highlands. J Saudi Soc Agric Sci 14: 182-188. DOI: 10.1016/j.jssas.2014.03.002.

Sharma T, Rajor A, Toor AP. 2014. Degradation of imidacloprid in liquid by *Enterobacter* sp. Strain ATA1 using co-metabolism. Bioremediat J 18: 227-235. DOI:1 0.1080/10889868.2014.918575.

Shetti A, Kaliwal BB, Kaliwal RB. 2021. Study on imidacloprid induced intoxication and its biodegradation by soil isolate *Bacillus weihenstephanensis*. Microbiol Biotechnol 4: 54-66. DOI: 10.9734/bpi/rpmb/v5/2039e.

Talpur FN, Unar A, Bhatti SK, Alsawalha L, Fouad D, Bashir H, Afridi HI, Ataya FS, Jefri OA, Bashir MS. 2023. Bioremediation of neonicotinoid pesticide, imidacloprid, mediated by *Bacillus cereus*. Bioengineering 10: 961. DOI: 10.3390/bioengineering10080951.

Tiwari S, Tripathi P, Mohan D, Singh RS. 2023. Imidacloprid biodegradation using novel bacteria *Tepidibacillus decaturensis* strain ST1 in batch and in situ microcosm study. Environ Sci Pollut Res 23: 36-40. DOI: 10.1007/s11356-022-24779-8.

Vu NT, Roh E, Thi TN, Oh CS. 2022. Antibiotic resistance of *Pectobacterium* Korean Strains Susceptible to the Bacteriophage phiPccP-1. Res Plant Dis 28: 166-171. DOI: 10.5423/RPD.2022.28.3.166.

Yadav DR, Adhikari M, Kim SW, Kim HS, Lee YS. 2021. Suppression of Fusarium Wilt caused by *Fusarium oxysporum* f. sp. *lactucae* and growth promotion on lettuce using bacterial isolates. J Microbiol Biotechnol 31: 1241-1255. DOI: 10.4014/jmb.2104.04026.

Yu B, Chen Z, Lu X, Huang Y, Zhou Y, Zhang Q, Wang D, Li J. 2020. Science of the total environment effects on soil microbial community after exposure to neonicotinoid insecticides thiamethoxam and dinotefuran. Sci Total Environ 725: 138328. DOI: 10.1016/j.scitotenv.2020.138328.

Zamule SM, Dupre CE, Mendola ML, Widmer J, Shebert JA, Roote CE, Das P. 2021. Bioremediation potential of select bacterial species for the neonicotinoid insecticides, thiamethoxam and imidacloprid. Ecotoxicol Environ Saf 209: 111814. DOI: 10.1016/j.ecoenv.2020.111814.

NUSANTARA BIOSCIENCE
Vol. 16, No. 2, pp. 292-296
November 2024

ISSN: 2087-3948
E-ISSN: 2087-3956
DOI: 10.13057/nusbiosci/n160216

Nutritional composition and antioxidant properties of calamansi (*Citrus microcarpa*) peels in different drying processes

KEZIA ESTHER T. ABAL[1], CASIANO H. CHORESCA JR.[2], FERNAND F. FAGUTAO[1], GWEN ANUEVO[3], MARY JANE S. APINES-AMAR[4], FERNIE A. CATIENZA[1], FIONA L. PEDROSO[1,♥]

[1]School of Marine Fisheries and Technology, Mindanao State University at Naawan. Pedro Pagalan St., Naawan, Misamis Oriental 9023, Philippines. Tel.: +63-20908-885-3500, ♥email: fionapedroso@gmail.com

[2]Fisheries Biotechnology Center, Department of Agriculture-National Fisheries Research and Development Institute. Science City of Munoz, Nueva Ecija 3119, Philippines

[3]Iloilo Science and Technology University ISAT-U. Burgos-Mabini-Plaza, Iloilo City 5000, Philippines

[4]Institute of Aquaculture, College of Fisheries and Ocean Sciences, University of the Philippines Visayas. Miagao, Iloilo City 5000, Philippines

Manuscript received: 8 March 2024. Revision accepted: 11 November 2024.

Abstract. *Abal KET, Choresca Jr. CH, Fagutao FF, Anuevo G, Apines-Amar MJS, Catienza FA, Pedroso FL. 2024. Nutritional composition and antioxidant properties of calamansi (*Citrus microcarpa*) peels in different drying processes. Nusantara Bioscience 16: 292-296.* Calamansi (*Citrus microcarpa* Bunge) is abundantly grown in the Philippines and is primarily utilized for its juice, resulting in peels as a waste product. This study aimed to evaluate the effects of different drying techniques (sun-drying, dehydration, and oven-drying) on the nutritional composition and antioxidant properties of calamansi peels. The dried samples were analyzed for nutritional content such as protein, fiber, fat, ash, carbohydrates, and moisture. Antioxidant properties were also measured through a DPPH scavenging activity assay, including total phenolic content and total flavonoid content. The results showed that Calamansi Dehydrated (CDD) had a significantly higher protein and fiber content than oven-dried and sundried, and calamansi oven-dried (COD) peels had the highest carbohydrate, fat, moisture, and ash content. Calamansi Sundried (CSD) has a significantly highest value of 21.04±2.44% scavenging activity, followed by CDD (20.79±5.43% scavenging activity), and then COD (8.91±1.89% scavenging activity) in DPPH assay. For Total Phenolic Content (TPC), CDD has a significantly higher value of 192.6±21.99 mg gallic acid equivalent (GAE) L^{-1} dry sample, followed by CSD and COD, with 145.7±6.54 mg GAE L^{-1} dry sample and 70.7±8.87 mg GAE L^{-1} dry sample, respectively. CSD had the highest value in Total Flavonoid Content (TFC) of 163.3±1.90 mg catechin equivalent (CE L-1 dry sample) mg catechin Equivalent (CE) L-1 dry sample, followed by COD (121.0±6.87 mg CE L^{-1} sample), and CDD (41.9±6.25 mg CE L^{-1} sample. The findings suggest sun-drying and dehydration as drying techniques resulted in higher antioxidant properties and economic viability.

Keywords: Antioxidant properties, calamansi, *Citrus microcarpa*, drying techniques, nutritional composition

Abbreviation: CDD: Calamansi Dehydrated, CE: Catechin Equivalent, COD: Calamansi Oven-Dried, CSD: Calamansi Sundried, GAE: Gallic Acid Equivalent, DPPH: 2,2-diphenyl-1-picrylhydrazyl, TFC: Total Flavonoid Content, TPC: Total Phenolic Content

INTRODUCTION

Fruit and vegetable consumption increases due to its significant benefits on human health (Angelino et al. 2019). In 2017, global fruit production reached 124.73 Million Metric Tons (MMT), bananas produced 114.08 MMT, apples yielded 84.63 MMT, grapes 74.49 MMT, the sum of 45.22 MMT for tropical fruits mangoes, mangosteens, and guavas, and pineapples 25.43 MMT (Sagar et al. 2018). Fruits and vegetables are the most consumed commodities, resulting in 42% of food waste (Ganesh et al. 2022).

Citrus fruits are widely grown and utilized for refreshing flavors, health benefits, and affordable prices (Tonogbanua et al. 2018). Citruses are mainly used to make fresh juice or citrus-flavored drinks, leading to a significant amount of waste from peels, pulp, and seeds yearly (Maqbool et al. 2023). Large amounts of waste were dumped in landfills or burned, which caused degraded soil quality and polluted and deoxygenated water. To address this concern, wastes are valorized into animal feed, essential oil extraction, production of biofuel, and biodegradable packaging films (Chavan et al. 2018). An average of 60% of processed citrus fruits discarded as waste contain valuable components like polyphenols and essential oils, making them nutritionally important and suitable for pharmaceutical applications (Kesbiç et al. 2022). These wastes contain bioactive compounds, such as phenolic acid and flavonoids, which affects various health benefits, including antioxidant, anti-inflammatory, and antibacterial properties (Wang et al. 2016).

The *Citrus* genus originated in Southeast Asia and has evolved into numerous varieties and hybrids through natural or artificial crossbreeding, including oranges, lemons, grapefruits, limes, and mandarins that have been extensively researched and are commercially cultivated (Zhong and Nicolosi 2020). Calamansi (*Citrus microcarpa* Bunge), also known as calamondin, is a natural hybrid of mandarin and oval kumquat (*Citrus reticulata* Blanco and *Citrus japonica* Thunb.) (Lim 2012). The climate and fertile soil of the Philippines allow for a year-round culture of citrus fruits

(Idquival et al. 2023). This species is widely cultivated as an alternative to lime due to its tolerance to pests and diseases and is commercially produced in syrups, juices, tea, concentrates, and purees. Additionally, calamansi is used for cough and a natural anti-inflammatory medication (Alinejhad et al. 2016). It is one of the staple fruit juices in the Philippines (Quijano et al. 2021). Calamansi peels have been tested for their efficiency in lowering the blood glucose level of albino rats *Rattus albus.* It also contains coumarin derivatives as an effective anticoagulant and can be utilized as an herbal remedy for managing blood glucose (Rocha et al. 2020).

Calamansi is included in the major fruit crops in the Philippines that are cultivated and exported (Mapalo and Rosillo-Magno 2018). From April to June 2023, calamansi production reached an estimated 14.24 thousand metric tons, showing a 4.0% increase from 13.69 thousand MT in the same quarter in 2022. Zamboanga Peninsula emerges as the leading producer, contributing 3.00 thousand metric tons, accounting for 21.1% of the total calamansi production in that quarter (PSA 2023). The Philippines is a significant exporter of calamansi juices in Japan, South Korea, Hong Kong, the USA, and Canada (Rodeo 2016).

The calamansi fruit peel, a byproduct of juicing, contains 1% flavonoids, 7.14% pectin, 0.51% limonin, 5.98% reducing sugar, and 4.25% essential oils (Zou et al. 2016). The calamansi peel is rich in pectin and essential oils, contributing to the fruit's overall flavor and nutritional profile. Calamansi peels from different regions were extracted using dichloromethane and hexane and analyzed for volatiles, aromatic profiles, and phenolic acids using gas chromatography-mass spectroscopy (Cheong et al. 2012). The results showed 79 identified compounds comprised over 98% of the volatiles. Malaysian calamansi peel had the highest level of a specific compound, methyl N-methylanthranilate. Principal component and canonical discriminant analyses were used to distinguish the peels from different regions. Additionally, ultra-fast liquid chromatography identified caffeic, p-coumaric, ferulic, and sinapic acids in the peels. The Philippines calamansi peel had the highest total phenolic acids, with p-coumaric acid being the most common free phenolic acid and ferulic acid being the primary bound phenolic acid.

Citrus byproducts contain a diverse selection of biologically active components, including essential oils, pectins, carotenoids, and limonoids, which can be extracted and utilized in various industries, such as food, feed, pharmaceuticals, and cosmetics (Panwar et al. 2021). Utilizing calamansi peel wastes can maximize the potential of the byproduct while addressing fruit waste disposal challenges in developing countries. Hence, this study aims to characterize the nutritional profile, specifically biomolecules carbohydrates, protein, lipid, ash, and fiber content of calamansi peels in different drying methods. It also aims to determine the antioxidant properties using DPPH scavenging activity assay, Total Phenolic Content (TPC), and Total Flavonoid Content (TFC) of calamansi peel waste as preliminary analyses in utilization of the calamansi byproduct.

MATERIALS AND METHODS

Collection and drying of samples

This study collected samples of unripe calamansi peels from a calamansi juice processing industry in Siay, Zamboanga Sibugay, Philippines. The collected samples were weighed, minced using a food processor (Kaisa Villa Electric Food Processor 2L), and stored at -4°C until the drying process began. Frozen samples were air-thawed first and then subjected to different drying methods. The codes were CSD-Calamansi Sundried, COD-Calamansi Oven-dried, and CDD-Calamansi Dehydrated. The study adopted a sun drying method by Farahmandfar et al. (2020), with some modifications, using a wooden frame and cloth drying rack placed in an open area and fresh calamansi peels were sun-dried around 15-37°C for 48 hours until they reached a 10% moisture content. After that, samples were processed into a fine powder using a 45-micron stainless sieve for further analysis.

Moreover, for dehydration, the fresh calamansi peels were loaded onto a food dehydrator (OneTwoFit Food Dehydrator Machine 5 Layers) and dried at 45°C for 48 hours to achieve a moisture content of 10%. After the drying, the samples were powdered and sieved into 45-micron and vacuum sealed for analysis. A laboratory oven (Isotherm® Forced Convection Laboratory Oven) was used for oven drying. Calamansi samples were then arranged in an aluminum tray and were dried at temperatures of 50 °C for an average of 36-40 hours to reach a moisture content of 10%. Then, samples were processed, sieved into fine powder using a 45-micron, and sealed for analysis.

Proximate analysis of the samples

For proximate analyses, 100 grams of each dried sample were sent to the National Fisheries Research and Development Institute (NFRDI)-Integrated Research Laboratory, Quezon City, to analyze protein, lipid, moisture, and ash. The fiber analysis was performed by a laboratory technician at Mindanao State University at Naawan-Institute of Fisheries Research and Development (MSUN-IFRD). Furthermore, the carbohydrate content was subtracted from the sum of the other components.

Protein content was determined using AOAC 954.01 by digesting the sample with sulfuric acid and a catalyst, then distilling and titrating the resulting ammonia. Lipid content was measured using AOAC 960.39 by extracting lipids with a solvent mixture, evaporating the solvents, and weighing the remaining lipids. Ash content was assessed following AOAC 938.08 by ashing the sample in a furnace and weighing the residue. Crude fiber was analyzed with AOAC 962.09 by treating the sample with acid and alkali, then drying and ashing. Carbohydrates were calculated by subtracting the percentages of protein, fat, moisture, ash, and fiber from 100%. Moisture content was determined by drying the sample and calculating the weight loss.

Antioxidant analyses of the samples

Ultrasound-assisted extraction

A method used by Mahmood et al. (2019), with some modifications, was used for the extraction process. Five

grams of the pulverized samples were added with 80% ethanol (100 mL) and placed at a sonicator power of 20 kHz for 15 min at room temperature. After sonication, the mixture was filtered and analyzed for its phytochemical composition and antioxidant activity.

Radical scavenging activity (DPPH)

With some modifications, Hossain and Rahman's (2010) protocol was used to analyze radical scavenging activity. About 1.6 mL ethanolic extract of the samples and 2.4 mL of 0.1 mM ethanolic solution of DPPH were mixed thoroughly. The control was prepared by mixing 1.6 mL 80% ethanol and 2.4 mL 0.1 mM ethanolic solution of DPPH. The mixture was left in the dark for 20 minutes at room temperature. At 517 nm, a UV-VIS spectrophotometer measured changes in absorbance. Ascorbic acid as a positive control was prepared but without the sample. The scavenging activity was measured with the formula shown below:

% Radical Scavenging Activity = (Control OD - sample OD divided by control OD) x 100.

Total Polyphenol Content (TPC)

For total phenolic content determination, Folin-Ciocalteu reagent in the concentration of 0.50mg/mL in distilled water was used. The 40 -µL of the extract was mixed with 200 -µL of Folin-Ciocalteu's phenol reagent and 600 -µL of 20% sodium carbonate. Then, it was diluted with water to a total volume of 5 mL. The mixture was left to stand for two hours, and the absorbance of the blue-colored solution was measured using a UV-VIS spectrophotometer at 765 nm. For TPC quantification, it was used with linear regression analysis, using gallic acid as the standard reference at concentrations ranging from 0 to 1000 mg L^{-1}. The analytical results represented milligrams of Gallic Acid Equivalents (GAE)/ liter (mg GAE L^{-1}).

Total flavonoid content

Total Flavonoid Content (TFC) was measured using the aluminum trichloride with catechin as the reference compound. One (1) mL of the calamansi extract was added to 300 µL of a 5% $NaNO_2$ solution and allowed to stand for 6 minutes; then, it was added with 300 µL of 10% aluminum trichloride and incubated for 5 minutes. After that, 2 mL of 1M NaOH was added to the solution and adjusted with distilled water to achieve a total volume of 5 mL. For 15 minutes, it was incubated. After the observation of the color of the solution, the absorbance was measured (510 nm). TFC concentration was evaluated using catechin as a standard, ranging from 0 to 500 mg L^{-1}. Values for total flavonoid content were expressed as mg CE L^{-1} dry sample.

Statistical design

Data were analyzed by utilizing one-way Analysis of Variance (ANOVA), and the mean values were ranked and compared using Duncan multiple range tests, employing the software program R Software version 4.2.2 for Windows. Significant differences were considered when $p < 0.05$. Values obtained in all analyses were expressed as mean ± Standard Error (M ± SE).

RESULTS AND DISCUSSIONS

Proximate analyses

The nutritional content of calamansi subjected to different drying techniques is shown in Table 1. Calamansi Oven-Dried (COD) samples showed the highest carbohydrate, fat, moisture, and ash content. Dehydrated calamansi (CDD) samples showed the highest protein and fiber content.

Antioxidant properties

The results showed a significant difference in antioxidant activity in three different drying methods (Table 2).

Table 1. Proximate composition of calamansi peels subjected to different drying methods

Drying method	Carbohydrates	Crude protein	Crude Fat	Moisture	Ash	Fiber
CSD	58.29±0.24b	8.26±0.11b	1.48±0.10a	14.31±0.51a	4.83±0.02b	12.83±0.46b
COD	63.21±0.33a	6.89±0.08c	1.55±0.12a	12.81±0.47b	6.14±0.02a	9.40±0.21c
CDD	57.34±1.24b	8.54±0.09a	1.20±0.02b	12.40±0.75b	4.86±0.03b	15.66±0.43a

Note: CSD: Calamansi Sundried, CDD: Calamansi Dehydrated, COD: Calamansi Oven-dried. Values are mean ± SE of triplicate determinations. Values with different superscripts in the same column significantly differ at $p<0.05$

Table 2. Antioxidant properties of calamansi peels in different drying methods

Drying method	DPPH (% Scavenging Activity)	TPC (mg GAE/L)	TFC (mg GAE/L)
CSD	21.04±1.41a	145.7±6.54a	163.3±1.90a
CDD	20.79±3.13a	192.6±21.99a	41.9±6.25b
COD	8.92±1.09b	70.7±8.87b	121.0±6.87c

Note: CSD: Calamansi Sundried, CDD: Calamansi Dehydrated, COD: Calamansi Oven-dried. Values are mean ± SE of triplicate determinations. Values with different superscripts in the same column significantly differ at $p<0.05$

Discussion

Sun-dried calamansi peels have comparable results with other methods regarding carbohydrates, crude fat, and ash. However, it has a significantly higher value in moisture. Sun drying is a traditional food preservation method, but it is less efficient in water removal due to reliance on environmental factors, slow evaporation rates, and risk of contamination (Elmsaad et al. 2024). A study by Siriwattananon and Maneerate (2016) showed that sun-drying retained higher amounts of dietary fiber in dried pumpkin, yardlong bean, red cabbage, and guava compared to hot air oven drying and freeze-drying. Moreover, a study by Wahdaningsih et al. (2023) showed that the highest total flavonoid content (22.5%) and total phenol content (37.35%) were found in sun-drying compared to oven-drying with total flavonoid content (20.698%) and total phenol content (36.648%). In contrast, some studies showed that sun-drying yielded the least antioxidant compared to freeze-drying, microwave oven, and oven-drying (Sarkar et al. 2024). The efficiency of sun drying and nutrient retention is greatly influenced by the prevailing environmental conditions, such as temperature, humidity, and sunlight availability (Elmsaad et al. 2024).

In the present study, dehydrated (CDD) samples showed the highest protein and fiber content. Moreover, dehydrated calamansi peels had the highest phenolic content (192.6 mg GAE/L). This is comparable to another study that measured the polyphenol content of lemons (160.57 mg/L), oranges (193.78 mg/L), and sweet limes (232 mg/L) (Ahn et al. 2020). A steady airflow during dehydration further aids in maintaining a low oxidizing environment, which is critical for preserving antioxidant properties (Muñoz-Fariña et al. 2023). High temperatures can lead to the rapid degradation of sensitive antioxidant compounds. Research indicates that retention of antioxidant capacity decreases with increasing dehydration temperature. By maintaining a dynamic flow of air, the oxygen concentration can be diluted or kept below critical levels necessary for oxidation, thus preventing the degradation of sensitive materials (Saini et al. 2014). Proper air circulation is essential to replace moisture-laden air with drier air, which is crucial for maintaining the efficiency of the drying process (Putra and Ajiwiguna 2017).

Calamansi oven-dried samples (COD) showed the highest carbohydrate, fat, moisture, and ash content. Convective oven drying is effective in moderate temperatures, typically between 60°C and 70°C, to remove moisture from food while minimizing nutrient degradation. This controlled temperature ensures that the essential constituents of dried fruits, vegetables, and other food products are maintained effectively (Onwude et al. 2022). However, this study observed oven-dried calamansi peels have significantly lower antioxidant activity than dehydrated and sun-dried peels. The preservation of antioxidants in dried fruits is related to the drying temperature. Kittibunchakul et al. (2023) found that lower temperatures enhance antioxidant activity, with temperatures below 50°C supporting better retention of bioactive compounds. High temperatures can accelerate oxidative reactions in polyphenols, leading to reduced antioxidant activity (Antony and Farid 2022). Studies show that increased temperatures negatively impact polyphenol content. Pascariu et al. (2014) examined dried grape pomace and found that the highest total polyphenol content occurred in grape pomace dried at 20°C, with degradation increasing as the temperature increased. Sarkar et al. (2024) showed that freeze-dried pomegranate peels contained t the highest values of total phenolic content, DPPH radical scavenging activity, vitamin C, and ferric-reducing antioxidant power compared to microwave drying, oven drying at 50°C, and sun drying, and sun drying was being the lowest quality.

Temperatures above 100°C negatively impact nutritional and sensory quality, although high temperatures accelerate drying; however, prolonged exposure results in lower nutrient retention (Turkmen et al. 2020; Jayawardena et al. 2022). This study used the lower temperature in sun-drying and dehydration at 37-40°C, and a higher temperature in oven drying (50°C) was employed. When considering energy efficiency and practicality, traditional sun-drying remains a practical choice. Additionally, dehydration using food dehydrators is a viable option due to its commercial availability and cost-effectiveness.

In conclusion, this study evaluated various drying techniques for calamansi peels: sun drying, dehydration, and oven drying. The oven-drying method effectively retains carbohydrates and fat but reduces antioxidant levels. Dehydration efficiently preserves protein and fiber, enhancing the overall nutritional profile. Additionally, sun drying demonstrates significant retention of flavonoids and higher DPPH scavenging activity, while dehydration preserves the polyphenols of the calamansi peels, highlighting its efficacy in preserving bioactive compounds. Hence, this study suggests that sun drying and dehydration present practical and cost-effective options for drying calamansi peels, particularly for future applications.

ACKNOWLEDGEMENTS

This study received funding support from the Inland Aquatic Resources Research Division (IARRD), the Philippine Council for Agriculture, Aquatic and Natural Resources Research and Development (PCAARRD), and the Department of Science and Technology (DOST)) for the project entitled “Utilization of fruit processing waste as a source of prebiotics and immunostimulants for the development of healthy and improved aquaculture feeds.” Also, this paper would like to acknowledge the support of the Department of Science and Technology Science Education Institute - Science and Technology Regional Alliance of Universities for National Development (DOST SEI-STRAND Program), Mindanao State University at Naawan-School of Marine Fisheries and Technology, National Fisheries Research and Development Institute, University of the Philippines Visayas-Institute of Aquaculture, and Iloilo Science and Technology University (ISAT-U).

REFERENCES

Ahn HY, Cho HD, Cho YS. 2020. Comparison of antioxidant effect and phenolic compounds in tropical fruits. SN Appl Sci 2: 1120. DOI: 10.1007/s42452-020-2927-5.

Alinejhad D, Asayesh MA, Asayesh, M. 2016. Determination of the anti-inflammatory property of tannins from the rind of calamansi (*Citrus microcarpa*, Rutaceae). J Intl Oral Health 8 (5): 546-553. DOI: 10.2047/jioh-08-05-04.

Angelino D, Godos J, Ghelfi F et al. 2019. Fruit and vegetable consumption and health outcomes: An umbrella review of observational studies. Intl J Food Sci Nutr 70 (6): 652-667. DOI: 10.1080/09637486.2019.1571021.

Antony A, Farid M. 2022. Effect of temperatures on polyphenols during extraction. Appl Sci 12 (4): 2107. DOI: 10.3390/app12042107.

Chavan P, Singh AK, Kaur G. 2018. Recent progress in the utilization of industrial waste and by-products of citrus fruits: A review. J Food Process Eng 41 (8): e12895. DOI: 10.1111/jfpe.12895.

Cheong MW, Chong ZS, Liu SQ, Zhou W, Curran P, Yu B. 2012. Characterisation of calamansi (*Citrus microcarpa*). Part I: Volatiles, aromatic profiles and phenolic acids in the peel. Food Chem 134 (2): 686-695. DOI: 10.1016/j.foodchem.2012.02.162.

Elmsaad E, Omran A, Emam A, Elmahi O, Amer B. 2024. Performance evaluation and analysis of different simple thermal modeling of greenhouse dryer. Front Sustain Food Syst 8: 1304584. DOI: 10.3389/fsufs.2024.1304584.

Farahmandfar R, Tirgarian B, Dehghan B, Nemati A. 2020. Comparison of different drying methods on bitter orange (*Citrus aurantium* L.) peel waste: Changes in physical (density and color) and essential oil (yield, composition, antioxidant and antibacterial) properties of powders. J Food Meas Charact 14: 862-875. DOI: 10.1007/s11694-019-00334-x.

Ganesh KS, Sridhar A, Vishali S. 2022. Utilization of fruit and vegetable waste to produce value-added products: Conventional utilization and emerging opportunities-A review. Chemosphere 287: 132221. DOI: 10.1016/j.chemosphere.2021.132221.

Hossain MA, Rahman SMM. 2010. Total phenolics, flavonoids, and antioxidant activity of tropical fruit pineapple. Food Res Intl 44 (3): 672-676. DOI: 10.1016/j.foodres.2010.11.036.

Idquival JLA, Layog PMP, Victoria CGC, Rosete MAL. 2023. An analysis of the citrus industry in Nueva Vizcaya, Philippines. Intl J Res Eng Sci Manag 6 (12): 144-153.

Jayawardena SR, Morton JD, Bekhit AEDA, Bhat ZF, Brennan CS. 2022. Effect of drying temperature on nutritional, functional and pasting properties and storage stability of beef lung powder, a prospective protein ingredient for food supplements. LWT 161: 113315. DOI: 10.1016/j.lwt.2022.113315.

Kesbiç OS, Acar Ü, Mohammady EY, Salem SM, Ragaza, JA, El-Haroun E, Hassaan MS. 2022. The beneficial effects of citrus peel waste and its extract on fish performance and health status: A review. Aquac Res 53 (12): 4217-4232. DOI: 10.1111/are.15945.

Kittibunchakul S, Temviriyanukul P, Chaikham P, Kemsawasd V. 2023. Effects of freeze drying and convective hot-air drying on predominant bioactive compounds, antioxidant potential and safe consumption of maoberry fruits. LWT 184: 114992. DOI: 10.1016/j.lwt.2023.114992.

Lim TK. 2012. *Citrus x microcarpa*. In: Lim TK (eds). Edible Medicinal and Non-Medicinal Plants. Springer, Dordrecht. DOI: 10.1007/978-94-007-4053-2_99.

Mahmood MH, Osama AK, Makky EA, Rahim MH, Ali NHM, Hazrudin ND. 2019. Phytochemical Screening, antimicrobial and antioxidant efficacy of some plant extracts and their mixtures. IOP Conf Ser Earth Environ Sci 346 (1): 012003. DOI: 10.1088/1755-1315/346/1/012003.

Mapalo NG, Rosillo-Magno AP. 2018. Morphological events on the development of flowers, fruits, and seeds of calamansi (*XCitrofortunella microcarpa* Bunge). J Sci Eng Technol 6: 160-168. DOI: 10.13140/RG.2.2.21298.12489.

Maqbool Z, Khalid W, Atiq HT, Koraqi H, Javaid Z, Alhag SK, Al-Farga A. 2023. Citrus waste as a source of bioactive compounds: Extraction and utilization in health and food industry. Molecules 28 (4): 1636. DOI: 10.3390/molecules28041636.

Muñoz-Fariña O, López-Casanova V, García-Figueroa O, Roman-Benn A, Ah-Hen K, Bastias-Montes JM., Quevedo-León R, Ravanal-Espinosa MC. 2023. Bioaccessibility of phenolic compounds in fresh and dehydrated blueberries (*Vaccinium corymbosum* L.). Food Chem Adv 2: 100171. DOI: 10.1016/j.focha.2022.100171.

Onwude DI, Iranshahi K, Rubinetti D, Schudel S, Schemminger J, Martynenko A, Defraeye T. 2022. How much do process parameters affect the residual quality attributes of dried fruits and vegetables for convective drying? Food Bioprod Process 131: 176-190. DOI: 10.1016/j.fbp.2021.11.005.

Panwar D, Saini A, Panesar PS, Chopra, HK. 2021. Unraveling the scientific perspectives of citrus byproducts utilization: Progress towards the circular economy. Trends Food Sci Technol 111: 549-562. DOI: 10.1016/j.tifs.2021.03.018.

Pascariu SM, Pop IM, Albu A. 2014. Degradation degree of polyphenols depending on drying temperature of the grape pomace. Bull Univ Agric Sci Vet Med Cluj-Napoca Anim Sci Biotechnol 71 (2): 212-217. DOI: 10.15835/buasvmcn-asb:10311.

Philippine Statistics Authority (PSA). Major Fruit Crops Quarterly Bulletin, April-June 2023 Vol.12 No.2. Retrieved January 23, 2024. URL: https://psa.gov.ph/system/files/csd/Major%20Fruit%20Crops%20Quarterly%20Bulletin%2C%20April-June%202023.pdf

Putra RN, Ajiwiguna TA. 2017. Influence of air temperature and velocity for drying process. Procedia Eng 170: 516-519. DOI: 10.1016/j.proeng.2017.03.082.

Quijano MF, Quijano G, Diaz R. 2021. Agricultural economic production of Philippine calamansi industry: A basis for production local development plan. Preprints 2021: 2021020388. DOI: 10.20944/preprints202102.0388.v1.

Rocha ICN, Roque SJR, Tanyag LG, Reyes KA, Sigui MAMM. 2020. Effect of *Citrofortunella microcarpa* (calamansi) peelings on whole blood coagulation using blood samples from albino mice. J Complement Altern Med Res 12 (1): 51-56. DOI: 10.9734/jocamr/2020/v12i130200.

Rodeo AJD. 2016. The Philippine fruit industry: An overview. Proc Conf Intl Train Workshop Cultiv Tech Fruit Trees 2016: 10-24.

Sagar NA, Pareek S, Sharma S, Yahia EM, Lobo MG. 2018. Fruit and vegetable waste: Bioactive compounds, their extraction, and possible utilization. Compr Rev Food Sci Food Saf 17 (3): 512-531. DOI: 10.1111/1541-4337.12330.

Saini RK, Shetty NP, Prakash M, Giridhar P. 2014. Effect of dehydration methods on retention of carotenoids, tocopherols, ascorbic acid and antioxidant activity in *Moringa oleifera* leaves and preparation of an RTE product. J Food Sci Technol 51 (9): 2176-2182. DOI: 10.1007/s13197-014-1264-3.

Sarkar A, Haque MA, Alam M. 2024. Unlocking the potential of pomegranate peels as a valuable source of bioactive compounds through effective drying strategies. Food Chem Adv 4: 100622. DOI: 10.1016/j.focha.2024.100622.

Siriwattananon L, Maneerate J. 2016. Effect of drying methods on dietary fiber content in dried fruit and vegetable from non-toxic agricultural field. GEOMATE J 11 (28): 2896-2900. DOI: 10.21660/2016.28.1372.

Tonogbanua KA, Espino RRC, Espino MRM. 2018. Diversity analysis of Philippine citrus collection using simple sequence repeat markers. PJCS 43 (3): 47-56.

Turkmen F, Karasu S, Karadag A. 2020. Effects of different drying methods and temperature on the drying behavior and quality attributes of cherry laurel fruit. Processes 8 (7): 761. DOI: 10.3390/pr8070761.

Wahdaningsih S, Rizkifani S, Untari EK, Rinaldi W. 2023. Effect of drying method on levels of antioxidant activity, total flavonoid levels, and total phenol levels in ethanol extract of bawang dayak (*Eleutherine americana*) leaves. Majalah Obat Tradisional 28 (1): 37-39. DOI: 10.22146/mot.80085.

Wang S, Tu H, Wan J, Chen W, Liu X, Luo J, Zhang H. 2016. Spatio-temporal distribution and natural variation of metabolites in citrus fruits. Food Chem 199: 8-17. DOI: 10.1016/j.foodchem.2015.11.113.

Zhong G, Nicolosi E. 2020. Citrus origin, diffusion, and economic importance. In: Gentile A, Malfa SL, Deng Z (eds). The Citrus Genome. Springer, Cham. DOI: 10.1007/978-3-030-15308-3_2.

Zou Z, Xi W, Hu Y, Nie C, Zhou Z. 2016. Antioxidant activity of *Citrus* fruits. Food Chem 196: 885-896. DOI: 10.1016/j.foodchem.2015.09.072.

NUSANTARA BIOSCIENCE
Vol. 16, No. 2, pp. 297-303
November 2024

ISSN: 2087-3948
E-ISSN: 2087-3956
DOI: 10.13057/nusbiosci/n160217

Biological features of *Spodoptera litura* fed on three vegetable host plants under controlled laboratory conditions

MELANIE MELANIE[1,2,♥], WAWAN HERMAWAN[1,2], HIKMAT KASMARA[1], FIRTRIA YUNITASARI[1], CAMELLIA PANATARANI[2,3], I MADE JONI[2,3]

[1]Department of Biology, Faculty of Mathematics and Natural Sciences, Universitas Padjadjaran. Jl. Raya Bandung Sumedang Km. 21, Sumedang 45363, West Java, Indonesia. Tel./fax.: +62-22-7796412, ♥email: melanie@unpad.ac.id

[2]Functional Nano Powder University Center of Excellence, Universitas Padjadjaran. Jl. Raya Bandung Sumedang Km. 21, Sumedang 45363, West Java, Indonesia

[3]Department of Physic, Faculty of Mathematics and Natural Sciences, Universitas Padjadjaran. Jl. Raya Bandung Sumedang Km. 21, Sumedang 45363, West Java, Indonesia

Manuscript received: 27 July 2024. Revision accepted: 17 November 2024.

Abstract. *Melanie M, Hermawan W, Kasmara H, Yunitasari F, Panatarani C, Joni IM. 2024. Biological features of* Spodoptera litura *fed on three vegetable host plants under controlled laboratory conditions. Nusantara Bioscience 16: 297-303.* Mass-rearing insects is necessary for biological control research, supporting the insect populations for effective in-vitro bioassay evaluations. The success of mass culture depends on the quality of insect feeding and environmental conditions. *Spodoptera litura* (Fabricius, 1775) larvae are notorious as major pests in horticultural crops. This study investigates the feeding preferences and developmental outcomes of *S. litura* larvae when fed on 3 different host plants (water spinach, spinach, and cabbage) with distinct nutritional compositions. The larvae were reared in a controlled insect-rearing cabinet, with parameters observed host-plant nutrition, total consumption, larval weight gain, and developmental duration from larvae to imago. The experimental design employed a completely randomized design with 3 host plants and 9 replications, analyzed with ANOVA and Duncan's multiple-range test. Results indicate that 4th-5th instar larvae showed highly consumed water spinach leaves compared to early larvae, which significantly preferred cabbage leaves. Larvae fed on water spinach leaves achieved the highest average weights for larvae, pupae, and imago, along with accelerated developmental times. However, no significant differences were observed in weight gain or developmental duration to imago among all feeding treatments. In conclusion, water spinach is an appropriate host plant for the controlled mass rearing of *S. litura*.

Keywords: Controlled insect-rearing, development time, host plants, *Spodoptera litura*, total consume, weight gain

INTRODUCTION

Spodoptera litura (Fabricius, 1775) is recognized as one of the economically significant polyphagous pests affecting crops, known for its resistance to various synthetic insecticides (Babu and Singh 2023). Recent studies on *Spodoptera* have spanned from molecular laboratory investigations to field-scale applications of biological control (Supartha et al. 2022). Establishing mass cultures of beneficial insects is crucial for effective biological control programs (Baratella et al. 2017). This requires the availability of mass-cultured insects at low cost and in healthy conditions suitable for bioassay preparations. Previously, We developed a controlled insect-rearing cabinet that promotes suitable physical environment conditions for insect culture, including air-conditioning systems, temperature and humidity, and lighting (Hermawan et al. 2017). In the successful mass culture of insects, the regulated environmental conditions and optimal nutritional feed sources play a crucial role (Belluco et al. 2023). Nutrition significantly influences the growth, development, reproduction, fecundity, and longevity throughout the life cycle of insects (Blackburn et al. 2016). For this reason, it is important in insect mass culture to fulfill appropriate feed with sufficient nutritional content (Carasi et al. 2014).

Several artificial diets to support insectary mass culture feed resources have been studied to supply nutrients needed and acceptable for insects including *S. litura* larvae. The soybean-based artificial diet effectively fed *S. frugiperda* (J.E.Smith, 1797) and affected pupal survival, sex ratio, and fecundity, but did not significantly influence survival or larval-pupal longevity (Thamrin et al. 2022). Research on the advantages of an artificial diet that contains gelatin, corn, wheat flour, yeast, and several chemical additives as a substitute feed for *S. litura* found that the survival rate of *S. litura* reached only 74.8% (Taufika et al. 2022). These facts show that fresh food as a host plant remains the best feed for *S. litura* culture.

Phytophagous insects depend on the host plant as their nutrition source (Kalaisekar et al. 2017). For instance, *S. littoralis* larvae demonstrated improved growth when fed castor beans with elevated nitrogen and phosphorus content (El-Refaie et al. 2024). Conversely, *Helicoverpa armigera* (Hübner, 1808) larvae displayed the slowest growth when fed red beans, which have the lowest protein and carbohydrate levels among the bean cultivars (Namin et al. 2014). The *S. litura* larvae are reported as polyphagous insects with a wide range of host plants, i.e., food crops, vegetables, fruit, and plantation, including soybeans,

eggplant, chili, tomatoes, cabbage, potatoes, peanuts, corn, tobacco, sugar cane, onions, cotton, and mustard (Patil et al. 2014; Rao et al. 2014; Fand et al. 2015; Ullah et al. 2016; Srivastava et al. 2018; Subiono 2020; Ramzan et al. 2021; Taufika et al. 2022; Ginting et al. 2024). The study of *S. frugiperda* feed sources in South America recorded 76 host plants, including the genera *Brassica*, *Amaranthus*, and *Ipomoea* spp. (Montezano et al. 2018). In Indonesia, cabbage plants (*Brassica oleracea* var. *Capitata* L.) have long been identified as host plants for *S. litura*. In contrast, water spinach (*Ipomoea reptans* (L.) Poir. ex G.Don.) and spinach (*Amaranthus hybridus* L.) are not primary hosts for this species. However, local farmers note that *S. litura* larvae can feed on water spinach and spinach. Several studies to investigate the influence of food plant sources on the biological characteristics of *S. litura* larvae have been carried out (Bayu and Krisnawati 2016; da Silva et al. 2017; Narvekar et al. 2018; Montezano et al. 2018; Subiono 2020; Taufika et al. 2022). According to available literature, no records exist of the consumed preference, growth, and development of *S. litura* larvae fed on *I. reptans*, *A. hybridus*, and *B. oleracea* var. *capitata* under controlled conditions in the insect-rearing instrument.

This paper aims to investigate the effects of different host plants on the mass culture of *S. litura* larvae in a controlled rearing cabinet for a suitable physical environment. The investigation focused on the evaluation of three types of host plants: *I. reptans*, *A. hybridus*, and *B. oleracea* var. *capitata* on *S. litura* larvae by determining the preferred consumed feed, the growth (increase the weight gain of larvae, pupa, and imago), and the development (accelerate the time development of larvae up to imago emergence). The nutritional content of the host plants related to their performances was discussed. This study is an important investigation to support sustainable pest control research by addressing biological and ethical considerations of test animals.

MATERIALS AND METHODS

Equipment and materials

The main equipment for rearing is a rearing cabinet (63.5×64×186.2 cm^3 equipped with an automatic control system for the humidity, temperature, and light and dark (L:D) (Figure 1) (Hermawan et al. 2017). The feeds under investigation for the *S. litura*. were water spinach leaves (*I. reptans*), spinach leaves (*A. hybridus*), and cabbage leaves (*B. oleracea* var. *capitata*) (Figure 2). The 10 % honey solution was used for imago feed.

Mass-culture *S. litura* in controlled rearing cabinet

The initial population of *S. litura* was obtained from the Indonesian Vegetable and Crops Research Institute (BALITSA) Lembang, West Java, Indonesia. It was reared from egg to hatch into larval stages (1^{st}-5^{th} instar larvae), developed into pupation and emergence as imago, under controlled laboratory conditions (Figure 3). The larvae were preserved in a container (14×5.5 cm^2) with a tissue pad. The feed plant leaves were washed before feeding to the larvae. When the larva reached the pupa phase, the pupa was inserted into a separate container enclosure with tissue. The female imago lays its eggs in host-plant leaves placed inside the imago cage. Finally, the larval and imago were placed in a rearing cabinet equipped with a temperature setting at 23°-25 °C, humidity at 70%, and photoperiodism (12 L:D) (Carasi et al. 2014). Moreover, the developmental period from oviposition to hatching was recorded. The population of 1^{st} instar larvae for each treatment was 100 hundred larvae. Each group of larvae was fed according to the treatment groups; water spinach leaves, spinach leaves, and cabbage leaves, respectively (Table 1). The feeds were given in ad-libitum and replaced every day. The weight of the feeds before and after daily consumption was weighed to obtain the average daily consumption. The weight of each larval instar phase was weighed up to the imago stage. When the pupa emerged into imago, the pupa was placed in a special cage provided with soil as pupation substrate, fed with 10% honey solution, and equipped with leaves overlap.

Figure 1. Insect-rearing cabinet with specified dimensions and controlled temperature, humidity, and lighting settings (Hermawan et al. 2017).

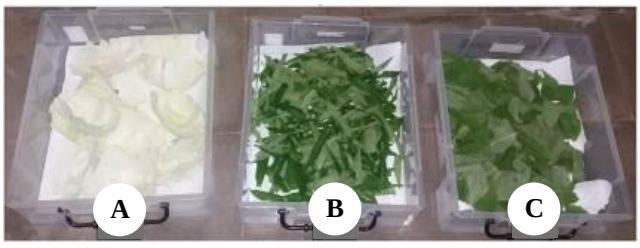

Figure 2. Host plants for feeding *Spodoptera litura*: A. Cabbage leaves (*Brassica oleracea* var. *capitata*), B. Water spinach leaves (*Ipomoea reptans*), C. Spinach leaves (*Amaranthus hybridus*)

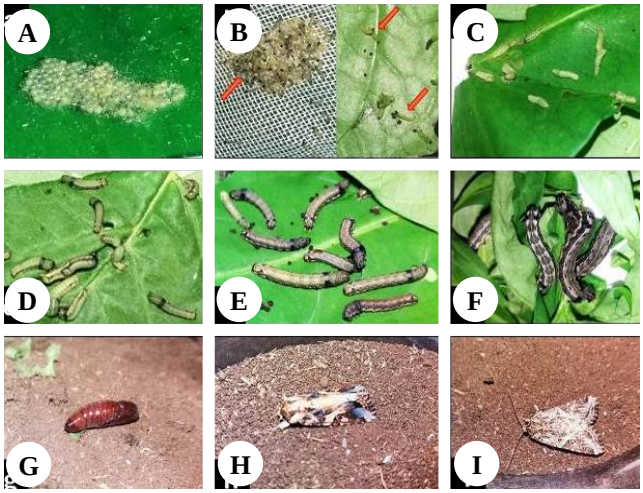

Figure 3. The life cycle of *Spodoptera litura* reared under controlled conditions from larval to imago stages: A. eggs, B. first instar larvae, C. second instar larvae, D. third instar larvae, E. fourth instar larvae, F. fifth instar larvae, G. pupae, H. ♂ imago, I. ♀ imago

Analysis of host plant nutritional content

A proximate analysis was conducted on the host plants to determine their water, ash, and nutritional contents. Water, ash, fat, carbohydrate, and protein contents were analyzed according to the SNI 01-2891-1992 standard test method (SNI 1992). The water content was determined by evaporating the leaves in an oven at a temperature of 100-105°C until the weight loss stabilized, indicating complete evaporation of the water content. The ash content was obtained by burning the leaves in a furnace at a temperature of 600°C for 5 hours, to remove all the main elements of the organic compounds (C, H, O, N). This ash represented the total mineral content in the leaves. The determination of crude protein content was based on the nitrogen content in the raw material. The fat content was obtained by extracting the leaves with a fat solvent, such as ether and acetone, using a Soxhlet apparatus for 16 hours. The extracted fat accumulated in the solvent (Soxhlet flask) was then separated from the solvent using a centrifuge and heated in an oven at a temperature of 105°C.

Data analysis

The experiment's design was completely randomized design with three types of feeding treatment on *S. litura* larvae. The data were analyzed by one-way ANOVA and Duncan's multiple ranges test ($p<0.05$). The parameters are the development time of larvae to imago; the weight of larvae, the weight of pupae and weight of imago, and the weight-average of feed consumed, respectively. Development of *S. litura* was observed in the population from the eggs hatched until imago. In contrast, growth was observed in the average weight of the *S. litura* population at each developmental phase. The feed consumed by insects was determined based on the dry weight of the leaves and was calculated using the formula in equation (1).

$$CPC = \sum_{i=0}^{j} BB_i \; x\%BK - BKS_i \quad (1)$$

Where:
CPC : percentage of the dry weight of feed (%)
BB_i : wet weight of feed (g)
BK : the dry weight of feed (g)
BKSi : the dry weight of residual feed (g)

The feed consumption was obtained by measuring the weight of the remaining feed which did not consume and was calculated using equation (2):

$$KMT = BB_i \; x\%BK - BKS_i \quad (2)$$

Where:
KMT : total feed consumption (g *BK*/individual)
BKSi : the dry weight of residual feed (g).

This study is an important investigation that addresses the biological and ethical considerations of test animals, supporting sustainable pest control research.

RESULTS AND DISCUSSION

The nutritional composition and benefits of *Spodoptera litura* host plants

The analysis of the nutritional content by proximate analysis of *S. litura* host plants reveals that each feed source has a diverse composition, described in Table 1. Comparatively, among the three types of feed, spinach leaves exhibited the highest carbohydrate and protein contents, although spinach had the lowest water content. Cabbage leaves had the highest water and fat contents compared to the others but had the lowest protein and carbohydrate levels. However, water spinach shows a more balanced composition among the three feed types. The notable variation shows in protein content among the 3 host plants (water spinach, spinach, and cabbage), while the contents of carbohydrates and fats are relatively the same (Table 1).

Table 1. The composition of nutrients, fiber, water, and ash contents in feeds for *Spodoptera litura*

Host plants	The nutrition content of fresh feeds					
	Protein (%)	Carbohydrate (%)	Fat (%)	Fiber (%)	Water (%)	Ash content (%)
Water spinach (p1)	2.67	3.97	0.34	2.85	91.91	1.11
Spinach (p2)	5.05	4.12	0.44	2.11	88.39	2
Cabbage (p3)	1.69	3.16	0.45	4.24	94.21	0.49

Spinach is one of the vegetables rich in protein according to the USA Food Center database (2021), spinach is included in the 10 groups of vegetables with the highest protein content, which protein accounts for 50% of its calories. Cabbage (*B. oleracea*) from the Cruciferae or Brassicaceae family group is characterized by its high water, fat, and fiber content (Ashfaq et al. 2018). Cabbage is a plant that requires a high water supply and a minimum rainfall of 500 mm. Consequently, cabbage has a high water-holding capacity (Huđ et al. 2023). Although water spinach grows on land, it can adapt well to muddy soils and slightly water-logged areas. Like cabbage and spinach, water spinach stems also exhibit a high water-holding capacity (Lakitan and Kartika 2020). The plant provides all the essential nutrients that herbivorous insects require; however, the specific amounts and ratios of these nutrients and water composition, especially macronutrients, can vary significantly (Deans et al. 2022).

Spodoptera litura, a polyphagous insect, relies on different host plants to meet its nutritional requirements. These plant nutrients are crucial for its development, growth, immune system, and survival (Vengateswari et al. 2020). This means that polyphagous insects like *Spodoptera* specialize in a diverse nutritional intake, and their adaptation to different feed sources supports their ability to regulate balanced water and nutrition (Deans et al. 2022). In general, insect herbivores can manage their nutritional intake. When confronted with an imbalanced diet, they adjust their nutrient consumption to address deficiencies and eliminate excesses, thus optimizing efficiency and survival. For instance, insect herbivores effectively utilize surplus proteins and fats for energy reserves. However, excessive protein can hinder optimal growth, so insects must effectively meet their protein requirements (Deans et al. 2022).

Macro and micronutrients play a crucial role in supporting the longevity of insects (Bayu and Krisnawati 2016). Carbohydrates promote general vitality, activity, and growth in insects (Le Gall and Behmer 2014). In the structure of glucose and glycogen, carbohydrates constitute the main energy source during metabolism. Proteins and lipids also provide alternative energy sources for insects (Bala et al. 2018). The protein content serves as an energy reserve and supports insect growth. Additionally, the amino acid composition of their diet influences their growth and reproduction (Kröncke and Benning 2023). Essential amino acids are crucial for forming cell membranes, enzymes, and hormones that regulate insect growth and development. A small amount of fat or sterol in the diet is sufficient to positively affect the growth and development of Lepidopteran larvae (Jing and Behmer 2020). In addition to being part of all cellular membranes, sterols are precursors for hormone regulation in insects. Insects require a high water intake for normal growth, development, and biological functions. Water content prevents dehydration and maintains the osmotic balance of cells, tissues, and organs (Benoit et al. 2022). The need for fiber in insects is primarily related to their digestive function.

Influence of different host plants on total *Spodoptera litura* consumption

Insect food preferences were measured quantitatively based on the amount of food consumed by the larvae. Total consumption was assessed by the average weight of feed consumed by *S. litura* larvae at each instar stage (Figure 3). Water spinach and cabbage had the same average weight consumed by 1st to 2nd instar larvae (0.004 g/larva). However, 2nd to 3rd instar larvae consumed the most cabbage, as indicated by the highest average weights of cabbage consumed compared to other feeds (0.035 g/larva). 3rd to 4th instar larvae consumed the most water spinach, with average weights of 0.072 g/larvae, and 4th to 5th instar larvae consumed 0.094 g/larvae (Duncan's multiple range test, $p<0.05$).

It is widely recognized that *Spodoptera* larvae consume larger quantities of feed with a softer surface texture and higher water content (da Silva et al. 2017), such as water spinach and cabbage, compared to spinach. The increased water content enhances food assimilation and promotes higher food intake. During the fourth and fifth instar stages, larvae favor water spinach over cabbage leaves. These stages also need significant nutritional reserves, obtained from water spinach, to prepare for pupation. As a polyphagous insect, *S. litura* demonstrates notable tolerance to various types of food with differing nutritional contents, whether high or low. This adaptability is supported by the larvae's ability to balance the nutrition requirements, ensuring survival through developmental phases (Le Gall and Behmer 2014). Test results showed that the highest carbohydrate and protein content in spinach limited larval food preferences, due to lower overall consumption during the instar stage compared to the other two feeds. Higher carbohydrate and protein intake for *S. litura* larvae can function as a large source of energy (calories) but can limit larval digestive efficiency. The feed with low carbohydrate and protein concentrations presents an opportunity to optimize digestive efficiency (Deans et al. 2022). Thus, insects do not require excessive intake if the nutritional content meets their needs. This is likely to cause variations in preferences and the quantity of food consumed by the *S. litura* larvae for their survival and development.

Influence of different host plants on insect growth in terms of larval, pupal, and imago weights

The qualitative assessment of larval growth was performed by measuring the average weight gain during each instar phase. Larvae fed with water spinach exhibited the greatest weight gain during the instar stages, followed by those fed with spinach, while the smallest weight gain was observed in larvae fed with cabbage (Figure 4). Water spinach leaves significantly enhanced larval weight gain, with average weight increments of 17.33, 155.11, 460, and 813.33 mg per larva for the 1st to 5th instar *S. litura* larvae. In comparison, the weight gains for the same instar stages with spinach and cabbage leaves were 12.22, 92.67, 288.44, and 667.56 mg per larva, and 8.22, 28.43, 137.04, and 295.28 mg per larva, respectively (Duncan's multiple range test, $p<0.05$). The type of feed similarly influenced the average weight of pupae. Water spinach resulted in the highest average weight gain (309.78 mg per pupa),

followed by spinach (303.56 mg per pupa), and cabbage, which produced the lightest weight gain (234.17 mg per pupa) (Figure 5.A). However, imago growth showed no significant difference in average weight among the 3 host plants—water spinach, spinach, and cabbage (ANOVA test, $p>0.05$), as shown in Figure 5.B.

The larval stage is a critical phase in the life cycle of Lepidopteran insects (El-Refaie et al. 2024). During this stage, larvae feed and grow significantly, accumulating essential nutrients and energy needed for metamorphosis into the imago stage. The pupal phase is characterized by a period of rest and no feeding. Therefore, the mass gain of pupae depends on the nutrient intake during the larval stage. The efficiency of nutrient utilization as a reserve affects the pupal mass gain. During the pupal phase, various processes occur, including developing new organs, leading to the imago stage. Feed consumption influences the intake of macronutrients, particularly carbohydrates and proteins (Le Gall and Behmer 2014; Blackburn et al. 2016).

Three groups of *S. litura* larvae fed with water spinach, spinach, and cabbage, showed no significant difference in weight gain among the imago stages. This suggests that the larvae adapt to variations in food sources and consume large amounts, reflecting efficient feeding behavior that optimizes nutrient use for imago growth. Insects require complete nutritional content in their feed for normal development. While normal growth can be maintained by addressing nutritional deficits or imbalances, herbivorous insects may face challenges due to suboptimal nutrition over time (Le Gall and Behmer 2014). Future studies could explore how insects compensate for nutritional deficiencies during development.

Influence of different host plants on insect development time

The viability of insect survival is indicated by the normal or shortened development period from larvae to imago. The results showed that the three types of food plants had significantly different effects on the average development time of *S. litura* larvae. Larvae fed with water spinach had the shortest average total development time from larvae to imago emergence, at 27.27 days (Duncan's multiple range test, $p< 0.05$) (Figure 6). This result aligns with earlier evidence that larvae fed water spinach achieved the highest food consumption and weight gain.

Optimal food intake ensures that *S. litura* larvae absorb essential nutrients in the midgut, and then circulate through the hemolymph system. The hemolymph carries these nutrients throughout the body, significantly impacting insect development. Proper nutritional content is crucial for metabolic processes (Bala et al. 2018). Carbohydrates and proteins are essential for effective growth and development (Le Gall and Behmer 2014; da Silva et al. 2017; Bala et al. 2018) Carbohydrates provide necessary metabolic energy and play a role in regulating developmental hormones. Proteins are vital for the secretion of Juvenile Hormone (JH), which governs the metamorphosis process, particularly during instar transitions (Le Gall and Behmer 2014). Therefore, *S. litura* larvae fed on water spinach, with their optimal levels of carbohydrates and proteins, benefit from improved nutrient intake that positively influences their development period. Our study found that *S. litura* takes approximately 27.27 days to develop from larvae to imago when fed water spinach, 28.62 days with spinach, and 33.8 days with cabbage. These durations are within the typical range for *S. litura* development from the first instar to imago emergence when using the main host plant as a food source (Ramzan et al. 2021). All emerging imago displayed normal sex ratios and morphological characteristics. This indicates that *S. litura* has effectively adapted to variations in the nutritional composition of its food intake, ensuring its survival and longevity.

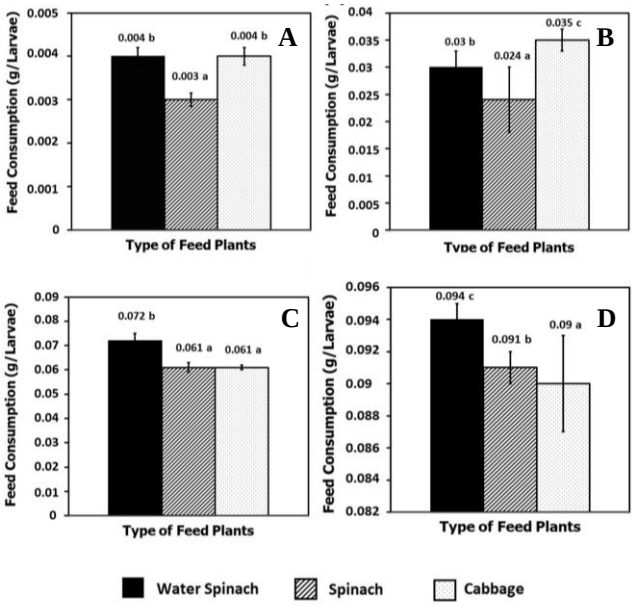

Figure 3. Total feed consumption of *Spodoptera litura* at different larval stages: A. 1st-2nd Instar, B. 2nd-3rd Instar, C. 3rd-4th Instar, D. 4th-5th Instar

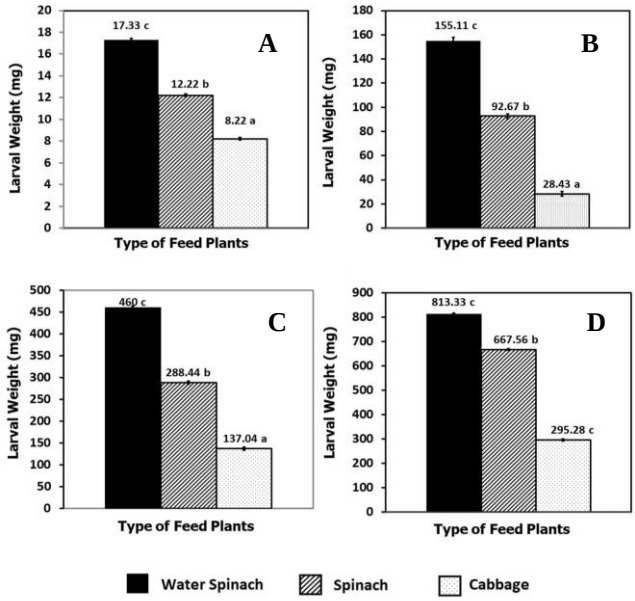

Figure 4. Average weight gain of *Spodoptera litura* larvae at various stages fed different host plants. A. 1st-2nd Instar, B. 2nd-3rd Instar, C. 3rd-4th Instar, D. 4th-5th Instar

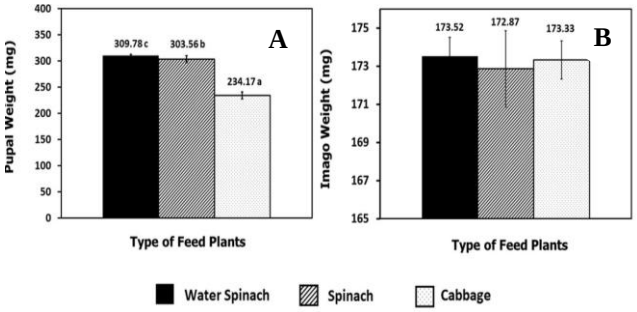

Figure 5. Average weight gain of *Spodoptera litura* pupae and imago at various stages fed different host plants. A. Pupal stage, B. Imago stage

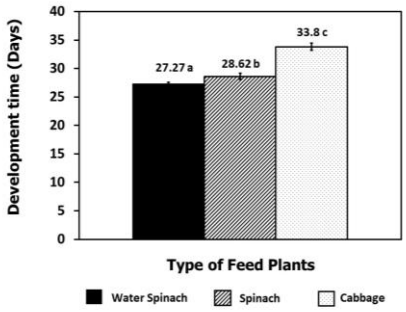

Figure 6. Development time from larvae to imago in *Spodoptera litura* influenced by different host plants

In conclusion, the nutritional content of food plants is essential for the growth, development, and survival of *S. litura* in a controlled rearing environment. Among the three host plants tested, water spinach offers a more balanced composition of carbohydrates, proteins, and water than spinach and cabbage. During the 4th to 5th instar stages, larvae exhibited a higher consumption of water spinach, while early instar 2nd to 3rd larvae showed a significant preference for cabbage leaves. The least consumed is spinach even though its protein composition is the highest. This demonstrates that *S. litura* as a phytophagous insect can adapt to various host plants with different nutritional compositions due to efficiently consumed behavior. The 4th to 5th instar *S. litura* larvae require sufficient carbohydrates and proteins from water spinach to support critical developmental stages leading to pupae and imago. The optimal nutrition from water spinach leads to higher average weights for all larval and pupal stages and shortens the development time. Despite these findings, no significant differences were observed in weight gain or developmental duration to imago across all feeding treatments. The total development period, sex ratio, and morphology of the surviving imago were all within normal ranges. Based on our findings, we recommend the three types of food plants as alternative main hosts for the mass rearing of *S. litura* in a controlled environment. Water spinach is preferred and demonstrates the finest growth and development from larvae to pupae relative to spinach and cabbage. Furthermore, water spinach provides an optimal nutritional composition that enhances the longevity of *S. litura*. Its benefits include ease of cultivation, adaptability to tropical and subtropical climates, widespread availability, and cost-effectiveness.

ACKNOWLEDGEMENTS

This research was funded by the Directorate of Research and Community Services of Universitas Padjadjaran for providing financial support under the Academic Leadership Grant and Functional Nano Powder University Center of Excellence, Universitas Padjadjaran, Sumedang, Indonesia.

REFERENCES

Ashfaq F, Butt MS, Nazir A, Jamil A. 2018. Compositional analysis of Pakistani green and red cabbage. Pak J Agric Sci 55 (1): 191-196. DOI: 10.21162/PAKJAS/18.6547.

Babu SR, Singh B. 2023. Resistance in *Spodoptera litura* (F) to insecticides and detoxification enzymes. Indian J Entomol 85 (1): 90-94. DOI: 10.55446/IJE.2022.519.

Bala K, Sood AK, Pathania VS, Thakur S. 2018. Effect of plant nutrition in insect pest management: A review. J Pharmacogn Phytochem 7 (4): 2737-2742.

Baratella V, Pucci C, Paparatti B, Speranza S. 2017. Response of *Bactrocera oleae* to different photoperiods and temperatures using a novel method for continuous laboratory rearing. Biol Control 110: 79-88. DOI: 10.1016/j.biocontrol.2017.04.010.

Bayu MSYI, Krisnawati A. 2016. The difference growth and development of armyworm (*Spodoptera litura*) on five host plants. Nusantara Biosci 8 (2): 161-168. DOI: 10.13057/nusbiosci/n080206.

Belluco S, Bertola M, Montarsi F, Martino GD, Granato A, Stella R, Martinello M, Bordin F, Mutinelli F. 2023. Insects and public health: An overview. Insects 14 (3): 240. DOI: 10.3390/insects14030240.

Benoit JB, McCluney KE, DeGennaro MJ, Dow JAT. 2022. Dehydration dynamics in terrestrial arthropods: From water sensing to trophic interactions Ann Rev Entomol 68: 129-149. DOI: 10.1146/annurev-ento-120120-091609.

Blackburn D, Shapiro-Ilan DI, Adams BJ. 2016. Biological control and nutrition: Food for thought. Biol Control 97: 131-138. DOI: 10.1016/j.biocontrol.2016.03.007.

Carasi RC, Telan IF, Pera BV. 2014. Bioecology of common cutworm (*Spodoptera Litura*) of Mulberry. Intl J Sci Res Publ 4 (4): 1-8.

da Silva DM, Bueno AF, Andrade K, Stecca CS, Oliveira PM, Neves J, de Oliveira MCN. 2017. Biology and nutrition of *Spodoptera frugiperda* (Lepidoptera: Noctuidae) fed on different food sources. Sci Agric 74 (1): 18-31. DOI: 10.1590/1678-992X-2015-0160.

Deans CA, Sword GA, Vogel H, Behmer ST. 2022. Quantity versus quality: Effects of diet protein-carbohydrate ratios and amounts on insect herbivore gene expression. Insect Biochem Mol Biol 145: 103773. DOI: 10.1016/j.ibmb.2022.103773.

El-Refaie RM, El-Sayed HS, Abd-Allah GE, Ebeid AA, Abouelnaga ZS. 2024. Effect of four host plants on the life history and nutritional indices of *Spodoptera littoralis* Intl J Trop Insect Sci 44: 1091-1101. DOI: 10.1007/s42690-024-01220-w.

Fand BB, Sul NT, Bal SK, Minhas PS. 2015. Temperature impacts the development and survival of common cutworm (S*podoptera litura*): simulation and visualization of potential population growth in India under warmer temperatures through life cycle modeling and spatial mapping. PLoS One 10 (4): e0124682. DOI: 10.1371/journal.pone.0124682.

Ginting S, Chozin M, Sudjatmiko S. 2024. Infestation of *Spodoptera frugiperda* on corn in Bengkulu at different elevations. J Trop Plant Pests Dis 24 (1): 38-47. DOI: 10.23960/j.hptt.12438-47.

Hermawan W, Kasmara H, Melanie M, Panatarani C, Joni IM. 2017. Recent advances of rearing cabinet instrumentation and control system for insect stock culture. AIP Conf Proc 1801 (1): 050005. DOI: 10.1063/1.4973103.

Huđ A, Šamec D, Senko H, Petek M, Brkljačić L, Pole L, Lazarević B, Rajnović I, Udiković-Kolić N, Mešić A, Palijan G, Salopek-Sondi B, Petrić I. 2023. Response of white cabbage (*Brassica oleracea* var. *capitata*) to single and repeated short-term waterlogging. Agronomy 13: 200. DOI: 10.3390/agronomy13010200.

Jing X, Behmer ST. 2020. Insect sterol nutrition: Physiological mechanisms, ecology, and applications. Ann Rev Entomol 65: 251-271. DOI: 10.1146/annurev-ento-011019-025017.

Kalaisekar A, Padmaja PG, Bhagwat VR, Patil JV. 2017. Insect Pests of Millets: Systematics, Bionomics, and Management. Academic Press Elsevier, London.

Kröncke N, Benning R. 2023. Influence of dietary protein content on the nutritional composition of mealworm larvae (*Tenebrio molitor* L.). Insects 14 (3): 1-19. DOI: 10.3390/insects14030261.

Lakitan B, Kartika K. 2020. Population density, multiple harvesting, and ability of *Ipomoea reptans* to compete with native weeds at tropical wetlands. Biodiversitas 21 (9): 4376-4383. DOI: 10.13057/biodiv/d210957.

Le Gall M, Behmer ST. 2014. Effects of protein and carbohydrate on an insect herbivore: The vista from a fitness landscape. Integr Comp Biol 54 (5): 942-954. DOI: 10.1093/icb/icu102.

Montezano DG, Specht A, Sosa-Gómez DR, Roque-Specht VF, Sousa-Silva JC, Paula-Moraes S, Peterson JA, Hunt TE. 2018. Host plants of *Spodoptera frugiperda* (Lepidoptera: Noctuidae) in the Americas. Afr Entomol 26 (2): 286-300. DOI: 10.4001/003.026.0286.

Namin FR, Naseria B, Razmjou J. 2014. Nutritional performance and activity of some digestive enzymes of the cotton bollworm, *Helicoverpa armigera*, in response to seven tested bean cultivars. J Insect Sci 14: 93. DOI: 10.1093/jis/14.1.93.

Narvekar PF, Mehendale SK, Golvankar GM, Karmarkar MS, Desai SD. 2018. Comparative biology of *Spodoptera litura* (Fab.) on different host plants under laboratory condition. Intl J Chem Stud 6 (6): 65-69.

Patil R, Mehta D, Jat B. 2014. Studies on life fecundity tables of *Spodoptera litura* Fabricius on tobacco *Nicotiana tabacum* Linnaeus. Entomol Ornithol Herpetol 3 (1): 1-5. DOI: 10.4172/2161-0983.1000118.

Ramzan M, Asghar MYN, Ijaz M, Abid M, Sardar MU, Latif MA, Hassan M, Akram MS, Moharvi MZ. 2021. The life cycle of armyworm, *Spodoptera litura* (Noctuidae: Lepidoptera) destructive pest of cabbage. Egypt Acad J Biol Sci A Entomol 14 (2): 191-194. DOI: 10.21608/EAJBSA.2021.191036.

Rao MS, Manimanjari D, Rao ACR, Swathi P, Maheswari P. 2014. Effect of climate change on *Spodoptera litura* Fab. on peanut: A life table approach. Crop Prot 66: 98-106. DOI: 10.1016/j.cropro.2014.09.004.

Srivastava K, Sharma D, Anal AKD, Sharma S. 2018. Integrated management of *Spodoptera litura*: A review. Intl J Life Sci Res 4 (1): 1536-1538. DOI: 10.21276/ijlssr.2018.4.1.4.

Standar Nasional Indonesia (SNI). 1992. Cara Uji Makanan dan Minuman. SNI 01-2891- 1992. Pusat Standar Industri. Departemen Perindustrian, Jakarta. [Indonesian]

Subiono T. 2020. Preferensi *Spodoptera frugiperda* (Lepidoptera: Noctuidae) pada beberapa sumber pakan. Jurnal Agroekoteknologi Tropika Lembab 2 (2): 130-134. DOI: 10.35941/jatl.2.2.2020.2813.130-134. [Indonesian]

Supartha IW, Susila IW, Sumiartha IK, Rauf A, Cruz LBD, Yudha IKW, Utama IWE, Wiradana PA. 2022. Preference, population development, and molecular characteristics of *Spodoptera exigua* (Lepidoptera: Noctuidae) on shallot cultivars: A field trial scale. Biodiversitas 23 (2): 783-792. DOI: 10.13057/biodiv/d230224.

Taufika R, Sumarmi S, Hartatie D. 2022. Pemeliharaan ulat grayak (*Spodoptera litura* Fabricius) (Lepidoptera: Noctuidae) menggunakan pakan buatan pada skala laboratorium. Agromix 13 (1): 47-54. DOI: 10.35891/agx.v13i1.2866. [Indonesian]

Thamrin S, Zuliana NS, Sjam S, Melina. 2022. The effect of artificial diet made of soybeans (*Glycine max* L.) on the rearing of *Spodoptera frugiperda* (Lepidoptera: Noctuidae). J Trop Plant Pests Dis 22 (2): 109-115. DOI: 10.23960/j.hptt.222109-115.

Ullah MI, Arshad M, Afzal M, Khalid S, Saleem M, Mustafa I, Iftikhar Y, Molin-Ochoa J, Foster JE. 2016. Incidence of *Spodoptera litura* (Lepidoptera: Noctuidae) and its feeding potential on various citrus (Sapindales: Rutaceae) cultivars in the Sargodha Region of Pakistan. BioOne Fla Entomol 99 (2): 192-195. DOI: 10.1653/024.099.0206.

USA Food Center. Department of Agriculture - Agricultural Research Service. 2021. FoodData Central Search Results, Category: Vegetables. https://fdc.nal.usda.gov/fdc-app.html#/food-details/1999633/nutrients

Vengateswari G, Arunthirumeni M, Shivaswamy MS, Shivakumar MS. 2022. Effect of host plants nutrients, antioxidants, and phytochemicals on growth, development, and fecundity of *Spodoptera litura* (Fabricius) (Lepidoptera: Noctuidae). Intl J Trop Insect Sci 42: 3161-3173. DOI: 10.1007/s42690-022-00868-6.